Journal of the Arkansas Academy of Science

Volume 57 Article 1

2003

Journal of the Arkansas Academy of Science - Volume 57 2003

Academy Editors

Journal of the

CODEN: AKASO
ISBN: 0097-4374

ARKANSAS ACADEMY OF SCIENCE

VOLUME 57
2003

ARKANSAS ACADEMY OF SCIENCE
DEPT. OF PHYSICAL SCIENCE
ARKANSAS TECH UNIVERSITY
RUSSELLVILLE, AR 72801

Library Rate

Arkansas Academy of Science, Dept. of Physical Sciences, Arkansas Tech University

PAST PRESIDENTS OF THE ARKANSAS ACADEMY OF SCIENCE

Charles Brookover, 1917
Dwight M. Moore, 1932-33, 64
Flora Haas, 1934
H. H. Hyman, 1935
L. B. Ham, 1936
W. C. Munn, 1937
M. J. McHenry, 1938
T. L. Smith, 1939
P. G. Horton, 1940
I. A. Willis, 1941-42
L. B. Roberts, 1943-44
Jeff Banks, 1945
H. L. Winburn, 1946-47
E. A. Provine, 1948
G. V. Robinette, 1949
John R. Totter, 1950
R. H. Austin, 1951
E. A. Spessard, 1952
Delbert Swartz, 1953
Z. V. Harvalik, 1954
M. Ruth Armstrong, 1955
W. W. Nedrow, 1956
Jack W. Sears, 1957
J. R. Mundie, 1958
C. E. Hoffman, 1959
N. D. Buffaloe, 1960
H. L. Bogan, 1961
Trumann McEver, 1962
Robert Shideler, 1963
L. F. Bailey, 1965
James H. Fribourgh, 1966
Howard Moore, 1967
John J. Chapman, 1968
Arthur Fry, 1969
M. L. Lawson, 1970
R. T. Kirkwood, 1971
George E. Templeton, 1972
E. B. Wittlake, 1973
Clark McCarty, 1974
Edward Dale, 1975
Joe Guenter, 1976
Jewel Moore, 1977
Joe Nix, 1978
P. Max Johnston, 1979
E. Leon Richards, 1980
Henry W. Robison, 1981
John K. Beadles, 1982
Robbin C. Anderson, 1983
Paul Sharrah, 1984
William L. Evans, 1985
Gary Heidt, 1986
Edmond Bacon, 1987
Gary Tucker, 1988
David Chittenden, 1989
Richard K. Speairs, Jr. 1990
Robert Watson, 1991
Michael W. Rapp, 1992
Arthur A. Johnson, 1993
George Harp, 1994
James Peck, 1995
Peggy R. Dorris, 1996
Richard Kluender, 1997
James Daly, 1998
Rose McConnell, 1999
Mostafa Hemmati, 2000
Mark Draganjac, 2001
John Rickett, 2002

INSTITUTIONAL MEMBERS

The Arkansas Academy of Science recognizes the support of the following institutions through their Institutional Membership in the Academy.

ARKANSAS STATE UNIVERSITY, Jonesboro
ARKANSAS STATE UNIVERSITY, Newport
ARKANSAS TECH UNIVERSTIY, Russellville
HARDING UNIVERSITY, Searcy
HENDERSON STATE UNIVERSITY, Arkadelphia
HENDRIX COLLEGE, Conway
JOHN BROWN UNIVERSITY, Siloam Springs
MISSISSIPPI COUNTY COMMUNITY COLLEGE, Blytheville
OUACHITA BAPTIST UNIVERSITY, Arkadelphia
SOUTHERN ARKANSAS UNIVERSITY, Magnolia
UNIVERSITY OF ARKANSAS AT FAYETTEVILLE
UNIVERSITY OF ARKANSAS AT LITTLE ROCK
UNIVERSITY OF ARKANSAS FOR MEDICAL SCIENCES, Little Rock
UNIVERSITY OF ARKANSAS AT MONTICELLO
UNIVERSITY OF ARKANSAS AT PINE BLUFF
UNIVERSITY OF CENTRAL ARKANSAS, Conway
UNIVERSITY OF THE OZARKS, Clarksville
UNIVERSITY OF ARKANSAS, Fort Smith

EDITORIAL STAFF

COVER: New AAS Logo. Designed by Renn Tumlison.

Arkansas Academy of Science 2003

April 4-5, 2003
87th Annual Meeting

University of Arkansas
Fayetteville, Arkansas

JOURNAL
ARKANSAS ACADEMY OF SCIENCE

ANNUAL MEETING 4-5 APRIL 2003
UNIVERSITY OF ARKANSAS AT FAYETTEVILLE

Secretary's Report

MINUTES OF THE 87TH MEETING

FIRST BUSINESS MEETING
University of Arkansas-Fayetteville BELL Center
APRIL 4, 2003

1. Call to Order: Walt Godwin, President of the AAS, called the meeting to order at 11:00 am with a welcome to all participants. He indicated that the very best thing that we could do as members is to PARTICIPATE and encourage our colleagues to PARTICIPATE in the Arkansas Academy of Science and to PUBLISH in the Journal as it is a PEER REVIEWED journal.

2. Historian: Henry Robison reported that this is the 87th annual meeting of the Arkansas Academy of Science, the 13th such meeting held at Fayetteville and that it had been 12 years since the meeting had last been on the University of Arkansas-Fayetteville campus. Previous meetings included 1937, '40, '48, '51, '54, '61, '65, '69, '72, '78, '84, and 1991.

3. Local Arrangements Chair: Greetings and welcome on behalf of the University to the AAS membership were given by Collis Geren. He expressed his thanks to the many people who have prepared to host the meeting and gave particulars about the facilities and activities planned.

4. Secretary: The minutes from 2002 business meetings at the UALR campus were compiled by Wayne Gray and distributed for approval by vote at the second business meeting. Jeff Robertson reported on the current membership list that included approximately 150 members and 50 student members to the Academy. A request for $200 was made to offset mailing charges incurred for the AAS mailings, the Newsletter, and Journals that were not picked up at the annual meeting which will be voted on at the second business meeting.

5. Treasurer: Joyce Hardin distributed the AAS 2002 Financial statement to the membership. She indicated that because of changes in checking and banking charges the AAS now uses Bank of Ozarks, Conway

2002 FINANCIAL STATEMENT

Ending Balance - December 31, 2002		**$ 28,720.77**
Beginning Balance - January 1, 2002		**$ 28,665.45**
Net Gain		**$ 55.32**

DISTRIBUTION OF FUNDS

Checking Account (Bank of Ozarks, Conway, AR)	**$ 1,017.72**
Certificates of Deposit	
Dwight Moore Endowment (Bank of Ozarks, Conway, AR)	**$ 4,757.24**
Life Membership Endowment (Bank of Ozarks, Conway, AR)	**$ 12,500.00**
CD Unrestricted (US Bank, Conway, AR)	**$ 5,000.00**
Phoebe and George Harp Endowment (Bank of Ozarks, Conway, AR)	**$ 5,445.81**
TOTAL	**$ 28,720.77**

INCOME:

1. ANNUAL MEETING		**$ 2,555.89**
2. ENDOWMENT DONATIONS		
a. AAS Unrestricted	$ 25.00	
b. Moore	$ 25.00	
	$ 50.00	**$ 50.00**
3. INTEREST		**$ 665.98**
4. INDIVIDUAL MEMBERSHIPS		
a. Associate/Student	$ 800.00	
b. Regular	$ 2,830.00	
c. Sustaining	$ 70.00	
d. Sponsoring	$ 0.00	
e. Life	$ 0.00	
	$ 3,700.00	**$ 3,700.00**

Secretary's Report

5. INSTITUTIONAL MEMBERSHIPS		**$ 2,100.00**
6. MISCELLANEOUS		
a. Memorial – John Rickett	$ 100.00	
b. Uncleared check (#699-18 months)	$ 50.00	
	$ 150.00	**$ 150.00**
7. JOURNAL		
a. Miscellaneous Sales	$ 2,850.00	
b. Page Charges	$ 6,120.00	
c. Subscriptions	$ 850.00	
	$ 9,820.00	**$ 9,820.00**
TOTAL INCOME		**$ 19,041.87**
EXPENSES:		
1. ANNUAL MEETING		**$ 0.00**
2. AWARDS		
a. Arkansas Science Fair (723)	$ 400.00	
b. Conway Trophy (1001)	$ 26.84	
c. Student Awards	$ 900.00	
d. Walt Godwin (1002)	$ 81.09	
	$ 1,407.93	**$ 1,407.93**
3. MISCELLANEOUS		
a. Checking account service charge	$ 16.00	
b. Checking account adjustment	$ 32.20	
	$ 48.20	**$ 48.20**
4. *NEWSLETTER*		**$ 0.00**
5. OFFICE EXPENSES		
Treasurer - Joyce Hardin (1007)		**$ 32.20**
6. *JOURNAL*		
a. Stan Trauth - Editorial Consultation and Travel Volume 55 (717)	$ 200.00	
b. Pinpoint Color Volume 55 (711)	$16,677.22	
c. Joy Trauth - Editorial Consultant Volume 56 (1004)	$ 600.00	
d. ATU Physical Science Volume 55 (1006)	$ 21.00	
	$17,498.22	**$17,498.22**
TOTAL EXPENSES		**$18,986.55**

AR. She also indicated that the Accounting committee now meets before the AAS business meetings to go over the books. Details on the income and expenses for the year were presented in addition to journal cost issues. There was a $200 donation to student research from UALR left over from the 2001 AAS meeting that is reflected in the budget.

6. *Journal* Editor-in-Chief: Stan Trauth introduces Chris McAllister as the new journal managing editor to replace the resigning David Saugey as voted on by the Executive Committee. He reports that Vol. 56 of the journal is 257 pages and that the current $40/page charges to publish need to be increased to $50/page. A request for the Academy to continue to support the *Journal* Editor-in-Chief with an allotment of $200 to cover incurred costs will be voted on at the second business meeting. Extra copies of the journal will be available at the annual meeting at a cost of $30/issue. Extra copies after the meeting and back issues will continue to be available for $50/issue.

7. *Journal* Managing Editor: David Saugey welcomes Chris McAllister as he passes the torch. David indicated that the current journal enlisted 70 peer reviewers. He also indicated that one of the national agencies to whom we share our journal with, congratulated the Academy on the quality (both scholarly and aesthetic) of our journal compared to other State Science Academy journals they collected. A request for $500 to cover incurred costs associated with being managing editor was made and will be voted on at the second business meeting. David also wanted to alert membership to the changes in the reprint order forms associated with the journal. Chris McAllister emphasized the need for members who wish to publish in the journal to "get their papers right!" *Journal* guidelines must be followed. If they are not, you will get your paper returned, no questions asked.

8. Newsletter Editor: Jeff Robertson mentioned that now he wears two hats (Newsletter editor and Secretary) there is an opportunity for an enthusiastic someone that desires to participate more fully in Academy business to become the newsletter editor. Jeff will continue happily to do both until such an individual makes themselves known.

9. Arkansas Science Fair Association: Joyce Hardin presented the report from Michael Rapp who requested that the Academy continue to allocate approximately $400 dollars to support the Arkansas Science Fair Association.

10. Junior Academy of Science: Joyce Hardin indicated that the current directors had resigned and that the Junior Academy was in need of new directorship. A request to continue to support the Junior Science and Humanities Symposium through an allotment of $200-400 was made to be voted on at the second business meeting.

11. Intel Talent Search: Joyce Hardin presented the report. The talent search has requested $90 for three plaques to given as awards, be supported by the Academy by vote at the second business meeting.

12. Committee Reports:

    a. Biota Committee: an announcement that the computerization of the Biota list is now complete was made.
    b. Nominations Committee: Mostafa Hemmati, Scott Kirkconnell and Robert Engelken suggested Vice-

Presidential nominees for inclusion in formal nominations at the second business meeting.

c. Science Education Committee: Mostafa Hemmati and Collis Geren indicated they would host a meeting of the committee and interested parties at 4pm after the sessions.

13. Old Business: The establishment of an AAS Young Investigator Award was tabled.

14. New Business: The Academy had asked Renn Tumlison to work on a design for a new logo for the AAS that better reflected the nature of the Academy as an Arkansas Science entity. The draft design was previewed and accepted by the executive committee and will be presented at the second business meeting for approval. Invitations are now well in the future (2006) for hosting annual meetings of the AAS as the Academy will meet at ASU-Jonesboro in 2004 and at Hendrix in 2005. Richard Speairs announced an OMBS meeting. David Saugey encouraged participation in the annual ONF Bat Blitz for faculty and students.

Jeff Robertson, AAS Secretary

SECOND BUSINESS MEETING
University of Arkansas-Fayetteville BELL Center
APRIL 5, 2003

1. Call to Order: Walt Godwin, President of the AAS, called the meeting to order at 11:40 am.

2. Historian: Henry Robison reported that this is the 87th annual meeting of the Arkansas Academy of Science, the 13th such meeting held at Fayetteville and that it had been 12 years since the meeting had last been on the University of Arkansas-Fayetteville campus. Previous meetings included 1937, '40, '48, '51, '54, '61, '65, '69, '72, '78, '84, and 1991.

3. Secretary: The minutes from 2002 business meetings at the UALR campus were approved. Jeff Robertson reported on the current membership list that included approximately 150 members and 50 student members to the Academy. A request for $200 was made to offset mailing charges incurred for the AAS mailings, the Newsletter, and Journals that were not picked up at the annual meeting was approved.

4. Treasurer: Bob Wiley, chair of the Accounting Committee, and Eric Sundell praised Joyce Hardin for the truth and accuracy of the Arkansas Academy of Science books. The financial report was unanimously accepted.

5. *Journal* Editor-in-Chief: Stan Trauth gave praise and thanks to outgoing journal managing editor David Saugey. Chris McAllister begins a 5-year appointment as the new journal managing editor. A motion to increase page charges from $40/page to $50/page was approved after an amendment to include a clause for hardship cases.

6. *Journal* Managing Editor: David Saugey indicated that one of the national agencies to whom we share our journal with, congratulated the Academy on the scholarly and aesthetic quality of our journal compared to other State Science Academy journals they collected. This is helped in part to the "wide spectrum" of peer reviewers in our acceptance process. A request for $500 to cover incurred costs associated with managing editor duties was approved.

7. Newsletter Editor: Jeff Robertson noted that there is an opportunity for a newsletter editor. Jeff will continue happily to do both the newsletter and secretary duties until someone desires to do the newsletter.

8. Arkansas Science Fair Association: Joyce Hardin presented the report from Michael Rapp and approval of $400 dollars to support the Arkansas Science Fair Association passed.

9. Junior Academy of Science: The Junior Academy is in need of new directorship. A request to continue to support the Junior Science and Humanities Symposium through an allotment of up to $400 was approved.

10. Intel Talent Search: A request of $90 from Jim Murray for three plaques to given as awards was approved.

11. Committee Reports:

    a. Biota Committee: the computerization of the Biota lists are now complete.
    b. Nominations Committee: Stan Trauth was elected by vote as Vice-President, joining Wayne Gray (President-Elect) and Betty Crump (current Vice President).
    c. Science Education Committee: Mostafa Hemmati and Collis Geren shared information about the science education discussions.

12. Local Arrangements Committee: Collis Geren announced the various scholarly awards presented to students for their research presented at the meeting symposia.

13. New Business: The new Arkansas Academy of Science LOGO designed by Renn Tumlison was accepted by

the membership. Boa-An Li from ASU-Jonesboro announced the dates of the 2004 meeting as April 2-3, 2004. Richard Spears suggested that more effort should be made to facilitate participation of the state's 2-year institutions in the Arkansas Academy of Science. David Saugey encouraged participation in the annual ONF Bat Blitz for faculty and students.

14. Closing: New president Wayne Gray accepted the gavel from former president Walt Godwin as Walt accepted a plaque from Wayne for his dedicated service. Wayne announced that everyone should develop plans to promote the activities of the Academy through advertising in every way shape and form. Meeting adjourned at 12:40 pm.

Jeff Robertson, AAS Secretary

APPENDIX A

2003 AAS Award Winners

GRADUATE STUDENT AWARDS

Engineering:

1st: Paul Millett
Computer Modeling of the Tornado-Structure Interaction: Investigations...
UAF

2nd: Ty McNutt
Silicon Carbide Power Device Models
UAF

3rd: Fisal Magableh
Effect of Design Parameters on Slow Wave Resonators
UAF

Life Science:

1st: David Williams
Molecular Systematics of Quercus Acerifolia UAF

2nd: M. L. McCallum
Can the Illinois Chorus Frog Survive in Arkansas ASU

3rd: T. E. Posey
Individual-Tree Green Weight Equations for the Loblolly Pine UAM

Physical Science:

1st: P. Rangarajan
Determinatin of Bile Acids in a Mixture by GC-MS
UALR

2nd: J. Annaratone
Preliminary IR Study of the Reaction ASU

3rd: A. Meier
Simulations of the Formation of Asteroids UAF

Poster Presentation:

1st: Emily Clark
Magnetohydrodynamics Studies UAF

2nd: Jennifer Lewter
DNA Sequence Analysis UAF

3rd: Eyutayo Fakunle
Low-Temperature Co-fired Cerami UAF

Honorable Mention: Muhammad Hossain
Assessment of Environmental Impact from the Wal-Mart
HS-UAPB

UNDERGRADUATE STUDENT AWARDS

Engineering:

1st: James Toland
A Development of a Generic Fatique Life Prediction Model
ATU

2nd: Pashupati Adhikari
A New Parameter for Fatique Crack Growth Rate Analysis
ATI

3rd: Bert Buford
Influence of Biological Factors in the Design of Hip Inplants
ATU

Life Science:

1st: K. A. Davis
Effects of Nectar on Energy Content of Monarch Butterflies
UALR

2nd: R. G. Neal
Calling Site Characterization of the Illinois Chorus Frog
ASU

3rd: S. M. Starnes
Response of Individual Plants to Fire in a Relicit Grassland
Hendrix

Physical Science:

1st: Pashupati Adhikar
Antiforce Wave Profile for Quasi-Neutral Region ATU

2nd: A. Ellison
Synthesis of a Trinuclear Ruthenium Complex UAF

Poster Presentation:
1st: Tiffany Ricks
Investigations of Stereoselectivity UAF

2nd: Amanda Suttle
Speciation of Chromate in Chromium ATU

3rd: Allan Holloway
Fabrication and Testing...CCD Spectography UCA

APPENDIX B

RESOLUTIONS

Be it resolved that we, the membership of the Arkansas Academy of Science, offer our sincere appreciation to the University of Arkansas-Fayetteville for hosting the 87th annual meeting of the Arkansas Academy of Science. We thank the Local Arrangements Committee: Chair Collis Geren, John Hehr, Duane Wolf, William Brown and all of the student workers and staff, who collectively contributed to such a successful meeting, particularly Gail Piaha of the Division of Continuing Education, as well as Benita Wolff, Patricia Koski and Shannon Stewart. Appreciation is expressed for the use of these excellent facilities, and the hospitality shown to us by the University of Arkansas personnel. We especially thank our Keynote Speaker, Dr. W. Frederick Limp for the technically informative and timely presentation entitled "A Sense of Where You Are: The Growing Role of Geospatial Technologies in Arkansas." We thank the University of Arkansas for their donations to the Social and Banquet, which were both excellent and thoroughly enjoyed by all. And we thank Provost Bob Smith for his thought provoking and entertaining welcome.

We appreciate the Program Chairs, who contributed to the organization and facility provision for this meeting: Stephen Boss (Geosciences), Dennis Brewer (Computer Science & Computer Engineering), Johnnie Gentry (University Museum/Biological Sciences), Dale Johnson (Chemistry & Biochemistry), Hameed Naseem (Electrical Engineering), Curt Rom (Horticulture), Richard Ulrich (Chemical Engineering), and Kenneth Vickers (Microelectronics-Photonics). The Academy recognizes the important role assumed by Session Chairs and expresses sincere appreciation to: Charles Rosenkrans, Steve Beaupre, Edith Hardcastle, Em Ward, Adnan Al-Shariah, Susan Burkett, Husam Abu-Safe, Richard Ulrich, Curt Rom, Laurent Bellasch, Dennis Brewer,Greg Tom, Robert Bittle, Frank Millett, William Brown, Fred Barlow, Stephen Boss, Eric Sundell and Don Culwell. A special appreciation is owed to these individuals who devoted considerable time and energy to judging the student papers: Dan Davis, Grover Paul Miller, Mostafra Hemmati, Bao-Ann Li, Tsunemi Yamashita, Russell Nordeen, Bill Durham, Lin Oliver, Frank Hardcastle, Paul Benoit, Collis Geren, Wayne Wahls, and Richard Ulrich.

We gratefully acknowledge the various directors of the science and youth activities which are supported or supervised by the Academy: Mostafa Hemmati, Chair of the Science Education Committee; Mike Rapp, Director of the Arkansas State Science Fair Association; Jim Murray, Director of the Intel Science Talent Search; and Rick Geraci and Mark Eakin, Co-Directors of the Junior Academy of Science. We wish to thank all those who served as directors at the regional science fairs and Junior Academy meetings including: Kathryn Shinn, Beverly Meinzer, Marty Huss, Lynne Hehr, Gary Earleywine, Jim Edson, Brian Monson and Mike Rapp.

The Academy appreciates the Arkansas Environmental Federation for donating to the undergraduate student awards and Sigma Xi for the graduate student awards. We congratulate all who presented papers and posters at this meeting. Student participants are especially recognized since their efforts contribute directly to the future success of the Academy and the improvement and advancement of science in Arkansas.

The continued success of the Academy is due to its strong leadership. We offer sincere thanks to our officers for another excellent year: Walt Godwin (President), Wayne Gray (President-Elect), Betty Crump (Vice-President), John Rickett, who will be with us in spirit for a very long time (Past-President), Jeff Robertson (Secretary), Joyce Hardin (Treasurer), Stan Trauth (*Journal* Editor-in-Chief), David Saugey (*Journal* Managing Editor), Jeff Robertson (Newsletter Editor), and Henry Robison (Historian).

Finally, the membership wishes to posthumously recognize Dr. Harvey E. Barton and Dr. Earl L. Hanebrink for their many years of numerous and valuable contributions and services to their students, to the Academy, and to the science and biology professions.

Respectfully submitted this 5th day of April, 2003.

Resolution Committee
Betty G. Crump, Chair
Wayne Gray
Walt Godwin

MEMBERS 2003

FIRST MI	LAST NAME	INSTITUTION
Robbin C.	Anderson	University of Arkansas-Fayetteville
Scott	Austin	University of Central Arkansas
Edmond J.	Bacon	University of Arkansas-Monticello
Gwen	Barber	Arkansas Tech University
Vernon	Bates	Ouachita Mtns. Biological Station
Melinda	Bodary	University of Arkansas-Pine Bluff
Wilfred J.	Braithwaite	University of Arkansas-Little Rock
Tom	Buchanan	University of Arkansas-Ft. Smith
Carrie	Cavenaugh	Arkansas State University
Michelle	Caviness	University of Arkansas-Fayetteville
David	Chittenden	Arkansas State University
Alan	Christian	Arkansas State University
Shawn	Cochran	U.S.D.A. Forest Service
Calvin	Cotton	Geographics Silk Screening Co.
Betty	Crump	U.S.D.A.
Donald	Culwell	University of Central Arkansas
James	Daly	University of Arkansas/Medical Sciences
Leo Carson	Davis	Southern Arkansas University
Robert H.	Dilday	University of Arkansas-Fayetteville
Paul	Doruska	University of Arkansas-Monticello
Mark	Draganjac	Arkansas State University
Brad	Edgar	Arkansas State University
Jim	Edson	University of Arkansas-Monticello
Rudolph	Eichenberger	Southern Arkansas University
Daniel R.	England	Southern Arkansas University
James	Engman	Henderson State University
William L.	Evans	University of Arkansas-Fayetteville
Kim	Fifer	University of Arkansas/Medical Sciences
James H.	Fribourgh	University of Arkansas-Little Rock
Arthur	Fry	University of Arkansas-Fayetteville
Linda	Gatti-Clark	Hendrix College
Johnnie	Gentry	University of Arkansas-Fayetteville
Collis	Geren	University of Arkansas-Fayetteville
David	Pace	Lyon College
Anthony	Grafton	Lyon College
John	Giese	Ark. Dept. of Env. Qual. (ret)
Walter	Godwin	University of Arkansas-Monticello
Dave	Gosse	The Nature Conservancy
Stephen	Grace	University of Arkansas-Little Rock
G.O.	Graening	Ozark Highlands Office
John	Graham	Arkansas Tech University
Wayne	Gray	University of Arkansas/Medical Sciences
Brian	Greuel	John Brown University
Joe M.	Guenter	University of Arkansas-Monticello
Franklin	Hardcastle	Arkansas Tech University
Joyce	Hardin	Hendrix College
Laurence	Hardy	LSU-Shreveport
George	Harp	Arkansas State University
Phoebe	Harp	Arkansas State University
Gary	Heidt	University of Arkansas-Little Rock
Ronnie	Helms	University of Arkansas-Fayetteville
Mostafa	Hemmati	Arkansas Tech University
William	Holimon	Arkansas Natural Heritage Commission
Philip	Hyatt	Kisatchie National Forest
Debra	Ingram	Arkansas State University
Jefremy	Jackson	FTN Associates
Carol	Jacobs	
Douglas	James	University of Arkansas-Fayetteville
David	Jamieson	ASU-Beebe/Newport
Arthur	Johnson	Hendrix College
George	Johnson	Arkansas Tech University
Ronald	Johnson	Arkansas State University
Cindy	Kane	University of Arkansas/Medical Sciences
Roger	Koeppe	University of Arkansas-Fayetteville
Janet	Lanza	University of Arkansas-Little Rock
Bao-An	Li	Arkansas State University
Michelle	Mary	Arkansas State University
Donald	Mattison	March of Dimes National Office
Donald	Mattison	March of Dimes National Office
Chris	McAllister	Texas A&M-Texarkana
Malcom	McCallum	Arkansas State University
Roland	McDaniel	FTN Associates
Dennis	McMasters	Henderson State University
Grover	Miller	UAMS
Herbert	Monoson	Ark. Science & Technology Authority
Clementine	Moore	
Matthew	Moran	Hendrix College
Alex	Nisbet	Ouachita Baptist University
Russell	Nordeen	University of Arkansas-Monticello
Gaylord	Northrop	University of Arkansas-Little Rock
Tom	Palko	Arkansas Tech University
James	Peck	University of Arkansas-Little Rock
Floyd	Perk	U.S. Public Health Service
Janet	Rader	Southern Arkansas University
Michael	Rapp	University of Central Arkansas
Scott	Reeve	Arkansas State University
Dennis	Richardson	Quinnipiac College
Jeff	Robertson	Arkansas Tech University
Henry	Robison	Southern Arkansas University
Dennis	Ruez	University of Texas-Austin
Blake	Sasse	Arkansas Game and Fish Com.
David	Saugey	U.S. Forest Service
Lothar	Schafer	University of Arkansas-Fayetteville
Stephen	Sewell	University of Mississippi
Paul	Sherman	Arkansas State University
Richard	Smith	University of Arkansas/Medical Sciences
Betty	Spears	Ouachita Mtns. Biological Station
Richard	Spears	Ouachita Mtns. Biological Station
Lori	Spencer	Mt. Magazine State Park
Frederick	Spiegel	University of Arkansas-Fayetteville
Richard	Standage	USDA Forest Service
Eric	Sundell	University of Arkansas-Monticello
George	Templeton	University of Arkansas-Fayetteville
Stanley	Trauth	Arkansas State University
Joy	Trauth	Arkansas State University
Gary	Tucker	FTN Associates
Renn	Tumlison	Henderson State University
Staria	Vanderpool	Arkansas State University
Brian	Wagner	Arkansas Game and Fish Commission
Wayne	Wahls	UAMS
Gerald	Walsh	
Rocky	Ward	Texas Parks and Wildlife Dept.
Hilary	Warley	Arkansas State University
Michael	Warriner	Arkansas Natural Heritage Commission
Benjamin	Wheeler	Arkansas State University
James	Wickliff	University of Arkansas-Fayetteville
Robert	Wiley	University of Arkansas-Monticello
Jim	Winter	University of Arkansas-Little Rock
Duane	Wolf	University of Arkansas-Fayetteville
Tsunemi	Yamashita	Arkansas Tech University
Bin	Zhang	Arkansas State University

SPONSORING MEMBERS

Bin	Zhang	Arkansas State University

LIFE MEMBERS

Robbin C.	Anderson	University of Arkansas-Fayetteville
Edmond J.	Bacon	University of Arkansas-Monticello
Vernon	Bates	Ouachita Mtns. Biological Station
Wilfred J.	Braithwaite	University of Arkansas-Little Rock
David	Chittenden	Arkansas State University
Calvin	Cotton	Geographics Silk Screening Co.
Betty	Crump	U.S.D.A.
James	Daly	University of Arkansas/Medical Sciences
Leo Carson	Davis	Southern Arkansas University
Robert H.	Dilday	University of Arkansas-Fayetteville
Mark	Draganjac	Arkansas State University
Jim	Edson	University of Arkansas-Monticello
Daniel R.	England	Southern Arkansas University
William L.	Evans	University of Arkansas-Fayetteville
Kim	Fifer	University of Arkansas/Medical Sciences
James H.	Fribourgh	University of Arkansas-Little Rock
Arthur	Fry	University of Arkansas-Fayetteville
Linda	Gatti-Clark	Hendrix College
Collis	Geren	University of Arkansas-Fayetteville
John	Giese	Ark. Dept. of Env. Qual. (ret)
Walter	Godwin	University of Arkansas-Monticello
Joe M.	Guenter	University of Arkansas-Monticello
Joyce	Hardin	Hendrix College
George	Harp	Arkansas State University
Phoebe	Harp	Arkansas State University
Gary	Heidt	University of Arkansas-Little Rock
Ronnie	Helms	University of Arkansas-Fayetteville

FIRST MI	LAST NAME	INSTITUTION
Mostafa	Hemmati	Arkansas Tech University
Carol	Jacobs	
Douglas	James	University of Arkansas-Fayetteville
Arthur	Johnson	Hendrix College
Cindy	Kane	University of Arkansas/Medical Sciences
Roger	Koeppe	University of Arkansas-Fayetteville
Donald	Mattison	March of Dimes National Office
Roland	McDaniel	FTN Associates
Herbert	Monoson	Ark. Science & Technology Authority
Clementine	Moore	
Gaylord	Northrop	University of Arkansas-Little Rock
Tom	Palko	Arkansas Tech University
James	Peck	University of Arkansas-Little Rock
Michael	Rapp	University of Central Arkansas
Jeff	Robertson	Arkansas Tech University
Henry	Robison	Southern Arkansas University
David	Saugey	U.S. Forest Service
Stephen	Sewell	University of Mississippi
Betty	Speairs	Ouachita Mtns. Biological Station
Richard	Speairs	Ouachita Mtns. Biological Station
George	Templeton	University of Arkansas-Fayetteville
Stanley	Trauth	Arkansas State University
Gary	Tucker	FTN Associates
Renn	Tumlison	Henderson State University
James	Wickliff	University of Arkansas-Fayetteville
Robert	Wiley	University of Arkansas-Monticello
Stephen A.	Walker	

STUDENT MEMBERS

Jan	Annaratone	ASU
Kirk	Babb	UALR
Ben	Ball	ASU
Marwan	Barghouti	UARK
Amanda	Bell	UARK
Ty	Blacklock	UALR
Michelle	Christy	UARK
Emily	Clark	UARK
Amanda	Crnkovic	OMBS
Sami	Eyuboglu	UALR
Tommy	Finley	UALR
Kristen	Greer	UARK
Darin	Gwartney	JBU
Lori	Hardcastle	ATU
Edith	Hardcastle	UARK
Allan	Holloway	UCA
Eran	Jones	UARK
Sandra	Kirchhoff	UALR
Kate	Ledbetter	ATU
Thalia	Madewell	UARK
Sharmila	Magan Lal	UARK
Travis	Marsisco	UARK
Shannan	Nilz	UALR
Sarah	Nunn	UARK
Eyitayo	Ofakunle	UARK
Travis	Posey	UAM
Zach	Ramsey	TAMUT
William	Reed	ASU
Tiffany	Ricks	UARK
Anindo	Roy	UALR
Shawn	Singer	TAMUT
Michael	Slay	UARK
Kristen	Sterba	UAMS
Amanda	Suttles	ATU
Stacie	Thomas	UALR
Kimberly	Trobaugh	UCA
David	Williams	UARK
Jeff	Wilson	UARK

PROGRAM

Arkansas Academy of Science

87th Annual Meeting
April 4-5, 2003
Fayetteville, Arkansas

SCHEDULE OF EVENTS

Friday, April 4, 2003		
9:00 am. - 3:00 p.m.	Registration	Bell Engineering
8:30 a.m. - 10:30 a.m.	Executive Committee Meeting	Upchurch Conf. Room, 3162 Bell Engineering
11:00 a.m. - 12:00 p.m.	First Business Meeting	Giffels Auditorium, Old Main
	Oral Presentations	
1:30 p.m. - 4:00 p.m.	Biology I	SCEN 403
1:30 p.m. - 4:15 p.m	Biology II	SCEN 406
1:30 p.m. - 4:30 p.m.	Arkansas Flora I	SCEN 407
1:30 p.m. - 4:30 p.m.	Geosciences, Science Education	SCEN 408
1:30 p.m. - 4:30 p.m.	Engineering I	BELL 268
1:30 p.m. - 2:30 p.m.	Chemistry I	BELL 269
1:30 p.m. - 3:00 p.m.	Physics	BELL 288
1:30 p.m. - 4:30 p.m.	Computer Science, Mathematics	BELL 288
1:30 p.m. - 4:00 p.m.	Poster Presentations	BELL 4008 Student Lounge
4:00 p.m.	AAS Science Ed. Committee	
4:30 p.m. - 5:30 p.m.	Keynote Address: Dr. Fred Limp *A Sense of Where You Are: The Growing Role of Geospatial Technologies in Arkansas*	BELL Auditorium
6:00 p.m. - 7:00 p.m.	Reception / Social Mixer	UARK Bowl
7:00 p.m. - 8:00 p.m.	Banquet	UARK Bowl
Saturday, April 5, 2003		
	Oral Presentations	
8:00 a.m. - 10:45 am.	Biology III	SCEN 403
8:00 a.m. - 10:45 am.	Biology IV	SCEN 406
8:00 a.m. - 10:45 am.	Biology V	SCEN 407
8:00 a.m. - 10:45 am.	Arkansas Flora II	SCEN 408
8:00 a.m. - 10:30 am.	Chemistry II	BELL 269
8:00 a.m. - 10:45 am.	Engineering II	BELL 268
8:00 a.m. - 10:30 a.m.	Engineering III	BELL 288
8:00 a.m. - 11:00 a.m.	Poster Presentations	BELL 4008 Student Lounge
11:30 a.m. - 12:30 p.m.	Second Business Meeting	BELL Auditorium

SECTION PROGRAMS

*** Undergraduate **Graduate**

ORAL PRESENTATIONS

Friday, April 4, 2003
Biology I: Plant Communities and Biology, and Fundamental Biology
Location: SCEN Room 403

Time — Topic

1:30 — Lauren P. Blair and Matthew D. Moran. Department of Biology, Hendrix College, 1600 Washington Ave., Conway, AR 72032. **PRIMARY FOREST IN ARKANSAS POST OAK SAVANNAS**

1:45 — Paul F. Doruska*, Robert C. Weih* Jr., Matthew D. Lane* and Don C. Bragg+, *University of Arkansas School of Forest Resources; Arkansas Forest Resources Center, PO Box 3468, Monticello, AR 71656, +USDA Forest Service Southern Research Station, P.O. Box 3516 UAM, Monticello, AR 71656. **QUANTIFYING FOREST GROUND FLORA BIOMASS USING PROXIMAL SENSING**

2:00 — Travis E. Posey, Paul F. Doruska, and David W. Patterson, University of Arkansas School of Forest Resources; Arkansas Forest Resources Center, PO Box 3468, Monticello, AR 71656. **INDIVIDUAL-TREE GREEN WEIGHT EQUATIONS FOR LOBLOLLY PINE SAWTIMBER IN THE COASTAL PLAIN OF ARKANSAS**

2:15 — C. Joan Patterson and Douglas A. James, Department of Biological Sciences, University of Arkansas, Fayetteville, AR 72701. **SPEED AND ACCURACY OF METHODS FOR OBTAINING FOREST STAND MEASUREMENTS**

2:30 — Sarah M. Starnes and Matthew D. Moran, Biology Department, Hendrix College, 1600 Washington Ave., Conway, AR 72032. **RESPONSE OF INDIVIDUAL PLANTS TO FIRE IN A RELICT GRASSLAND**

2:45 — K.M. Greer[1], P.M. White, Jr.[1], D.C. Wolf[1], G.J. Thoma[2], and S.E. Ziegler[3], Univ. of Arkansas, [1]Dept. of Crop, Soil, & Env. Sci., [2]Dept. of Chem. Engr., and [3]Dept. of Biol. Sci. Fayetteville, AR 72701. **EVALUATION OF FIELD SCALE PHYTOREMEDIATION OF CRUDE OIL-CONTAMINATED SOIL**

3:15 — Eric T. Stafne[1], Allen L. Szalanski[2], and John R. Clark[1], [1]Department of Horticulture, University of Arkansas, Fayetteville, AR 72701, [2]Department of Entomology, University of Arkansas, Fayetteville, AR 72701. **NUCLEAR**

RIBOSOMAL ITS REGION SEQUENCES FOR DIFFERENTIATION OF *RUBUS* GENOTYPES

3:30 Terry Hostetler,* Timothy O'Brien**, Max Baker+, and James Daly Sr*. Departments of Microbiology and Immunology*, Obstetrics and Gynecology**, and Radiology+; University of Arkansas for Medical Sciences, Little Rock AR 72205. **THE USE OF IRRADIATED AND FORMALIN-FIXED *TRICHOMONAS VAGINALIS* TO EXAMINE PROTECTIVE IMMUNE RESPONSES IN THE MOUSE MODEL**

3:45 Kristen M. Sterba[1], Samuel G. Mackintosh[1], Jon S. Blevins[2], Barry K. Hurlburt[1,3], and Mark S. Smeltzer[2], Departments of Biochemistry and Molecular Biology[1] and Microbiology and Immunology[2], University of Arkansas for Medical Sciences, Little Rock, AR 72205 and United States Department of Agriculture, Southern Regional Research Center, New Orleans, Louisiana, 70124. **CHARACTERIZATION OF SARA BINDING SITES IN *STAPHYLOCOCCUS AUREUS***

Friday, April 4, 2003
Biology II: Mammalian and Avian Communities and Biology
Location: SCEN Room 406

Time Topic

1:30 Erin E. McCammon, Philip A. Tappe, And Robert E. Kissell, Jr., Arkansas Forest Resources Center and School Of Forest Resources, University Of Arkansas, Monticello, AR 71656. **A COMPARISON OF GROUND-BASED THERMAL-INFRARED IMAGING WITH SPOTLIGHT COUNTS OF WHITE-TAILED DEER**

1:45 Donald I. M. Enderle and Philip A. Tappe, Arkansas Forest Resources Center and School of Forest Resources, University of Arkansas-Monticello, AR 71656. **SITE-LEVEL HABITAT AND HIGHWAY FACTORS CONTRIBUTING TO DEER-VEHICLE COLLISIONS ON STATE AND FEDERAL HIGHWAYS IN ARKANSAS**

2:00 Michael C. Farrell and Philip A. Tappe, Arkansas Forest Resources Center and School of Forest Resources, University of Arkansas at Monticello, School of Forest Resources, Arkansas Forest Resources Center, Monticello, AR 71656. **A MULTIVARIATE ANALYSIS OF COUNTY-LEVEL FACTORS THAT CONTRIBUTE TO DEER-VEHICLE COLLISIONS IN ARKANSAS**

2:15 Zachary D. Ramsey and Chris T. McAllister, Department of Biology, Texas A&M University-Texarkana, Texarkana, TX 77505. **BATS OF THE ARK-LA-TEX, WITH A NOTEWORTHY RECORD OF THE SEMINOLE BAT, *LASIURUS SEMINOLUS* (CHIROPTERA: VESPERTILIONIDAE), FROM EXTREME SOUTHWESTERN ARKANSAS**

2:30 W. Drew Reed[1], Tammy Jones[1], J.D. Wilhide[1], Roger Buchanan[1], Betty Crump[2], Blake Sasse[3], and David A. Saugey[4]. [1]Department of Biological Sciences, Arkansas State University, P.O Box 599, State University, AR 72467; [2] U.S. Forest Service, P.O. Box 1270, Hot Springs, AR 71902; [3] Arkansas Game and Fish Commission, #2 Natural Resources Drive, Little Rock, AR 72205; [4] U.S. Forest Service, P.O. Box 189, Jessieville, AR 71949. **BRIDGE AND MINE USE BY SOUTHEASTERN MYOTIS (MYOTIS USTRORIPARIUS) IN SOUTHWEST ARKANSAS**

2:45 William C. Holimon, Arkansas Natural Heritage Commission, 1500 Tower Building, 323 Center Street, Little Rock, AR 72201, and Douglas A. James, Department of Biological Sciences, University of Arkansas, Fayetteville, AR 72701. **NESTING WILLOW FLYCATCHERS DISCOVERED AT HARRISON, ARKANSAS**

3:15 William C. Holimon, Arkansas Natural Heritage Commission, 1500 Tower Building, 323 Center Street, Little Rock, AR 72201, Warren G. Montague, Poteau Ranger District-Ouachita National Forest, USDA-Forest Service, P.O. Box 2255, Waldron, AR 72958. **RECIPROCAL TRANSLOCATION REESTABLISHES BREEDING STATUS OF MISSISSIPPI ALLUVIAL PLAIN POPULATION OF RED-COCKADED WOODPECKER IN ARKANSAS**

3:30 Lori Spencer and Don Simons, Mount Magazine State Park, 16878 Highway 309 South, Paris, AR 72855. **STATUS OF WILDLIFE MANAGEMENT AT MOUNT MAGAZINE STATE PARK**

3:45 Ty D. Blacklock[1], Gary A. Heidt[1], and David A. Saugey[2], [1]Dept. of Biology, University of Arkansas at Little Rock, Little Rock, AR 72204 and [2]USFS, Jessieville, AR 71949 **REPORTED ANIMAL RABIES IN ARKANSAS: 1991-2000**

4:00 Sandra J. Kirchhoff, Marie Greene, and Gary A. Heidt, Little Rock Zoo, Little Rock, AR 72205 and Dept. of Biology, University of Arkansas at Little Rock, Little Rock, AR 72204. **SEASONAL ACTIVITY AND EXHIBIT USE BY THE CAPYBARA (*HYDROCHOERUS HYDROCHAERIS*) AT THE LITTLE ROCK ZOO**

Friday, April 4, 2003
Arkansas Flora I
Location: SCEN Room 407

Time Topic

1:30 Johnnie L. Gentry, University of Arkansas Herbarium, University of Arkansas, Biomass Research Center 141, Fayetteville, AR 72701, James H. Peck, Department of Biology, University of Arkansas at Little Rock, 2801 S. University Ave., Little Rock, AR 72204 and Sarah Nunn, University of Arkansas Herbarium, University of Arkansas, Biomass Research Center 141, Fayetteville, AR 72701. **WAIFS, WEEDS AND INVASIVES: A PRELIMINARY REVIEW OF ARKANSAS' NON-NATIVE VASCULAR FLORA**

1:45 Gary Tucker. **HISTORY OF ARKANSAS BOTANY: ROLE OF UNIVERSITY OF ARKANSAS**

2:00 James H. Peck, Department of Biology, University of Arkansas at Little Rock, 2801 S. University Ave., Little Rock, AR 72204. **HOW TO STUDY THE ARKANSAS FLORA: A 22 YEAR STUDY OF PTERIDOPHYTES**

2:15 James H. Peck, Department of Biology, University of Arkansas at Little Rock, 2801 S. University Ave., Little Rock, AR 72204. **ARKANSAS VASCULAR FLORA: ADDITIONS, RE-INSTATEMENTS, EXCLUSIONS, and RE-EXCLUSIONS**

2:30 George P. Johnson, Herbarium (APCR), Arkansas Tech University, McEver Building Room 37A, 1701 North Boulder Avenue, Russellville, AR 72801-2222. **ARKANSAS' ORCHIDS: THE STATE OF THE STATE**

2:45 James S. Pringle, Royal Botanical Gardens, P.O. Box 399,

Hamilton, Ontario, Canada, L8N 3H8; C. Theo Witsell, Arkansas Natural Heritage Commission, 1500 Tower Building, 323 Center St., Little Rock, AR 72201, USA. **A NEW SPECIES OF *SABATIA* (GENTIANIACEAE) FROM CENTRAL ARKANSAS**

3:15 Theo Witsell, Arkansas Natural Heritage Commission, 1500 Tower Building, 323 Center St., Little Rock, AR 72201. **ADDITIONS AND NOTEWORTHY COLLECTIONS FOR THE FLORA OF ARKANSAS**

3:30 Edith L. Hardcastle, University of Arkansas, Fayetteville, Department of Biological Sciences, Fayetteville, Arkansas 72701. **CONSERVATION GENETICS OF DELPHINIUM NEWTONIANUM (RANUNCULACEAE)**

3:45 Travis Marsico, University of Arkansas Herbarium (UARK), Biomass Research Center 141, Fayetteville, AR 72701, (479) 575-4372, tmarsic@uark.edu. **ON THE RARE ENDEMIC *HYDROPHYLLUM BROWNEI* KRAL & BATES (BROWNE'S WATERLEAF) NEW POPULATION INFORMATION AND A RECOMMENDATION FOR CHANGE IN STATUS**

4:00 David X. Williams, Dept. of Biological Sciences, University of Arkansas, Fayetteville, AR, 72701. **MOLECULAR SYSTEMATICS OF *QUERCUS ACERIFOLIA*: IS MAPLE-LEAF OAK REALLY A SPECIES?**

4:15 Brent Baker, University of Central Arkansas, Conway, AR 72035. **A PRELIMINARY SURVEY OF THE VASCULAR FLORA OF YELL COUNTY, ARKANSAS**

Friday, April 4, 2003
Geosciences, Science Education
Location: SCEN Room 408

Time Topic

1:30 David Jamieson, Arkansas State University-Newport, Department of Biological Sciences, 7648 Victory Boulevard, Newport, Arkansas 72112. **TEACHING DARWIN'S THEORY OF EVOLUTION AT THE TWO-YEAR COLLEGE (Part II)**

1:45 Natalie Casey, University of Arkansas, Department of Anthropology, Fayetteville, Arkansas, 72701. **SEXUAL DIVERSITY AND UNIVERSITY CULTURE**

2:00 Thalia M. Madewell and Mary C. Savin, Department of Crop, Soil, and Environmental Sciences, University of Arkansas, Fayetteville, Arkansas 72701. **ALUMNI AND EMPLOYER PERCEPTION OF THE CSES CURRICULA: SURVEY RESULTS**

2:15 Blaine W. Schubert, Environmental Dynamics Program, 113 Ozark Hall, University of Arkansas, Fayetteville, AR, 72701, bschube@uark.edu. **FIRST RECORD OF JAGUAR (*Panthera onca*) FROM ARKANSAS**

2:30 Gregory Vogel, Environmental Dynamics Program, 113 Ozark Hall, University of Arkansas, Fayetteville, AR, 72701; gvogel@uark.edu. **RATES OF BIOMANTLE FORMATION AND ARTIFACT DEPTH DISTRIBUTIONS IN THE OZARK UPLANDS**

2:45 Melinda Bodary, University of Arkansas at Pine Bluff, Department of Aquaculture and Fisheries, 1200 N. University Drive, P.O. Box 4912, Pine Bluff, Arkansas, 71611. Mbodary@uaex.edu. **WATER QUALITY AND MACROINVERTEBRATE COMMUNITY ASSESSMENT IN A CENTRAL ARKANSAS BAYOU ASSOCIATED WITH URBANIZATION AND AQUACUULTURE EFFLUENT**

3:15 A.D. Christian[1], N. Bickford[1], J. Bouldin[1], L. Kanieski[2], A. McBride[2], A. Sako and J.L. Farris[1]. [1]Department of Environmental Sciences, Arkansas State University, P.O. Box 847, State University Arkansas, 72467. [2]Department of Biological Sciences, Arkansas State University, P.O. Box 599, State University, Arkansas 72467. **WINTER AND SPRING WATER QUALITY OF THE BIG CREEK WATERSHED, CRAIGHEAD COUNTY, ARKANSAS: NUTRIENTS, HABITAT, AND MACRO-INVERTEBRATES**

3:30 Eileen G. Ernenwein, Environmental Dynamics Program, 113 Ozark Hall, University of Arkansas, Fayetteville, AR 72701; eernenw@uark.edu. **HIGH-TECH ARCHAEOLOGY: MULTI-DIMENSIONAL REMOTE SENSING AT ARMY CITY, KANSAS: FUSING GROUND, AIR, AND SATELLITE DATA**

3:45 Angela M. Polly and Stephen K. Boss, Department of Geosciences, 113 Ozark Hall, University of Arkansas, Fayetteville, AR 72701. **ACOUSTIC MAPPING OF SEDIMENT AND AQUATIC VEGETATION IN LAKES: AN EXAMPLE FROM NORTHWEST ARKANSAS**

4:00 Dorothy G. Neely and Stephen K. Boss, Environmental Dynamics Program, 113 Ozark Hall, University of Arkansas, Fayetteville, AR 72701; dgneely@uark.edu. **ACOUSTIC IMAGING OF SUBMERGED TOPOGRAPHY AND MASS WASTING FEATURES IN BEAVER LAKE, NORTHWEST ARKANSAS**

4:15 Abbas S. Eyuboglu and Haydar J. Al-Shukri, University of Arkansas at Little Rock, 2801 South University Avenue, Little Rock, AR 72204. **DETECTION OF WATER LEAKS BY USING GROUND PENETRATING RADAR**

Friday, April 4, 2003
Engineering I
Location: BELL Room 268

Time Topic

1:30 Gustavo Rehder, Dr. Robert Engelken, Randy Stidham, Richard Tanner, Brandon Passmore, and Anil Baral, Optoelectronic Materials Research Laboratory, College of Engineering, Arkansas State University, P.O. Box 1740, State University (Jonesboro), AR 72467. **INVESTIGATION OF PHOTOCONDUCTIVITY OF INDIUM (III) SULFIDE FILMS ONTO LOW DIFFUSION, COPPER-FREE PHOTOCELL CONTACTS**

1:45 Brandon Passmore, Dr. Robert Engelken, Gustavo Rehder, Randy Stidham, Richard Tanner, and Anil Baral, Optoelectronic Materials Research Laboratory, Arkansas State University – Jonesboro, P.O. Box 1740, State University, AR 72467, (870) 972-2088 bdengens@astate.edu. **LIQUID AND SOLID PHASE SYNTHESIS OF THE PYRRHOTITE PHASE OF IRON SULFIDE FOR SEMICONDUCTOR AND FERROMAGNETIC APPLICATIONS**

2:00 Richard Tanner, Dr. Robert Engelken, Brandon Passmore, Gustavo Rehder, and Randy Stidham; Arkansas State University, College of Engineering, P.O. Box 1740, State University, AR 72467. **ELECTROLESS DEPOSITION OF**

NICKEL CONTACT PATTERNS ON PRINTED CIRCUIT BOARDS FOR USE IN PHOTOCONDUCTIVE CELLS

2:15 Anil Baral, Dr. Robert Engelken, Richard Tanner, Randy Stidham, Gustavo Rehder, and Brandon Passmore, Environmental Sciences Program/ College of Engineering, Arkansas State University, P.O. Box 1740, State University (Jonesboro), AR 72467. **OPTIMIZATION OF AMINO ACID-BASED TRIVALENT CHROMIUM ELECTRODEPOSITION**

2:30 Vikram Bedekar, Deepak G. Bhat, Stephen A. Batzer; Department of Mechanical Engineering, University of Arkansas. **EPMA STUDIES OF NEW CERAMIC MATERIAL FOR MACHINING TITANIUM ALLOYS**

2:45 Kalyana Chittineni, Frank Paolino and Deepak G Bhat, Department of Mechanical Engineering, University of Arkansas, Fayetteville, AR 72701. **INITIAL STUDY OF MECHANICAL ALLOYING FOR THE SYNTHESIS OF Al-Cu AGE HARDENABLE ALLOYS BY POWDER METALLURGY**

3:15 A. M. Shariah [a,b], H. A. Naseem[b] and S. P. Singh [c] ; [a]Visiting Professor, Physics Department, Jordan University of Science and Technology, Irbid-Jordan, [b]3217 Bell Engineering Center, University of Arkansas, Fayetteville, Arkansas 72701, USA, [c]Department of Physics, University of Arkansas, Fayetteville, Arkansas 72701, USA. **CRYSTALLIZATION OF a-Si FILMS IN CONTACT WITH ALUMINUM METAL BY CW LASER**

3:30 Marwan Barghouti, Husam Abu-safe, and Hameed Naseem, Department of Electrical Engineering, Bell Engineering, University of Arkansas 72701. **EFFECT OF SILICON DIOXIDE INTERFACE ON ALUMINUM INDUCED CRYSTALLIZATION OF HYDROGENATED AMORPHOUS SILICON**

3:45 Mohammad Saad Abbasi, H. A. Naseem, H. Abu Safe, W. D. Brown, Arkansas Photovoltaic Research Center, Department of Electrical Engineering, University of Arkansas, Fayetteville, AR, 72701. **ANALYSIS AND MODELING OF ALUMINUM ENHANCED LATERAL CRYSTALLIZATION OF HYDROGENATED AMORPHOUS SILICON**

4:00 Husam Abu-Safe, Marouf Hossain, Hameed Naseem, and William Brown, Electrical Engineering Department, University of Arkansas, Fayetteville, AR 72701, and Abdullah Al-Dhafiri, Department of Physics, King Saud University, Riyadh, Saudia Arabia. **CHLORINE DOPED CdS THIN FILMS FROM $CdCl_2$ MIXED CdS POWDER**

4:15 Sunny N. Wallace, Danielle Julie Carrier, Edgar C. Clausen, Biological and Agricultural Engineering, University of Arkansas, 203 ENGR Hall, Fayetteville, AR 72701, Chemical Engineering, University of Arkansas, 3202 Bell Engineering Center, Fayetteville, AR 72701. **LOW TEMPERATURE SOLVENT EXTRACTION OF MILK THISTLE (*SILYBUM MARIANUM* L.) AND FLAVANOLIGNAN STABILITY**

Friday, April 13, 2001
Chemistry I
Location: BELL Room 269

Time Topic

1:30 A. Meier, P.H. Benoit, A. Kracher, and D.W.G. Sears. Arkansas-Oklahoma Center for Space and Planetary Sciences. Dept. Chemistry and Biochemistry, University of Arkansas, Fayetteville, AR 72701. **SIMULATIONS OF THE FORMATION OF ASTEROIDS IN THE EARLY SOLAR SYSTEM**

1:45 Amy Ellison, Bill Durham and Frank Millett, Department of Chemistry and Biochemistry, University of Arkansas, Fayetteville, AR 72701. **SYNTHESIS OF A TRINUCLEAR RUTHENIUM COMPLEX AS A PHOTOINITIATOR FOR ELECTRON TRANSFER IN METALLOPROTEINS**

2:00 Jan Annaratone and M. Draganjac, Department of Chemistry and Physics, Arkansas State University, State University, AR 72467. **PRELIMINARY IR STUDY OF THE REACTION OF $CpRu(CO)_2^+$ WITH ORGANIC THIOLS**

2:15 K.S. Trauth, W.A. Burns, and S.W. Reeve, Department of Chemistry, Arkansas State University, PO Box 419, State University, AR, 72467. **ROTATIONAL ANALYSIS OF SEVERAL VIBRATIONAL BANDS OF COBALT TRICARBONYL NITROSYL OBTAINED UNDER JET COOLED CONDITIONS**

2:30 Franklin D. Hardcastle*, Amanda Suttles, Kenneth Trantham, and John P. Graham, Department of Physical Sciences, Arkansas Tech University, Russellville, AR 72801. **RAMAN SPECTROSCOPY OF CHROMIUM CONVERSION COATINGS**

Friday, April 4, 2003
Physics
Location: BELL Room 288

Time Topic

1:30 Scott Austin, University of Central Arkansas, Department of Physics and Astronomy, 201 Donaghey St, Conway, AR 72035. **UCA FIBER-FED CCD SPECTROGRAPH FOR ASTRONOMICAL RESEARCH**

1:45 Bao-An Li, Department of Chemistry and Physics, Arkansas State University, State University, Arkansas 72467-0419. **PROBING NUCLEAR SYMMETRY ENERGY WITH HIGH ENERGY RADIOACTIVE BEAMS**

2:00 Dr. Wilson J. Gonzalez-Espada and Dr. Jeff Robertson, Department of Physical Science, School of Physical and Life Science, Arkansas Tech University, 1701 North Boulder Avenue, Russellville, AR 72801. **THE DOPPLER EFFECT FOR A CONSTANTLY ACCELERATING SOUND SOURCE RECEDING FROM A STATIONARY OBSERVER: DETERMINING THE ACCELERATION OF GRAVITY BASED ON ACOUSTIC DATA**

2:15 Scott Arther Ryan and Mostafa Hemmati, Department of Physical Sciences, Arkansas Tech University, Russellville, Arkansas 72801. **ANTIFORCE WAVE PROFILE FOR QUASI-NEUTRAL REGION**

2:30 A. M. Shariah [a,b], H. A. Naseem[b] and S. P. Singh [c] , [a]Visiting Professor, Physics Department, Jordan University of Science and Technology, Irbid-Jordan, [b]3217 Bell Engineering Center, University of Arkansas, Fayetteville, Arkansas 72701, USA, [c]Department of Physics, University of Arkansas, Fayetteville, Arkansas 72701, USA. **CRYSTALLIZATION OF a-Si FILMS IN CONTACT WITH ALUMINUM METAL BY CW LASER**

2:45 Bin Zhang, Bao-An Li, Donald Johnson, Department of

Chemistry and Physics, Arkansas State University, P.O. Box 419, State University, AR 72467-0419. **CHARMONIUM PRODUCTION FROM QUARK COALESCENCE IN A BJORKEN HYDRODYNAMICAL MODEL**

Friday, April 4, 2003
Computer Science, Mathematics
Location: BELL Room 288

3:30 Son Nguyen and Magda-El-Shenawee, Electrical Department, University of Arkansas, Fayetteville, Arkansas 72701. **A RAPID ALGORIMTHM FOR SEARCHING THE MINIMUM POINTS OF DISCRETE FUNCTIONS**

3:45 Steffany Belcher-Novosad and Debra Ingram, Department of Computer Science and Mathematics, Arkansas State University, P.O. Box 70, State University, AR 72467. **MINIMUM *G* ABERRATION DESIGNS FROM HADAMARD MATRICES OF ORDER 28**

4:00 Katrina Corley and Miah Adel, University of Arkansas at Pine Bluff, Pine Bluff, AR 71601; Miah Adel, Department of Chemistry & Physics, University of Arkansas at Pine Bluff, Pine Bluff, AR 71601. **FALLOUT DISTANCES AND CONCENTRATIONS OF FLUE GASES FROM THE INTERNATIONAL PAPER MILL**

4:15 Lyska Dilworth, Department of Mathematical Sciences, UAPB, Pine Bluff, AR 71601; Miah Adel, Department of Chemistry & Physics, UAPB, Pine Bluff, AR 71601. **GAUSSIAN PLUME DISTRIBUTION OF THE NANHAZARDOUS MATERIAL INCINERATION AT THE PINE BLUFF ARSENAL**

POSTER PRESENTATIONS

Friday, April 4, 2003
Location: BELL 4008 Student Lounge

Time — Topic

1:30 Blythe Bowman, Jason Fechter, Julie Carter, John Frank, Barbara Clancy, University of Central Arkansas, Department of Biology, 150 Lewis Science Center, Conway, Arkansas 72035. **SURVIVING SUBPLATE CELLS IN SWISS WEBSTER MICE**

Charles R. McDowell[1], Malcolm L. McCallum[2] (mmccallu@astate.edu), Stanley E. Trauth[1], Benjamin A. Wheeler[2], and Richard L. Shelton[3]; [1]Department of Biological Sciences, Arkansas State University, P.O. Box 599, State University, AR 72467, [2]Environmental Sciences Ph.D. Program, Arkansas State University, P.O. Box 847, State University, AR 72467, [3]Mammoth Spring National Fish Hatchery, P.O. Box 160, Mammoth Spring, AR 72554. **LENGTH-MASS ASSOCIATIONS OF HATCHLING ALLIGATOR SNAPPING TURTLES AT VARIOUS STAGES OF METABOLIC BONE DISEASE, WITH NOTES ON BEHAVIORAL OBSERVATIONS**

Sandra J. Kirchhoff, Marie Greene, and Gary A. Heidt, Little Rock Zoo, Little Rock, AR 72205 and Dept. of Biology, University of Arkansas at Little Rock, Little Rock, AR 72204. **SEASONAL ACTIVITY AND EXHIBIT USE BY THE CAPYBARA (*HYDROCHOERUS HYDROCHAERIS*) AT THE LITTLE ROCK ZOO**

2:30 D. Blake Sasse, Arkansas Game and Fish Commission, # 2 Natural Resources Drive, Little Rock, AR 72205. **NEW RECORDS OF THE EASTERN CHIPMUNK (*TAMIAS STRIATUS*) IN ARKANSAS**

Mari K. Davidson, Harish K. Shandilya[1], Kouji Hirota[2], Kunihiro Ohta[2], and Wayne P. Wahls[1], [1]Department of Biochemistry and Molecular Biology, University of Arkansas for Medical Sciences, Little Rock, AR 72205, USA; [2]Genetic Dynamics Research Unit-Laboratory, RIKEN Institute, Wako, Saitama 351-0198, Japan. **ATF1•PCR1•*M26* COMPLEX DIRECTLY LINKS STRESS-ACTIVATED MAPK AND PKA PATHWAYS *VIA* CHROMATIN REMODELING OF *CGS2*$^+$**

Lewter, Jennifer A.[1], Tsunemi Yamashita[2], and Allen L. Szalanski[1], [1]Department of Entomology, University of Arkansas, Fayetteville, AR 72701, [2]Department of Biology, Arkansas Tech University, Russellville, AR 72801. **DNA SEQUENCE ANALYSIS OF THE FRESHWATER MUSSEL *LAMPSILIS HYDIANA* (BIVALVIA: UNIONIDAE) IN SELECT OZARK AND OUACHITA MOUNTAIN STREAMS OF ARKANSAS**

3:30 Jun Gao and Grover Paul Miller, Department of Biochemistry and Molecular Biology, University of Arkansas for Medical Sciences, Little Rock, AR 72205. **PROTEIN CHIMERAS AS A TOOL TO ELUCIDATE THE ROLE OF CYTOCHROME P450 REDUCTASE STRUCTURE IN THE P450-REDUCTASE COMPLEX**

Kirk B. Babb, PhD Candidate, Applied Science Department, University of Arkansas at Little Rock, 2801 S. University, ETAS 575, Little Rock, AR 72204. **DETERMINING THE ROLE OF 7,12-DIMETHYLBENZ[A]ANTHRACENE IN BREAST CANCER**

Anindo Roy*, PhD Candidate, and Kamran Iqbal**, Assistant Professor, *Department of Applied Science, Univ. of Arkansas at Little Rock, 2801 S. Univ. Ave., Little Rock, AR 72204, ** Department of Systems Engineering, Univ. of Arkansas at Little Rock, 2801 S. Univ. Ave., Little Rock, AR 72204. **PID STABILIZATION OF A POSITION-CONTROLLED ROBOT MANIPULATOR ACTING INDEPENDENTLY OR IN COLLABORATION WITH HUMAN ARM**

ORAL PRESENTATIONS

Saturday, April 5, 2003
Biology III: Aquatic Communities and Biology
Location: SCEN Room 403

Time — Topic

8:00 Thomas M. Buchanan, Department of Biology, University of Arkansas – Fort Smith, Fort Smith, AR 72913, Drew Wilson and L.G. Claybrook, Arkansas Game and Fish Commission, 2 Natural Resources Drive, Little Rock, AR 72205, and William G. Layher, Layer BioLogics RTEC, Inc., 7233 Camden Cutoff Road, Pine Bluff, AR 71603. **FISHES OF THE RED RIVER IN ARKANSAS**

8:15 Thomas M. Buchanan, Department of Biology, University of Arkansas - Fort Smith, Fort Smith, AR 72913, and Michael M. Stevenson, Department of Biological Sciences, University of New Orleans, New Orleans, LA 70148. **DISTRIBUTION OF THE BIGSCALE LOGPERCH, *PERCINA MACROLEPIDA* (PERCIDAE), IN THE ARKANSAS RIVER BASIN**

8:30 Carrie Cavenaugh and Ronald Johnson, Arkansas State University, Department of Biological Sciences, State University, AR 72467. **GENETIC RELATIONSHIPS OF THE ROCK BASSES (AMBLOPLITES) AS DETERMINED BY MITOCHONDRIAL DNA ANALYSIS**

8:45 Dr. Wilson J. Gonzalez-Espada and Dr. Jeff Robertson, Department of Physical Science, School of Physical and Life Science, Arkansas Tech University, 1701 North Boulder Avenue, Russellville, AR 72801. **THE DOPPLER EFFECT FOR A CONSTANTLY ACCELERATING SOUND SOURCE RECEDING FROM A STATIONARY OBSERVER: DETERMINING THE ACCELERATION OF GRAVITY BASED ON ACOUSTIC DATA**

9:00 Robin L. Stingley[1], Billy R. Griffin[2], Reid Landes[3], and Wayne L. Gray[1]. Dept. of Microbiology and Immunology[1], and Division of Biometry[3], Univ. of Arkansas for Medical Sciences, Little Rock, AR, 72205, and Stuttgart National Aquaculture Research Center[2], Stuttgart, AR 72160. **EXPERIMENTAL CHANNEL CATFISH VIRUS INFECTION MIMICS NATURAL INFECTION OF CHANNEL CATFISH**

9:15 Chris L. Davidson[1] and Dave Gosse[2], [1]200 Hazelwood Drive, Sheridan, Arkansas 72150, [2]The Nature Conservancy, Arkansas Field Office, 601 N. University, Little Rock, Arkansas 72205. **STATUS AND DISTRIBUTION OF FRESHWATER MUSSELS (BIVALVIA: UNIONACEA) INHABITING THE SALINE RIVER/HOLLY CREEK BOTTOMS AREA, SALINE COUNTY, ARKANSAS.**

9:45 Elizabeth Pope and James Engman, Biology Department, Henderson State University, Box 7520, Arkadelphia, AR, 71999. **FRESHWATER SPONGE SPECIES OCCURRENCE ON *EGERIA DENSA* IN DEGRAY LAKE, ARKANSAS**

10:00 Teri Tuxson and James Engman, Biology Department, Henderson State University, Box 7520, Arkadelphia, AR, 71999. **SEASONAL VARIATION IN FRESHWATER SPONGE ABUNDANCE ON AQUATIC VEGETATION IN DEGRAY LAKE, ARKANSAS**

10:15 Jane Dunn, Department of Biology, Henderson State University, Box 7680 HSU, Arkadelphia, AR 71999-0001. ***GYRATRIX HERMAPHRODITUS*: A STATE RECORD FOR ARKANSAS**

10:30 Adam Rivers and James Engman, Biology Department, Henderson State University, Box 7520, Arkadelphia, AR, 71999. **ANALYSIS OF *DIADEMA ANTILLARUM* PHILIPPI (ECHINODERMATA: ECHINOIDEA) ABUNDANCE AND MACROALGAL COVER IN ST. ANN'S BAY, JAMAICA**

Biology IV: Amphibian and Invertebrate Communities and Biology

Location: SCEN Room 406

Time — Topic

8:00 Malcolm L. McCallum[1], Robert G. Neal[2], Stanley E. Trauth[2], and Vernon Hoffman[3], [1]Environmental Sciences Ph.D. Program, Arkansas State University, P.O. Box 847, State University, AR 72467, [2]Department of Biological Sciences, Arkansas State University, P.O. Box 599, State University, AR 72467, [3]Department of Biological Sciences, University of Arkansas Community College at Batesville, P.O. Box 3350, Batesville, AR 72503. **AN INVENTORY OF AMPHIBIANS AND REPTILES AT THE ARKANSAS POST NATIONAL MEMORIAL**

8:15 Robyn Konvalinka and Stanley E. Trauth, Department of Biological Sciences, Arkansas State University, P.O. Box 599, State University, AR 72467-0599. **EGG DISCRIMINATION IN THE WESTERN SLIMY SALAMANDER, *PLETHODON ALBAGULA***

8:30 Michelle N. Mary, Department of Biological Sciences, Arkansas State University, P.O Box 599, State University, AR 72467, USA, Dr. Stanley E. Trauth, Department of Biological Sciences, Arkansas State University, P.O. Box 599, State University, AR 72467, USA. **HISTOLOGY AND HISTOCHEMISTRY OF CAUDAL COURTSHIP GLANDS IN *PLETHODON ALBAGULA, P. OUACHITAE*, AND *DESMOGNATHUS BRIMLEYORUM***

8:45 Tobin Fulmer and Renn Tumlison, Department of Biology, Henderson State University, Arkadelphia, AR 71999. **IMPORTANT RECORDS OF THE BIRD-VOICED TREEFROG (*HYLA AVIVOCA*) IN THE HEADWATERS OF THE OUACHITA RIVER DRAINAGE OF SOUTHWESTERN ARKANSAS**

9:00 Malcolm L. McCallum[1] (mmccallu@astate.edu), Tracey Klotz[2], Stanley E. Trauth[2], William Stephens[1], Jennifer Bouldin[1], Benjamin A. Wheeler[1], Kenneth Gillespie[2], and David Feldman[2], [1]Environmental Sciences Ph.D. Program, Arkansas State University, P.O. Box 847, State University, AR 72467, [2]Department of Biological Sciences, Arkansas State University, P.O. Box 599, State University, AR 72467. **A THREE-YEAR STUDY ON WOOD FROG DEATHS IN THE SYLAMORE**

9:15 Robert G. Neal[1], Malcolm L. McCallum[2], Stanley E. Trauth[1], Charles R. McDowell[1], and Tracey L. Klotz[1], [1]Department of Biological Sciences, Arkansas State University, P.O. Box 599, State University, AR 72467, [2]Environmental Sciences Ph.D. Program, Arkansas State University, P.O. Box 847, State University, AR 72467. **CALLING SITE CHARACTERIZATION OF THE ILLINOIS CHORUS FROG (*PSEUDACRIS STRECKERI ILLINOENSIS*)**

9:45 Malcolm L. McCallum, Environmental Sciences Ph.D. Program, Arkansas State University, P.O. Box 847, State University, AR 72467, Stanley E. Trauth, Department of Biological Sciences, Arkansas State University, P.O. Box 599, State University, AR 72467. **CAN THE ILLINOIS CHORUS FROG SURVIVE IN ARKANSAS?**

10:00 Benjamin A. Wheeler[1], Malcolm L. McCallum[1], Stanley E. Trauth[2], Michelle N. Mary[2], and Charles R. McDowell[2], [1]Environmental Sciences Ph.D. Program, Arkansas State University, P.O. Box 847, State University, AR 72467, [2]Department of Biological Sciences, Arkansas State University, P.O. Box 599, State University, AR 72467. **FALL BREEDING OF *RANA SPHENOCEPHALA* IN NORTHEAST ARKANSAS**

10:15 G. O. Graening, The Nature Conservancy, 1037 North Main Avenue, Suite 7, Fayetteville AR 72701; Michael Slay, Dept. of Biological Sciences, University of Arkansas, 601 Science-Engineering, Fayetteville AR 72701; Kare Tinkle, Sylamore Ranger District, U.S. Forest Service, P.O. Box 1279, Mountain View AR 72560. **SUBTERRANEAN FAUNA OF ARKANSAS, PART 1: SUBTERRANEAN BIODIVERSITY OF THE SYLAMORE RANGER DISTRICT, OZARK NATIONAL FOREST, ARKANSAS**

10:30 G. O. Graening, The Nature Conservancy, 1037 North Main

Avenue, Suite 7, Fayetteville AR 72701. **SUBTERRANEAN BIODIVERSITY OF ARKANSAS, PART 2: STATUS UPDATE OF THE FOUSHEE CAVESNAIL (AMNICOLA CORA)**

Biology V: Arthropod Communities and Biology
Location: SCEN Room 407

Time	Topic
8:00	Michael D. Warriner and C. Theo Witsell, Arkansas Natural Heritage Commission, 1500 Tower Building, 323 Center Street, Little Rock, AR 72201. **BUTTERFLIES (LEPIDOPTERA) OF CONSERVATION CONCERN IN ARKANSAS: DISTRIBUTION AND LARVAL HOST PREFERENCES**
8:15	Kara A. Davis, and Janet Lanza. Biology Department, University of Arkansas at Little Rock, Little Rock, Arkansas 72204. **EFFECTS OF NECTAR ON ENERGY CONTENT OF MONARCH BUTTERFLIES**
8:30	Marjorie Stephen[1], Mylinda L. Terry, and Janet Lanza. Biology Department, University of Arkansas at Little Rock, Little Rock, Arkansas 72204. [1]Current address: Arkansas Baptist Middle School, 8400 Ranch Road, Little Rock, Arkansas 72223. **NECTAR-BORNE AMINO ACIDS INCREASE REPRODUCTION BY MONARCH BUTTERFLIES**
8:45	George L. Harp and Phoebe A. Harp. Dept. of Biological Sciences, Arkansas State University, State University, AR 72467. **DRAGONFLIES (ODONATA) OF THE OUACHITA NATIONAL FOREST**
9:00	James A. Engman, Biology Department, Henderson State University, Box 7520, Arkadelphia, AR, 71999. **NESTING ACTIVITY OF *OSMIA LIGNARIA* (HYMENOPTERA: MEGACHILIDAE) PROVIDES AN EXPLANATION FOR APPARENT SABOTAGE OF AIRCRAFT FUEL**
9:15	Blake K. Stevenson and Matthew D. Moran, Biology Department, Hendrix College, 1600 Washington Ave., Conway, AR 72032. **FIRE EFFECTS ON AN ARTHROPOD COMMUNITY IN A RELICT GRASSLAND**
9:45	Chris T. McAllister, Rowland M. Shelley, and James T. McAllister, III, Department of Biology, Texas A&M University-Texarkana, Texarkana, TX 75505; Research Laboratory, North Carolina State Museum of Natural Sciences, Raleigh, NC 27607; and W. T. White High School, 1244 Forest Lane, Dallas, TX. 75228. **GEOGRAPHIC DISTRIBUTION RECORDS FOR SCOLOPENDROMORPH CENTIPEDES (ARTHROPODA: CHILOPODA) FROM ARKANSAS, OKLAHOMA, AND TEXAS**
10:00	Chris T. McAllister, Rowland M. Shelley, and James T. McAllister, III, Department of Biology, Texas A&M University-Texarkana, Texarkana, TX 75505; Research Laboratory, North Carolina State Museum of Natural Sciences, Raleigh, NC 27607; and W. T. White High School, 1244 Forest Lane, Dallas, TX. 75228. **ADDITIONAL MILLIPED RECORDS (ARTHROPODA: DIPLOPODA) FOR ARKANSAS AND OKLAHOMA**
10:15	Tsunemi Yamashita, Department of Biological Sciences, Arkansas Tech University, Russellville, AR 72801. **PHYLOGEOGRAPHY OF THE STRIPED SCORPION, *CENTRUROIDES VITTATUS***
10:30	S. Jill James, Marta Pogribna, Stepan Melnyk, William Slikker III, Elizabeth New, and Stefanie Jernigan. National Center for Toxicological Research, Jefferson AR, 72079. **PREVENTION OF TIMEROSAL-INDUCED NEUROTOXICITY BY GLUTATHIONE (GSH) AND CYSTEINE, BUT NOT METHIONINE**

Arkansas Flora II
Location: SCEN Room 408

Time	Topic
9:00	Staria S. Vanderpool, Department of Biological Sciences, Arkansas State University, P. O. Box 599, State University, Arkansas 72467-0599. **PLANTS NEW TO THE STATE OF ARKANSAS**
9:15	Staria S. Vanderpool, J. D. Wilhide, Lynn E. Alterman, Steven C. Fowler, Jeremy L. Jackson, Tammy R. Jones, William D. Reed, James R. Samples, Lann M. Wilf, Adam S. Chappell, Ronald E. Cossey, Marcelle L. Daggett, James W. Gore, Michaeal A. Reed, Mary C. Scott, and Joshua H. Seagraves. Department of Biological Sciences, Arkansas State University, P. O. Box 599, State University, Arkansas 72467-0599. **AN INVENTORY OF WOODY TAXA AND SPRING FOREST EPHEMERALS IN THE PROPOSED LAKE BONO SITE, CRAIGHEAD COUNTY**
9:45	Michelle Parker and Brett E. Serviss. Department of Biology. Henderson State University. Arkadelphia, AR 71999–0001. **OCCURRENCE AND STATUS OF HYDRILLA VERTICILLATA (L. F.) ROYLE (HYDROCHARITACEAE) IN ARKANSAS**
10:00	Thomas D. Slaughter, Jason Wilis, and Brett E. Serviss. Department of Biology. Henderson State University. Arkadelphia, AR 71999–0001. **IDENTIFICATION AND ECOLOGY OF NATURALIZED SPECIES OF NARCISSUS (LILIACEAE) IN ARKANSAS**
10:15	Joe B. Pagan, Jr., Natural Resources Conservation Service, 700 W. Capitol, Little Rock AR 72201; Thomas L. Foti, Arkansas Natural Heritage Commission, 323 Center St., Little Rock AR 72201. **A COMPREHENSIVE FLORISTIC INVENTORY AND DISTRIBUTION MODEL OF UNIQUE WETLAND COMMUNITIES ON TERRACES ALONG THE OUACHITA RIVER IN SOUTHERN ARKANSAS**
10:30	Thomas L. Foti, Arkansas Natural Heritage Commission, 323 Center St., Little Rock AR 72201; Joe B. Pagan, Natural Resources Conservation Service, 700 W. Capitol, Little Rock AR 72201. **RELATIONSHIPS OF BOTTOMLAND HARDWOOD FOREST COMMUNITIES TO FLOODING ALONG THE WHITE RIVER NEAR CLARENDON, ARKANSAS**

Chemistry II
Location: BELL Room 269

Time	Topic
8:00	Amit Shah, Brian C. Berry, Tito Viswanathan and Ali U. Shaikh; Department of Chemistry, University of Arkansas at Little Rock, Little Rock, AR 72204. **STABILIZATION OF POLYVINYL CHLORIDE BY SOME CONDUCTING POLYMERS**

8:15 Pradeepa Rangarajan[1], Gary A. Heidt[2] and Ali U. Shaikh[3], [1,3]Department of Chemistry, [2]Department of Biology, University of Arkansas at Little Rock, Little Rock, AR 72204. **DETERMINATION OF BILE ACIDS IN A MIXTURE BY GAS CHROMATOGRAPHY-MASS SPECTROMETRY**

8:30 Matt Flynt and Ali U. Shaikh, Department of Chemistry, University of Arkansas at Little Rock, Little Rock, AR 72204. **AN EVALUATION OF IN-SITU GENERATION OF HYDROGEN SULFIDE IN A FISH POND USING A SULFIDE ION-SELECTIVE ELECTRODE**

8:45 Amanda Bell, Marilyn Davis, Marti Scharlau, and Lois Geren. Department of Chemistry and Biochemistry, University of Arkansas, Fayetteville, AR 72701. **DESIGN OF A PHOTOACTIVE RUTHENIUM-CYTOCHROME B5 DERIVATIVE TO STUDY ELECTRON TRANSFER TO CYTOCHROME C**

9:00 Jun Gao and Grover Paul Miller, Department of Biochemistry and Molecular Biology, University of Arkansas for Medical Sciences, Little Rock, AR 72205. **PROTEIN CHIMERAS AS A TOOL TO ELUCIDATE THE ROLE OF CYTOCHROME P450 REDUCTASE STRUCTURE IN THE P450-REDUCTASE COMPLEX**

9:15 Erin M Scherer, Haiyan Sun and Roger E. Koeppe, II, Department of Chemistry and Biochemistry, University of Arkansas, Fayetteville, AR 72701. **GRAMICIDIN CHANNELS WITH TRYPTOPHAN (TRP) SUBSTITUTED BY 7-AZA-TRP OR 1-METHYL-TRP OR 1-METHYL-7-AZA-TRP**

9:45 Mari K. Davidson, Wallace D. Sharif and Wayne P. Wahls, Department of Biochemistry and Molecular Biology, University of Arkansas for Medical Sciences, 4301 W. Markham Street (slot 516), Little Rock, AR 72205-7199. **RECOMBINASE REC12 (SPO11) ACTIVATES A MEIOSIS I NONDISJUNCTION / DISTRIBUTIVE SEGREGATION CHECKPOINT**

10:00 Yang Ou and Wayne L. Gray, Department of Microbiology and Immunology, University of Arkansas for Medical Sciences, Little Rock, AR 72205. **SIMILAR PROPERTIES OF GENE 29 PROMOTER IN VARICELLA-ZOSTER VIRUS AND SIMIAN VARICELLA VIRUS**

10:15 Lothar Schäfer, Department of Chemistry and Biochemistry, University of Arkansas, Fayetteville, AR 72701. **THE IMPORTANCE OF THE QUANTUM PROPERTIES OF BIOMOLECULES FOR A COMPREHENSIVE VIEW OF EVOLUTION: QUANTUM SELECTION DRIVES EVOLUTION IN TANDEM WITH NATURAL SELECTION**

10:30 Stephen C. Grace, Department of Biology, University of Arkansas at Little Rock, Little Rock, Arkansas 72204. **METAL CATALYZED HYDROXYL RADICAL FORMATION AND DNA STRAND SCISSION BY HYDROXYCINNAMIC ACIDS**

Engineering II
Location: BELL Room 268

Time Topic

8:00 J. Duck; R. Schupbach and J. Balda; University of Arkansas, College of Engineering, 3217 Bell Engineering Center, Fayetteville AR, 72701. **A REGENERATIVE HIGH-POWER ELECTRONIC LOAD FOR BATTERIES AND ULTRACAPACITORS TESTING USING THE TMS320C240**

8:15 D. Robinson; R. Schupbach and J. Balda; University of Arkansas, College of Engineering, 3217 Bell Engineering Center, Fayetteville AR, 72701. **MODELING OF AN ULTRACAPACITORS BANK**

8:30 Roberto M. Schupbach and Juan C. Balda; University of Arkansas, College of Engineering, 3217 Bell Engineering Center, Fayetteville AR, 72701. **A VERSATILE LABORATORY TEST BENCH FOR DEVELOPING POWERTRAINS FOR ELECTRIC VEHICLES**

8:45 Jie Zhu and Wookwon Lee, Department of Electrical Engineering, University of Arkansas, 3217 Bell Engineering Center, Fayetteville, AR 72701, Email: {zhu, wookwon}@uark.edu. **CHANNEL ESTIMATION FOR OFDM SYSTEMS**

9:00 Mohammad A Khan, Wookwon Lee, Department of Electrical Engineering, University of Arkansas, 3217 Bell Engineering Center, Fayetteville, AR 72701, USA, Email: mak07, wookwon}@uark.edu. **CSMA/CA WITH SHORTEND CONTENTION WINDOW FOR MIXED TRAFFIC IN IEEE802.11 W LANS**

9:15 Muhammad T. Hossain, Junior, Pine Bluff High School, Pine Bluff, AR 71601; Miah M. Adel, Department of Chemistry & Physics, University of Arkansas at Pine Bluff, Pine Bluff, AR 71601. **ASSESSMENT OF ENVIRONMENTAL IMPACT FROM THE WAL-MART SUPERCENTER CONSTRUCTION BY THE STATE HIGHWAY 15 AND THE INTERSTATE HIGHWAY 530 N**

9:45 Paul C. Millett and R. Paneer Selvam, Computational Mechanics Laboratory, Bell 4190, University of Arkansas, Fayetteville, AR 72701, Phone: (479)-575-2229; Fax: (479)-575-7168, E-mail: rps@engr.uark.edu, pmillet@engr.uark.edu. **COMPUTER MODELING OF THE TORNADO-STRUCTURE INTERACTION: INVESTIGATION OF STRUCTURAL LOADING ON CUBIC BUILDING**

10:00 Yangki Jung and R. Panneer Selvam, High Density Electronics Center, Bell 4190, University of Arkansas, Fayetteville, AR, 72701, Phone: 479-575-2229; Fax: 479-575-7168, E-mail: yjung@ engr.uark.edu. **NUMERICAL ANALYSIS OF MICRO-JET ARRAY COOLING DEVICE WITH VARIOUS CONFIGURATIONS**

10:15 Nathan B. Edgar and Paul S. Sherman, Asst. Prof. of Mech. Engr., Assoc. Prof. of Mech. Engr., College of Engineering, Arkansas State University, P.O. Box 1740, State University, AR 72467. **HIGH-ORDER COMPACT DIFFERENCE OPERATORS FOR COMPUTATIONAL ACOUSTICS**

10:30 Paul S. Sherman and Nathan B. Edgar, Assoc. Prof. of Mech. Engr. , Asst. Prof. of Mech. Engr., Arkansas State University, College of Engineering, PO Box 1740, State University, AR 72467. **INTERPOLATION TECHNIQUES FOR OVERSET GRIDS**

Engineering III
Location: BELL Room 288

Time Topic

8:00 F. Magableh, Ceramic Electronic PAckaging Laboratory (CEPAL), University of Arkansas, Fayetteville, AR 72701, Phone: 501-575-2374 Fax: 501-575-7967, e-mail: fmagabl@uark.edu. **EFFECT OF DESIGN PARAMETERS ON SLOW WAVE RESONATORS**

8:15 Eran J. Jones, University of Arkansas, Microelectronics-

Photonics, Physics Building, Room 226, Fayetteville, AR 72701. **GEOMETRY AND LAYERING EFFECTS ON THE OPERATING CHARACTERISTICS OF SPIRAL INDUCTORS**

8:30 Son Nguyen and Magda-El-Shenawee, Electrical Engineering Department, University of Arkansas, Fayetteville, Arkansas 72701. **A RAPID ALGORIMTHM FOR SEARCHING THE MINIMUM POINTS OF DISCRETE FUNCTIONS**

8:45 Vasanth Sarathy, Milos Jankovic and Magda El-Shenawee, Department of Electrical Engineering, University of Arkansas, Fayetteville, AR 72701. **FULL WAVE ANALYSIS OF MICROSTRIP TRANSMISSION LINES USING METHOD OF LINES**

9:00 Ty R. McNutt, Alan Mantooth, University of Arkansas, BEC 3217, Fayetteville, AR 72701. **SILICON CARBIDE POWER DEVICE MODELS AND PARAMETER EXTRACTION ROUTINES FOR CIRCUIT SIMULATION**

9:15 Kevin M. Speer, Ty R. McNutt, Alex B. Lostetter, H. Alan Mantooth, University of Arkansas, Department of Electrical Engineering, 3217 Bell Engineering Center, Fayetteville, AR 72701. **A NOVEL HIGH FREQUENCY SILICON CARBIDE (SIC) STATIC INDUCTION TRANSISTOR (SIT) BASED TEST-BED FOR THE ACQUISITION OF SIC POWER DEVICE REVERSE RECOVERY CHARACTERISTICS**

9:45 Avinash Kashyap and Sharmila Maganlal, University of Arkansas, Dept. of Electrical Engineering, Fayetteville, Ar 72701. **TESTING AND MODELING ELECTRICAL CHARACTERISTICS OF NOVEL SILICON CARBIDE (SIC) STATIC INDUCTION TRANSISTORS (SITS)**

10:00 Xiaoling Huang, Yongfeng Feng, Wei Zheng, Jianhua Mao, H. Alan Mantooth, University of Arkansas, 3217 Bell Engineering Center, Fayetteville, Arkansas 72701, USA. **MODELING OF NONLINEAR DYNAMICAL BEHAVIOR IN ANALOG CIRCUITS**

10:15 Maruf Hossain, Ty McNutt, H.Alan Mantooth, Edgar Cilio, Department of Electrical Engineering, University of Arkansas, 3217 Bell Engineering Center, Fayetteville, AR-72701. **PARAMETER EXTRACTION SOFTWARE FOR COMPACT DIODE MODEL**

POSTER PRESENTATIONS

Saturday, April 5, 2003
Location: BELL 4008

Time Topic

8:00 Allan Holloway, University of Central Arkansas, Department of Physics and Astronomy, 201 Donaghey St., Conway, AR, 72035. **FABRICATION AND TESTING OF THE UCA FIBER-FED CCD SPECTROGRAPH**

Jeff Robertson, Arkansas Tech University, 1701 N. Boulder, Russellville, AR 72801, Mark Pitts, Kent Honeycutt % Stella Kafka, Indiana University, Swain Hall West 319, Bloomington, IN 47405, Tut & Jeannie Campbell, ATU, 7021 Whispering Pine, Harrison, AR 72601. **SYSTEMATICS OF SUPERHUMPS IN THE SU UMA DWARF NOVA V1159 ORIONIS**

John P. Graham and Glen Henke, Department of Physical Science, Arkansas Tech University, Russellville, AR 72801. **AN APPROXIMATE MOLECULAR ORBITAL DESCRIPTION OF A NOVEL CHELATING CARBENE COMPLEX**

9:00 Kate Ledbetter, John P. Graham, and Franklin D. Hardcastle, Department of Physical Sciences, Arkansas Tech University, Russellville, AR 72801. **SPECIATION OF CHROMATE IN CHROMIUM CONVERSION COATING SOLUTIONS**

Jaime L. Hardcastle, Kate Ledbetter, and Franklin D. Hardcastle, Department of Physical Sciences, Arkansas Tech University, Russellville, AR 72801. **MONITORING THE LEACHING OF CHROMIUM CONVERSION COATINGS INTO THE ENVIRONMENT BY ION CHROMATOGRAPHY**

Briley Charette, Kenneth Trantham, and Franklin D. Hardcastle, Department of Physical Sciences, Arkansas Tech University, Russellville, AR 72801. **ELECTROCHEMICAL MEASUREMENTS OF CHROMIUM CONVERSION COATINGS ON ALUMINUM**

10:00 Emily A. Clark and Ingrid Fritsch, Department of Chemistry and Biochemistry, University of Arkansas, Fayetteville, AR 72701. **MAGNETOHYDRODYNAMIC STUDIES TOWARD THE DEVELOPMENT OF MICROFLUIDIC DEVICES**

Eyitayo Fakunle, Fred Barlow and Ingrid Fritsch, Department of Chemistry and Biochemistry, Department of Electrical Engineering, University of Arkansas, Fayetteville, AR 72701. **LOW TEMPERATURE CO-FIRED CERAMIC WITH SCREEN PRINTED ELECTRODES AS A PLATFORM FOR MICRO-TOTAL ANALYSIS SYSTEMS**

Avinash Kashyap & Sharmila Maganlal, University of Arkansas, Dept. of Electrical Engineering, Fayetteville, Ar 72701. **TESTING AND MODELING ELECTRICAL CHARACTERISTICS OF NOVEL SILICON CARBIDE (SIC) STATIC INDUCTION TRANSISTORS (SITS)**

Fishes of the Red River in Arkansas

Thomas M. Buchanan*
Department of Biology
University of Arkansas-Fort Smith
Fort Smith, AR 72913

Drew Wilson and **L. G. Claybrook**
Arkansas Game and Fish Commission
2 Natural Resources Drive
Little Rock, AR 72205

William G. Layher
Layher BioLogics RTEC, Inc.
7233 Camden Cutoff Road
Pine Bluff, AR 71603

* Corresponding Author

Abstract

Fishes were collected from Red River mainstem habitats in Arkansas with seines, rotenone, hoop nets, gill nets, and trotlines from 1995 through 2001. Seventy-two species were identified distributed among 17 families, and 15 species were new records for the Red River in Arkansas. Eighty-three species are now historically known from the Arkansas segment of the Red River. Approximately 67% of the fishes known from the entire Red River have been found in the Arkansas segment, which is only 11% of the entire river length. Baseline data on the fish fauna of the Red River is critical for the analysis of potential effects to aquatic systems, and because of the potential for deleterious effects from alteration of aquatic habitats by a proposed project to extend the Red River Navigation System upstream from Shreveport, Louisiana to Index, Arkansas and by desalination projects upstream in Texas.

Introduction

The fish communities of large rivers are the least studied ichthyofaunas of all aquatic habitats in Arkansas. This study was the first comprehensive sampling to determine fish species distribution and abundance within the entire Arkansas segment of the Red River. An up-to-date survey of the fishes of the Red River in Arkansas is especially important because of the proposed construction of a navigation channel from Shreveport, Louisiana through the lower half of the Red River in Arkansas.

Description of the Red River and the Study Area in Arkansas.--The Red River originates in eastern New Mexico and flows easterly across the Texas panhandle, along the boundary between Texas and Oklahoma, through the southwestern corner of Arkansas, and across Louisiana to join the Atchafalaya River near Simmesport, Louisiana. The Red River formerly flowed directly into the Mississippi River, but the flood of 1927 and the subsequent construction of levees diverted the Red River southward into the Atchafalaya River (Douglas, 1974). Today, the Red River is accessible from the Mississippi River through its old channel because part of the Mississippi River flow is diverted through the old channel (11.3 km) into the Atchafalaya River, forming the first segment of the Red River Navigation System.

The Red River is 1,945 km long and drains an area of 179,308 km^2. The Arkansas segment of the river is 217 km long with a drainage area of 11,484 km^2. Compared to the other big rivers in Arkansas (e.g., the Arkansas and Mississippi Rivers), the Red River has been least altered by human activity. A number of anthropogenic alterations, however, have occurred in the Red River upstream and downstream from Arkansas. The upper Red River in Texas and Oklahoma contains salt concentrations approaching that of seawater with decreasing salinities occurring downstream (Matthews, 1998). The Echelle et al. (1972) fish surveys indicated that the species composition of the upper Red River reflected differences in the fish assemblages along the salinity gradient. Those assemblages are currently threatened to be influenced by a project underway to decrease the amount of salt in the Red River by building dams, brine reservoirs, pipelines and pumps on west Texas tributaries that feed the Red River. The natural flow regime has been changed by the construction of Denison Dam, which impounded Lake Texoma on the Red River in Oklahoma, by seven large impoundments in the Little River drainage in Arkansas and Oklahoma, and by several other small impoundments on Red River tributaries in Oklahoma. The lower portion of the Red River in Arkansas downstream from the U.S. Hwy 71 bridge has been modified by manmade levees and numerous areas of revetted banks and wing dikes. Upstream from U.S. Hwy 71 in Arkansas, however, few channel modification structures exist. Downstream from Arkansas, a series of locks and dams maintains a 2.7 m deep navigation channel from the Mississippi River through Old River and the Red River to Shreveport, Louisiana, a distance of approximately 377 km.

Chronological History of Red River Fish Sampling in Arkansas.--The earliest reported scientific collection of fishes from the Arkansas portion of the Red River was by Jordan and Gilbert (1886). During September 1884, David Starr Jordan assisted by Charles H. Gilbert, Joseph Swain, and Seth E. Meek collected fishes "with a fine-meshed seine of large size" from a number of streams in Arkansas, Indian Territory (Oklahoma), and Texas for the U. S. National Museum and the U.S. Fish Commission. The Red River at Fulton, Arkansas was one of their collecting sites. They judged the water to be at its lowest point and referred to the Red River at this site as "singularly barren of fish life"

although they collected 23 species. *Hybognathus nuchalis* was listed as "by far more numerous in individuals than any other species in the river." *Notropis atherinoides*, *Macrhybopsis hyostoma*, and *M. storeriana* were also reported to be rather common or abundant. All 23 species reported by Jordan and Gilbert (1886) were collected from the Red River in the 1990s.

The next reported collections of fishes from the Arkansas segment of the Red River were in 1938 and 1939 by John D. Black (1940), 54 years after Jordan's expedition. Black collected fishes at three mainstem sites and reported 34 currently recognized fish species from those localities, 18 of which had not been reported from the Red River mainstem by Jordan and Gilbert (1886). This increased the number of species known from the Red River in Arkansas to 41. Black's collections included the first known records of the Red River shiner, *Notropis bairdi*, from Arkansas (two adult specimens taken at Spring Bank Ferry, 8 km north of the Louisiana state line on 8 July 1939). Black also reported the only specimens of the plains minnow, *Hybognathus placitus*, ever taken from the Red River in Arkansas (three young and adult specimens collected at Spring Bank Ferry on 8 July 1939).

On 18 August 1940, Reeve M. Bailey and M. E. Davis collected 15 species of fishes from the Red River at Fulton. The results of this collection were not published, but the specimens were deposited in the University of Michigan Museum of Zoology. This collection added three species to the list of fishes known from the Red River in Arkansas, bringing the total known species to 44. The most noteworthy record from this sample was the second (and last known) report of *Notropis bairdi* from Arkansas (three

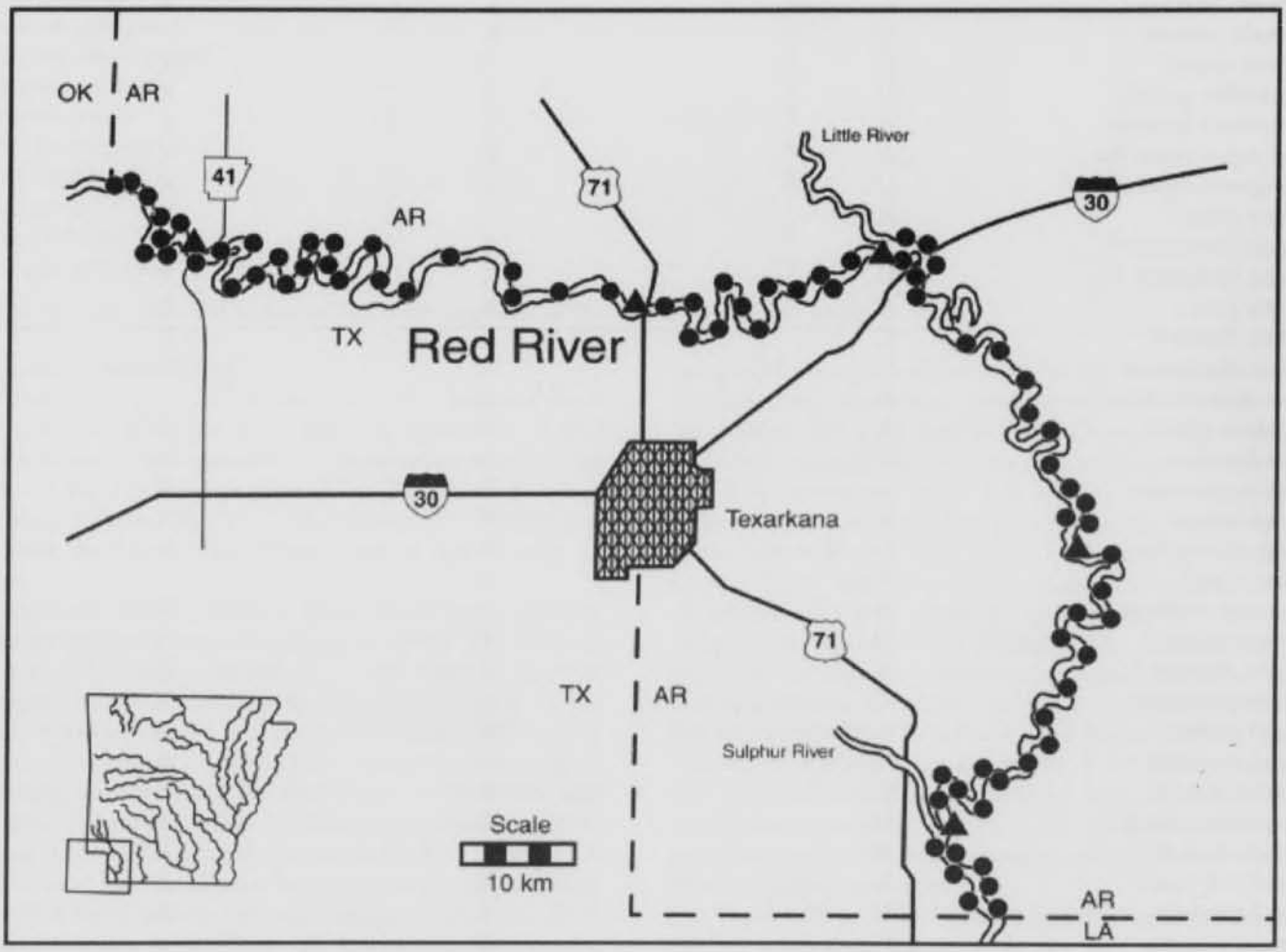

Fig. 1. Red River fish collecting sites in Arkansas, 1995-2001. Solid circles are localities sampled by seine and/or rotenone, solid triangles are localities sampled by hoop nets, gill nets, and/or trotlines. Collecting locales included the following counties in AR: Hempstead, Lafayette, Little River, and Miller.

Table 1. Fish species collected from the Red River in Arkansas, 1995-2001. Status of each species is designated as abundant (A), common (C), uncommon (U), or rare (R).

Species	Status	Collected upstream from Little R. mouth	Collected downstream from Little R. mouth
Scaphirhynchus platorynchus	C	X	X
Polyodon spathula	R		X
Atractosteus spatula	R	X	X
Lepisosteus oculatus	U	X	X
Lepisosteus osseus	A	X	X
Lepisosteus platostomus	U	X	X
Hiodon alosoides	R	X	
Alosa chrysochloris	U	X	X
Dorosoma cepedianum	C	X	X
Dorosoma petenense	A	X	X
*Ctenopharyngodon idella**	R		X
Cyprinella lutrensis	A	X	X
Cyprinella venusta	U	X	X
Cyprinus carpio	U	X	X
Hybognathus nuchalis	U	X	X
Macrhybopsis hyostoma	U	X	X
Macrhybopsis storeriana	A	X	X
Notemigonus crysoleucas	U	X	X
*Notropis amnis**	R		X
Notropis atherinoides	A	X	X
Notropis buchanani	U	X	X
Notropis potteri	A	X	X
Notropis shumardi	C	X	X
Opsopoeodus emiliae	U	X	X
*Phenacobius mirabilis**	R	X	
Pimephales vigilax	A	X	X
Carpiodes carpio	A	X	X
Cycleptus elongatus	A	X	X
Ictiobus bubalus	C	X	X
Ictiobus cyprinellus	U	X	X
*Ictiobus niger**	R	X	
Minytrema melanops	R		X
*Ameiurus natalis**	U	X	X
Ictalurus furcatus	A	X	X
Ictalurus punctatus	C	X	X
Noturus gyrinus	U	X	X
*Noturus nocturnus**	U	X	X
Pylodictis olivaris	C	X	X
Aphredoderus sayanus	U	X	X
*Fundulus blairae**	R		X
Fundulus chrysotus	R	X	X
Fundulus notatus	U	X	X
Fundulus olivaceus	R	X	
Gambusia affinis	C	X	X
*Labidesthes sicculus**	U	X	X
Menidia beryllina	A	X	X

Table 1. Continued

Morone chrysops	A	X	X
Morone mississippiensis	C	X	X
Morone saxatilis	C	X	X
Elassoma zonatum	U	X	X
Lepomis cyanellus	U	X	X
Lepomis gulosus	C	X	X
Lepomis humilis	C	X	X
Lepomis macrochirus	C	X	X
Lepomis megalotis	C	X	X
Lepomis microlophus	U	X	X
Lepomis miniatus	R	X	X
*Lepomis symmetricus**	U	X	X
*Micropterus punctulatus**	U	X	X
Micropterus salmoides	C	X	X
Pomoxis annularis	C	X	X
Pomoxis nigromaculatus	U	X	X
Ammocrypta clara	U	X	
*Etheostoma asprigene**	R	X	X
*Etheostoma chlorosomum**	U	X	X
*Etheostoma collettei**	R	X	
Etheostoma gracile	C	X	X
*Percina macrolepida**	U	X	X
*Percina maculata**	R	X	X
Percina sciera	U	X	
Percina shumardi	U	X	X
Aplodinotus grunniens	A	X	X

* A species first collected from the Arkansas segment of the Red River in this study.

specimens, UMMZ 170013).

Reeves (1953) provided records for the Alabama shad, *Alosa alabamae*, from the Little River of Oklahoma, a Red River tributary. *Alosa alabamae*, an anadromous species, had to ascend the Arkansas portion of the Red River to reach spawning habitat in the Little River of Oklahoma, increasing the known Red River fauna of Arkansas to 45 species.

Buchanan (1973) provided distribution maps showing all known species records and localities for the Red River in Arkansas. This was a summary of all known previous collections, but nine additional species were added to the list of fishes known from the Red River. These nine new species came from Arkansas Game & Fish Commission records of gill netting samples from the Red River in the 1960s and from seine collections at five localities by Buchanan in 1972, bringing the total known fish species in the Red River to 54.

The next, and until now most intensive, fish sampling on the Red River in Arkansas was a survey of the fishes from Index, Arkansas (U.S. Hwy. 71 bridge) to Shreveport, Louisiana by Kelly H. Oliver from December 1978 through July 1979 (Dorris et al., 1979). Oliver sampled 13 mainstem sites in the lower half of the Arkansas portion of the Red River and four mainstem sites in Louisiana. Each site was sampled from one to three times by gill nets, seines, and/or electrofishing; occasional creel censuses were made when local fishermen were encountered. Oliver's field notes and collection site species lists were lost, and it is not possible to precisely determine which fish species were found in the Arkansas portion of the Red River from the data presented in the report (Dorris et al., 1979). Eight species reported by Oliver from the Red River mainstem were possibly misidentified. No voucher specimens of the eight questionable species were available for examination, and those species were not considered as part of the documented Red River fauna. Because 57 of the 58 species reported from the mainstem of the Red River were found in the Arkansas segment of the river, we accept 10 of the species listed by Oliver as new Red River records for Arkansas, bringing the total known mainstem species to 64. All 10 of Oliver's new species records were subsequently confirmed from the Red River by other collectors.

From 1973 to 1987, Robison and Buchanan (1988) made 27 fish collections by seine in the Red River mainstem between the Oklahoma and Louisiana state lines. These collections added four additional species to the known Red River fish fauna of Arkansas, bringing the known species total to 68.

Table 2. Fish species historically known from the Red River in Arkansas but not collected in the 1995-2001 sampling.

Species	Collector and/or author first reporting species
Ichthyomyzon castaneus	Robison and Buchanan (1988)
Amia calva	Bailey, 1940 (Buchanan, 1973)
Anguilla rostrata	Buchanan (1973)
Alosa alabamae	Reeves (1953)
Campostoma anomalum	Oliver (Dorris et al., 1979)
Hybognathus placitus	Black (1940)
Luxilus chrysocephalus	Black (1940)
Notropis bairdi	Black (1940)
Pimephales promelas	Oliver (Dorris et al., 1979)
Ameiurus melas	Black (1940)
Mugil cephalus	Oliver (Dorris et al., 1979)

Methods

Main channel Red River habitats in four counties of Arkansas from the Oklahoma state line to the Louisiana state line were sampled by seines and rotenone from 1995 through 2001 and by gill nets, hoop nets, and trotlines in 1997 and 1998 (Fig. 1). Ninety-one seine and/or rotenone samples were taken in the following four mainstem habitats: main river channel in slow to swift current along point bars and islands, chutes, backwaters adjacent to main channel, and sandbar pools. Seine collections were made with 6 x 1.5 m and 9 x 1.5 m nylon seines of 3.2 mm mesh. Small-scale samples were made with rotenone in areas of little or no current. Sampling time by seine and rotenone averaged 1.0 hour per site and ranged from 0.5 to 2.0 hours. Specimens were preserved in 10% formalin and later transferred to 45% isopropanol. All preserved fishes were identified in the laboratory, and specimens were deposited in the Zoology Collection of the University of Arkansas – Fort Smith.

Five localities in the Arkansas segment of the Red River were sampled with gill nets and hoop nets between March and June 1997, and the three most downstream of those localities were sampled with gill nets and hoop nets between January and July 1998 (Fig. 1), for a total of eight site-samples during the two sampling periods. Each site included a river reach of approximately 8 km. Hoop nets 1.2 m in diameter with 3.8 cm bar mesh were used in deep water, and hoop nets 0.9 m in diameter with 3.8 cm bar mesh were used in shallow water. The hoop nets were checked twice daily, just after sunrise and just before sunset. Experimental gill nets consisting of three 30 m panels one each of 5.1, 7.6, and 10.2 cm monofilament webbing were checked at approximately two-hour intervals. At the two most downstream sampling localities, trotlines baited with golden shiners were used in 1997. A total of 378 hoop net nights, 24 gill net nights, and 8 trotline nights represented approximately 5000 hours of sampling at the five sites.

Present status in the Red River was assigned to each fish species collected in this study (Table 1) based on a combination of habitats sampled, sampling methods used, and number of individuals collected. Species collected mainly by seines and/or rotenone were assigned a status as follows: (1) Abundant – more than 700 specimens collected and the species taken in more than 60 samples, (2) Common – 100-700 specimens collected and taken in 25-59 samples, (3) Uncommon – 11-99 specimens collected and taken in 5-24 samples, and (4) Rare – 1-10 specimens collected and taken in 1-4 samples.

Species taken almost exclusively by hoop nets, gill nets, and trotlines were assigned a status as follows: (1) Abundant – more than 100 specimens collected and taken in seven or eight of the eight site-samples during 1997 and 1998, (2)

Common – 30-99 specimens collected and taken in five or six site-samples, (3) Uncommon – 5-15 specimens collected and taken in three or four site-samples, and (4) Rare – 1-4 specimens collected and taken in one or two site-samples.

Species meeting only one of the two criteria (number of specimens and number of sites) for a given rank in the above two ranking systems were assigned to the next lower ranked category. A few species, which were taken in a variety of habitats and by a variety of methods, were assigned a rank by using a combination of the two previously described ranking systems.

To compare fish species richness and distribution of the Arkansas segment of the Red River with the much longer Red River segments upstream and downstream from Arkansas, several data sources were consulted. Fish distribution records in the Red River upstream from Arkansas were obtained from Hargrave (2000), Miller and Robison (1973), Riggs and Bonn (1959), Sublette et al. (1990), the University of Oklahoma Museum of Natural History, and the Oklahoma Department of Environmental Quality records from Red River fish sampling stations. Fish distribution records in the Red River downstream from Arkansas came from Douglas (1974) and the University of Louisiana at Monroe and Tulane University fish collection databases. Fish species similarity of the Red River segments upstream and downstream from Arkansas was compared with the Arkansas segment by using the index of similarity (S) of Odum (1971), S=2C/A+B, where C is the number of fish species common to two segments being compared, A is the total number of species in one segment, and B is the total number of species in the other stream segment.

Results

Seventy-two fish species and one hybrid combination (38 specimens of *Morone chrysops* x *M. saxatilis*) were collected from the Red River mainstem in Arkansas (Table 1). Fifteen species were new records, bringing the total number of species historically known from the Red River in Arkansas to 83. Prior to this study, 68 fish species were historically reported from the Red River in Arkansas, and 11 of those species were not collected in our 1995-2001 sampling (Table 2). Fish sampling in the Arkansas segment of the Red River in 1999 and 2000 by the U.S. Army Corps of Engineers produced no additional new species records (pers. comm., J. Kilgore, U.S. Army Corps of Engineers Waterways Experiment Station, Vicksburg, MS).

The species collected in this study were distributed among 17 families. More than 84% of the specimens collected were in the minnow family, Cyprinidae. The four next most abundant families by number of specimens collected were Centrarchidae (5%), Clupeidae (3%), Catostomidae (1.7%), and Atherinopsidae (1.4%). The ten most abundant species in decreasing order of number of specimens collected were as follows: *Notropis atherinoides*, *N. potteri*, *Cyprinella lutrensis*, *Pimephales vigilax*, *N. shumardi*, *Lepomis humilis*, *Dorosoma petenense*, *Macrhybopsis storeriana*, *Menidia beryllina*, and *Carpiodes carpio*. Six species represented by only a single specimen each were as follows: *Polyodon spathula*, *Ctenopharyngodon idella*, *Phenacobius mirabilis*, *Ictiobus niger*, *Fundulus blairae*, and *F. olivaceus*.

In general, the 10 most abundant species were also the most widely distributed species in the study area based on the number of collections in which they were found. Only *N. shumardi* among the 10 most abundant species was not among the 10 most widely distributed species (falling to twelfth most widely distributed). The ten species appearing in the greatest number of collections in decreasing order were as follows: *C. lutrensis*, *P. vigilax*, *N. atherinoides*, *M. beryllina*, *D. petenense*, *M. storeriana*, *D. cepedianum*, *N. potteri*, *C. carpio*, and *L. humilis*.

Discussion

The Red River exhibits the well-documented pattern of increasing fish species richness from headwaters to downstream (Horwitz, 1978; Matthews, 1998), and the Arkansas segment of the Red River has high fish species richness. Approximately 124 fish species are historically known from the entire Red River. Eleven percent of the Red River mainstem length and 6.4% of the total Red River drainage area are in Arkansas, and 83 species are historically known from the Arkansas segment. This is approximately 67% of the entire Red River fish fauna, and 58% percent of the mainstem fish fauna was found in this study. Ninety fish species are known from the Red River upstream from Arkansas, and 106 species are known from the Red River downstream from Arkansas. Two species *Etheostoma collettei* and *Percina maculata* have been reported only from the Arkansas segment, 11 species from the Arkansas segment have not been reported upstream from Arkansas, and seven species found in Arkansas have not been reported from the Red River in Louisiana. In this study, the Arkansas segment of the Red River had 61% of the species known from the downstream segment and 68% of the species reported from the upstream reaches. Based on the similarity index (S) of Odum (1971), the fish species composition of the Arkansas segment of the Red River is slightly more similar to the river segment upstream from Arkansas (S=.83) than to the downstream segment (S=.80). Species historically known from the Arkansas segment comprise 80% and 72% of the species reported from the upstream and downstream segments, respectively.

One currently abundant species, *Notropis potteri*, occurs in the Arkansas portion of its range only in the main channel of the Red River. This species occurred throughout the

study reach and was the second most abundant species found with nearly 10,000 specimens collected. A single specimen of *Phenacobius mirabilis* was the first record of that species from the mainstem Red River in Arkansas and was only the second specimen of that species collected in Arkansas in the last 50 years. The bigscale logperch, *Percina macrolepida*, was first reported in Arkansas from the upper portion of the Red River (Buchanan et al., 1996) and was found throughout the Arkansas segment of the Red River in this study.

The blue sucker, *Cycleptus elongatus*, was the most abundant large species caught by hoop nets and was the third most common large species (after *Carpiodes carpio* and *Aplodinotus grunniens*) collected by all methods. The range of *C. elongatus* has drastically declined in recent decades, and it is currently more abundant in the Red River than in any other river in Arkansas. Two specimens of alligator gar, *Atractosteus spatula*, another declining big river fish were collected. Layher (1998) provided additional data on large species collected from the Red River by hoop nets, gill nets, and trotlines.

Eleven species previously reported from the Red River in Arkansas were not found in this study (Table 2). Two of those species, *Campostoma anomalum* and *Luxilus chrysocephalus*, probably are accidentals from tributaries. It is likely that additional Red River floodplain and tributary species could occasionally be taken in future main channel sampling.

Three of the historically reported species not found in our study have probably been extirpated from the Arkansas segment of the Red River. The Alabama shad, *Alosa alabamae*, was reported from the Little River, a Red River tributary in Oklahoma (Reeves, 1953; Miller and Robison, 1973). That anadromous species is no longer able to ascend the Little River to reach its former spawning areas in Oklahoma due to the 1963 construction of Millwood Dam on Little River in Arkansas. *Alosa alabamae* still successfully ascends the lower 55 km of the Red River Navigation System in Louisiana to enter and spawn in the Ouachita River in Arkansas (Buchanan et al., 1999). The plains minnow, *Hybognathus placitus*, and the Red River shiner, *Notropis bairdi*, have not been reported from the Arkansas segment of the Red River in more than 60 years. Both of those primarily Great Plains species are common today in the Red River upstream from Lake Texoma, and small populations of those species persisted into the mid 1990s in the Red River of Oklahoma downstream from Lake Texoma (pers. comm., J. Pigg, Oklahoma Department of Environmental Quality). It is possible that future fish sampling could produce sporadic records of *H. placitus* and *N. bairdi* in the Red River of Arkansas because both species were taken at an Oklahoma Department of Environmental Quality fish sampling site on the Red River near DeKalb, Texas, 18 km upstream from the Arkansas state line as recently as 1995. Unsuccessful attempts were made to collect both species in the Arkansas portion of the Red River near the Oklahoma state line in each year of this study.

Human alteration of the Red River has likely caused the extirpation of *A. alabamae*, *H. placitus*, and *N. bairdi* from the Arkansas segment of that river. Construction of the Red River Navigation System in Louisiana impedes or blocks access of *A. alabamae* to former upstream tributaries of the Red River in Arkansas and Oklahoma, and dams on Little River also block access to former spawning sites. The impoundment of Lake Texoma by Denison Dam on the Red River in Oklahoma in 1944 fragmented the ranges of *H. placitus* and *N. bairdi*, creating a more precarious situation for populations of those species downstream from Denison Dam. Great Plains streams typically experience environmental fluctuations that can lead to the extirpation of local populations of fish species (Luttrell et al., 1999). A species whose range has been fragmented by a dam has little possibility of repopulation if populations above or below the dam are lost. Winston et al. (1991) documented major changes in the fish community in the North Fork of the Red River in Oklahoma, including extirpation of four minnow species following construction of Altus Dam on that river. The small populations of *H. placitus* and *N. bairdi*, known from the Red River in Oklahoma below Denison Dam as recently as the 1990s, have little chance of repopulation from the larger populations of those species upstream from Lake Texoma if they are extirpated.

The mouth of the Little River, just west of Interstate Hwy 30, divides the Arkansas segment of the Red River into two nearly equal parts. The Red River upstream from the Little River mouth, especially upstream from the U.S. Hwy 71 bridge, has been altered very little by manmade structures, whereas the Red River downstream from the Little River mouth has numerous levees, wingdikes, and revetted banks. We found no substantial differences in fish species richness between the upstream (67 species) and downstream (65 species) segments in Arkansas. Seven species were found only in the upstream segment, and five species were found only in the downstream segment (Table 1). Some species found in both river segments in Arkansas were more abundant in one segment based on number of specimens taken and the number of samples in which they occurred. *Macrhybopsis hyostoma*, *Notropis buchanani*, *Labidesthes sicculus*, *Etheostoma asprigene*, and *E. chlorosomum* were more abundant in the upstream segment of the Red River in Arkansas, and *Lepisosteus oculatus*, *Cyprinella venusta*, and *Morone mississippiensis* were more abundant in the downstream segment.

The U.S. Army Corps of Engineers has proposed a project to extend the Red River Navigation System 217 km

upstream from Shreveport, Louisiana to Index, Arkansas near U.S. Highway 71. This project, currently estimated to cost one billion dollars, would require the construction of three to five locks and dams, over 100 dikes, extensive rock revetments, and other channel modification structures. It is not possible to precisely predict the effects of such a project on the fish community of the Red River; however, such a drastic modification of the environment would likely have major impacts on fish species richness, diversity, and distribution. Some species would increase in abundance, while others would decrease or even be extirpated from large sections of the river. This study of the fishes of the Arkansas segment of the Red River should provide a baseline for determining future changes in fish species distribution and abundance.

ACKNOWLEDGMENTS.—We are grateful to the University of Arkansas – Fort Smith for partially funding this study through the Scholar-Preceptor Program and a faculty development grant. Additional funding was provided by a National Science Foundation grant through South Central Partnership for Environmental Technology Education. We thank Chad Hargrave of the Sam Noble Museum of Natural History, University of Oklahoma; Henry L. Bart, Jr. of the Tulane University Museum of Natural History; and Frank Pezold of the University of Louisiana at Monroe Museum of Natural History for providing records of Red River fishes from their respective museum databases. The late Jimmie Pigg provided data from Red River fish sampling in Oklahoma by the Oklahoma Department of Environmental Quality. Jack Kilgore provided data on Red River fish collections made in Arkansas in 1999 and 2000 by the U.S. Army Corps of Engineers Waterways Experiment Station. Henry Robison contributed information on *Alosa alabamae* in Oklahoma, Chris Jones prepared Fig. 1, and the following persons assisted with the fieldwork: Phillip W. Penny, Jr., Chad Hargrave, Laura Hudson, Josh Nichols, Joseph Hyland, Cheryl Jackson, Patrick Harrison, and Kim Lankford.

Literature Cited

Black, J. D. 1940. The distribution of the fishes of Arkansas. Unpublished Ph.D. Dissertation. Univ. Michigan, Ann Arbor. 243 pp.

Buchanan, T. M. 1973. Key to the fishes of Arkansas. Arkansas Game & Fish Commission, Little Rock. 68 pp.

Buchanan, T. M., C. Hargrave, D. Wilson, L. G. Claybrook, and **P. W. Penny, Jr.** 1996. First Arkansas records for bigscale logperch, *Percina macrolepida* Stevenson (Pisces: Percidae), with comments on habitat preference and distinctive characters. Proc. Arkansas Acad. Sci. 50:28-35.

Buchanan, T. M., J. Nichols, D. Turman, C. Dennis, S. Wooldridge, and **B. Hobbs.** 1999. Occurrence and reproduction of the Alabama shad, *Alosa alabamae* Jordan and Evermann, in the Ouachita River system of Arkansas. Proc. Arkansas Acad. Sci. 53:21-26.

Dorris, P. R., K. H. Oliver, J. D. Bragg, D. L. Marsh, D. W. McMasters, and **W. W. Fitzgerrel.** 1979. Biological inventory of the Red River waterway from Index, Arkansas to Shreveport, Louisiana. Unpublished Report to U.S. Army Corps of Engineers, New Orleans District. 106 pp.

Douglas, N. H. 1974. Freshwater fishes of Louisiana. Claitor's Publ. Div., Baton Rouge. 443 pp.

Echelle, A. A., A. F. Echelle, and **L. G. Hill.** 1972. Interspecific interactions and limiting factors of abundance and distribution in the Red River pupfish, *Cyprinodon rubrofluviatilis*. Am. Midl. Nat. 88:109-130.

Hargrave, C. W. 2000. A decade of stability in fish assemblages of a harsh, prairie river system. Unpubl. M.S. Thesis. Univ. Oklahoma, Norman. 102 pp.

Horwitz, R. J. 1978. Temporal variability patterns and the distributional patterns of stream fishes. Ecol. Monogr. 48:307-321.

Jordan, D. S., and **C. H. Gilbert.** 1886. List of fishes collected in Arkansas, Indian Territory, and Texas, in September, 1884, with notes and descriptions. Proc. U.S. Nat. Mus., 9(549):1-25.

Layher, W. G. 1998. Status and distribution of pallid sturgeon, blue sucker and other large river fishes in the Red River, Arkansas. Unpublished report to Arkansas Game and Fish Commission, Little Rock, Arkansas. 31 pp.

Luttrell, G. R., A. A. Echelle, W. L. Fisher, and **D. J. Eisenhour.** 1999. Declining status of two species of the *Macrhybopsis aestivalis* complex (Teleostei: Cyprinidae) in the Arkansas River Basin and related effects of reservoirs as barriers to dispersal. Copeia 1999:981-989.

Matthews, W. J. 1998. Patterns in freshwater fish ecology. Chapman & Hall, New York. 756 pp.

Miller, R. J., and **H. W. Robison.** 1973. The fishes of Oklahoma. Oklahoma State Univ. Museum of Natural and Cultural History, Series No. 1. 246 pp.

Odum, E. P. 1971. Fundamentals of ecology. W.B. Saunders Co., Philadelphia. 574 pp.

Reeves, J. D. 1953. The fishes of the Little River system in Oklahoma. Unpubl. Ph.D. Dissertation. Oklahoma State Univ., Stillwater. 95 pp.

Riggs, C. D., and **E. W. Bonn.** 1959. An annotated list of the fishes of Lake Texoma, Oklahoma and Texas. Southwest. Nat. 4:157-168.

Robison, H. W., and **T. M. Buchanan.** 1988. Fishes of Arkansas. Univ. Arkansas Press, Fayetteville. 536 pp.

Sublette, J. E., M. D. Hatch, and **M. Sublette.** 1990. The fishes of New Mexico. Univ. New Mexico Press,

Albuquerque. 393 pp.

Winston, M. R., C. M. Taylor, and **J. Pigg.** 1991. Upstream extirpation of four minnow species due to damming of a prairie stream. Trans. Am. Fish. Soc. 120:98-105.

Winter and Spring Water Quality of the Big Creek Watershed, Craighead County, Arkansas: Nutrients, Habitat, and Macroinvertebrates

Alan D. Christian*, **Jennifer Bouldin, Nate Bickford**
Samuel B. McCord, Aboubakar Sako and **Jerry L. Farris**
Department of Environmental Sciences
Arkansas State University
P.O. Box 847
State University, AR 72467

Lynn Kanieski and Ashley McBride
Department of Biological Sciences
Arkansas State University
P.O. Box 599
State University, AR 72467

* Corresponding Author

Abstract

The objective of this study was to assess the water quality of the Big Creek watershed during the winter and spring of 2002 by analyzing water physical, chemical variables, aquatic macro-invertebrates, and habitat. The Big Creek watershed, arising on Crowley's Ridge in northeast Arkansas, is a small deltaic watershed and is an area of intense cultivation. Four stations, Big Creek Upper (BCU), Mud Creek (MC), Lost Creek (LC), and Big Creek Lower (BCL) were established for this study from Big Creek, Mud Creek and Lost Creek. Water samples were collected on a weekly basis for 10 weeks from January 2002 through March 2002. We analyzed these streams for temperature, pH, D.O., conductivity, TSS, chlorophyll-*a*, DOC, total N and P, total dissolved N and P, nitrate, ammonium, and soluble reactive phosphorus. During this time period, we also sampled aquatic macroinvertebrates and assessed stream habitat according to USEPA rapid bioassessment protocols. Overall, nutrients and TSS were high, pH fluctuated from 5.8 to 7.8, and D.O. was moderate to high, ranging from 6.75 to 13.24 mg/L. Generally, physical and chemical water variables were correlated with changes in stream discharge. For a 20-jab dip-net sample, macroinvertebrate species richness ranged from 9 to 23 taxa, while abundance ranged from 38 to 209 individuals per station. Physical habitat index scores ranged from 75 to 104 (maximum of 200) indicating marginal physical habitat. We report that this watershed has high concentrations of nutrients and suspended solids during the winter and spring wet season and that the macroinvertebrate communities are influenced by stream conditions, including marginal physical habitat.

Introduction

Aquatic macroinvertebrate and fish faunal groups have been studied historically and used as indicators of water quality in the Big Creek watershed (Beadles, 1970; Jenkins and Harp, 1971; Cather and Harp, 1975; Arkansas Pollution Control and Ecology Commission, 1998). Cather and Harp (1975) reported lower macroinvertebrate taxa richness and species diversity at two stations on Big Creek in comparison to a high quality Ozark stream. In 1998 the Arkansas Department of Pollution Control and Ecology reported 9 to 20 aquatic macroinvertebrate taxa from three stations on Big Creek Ditch and 1 station on Lost Creek Ditch (Arkansas Pollution Control and Ecology Commission, 1998). Beadles (1970) observed only eight species of fish, several of which are considered tolerant to moderate amounts of domestic effluents, at 5 sampling stations on Lost Creek, a tributary of Big Creek. Jenkins and Harp (1971) reported low (11) to moderate (17) fish richness from Big Creek and its two major tributaries, Mud and Lost creeks, with several species that are known to withstand high turbidity. More recently, the Arkansas Department of Pollution Control and Ecology reported 6 to 20 taxa at four stations in the watershed (Arkansas Pollution Control and Ecology Commission, 1998).

Because habitat provides the template for the distribution of organisms, assessment of habitat quality is important in determining if habitat degradation is a factor influencing aquatic organism composition (Resh et al., 1996; Barbour et al., 1999). High nutrient concentrations also have been shown to influence fish and aquatic macroinvertebrates. For instance, Miltner and Rankin (1998) have shown that there is high negative correlation between biotic integrity and nutrient concentrations. One land use type that has been shown to be a source of high nutrient fluxes is the agriculture dominated watershed, which has been shown to be orders of magnitude higher in nutrient fluxes than the undisturbed forest watershed (Beaulac and Reckhow, 1982; Vanni et al., 2001).

Big Creek and its tributaries originate on Crowley's Ridge in southcentral Greene County and northeast Craighead County. It is 36.8 km long, has an average gradient of 1.6 m/km, and ultimately becomes Bayou DeView Ditch 8 km east of Cache, Craighead County, Arkansas (Jenkins and Harp, 1971; Cather and Harp, 1975). Big Creek is impounded by Lake Frierson before flowing

into Craighead County. Lost Creek and Mud Creek are major tributaries of Big Creek, and like Big Creek, are channelized for most of their length (Jenkins and Harp, 1971). Mud Creek enters into Big Creek 4.2 km north of Jonesboro, Craighead County, Arkansas, has a total length of 12 km, and has an average gradient of 1.5 m/km (Jenkins and Harp, 1971). Lost Creek enters Big Creek 3.2 km west-southwest of Jonesboro, has a total length of 14 km, and an average gradient of 1.7 m/km. Between the confluences of Mud and Lost creeks with Big Creek, Jonesboro West Wastewater Treatment Facility (WWTF) discharges effluent into an unnamed tributary which then enters into Big Creek. The predominant soils of the watershed are Falaya-Collins association washed from loess, which are deep, poorly to moderately well drained, moderately permeable, and silty bottomed (Jenkins and Harp 1971). Land use in the watershed is mostly agriculture with rice, soybeans, and cotton crops. Streams in the Big Creek watershed have been extensively channelized and have been classified by the Arkansas Department of Pollution Control and Ecology as a channel-altered Delta Ecoregion fishery with designated beneficial uses for: primary and secondary contact recreation; and as domestic, industrial, and agricultural water supplies (Arkansas Pollution Control and Ecology Commission, 1998). National pollution discharge elimination system permit holders in the watershed include Jonesboro-West WWTF, Northern Mobile Home Park, and Olivetan Benedictine Sisters (Arkansas Department of Pollution Control and Ecology, 1998).

The objective of this study was to assess the water quality of the Big Creek watershed during the winter and spring of 2002 by analyzing select physical-chemical variables, aquatic macroinvertebrates, and habitat. We expect that the aquatic macroinvertebrate fauna will be impaired due to loss of habitat through channelization and due to high nutrient concentrations typically associated with agriculturally dominated watersheds.

Materials and Methods

Four stations were used in this study. The Big Creek upper (BCU) station is located in SE 1/4, SW1/4, Sec. 13, T 15 N, R 3 E, Craighead County, Arkansas [GPS: N 35" 54.064'; W 90" 43.063'], and has an elevation of 97.5 m. The Big Creek lower (BCL) station is located in NE1/4 NW1/4, Sec. 25, T 14 N, R 2 E, Craighead County, Arkansas [GPS: N 35" 49.277'; W 90" 50.045"], and has an elevation of 77.4 m. The Lost Creek (LC) station is located in NW1/4, NW1/4, Sec. 13, T 14 N, R 3 E, Craighead County, Arkansas [GPS: N 35" 50.915' W 90" 43.819'], and has an elevation of 91.4 m. The Mud Creek (MC) station is located in SW1/4, SW1/4, Sec. 18, T 15 N, R 4 E, Craighead County, Arkansas [GPS: N 35" 54.058; W 90" 42.779'], and has an elevation of 97.5 m.

The four stations were sampled on a weekly basis from 26 January to 30 March 2002. Stream stage and depth of water column, at a standard center stream location, also was determined weekly by using a weighted steel cable and subtracting the distance from the top of the bridge to the bottom of the stream from the distance from the top of the bridge to the water surface. Water samples were collected at 3 locations along a transect at the 25, 50, and 75% stream width, and transported back to the lab for particulate and dissolved nutrient analyses. At the same time, dissolved oxygen (D.O.), temperature, pH, and conductivity were determined in the field for each sample using a Hach sensION™ 156 Portable Multiparameter meter. Rainfall gauges were established streamside the first week of the study, and rainfall data were recorded on a weekly basis thereafter.

For particulate variable analyses, known volumes (between 100 and 500 ml) of sample water were filtered through pre-weighed combusted 22 or 47 mm Gelman A/E glass fiber filters (nominal pore size = 1.0 µm). Total suspended solids (TSS) dry mass for each sample was obtained by drying the 47-mm filters at 60°C for 48 hours or longer until dry mass stabilized. Ash-free dry mass for each water sample was obtained by drying 47-mm glass fiber filters at 60°C for 48 hours or until dry mass stabilized, recording a mass, cooking these filters in a muffle furnace at 550°C for 4 hours, and then recording a final mass (Clesceri et al., 1998).

For chlorophyll-*a* concentrations, a known volume of water was filtered onto a 47-mm glass fiber filter (Pall Corporation, Type A/E). Filters were subsequently wrapped, labeled, and frozen until analysis was performed. For analysis, filters were placed in test tubes and frozen for at least 24 hours. Chlorophyll-*a* was extracted in 5 mL of 90% acetone in the refrigerator for 2 to 24 hours prior to analysis. Chlorophyll-*a* concentrations were determined on extracted chlorophyll samples using absorbance at 663 nm (Clesceri et al., 1998).

Dissolved nutrient concentration determinations, including total phosphorus (TP), soluble reactive phosphorus (SRP), total nitrogen (TN), nitrate, and ammonium, were conducted on the filtrate of samples filtered for fine particulate organic matter (FPOM). Filtrate was stored in 250-ml, acid-washed Nalgene bottles and preserved using a 1.5 ml/L concentration of concentrated H_2SO_4. Ammonium and SRP were determined by the Solorzano Colorimetric technique (Soloranzo, 1969) and the acid molybdate method (Stainton et al., 1974) respectively, and are reported as µg NH_4-N/L and µg PO_4-P/L, respectively. Nitrate concentrations were determined using second derivative spectroscopy methodology (Crumpton et al., 1992) and are reported as µg NO_4-N/L. Total phosphorus was determined on a whole water sample by digesting the samples with potassium persulfate and

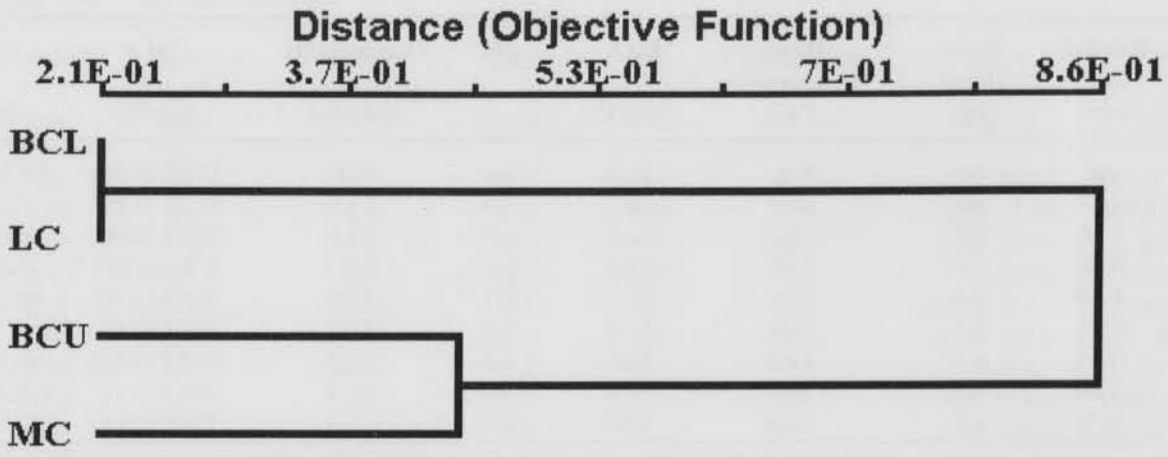

Fig. 1. A cluster dendogram based on Sorensen's distance of the aquatic macroinvertebrate fauna collected on 22 January 2002 at the Big Creek Lower (BCL), Big Creek upper (BCU), Lost Creek (LC), and Mud Creek (MC) stations.

analyzing the resulting orthophosphate using the acid molybdate method mentioned above (Stainton et al., 1974). Total nitrogen concentration of the filtrate was determined by digesting with low N potassium persulfate, followed by nitrate determination using second-derivative spectroscopy (Crumpton et al., 1992). Total dissolved carbon (TDC), total dissolved organic carbon (TDOC), and total dissolved inorganic carbon (TDIC) also were determined for each station on each sampling date using standardized methods (Clesceri et al., 1998).

We used the US Environmental Protection Agency (USEPA) rapid bioassessment protocol to qualitatively assess habitat on 26 January 2002 at each of four stations (Barbour et al., 1999). These habitat assessments were conducted along a 200 m stretch at each station. This qualitative assessment incorporates 10 metrics, each with a maximum score of 20 for a possible total of 200 points. Scores ranging from 200-160 represent optimal habitat conditions, 159-110 represent sub-optimal habitat conditions, 109-60 represent marginal habitat conditions, and scores below 60 represent poor habitat conditions.

We used the USEPA rapid bioassessment protocol to assess the macroinvertebrate community on 26 January 2002 at each of four stations (Resh et al., 1996; Barbour et al., 1999). This protocol calls for a composite 20-jab sample over a variety of microhabitats present along the 200-m

Table 1. Physical, chemical, and biological variables (± 1 SD, if applicable) of the Big Creek Lower station across ten weeks in winter and early spring 2002. na = not analyzed

Date	Rainfall (cm)	Water Depth (m)	Water Temperature (°C)	D.O. (mg/L)	pH	Conductivity (µS/cm)	Chl *a* (mg/L)	TSS (mg/L)
26 Jan.	na	na	na	na	na	na	9.46 (4.39)	43.00 (9.93)
01 Feb.	3.43	0.6	9.3	9.7	7.5	59.7	7.99 (0.90)	na
08 Feb.	1.24	0.6	8.5	9.1	7.8	104.5	4.36 (0.63)	2.23 (1.32)
16 Feb.	0.00	0.6	7.5	11.8	6.6	152.2	31.37 (25.02)	1.93(0.65)
22 Feb.	na	0.6	9.0	8.9	6.8	100.4	11.76 (1.19)	na
01 March	0.64	0.5	9.2	10.0	6.5	79.9	6.08 (0.28)	67.18 (22.10)
08 March	0.64	0.5	9.4	11.0	6.7	104.0	10.37 (1.71)	39.02 (12.13)
22 March	8.13	0.5	9.0	9.8	6.6	108.0	11.23 (0.23)	30.33 (1.93)
29 March	5.00	0.4	9.3	9.5	6.8	110.0	4.65 (1.27)	87.78 (9.40)

Table 2. Physical, chemical, and biological variables (± 1 SD, if applicable) of the Big Creek Upper station across 10 weeks in winter and early spring 2002. na = not analyzed

Date	Rainfall (cm)	Water Depth (m)	Water Temperature (°C)	D.O. (mg/L)	pH	Conductivity (µS/cm)	Chl *a* (mg/L)	TSS (mg/L)
26 Jan.	na	na	6.4	12.4	na	40.0	11.67 (0.58)	65.70 (23.33)
01 Feb.	3.87	na	10.9	10.7	5.8	41.7	13.13 (0.19)	77.60 (na)
08 Feb.	1.14	0.7	7.1	12.2	6.3	59.1	13.70 (2.06)	3.22 (1.03)
16 Feb.	0.00	0.7	5.3	12.5	6.7	103.1	8.22 (0.39)	2.21 (1.69)
22 Feb.	4.39	0.8	7.9	12.1	6.7	47.0	18.90 (0.56)	48.36 (8.04)
01 March	0.71	0.5	4.7	13.2	6.9	81.0	10.74 (0.45)	na
08 March	0.63	0.5	14.9	12.6	7.8	31.2	10.46 (0.35)	16.36 (4.90)
22 March	7.48	0.8	8.5	11.1	7.0	46.9	16.54 (1.11)	118.56 (41.41)
29 March	4.52	0.8	12.3	8.66	6.7	52.0	17.68 (0.44)	22.29 (5.66)

Table 3. Physical, chemical, and biological variables (± 1 SD, if applicable) of the Lost Creek station across 10 weeks in winter and early spring 2002. na = not analyzed

Date	Rainfall (cm)	Water Depth (m)	Water Temperature (°C)	D.O. (mg/L)	pH	Conductivity (µS/cm)	Chl *a* (mg/L)	TSS (mg/L)
26 Jan.	na	0.0	6.4	12.4	na	42.5	36.95 (50.36)	70.56 (0.33)
01 Feb.	3.30	0.3	9.6	7.6	6.9	53.4	5.04 (0.26)	81.91 (65.72)
08 Feb.	1.02	0.3	8.1	6.8	7.0	62.5	1.78 (0.17)	4.82 (4.50)
16 Feb.	0.00	0.2	6.6	11.9	6.8	61.1	14.69 (20.47)	2.48 (0.87)
22 Feb.	7.87	0.2	8.4	10.0	6.8	60.0	6.66 (0.38)	18.69 (20.34)
01 March	1.14	0.2	8.6	11.0	6.7	64.0	8.19 (0.17)	11.73 (6.17)
08 March	0.51	0.1	9.8	10.5	6.8	71.1	9.04 (0.49)	18.93 (3.47)
22 March	8.38	0.1	9.9	10.1	7.3	68.0	8.28 (0.35)	18.96 (3.33)
29 March	5.00	0.3	10.1	9.8	7.1	65.0	7.49 (1.73)	70.62 (6.16)

stretch at each station. Taxa richness, total abundance, % Ephemeroptera, Plecoptera, and Trichoptera (EPT), % Diptera, % Chironomidae, functional feeding groups (i.e. % Shredders, % Collectors, % Filterers, % Scrapers, % Predators), and Family Level Tolerance Values (Hilsenhoff, 1988; Resh et al., 1996) were determined on the entire jab sample at each station. Sorensen community similarity distances were also calculated on the four assemblages using the software program PC-Ord (McCune and Mefford, 1999).

Results

Rainfall for the 10 week period ranged from 0.0 to 9.2 cm across all stations and water column depth ranged from 0.03 to 1.0 m (Tables 1-4). Water temperatures ranged from 5.0 to 14.9 °C across all stations over the 10-week period (Tables 1-4). Dissolved oxygen concentrations ranged from 6.8 to 13.2 mg/L and generally were lowest at BCL (Tables 1-4). The pH at the four stations ranged from 5.8 to 7.8 and generally was below 7.0 (Tables 1-4). Conductivity ranged from 31.2 to 152.0 µS/cm and generally was highest at BCL (Tables 1-4). Chlorophyll *a* concentrations ranged from 1.75 to 36.95 mg / L and was consistently above 10 mg/L at BCU (Tables 1-4). Total suspended solids ranged from 1.18 to 144.91 mg/L across all sampling stations (Tables 1-4).

Total dissolved organic carbon concentrations ranged from a low of 2.0 mg TDOC-C/L at BCL to a high of 8.6 mg TDOC-C/L at BCU (Tables 5-8). Total dissolved inorganic carbon concentrations ranged from a low of 0.7 mg TDOC-C/L at BCL to a high of 4.9 mg TDIC-C/L at BCU (Tables 5-8). Ammonium concentrations ranged from a low of 34.6 µg NH_4-N/L at LC to a high of 269.8 µg NH_4-N/L at BCL (Tables 5-8). Nitrate concentrations ranged from a low of 3.5 µg NO_3-N/L at BCL and BCU to a high of 1,294.3 µg NO_3-N/L at LC (Tables 5-8). Total nitrogen concentrations ranged from a low of 381.8 µg TN-N/L at

Table 4. Physical, chemical, and biological variables (± 1 SD, if applicable) of the Mud Creek station across 10 weeks in winter and early spring 2002. na = not analyzed

Date	Rainfall (cm)	Water Depth (m)	Water Temperature (°C)	D.O. (mg/L)	pH	Conductivity (µS/cm)	Chl *a* (mg/L)	TSS (mg/L)
26 Jan.	na	na	6.1	12.3	na	46.8	5.05 (0.15)	62.47 (21.31)
01 Feb.	4.06	na	10.3	10.3	6.3	57.4	4.83 (1.82)	144.91 (13.15)
08 Feb.	1.63	0.7	6.0	12.9	5.8	56.0	2.24 (0.56)	1.38 (0.47)
16 Feb.	0.00	0.9	5.0	12.3	6.7	78.4	1.75 (0.36)	1.18 (0.53)
22 Feb.	6.77	0.8	8.4	11.4	6.6	50.4	10.73 (0.32)	16.00 (4.22)
01 March	2.03	0.7	5.0	12.2	7.4	70.0	4.46 (0.11)	na
08 March	0.86	0.7	13.4	12.7	7.2	83.1	7.56 (0.42)	11.31 (0.54)
22 March	9.20	1.0	7.8	12.2	6.3	47.8	8.07 (0.44)	66.92 (17.84)
29 March	4.52	1.0	12.2	7.9	6.5	53.1	11.69 (0.56)	32.38 (2.16)

Table 5. Mean (± 1 SD) nutrient concentrations for the Big Creek Lower station across 10 weeks in winter and early spring 2002. na = not analyzed

Date	TDOC-C (mg/L)	TDIC-C (mg/L)	NH_4-N (µg/L)	NO_3-N (µg/L)	TN-N (µg/L)	PO_4-P (µg/L)	TP-P (µg/L)
26 Jan.	4.38 (0.09)	1.60 (0.08)	47.11 (5.80)	na	9868.32 (7887.29)	1993.49 (282.68)	3121.62 (746.07)
01 Feb.	2.08 (0.05)	2.34 (0.03)	50.07 (14.56)	221.08 (8.19)	618.83 (536.64)	1694.58 (164.51)	2866.03 (24.25)
08 Feb.	6.77 (0.05)	1.56 (0.08)	53.22 (8.17)	444.95 (27.31)	1451.96 (350.36)	9333.40 (694.51)	5372.77 (167.90)
16 Feb.	6.51 (0.36)	4.58 (0.34)	165.80 (95.13)	681.43 (23.33)	1333.08 (73.36)	13,961.86 (410.83)	8946.07 (115.21)
22 Feb.	2.03 (0.03)	4.81 (0.11)	120.29 (4.84)	355.09 (17.91)	998.96 (79.94)	3267.90 (132.71)	5411.97 (139.81)
01 March	7.33 (0.10)	3.64 (0.08)	84.27 (20.70)	921.06 (20.62)	2015.46 (259.61)	15,229.45 (414.41)	14,968.05 (349.85)
08 March	8.40 (0.06)	0.68 (002)	269.83 (29.24)	832.78 (10.92)	1624.72 (147.30)	4229.82 (87.85)	5295.22 (1038.15)
22 March	5.40 (0.05)	2.85 (0.08)	73.09 (6.97)	233.42 (18.82)	729.35 (14.82)	2213.59 (105.39)	2573.38 (36.80)
29 March	5.63 (0.17)	2.85 (0.10)	149.29 (19.01)	256.64 (5.36)	na	2767.92 (136.04)	na

BCU to a high of 9,868.3 µg TN-N/L at BCL (Tables 5-8). SRP concentrations ranged from a low of 272.5 µg PO_4-P/L at MC to a high of 15,229.5 µg PO_4-P/L at BCL (Tables 5-8). Total phosphorus concentrations ranged from a low of 717.2 µg TP-P/L to a high of 14,968.1 µg TP-P/L at BCL (Tables 5-8).

Habitat assessment total scores ranged from a low of 75 at LC to a high of 104 at BCL (Table 9). These total scores fall into the range of "Marginal" habitat quality. Habitat metrics that reflect variables that limit aquatic macroinvertebrates such as epifaunal substrate / available cover, pool substrate, and substrate deposition generally were low (i.e. marginal)(Table 9).

Macroinvertebrate taxa richness ranged from a low of 9 to a high of 23 at BCL and MC, respectively (Tables 10-11). Total abundance per station ranged from 38 to 207 (Table 10). Family Biotic Index scores for all stations ranged from 4.8 (i.e. good water quality) at MC to 6.2 (i.e. fairly poor water quality) at LC (Table 11). Evenness, Shannon's Diversity, and Simpson's Diversity were lowest at BCU and higher and variable at the other sites (Table 11). The % of EPT was lowest at LC and highest at BCL, whereas % Diptera was highest at the BCU. Chironomidae composition, a component of % Diptera, was lowest at BCU and highest at BCL (Table 11). Collectors comprised the highest % and shredders comprised the lowest % of macroinvertebrates at all stations with all stations being similar in % composition for all 5 functional feeding groups (Table 11). Sorensen's distance analysis reveled that BW and MC macroinvertebrate assemblages were 0.395 dissimilar, whereas the BCL and LC macroinvertebrate assemblages were 0.210 dissimilar (Fig. 1). The clusters of BCU and MC were 0.830 dissimilar to the BCL and LC group (Fig. 1).

Discussion

Nutrient concentrations in this study were high and typical of agriculturally dominated watersheds (Beaulac and

Table 6. Mean (± 1 SD) nutrient concentrations for the Big Creek Upper station across 10 weeks in winter and early spring 2002. na = not analyzed

Date	TDOC-C (mg/L)	TDIC-C (mg/L)	NH_4-N (µg/L)	NO_3-N (µg/L)	TN-N (µg/L)	PO_4-P (µg/L)	TP-P (µg/L)
26 Jan.	8.56 (0.44)	4.90 (0.36)	43.18 (5.88)	na	556.21 (129.14)	971.78 (60.17)	1929.43 (196.16)
01 Feb.	2.71 (0.60)	3.75 (0.61)	42.45 (0.32)	69.73 (4.73)	697.65 (122.83)	880.30 (140.99)	4871.52 (2381.64)
08 Feb.	3.62 (0.05)	1.80 (0.11)	57.58 (4.36)	83.92 (0.00)	593.11 (12.30)	704.58 (109.45)	1688.54 (486.87)
16 Feb.	3.50 (0.02)	3.17 (0.12)	52.82 (4.07)	76.04 (2.73)	453.73 (69.93)	527.05 (49.14)	1346.40 (61.50)
22 Feb.	3.55 (0.06)	1.40 (1.40)	57.38 (1.35)	255.77 (5.46)	595.16 (87.04)	499.88 (74.76)	1520.33 (154.34)
01 March	2.42 (0.02)	1.06 (0.06)	35.60 (2.02)	14.56 (2.73)	513.36 (125.84)	677.41 (20.39)	1047.09 (211.53)
08 March	5.91 (0.09)	4.48 (0.47)	51.41 (0.82)	3.52 (0.00)	381.81 (39.22)	579.58 (141.52)	1135.71 (12.33)
22 March	4.14 (0.20)	2.91 (0.06)	41.04 (4.36)	60.12 (3.09)	542.82 (42.61)	961.82 (27.58)	1751.29 (107.74)
29 March	3.76 (0.06)	2.61 (0.08)	41.51 (3.64)	147.66 (74.33)	572.27 (18.00)	997.14 (36.56)	1524.20 (154.73)

Table 7. Mean (± 1 SD) nutrient concentrations for the Lost Creek station across 10 weeks in winter and early spring 2002. na = not analyzed

Date	TDOC-C (mg/L)	TDIC-C (mg/L)	NH_4-N (µg/L)	NO_3-N (µg/L)	TN-N (µg/L)	PO_4-P (µg/L)	TP-P (µg/L)
26 Jan.	3.08 (0.03)	1.88 (0.02)	34.62 (4.20)	na	716.10 (221.97)	949.14 (68.38)	1842.87 (428.27)
01 Feb.	6.07 (0.10)	1.98 (0.03)	70.17(14.05)	1294.39 (320.76)	778.71 (674.39)	894.79 (142.76)	2656.58 (337.78)
08 Feb.	2.77 (0.10)	3.27 (0.10)	60.24 (5.56)	1033.94 (40.38)	904.68 (103.14)	624.87 (205.49)	1949.84 (162.42)
16 Feb.	7.30 (0.19)	0.72 (0.27)	89.04 (45.87)	762.32 (19.60)	787.84 (193.71)	872.15 (71.27)	1650.16 (95.71)
22 Feb.	5.22 (0.06)	2.20 (0.12)	97.76 (21.35)	1015.33 (250.66)	1068.66 (381.32)	701.86 (46.86)	1944.94 (69.76)
01 March	5.06 (0.05)	4.71 (0.44)	174.80 (146.85)	898.26 (80.18)	996.39 (172.98)	1274.31 (327.65)	1884.21 (194.62)
08 March	4.62 (0.10)	2.02 (0.36)	124.18 (15.03)	789.70 (76.47)	770.58 (85.84)	1113.99 (63.90)	2120.79 (84.29)
22 March	4.88 (0.09)	2.32 (0.10)	56.72 (7.33)	873.56 (63.30)	752.91 (23.81)	1399.30 (57.56)	1609.66 (27.51)
29 March	4.15 (0.17)	4.14 (0.28)	74.71 (9.75)	933.47 (93.58)	622.37 (539.12)	1601.29 (19.09)	2061.09 (1835.38)

Reckhow, 1982; Vanni et al., 2001). Arkansas Department of Environmental Quality has not set any nutrient standards other than for total phosphorus (≤ 100 mg TP/L) in clear flowing streams and does not have any criteria established in streams with high natural silt loads or color (Arkansas Pollution Control and Ecology Commission, 2001). Since no nutrient criteria are established for these streams, we used literature values to determine if nutrient concentrations in the ranges we observed in this study have the potential to impair stream organisms. For example, Miltner and Rankin (1998) reported that fish communities in small streams begin to show deleterious effects of increasing nutrient concentrations when total inorganic nitrogen exceeds 0.61 mg N/L and total phosphorus exceeds 0.06 mg TP/L. Both of these concentrations were exceeded consistently during this study. Our results indicate high levels of nutrient and suspended solids fluxes during the winter and early spring rainy season in the Big Creek watershed, and this information may be important for future management decisions because of the development of total maximum daily load initiatives across the state and nation as part of the Clean Water Act.

Our low taxa richness (Barbour et al., 1999), moderate Shannon's Species Diversity (Wilhm and Dorris, 1968), low % EPT (Barbour et al., 1999), moderate Family Biotic Index (Hilsenhoff, 1988), and high % Diptera and % Chironomidae (Barbour et al., 1999) indicate an impaired aquatic macroinvertebrate fauna. The species diversity values for the macroinvertebrate fauna in this study were similar to or slightly lower than those of Cather and Harp (1975) at two stations on Big Creek. They reported species diversity values that ranged from a low of 1.882 to a high of 2.905 during the summer and fall. They attributed their relatively low aquatic macroinvertebrate diversity values to a lack of microhabitats and related loss of ecological niches for aquatic invertebrates as compared to the high microhabitat diversity Ozark stream, Janes Creek, in which they reported species diversity index values over 3.272

Table 8. Mean (± 1 SD) nutrient concentrations for the Mud Creek station across 10 weeks in winter and early spring 2002. na = not analyzed

Date	TDOC-C (mg/L)	TDIC-C (mg/L)	NH_4-N (µg/L)	NO_3-N (µg/L)	TN-N (µg/L)	PO_4-P (µg/L)	TP-P (µg/L)
26 Jan.	3.88 (0.11)	0.83 (0.21)	46.61 (17.73)	na	618.32 (188.39)	665.63 (82.91)	1830.62 (243.05)
01 Feb.	2.61 (0.49)	3.16 (2.03)	35.09 (6.45)	131.22 (4.73)	652.55 (52.30)	757.11 (68.00)	3037.51 (581.90)
08 Feb.	2.19 (0.03)	2.26 (0.17)	42.95 (13.30)	145.41 (0.00)	558.26 (110.23)	467.27 (60.70)	1240.25 (133.04)
16 Feb.	2.78 (0.13)	1.83 (0.13)	58.36 (13.15)	219.51 (7.22)	740.69 (117.32)	402.05 (86.40)	949.55 (66.88)
22 Feb.	3.63 (0.09)	0.88 (0.10)	40.00 (26.90)	251.04 (9.85)	562.36 (22.17)	272.53 (23.43)	1438.67 (87.83)
01 March	2.51 (0.02)	2.49 (0.01)	34.93 (6.58)	159.60 (9.46)	444.64 (10.20)	306.95 (80.47)	775.70 (27.52)
08 March	2.23 (0.03)	2.06 (0.02)	37.14 (9.61)	146.98 (2.73)	554.60 (212.17)	351.33 (48.94)	717.15 (422.77)
22 March	2.78 (0.06)	1.96 (0.07)	40.33 (11.32)	115.51 (8.19)	487.84 (63.53)	866.71 (24.91)	1173.69 (68.84)
29 March	2.66 (0.01)	2.12 (0.02)	43.92 (13.65)	144.09 (0.00)	758.80 (14.82)	751.68 (50.13)	1073.99 (98.24)

Table 9. Habitat assessment at the Big Creek Lower (BCL), Big Creek Upper (BCU), Lost Creek (LC), and Mud Creek (MC) stations sampled on 22 January 2002 in the Big Creek Watershed of northeast Arkansas.

Metric	Variable	BCL	BCU	LC	MC
1	Epifaunal Substrate / Available Cover	7	7	6	8
2	Pool Substrate	8	7	6	8
3	Pool Variability	13	13	3	16
4	Sediment Deposition	9	4	12	16
5	Channel Flow	11	7	8	7
6	Channel Alteration	14	18	13	16
7	Channel Sinuosity	10	13	3	13
8	Bank Stability	18	4	15	4
9	Vegetative Protection	14	8	9	8
10	Riparian Vegetative Zone	16	4	12	2
Total		104	81	75	96

(Cather and Harp, 1975). This anecdotal lack of micro- and macro-habitat in the Big Creek watershed discussed by Cather and Harp (1975) for macro-invertebrates and by Beadles (1970) and Jenkins and Harp (1971) for fishes was also observed in this study and quantified by the "marginal" designation of our habitat assessment. Big Creek and its tributaries lack riffle-run-pool development due to the extensive historical and current channelization for flood control. Substrates of Big Creek consist of hard clays, mud, and silt.

Our species richness was slightly lower than the 55 taxa reported from two stations across four summer and fall months (by Cather and Harp 1975). Their sampling consisted of 38 quantitative and 16 qualitative dip net samples in Big Creek; we however, sampled four stations in the watershed on one date in mid-winter using qualitative sampling dip-nets. Another explanation in the difference in taxa richness is that Cather and Harp (1975) identified many of their taxa to the species level, whereas we have only identified to the generic level. The higher degree of taxonomic resolution also could have been a reason for the higher diversity values reported by Cather and Harp (1975).

Our taxa richness (9 to 23 taxa) and Family Level Biotic Index values (4.8 to 6.2) were similar to those reported by the Arkansas Department of Pollution Control and Ecology (9 to 20 taxa; 4.3 to 6.4) using a similar 20 jab sampling technique (Arkansas Pollution Control and Ecology Commission, 1998). Our taxonomic composition is similar to theirs as well, with overlaps in ranges. They also reported similar relative percentages of functional feeding groups to ours, except that their % collectors ranged from 19.0 to 48.4%, whereas ours ranged from 66 to 89%. Overall, they

Table 10. Aquatic macroinvertebrate abundance collected on 22 January 2002 for the Big Creek Lower (BCL), Big Creek Upper (BCU), Lost Creek (LC) and Mud Creek (MC) stations.

Taxon			BCL	BCU	LC	MC
Oligochaeta		Oligochaeta	3	5	15	
Cladocera	Daphnidae	Daphnidae		1		
Isopoda	Asellidae	*Caecidotea*			1	
		Lirceus		1		1
Amphipoda	Talitridae	*Hyalella*				5
	Gammaridae	*Gammarus*			5	
	Crangonyctidae	*Synurella*				2
	Crangonyctidae	*Crangonyx*		1		1
Decapoda	Cambaridae	*Cambaridae*		1	2	
	Cambaridae	*Procambarus*				1
Ephemeroptera	Baetidae	Baetidae		1		1
	Heptageniidae	*Stenacron*		4		
	Heptageniidae	*Stenonema*				1
	Caenidae	*Caenis*	1	1		12
Odonata	Calopterygidae	*Calopteryx*				1
	Coenagrionidae	*Argia*				1
	Macromiidae	*Macromia*				1
	Corduliidae	*Epitheca*	1			
Plecoptera	Perlodidae	*Isoperla*			1	3
Hemiptera	Corixidae	*Trichocorixa*			4	
	Corixidae	*Ramphocorixa*		1		
	Notonectidae	*Notonecta*			1	
Trichoptera	Hydrophsychidae	*Cheumatopsyche*	5	2		
	Limnephilidae	*Ironoquia*				1
Coleoptera	Dytiscidae	*Brachyratus*			2	
	Carabidae	Carabidae			1	
	Hydrophilidae	*Tropisternus lateralis nimbatus*			1	2
	Elmidae	*Stenelmis*		1		1
Diptera	Tipulidae	*Tipula*			1	
	Simuliidae	*Cnephia*			9	
	Simuliidae	*Prosimulium*	5	74	6	19
	Simuliidae	*Simulium*		101		20
	Ceratopogonidae	*Mallochohelea*		1		
	Chironomidae	Tanypodinae	5	4		1
	Chironomidae	Orthocladiinae	16		53	
	Chironomidae	Chironomini		3		26
	Chironomidae	Tanytarsini	1			
	Tabanidae	Tabanidae		1		
	Stratiomyidae	*Allognosta*		1		
Mollusca	Lymnaeidae	*Pseudosuccinea columella*				1
	Ancylidae	Ancylidae				1
	Physidae	*Physa*			2	
	Corbiculidae	*Corbicula fluminea*		2		4
	Unionidae	*Toxolasma lividus*				1
	Sphaeridae	*Sphaerium*	1		2	

Table 11. Macroinvertebrate assemblage characteristics collected on 22 January 2002 at the Big Creek Lower (BCL), Big Creek Upper (BCU), Lost Creek (LC), and Mud Creek (MC)stations sampled in the Big Creek Watershed of northeast Arkansas.

Variable	BCL	BCU	LC	MC
Richness	9	19	16	23
Family Biotic Index	5.9	5.9	6.2	4.8
Evenness	0.796	0.474	0.659	0.745
Shannon's Diversity	1.748	1.397	1.827	2.336
Simpson's Diversity	0.762	0.629	0.714	0.856
% EPT	16.0	3.8	0.9	5.4
% Diptera	71.0	89.0	65.0	62.0
% Chironomidae	58.0	3.0	50.0	25.0
% Shredders	3.0	0.0	1.0	0.0
% Collectors	71.0	89.0	66.0	74.0
% Filterers	3.0	1.0	2.0	5.0
% Scrapers	0.0	2.0	0.0	4.0
% Predators	3.0	3.0	9.0	8.0

reported higher % EPT (8.9 to 39.1) than we did (0.9 to16). Based on samples collected using similar methods, we can say that our winter results overlap with their summer samples (Arkansas Pollution Control and Ecology Commission, 1998). The Arkansas Department of Pollution Control and Ecology stated that based on the biological assessment of Big Creek and Lost Creek ditches, that the fish and macroinvertebrate communities generally were below expectations for a channel-altered Delta fishery (Arkansas Pollution Control and Ecology Commission, 1998). They also noted the high concentrations of nutrients and TSS as potential impacts to the Big Creek Ditch system.

The aquatic macroinvertebrates of Big Creek and its tributaries are impacted by both physical and chemical variables. Nutrients and suspended solids are high and have the potential to impair macro-invertebrate communities. Furthermore, the lack of macro- and micro-habitat also limits the diversity of habitat that can be used by taxa compared to unaltered or less altered streams. Nevertheless, over the last 25 plus years, water quality based on the aquatic macroinvertebrate fauna of the Big Creek watershed does not appear to have changed.

ACKNOWLEDGMENTS.—Financial support was provided by the ASU Departments of Biological Science, Chemistry and Physics, and Environmental Sciences. We thank R. Hannigan for use of equipment and L. Harding and S. Seagraves for their laboratory assistance.

Literature Cited

Arkansas Pollution Control and Ecology Commission. 1998. TMDL investigation of water quality impairments to Big Creek Ditch and Lost Creek Ditch Craighead County, Arkansas. Arkansas Department of Pollution Control and Ecology Commission, Little Rock, Arkansas.

Arkansas Pollution Control and Ecology Commission. 2001. Regulation 2: Regulation establishing water quality standards for surface waters of the state of Arkansas. Arkansas Pollution Control and Ecology Commission, Little Rock, Arkansas.

Barbour, M. T., J. Gerritsen, B. D. Snyder, and **J. B. Stribling.** 1999. Rapid bioassessment protocols for use in streams and wadeable rivers: periphyton, benthic macroinvertebrates, and fish. Second edition. EPA 841-B-99-002. U.S. Environmental Protection Agency: Office of Water, Washington D.C.

Beaulac, M. N., and **K. H. Reckhow.** 1982. An examination of land use-nutrient export relationships. Water Res. Bull. 18:1013-1024.

Beadles, J. K. 1970. The effect of domestic effluent on two spring surveys of fishes in Lost Creek, Craighead County, Arkansas. Proc. Arkansas Acad. Sci. 14:74-75.

Cather, M. R., and **G. L. Harp.** 1975. The aquatic macroinvertebrate fauna of an Ozark and Deltaic stream. Proc. Arkansas Acad. Sci. 29:30-35.

Clesceri, L. S., A. E. Greenberg, A. D. Eaton, and **M. A. H. Franson, editors.** 1998. *Standard methods for the examination of water and wastewater*, Twentieth edition. American Public Health Association, American Water Works Association, and Water Environment Federation, Washington D.C.

Crumpton, W. G., T. M. Isenhart and **P. D. Mitchell.** 1992. Nitrate and organic N analysis with second-derivative spectroscopy. Limnol. Oceanog. 37:907-913.

Hilsenhoff, W. L. 1988. Rapid field assessment of organic pollution with a family-level biotic index. J. N. Amer. Benthol. Soc. 7:65-68.

Jenkins, J. T., and **G. L. Harp.** 1971. Ichthyofaunal diversification and distribution in the Big Creek Watershed, Craighead and Greene Counties, Arkansas. Proc. Arkansas Acad. Sci. 25:79-87.

McCune, B., and **M. J. Mefford.** 1999. PC-ORD. Multivariate analysis of ecological data, Version 4 edition. MjM Software Design, Gleneden Beach, Oregon, USA.

Miltner, R. J., and **E. T. Rankin.** 1998. Primary nutrients and biotic integrity of rivers and streams. Freshwater Biol. 40:145-158.

Resh, V. H., M. J. Myers, and **M. J. Hannaford.** 1996. Macroinvertebrates as biotic indicators of environmental quality. Pages 647-667 *In:* F. R. Hauer and G. A. Lamberti, editors *Methods in stream ecology.* Academic Press, Inc, San Diego.

Soloranzo, L. 1969. Determination of ammonia in natural

waters by the phenolthypochlorite method. Limnol. Oceanog. 14:799-801.

Stainton, M. P., M. J. Capel, and **F. A. J. Armstrong.** 1974. The chemical analysis of freshwater. Fisheries Research Board of Canada. Misc. Spec. Publ. No. 25.

Vanni, M. J., W. H. Renwick, J. L. Headworth, J. D. Auch, and **M. H. Schaus.** 2001. Dissolved and particulate nutrient flux from three adjacent agricultural watersheds: A five-year study. Biogeochem. 54:85-114.

Wilhm, J. L., and **T. C. Dorris.** 1968. Biological parameters for water quality. BioScience 18:477-481.

Quantifying Forest Ground Flora Biomass Using Proximal Sensing

Paul F. Doruska* and **Robert C. Weih Jr.**
Arkansas Forest Resources Center
University of Arkansas School of Forest Resources
P.O. Box 3468
Monticello, AR 71656

Matthew D. Lane
Landscape Analysis Laboratory
University of the South
P.O. Box 222
Sewanee, TN 37375

Don C. Bragg
USDA Forest Service Southern Research Station
P.O. Box 3516
Monticello, AR 71656

*Corresponding Author

Abstract

Current focus on forest conservation and forest sustainability has increased the level of attention given to measures of ground flora in forest ecosystems. Traditionally, such data are collected via time- and resource-intensive methods of field identification, clipping, and weighing. With increased focus on community composition and structure measures of forest ground flora, the manner in which these data are collected must change. This project uses color and color infrared digital cameras to proximally sense forest ground flora and to develop regression models to predict green and dry biomass (g/m^2) from the proximally sensed data. Traditional vegetative indices such as the Normalized Difference Vegetative Index (NDVI) and the Average Visible Reflectance Index (AVR) explained 35-45% of the variation in forest ground flora biomass. Adding individual color band variables, especially the red and near infrared bands, to the regression model allowed the model to explain 66% and 58% of the variation in green and dry biomass, respectively, present.

Introduction

Many forest research projects estimate forest ground flora biomass via the labor-intensive technique of clipping, drying and weighing vegetative samples (Brower et al., 1990). When combined with species identification, such work is used to calculate a variety of community composition and structure measures (Magurran, 1988; Reed and Mroz, 1997; Elzinga et al., 1998) used in ecosystem studies and reporting. Such information is also used when assessing wildlife habitat (National Wildlife Research Center, 2000). The need to rapidly and preferably nondestructively determine such attributes has become apparent with the increased focus conservation and sustainability.

Satellite or airborne imagery combined with computer algorithms can be used to estimate forest biomass (Baret et al., 1989; Ahern et al., 1991). However, such imagery cannot be used to estimate forest ground flora biomass for two primary reasons. First, the scale of the imagery is too coarse to adequately examine forest ground flora. Second, the presence of a forest canopy often prevents a satellite or airborne camera from capturing forest ground flora in its imagery. This project examines whether techniques used to estimate forest biomass from satellite or airborne imagery can be used to estimate forest ground flora biomass using proximally sensed data obtained from color and color infrared imagery.

Photoplots have been used in ecological research for change detection (Schwegman, 1986; Windas 1986). This project combines the idea of photoplots, utilizing both color and color infrared digital images of forest ground flora, with vegetative indices typically calculated from satellite images to estimate forest ground flora aboveground biomass in g/m^2 via regression models.

Materials and Methods

Equipment and Software.--Two digital cameras were used with this project. A Kodak DCS760 camera with a Nikon F5 body was used to take color digital images at a 6 million pixel (3038 x 2028) resolution. A Kodak DCS420CIR camera with a Nikon F90 body camera operating at a 1.5 million pixel (1524 x 1020) resolution was used to take color infrared images. 20 mm auto-focus lenses were used on both cameras and an Omega Optical band pass filter (500-900 nm) was used with the DCS420CIR camera. A GER2600 spectroradiometer was used to assist in image standardization.

An aluminum stand was constructed to mount the

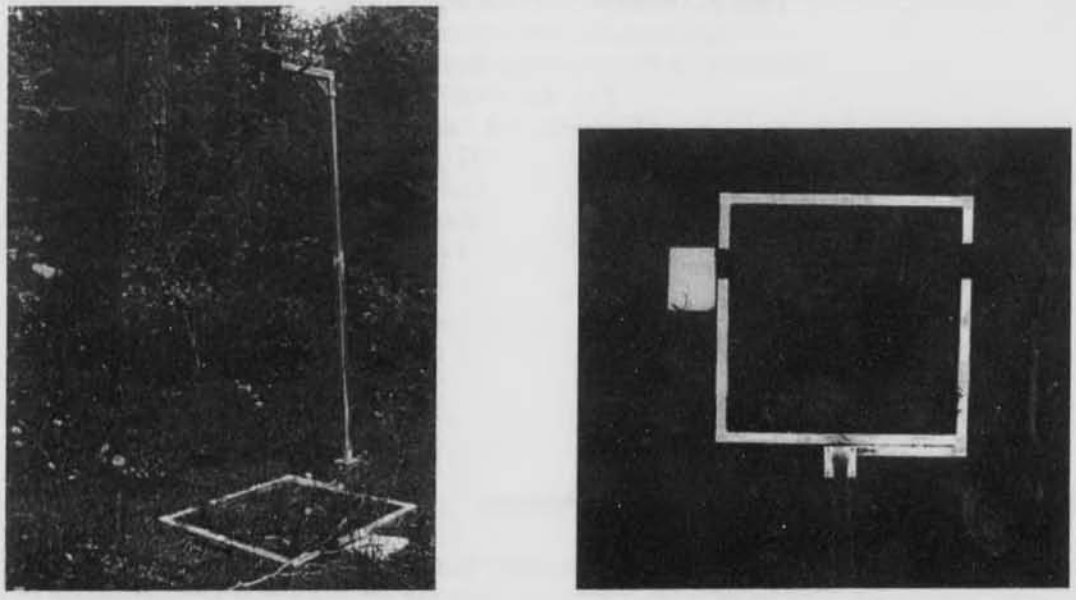

(A) (B)

Fig. 1. The frame (A) used to photograph the plots and an image (B) taken with the color camera (grayscale version shown here).

cameras and frame plots 1 m^2 in size. The actual frame size was 0.966 m^2 but hereafter it will be referred to as 1 m^2. The cell size for the imagery was 0.1015 cm. Black and white bands were painted onto the frame to calibrate image values from 0 to 255 to take into account variations in illuminations. Cross hairs (or tic marks) were drawn onto the frame in order to develop a local coordinate system for image comparisons. ESRI ArcGIS™ 8.x and ERDAS Imagine® 8.5 software were used to process the imagery and calculate the vegetative indices used herein.

Image Acquisition and Vegetation Collection.--A total of 75 1-m^2 plots was randomly established throughout the summer and early fall of 2002 in a variety of forest stands in the University Forest at the Univ. of Arkansas-Monticello, Monticello, AR (Drew County), near the Crossett Experimental Forest in Crossett, AR (Ashley County), and in established research areas in the Ouachita Mountains (Perry County). Young pine plantations, mature pine plantations, mixed pine-hardwood forests, and hardwood forests were visited. Once a plot location was established, the aluminum camera stand was set up (Fig. 1A), and any vegetation overlapping or extending beyond the border of the frame was removed to ensure only vegetation within the plot would appear in the images. For the purposes of this study, forest ground flora was defined as all vegetation less than 1 meter in height.

Each camera was then mounted to the frame separately and raised to the appropriate level to digitally capture an image of the plot. Three pictures were taken per camera to be sure at least one usable image was captured for each camera on each plot (Fig. 1B). After the images were taken, the vegetation in the plots was identified, clipped at ground level, sorted by species, placed into labeled plastic bags, and sealed for laboratory analysis. No protected species were encountered so all vegetation could be clipped for subsequent mass determination.

Mass Determination.--The green mass of the contents of each bag was determined immediately upon return to the laboratory. The contents of each plastic bag were then transferred to labeled paper sacks and placed in a drying oven at 60°C for three to four days. Upon completion of the drying process, the dry mass of the contents of each bag was determined and summed to obtain plot-level values.

Image Registration and Standardization.--The camera stand used in this study had a set of seven tick marks on its frame. These tick marks were measured to within 0.025 cm and placed in a shapefile to represent a local coordinate system for the camera stand. Each collected image was then registered to that coordinate system within ArcGIS™ ArcMap® using the georeferencing extension. The referencing was accomplished by aligning the measured tick marks with the marks seen on the image. Doing so insured that all images would align exactly with each other and could be compared.

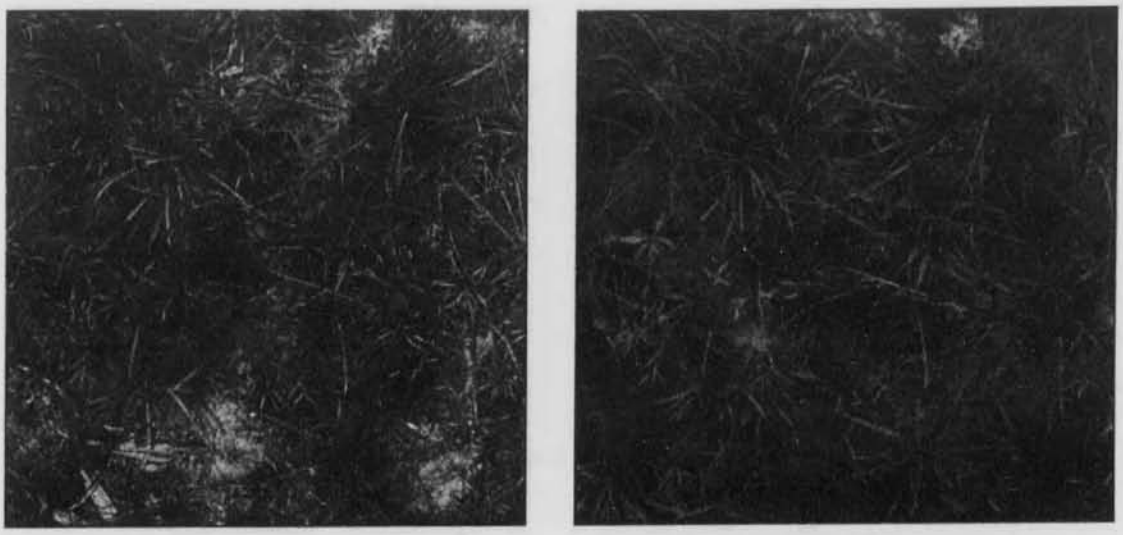

(A) (B)

Fig. 2. Color (A) and color infrared (B) images of an area of interest (grayscale versions shown here).

The camera stand also had black and white painted regions on it so that the illumination of images could be standardized, as the amount of solar energy incident on the plots changed. A GER2600 spectroradiometer was used to determine the reflectance of the painted regions for 4 bands (Near Infrared [NIR], Red [R], Green [G], and Blue [B]) and represented the extremes of the range of colors present in any image for any band. A simple linear regression was created per band per image to convert the range of values present within a given band/image combination to the range defined via the spectroradiometer. The regressions were used to calibrate each image. Upon completion of the

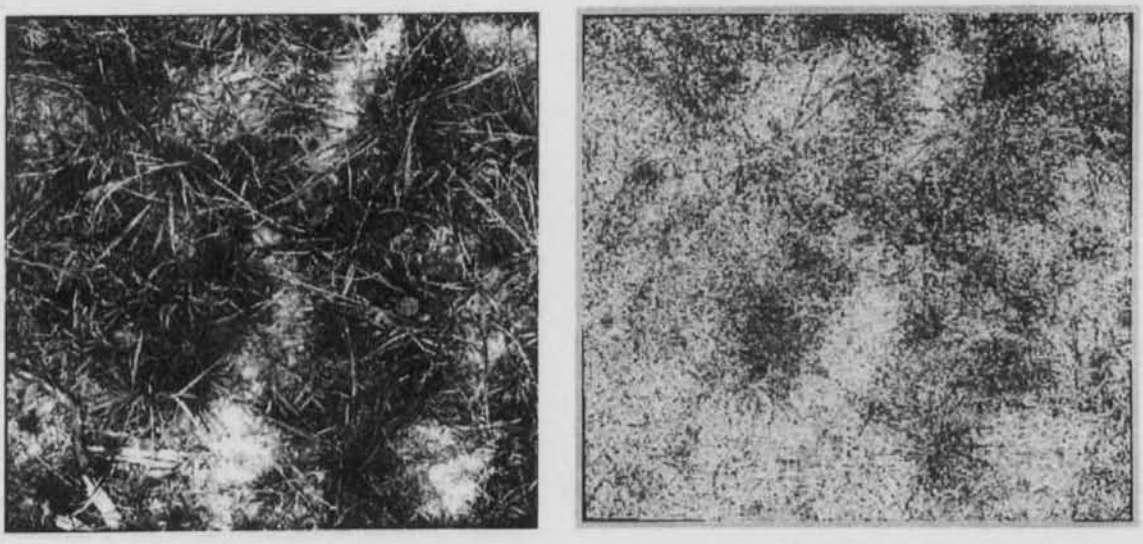

(A) (B)

Fig. 3. AVR (A) and NDVI (B) images created for the area of interest shown in Fig. 2 (a grayscale version of the NDVI image is shown here).

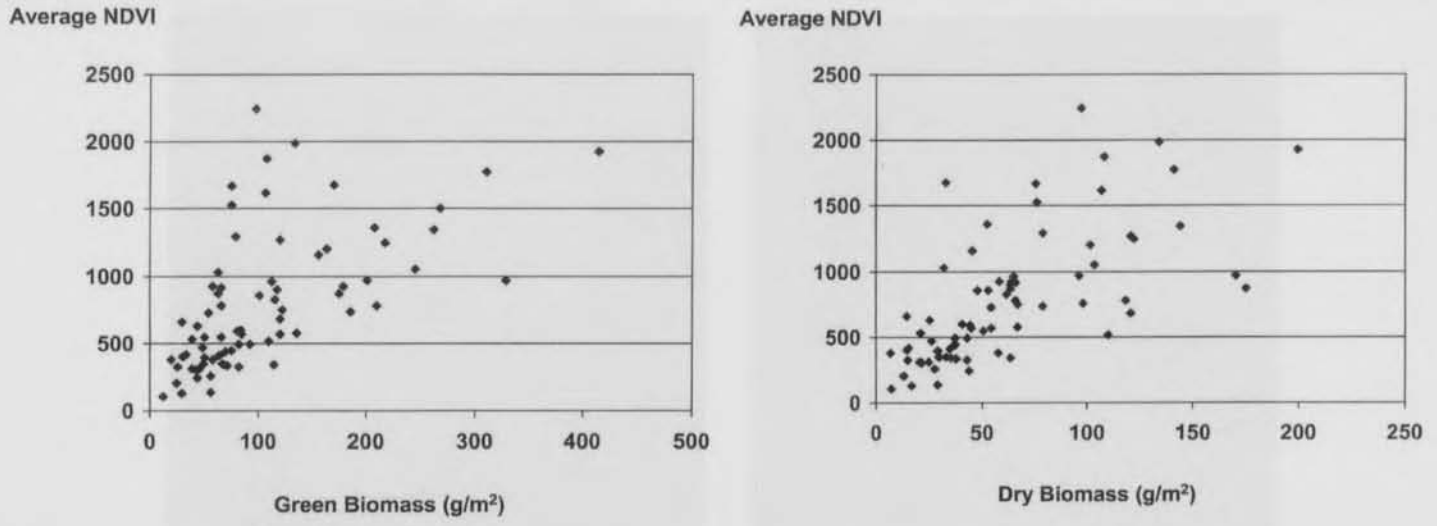

Fig. 4. Average NDVI values from each of the 75 forest ground flora plots versus (A) green biomass and (B) dry biomass in g/m^2.

calibration, the digital values were standardized and represented the same colors from one image to the next.

Images were then cropped to areas of interest (AOI's) created manually in Imagine®. The AOI's contained only that portion of each image that was inside the frame of the camera stand, and only that was used for all subsequent analyses (Fig. 2). When applying the regression models to the areas of interest for each respective band/image combination, any values in the output grid that were less than 0 were reset to equal 0 (negative values can disrupt calculation of certain vegetation indices). A vegetation mask was applied to better distinguish vegetation from non-vegetation in the images. The final output grid was a 6-band image consisting of standardized NIR, red and green bands from the color infrared image, and the red, green, and blue bands from the color image.

Vegetation Indices and Regression Modeling.--The CIR camera images were used to calculate the Normalized Difference Vegetation Index(NDVI), and the color camera images were used to calculate the Average Visible Reflectance(AVR) index for each pixel in each image.

$$NDVI = (NIR-R)/(NIR+R) \quad (1)$$
$$AVR = (G+R+B)/3 \quad (2)$$

The output image from this step was a two band grid (NDVI and AVR) with a cell size of 0.1015 cm by 0.1015 cm (Fig. 3). Once the NDVI and AVR values for the images were calculated, they were summed and averaged for use as potential independent variables in regression equations to predict green or dry biomass. Typical regression diagnostics (Myers, 1990) were used to construct models to predict green and dry biomass (g/m^2) of the forest ground flora from independent variables derived from the imagery.

Results

The green biomass data collected from the plots averaged 106.06 g/m^2, possessed a standard deviation of 77.95 g/m^2, and ranged from 12.90 to 413.60 g/m^2. The corresponding dry biomass observations averaged 53.68 g/m^2, possessed a standard deviation of 39.82 g/m^2, and ranged from 6.90 to 199.50 g/m^2. The green and dry biomass observations served as the dependent variables in the regression models constructed. The scatter plots of average NDVI versus green and dry biomass are depicted in Fig. 4, while Fig. 5 depicts the relationship between average AVR and green and dry biomass. Initial regression models used average NDVI and average AVR in an attempt to predict observed biomass.

Sole use of either of these averaged vegetative indices as independent variables did not result in very strong simple linear regressions, as the R^2 from such models were in the 25% to 35% range. Even after the non constant variance issues present in Figs. 4 and 5 were addressed by using a natural log transformation of the respective dependent variables (the biomass measures), the R^2, or the proportion of variation in biomass explained by the model (the respective averaged vegetative indices) were well under 50%. Clearly, alternate model forms or use of additional

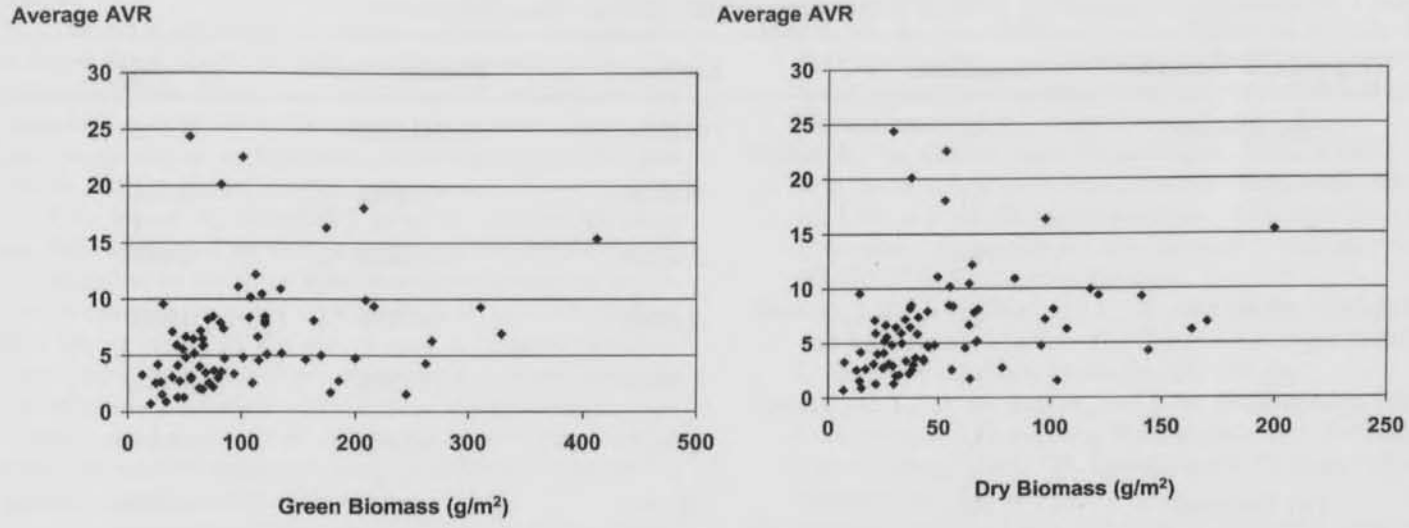

Fig. 5. Average AVR values from each of the 75 forest ground flora plots versus (A) green biomass and (B) dry biomass in g/m^2.

independent variables were needed to improve model performance.

Several nonlinear model forms (Sit and Poulin-Costello, 1994) were examined in order to improve the fit of the regression model. None of the nonlinear forms, which used just average NDVI or average AVR as independent variables, outperformed the simple linear regression models already developed.

In addition to the average NDVI value and average AVR value for each image, additional attributes were available for use as potential independent variables. The following attributes were available for each image taken using the color infrared camera: average of the NIR band, average of the G band, and average of the B band. Similarly, averages of the R, G, and B bands were available for each image taken with the color camera. These attributes were used in conjunction with the average NDVI and AVR attributes previously described to build a regression model via a stepwise regression procedure.

Upon successful completion of the stepwise regression procedure, the following linear regression model performed best with respect to estimating either green or dry biomass.

$$\hat{Biomass}_i = b_0 + b_1(A\_NDVI_i) + b_2(A\_AVR_i) + b_3(A\_NIR420_i) + b^4(A\_G420_i) + b_5(A\_R760_i) \quad (3)$$

where $\hat{Biomass}_i$ = predicted biomass, green or dry (g/m^2) for plot i,

A_NDVI_i = average NDVI value for plot i,

A_AVR_i = average AVR value for plot i,

A_NIR420_i = average NIR band value from the color infrared image for plot i,

A_G420_i = average G band value from the color infrared image for plot i,

A_R760_i = average R band value from the color image for plot i, and

$b_0, b_1, b_2, b_3, b_4, b_5$ = parameters to be estimated.

Fit statistics for equation (3), when fit to the green and dry biomass data, respectively, can be found in Table 1. The standard error of the estimate was 48.00 g/m^2, and R^2 equaled 66% for the regression fit to the green biomass data, whereas those statistics for the dry biomass regression fit were 25.50 g/m^2 and 58%, respectively. All parameter estimates are significantly different than 0 at the 0.05 α-level. Clearly, both of these model fits perform considerably better than the models using just NDVI or AVR as the sole independent variable.

Variance Inflation Factors (VIFs) were used to assess the potential presence of multicollinearity between the independent variables in the fitted models. Since none of the VIFs in either model exceeded 10, multicollinearity issues are not present in either model (Myers, 1990). The presence of outliers and influential data points were addressed by examining studentized residuals, difference in fits (DIFFITs) values, and difference in betas (DFBETAs) values (Myers, 1990), and no outliers or influential points were detected. Therefore, the parameterizations of equation

Table 1. Fit statistics for equation (3) when fit to the green and dry biomass data, respectively.

Dependent Variable	Parameter	Estimate	Standard Error	p-value
Green Biomass	b_0	97.8778	30.0038	0.0017
	b_1	0.1338	0.0182	<0.0001
	b_2	4.9456	1.5056	0.0016
	b_3	-2.5581	0.7175	0.0007
	b_4	2.4904	1.1584	0.0351
	b_5	-2.0427	0.3893	<0.0001
Dry Biomass	b_0	48.5839	16.2102	0.0038
	b_1	0.0627	0.0099	<0.0001
	b_2	2.4722	0.8135	0.0034
	b_3	-1.3929	0.3877	0.0006
	b_4	1.2709	0.6258	0.0461
	b_5	-0.7762	0.2104	0.0004

(3) shown in Table (1) are the final regression models examined for these data.

Discussion and Conclusions

The ability to quantify forest ground flora attributes, such as the amount of biomass present is becoming increasingly important (Reed and Mroz, 1997). Such attributes are commonly estimated using the time- and labor-intensive method of field identification, clipping, drying, and mass determination in the lab. That technique poses three problems as the intensity of this type of research/reporting increases: the nature of destructive sampling, the amount of time involved to collect such data, and the necessity of field identification.

In certain areas destructive sampling is acceptable; in others it is not, such as in ecologically-sensitive areas or areas where vegetation is sparse (thus impact of removal would be great). This project attempts to address this issue. By using proximally-sensed data of subsequently clipped forest ground flora and building regression models to predict biomass from image characteristics, this work is setting the stage for future research and improvements in this data collection arena. While R^2 of 58% - 66% may at first seem a bit low, the authors are quite pleased with these results given the truly experimental nature of this work. The ability to explain variation in forest ground flora biomass, even to the degrees achieved herein, via a regression equation that requires no destructive sampling to apply is a very positive development. It should be noted that plots with much overlapping foliage were problematic because the images acquired only captured the top level of foliage. Future improvements in the data collection procedure (such as employing plots smaller than 1 m^2 in size) could positively impact results by reducing the amount of overlap that may be present in a given plot. More total plots would need to be employed to offset a reduction in plot size in any such sampling scenario.

The ability to better estimate green biomass than dry biomass as evidenced by the R^2 values is at first a somewhat surprising result because many biomass studies do far better at estimating dry biomass than green biomass. In this study, the vast majority of the forest ground flora sampled was herbaceous. Reflectance in the NIR band is particularly sensitive to moisture content fluctuations in the complex internal structure of foliage (Swain and Davis, 1978). Therefore, use of the NIR band may have led to better green biomass estimation than dry biomass estimation

because biomass in the green condition was captured in the images.

The time necessary to sample a plot is dramatically reduced if just images are taken and no vegetation is actually clipped. While times were not directly studied in this endeavor, a time versus accuracy comparative study has been suggested as an interesting follow-up project (Dr. Jim Guldin, USDA Forest Service, pers. comm.).

One aspect of community structure and composition not fully addressed by this project is species identification. Identification of the three most dominant species on a plot or determining the cover type (graminoid versus broadleaf forb versus shrub) of the plot is used to generate species-abundance or cover-type abundance curves. Species identification combined with biomass observations can be used to calculate similarity indices (Reed and Mroz, 1997). However, this project is providing valuable information that might be used to address this issue over time.

Over the course of this project, nearly 120 forest ground flora species were identified and digitally captured. Spectral attributes of some of these species have been identified. As work continues in this arena and more observations are taken throughout the entire growing season, computer algorithms and perhaps other equipment will be used in an attempt to better identify species thus addressing the third issue with collecting these data: species identification. With the traditional method of data collection, a botanist, or someone well-versed in forest ground flora species identification, must participate in the field identification process. In the future, perhaps some, but most likely not all, of this identification could be done from the images as well.

As interest in and reporting of herbaceous plant community and structure measures in forested ecosystems continues to increase, the need to more rapidly and nondestructively quantify such measures is apparent. This project has attempted to set the stage for using proximal sensing as the technique to satisfy that need, and has suggested means to pursue to improve model performance in the future.

ACKNOWLEDGMENTS.—The authors would like to thank the National Science Foundation Biodiversity and Ecosystem Informatics program for primary financial support of this project (EIA/0131801). Any opinions, findings, and conclusions or recommendations expressed in this material are those of the author(s) and do not necessarily reflect the views of the National Science Foundation. The Arkansas Forest Resources Center is also hereby acknowledged for providing additional financial support. The assistance of Dr. Michael Shelton when identifying available study areas is also greatly appreciated. This manuscript is approved for publication by the Director of the Arkansas Agricultural Experiment Station.

Literature Cited

Ahern, F. J., T. Erdle, D. A. McLean, and **I. D. Kneppeck.** 1991. A quantitative relationship between forest growth rates and thematic mapper reflectance measurements. Int. J. Rem. Sens. 13:699-714.

Baret, F., G. Guyot, and **D. J. Major.** 1989. TSAVI: A vegetation index which minimizes soil brightness effects on LAI and APAR estimation. Pp. 1355 1358 *In:* 12th Canadian symposium on remote sensing and IGARSS'90, Vancouver, Canada.

Brower, J. E., J. H. Zar, and **C. N. von Ende.** 1990. Field and Laboratory Methods for General Ecology. William C. Brown Publishers, Dubuque, IA. 237 pp.

Elzinga, C. L., D. W. Salzer, and **J. W. Willoughby.** 1998. Measuring and Monitoring Plant Populations. Bureau of Land Management, US Government Printing Office, Washington, D.C. 477 pp.

Magurran, A. E. 1988. Ecological Diversity and its Measurement. Princeton University Press, Princeton, NJ. 179 pp.

National Wildlife Research Center. 2000. web; http://www.nwrc.gov/wdb/pub/hsi/hsiindex.html Accessed 2002 December 1.

Myers, R. H. 1990. Classical and Modern Regression with Applications, 2nd Edition. PWS-Kent Publishing, Boston, MA. 488 pp.

Reed D. D., and **G. D. Mroz.** 1997. Resource Assessment in Forested Landscapes. John Wiley & Sons, Inc., NY. 386 pp.

Schwegman, J. 1986. Two types of plots for monitoring individual herbaceous plants over time. Natural Areas J. 6:64-66.

Sit, V., and **M. Poulin-Costello.** 1994. Catalog of Curves for Curve Fitting. Biometrics Information Handbook No. 4. Province of British Columbia Ministry of Forests, Victoria B.C. 110 pp.

Swain, P. H., and **S. M. Davis** (eds). 1978. Remote Sensing: the Quantitative Approach. McGraw-Hill, Inc., NY. 396 pp.

Windas, J. L. 1986. Photo-quadrat and compass mapping tool. Natural Areas J. 6:66-67.

Subterranean Biodiversity of Arkansas, Part 1: Bioinventory and Bioassessment of Caves in the Sylamore Ranger District, Ozark National Forest, Arkansas

G. O. Graening*
The Nature Conservancy
Arkansas Field Office
601 North University Avenue
Little Rock, AR 72205

Michael E. Slay
Department of Biological Sciences
University of Arkansas
601 Science-Engineering
Fayetteville, AR 72701

Karen K. Tinkle
Sylamore Ranger District
U.S. Forest Service
P.O. Box 1279
Mountain View, AR 72560

*Corresponding Author

Abstract

Inventory and assessment of subterranean ecosystems of the Sylamore Ranger District (within Baxter, Marion, Searcy, and Stone counties), Ozark National Forest, was performed 2000 to 2002. The Sylamore District, completely underlaid in karst topography (occurring in Mississippian to Ordovician carbonates), contains approximately 10% of the known caves in Arkansas. Thirty-five sites were inventoried, six of which were sampled for environmental quality. These were combined and analyzed with previous studies, creating a database of 1,238 total species occurrences, 230 species, and 61 total sites. Most common were cave crickets, pipistrelle bats, woodrats, mosquitoes, and spiders. Fourteen species obligate to caves or groundwater were found, including four new to science, although a collector's curve showed that sampling effort to date has not reached maximum species richness. Richness was significantly greater in caves developed in Ordovician carbonates, in caves with organic inputs (especially bat guano), and as cave passage length increased. Richness was not significant between watersheds (Buffalo versus White Rivers), nor by water resource, nor by degree of recreational use. Caves were ranked by passage length, total and obligate richness, and overall biological significance. Blanchard Springs Caverns ranked highest and is the most biologically rich cave in Arkansas with 96 total and nine obligate species. Recommendations include continuation of physical and biological inventories, increased protection of high-ranking sites, and increased public education/outreach. The US Forest Service has invested 0.6 million dollars in cave research, monitoring, and protection on the Sylamore District to date.

Introduction

The subterranean fauna of Arkansas are inadequately documented and protected, yet are important for many reasons. These animals are extremely rare and highly endemic, and are a significant part of the natural heritage of the region and nation. In the United States, cave-limited fauna (troglobites) and ground-water-limited fauna (stygobites) represent more than half of the imperiled (heritage ranks of G1 and G2) species listed in the Natural Heritage Program, yet less than 4% are under federal protection (Culver et al., 2000; NatureServe, 2002). Furthermore, these animals, with their unique morphological adaptations to subterranean habitats, are important subjects of medical and evolutionary research. These animals can also serve as ground water quality indicators (Malard et al., 1996), and ground water is a major water resource for communities, agriculture, and industry in Arkansas. To address these data deficiencies, a regional inventory of subterranean habitats was initiated by a multi-agency consortium (the Ozark Subterranean Biodiversity Project), the results of which are being presented in this manuscript series. This study focused upon one of the most cave-dense areas of the Ozark plateaus ecoregion.

Public lands managed by the US Department of Agriculture, Forest Service (USFS) harbor the greatest number of populations of imperiled and endangered species of any federal agency - 40% of imperiled species and 50% of federally listed species (Stein et al., 2000). Of all of the national forests in the US, the Ozark National Forest (ONF) is one of the richest in caves. The Sylamore Ranger District of the ONF (Sylamore District) is located within Baxter, Marion, Searcy, and Stone counties (Fig. 1). It contains the majority of caves on the ONF, and an estimated 10% of all reported caves in Arkansas, a state that is itself very rich in caves, ranking 13th in cave richness by state in the US (Harris, 2003). Thus, the Sylamore District has a unique resource and management challenge with its diversity of subterranean habitats and fauna.

Methods

The objectives of this study were as follows: to bioinventory as many caves as possible in a two-year period, with special focus upon caves containing endangered species; in select sites, assess environmental quality,

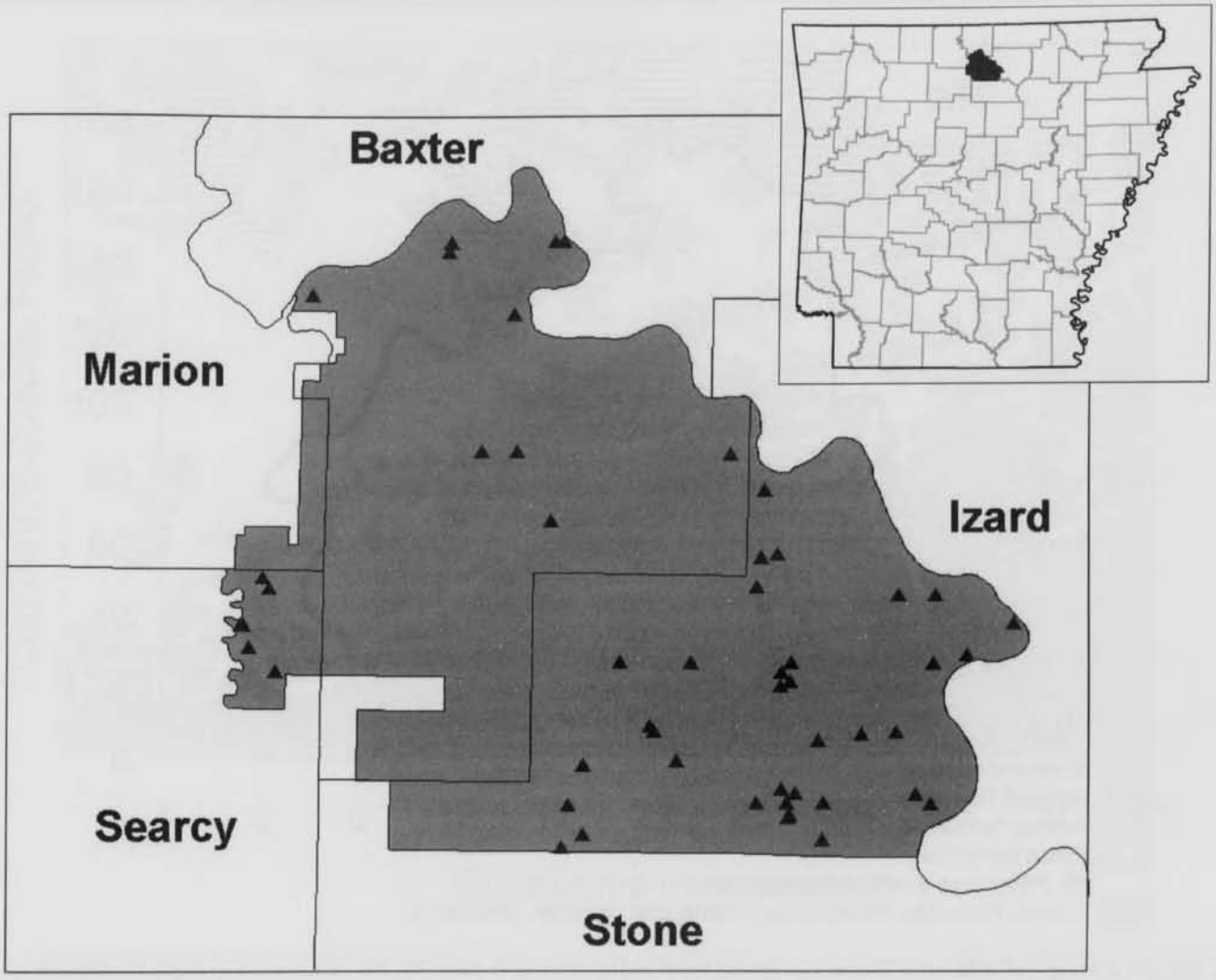

Fig. 1. Inset map shows the location of the Sylamore District within Arkansas. Larger map shows the Sylamore District shaded in gray in relation to Baxter, Marion, Searcy, and Stone counties. Black triangles demarcate the locations of 61 total sites inventoried in this study or previous studies.

focusing upon parameters that might indicate pollution from land-use practices; assemble this new data into a database and, combined with historic information, discern patterns in the distribution of cave fauna, their limiting factors, and the effect of any habitat stressors.

The Sylamore District lies within a dramatic geologic setting – the entire district (*circa* 130,000 acres) lies in karst topography (Fig. 2), a landscape formed by acidic ground water dissolving the carbonate bedrock. This creates a system of voids and conduits that transport enormous amounts of ground water and sediment. The Eureka Springs Escarpment divides the Sylamore District and demarcates the abrupt change from the Springfield Plateau down into the Salem Plateau. Three rivers (the White River, Sylamore Creek, and Big Creek) divide the Sylamore District into the Middle White River Basin and the Buffalo River Basin and have dissected deeply the plateaus that contain them.

Sites were assessed for the following parameters: level of human visitation - none, little, moderate, and heavy use; presence/absence of vandalism, defined as spray paint or other graffiti, damage to speleothems or fauna, refuse, or smoke damage; presence/absence of organic matter, including leaf and woody debris or guano and other feces; and water resource - dry, drip pool, intermittent stream, or perennial stream. Water samples were taken on 19 - 20 February 2000 at Bald Scrappy Cave, Biology Cave, Blanchard Springs Caverns, Clark Spring, Hell Creek Cave, Nesbitt Spring, and Rowland Cave. Water and sediment samples were taken on 7-8 April 2001 at Blanchard Springs Caverns, Clark Spring, Gunner Cave, Hell Creek Cave, Nesbitt Spring, and Rowland Cave and again on 29 March 2002 at Blanchard Springs Caverns, Clark Spring, and

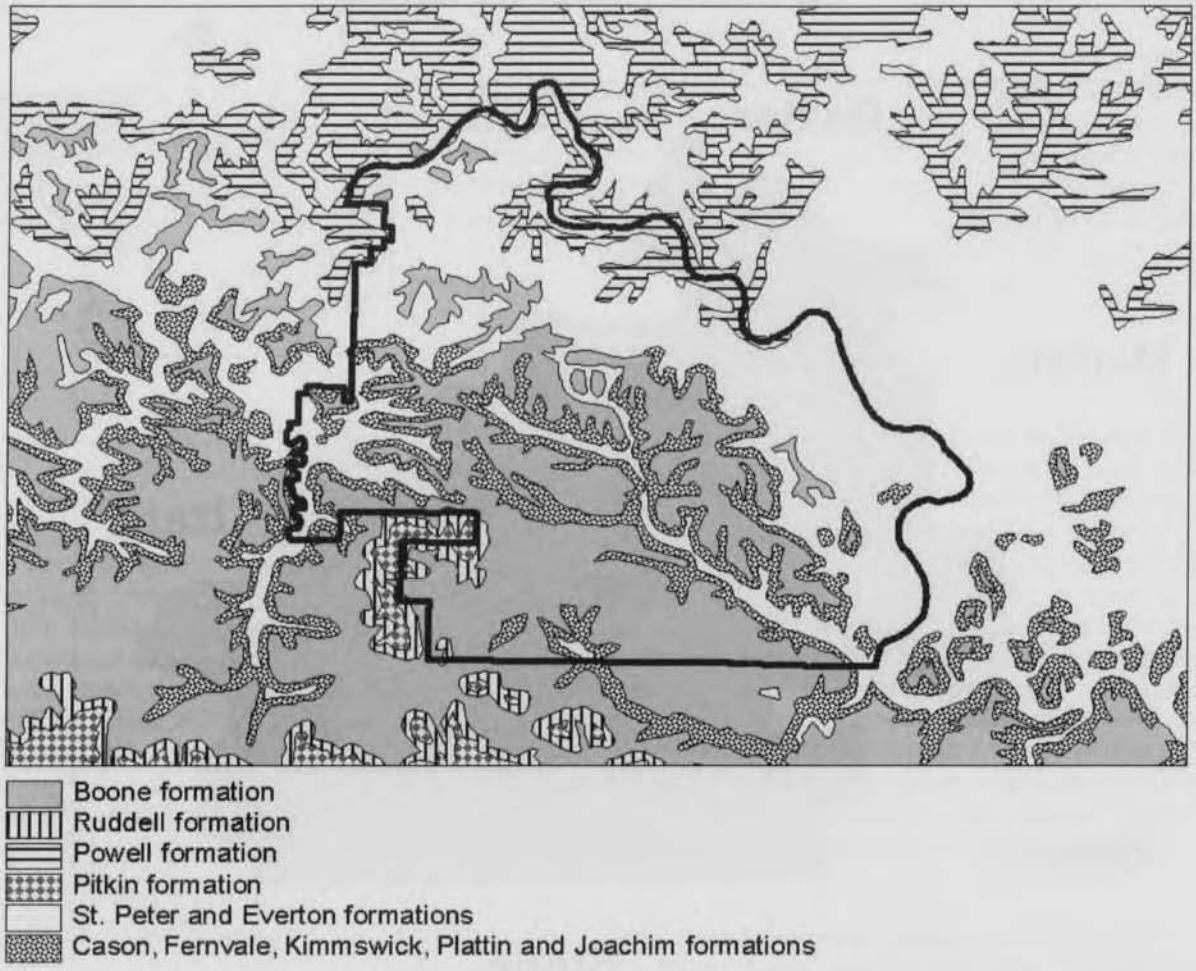

Fig. 2. Surface geology of Sylamore District, adapted from a digital map created by the Arkansas Geologic Commission.

Partee Spring. For flowing cave streams, water samples were collected manually where discharge was greatest for the stream cross-section, and for still water, the samples were collected in the largest accessible pool. The following parameters were analyzed: metals in sediments and water column; nitrate and ammonia-nitrogen, total and ortho-phosphate, chloride, fluoride, sulfate, and hardness (all in mg/L); total coliform and *Escherichia coli* densities (each as colony-forming unit / 100 mL), temperature (± 0.5 °C); pH (± 0.5 unit); turbidity (± 0.5 Nephlometric Turbidity Unit); and specific conductivity (± 1 µSiemens/cm). Sampling techniques and analytical procedures followed approved US Environmental Protection Agency methods. Analyses were performed at the Arkansas Department of Environmental Quality's Environmental Chemistry Laboratory, the Arkansas Water Resources Center's Water Quality Laboratory, and the Center of Excellence in Poultry Science's Central Analytical Laboratory. Appropriate quality assurance and quality control measures were taken.

Biological inventories of macrofauna were performed from September 2000 to December 2002. During this two-year study, over 40 field trips were taken and at least 35 caves and springs were inventoried (Fig. 1). They are: Albino Orchid Cave, Alexander Cave, Almus Knob Cave, Almus Knob Annex Cave, Bald Scrappy Cave, Barfing Vulture Cave, Big Creek Cave, Biology Cave, Bird's Nest Cave, Black Gum Cave, Blanchard Springs Caverns, Blowing Spring Cave, Bonanza Cave, Breakdown Cave, Bud Wallis Cave, Clark Spring – Alexander Cave, Dead Bear Cave, Double Barrel Cave, Gunner Cave, Gustafson Cave, Hammer Springs Cave, Hanger Cave, Herald Hollow Cave, Hidden Spring Cave, Lower Shelter Cave, Norfork Bat Cave, Optimus Cave, Partee Spring, Rowland Cave, Saltpeter Cave, Shelter Cave, Thruway Cave, Upper Shelter Cave, and Wood's Hollow Caves No. 1 and No. 2. Sites were georeferenced in Universal Transverse Mercator

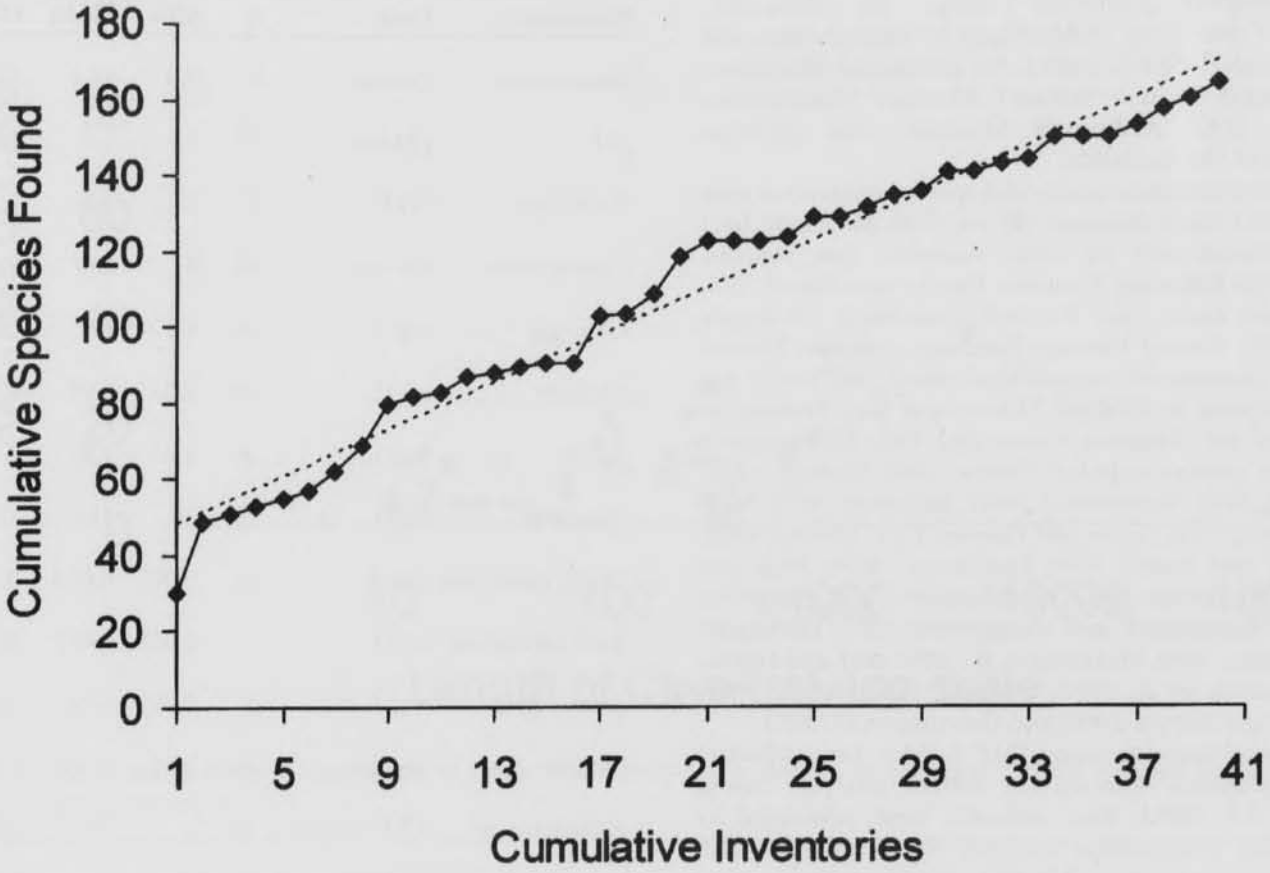

Fig. 3. Collector's curve for this inventory effort (40 bioinventories performed from September 2000 to December 2002), where cumulative number of inventories were plotted against cumulative number of unique species found, with a line fitted to the curve.

coordinates using North America Datum 1983 with a global positioning system handheld unit (Garmin III Plus GPS), and the estimated position error was recorded (range of 1 - 20 m). In each cave surveyed, fauna were inventoried using the most unobtrusive methods possible and at times when endangered bats were not hibernating or birthing. Macrofauna were counted visually with helmet-mounted lights, using snorkeling gear and dive lights for deep pools. For submerged passages, SCUBA was necessary, and those portions of the surveys were sub-contracted to certified cave divers as funds permitted. Collections were limited to those fauna that were impossible to identify on site and were made possible by the following permits: Federal Fish and Wildlife Permits PRT-834518, TE834518-3, TE834518-2 and TE834518-1, Arkansas Natural Heritage Commission Permit S-NHCC-98-009 and S-NHCC-97-009, and Arkansas Game and Fish Commission Educational Collecting Permits 1082 and 1476. Voucher specimens were collected by hand, aspirator, or net, preserved in 75% ethanol, and brought back to the University of Arkansas at Fayetteville (UAF) for identification and cataloging. Specimens were identified at UAF by Graening and Slay, by Jeffrey Barnes (UAF Dept. of Entomology), or sent to taxonomic specialists, including the following: Kenneth Christiansen (Grinnell College) and Jeffrey Battigelli (Earthworks Research Group) for collembolans; Horton Hobbs III (Wittenburg Univ.) for decapods; John Holsinger (Old Dominion Univ.) for amphipods; Jerry Lewis (Lewis Consulting, Inc.) for isopods; William Shear (Hampdra-Sydney College) for diplopods; Jeffrey Battigelli for acari; William Muchmore (University of Rochester) for pseudoscorpions; Henry Robison (Southern Arkansas Univ.) for fishes; Stewart Peck (Carleton Univ.) for coleopterans; James Cokendolpher (Museum of Texas Tech

Univ.) and Darrell Ubick (California Academy of Sciences) for opilionids; Lynn Ferguson (Longwood College) and Mark Muegge (Texas Cooperative Extension) for diplurans; Anne Hampton (Castleton College) for planarians; Theodore Cohn (Univ. of Michigan) for orthopterans; and Gerald Walsh (USEPA, retired) for gastropods. Specimens were curated in the National Museum (Smithsonian Institute), UAF Arthropod Museum, and personal collections of the specialists.

The environmental quality and species' occurrence data were entered into a database (Access 2000, Microsoft, Inc.) and combined with all other available data sources, including the following: Sylamore District cave files (USFS, unpublished data); Cave Research Foundation (Welbourn 1980, 1983); Natural Heritage Database (Arkansas Natural Heritage Commission, unpublished data); and yearly bat surveys (reports by Michael Harvey and Ron Redman to USFS and the Arkansas Game and Fish Commission). Other data sources included: Wilson, 1967; Dickson, 1971; Flemming, 1972; Schuier et al., 1972; McIntosh, 1973; Peck, 1973; Grove, 1974; Grove and Harvey, 1974; Harvey, 1975; McDaniel and Smith, 1976; Muchmore, 1976; Peck and Russell, 1976; Stotler and Crandall-Stotler, 1977; Saugey et al., 1978; Youngsteadt and Youngsteadt, 1978; Darlington and Chandler, 1979; McDaniel et al., 1979; Beck and Dorris, 1982; Dunivan et al., 1982; Waddell, 1982; Smith, 1984; Graening and Brown, 2000; and Graening et al., 2001.

Statistical analyses (using JMP 5, SAS, Inc., software) and geographical information system analyses (using ArcView 3.2, ESRI, Inc., software) were performed to discern any relationships between the distribution and richness of cave fauna and factors such as geologic setting and watershed, water quality, level of disturbance, *etc.* Statistics used included linear and logistic regression, pair-wise correlation, *t*-test, and the chi-square test (where water and sediment quality parameters that were below detection were set to the detection limit). For some of the analyses in this study, data for Rowland Cave and Blanchard Springs Caverns were analyzed separately, and in other instances data were combined. Dye tracing has shown that these two cave systems are hydrologically connected by sharing the same subterranean stream (Aley, 1980), and mapping surveys have converged the systems within 300 feet of a traversable connection. Similarly, data for Clark Spring and Alexander Cave were combined for some analyses because divers have connected the spring resurgence owned by USFS (Clark Spring) to the upstream cave system owned privately (Alexander Cave).

Results

Summary of water and sediment quality analyses are presented in Tables 1 and 2, and the complete data set is available in Graening et al. (2003). Surficial geology was determined for 208 solution caves, one crevice cave, three springs, one sinkhole, two pits, and one bluff shelter by site reconnaissance and by using GIS analyses upon the Arkansas Geologic Commission's digital version of the 1976 Geologic Map of Arkansas, scale 1:500,000 (Fig. 2). Sixty caves were formed in Mississippian Period limestone (Boone formation), 51 were formed in Ordovician limestones and dolomites (Fernvale, Plattin, and Joachim formations), and 96 were formed in Ordovician limestone (Everton formation) with a few caves each in other carbonates (Cotter, Jefferson City, Powell formations). Of the 52 mapped caves, mean total passage length was 637 m, the longest cave in the data set was the Rowland – Blanchard Springs Caverns complex at over 17,000 m of combined, mapped passages, and the shortest was Partee Spring at 5 m.

Table 1. Summary statistics of water quality parameters of select cave streams and springs on the Sylamore District.

Parameter	Unit	n	Min.	Mean	Max.
Temperature	Celsius	8	9.0	13.4	15.0
pH	pH unit	13	5.5	6.5	7.0
Turbidity	NTU	7	1.5	2.7	7.0
Conductivity	µS/cm	16	8	190	305
Chloride	mg/L	16	1.5	3.9	6.1
Fluoride	mg/L	10	0.05	0.06	0.08
Sulfate	mg/L	16	2.45	4.97	8.44
Hardness	mg/L	15	26	115	175
Ortho-phosphate	mg/L	16	0.007	0.024	0.084
Total phosphate	mg/L	7	0.056	0.077	0.111
Ammonia	mg/L	3	0.01	0.01	0.02
Nitrate	mg/L	16	0.07	0.91	3.78
Escherichia coli	CFU/100mL	16	4	79	199
Total coliforms	CFU/100mL	16	20	524	2540

Species occurrence data obtained from our study and others produced a total of 1,238 species occurrences, 230 unique species reported, 61 sites with some amount of species occurrence data, and 40 sites with intensive

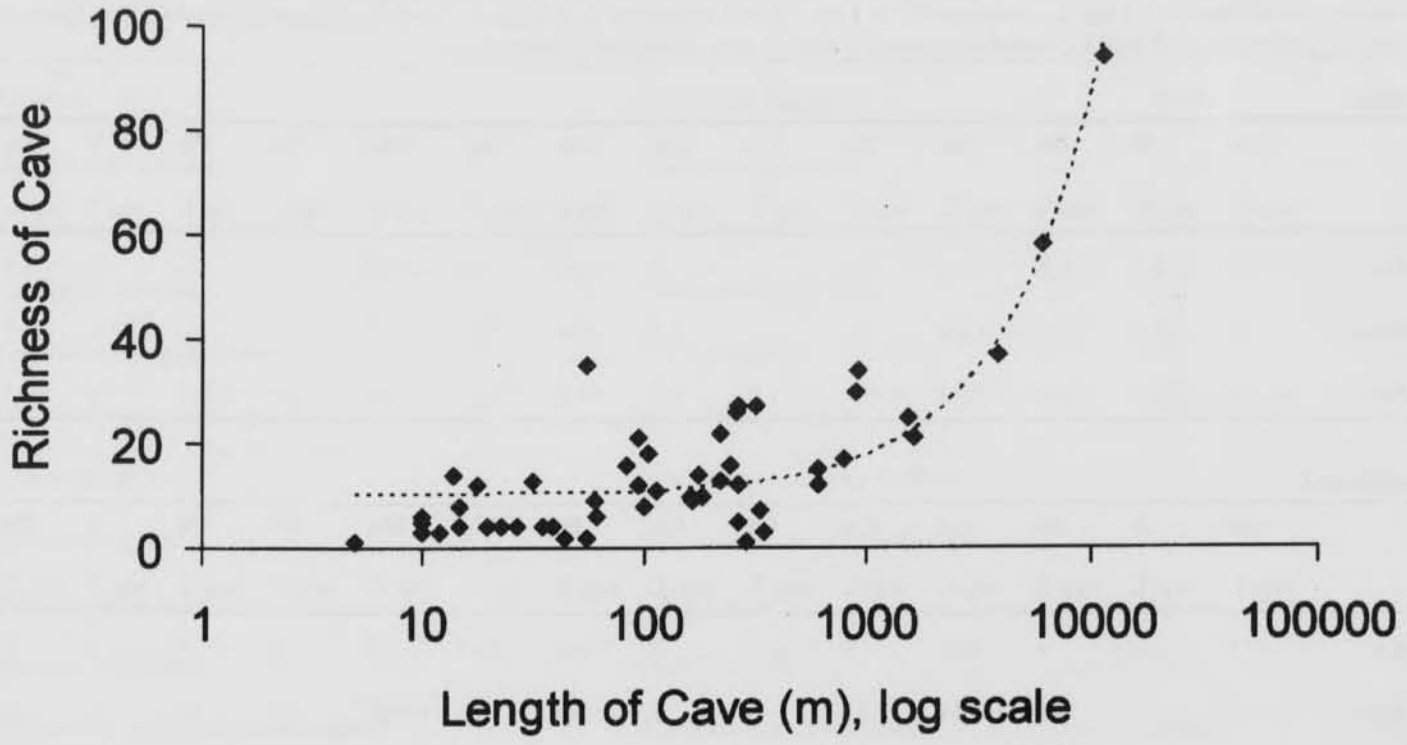

Fig. 4. Total mapped passage lengths (m) of caves in this study were directly proportional to their richness (total number of unique species per cave).

bioinventories - see Graening et al. (2003) for a detailed faunal list. A collector's curve was created, whereby each novel species found during consecutive collecting trips was added to the cumulative number of species found and plotted against cumulative number of collecting trips (Fig. 3) and assuming consistent search effort. The number of cumulative species found increased linearly with every additional inventory (species = 45.235 + 3.111 x number of inventories, $r^2 = 0.973$, $P < 0.001$), suggesting that this study did not exhaustively inventory all animals inhabiting Sylamore District caves.

Of 52 cave habitats with at least partial inventory data, the mean species per habitat (alpha diversity) was 15, with a maximum of 81 (Blanchard Springs Caverns), a median of 12, and a mode of 4. The Rowland Cave - Blanchard Springs Cavern complex was the richest with 96 species, and second was Bud Wallis Cave with 34 species. The relationship between species richness and number of caves having that richness was significant, indicating that an exponentially fewer number of caves have an increasingly greater number of species [log (number of caves) = 0.703 – (0.013 x richness), n = 29, $P = 0.006$, $r^2 = 0.252$]. Regional species richness (gamma diversity) was difficult to estimate, but at least 14 stygobites and troglobites and at least 215 other, non-cave adapted species occurred on the Sylamore District (Table 3). The Rowland-Blanchard Springs Caverns complex had the most obligates per cave with a count of nine. Second were the Clark Spring - Alexander Cave complex and Gunner Cave, both with six, followed by Hammer Spring Cave, Biology Cave, Breakdown Cave, Norfork Bat Cave, and Woods Hollow Cave No. 1, all with four.

The pooled faunal occurrences (n = 1,238) were examined for most abundantly occurring species, irrespective of habitat. Overall, arthropods dominated the cave habitats, especially crickets, mosquitoes, spiders, and springtails. The most common invertebrates were cave crickets of the genus *Ceuthophilus* with 59 site occurrences. The most common vertebrates were eastern pipistrelle bats (*Pipistrellus subflavus*) with 41 occurrences and eastern woodrats (*Neotoma floridana*) with 31 occurrences. In aquatic habitats, plethodontid salamanders and crustaceans dominated. Significant species found and their number of occurrences include the following: cave salamander (*Eurycea lucifuga*) - 23 occurrences; grotto salamander (*Typhlotriton*

Table 2. Summary statistics of metals concentrations in water samples (n = 15) and sediment samples (n = 9) in select cave streams and springs on the Sylamore District. Other metal concentrations measured were below detectable limits in water samples - beryllium (< 0.3 µg/L), cadmium (< 0.4 µg/L), and selenium (< 3.0 µg/L) - and in sediment samples - beryllium (< 1 mg/L), cadmium (< 1 mg/L), molybdenum (< 2 mg/L), and selenium (< 0.6 mg/L).

Water

	As	B	Ba	Ca	Co	Cr	Cu	Fe	Mg	Mn	Ni	Pb	V	Zn
	µg/L	µg/L	µg/L	mg/L	µg/L	µg/L	µg/L	µg/L	mg/L	µg/L	µg/L	µg/L	µg/L	µg/L
Min.	---	< 4.5	< 8.8	6.4	---	---	< 0.5	< 15.0	0.8	< 0.5	---	---	---	3.3
Mean	---	69.0	15.2	42.4	---	---	1.5	17.0	2.2	1.0	---	---	---	11.1
Max.	< 1.0	203.8	22.6	53.2	< 0.5	< 1.0	3.9	44.2	13.4	3.4	< 2.5	< 0.6	< 1.0	39.3

Sediment

	As	B	Ba	Ca	Co	Cr	Cu	Fe	Mg	Mn	Ni	Pb	V	Zn
	mg/L	mg/L	mg/L	mg/L	mg/L	mg/L	mg/L	mg/L	mg/L	mg/L	mg/L	mg/L	mg/L	mg/L
Min.	< 1	---	4	647	1	< 1	3	1152	260	59	2	2	6	4
Mean	4	---	60	15284	11	5	7	18915	512	10087	27	14	62	33
Max.	11	< 1.0	99	37373	27	15	17	91261	1541	84501	81	27	96	62

spelaeus) - 16 occurrences; cave isopods (*Caecidotea* spp.) - 10 occurrences; and cave amphipods (*Stygobromus* spp.) - 10 occurrences.

Logistic regression of surface geology category by species richness revealed that sites underlaid by Ordovician Period formations (Fernvale, Kimmswick, Plattin, and Joachim carbonates) were significantly richer in species than sites underlaid by other formations (Boone, Cotter, Jefferson City, or Everton) (n = 52, $P = 0.030$, $r^2 = 0.169$). Analysis revealed that species richness was significantly greater when organics were present (n = 52, $P = 0.001$, $r^2 = 0.222$, $t = -3.795$) and when bat guano was present (n = 52, $P = 0.001$, $r^2 = 0.220$, $t = -3.753$). Species richness did not significantly differ between Buffalo River and Middle White River watersheds ($P = 0.547$), nor by water resource category ($p = 0.383$), nor by degree of recreational use ($P = 0.100$). Species richness of a site was directly proportional to its passage length (m) (richness = 10.067 + 0.007 x length, n = 52, $r^2 = 0.76$, $t = 12.71$, $P < 0.001$); approximately one more species is added for every additional 100 m of cave passage (Fig. 4).

Discussion

A diverse array of arachnids, crustaceans and insects dominate the species composition of cave faunas in Arkansas (Graening et al., 2001) and in the U.S. in general (Culver et al., 2000). In a survey of cave streams of the Springfield plateau, Willis and Brown (1985) found that isopods (*Caecidotea* spp.) were the most common benthic invertebrates, and chironomids were second. Graening et al. (2001) also found isopods to be the most abundant benthic invertebrates in a survey of Arkansas cave streams, while cave crickets were the most common terrestrial invertebrates and bats and salamanders were the most abundant vertebrates. Similar findings are reported here. The Sylamore District is one of the most biologically important karst areas of the Ozark Plateaus ecoregion. Several species with federal status under the Endangered Species Act rely upon subterranean habitats of the Sylamore District: two endangered bat species, the gray bat (*Myotis grisescens*) and the Indiana bat (*M. sodalis*), utilize many caves for hibernation and reproduction; the endangered Ozark big-eared bat (*Corynorhinus townsendii ingens*) has occasionally been reported in crevice and solution caves; and the endangered Hell Creek cave crayfish (*Cambarus zophonastes*) is rumored to exist in Blanchard Springs Caverns, and its designated habitat (Hell Creek Cave recharge zone) is contiguous with the district boundary. At least 14 subterranean-obligate species exist on the Sylamore District, including two new species of troglobitic diplurans

Table 3. At least 16 species are known to be limited to, or adapted to, groundwater habitats (stygobites) or caves (troglobites) on the Sylamore District. Also shown are the global heritage status ranks assigned by The Nature Conservancy and NatureServe: G1- critically imperiled; G2 – imperiled; G3 – vulnerable; G4 – apparently secure; G5 – demonstrably secure; GU - unranked (NatureServe, 2002).

Species	Common Name	Rank
Apochthonius titanicus	Cave false scorpion	G1G2
Caecidotea antricola	Cave isopod	G3G4
Causeyella causeyae	Cave milliped	GU
Causeyella youngsteadtorum	Cave milliped	GU
Hesperochernes occidentalis	Cave false scorpion	G4G5
Litocampa sp. nov. 1	New species of cave dipluran	GU
Litocampa sp. nov. 2	New species of cave dipluran	GU
Phanetta subterranea	Cave spider	G4
Spelobia tenebrarum	Cave dung fly	GU
Stygobromus alabamensis alabamensis	Alabama cave amphipod	G4G5
Stygobromus sp. nov.	Undescribed amphipod	GU
Tricladida	Unidentified cave flatworm	GU
Typhlichthys subterraneus	Southern cavefish	G4
Typhlotriton spelaeus	Grotto salamander	G4

(*Litocampa* spp.) that await taxonomic description. However, the bioinventory effort is far from complete, and much taxonomic study remains to be done. Continuation of biologic and geologic inventories is highly recommended in order to accurately assess and manage these karst resources.

Caves have often been likened to islands due to their insular features, especially their hydrologic and geologic barriers (e.g., Culver, 1970). As a general pattern, larger islands carry more species than smaller ones, and this species-area relationship is well documented in diversity studies (e.g., MacArthur and Wilson, 1967). Similarly, the largest caves (measured as passage length) are often the most diverse - the world's longest cave, Mammoth Cave, at over 571 km of passage, has the greatest known number of stygobites and troglobites (Culver and Sket, 2000). Longer caves imply more habitat types and trophic resources, which may increase the few niches available and increase carrying capacity (Culver and Sket, 2000). Cave length was significantly correlated to richness in this study and in Arkansas caves in general (Graening et al., 2001). For this reason, length was used as the primary criterion for biological significance ranking. However, this constitutes a significant management challenge because the longest caves are usually the most attractive for recreational caving. The richness of obligate species is often used to rank the importance of the world's caves (*e.g.* Culver and Sket, 2000), and this criterion was also used in this study. The third criterion was total species richness, which is a common measure of biological significance, and in this study, significantly fewer caves had high species counts. The 61 caves that had been bioinventoried adequately were ranked according to these three criteria if they had a minimum of at least two obligate species, at least 20 total species, and at least 600 m of cave passage (Table 4). The Rowland Cave-

Blanchard Springs Caverns complex ranked highest with 96 species (Table 5), nine of which were stygobites or troglobites.

The best-studied caves tend to be the most biologically rich caves (see summary by Graening et al., 2001). Blanchard Springs Caverns is undoubtedly Arkansas' most thoroughly studied cave, although we agree with McIntosh (1973) who states, "*The inventory of biologic features of Blanchard Springs Caverns will never be complete.*" Ignoring this and other biases, this cave complex is the most species rich cave documented in Arkansas to date and second only to Tumbling Creek Cave, Taney County, Missouri, for the entire Ozark plateaus ecoregion; Tumbling Creek Cave has approximately 105 species, 12 of which are stygobites or troglobites (William Elliot, pers. comm.). Blanchard Springs Caverns also has at least two single-site endemics - a liverwort, *Plagiochila acanthophylla ciliigera*, (Stotler and Crandall-Stotler, 1977) and a cellular slime mold, *Dictyostelium caveatum*, (Waddell, 1982). Surprisingly, it is also a very impacted cave. Blanchard Springs Caverns is the most visited cave in Arkansas with an estimated 88,000 visitors per year (Bob Reeves, Caverns Administrator, pers. comm.). It has been modified in many ways including the paving of passages, extensive illumination of surfaces, and the creation of two artificial entrances and other tunnels and shafts by use of explosives.

The impact of trespass, archaeological looting, and vandalism in caves of the Sylamore District is of special concern. Approximately 30 recreational caving permits per year and 50 scientific study permits per year are issued, and Tinkle estimates over 100 recreational caving trips per year are undertaken illegally (without permits). The Arkansas Cave Resources Protection Act of 1989 affords limited protection to caves, and subterranean fauna are protected by Arkansas Game and Fish Commission Regulation No.1817 - Wildlife Pet Restrictions and the federal Endangered Species Act of 1973. Protection for Arkansas caves also necessitates the enforcement of state and federal water quality and solid waste disposal regulations, although water and sediment analyses of the study caves did not reveal any major pollution concerns on the Sylamore District. The Federal Cave Resources Protection Act protects caves designated as "significant" on federal lands by allowing federal land managers to keep cave locations and names confidential and assign a penalty of up to $10,000 for abuses. All surveyed caves on the Sylamore District have been designated "significant." All caving and related activities on Forest Service lands are by permit only and permits can be acquired by contacting the District Office.

Other management recommendations include increasing protection of vulnerable, high-ranking sites, such as Alexander Cave which is not under public ownership, and the improvement of public outreach regarding wise use of karst resources. The USFS has invested approximately 0.6 million dollars in protection of karst resources on the Sylamore District, including the following: endangered bat species monitoring and research at approximately $10,000 per year for at least 12 years; four cave gates at approximately $50,000 each; monitoring, research, and educational products at approximately $15,000 per year for the last 10 years; and $102,000 spent on the protection, development, and maintenance of Blanchard Springs Caverns since its dedication, and another $35,000 was spent for research and continuing water and air quality monitoring.

ACKNOWLEDGMENTS.—Funding for this study was provided by a USFS challenge-cost share grant, whereby funds were matched in-kind by donation of time by the authors and cavers, and administration costs were matched by UAF. The cost of taxonomic subcontracts was augmented by a U.S. Fish and Wildlife Service grant. Water and sediment analyses were donated by Richard Thompson and Tim Kresse (both of the Arkansas Department of Environmental Quality) as project cooperators. Computer mapping and GIS analyses were performed by Shelley McGinnis (The Nature Conservancy). The generous donation of data and fieldwork by Ron Redman (Arkansas Soil and Water Conservation Commission), Michael Harvey (Tennessee Technical Univ.), David Taylor (Association for Arkansas Cave Studies), and Bill Puckette (Tulsa Regional Oklahoma Grotto) greatly enhanced this project. Cave diving was performed by the Mid-Ozark Sump Team: Jeff Disler, Brian Moore, Bob Koch, R. D. Millhollin, and Gene Herd. Bob Reeves (Caverns Administrator, Sylamore District) coordinated the bioinventory of Blanchard Springs Caverns. Many cavers graciously donated their time to this project, especially Charles Brickey (with 22 field trips), Dante Fenolio (10), Shelley McGinnis (8), David Kampwerth (6), Brian Wagner (3), and Matt Covington (2).

Literature Cited

Aley, T. 1980. Delineation of the recharge area for Blanchard Springs: the identification, location, and evaluation of water quality hazard areas. Report to the U. S. Forest Service, Mountain View, Arkansas.

Beck, M., and **P. Dorris.** 1982. A continuation of spider research in Arkansas: east central Ozark Mountain Area. Proc. Ark. Acad. Sci. 36:20-22.

Culver, D. C. 1970. Analysis of simple cave communities I: Caves as islands. Evolution 24:463-474.

Culver, D. C., and **B. Sket.** 2000. Hotspots of subterranean biodiversity in caves and wells. Jour. Cave. Karst Stud. 62:11-17.

Culver, D. C., L. Master, M. Christman, and **H. Hobbs III.** 2000. The obligate cave fauna of the 48 contiguous United States. Conserv. Biol. 14: 386-401.

Darlington, J., and **C. Chandler.** 1979. A survey of the

planarians (Tricladida: Paludicola) of Arkansas. Southw. Nat. 24(1):141-148.

Dickson, J. W. 1971. The reptiles of the Sylamore Ranger District, Ozark National Forest, Arkansas. Unpubl. Masters Thesis, Memphis State University, Memphis, Tennessee.

Dunivan, J. D., C. R. Tumlison, and **V. R. McDaniel.** 1982. Cave fauna of Arkansas: further records. Proc. Ark. Acad. Sci. 36:87-88.

Flemming, L. 1972. The evolution of the eastern North American isopods of the genus *Asellus* (Crustacea: Asellidae) Part I. Int. Journ. Speleol. 4:22-256.

Graening, G. O., and **A. V. Brown.** 2000. Status survey of aquatic cave fauna in Arkansas. A report submitted to the Arkansas Game and Fish Commission. Publication No. MSC-286. Arkansas Water Resources Center, University of Arkansas, Fayetteville. 44 pp.

Graening, G. O., M. E. Slay, and **A. V. Brown.** 2001. Subterranean biodiversity in the Ozark Plateaus of Arkansas. A report submitted to Arkansas Game and Fish Commission and Arkansas Department of Natural Heritage.University of Arkansas, Fayetteville. 28 pp.

Graening, G. O., M. E. Slay, and **K. K. Tinkle.** 2003. Bioinventory and bioassesment of caves in the Sylamore Ranger District, Ozark National Forest, Arkansas. Final report to the U. S. Forest Service, Mountain View, Arkansas. 35 pp.

Grove, J. 1974. Ecology of Blanchard Springs Caverns, Ozark National Forest, Arkansas. Masters thesis, Memphis State University, Memphis, Tennessee. 27 pp.

Grove, J., and **M. J. Harvey.** 1974. Ecology of Blanchard Springs Caverns, Ozark National Forest, Arkansas. Report to the U. S. Forest Service, Mountain View, Arkansas.

Harris, K. 2003. The top twenty cave states in the United States by length. Nat. Speleol. Soc. News 61: 25-26.

Harvey, M. J. 1975. Distribution and ecology of vertebrates inhabiting caves of the Sylamore Ranger District, Ozark National Forest. Report to the U. S. Department of Agriculture, Forest Service, Ozark National Forest, Mountain View, Arkansas. 35 pp.

MacArthur, R., and **E. Wilson.** 1967. The theory of island biogeography. Princeton University Press, Princeton, New Jersey.

Malard, F., S. Plenet, and **J. Gibert.** 1996. The use of invertebrates in groundwater monitoring: a rising research field. Groundw. Mon. Remed. 16:103-113.

McDaniel, V. R., and **K. L. Smith.** 1976. Cave fauna of Arkansas: selected invertebrate taxa. Proc. Ark. Acad. Sci. 30:57-60.

McDaniel, V. R., K. Paige, and **C. R. Tumlison.** 1979. Cave fauna of Arkansas: additional invertebrate and vertebrate records. Proc. Ark. Acad. Sci. 33:84-85.

McIntosh, P. 1973. Inventory of biological features of Blanchard Springs Caverns. Unpubl. report. US Forest Service, Mountain View, Arkansas.

Muchmore, W. B. 1976. New species of *Apochthonius*, mainly from caves in central and eastern United States (Pseudoscorpionida, Chthoniidae). Proc. Biol. Soc. Wash. 89:67-80.

NatureServe. 2002. NatureServe Explorer: An online encyclopedia of life. Version 1.6. NatureServe, Arlington, Virginia. URL: http://www.natureserve.org/explorer.

Peck, S. B. 1973. A systematic revision and the evolutionary biology of the *Ptomaphagus* (Adelops) beetles of North America (Coleoptera; Leiodidae; Catopinae), with emphasis on cave-inhabiting species. Bull. Mus. Comp. Zoology 145:29-162.

Peck, S. B., and **D. Russell.** 1976. Life history of the fungus gnat *Macrocera nobilis* in American caves (Diptera: Mycetophilidae). Can. Ent. 108:1235-1241.

Saugey, D., R. Baber, and **V. McDaniel.** 1978. An unusual accumulation of bat remains from an Ozark cave. Proc. Ark. Acad. Sci. 32:92-93.

Schuier, J. P., J. W. Dickson, and **M. J. Harvey.** 1972. Herpetofauna of Sylamore Ranger District, Ozark National Forest, Arkansas: preliminary report. Proc. Ark. Acad. Sci. 26:61-66.

Smith, K. L. 1984. The status of *Cambarus zophonastes* Hobbs and Bedinger, an endemic cave crayfish from Arkansas. Arkansas Natural Heritage Commission. Little Rock, Arkansas. 15 pp.

Stein, B. A., L. S. Kutner, and **J. S. Adams**, editors. 2000. Precious heritage: the status of biodiversity in the United States. The Nature Conservancy and Association for Biodiversity Information. Oxford University Press, New York, New York. 399 pp.

Stotler, R., and **B. Crandall-Stotler.** 1977. A checklist of liverworts and hornworts of North America. Bryologist 76:405-428.

Waddell, D. R. 1982. A predatory slime mold. Nature 298:464-466.

Welbourn, W. C. 1980. Summary report for the cave resource inventory on the Sylamore District, Ozark-St. Francis National Forest. Prepared for the US Dept. of Agriculture, Forest Service, Mountain View, Arkansas. Cave Research Foundation, Dallas, Texas.

Welbourn, W. C. 1983. Summary report for the cave resource inventory on the Sylamore District, Ozark-St. Francis National Forest, Part 2. Prepared for the USDA, Forest Service, Mountain View, Arkansas. Cave Research Foundation, Dallas, Texas.

Willis, L. D., and **A. V. Brown.** 1985. Distribution and habitat requirements of the Ozark cavefish (*Amblyopsis rosae*). Am. Mid. Nat. 114:311-317.

Wilson, S. N. 1967. Faunal collections in Blanchard Springs Caverns with some ecological notes. Unpubl. report. U. S. Forest Service, Ozark National Forest, Mountain

View, Arkansas. 8 pp.

Youngsteadt, N. W., and **J. O. Youngsteadt**. 1978. A survey of some invertebrates from northern Arkansas. The Association for Arkansas Cave Studies, Inc. Arkansas Cave Studies, Number 1. 13 pp.

Table 4. Ranking of the top 20 most biologically significant caves on the Sylamore District, with and without Blanchard Springs Caverns and Rowland Cave combined. Sites were scored according to the following formula: (number of obligate species x 10) + (number of total species) + (square root of length in meters).

Site Name	No. of obligates	No. of Species	Length	Score	Rank
Rowland – BSC Cave complex	9	96	17381	318	1st
Blanchard Springs Caverns	8	81	11265	267	1st
Rowland Cave	7	58	6116	206	2nd
Clark Spring – Alexander Cave	6	29	5633	164	3rd
Gunner Cave	6	31	3891	153	4th
Norfork Bat Cave	4	27	900	97	5th
Biology Cave	4	17	789	85	6th
Bonanza Cave	2	24	1536	83	7th
Gustafson Cave	2	33	906	83	7th
Hammer Springs Cave	4	25	321	83	7th
Hidden Spring Cave	2	21	1629	81	8th
Breakdown Cave	4	15	605	80	9th
Big Creek Cave	3	27	265	73	10th
Saltpeter Cave	3	11	900	71	11th
Herald Hollow Cave	3	24	262	70	12th
Woods Hollow Cave No. 1	4	18	105	68	13th
Bud Wallis Cave	2	34	55	61	14th
Bald Scrappy Cave	2	22	220	57	15th
Woods Hollow Cave No. 2	3	16	84	55	16th
Double Barrel Cave	2	21	94	51	17th
Panther Mountain Cave	2	9	167	42	18th

Table 5. All known animal species (96) found in Rowland – Blanchard Springs Cavern complex, with obligate species emboldened (data from this study and those cited in Methods). Columns are scientific name of species, common name of species, degree of adaptation to subterranean environments (obligate – troglobite or stygobite; tolerant – troglophile or stygophile; intolerant or transitory – incidental; or unknown), and site of species' occurrence – Blanchard Springs Caverns (BSC), Rowland Cave, or both caves.

Species	Common Name	Adaptation	Site
Achaearanea tepidariorum	Common house spider	Troglophile	BSC
Aecothea specus	Cave fly	Troglophile	BSC
Agkistrodon contortrix contortrix	Southern copperhead	Incidental	Rowland Cave
Ambystoma maculatum	Spotted salamander	Troglophile	BSC
Amoebalaria defessa	Fly	Troglophile	Both
Amphipoda - stygophilic	Surface amphipod	Stygophile	BSC
Apochthonius titanicus	**Cave false scorpion**	**Troglobite**	**BSC**
Arrhopalites clarus	Springtail	Troglophile	Rowland Cave
Athetini sp.	Rove beetle	Unknown	Rowland Cave
Bibio albipennis	Beetle	Unknown	BSC
Brevicornu sp.	Fungus gnat	Unknown	BSC
Caecidotea antricola	**Cave isopod**	**Stygobite**	**Rowland Cave**
Calliphoridae	Unidentified blow fly	Unknown	BSC
Camponotus americanus	Ant	Unknown	BSC
Causeyella causeyae	**Cave milliped**	**Troglobite**	**Both**
Ceuthophilus gracilipes	Cave cricket	Troglophile	Both
Chironomidae	Unidentified blood worm	Unknown	Both
Chrysomelidae sp. 1 and 2	Unidentified beetles	Unknown	BSC
Corynoptera sp.	Dark-winged fungus gnat	Troglophile	Both
Curculionidae	Unidentified weevil	Unknown	BSC
Decapoda - crayfish	Unidentified crayfish	Stygophile	BSC
Drosophila melanogaster	Fruit fly	Unknown	BSC
Elaphe obsoleta	Black rat snake	Incidental	BSC

Species	Common Name	Adaptation	Site
Eptesicus fuscus	Big brown bat	Troglophile	Both
Eurycea longicauda melanopleura	Dark-sided salamander	Troglophile	Both
Eurycea lucifuga	Cave salamander	Troglophile	Both
Eurycea multiplicata multiplicata	Many-ribbed salamander	Troglophile	BSC
Exechia sp.	Fungus gnat	Unknown	BSC
Exechiopsis sp.	Fungus gnat	Unknown	Rowland Cave
Formicidae	Unidentified ant	Unknown	BSC
Gastropoda - aquatic snail	Unidentified aquatic snail	Unknown	BSC
Ichneumonidae	Unidentified wasp	Incidental	BSC
Lasionycteris noctivagans	Silver-haired bat	Troglophile	Rowland Cave
Lasiurus borealis	Eastern red bat	Troglophile	Both
Lasiurus cinereus	Hoary bat	Troglophile	Both
Leiobunum sp.	Eastern harvestman	Troglophile	BSC
Lepidoptera	Unidentified moth	Unknown	BSC
Leptocera caenosa	Small dung fly	Unknown	BSC
Leptoneta arkansa	Spider	Troglophile	BSC
Ligidium elrodii elrodii	Sow bug	Troglophile	BSC
Lithobiomorpha	Unidentified centipede	Unknown	BSC
***Litocampa* sp. nov. 1 and 2**	**New species cave diplurans**	**Troglobite**	**Rowland Cave**
Lumbricidae	Unidentified earthworm	Troglophile	Both
Macrocera nobilis	Fungus gnat	Troglophile	Both
Megapallifera ragsdalei	Ozark mantleslug	Unknown	BSC
Megaselia cavernicola	Humpbacked fly	Troglophile	Rowland Cave
Mephitis mephitis	Striped skunk	Incidental	Rowland Cave
Microtus pinetorum	Woodland vole	Troglophile	BSC
Mus musculus	House mouse	Troglophile	BSC

Species	Common Name	Adaptation	Site
Myotis grisescens	Gray bat	Troglophile	Both
Myotis lucifugus	Little brown bat	Troglophile	Both
Myotis septentrionalis	Northern long-eared bat	Troglophile	Both
Myotis sodalis	Indiana bat	Troglophile	Both
Nematomorpha	Horsehair worm	Unknown	BSC
Neotoma floridana	Eastern woodrat	Troglophile	Rowland Cave
Nycticeius humeralis	Evening bat	Troglophile	Rowland Cave
Patera perigrapta	Engraved bladetooth snail	Unknown	BSC
Pentatomidae	Unidentified stinkbug	Unknown	BSC
Pericoma signata	Dark-winged fungus gnat	Unknown	BSC
Phagocata gracilis	Flatworm	Stygophile	BSC
Phoridae	Humpbacked fly	Unknown	BSC
Pipistrellus subflavus	Eastern pipistrelle	Troglophile	Both
Platynus sp.	Ground beetle	Troglophile	BSC
Plecoptera	Stonefly larva	Unknown	BSC
Plethodon albagula	Slimy salamander	Troglophile	BSC
Plethodon angusticlavius	Ozark zigzag salamander	Troglophile	BSC
Procyon lotor	Northern raccoon	Troglophile	Rowland Cave
Pseudopolydesmus pinetorum	Milliped	Troglophile	BSC
Psychoda satchelli	Moth fly	Unknown	BSC
Ptomaphagus cavernicola	Round fungus beetle	Troglophile	Rowland Cave
Rana catesbeiana	BullFrog	Incidental	BSC
Rana clamitans melanota	Green frog	Incidental	BSC
Rana sphenocephala	Southern leopard frog	Incidental	BSC
Rana sylvatica	Wood frog	Incidental	BSC
Rhagidia sp.	Mite	Unknown	Rowland Cave

Species	Common Name	Adaptation	Site
Sabacon cavicolens	Harvestman	Troglophile	Rowland Cave
Sayornis phoebe	Eastern phoebe	Troglophile	Both
Sciaridae	Dark-winged fungus gnat	Unknown	BSC
Sciurus carolinensis	Eastern gray squirrel	Incidental	BSC
Soricidae	Shrew	Troglophile	BSC
Spelobia tenebrarum	**Cave dung fly**	**Troglobite**	**Rowland Cave**
Sphingidae	Unidentified sphinx moth	Unknown	BSC
Storeria occipitomaculata	Red-belly snake	Incidental	BSC
Stygobromus a. alabamensis	**Alabama cave amphipod**	**Stygobite**	**BSC**
***Stygobromus* sp. nov.**	**Undescribed cave amphipod**	**Stygobite**	**Rowland Cave**
Tamias striatus	Eastern chipmunk	Incidental	BSC
Tipulidae	Unidentified crane fly	Troglophile	Both
Tomoceridae	Unidentified springtail	Unknown	BSC
Trichoceridae	Winter crane fly	Incidental	BSC
Turbellaria	Stream flatworm	Stygophile	BSC
Typhlotriton spelaeus	**Grotto salamander**	**Troglobite**	**Both**
Ventridens ligera	Globose dome snail	Unknown	BSC
Virginia valeriae	Smooth earth snake	Incidental	BSC
Zonitoides arboreus	Quick gloss snail	Unknown	Rowland Cave

Fenske-Hall Approximate Molecular Orbital Analysis of the Chelating Carbene Complex η^5-Cp′(CO)Mn{C(OEt)CH_2PPh_2}

John P. Graham
Department of Physical Science
Arkansas Tech University
Russellville, AR 72801

Abstract

The novel three legged piano stool chelating carbene complex, Cp′(CO)Mn{C(OEt)CH_2PPh_2}, 1, exhibits interesting structural, spectroscopic and electrochemical properties. It also readily undergoes reaction with CO to produce the three-legged piano stool complex Cp′$(CO)_2${PPh_2C(OEt)=CH_2}, 2. This is in contrast to the analogous non-chelating complex Cp(CO)(PPh_3)Mn{C(OMe)CH_2CH_3}, 3, which does not react with CO. This paper discusses the results of Fenske-Hall approximate molecular orbital calculations on model complexes for 1 and 3. The differences in spectroscopic and electrochemical properties are explained using molecular orbital analysis. Possible reasons for the enhanced reactivity of 1 are also presented.

Introduction

Transition metal carbene complexes have been the subject of extensive study for many years (Schrock, 2001; Frenking and Froelich, 2000). Fenske and Kostic (1982) and Schilling et al. (1979) described the conformational preferences of the carbene ligand in transitional metal - carbene complexes: For carbene complexes of the type $CpM(L)_2(CB)$ (L= π acceptor ligand such as CO, CB = carbene), the orientation of the carbene plane relative to the ligands L has been shown to have considerable effect on the electronic structure. The two extreme orientations of interest are illustrated in Fig. 1. It has been shown that the vertical orientation is more stable than the horizontal orientation, based on energetic and orbital overlap arguments.

Complexes of the form CpMLL′(CB), where L and L′ differ considerably in π acceptor ability, have been shown to adopt an orientation in which the plane of the carbene ligand is parallel to the M-L vector, where L is the better π accepting ligand (Kiel et al., 1980). The two extreme orientations labeled 'parallel' and 'perpendicular' are illustrated in Fig. 2.

The recently synthesized complexes 1 and 3 exhibit different carbene orientations (Lugan, pers. comm.): Complex 3 exhibits the standard conformation with the carbonyl ligand parallel to the plane of the carbene ligand. Complex 1 is forced, by the chelating nature of the carbene, to adopt the normally unfavorable orientation with the CO perpendicular to the carbene plane. The structure of complex 1 is represented by a ball and stick description in Fig. 3. It is noteworthy that the C1-C-P angle in the chelating ligand is unusually small (89°) and that the C-P distance indicated by the dashed line is quite short (2.36 Å). It has been observed that complex 1 exhibits enhanced reactivity, a higher oxidation potential, and lower CO stretching frequency than complex 3 (Lugan, pers. comm.). These differences in observed properties could arise from strain within the chelating ligand of 1 or from the unfavored orientation of the chelating ligand with respect to CO. The

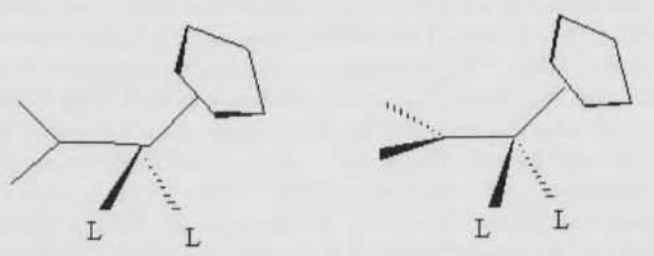

Fig. 1. Extreme orientations of the complex $CpM(L)_2CB$, L= strong π acid ligand.

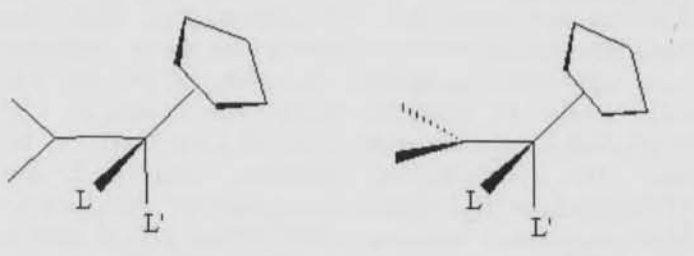

Fig. 2. Extreme orientations of the complex CpMLL′CB, where L and L′ differ considerably in π acidity.

Fenske-Hall Approximate Molecular Orbital Analysis of the Chelating Carbene Complex η^5-Cp′(CO)Mn{C(OEt)CH_2PPh_2}

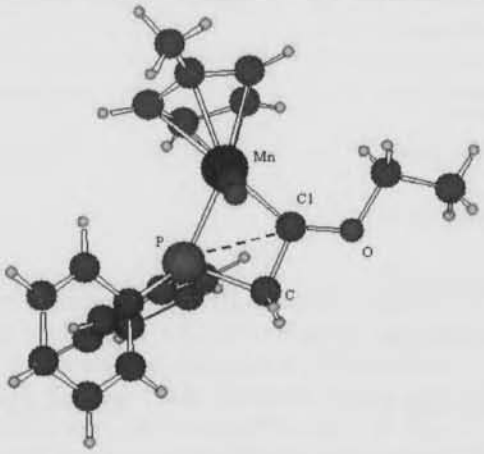

Fig. 3. A ball-and-stick representation of complex 1. The dashed line between P and C1 indicates a weak interaction.

origin of the observed differences between complexes 1 and 3 will be the main focus of this paper.

To simplify the calculations, model complexes have been used. The model for complex 1 is Cp(CO)Mn{C(OMe)CH_2PH_2)} and labelled 1a. The model for complex 3 is Cp(CO)Mn(C(OMe)Me)PH_3. To help study the effect of carbene orientation without the necessity to consider other factors, two structures are considered; the observed 'parallel' orientation, 3a, and the unfavorable 'perpendicular' orientation, 3b. We will initially compare model complex 3a with the unfavorable model isomer 3b. Comparisons will then be made between 3b and the model complex 1a.

Methods

The Fenske-Hall approximate molecular orbital method was used for all calculations (Hall and Fenske, 1972). All atomic basis functions were generated by a least-squares fit of Slater-type orbitals to the atomic orbitals from Herman-Skillman atomic calculations (Bursten et al., 1978). Contracted double ζ representations were used for the Mn 3d, C 2p, O 2p and P 3p atomic orbitals. An exponent of 1.16 was used for the H 1s AO's (Hehre et al., 1969). The basis functions for Mn were derived from the +1 oxidation state with fixed 4s and 4p exponents of 2.0 and 1.8, respectively. In modeling complexes 1 and 3, Cp′ ($C_5H_4CH_3$) was replaced by Cp (C_5H_5), Ph (C_6H_5) by H, and OEt by OMe. In modeling complex 2, the {$PPh_2C(OEt)=CH_2$} ligand was replaced by PH_3, and L-Mn-L angles were idealized to 90°. Where PH_3 is used to model PPh_3, a H-P-H angle of 102° is employed (Clayton, 1989). The 3σ and 6σ orbitals of CO and all Cp orbitals below the lowest occupied π orbital and above the highest unoccupied π orbital were deleted from the set of variational

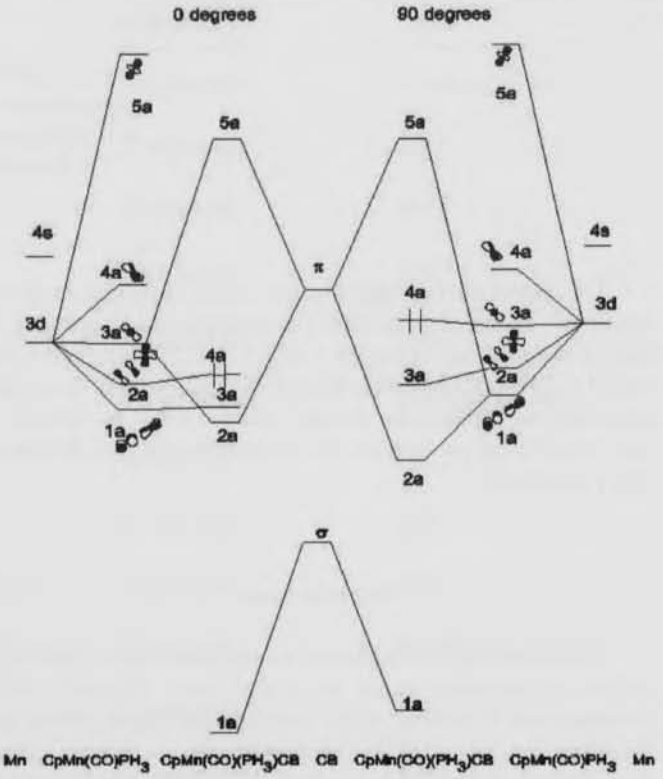

Fig. 4. A molecular orbital diagram complexes 3a and 3b.

orbitals (Lichtenberger and Fenske, 1976). The carbene plane - CO vector angles were idealized at 90° or 0° where appropriate. All other bond distances and angles were preserved as in the crystal structures (Lugan, N., Laboratorie de Chemie de Coordination, Toulouse, France. pers. comm.)

Results and Discussion

Comparison of model complexes 3a and 3b.--A molecular orbital description of complexes 3a and 3b is given in Fig. 4. The results are presented in a fragment approach, in which each molecule is represented by the interaction of a $CpMn(CO)_2$ fragment with a CMe(OMe) carbene fragment. The frontier orbitals of primary interest of the $CpMn(CO)_2$ fragment are the largely metal based 1a, 2a, and 3a orbitals. The local coordinate system used for the metal center is such that the local z axis points towards the carbonyl ligand. The local y axis points in-between the phospine and carbene ligands. The local x axis is perpendicular to the plane of the page. In this coordinate system, the composition of the metal based frontier orbitals of $CpMn(CO)_2$ are as follows: The orbitals 1a and 2a are the Mn d_{xz} - $CO2\pi_x$ and Mn d_{yz} - $CO2\pi_y$ bonding molecular orbitals respectively; orbital 3a is an essentially

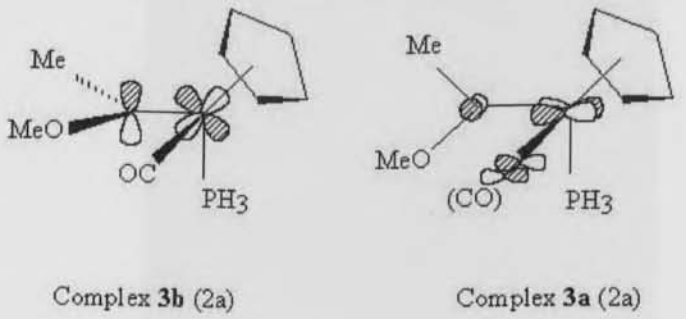

Complex **3b** (2a) Complex **3a** (2a)

Fig. 5. The carbene π^* - $CpMn(CO)(PH_3)$ interactions in complexes 3a and 3b.

non-bonding Mn $d_{x^2-y^2}$ based orbital. The principal frontier orbitals of the carbene ligand are those labeled σ and π^*. The carbene σ orbital is essentially a lone pair of electrons localized largely on the carbene C1 (the C bound to Mn) atom. The π^* orbital is a virtual orbital perpendicular to the plane of the carbene ligand and is antibonding between C1 and O, mostly localized on C1. In complex 3a, the Mn $d_{x^2-y^2}$ based non-bonding HOMO (Highest Occupied Molecular Orbital) of $CpMn(CO)_2$ donates electron density to the π^* orbital of the carbene ligand. The resultant stabilized molecular orbital 2a has considerable metal and carbene character. The 5a antibonding counterpart of this interaction constitutes the LUMO (Lowest Unoccupied Molecular Orbital) of the complex. The 4a HOMO and 3a SHOMO (Second Highest Occupied Molecular Orbital) of 3a are the essentially unperturbed 1a and 2a orbitals of the $CpMn(CO)_2$ fragment. The carbene lone pair orbital σ is strongly stabilized through donation to the Mn d_{xy} based 4a orbital.

When the carbene ligand is rotated 90°, as in complex 3b, the resultant molecular orbitals of the complex are significantly different: The carbene π^* ligand now interacts with the $CpMn(CO)_2$ 1a orbital. The resultant strongly stabilized molecular orbital 2a is largely Mn d_{xz} based with contributions from both the $CO2\pi_x$ and carbene π^*. The 3a molecular orbital is similar to that in complex 3a, a largely Mn d_{yz}-$CO2\pi_y$ based orbital. The HOMO 4a is essentially the unperturbed 3a non-bonding HOMO of $CpMn(CO)_2$. The LUMO 5a is a largely carbene π^* based orbital with some contribution from Mn d_{xz} and $CO2\pi_x$. A diagrammatic comparison of the carbene π^* - $CpMn(CO)_2$ interactions for complexes 3a and 3b is given in Fig. 5. The contour plots given in Fig. 6 illustrate the C1 localized nature of the LUMO. The composition of the molecular orbitals of 3a and 3b are summarized in Tables 1 and 2.

The Mulliken populations listed in Table 3 indicate that both the σ and π interactions of the carbene ligand with Mn are slightly weakened in complex 3b relative to 3a. It is noted that backdonation to the CO 2π is reduced by 0.04 in 3b relative to 3a due to competition between CO and the carbene for bonding with the Mn d_{xz} orbital.

The overlap integral between the carbene π^* and $CpMn(CO)_2$ 3a in 3a is 0.117. The overlap between carbene π^* and $CpMn(CO)_2$ 1a in 3b is 0.116. The carbene σ - $CpMn(CO)_2$ 4a overlap integrals in 3a and 3b are 0.309 and 0.304, respectively. Clearly the difference in stability of the two conformers cannot be attributed to changes in frontier orbital overlap on rotation.

The energies of the frontier molecular orbitals of 3a and 3b are given in Table 4. The average energy of the occupied metal based orbitals is relatively unchanged upon rotation of the carbene ligand (-5.78eV and -5.58eV for 3a and 3b, respectively). This indicates that stability lost by elimination of the carbene π^*- 3a interaction is approximately countered

Table 1: Percent character of valence MOs of complex 3a.

	THOMO	SHOMO	HOMO	LUMO	SLUMO	TLUMO
Energy (eV)	-6.12	-5.85	-5.35	-1.58	0.01	0.14
% Mn	63.7	80.0	80.3	45.8	62.1	61.1
%Mn 3d	62.2	76.4	77.9	43.9	53.5	47.6
% Cp (e_1'')	****	****	2.2	5.5	10.6	13.0
%CO 2π	****	18.0	13.9	****	11.2	13.0
% CB lp	****	****	****	****	2.3	****
% CB pz	31.6	****	****	46.6	8.8	6.6

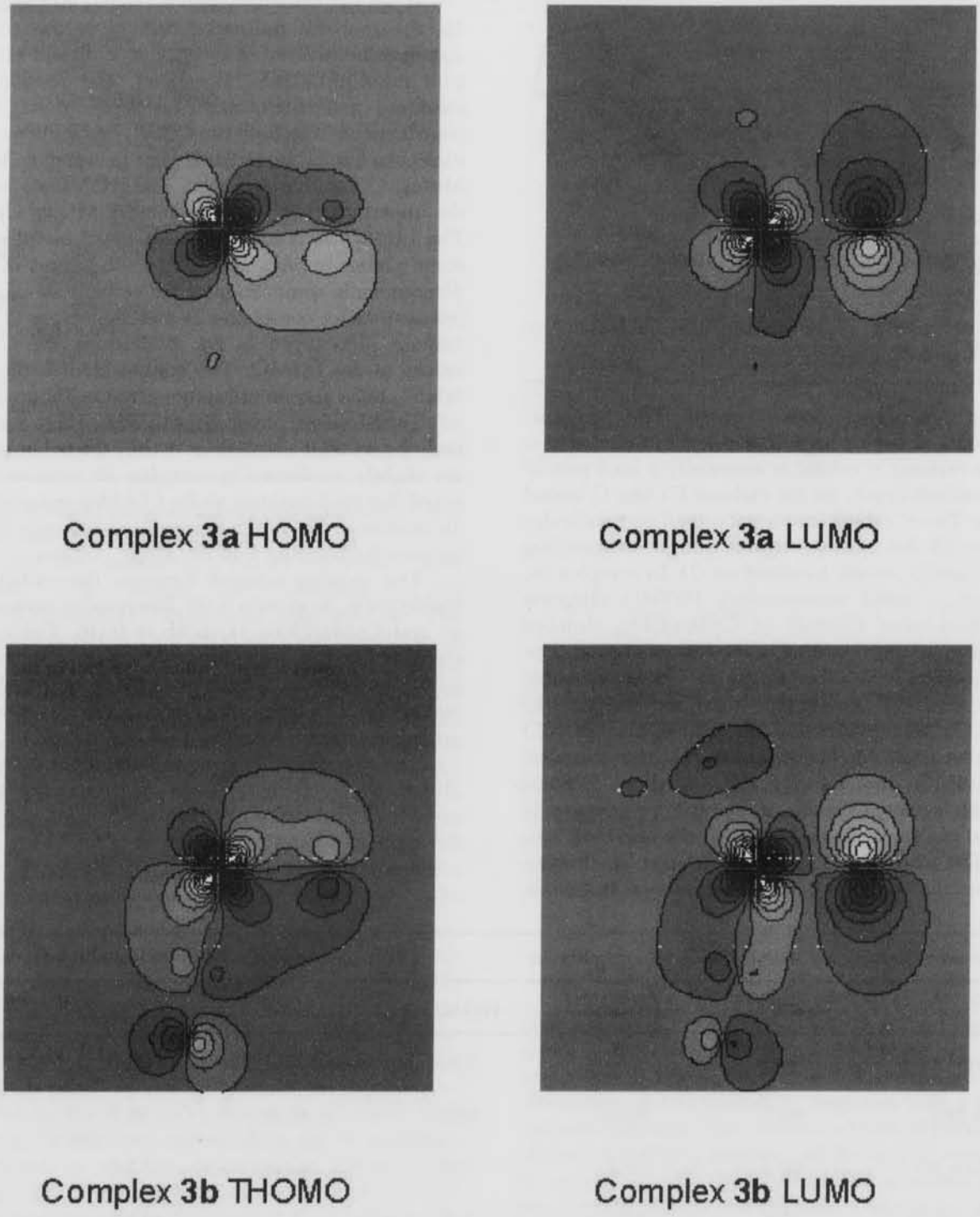

Fig. 6. Contour plots of the metal carbene π bonding and antibonding interactions in complexes 3a and 3b.

by that gained by the introduction of the carbene π*-1a interaction on going from 3a to 3b. Such a result is consistent with ligand additivity models such as that of Bursten and Green (1988). The principal factor to which we attribute the stability of 3a over 3b is the difference in HOMO energy between the complexes. In complex 3a, the orbital stabilized by the π* of the carbene ligand is the 3a non-bonding HOMO of the $CpMn(CO)_2$ fragment. This

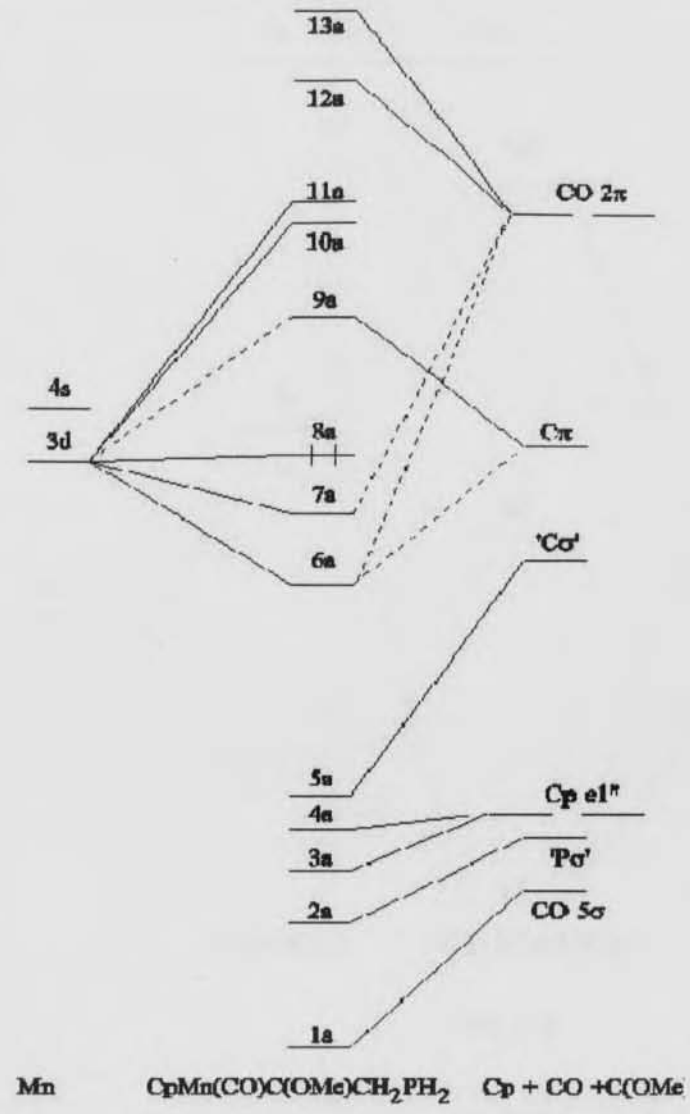

Fig. 7. A molecular orbital description of complex 1a.

results in a HOMO for complex 3a which is a Mn-CO2π stabilized orbital. In complex 3b, the carbene π* interacts with the already CO stabilized $CpMn(CO)_2$ 1a orbital, leaving a non-bonding 3a orbital as the HOMO of the complex while further stabilizing the THOMO (Third Highest Occupied Molecular Orbital). It is well known (Pearson, 1987) that the stability of organometallic complexes can be related to the magnitude of the energy difference between the HOMO and LUMO (HOMO-LUMO gap). Complex 3a has a calculated HOMO-LUMO gap of 3.77eV, considerably higher than that of complex 3b (2.91eV). As the LUMO energies in each complex are similar, this effect can be attributed mainly to the metal – carbene bonding π* interactions. These observations are consistent with those in Fenske's and Kostic's (1982) account of the importance of non-bonding and antibonding molecular orbitals in the stereochemistry of organometallic complexes.

Comparison of the model complexes 1a and 3.--A molecular orbital diagram for the chelating complex 1a, given as the interaction between the fragments Mn, CO, Cp, and $C(OMe)CH_2PH_2$ is given in Fig. 7. The composition of the molecular orbitals is summarized in Table 5. The largely metal based 6a, 7a, and 8a orbitals are similar to in energy and composition to the analogous 2a, 3a, and 4a orbitals of 3b. The HOMO-LUMO gap in complex is 2.63eV. The Mulliken population of the CO 2π orbitals in 1a is also similar to that in 3b. The most distinct difference in the molecular orbital diagrams of 1a and 3b is the energy of the Cσ fragment orbital of the carbene ligand. In complex 3b, the Cσ orbital is found at -7.91eV compared to -6.28eV in 1a. This increased basicity of the carbene C lone pair arises from a C1-P interaction in the chelating ligand and is discussed below. The Mulliken population of the 'Cσ' orbital in 1a is considerably lower than that in 3b, which also reflects the increased donor ability of the ligand. The carbene π* Mulliken population in the chelating ligand is considerably higher than that in 3a or 3b. We suggest this increase in backdonation to the carbene ligand is a result of the increased electron density at the metal center due to the more basic Cσ orbital. Despite these differences, the most interesting features of the molecular orbital diagram (the largely metal based orbital energies and compositions) are very similar to those of complex 3b. This suggests that the observed differences in properties of complexes 1 and 3 arise largely from the orientation of the carbene ligand.

A molecular orbital diagram of the chelating carbene ligand $C(OMe)CH_2PH_2$, depicted as the interaction of $C(OMe)CH_2$ and PH_2 fragments, is presented Fig. 8. The picture on the right shows the ligand with the C-C-P angle the same as in complex 1 (89^o). The left-hand picture shows the ligand with a C-C-P angle relaxed to 109^o. In each case the 1a′ orbital is clearly the CH_2-PH_2 bond. When $\theta = 109^o$, we see that the 2a′ and 3a′ orbitals are essentially unperturbed P and C1 lone pairs respectively. When $\theta = 89^o$, the P and C1 lone pairs are brought closer together, resulting in a filled-filled interaction. The resulting molecular orbitals, 2a′ and 3a′, have considerable C1 and P character. The 2a′ orbital is more localized on the P atom and slightly lower in energy than the corresponding 2a′ orbital at 109^o. The 3a′ molecular orbital, the C1-P antibonding combination, is considerably destabilized and largely localized on the C1 atom. The 1a′ LUMO in each case is the C-O antibonding π orbital of the carbene fragment. The net effect of closing the C-C-P angle is the formation of a strongly basic frontier orbital, C1-P

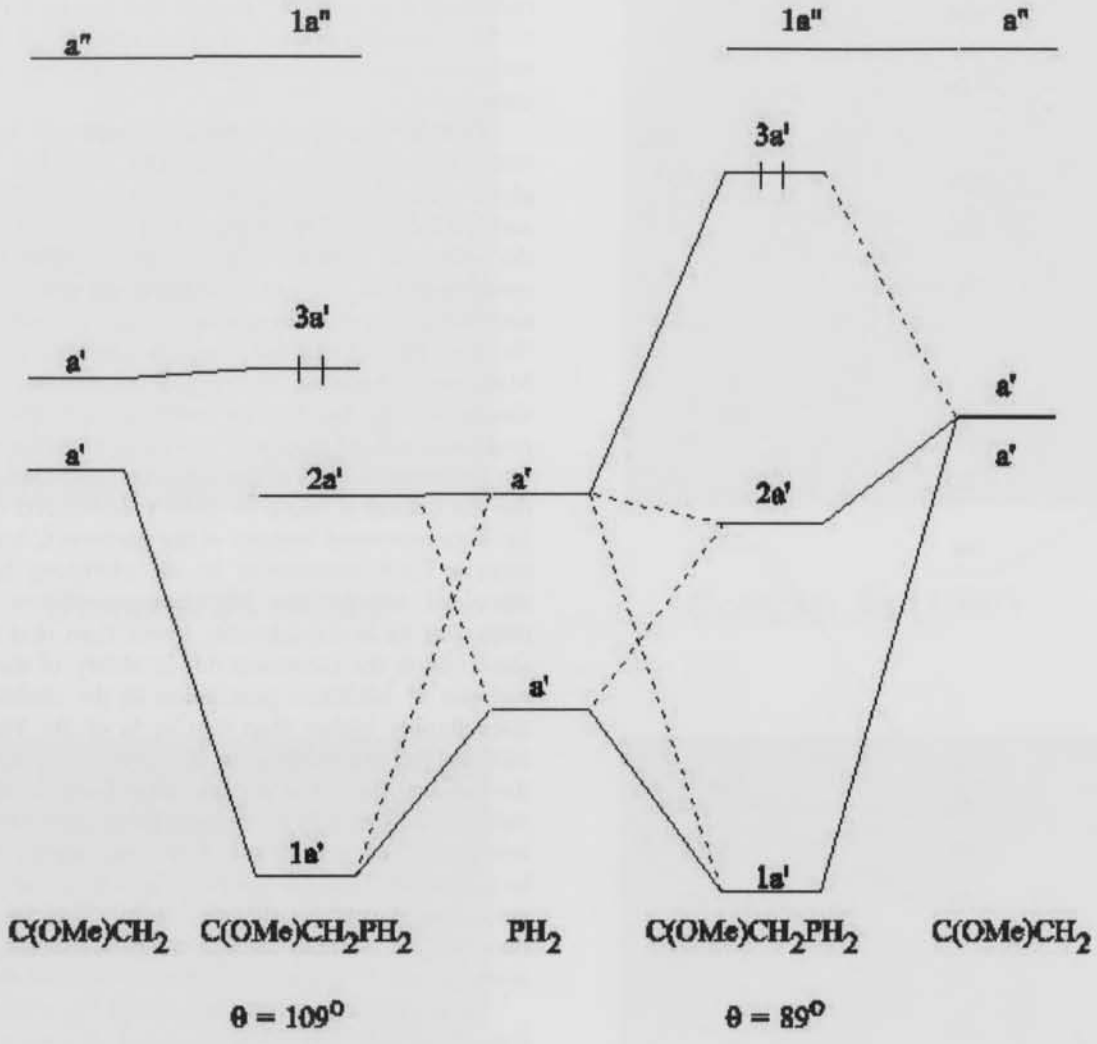

Fig. 8. A molecular orbital description of the chelating ligand $C(OMe)CH_2PH_2$ at $\theta = 89^o$ and 109^o.

antibonding in nature, more heavily localized on C1. This accounts for the enhanced basicity observed in the molecular orbital diagram of 1a.

The nonbonding HOMO of complex 1a should result in an increased oxidation potential relative to complex 3a. We would also expect a reversible 2e oxidation process in 1a. Indeed, the oxidation potential of 1 has been determined to be 0.54V greater than that for 3. It has been observed that the oxidation potential for Mn(I) complexes changes approximately half as fast as the HOMO energy (Lichtenberger and Fenske, 1976). The difference in HOMO energies between 1a and 3a (1.09eV) is remarkably consistent with this trend. We would expect to see a red-shift in ligand field transition energies for 1 relative to 3 because the of difference in HOMO-LUMO gaps in model complexes 1a and 3a. This is consistent with experimental data also. The C-O stretching frequency observed in 1 is $43cm^{-1}$ lower than that found in 3. Correlation with the C-O force constant and CO2π and 5σ Mulliken populations had been shown (Hall and Fenske, 1972) to follow the form

$$k_{co} = a(5\sigma) + b(2\pi) + c.$$

Donation from the CO 5σ orbital strengthens the C-O bond, and π backbonding to the CO2π weakens the bond. The 5σ populations in complexes 1a, 3a, and 3b are

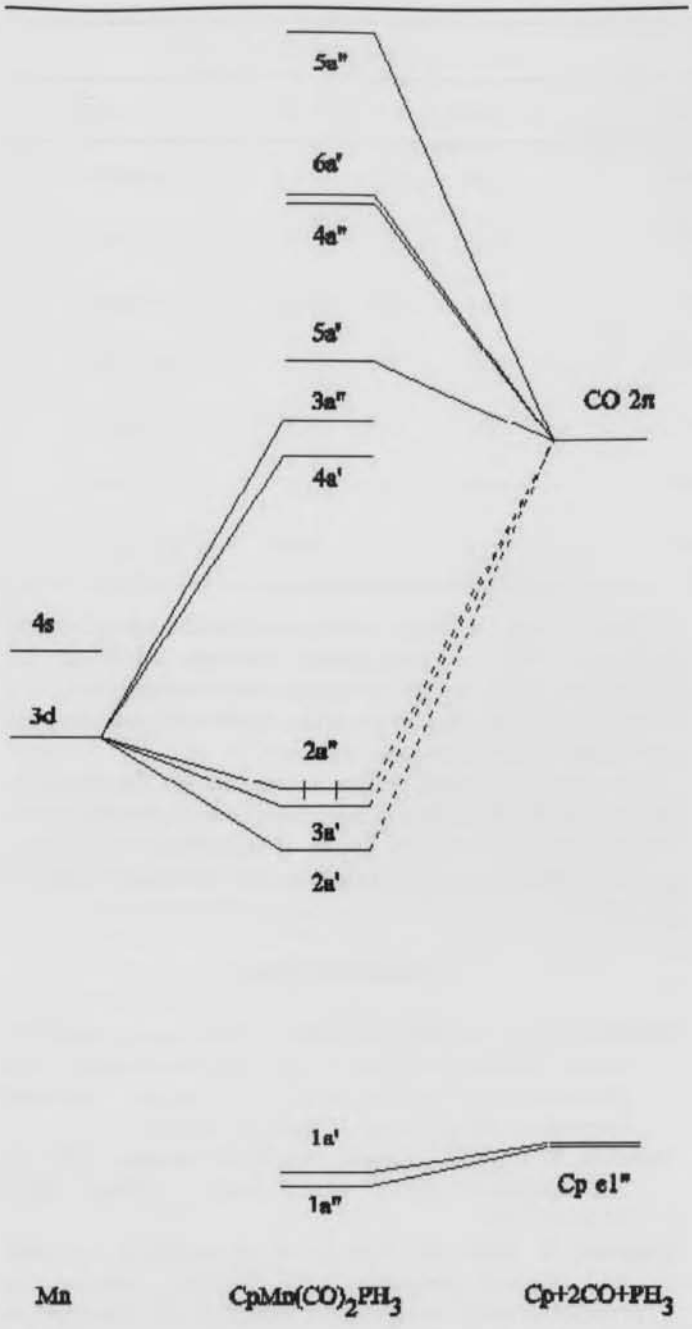

Fig. 9. A molecular orbital description of complex 2a.

essentially invariant. Hence, we would expect the increase in CO 2π population of 1a relative to 3a (+0.037) to give rise to a lower C-O stretching frequency, as experimentally observed. The magnitude of this change in ν(CO) is difficult to estimate, but it should also be noted that the presence in Cp′ in complex 1 vs. Cp in complex 3 would also be expected to contribute to lowering ν(CO).

Reactivity.--In the presence of CO, complex 1 undergoes a carbene insertion reaction to give the three legged piano stool complex 2. The reaction involves the breaking and formation of several bonds and would be difficult to address using molecular orbital analysis without access to detailed mechanistic information. A molecular orbital description for the model complex 2a, CpMn(CO)2(PH3), is given in Fig. 9. The molecule is represented by the interaction of CpMn, 2xCO, and PH3 fragments. All three metal based dπ orbitals are stabilized through interaction with the CO ligands. The resultant HOMO is bonding, and the pattern of dπ based MO's resembles that in the complex 3a (favorable carbene orientation). Factors that we would expect to contribute to the enhanced reactivity of 1a over 3a include the nonbonding nature of the HOMO in 1a and the ring-strain within the carbene ligand (and resultant filled-filled interaction between the carbene C1 and P). The LUMO of 1a is the carbene - Mn π antibonding orbital. Frontier orbital controlled nucleophilic attack on complex 1a would be expected to occur at the carbene C atom (which gives the larger contribution to the LUMO). Hence donation from CO to the LUMO would be expected to weaken the Mn-carbene bond. However the LUMO of complex 3a is also carbene-Mn π-antibonding and is of similar energy. As CO attack is not observed in 3, the nature of the LUMO alone is insufficient to explain the difference in reactivity. However, upon nucleophilic attack at the Mn-carbene antibonding LUMO, Mn-carbene bond cleavage may be facilitated by the ring strain and C1-P interaction within the chelating ligand of 1. Although apparently not the most important differentiating factor in the electrochemistry or spectroscopic properties of 1 and 3, it appears that this ring strain and C1-P antibonding interaction within the chelating carbene ligand may contribute significantly to the observed reactivity of 1. Higher level calculations are currently underway to further study possible mechanisms of nucleophilic attack on complex 1.

Conclusions

The molecular orbital analysis of complexes 3a, 3b, and 1a suggests that the conformational preferences of carbene ligands in complexes of the form CpMLL′CB, where L and L′ differ significantly in π acceptor ability, arises from the presence of a non-bonding HOMO in the 'perpendicular' conformation. There are no significant differences in overlap between the carbene and metal fragment in the two model isomers of 3. The metal based orbitals in 1a may be modeled satisfactorily using complex 3b. From comparisons of the bonding in 3a and 3b, electrochemical and spectroscopic differences between 1 and 3 can be explained. The principal difference between complexes 1a and 3b lies

Table 2: Percent character of valence MOs of complex 3b.

	THOMO	SHOMO	HOMO	LUMO	SLUMO	TLUMO
Energy (eV)	-6.70	-5.49	-4.48	-1.58	-0.24	0.45
% Mn	51.7	78.4	94.9	35.4	71.6	58.1
%Mn 3d	49.5	76.5	93.2	33.4	63.2	44.5
% Cp (e_1'')	****	****	****	8.5	13.7	7.6
%CO 2π	14.2	16.4	****	5.4	8.3	21.8
% CB l.p.	****	****	****	****	1.7	****
% CB p_z	31.0	1.0	****	50.8	****	6.7

Table 3: Mulliken populations of frontier ligand fragment orbitals in complexes 3a, 3b, and 1a.

	Complex 3a	Complex 3b	Complex 1a
Carbene σ	1.353	1.369	1.200
Carbene π*	0.706	0.683	0.756
CO 2π	0.783	0.743	0.750
CO 5σ	1.420	1.421	1.420

Table 4: Frontier MO energies for complexes 1a, 3a and 3b.

	Complex 3a	Complex 3b	Complex 1a
LUMO	-1.58	-1.59	-1.63
HOMO	-5.35	-4.50	-4.26
SHOMO	-5.86	-5.52	-5.37
THOMO	-6.12	-6.73	-6.69

in the interactions within the chelating ligand of 1a. It is suggested that the filled-filled P-C1 interaction in the chelating ligand, along with the considerable ring strain, contributes to the enhanced reactivity of 1 over 3. The LUMO of 1a, a spatially localized and energetically isolated orbital, is an ideal site for nucleophilic attack. Attack at the LUMO, which is Mn - carbene π antibonding, would encourage Mn - carbene bond cleavage. Although the LUMO of 3a is similar in energy and composition, it is suggested that the ring strain in the chelating ligand may aid Mn-carbene bond cleavage in 1.

ACKNOWLEDGMENTS.—The author thanks Dr. Bruce E. Bursten of the Ohio State University for his valuable advice and insights and Dr. Noel Lugan of Laboratorie de Chemie de Coordination for providing data and creating the basis of this study.

Literature Cited

Bursten, B. E., and **M. R. Green.** 1988. Ligand additivity in the vibrational spectroscopy, electrochemistry and photoelectron spectroscopy of metal carbonyl derivatives. Prog. Inorg. Chem. 36:393-485.

Bursten, B. E., J. R. Jensen, and **R. F. Fenske.** 1978. An Xα optimized atomic orbital basis. J. Chem. Phys. 68:3320-3321.

Clayton, T. 1989. The correlation of structure, reactivity and physical properties with electronic structure in transition metal complexes. Unpubl. Ph.D. Dissertation. The Ohio State University, Columbus, OH.

Fenske, R. F., and **N. M. Kostic.** 1982. Criteria of maximum overlap and minimum orbital energy in molecular orbital studies of conformations of transition-metal carbene and carbyne complexes. J. Am. Chem. Soc. 104:3879-3884.

Frenking, G., and **N. Froelich.** 2000. The nature of bonding in transition metal compounds. Chem. Rev. 100:717-774.

Hall, M. B., and **R. F. Fenske.** 1972. Electronic structure and bonding in methyl- and perfluoromethyl-

Table 5: Percent character of valence MOs of complex 3a.

	THOMO	SHOMO	HOMO	LUMO	SLUMO	TLUMO
Energy (eV)	-6.69	-5.37	-4.26	-1.63	0.16	0.55
% Mn	48.9	76.4	96.5	37.0	67.0	59.7
%Mn 3d	46.6	74.4	95.0	35.3	57.2	45.7
% Cp (e_1'')	****	****	****	7.3	12.9	8.1
%CO 2π	13.4	17.3	****	5.8	14.0	20.8
% CB 'lp'	****	****	****	****	4.7	****
% CB p_z	34.7	1.0	****	49.0	****	5.9

(pentacarbonyl)manganese. Inorg. Chem. 11:768-775.

Hall, M. B., and **R. F. Fenske.** 1972. Force constants and the electronic structure of carbonyl groups. d^6 carbonyl halides and dihalides. Inorg. Chem. 11:1619-1624.

Hehre W. J., R. F. Stewart, and **J. A. Pople.** 1969. Self-consistent molecular-orbital methods. I. use of gaussian expansions of Slater-type atomic orbitals. J. Chem. Phys. 51:2657-2665.

Kiel, W. A., L. Gong-Yu, and **J. A. Gladysz.** 1980. Unprecedented regiospecificity and stereospecificity in reactions of $Ph_3C^+PF_6^-$ with rhenium alkyls of the formula $(\eta^5\text{-}C_5H_5)Re(NO)(PPh_3)(CH_2R)$. J. Am. Chem. Soc. 102:3299-3301.

Lichtenberger, D. L., and **R. F. Fenske.** 1976. The transferability of molecular fragment canonical orbitals. J. Chem. Phys. 64:4247-4264

Pearson, R. G. 1987. Recent advances in the concept of hard and soft acids and bases. J. Chem. Ed. 64:561-567.

Schilling, B. E. R., R. Hoffmann, and **D. L. Lichtenberger.** 1979. $CpM(CO)_2$(ligand) complexes. J. Am. Chem. Soc. 101:585-591.

Schrock, R. R. 2001. Transition metal-carbon multiple bonds. J. Chem. Soc., Dalton Trans. 18:2541-2550.

Dragonflies (Odonata) of the Ouachita National Forest

George L. Harp* and **Phoebe A. Harp**
Dept. of Biological Sciences
Arkansas State University
State University, AR 72467

*Corresponding Author

Abstract

The Ouachita National Forest (ONF) was established in 1907 and encompasses 1.8 million acres (728,450 ha) in Arkansas and Oklahoma, almost entirely within the Ouachita Mountains Natural Division. The adult dragonfly species richness, seasonal and spatial distribution, and relative abundance were surveyed during 2002. Fifty-four collections were made at 43 sites during 10-19 May (20 collections), 10-22 July (19 collections) and 9-17 September (15 collections). Literature records were searched, as well as records from pertinent museums and individuals. Eighty-three species are reported here for the ONF, 77 of which were collected during 2002. *Nehallenia integricollis* is newly reported for Arkansas, as are several species for the six Arkansas and two Oklahoma counties that encompass the ONF. The species richness results from a diversity of aquatic habitats, particularly within the Caddo Ranger District. Plastic species (e.g. *Plathemis lydia*) typically are widely distributed and have long flight seasons. More specialized species (e.g. *Ophiogomphus westfalli*) often are quite restricted in both distribution and flight season. Maintenance of good water quality in all aquatic habitat types will ensure species richness for dragonflies and the invertebrates upon which they feed.

Introduction

All life has value, and genetic diversity should be conserved (Moore, 1997). Biodiversity surveys are one response to this realization. Their size, intricate coloration and incredible aerial acrobatics have made dragonflies specific subjects of the folklore of countries such as China and Japan, as well as Native Americans, for whom odonates are often the subjects of art and poetry (Moore, 1997). Because of their aerial maneuverability, dragonflies have prompted considerable study by aeronautical engineers, often funded by the U.S. Air Force or similar agencies (Moore, 1997). Their size facilitates biological research, particularly in behavioral and ecological studies. They have potential as bio-indicators, because species differ both in their preference for specific habitats and their sensitivity to various types of pollutants. Finally, dragonflies eat prodigious numbers of insects that are harmful to man's food supplies, forests (e.g. moths), and health (e.g. mosquitoes as vectors) (Moore, 1997).

Description of the Area.--The Ouachita Mountain Natural Division, lying entirely within Arkansas and Oklahoma, was formed by uplifting, folding, and faulting processes during the Pennsylvanian Period approximately 300 mya. These mountains are a series of long, narrow ridges with east-west axes. The ridges are separated by wide valleys, each drained by a river or stream. Principle geologic formations in these Mountains are Paleozoic sedimentary sandstone and shale ranging in age from Cambrian or Ordovician through Pennsylvanian, which were warped, twisted and folded under tremendous pressure. Soils are derived from shale and sandstone, with recent alluvium in the bottomlands of the main rivers. Shortleaf pine, upland hardwood and bottomland hardwood forests predominate (Robison and Buchanan, 1988). Water hardness, alkalinity, and pH all tend to be relatively unbuffered.

The Ouachita National Forest (ONF), the South's oldest and largest national forest, was established in 1907 and encompasses 1.8 million acres (728,450 ha), almost entirely within the Ouachita Mountain Natural Division. The ONF is managed through 12 ranger districts, nine in Arkansas and three in Oklahoma. These districts range in area from 118,921 (Winona) to 194,551 (Mena) acres (48,127-78,731 ha). Mean rainfall varies among districts, but the Caddo Ranger District receives the greatest amount.

The primary purpose of this survey was to establish a biodiversity list for dragonflies of the ONF. Secondary goals were to determine the seasonal occurrence, relative abundance and preferred habitat for at least the more common species. Finally, several areas heavily damaged by southern pine beetles were surveyed to determine extent of dragonfly utilization.

Materials and Methods

Fifty-four collections were made at 43 sites within the ONF during 2002 (Table 1). Collections were distributed seasonally, during 10-19 May (20 collections), 10-22 July (19

collections), and 9-17 September (15 collections). Voucher specimens are housed in the Adult Odonata Collection of the Arkansas State University Museum of Zoology (ASUMZ). Additionally the ASUMZ was searched for previous collections from the ONF. Records were also acquired from the Florida State University Collection of Arthropoda (FSCA) through Bill Mauffray. Literature records were searched. Finally, personal records from John Abbott (University of North Texas), Sidney W. Dunkle (Collin Co. Comm. College, Plano, TX), and Roy J. Beckemeyer (Wichita, KS) were acquired. These odonatists have collected extensively in the Ouachita Mountains.

Results and Discussion

Eighty-three species of dragonflies are reported here for the ONF (Table 2). Of these, 77 species were collected during 2002, while voucher specimens of six additional species are housed in the ASUMZ, FSCA, or private collections. The 83 species comprise 61% of the species known to occur in Arkansas (Harp and Harp, 1996; Westfall and May, 1996, Needham et al., 2000). The species richness results from a diversity of aquatic habitats (seeps, springs, ponds, lakes, creeks, and rivers), particularly within the Caddo Ranger District.

Nehalennia integricollis, collected at the retention pond immediately above Caddo Pond on 18 May, is reported for the first time in Arkansas. Several new records are reported for the six Arkansas counties in the ONF (Table 3). Montgomery County is particularly species rich for two related reasons. First, the Caddo Ranger District lies within southern Montgomery County. Second, because of its great diversity of aquatic habitats, this district has been more thoroughly collected than perhaps any other area of comparable size in Arkansas. *Ladona deplanata* is a new record for LeFlore Co., OK, as are *Ischnura ramburii* and *Arigomphus lentulus* for McCurtain Co., OK (R.J. Beckemeyer, pers. comm.).

Common species are often referred to as generalists, or plastic species, because they tolerate a wide range within many environmental parameters. The ability of their nymphs to survive relatively low dissolved oxygen (DO) concentrations is of primary importance. Because of this, they can inhabit a wide range of current speeds and are characteristically found in both lentic (standing water) and lotic (running water) habitats. For these species, moderate turbidity is not a problem. Their plasticity is reflected in the number of sites at which they were found in the ONF. Foremost among these species are *Erythemis simplicicollis* (34 sites), *Ischnura posita* (30), *Pachydiplax longipennis* (30), *Libellula incesta* (25), *Plathemis lydia* (24), and *Perithemis tenera* (19) (Table 2).

Other species are widespread and common because, in addition to their broad tolerance of environmental conditions, they are strong fliers and thus are better able to disperse widely. These species are represented in the ONF by *Anax junius* and *Tramea lacerata* (21 and 19 sites, respectively) (Table 2).

Plastic species often have a long flight season, in Arkansas extending perhaps from April through September (e.g. *Ischnura posita*, *Erythemis simplicicollis*, *Plathemis lydia*). Other species, although they may be common as revealed by the presence of their nymphs, are not found as adults as often because of their short flight seasons, usually in the spring or fall. Typical spring fliers, found almost exclusively during the May samples in this study, include *Basiaeschna janata* (springtime darner), *Gomphus ozarkensis*, *Gomphus oklahomensis*, *Epitheca costalis*, *Epitheca cynosura*, *Ladona deplanata*, and *Libellula semifasciata* (Table 2). Fall fliers found in the ONF include *Boyeria vinosa*, *Sympetrum ambiguum* and *Sympetrum vicinum* (Table 2).

Species strongly adapted to either lentic or lotic habitats obviously will be less common than generalist species. Species characteristic of lentic habitats are typically more tolerant than those of lotic habitats, however. The latter tend to require at least some current but less turbid water, with concomitant higher DO levels. Because of this, stream species are somewhat better indicators of water quality. Strongly lentic species include *Lestes disjunctus australis*, *Enallagma aspersum*, *Enallagma traviatum*, *Anax longipes* and *Celithemis* spp. (Table 2) (Westfall and May, 1996). Strongly lotic species of the ONF include *Hetaerina americana*, *Argia sedula*, *Enallagma exsulans* (stream bluet), *Basiaeschna janata*, *Hagenius brevistylus* and *Stylogomphus* n. sp. (Table 2).

Seeps are sensitive habitats, usually small aquatic ecosystems with a substrate of organic mud is often present, which limits DO. Drought, recreational off-road vehicular use and/or land management practices, such as timber harvesting without adequate protective buffers, obviously are detrimental to their flora and fauna. Thus species adapted to this distinct habitat type are often uncommon. Species of the ONF in this habitat type include *Argia bipunctulata* (seepage dancer), and *Tachopteryx thoreyi*. Also included are *Cordulegaster obliqua* and *Cordulegaster* n. sp. *Cordulegaster* species characteristically inhabit woodland headwater streams, and these may originate at seeps. Currently, *Cordulegaster* n. sp. is known only from the Caddo Ranger District. This species is being described by Ken Tennessen, Florence, AL.

Argia plana (springwater dancer) is only found at springs or streams heavily influenced by springs. The lilypad forktail (*Ischnura kellicotti*) is quite unusual in that its lifecycle is closely associated with lily pads of the genera *Nuphar* and *Nymphaea* (Harp, 1983). Its distribution, therefore, tends to be disjunct, although it can be abundant locally. While *A. plana* was recorded from only one site in the ONF (Table 2), it should be widely distributed because of the abundance of springs and spring-fed streams. *Ischnura kellicotti* was

recorded from only one site in the ONF also. Lily pads occur quite infrequently in the ONF.

The Interior Highlands (Ozark Plateaus and Ouachita Mountains) support several endemic invertebrate species (Smith, 1984). Those endemic dragonflies found within the ONF include *Gomphus ozarkensis*, *Ophiogomphus westfalli*, and *Somatochlora ozarkensis*. Another endemic species occurring in the ONF, *Gomphus oklahomensis*, is known only from extreme eastern Texas, southeastern Oklahoma, southwestern Arkansas, and northwestern Louisiana. It inhabits mud-bottomed ponds, lakes, creeks and rivers (Dunkle, 2000).

Many *Neurocordulia* spp. (shadowdragons) are common, but the adults spend most of the day hanging from twigs in forested areas. They actively fly only at dawn and dusk, thus escaping the collecting efforts of most odonatists. The result is fewer records for them.

In recent years, the southern pine beetle (SPB) has caused particular damage within Arkansas pine-dominate forests. The most effective control of this pest includes quickly felling pine trees where the beetle is concentrated. These southern pine beetle spots are referred to as SPBs. Of 33 SPBs in the Caddo Ranger District, three were closed due to turkey nesting and three were inaccessible due to terrain. Of the 27 SPBs surveyed, 23 had no dragonflies on site. For six of these 23 sites 1-4 species were found on the access road, near the sites. Only four SPBs had dragonflies on the site proper (1-8 species, Harp and Harp, 2002). In all circumstances, dragonfly presence or absence was due to the presence, proximity or absence of water. A permanent stream bordered the SPB where eight species were found, all being at streamside. In most instances, the dragonflies present were generalists, i.e. the most hardy. The SPBs possessed no features that would encourage dragonfly utilization.

The most important requirement for dragonfly diversity is diversity of aquatic habitat. Seeps and springs are most sensitive, and they typically harbor the least common dragonflies. While dragonflies as a group (Odonata) are not as sensitive to water quality degradation as stoneflies or caddisflies, good water is important. Also of importance are shorelines with relatively shallow gradients. These tend to promote development of beds with diverse aquatic vegetation, which in turn function as oviposition and resting sites, as well as areas of warm, sunny water with good DO concentrations, all beneficial to dragonflies and the organisms upon which they feed.

ACKNOWLEDGMENTS.—Funding was provided by the Ouachita National Forest. John Abbott, Roy J. Beckemeyer, Sidney Dunkle, and Bill Mauffray (FSCA) graciously have given permission for their records to be used.

Literature Cited

Cook, C., and **J. J. Daigle.** 1985. *Ophiogomphus westfalli* spec. nov. from the Ozark Region of Arkansas and Missouri, with a key to the *Ophiogomphus* species of eastern North America (Anisoptera: Gomphidae). Odonatologica 14:89-99.

Dunkle, S. W. 2000. Dragonflies through binoculars: a field guide to dragonflies of North America. Oxford Univ. Press. 266 pp.

Harp, G. L. 1983. A preliminary report on the Zygoptera (Damselflies) of Arkansas. Proc. Arkansas Acad. Sci. 37:87-88.

Harp, G. L., and **P. A. Harp.** 1996. Previously unpublished Odonata records for Arkansas, Kentucky and Texas. Notul. Odonatol. 4(8):127-130.

Harp, G. L., and **P. A. Harp.** 2002. Dragonflies of the Ouachita National Forest. Final Report. 16pp. + app.

Harp, G. L., and **J. D. Rickett.** 1985. Further distributional records for Arkansas Anisoptera. Proc. Arkansas Acad. Sci. 39:131-135.

Moore, N. W. 1997. Dragonflies – Status survey and conservation action plan. IUCN/SSC Odonata Specialist Group. IUCN, Gland, Switzerland and Cambridge, UK. v + 28 pp.

Needham, J. G., M. J. Westfall, Jr., and **M. L. May.** 2000. Dragonflies of North America. Scientific Publishers, Gainesville, Florida. 939 pp.

Robison, H. W., and **T. M. Buchanan.** 1988. Fishes of Arkansas. University of Arkansas Press, Fayetteville. 536 pp.

Smith, K. L. 1984. Animals. *In*: Shepherd, B. (Coord. Ed.) 1984. Arkansas's Natural Heritage. August House, Little Rock. 116pp.

Westfall, M. J., Jr., and **M. L. May.** 1996. Damselflies of North America. Scientific Publishers, Gainesville, Florida. 650pp.

Table 1. Collecting sites for Odonata, Ouachita National Forest, May-September 2002.

1. Shady Lake at Shady Lake Recreation Area, NE1/4Sec31, T4S, R28W, Polk Co., AR, 10 May (1a), 15 May (1b).

2. Wetland at NE corner of jct. US Hwy 270/FS 929, NW1/4Sec20, T1N, R28W, Scott Co., AR, 11 May (2a), 21 July (2b), 12 Sept. (2c).

3. Mill Creek at FS 929, NW 1/4Sec20, T1N, R28W, Scott Co., 11 May
4. Lake Hinkle at Little Pines Rec. Area, NE1/4Sec3, T2N, R31W, Scott Co., AR, 11 May (4a), 18 July (4b).
5. Cedar Lake North Shore, NE1/4Sec32, T4N, R25E, Le Flore Co., OK, 12 May.
6. Red Slough, E 1/2Sec25, T9S, R25E, McCurtain Co., OK, 13 May.
7. Mt. Fork River at The Narrows (FS 28000), E1/2Sec9, T2S, R25E, McCurtain Co., OK, 15 May (7a), 19 July (7b).
8. C-25 Pond, SE1/4Sec26, T3S, R23W, Montgomery Co., AR, 16 May.
9. Pond at end of FS C-25, NW1/4Sec36, T3S, R23W, Montgomery Co., AR, 16 May.
10. Beaver pond near Fancy Hill Lake, SW1/4Sec22, T4S, R26W, Montgomery Co., AR, 16 May (10a), 10-11 Sept (10b).
11. Fancy Hill Lake, SW1/4Sec22, T4S, R26W, Montgomery Co., AR, 16 May (11a), 10 Sept (11b).
12. Caddo Pond, SE1/4Sec19, T4S, R23W, Montgomery Co., AR, 18 May (12a), 12 July (12b), 9 Sept (12c).
13. Pond above Caddo Pond, SE1/4Sec19, T4S, R23W, Montgomery Co., AR, 18 May.
14. Caddo River 1mi SE of Caddo Gap, southcentral Sec19, T4S, R24W, Montgomery Co., AR, 18 May (14a), 10 Sept (14b).
15. FS 476, E1/2Sec22, T3S, R23W, Montgomery Co., AR, 17-19 May.
16. Stream paralleling FS 476 on the north, E1/2Sec22, T3S, R23W, Montgomery Co., AR, 19 May.
17. Collier Creek at Buttermilk Springs Rd., SE1/4Sec31, T3S, R24W, Montgomery Co., AR, 18 May (17a), 19 May (17b).
18. Seep 1mi E of Alamo, Sec151/4, T3S, R23W, Montgomery Co., AR, 19 May.
19. Caney Creek ~ 8km NNE of Glenwood, NW 1/4Sec 18, T4S, R23W, Montgomery Co., AR, 10 July.
20. C-12 Pond, NE 1/4Sec33, T3S, R22W, Garland Co., AR, 11 July.
21. East Fork Caney Creek, Sec18, T4S, R23W, Montgomery Co., AR, 11 July.
22. Meyers Creek along Co Hwy103, Sec16, T3S, R22W, Garland Co., AR, 12 July.
23. Mazarn Creek at St Hwy 227, SE1/4Sec15, T3S, R21W, Garland Co., AR, 14 July.
24. Mazarn Creek from Co Hwy 38 upstream ~ 400m, Montgomery Co., AR, 9 Sept.
25. Richardson Bottoms, on FS 37300, NE1/4Sec12, T1S, R23W, Montgomery Co., AR, 15 July.
26. Dutch Creek 0.4km N St Hwy 80, NE1/4Sec14, T1S, R23W, Yell Co., AR, 16 July.
27. Dutch Creek 0.4km N St Hwy 80, NE1/4Sec29, T4N, R25W, Yell Co., AR 16 July.
28. Southernmost lake of the Blue Moon Wildlife Demo Area (Keith's Pond), 11km W of Waldron, 1/8mi N St Hwy 248, SE 1/4Sec19/NE 1/4Sec30, T3N, R30W, Scott Co., AR, 16 July.

29. Westernmost lake of the Blue Moon Wildlife Demo Area (Moist Soils Wetland), 11km W Waldron, 1/4mi N St Hwy 248, SW1/4Sec 19, T3N, R30W, Scott Co., AR, 18 July.

30. Cedar Lake South Shore, NE1/4Sec32, T4N, R25E, LeFlore Co., OK, 19 July.

31. Cossatot River at FS 30 (Gillham Spgs), NW1/4Sec22, T4S, R30W, Polk Co., AR, 20 July.

32. Westernmost (larger) pond of Mauldin Ponds, N side of FS 37, SE1/4Sec4, T2S, R25W, Montgomery Co., AR, 22 July.

33. Easternmost (smaller) pond of Mauldin Ponds, N side of FS 37, SE1/4Sec4, T2S, R25W, Montgomery Co., AR, 22 July.

34. Camp Clearfork, incl. Clearfork Lake, spring branch at its upper end and Walnut Creek immediately below dam, NE1/4Sec6, T3S, R22W, Montgomery Co., AR, 22 July.

35. Unnamed trib. of South Fk Caddo R., N of C-99 Rd, NCSec29, T4S, R26W, Montgomery Co., AR, 11 Sept.

36. Jones Creek at FS Rd. 837, 1.3km below Lake Hinkle, NE 1/4Sec12, T2N, R31W, Scott Co., AR, 12 Sept.

37. Northernmost lake of the Blue Moon Wildlife Demo Area (Bee Tree Pond), 11km W Waldron, 1.6km N St Hwy 248, NE1/2Sec19, T3N, R30W, Scott Co., AR, 13 Sept.

38. Woodland Pond nr Bee Tree Pond, Blue Moon Wildlife Demo Area, 11km W Waldron, 1.6km N St Hwy 248, NW 1/4Sec19, T3N, R30W, Scott Co., AR, 13 Sept.

39. Fourche LaFave R. 2.9km WNW of Y City, SW 1/4Sec17, T1N, R29W, Scott Co., AR, 13 Sept.

40. Moss Creek Road Pond, N side of FS 159, SW 1/4Sec7, T4N, R24W, Yell Co., AR, 16 Sept.

41. Fourche LaFave R. at St Hwy 307, 3km S Briggsville, Yell Co., AR, 16 Sept.

42. Fourche LaFave R. at St Hwy 7, just below Lake Nimrod dam, SW 1/4Sec32, T4N, R20W, Perry Co., AR, 17 Sept.

43. Cove Creek Lake, FS 210, 9.6km SE Lake Nimrod dam, NW 1/4Sec18, T3N, R19W, Perry Co., AR, 17 Sept.

Table 2. Species list and distributions for Odonata, Ouachita National Forest.

Scientific Name	Common Name	Location
Calopteryx maculata	ebony jewelwing	1a**s*** 17a**s**, 19**s**, 22**s**, 24**s**, 31**s**, 34**s**, 35**s**
Hetaerina americana	American rubyspot	7a, 7b**s**, 14a**s**, 14b**s**, 17a**s**, 23, 31**s**, 36**s**, 41**s**, 42**s**
Archilestes grandis	Great spreadwing	Mazarn[ASUMZ]
Lestes disjunctus australis	common spreadwing	2a, 2b, 2c, 6, 8**s**
Lestes vigilax	swamp spreadwing	9, 10b
Argia apicalis	blue-fronted dancer	4b, 30**s**, 42, 43**s**
Argia bipunctulata	seepage dancer	18
Argia fumipennis violacea	variable dancer	5, 10b, 11b**s**, 30**s**, 32**s**, 33**s**, 34**s**, 36**s**, 38**s**, 39**s**, 40**s**, 41**s**
Argia moesta	powdered dancer	3, 7a, 7b**s**, 12a**s**, 14a**s**, 14b**s**, 17a**s**, 19**s** 23**s**, 24**s**, 26**s** 27**s**, 31**s**, 36**s**, 39**s**, 41**s**, 42**s**
Argia plana	springwater dancer	19
Argia sedula	blue-ringed dancer	14b, 23**s**, 31, 34**s**, 39
Argia tibialis	blue-tipped dancer	23, 27**s**

Argia translata	dusky dancer	14b**s**, 19**s**, 23, 24**s**, 31**s**, 34**s**, 39**s**, 41, 42**s**, Jack Cr. Campground (Logan Co.)[RJB]
Chromagrion conditum	openwing damsel	2a
Enallagma aspersum	azure bluet	2a, 2b, 20, Jack Cr. Campground (Logan Co.)[RJB]
Enallagma basidens	double-striped bluet	11b, 29
Enallagma civile	familiar bluet	1b, 11b, 40, 43
Enallagma daeckii	attenuated bluet	10a
Enallagma divagans	turquoise bluet	5, 13
Enallagma exsulans	stream bluet	4b, 7a, 14a**s**, 14b, 17a, 19, 23, 27, 31, 36, 39, 41, 42
Enallagma geminatum	skimming bluet	34
Enallagma signatum	orange bluet	4a, 5, 6, 11b, 14b, 29, 40, 41, 42, 43
Enallagma traviatum	slender bluet	Lake Sylvia (Polk Co.)[FSCA], Shady[FSCA]
Ischnura hastata	citrine forktail	2a**s**, 2b**s**, 4a**s**, 4b**s**, 6, 10b, 11a**s**, 11b**s**, 12a**s**, 38**s**
Ischnura kellicotti	lilypad forktail	25
Ischnura posita	fragile forktail	1a**s**, 1b**s**, 2a**s**, 2b**s**, 4a**s**, 4b**s**, 5, 6**s**, 9**s**, 10b**s**, 11b**s**, 12a**s**, 12c**s**, 14a**s**, 14b**s**, 17a**s**, 25**s**, 26**s**, 27**s**, 28**s**, 30**s**, 32**s**, 33**s**, 36**s**, 37**s**, 38**s**, 39**s**, 40**s**, 42**s**, 43**s**
Ischnura ramburii	Rambur's forktail	6, 9**s**, 11b, 41
*Nehallenia integricollis***	southern sprite	13
Tachopteryx thoreyi	gray petaltail	15, 17a**s**, 22, 33**s**, 34**s**
Anax junius	green darner	2b**s**, 3, 4a**s**, 10b**s**, 11a**s**, 11b**s**, 12a**s**, 12b**s**, 14a, 14b**s**, 25**a**, 28**s**, 32**s**, 33**s**, 34**s**, 36**s**, 37**s**, 39**s**, 40**s**, 41**s**, 42**s**
Anax longipes	comet darner	9**s**, 12a**s**, 12b**s**, 20, 28, 33
Basiaeschna janata	springtime darner	4a, 16**s**
Boyeria vinosa	fawn darner	36, 41
Epiaeschna heros	swamp darner	1a, 1b**s**, 14a**s**, 15**s**, 17a**s**, 18**s**
Arigomphus lentulus	stillwater clubtail	6
Dromogomphus spinosus	black-shouldered spinyleg	4b**s**, 22**s**, 23**s**, 25, 27**s**, 30, 31, 39**s**
Dromogomphus spoliatus	flag-tailed spinyleg	11b
Gomphus externus	plains clubtail	15
Gomphus ozarkensis	Ozark clubtail	3, 7a, 12a, 14a, 17b
Gomphus graslinellus	pronghorn clubtail	3, 15, 17b
Gomphus oklahomensis	Oklahoma clubtail	3, 11a, 12a
Hagenius brevistylus	dragonhunter	14b**s**, 19**s**, 22**s**, 23**s**, 24**s**, 31**s**, 34**s**, 39**s**, 41, 42**s**, 43**s**
Ophiogomphus westfalli	Arkansas snaketail	Caddo R @ St Hwy 240 (Montgomery Co)[LIT]
Progomphus obscurus	common sanddragon	31
Stylogomphus albistylus	least clubtail	17a, 22, 31
Cordulegaster obliqua	arrowhead spiketail	12a, 12b**s**, 15, 17b, 21, 29
Cordulegaster n. sp.	undescribed spiketail	15
Macromia alleghaniensis	Allegheny River cruiser	23, 29
Macromia illinoiensis	Illinois River cruiser	17a
Epitheca costalis	stripe-winged baskettail	12a, 15
Epitheca cynosura	common baskettail	1a, 1b, 2a, 3, 4a, 6, 12a, 15
Epitheca princeps	prince baskettail	4b, 23**s**, 26
Neurocordulia xanthosoma	orange shadowdragon	27, Ouachita R @ US 270 (Montgomery Co.)[SWD], S Fourche LaFave R @ St Hwy 7 (Perry Co.)[SWD], Fourche LaFave R @ US 71 (Scott Co.)[SWD]
Somatochlora linearis	mocha emerald	11km NE Glenwood (Montgomery Co.)[SWD]
Somatochlora ozarkensis	Ozark emerald	11km NE Glenwood (Montgomery Co.)[SWD], 13km N Jessieville (Saline Co.)[RJB]
Somatochlora tenebrosa	clamp-tipped emerald	11km NE Glenwood (Montgomery Co.)[SWD]

Celithemis elisa	calico pennant	1b, 11bs, 12as, 14as, 20s, 29s, 37s, 43s
Celithemis eponina	Halloween pennant	4bs, 11bs, 15s, 25, 28, 29s, 34s, 37s
Celithemis fasciata	banded pennant	4b, 12b, 28, 29, 37, 32, 36, 40, 43
Celithemis verna	double-ringed pennant	6, 13, 33
Dythemis velox	swift setwing	30
Erythemis simplicicollis	eastern pondhawk	1as, 1b, 2bs, 4bs, 7bs, 10bs, 11as, 11bs, 12as, 12bs, 12cs, 14as, 14bs, 15, 17as, 23, 24s, 25s, 26, 27s, 28s, 29s, 30s, 31s, 32s, 33s, 34s, 36s, 37s, 38s, 40s, 41s, 42s, 43s
Erythrodiplax umbrata	band-winged dragonlet	6, 15
Ladona deplanata	blue corporal	1a, 1b, 4a, 5, 12as, 11a
Libellula auripennis	golden-winged skimmer	11b
Libellula cyanea	eastern spangled skimmer	2a, 2b, 4b, 6, 12a, 12b, 11a, 15, 28, 33
Libellula flavida	yellow-sided skimmer	15, 32s, 33s, 34, Mazarn[ASUMZ]
Libellula incesta	slaty skimmer	2bs, 4bs, 6, 10bs, 11bs, 12as, 12bs, 12cs, 23s, 25s, 27s, 28s, 29s, 30s, 31s, 32s, 33s, 34s, 36s, 37s, 38s, 40s, 41s, 42s, 43s
Libellula luctuosa	widow skimmer	4bs, 12bs, 14bs, 20s, 23s, 25s, 26s, 27s, 28s, 29s, 30s, 31s, 33s, 34s, 37s, 39s, 43s
Libellula pulchella	twelve-spotted skimmer	6, 11bs, 14bs, 37s, 39s, 40s, 41s, 43s
Libellula semifasciata	painted skimmer	15
Libellula vibrans	great blue skimmer	1b, 6, 19s, 31
Orthemis ferruginea	roseate skimmer	36s
Pachydiplax longipennis	blue dasher	1bs, 2as, 2bs, 4bs, 6, 10bs, 11as, 11bs, 12as, 12bs, 12cs, 14as, 14bs, 20s, 24s, 25s, 26s, 27s, 28s, 29s, 30s, 32s, 33s, 34s, 36s, 37s, 40s, 41s, 42s, 43s
Pantala flavescens	globe glider	7bs, 14bs, 26s, 31, 37s
Pantala hymenaea	spot-winged glider	7b, 26s
Perithemis tenera	eastern amberwing	4bs, 6, 10bs, 11bs, 12as, 12bs, 12cs, 14as, 28s, 29s, 30s, 33s, 34s, 36s, 37s, 40s, 41s, 42s, 43s
Plathemis lydia	common whitetail	1as, 2bs, 3s, 4bs, 11bs, 12as, 12bs, 12cs, 14as, 15, 17as, 19s, 20s, 22s, 23s, 25s, 26s, 30s, 31s, 32s, 34s, 37s, 40s, 43s
Simpetrum ambiguum	blue-faced meadowhawk	4bs, 28, 34, 43
Sympetrum corruptum	variegated meadowhawk	6s
Sympetrum vicinum	yellow-legged meadowhawk	35s
Tramea carolina	violet-masked glider	1b, 12b, 25, 33
Tramea lacerata	black-mantled glider	1bs, 3s, 6s, 10as, 10bs, 11bs, 20, 25s, 27s, 28s, 29s, 30s, 31s, 32, 33s, 36s, 37s, 40s, 43s

*Sight identification – no voucher specimen. These species can be field identified reliably
**New record for Arkansas
[ASUMZ]Record from specimen in the ASUMZ
[LIT]Literature record from Cook and Daigle, 1985.
[FSCA]Record from specimen in the Florida State Collection of Arthropoda
[RJB]Record from specimen in the personal collection of Roy J. Beckemeyer.
[SWD]Record from specimen in the personal collection of Sidney W. Dunkle.

Table 3. Number of new species for Arkansas counties in the Ouachita National Forest.

County	No. Anisoptera spp[1]	New	No. Zygoptera spp.[2]	New	Total Odonata
Garland	28	3	6	5	42
Logan	20	0	6	2	28
Montgomery	35	16	12	10	73
Perry	14	7	4	5	30
Polk	24	6	8	2	40
Saline	37	1	9	0	47
Scott	15	16	4	10	45
Yell	24	3	7	6	40

[1]Harp and Rickett (1985)
[2]Harp (1983)

Antiforce Wave Profile for Quasi-Neutral Region

Mostafa Hemmati*, **Pashupati Adhikari, Jeremy Eckart** and **Marcus Ilbara**
Department of Physical Science
Arkansas Tech University
Russellville, AR 72801

*Corresponding Author

Abstract

This article will present a fluid dynamical theory for breakdown waves in which the direction of electric field force on electrons is in the opposite direction of wave propagation. We will refer to such waves as antiforce waves. The set of equations describing the model will include the equation of particle mass balance, equation of conservation of momentum, and equation of conservation of energy, coupled with Poisson's equation. This model treats the potential wave front as an electron shock wave propagating forward mainly due to the electron impact ionization. The shock front is succeeded by a thin dynamical transition region (sheath region) in which the electric field reduces to zero and the electron velocity approaches that of heavy particle velocity. Following the sheath region, ionization continues as long as electrons possess sufficient thermal energy. This thermal region is referred to as the quasi-neutral region. For antiforce waves, we have been able to integrate the set of electron fluid dynamical equations through the sheath region and through the quasi-neutral region. Our results conform to the expected physical conditions at the end of the sheath region and at the end of the quasi-neutral region. For three wave propagation velocities we will present the wave profile for each of the following: the electric field as a function of electron velocity inside the sheath, the ionization rate inside the sheath region and the quasi-neutral region, and the electron temperature and number density inside the quasi-neutral region.

Introduction

Hauksbee (1706) is believed to be the first person to study luminous pulses caused by a large potential difference between two electrodes in evacuated chambers. Hauksbee's research led him to discover the conditions for producing luminous pulses in gases.

Snoddy et al. (1937) made extensive measurements on the speed of propagation of breakdown waves in long discharge tubes containing dry air at different air pressures. In their experiments, they used discharge tubes with three different diameters. They observed that at approximately constant applied potential of 1.25×10^5V and low air pressure range, the breakdown wave speed increases with increasing air pressure. Keeping their tube diameter constant, they did not detect a considerable change in wave propagation speed when they conducted their experiments in dry air, CO_2 or H_2. However, they did discover a linear relationship between breakdown wave speed and applied potential at constant pressure in dry air. They observed that immediately following the initial wave, which propagates from the high voltage end to the grounded end of the tube, a second return stroke would propagate in the opposite direction. For the return stroke, the electric field force on electrons is in the opposite direction of wave propagation. This electric field force, however, is overcome by the electron gas partial pressure, which being very large provides the driving force for wave propagation. Snoddy et al. (1937) reported a wave speed of approximately 10^8 m/s for return discharge waves.

Asinovski et al. (1994) reported that an increase in the applied voltage leads to an increase in wave velocity. They also reported that in a low-pressure region, the propagation speed of breakdown waves of positive polarity is less than those of negative polarity.

A lack of Doppler shift in the spectral lines of the radiation emitted during the gas electrical discharge indicates an absence of heavy particle (ions and neutral particles) motion. The breakdown wave propagation therefore must be due to the electron mobility only. Consequently, Shelton et al. (1968) referred to such waves as Electron Fluid Dynamical Waves. They assumed that the high temperature electron gas expands very rapidly producing an electron shock wave. Therefore, they formulated a set of one-dimensional, steady state, fluid equations to describe breakdown waves. Shelton's set of electron fluid dynamical equations consist of the equation of conservation of mass, momentum, and energy plus Poisson's equation. Using an approximation method, Shelton et al. (1968) solved the set of electron fluid dynamical equations and the results of their approximate solutions conform to experimental results reasonably well.

Fowler et al. (1984) completed Shelton's set of electron fluid dynamical equations, adding several terms to the energy equation, among which the heat conduction term proved to be the most significant one. Also, Fowler et al. (1984) allowed for temperature derivative discontinuity at the shock front. Their allowance for temperature derivative

discontinuity proved to be essential in integration of the electron fluid dynamical equations through the sheath region.

Analysis

Fowler's (1984) set of electron fluid dynamical equations: equations of conservation of mass, momentum, and energy plus Poisson's equation for proforce waves respectively are

$$\frac{d(n\upsilon)}{dx} = \beta n, \tag{1}$$

$$\frac{d}{dx}\{nm\upsilon(\upsilon - V) + nkT_e\} = -enE - KmnV(\upsilon - V), \tag{2}$$

$$\frac{d}{dx}\left\{nm\upsilon(\upsilon - V)^2 + nkT_e(5\upsilon - 2V) + 2e\phi n\upsilon + \varepsilon_0 VE^2 - \frac{5nk^2T_e}{mk}\frac{dT_e}{dx}\right\}$$

$$= -3(m/M)nKkT_e - (m/M)nmK(\upsilon - V^2), \text{ and} \tag{3}$$

$$\frac{dE}{dx} = \frac{en}{\varepsilon_0}\left(\frac{\upsilon}{V} - 1\right). \tag{4}$$

Where E_0 is electric field magnitude at the wave front, m is the electron mass, e is the electron charge, n is the electron number density, E is the electric field inside the sheath, υ is the electron velocity, T_e is the electron temperature, k is the Boltzman's constant, M is the neutral particle mass, K is the elastic collision frequency, x is the position in the wave profile, β is the ionization frequency, ϕ is the ionization potential of the gas, and V is the wave velocity.

For antiforce waves, the electron fluid dynamical equations have to be modified due to the change in the electric field direction at the shock front. Also, we introduce an appropriate set of non-dimensional variables, which takes the direction of the electric field force on electrons into consideration. The non-dimensional variables employed are

$$\eta = \frac{E}{E_0}, \quad \nu = \frac{2e\phi}{\varepsilon_0 E_0^2}n, \quad \psi = \frac{\upsilon}{V}, \quad \theta = \frac{Tek}{2e\phi}, \quad \xi = -\frac{eE_0x}{mV^2}, \quad \omega = \frac{2m}{M},$$

$$\kappa = -\frac{mVK}{eE_0}, \quad \mu = \frac{\beta}{K}, \quad \alpha = \frac{2e\phi}{mV^2}.$$

Where υ is the non-dimensional electron number density, η is the net electric field (applied plus space charge field), ψ is the electron velocity, θ is the electron gas temperature, ξ is the position within the sheath, μ is the ionization rate, κ and α are wave parameters.

In non-dimensional form, the electron fluid dynamical equations representing antiforce waves become:

$$\frac{d(\nu\psi)}{d\xi} = \kappa\mu\nu, \tag{5}$$

$$\frac{d}{d\xi}\{\nu\psi(\psi - 1) + \nu\alpha\theta\} = \nu\eta - \kappa\nu(\psi - 1), \tag{6}$$

$$\frac{d}{d\xi}\{\nu\psi(\psi-1)^2 + \alpha\nu\theta(5\psi - 2) + \alpha\nu\psi + \alpha\eta^2 - \frac{5\alpha^2\nu\theta}{\kappa}\frac{d\theta}{d\xi}\}$$

We will define the variable values at the wave front with a subscript (1), the variable values at the end of the sheath with a subscript (2), and the variable values at the end of the quasi-neutral region with a subscript (f).

$$= -\omega\kappa\nu\left\{3\alpha\theta + (\psi - 1)^2\right\}, \text{ and} \tag{7}$$

$$\frac{d\eta}{d\xi} = -\frac{\nu}{\alpha}(\psi - 1). \tag{8}$$

At the wave front the electron velocity is less than the wave velocity ($\psi_1 < 1$); therefore, according to Equation 8, the net electric field intensity will increase $\{(\frac{d\eta}{d\xi}) > 0\}$ until electrons gain speeds in excess of ions and heavy particles ($\psi > 1$). The electric field then will start decreasing. Since a conductor cannot support an electric field, the magnitude of the electric field has to approach zero at the end of the sheath region ($\eta_2 \to 0$). Without the supporting potential of the electric field the electrons gradually slow down due to collisions with neutral particles until their speeds compare with that of the ions and heavy particles ($\psi_2 \to 1$).

Successful integration of the non-dimensional electron fluid dynamical equations makes it possible to attain values of the variables including electron number density, ionization rate, electron temperature, and position at the end of the sheath region. The variable values at the end of the sheath region will constitute the initial conditions for integration of the set of electron fluid dynamical equations through the quasi-neutral region. The electron number density, ν_f, should approach one at the end of the quasi-neutral region, because the hot electron gas following the sheath region ionizes neutral particles during its cooling. Electrostatic energy density, therefore, is converted into ionization density behind the wave, resulting in neutral plasma. Electrons at the end of the quasi-neutral region reach thermal equilibrium with surrounding heavy particles. The dimensionless electron temperature, θ_f, in this region has to approximately reduce to 0.065.

All attempts in integration of Equations (5-8) through the quasi-neutral region failed. In our final attempt in integration of the set of electron fluid dynamical equations through the quasi-neutral region we chose to utilize the original form of the equations. Expressed in dimensionless variables, these original equations are

$$\frac{d(\nu\psi)}{d\xi} = \kappa\mu\nu, \tag{9}$$

$$\frac{d}{d\xi}\{\nu\psi^2 + \alpha\nu\theta\} = -\nu\eta - \kappa\nu(\psi - 1) + \kappa\mu\nu, \tag{10}$$

$$\frac{d}{d\xi}\left\{\nu\psi^3 + 5\nu\psi\alpha\theta - \frac{5\alpha^2\nu\theta}{\kappa}\frac{d\theta}{d\xi}\right\}$$

$$= -2\nu\psi\eta - 2\kappa\nu(\psi - 1) + \kappa\mu\nu(\psi - 1) - \omega\kappa\nu\left\{3\alpha\theta + (\psi - 1)^2\right\}, \text{ and} \tag{11}$$

$$\frac{d\eta}{d\xi} = -\frac{\nu}{\alpha}(\psi - 1). \tag{12}$$

We will use Ibarra et al.'s (2002) approach to integrate the set of equations through the quasi-neutral region. Expanding the momentum balance equation (Equation 6) and using the equation of conservation of mass balance in the expanded form to solve for $(\frac{d\psi}{d\xi})$, the singularity inherent in the set of equations appears in the denominator of the equation

$$\frac{d\psi}{d\xi} = \frac{\kappa(1+\mu)(1-\psi)\psi - \kappa\mu\alpha\theta - \eta\psi - \alpha\psi\theta'}{\psi^2 - \alpha\theta}.$$

When the denominator in $(\frac{d\psi}{d\xi})$ approaches zero, $(\frac{d\psi}{d\xi})$ approaches infinity. This would indicate a shock within the sheath region. Since no new shock is possible inside the sheath, therefore, the denominator and numerator must both approach zero at the same time. This condition allows one to choose a starting value for $\psi 1$, for a given value of κ, α, and υ_1, by trial and error. We note that, at the end of the sheath region, the electron velocity, ψ, becomes equal to one and $(\frac{d\psi}{d\xi})$ approaches zero. Also, the electric field, ξ, and its derivative, $(\frac{d\eta}{d\xi})$, both approach zero at the end of the sheath region. The resulting formulated equations with respect to previously noted conditions are

$$(\frac{d\nu}{d\xi})_2 = \kappa\mu_2\nu_2, \quad (13)$$

$$(\frac{d\theta}{d\xi})_2 = -\kappa\mu_2\theta_2. \quad (14)$$

We have been successful in integrating equations (13-14) through the quasi-neutral region for antiforce waves propagating into a non-ionized medium. For three wave speeds, our solutions meet the expected conditions at the trailing edge of the wave ($\nu_f \approx 1$, and $\theta_f \approx 0.065$).

Results

For wave speeds of $\alpha = 0.05$, $\alpha = 0.1$, and $\alpha = 1.0$, we have successfully integrated the electron fluid dynamical equations through both the sheath and quasi-neutral region. After integration of Equations (5-8) throughout the sheath region we needed to integrate Equations (13) and (14) through the quasi-neutral region. The following initial values for electron number density (ν_1), electron velocity (ψ_1), and wave parameter (κ) were utilized in order to obtain solutions that met the expected physical conditions at the end of the sheath region and the quasi-neutral region.

α	ν_1	ψ_1	κ
0.05	0.09	0.95	0.3511
0.10	0.14	0.8679	0.2995
1.0	0.40	0.97501	0.175

The data indicates that sheath thickness increases as wave velocity decreases. A value of $\alpha = 0.01$ represents a wave speed of 3×10^7 m/s and $\alpha = 2.0$ represents a moderately slow wave possessing a velocity of 2×10^6 m/s. We were also able to integrate the set of equations through the sheath and quasi-neutral region for $\alpha = 0.005$. $\alpha = 0.005$ represents a fast wave speed of $V = 10^8$ m/s.

Figure 1 is a graph of the electric field, η, as a function of electron velocity, Ψ, inside the sheath region. Figure 2 is a graph of the ionization rate, μ, as a function of position, ξ, inside the sheath region. $\xi = 5.72$ represents a sheath thickness of 0.03 mm.

Figure 3 is a graph of the ionization rate, μ, as a function of position, ξ, inside the quasi-neutral region. Figure 4 is a log-log plot of the electron temperature, θ, as a function of position, ξ, inside the quasi-neutral region. $\theta = 20$ represents an electron temperature of approximately 10^7 K. Figure 5 is a plot of electron number density, ν, as a function of position, ξ, inside the quasi-neutral region. $\nu = 1$ represents an electron number density of approximately 10^{20} electrons/m^3.

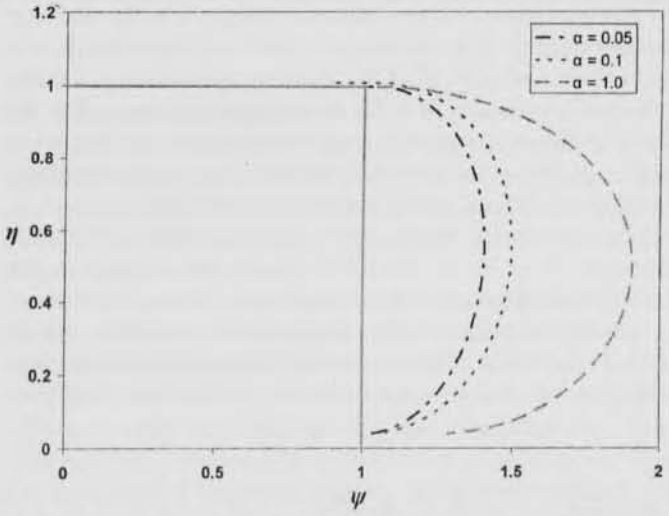

Fig. 1. Electric field, η, as a function of electron velocity, ψ, inside the sheath region for $\alpha = 0.05$, $\alpha = 0.1$, and $\alpha = 1$.

Our study of antiforce waves, or waves that propagate in the opposite direction as the electric field force on electrons, is exemplified in nature by lightning's return stroke. The range of speed for which our integration of the set of electron fluid dynamical equations has been successful, conform to the experimental results reported by Rakov et al. (1998). They employed triggered-lightning experiments to make measurements on lightning propagation speeds, temperatures, light intensity, and electric fields, and their average return stroke speeds are indeed on the order of 10^8 m/s.

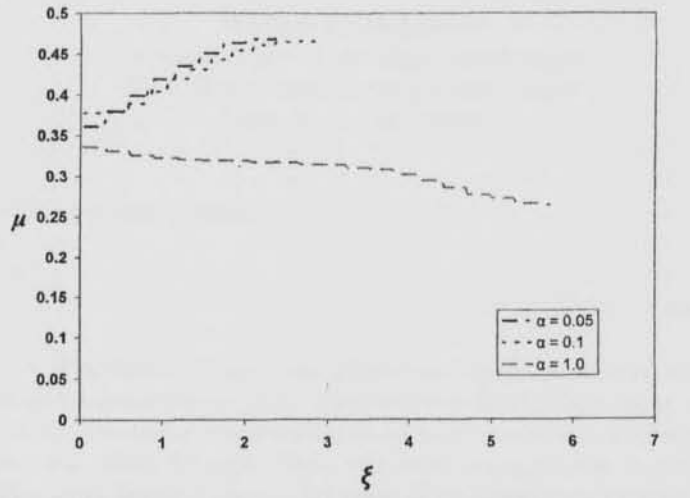

Fig. 2. Ionization rate, μ, as a function of position, ξ, inside the sheath region for $\alpha = 0.05$, $\alpha = 0.1$, and $\alpha = 1$.

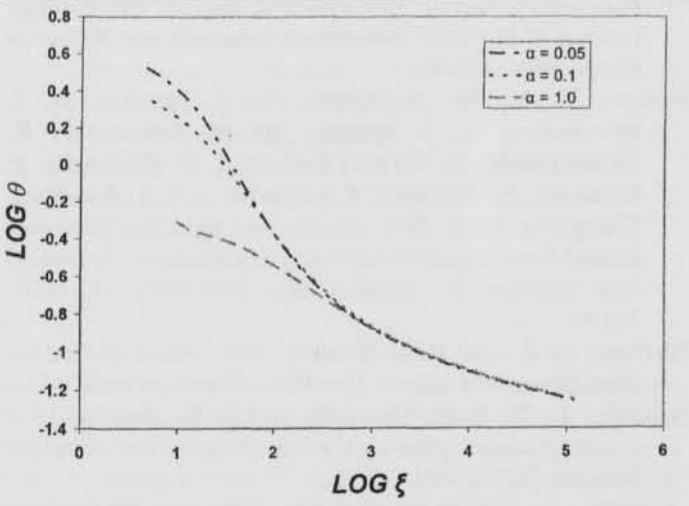

Fig. 4. Electron temperature, θ, as a function of position, ξ, inside the quasi-neutral region for α=0.05, α=0.1, and α=1.

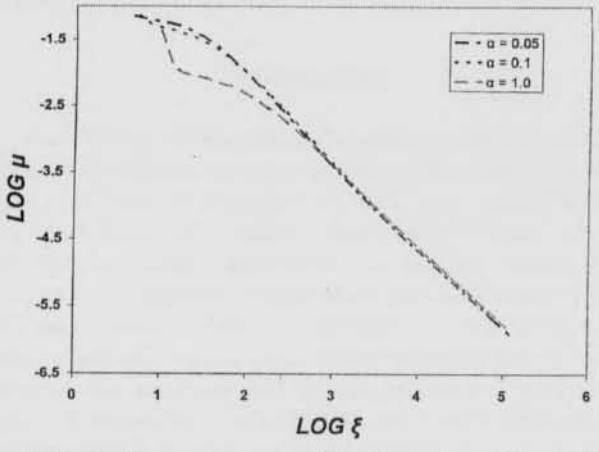

Fig. 3. Ionization rate, μ, as a function of position, ξ, inside the quasi-neutral region for α=0.05, α=0.1, and α=1.

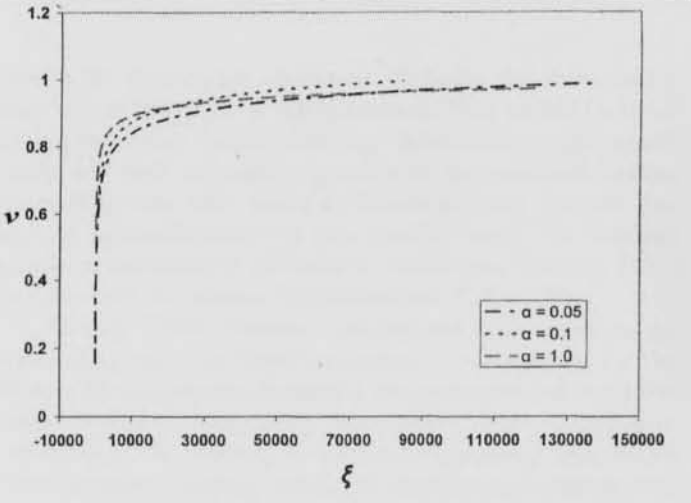

Fig. 5. Electron number density, ν, as a function of position, ξ, inside the quasi-neutral region for α=0.05, α=0.1, and α=1.

Conclusions

For antiforce waves, we have been able to integrate the set of electron fluid dynamical equations through both the sheath region and the quasi-neutral region for a range of wave speeds. The solutions meet the expected physical conditions at the end of the sheath region and the quasi-neutral region. The range of speeds for which integration of the set of electron fluid dynamical equations become possible conforms to the experimental results. This is another confirmation on the validity of the application of fluid equations to breakdown waves.

ACKNOWLEDGMENTS.—The authors would like to express their gratitude to the Arkansas Space Grant Consortium and the Scientific Information Liaison Office for their financial support of this project.

Literature Cited

Asinovsky, E. I., A. N. Lagarkov, V. V. Markovets, and **I. M. Rutkevich.** 1994. On the similarity of electric breakdown waves propagating in shielded discharge tubes. Plasma Sources Sci. Technol. 3:556-563.

Fowler, R. G., M. Hemmati, R. P. Scott, and **S. Parsenajadh.** 1984. Electric breakdown waves: Exact numerical solutions. Part I. Phys. Fluids. 27:1521-1526.

Hauksbee, F. 1706/7. An account of an experiment, confirming one lately made, touching the production of light, by the effluvia of one glass falling on another in motion. Phil. Trans. Roy. Soc. 25:2413.

Ibarra, M., R. C. Cook, and **M. Hemmati.** 2002.

Breakdown waves: quasi-neutral region. Proceedings Journal of the 2002 Arkansas Undergraduate Research Conference. 143-151.

Rakov, V. A., M. A. Uman, K. J. Rambo, M. I. Fernandez, R. J. Fisher, G. H. Schnetzer, R. Thottappillil, A. Eybert-Berard, J. P. Berlandis, P. Lalande, A. Bonamy, P. Laroche, and **A. Bondiou-Clergerie.** 1998. New insights into lightning processes gained from triggered-lightning experiements in Florida and Alabama. J. Geophys. Res. NO. D12. 100:14117-14130.

Shelton, G. A., and **R. G. Fowler.** 1968. Nature of electron fluid dynamical waves. The Phys. Fluids. 11:740-746.

Snoddy, L. B., J. R. Dietrich, and **J. W. Beams.** 1937. Propagation of potential in discharge tubes. Physical Review. 52:739-746.

Nesting Willow Flycatchers Discovered at Harrison, Arkansas

William C. Holimon*
Arkansas Natural Heritage Commission
1500 Tower Building, 323 Center Street
Little Rock, AR 72201

Douglas A. James
Department of Biological Sciences
University of Arkansas
Fayetteville, AR 72701

*Corresponding Author

Abstract

The Willow Flycatcher, *Empidonax traillii* (Audubon), was a newly discovered species when John James Audubon found it at Arkansas Post in 1822. The bird was fairly common in summer in prairie-scrub habitat around Arkansas at least until the 1950s. Thereafter numbers declined until one or two individuals were found occasionally at a single site in Benton County in the late 1980s through 1990s. We found a population consisting of three nesting territories on Baker Prairie Natural Area in Harrison, Boone County, Arkansas. This represents the first confirmed nesting since 1990 and only the second since 1969. A nest with eggs was located 10 July 2002; fledglings were being fed by parents in two territories on 6 August, and only an empty nest was found in the third territory. Baker Prairie is protected by the Arkansas Natural Heritage Commission and The Nature Conservancy. The habitat, tallgrass prairie fringed with woody scrub vegetation, will be managed to benefit the flycatcher.

Introduction

The Willow Flycatcher, *Empidonax trailli* (Audubon), was a newly discovered species when John James Audubon found it at "Fort of Arkansas" in 1822, now called Arkansas Post (Audubon, 1831, 1839; Arthur, 1937). This is the only bird species newly described for science based on a discovery in Arkansas. Audubon found the bird on 17 April 1822 and characterized it as residing "in the skirts of the woods along the prairie lands of the Arkansas River," which describes the southern end of the Arkansas Grand Prairie region. A female bird he collected was listed as having "five pea sized eggs" developing in the ovary.

There has always been consternation concerning Audubon's date because in recent times the summer resident Willow Flycatcher, a late migrant, does not reach Arkansas until May, often well into May (James and Neal, 1986; White, 1995). To investigate this puzzle, Thomas Foti and the late Jane Stern organized a team of observers to monitor Willow Flycatcher activity periodically in 1969 at the last known nesting area in the Grand Prairie area (Foti, 1971), a site now preserved as the Konecny Grove Natural Area at Slovak in Prairie County, Arkansas. Investigators visited the site at frequent intervals from early April into July. The first Willow Flycatchers arrived in early May, nesting occurred in late May into June, and young birds were fledged in late June into July (James and Neal, 1986). Brooke Meanley had earlier also made frequent visits (Meanly, 1952) to a Grand Prairie site. The first pair of flycatchers he found arrived 10 May, nests were built by 28 May, and the first eggs were found in nests 31 May. All this evidence suggests that Audubon may have stated the wrong month for his female specimen. Perhaps the more likely date was 17 May, not 17 April, because May would be more appropriate for females having developing eggs nearly ready for nest deposition given the documented nesting chronology for this species. However, this species has arrived unusually early in two nearby states. The earliest known arrival date is 20 April in Oklahoma (Sutton, 1967) and 24 April in Indiana (Mumford and Keller, 1984).

Aldrich (1951) further complicated this situation by concluding that Audubon's museum type specimen for the Willow Flycatcher was actually a long winged dark northern form probably migrating northward when Audubon collected it. According to present taxonomy (American Ornithologists' Union, 1998), if Aldrich was correct this would make the specimen a different species, the present Alder Flycatcher now named *Empidonax alnorum* (Brewster, 1895) rather than the Willow Flycatcher, *Empidonax traillii* (Audubon). However, Browning (1993) concluded that the specimen Aldrich inspected was not the same one Audubon collected from Arkansas in 1822. Browning stated that measurements of the specimen did not conform to those given by Audubon and that the specimen's worn plumage suggests that it was collected much later than April. Browning further concluded that the actual type of the Willow Flycatcher collected by Audubon was lost and that the alleged type USNM 1865 did not meet criteria to be a type specimen. In addition, Browning speculated that because birds do not migrate with developing eggs and because the Alder Flycatcher is not known to nest in Arkansas, that the bird Audubon observed and described in 1822 was a Willow Flycatcher that arrived and nested early. Moreover, because the Willow Flycatcher is the only species

that resembles Audubon's illustration and breeds in Arkansas, Browning concluded that nomenclature stability was best served by retaining the name *traillii* Audubon as the specific name for this species.

The American Ornithologists' Union (1973), following the opinion of Eisenmann (committee chairman), reached the same conclusion as Browning using similar reasons when it divided *Empidonax traillii* into two species and retained *traillii* Audubon as the specific name for the Willow Flycatcher (Banks, pers. comm.). However, Eisenmann did not subsequently publish on this opinion. The work by Browning (1993) is therefore considered the authority on this subject (Banks, pers. comm.). The type specimen USNM 1865 of the Willow Flycatcher was refuted by the American Museum of Natural History based on Browning's work (Dean, pers. comm.). Because the only other two type specimens for this species were collected in Oregon and represent *E. t. brewsteri*, the illustration from Arkansas in Audubon's elephant portfolio now serves as the type specimen for the subspecies *E. t. traillii* (Browning, 1993).

Regardless of the date puzzle, this present paper is devoted to documenting the recolonization of the Willow Flycatcher as a nesting bird in Arkansas after its apparent disappearance or near disappearance for about 30 years from around the 1970s to the 2000s. The species probably was abundant in Arkansas when Audubon discovered it because it was subsequently reported to be numerous in suitable habitat around the state until the 1950s (James and Neal, 1986). After which, a rapid decrease followed (James, 1974; James and Neal, 1986).

Methods

We conducted field investigations at Baker Prairie Natural Area, a 71-acre nature preserve co-owned and managed by the Arkansas Natural Heritage Commission and The Nature Conservancy, located in Harrison, Boone County, in northern Arkansas. This site protects a small remnant of tallgrass prairie, which was part of the Osage Prairie that historically covered a large portion of Boone County (Marsh, 1978; Arkansas Natural Heritage Commission, 2001), but now is mostly converted to other land uses. In addition to tallgrass prairie, various shrubs, saplings, and trees grow along a fencerow that borders a pasture adjacent to the western side of the prairie and along an abandoned fencerow within the western half of the Natural Area.

We used territory mapping (Bibby et al., 1997) to determine the number of Willow Flycatcher territories. Males engaged in territorial behavior (song, courtship, and defense) were noted and their locations marked on a study-area map. Locations of adults provisioning nestlings or young juveniles also were mapped. Territorial mapping was conducted between 21 June and 29 August 2002 with resulting territories delineated using the total mapping technique (Lancia et al., 1994).

We searched for and monitored nests between 27 June and 29 August 2002 to determine nesting success and productivity. These searches were accomplished by following adults carrying food or nesting material and by inspecting habitat suitable for nest sites. Once a nest was discovered, we minimized nest disturbance by making only a limited number of subsequent nest visits, about once a week. A hand-held vanity mirror was used to check nest contents for nest heights above eye level. We checked nests for number of eggs and nestlings, brood parasitism, signs of predation, with type of substrate and nest height also noted. Nests were considered successful if at least one young fledged. To confirm nest success, we made observations of adults feeding young fledglings within territories.

Results

At least six Willow Flycatchers representing three active territories were found on Baker Prairie (Fig. 1). Nests were located in two of the territories, and fledglings being fed were seen in the third one. All three territories produced young birds that successfully fledged. Territory sizes were estimated as 0.64 ha, 1.41 ha, and 0.80 ha for an overall average of 0.95 ha ± 0.40 SD. These territory-size estimates were consistent with those reported from the literature for other Willow Flycatcher populations (Sedgwick, 2000). The center of territory A ran north-south along the interior fencerow within the western half of the natural area and was 284 m northeast of the center of territory B. Territory B was located in the southwestern corner of the natural area with much of the territory running north-south along the western fencerow. The center of territory C was 240 m east of the center of territory B and ran east-west along a fencerow until it intersected a second fencerow, at which point it turned south. The center of territory C was 233 m south of the center of territory A. For all territories, mean distance from the center of one territory to the other was estimated as 252.3 m ± 27.6 SD.

One active nest with four flycatcher eggs and no Brown-headed Cowbird (*Moluthrus ater*) eggs was found in territory A on 10 July 2002. The nest was approximately 3.0 m above the ground in the lowest crotch of the main stem in the upper portion of a smooth sumac (*Rhus glabra*). Nest dimensions were 3.18 cm for inner height, 5.72 cm for outer height, 5.93 cm for inner diameter, and 6.79 cm for outer diameter. On 6 August 2002 three fledglings were seen being provisioned by parent birds within a few meters of this nest. The fledglings on this date had a tail length about 2/3 that of an adult, a clearly visible juvenile gape, and flicked their tails much like adults. No Willow Flycatcher fledglings or adults were observed in this territory on 29 August 2002.

Although no nests were found in territory B, we observed adults provisioning at least three fledglings there on 6 August 2002. These fledglings had a tail length approximately 3/4 that of an adult and a barely visible juvenile gape. The fledglings constantly followed the adults, but were never observed being fed by them. Two Willow Flycatchers were observed in this territory on 29 August 2002, but we could not determine if they were juveniles or adults. No juvenile cowbirds were observed in this territory, though two cowbird eggs were found on 27 June 2002 in a Bell's Vireo (*Vireo bellii*) nest located within the flycatcher territory.

A second flycatcher nest, already abandoned, was discovered on 6 August 2002 in territory C. The nest was approximately 1.27 m above the ground in a crotch of the upper portion of a smooth sumac. Nest dimensions were not measured. A pair of adult Willow Flycatchers was observed in this territory, but was never seen provisioning fledglings. On 29 August 2002, a single Willow Flycatcher fledgling was seen foraging in the vicinity of one of the adults.

Discussion

Our observations show that the Willow Flycatcher is again nesting in Arkansas after being assumed extirpated since the early 1980s (James and Neal, 1986), though sporadic observations have been reported at Lake Bentonville near Rogers, Arkansas (Arkansas Audubon Society Bird Record Files). The bird once was a common breeder across much of Arkansas, particularly in patchy, shrubby areas of prairies and other open habitats. Unfortunately, this species began to decline rapidly in the mid-1900s and by the early 1970s was considered to be endangered in Arkansas (James, 1974). The Arkansas Natural Heritage Commission, based on input from ornithologists across the state, lists the breeding populations of the Willow Flycatcher in Arkansas as extremely rare and especially vulnerable to extirpation. Though occasional sightings of singing males have occurred over the last two decades, the last known definite nesting success in Arkansas was in 1969 at the Konecny Grove Natural Area, near Slovak in Prairie County (James and Neal, 1986). A few birds lingered there through 1982, but no nest searching was performed after 1969, and no birds were found after 1982 (James and Neal, 1986; Foti, pers. comm.). In addition, Mike Mlodinow observed one to two pair of Willow Flycatchers in the nesting season at a site near Rogers, Benton County, Arkansas (Lake Bentonville area) from 1986-1999, and Jimmy Woodard found a nest with nestlings there in 1990 (Arkansas Audubon Society Bird Record Files). The nest was not monitored subsequently, so its fate is unknown.

Our data, combined with anecdotal evidence from the prior two years, suggest that Willow Flycatchers have become fairly well established at Baker Prairie. At least three pair attempted to nest in 2002 and all three were successful. The site of territory B, where there was confirmed breeding in 2002, was found to have birds in 2001 (Stewart, pers. comm.) and in 2000 (Holimon, pers. obs.). It therefore seems that the Willow Flycatcher has been established at Baker Prairie for at least three years. Bird watchers and ornithologists often visit the prairie but did not find Willow Flycatchers there until 2000.

Chief threats to the Willow Flycatcher are habitat loss, brood parasitism by brown-headed cowbirds, and predation. These threats led to the listing of the southwestern subspecies of this bird as federally endangered (U.S. Fish and Wildlife Service, 1995). In contrast, eastern populations, with the exception of those in Arkansas, are relatively stable and have shown only a slight trend in population declines over the past three decades (Sauer et al., 2001). Eastern populations are not as greatly impacted by cowbird parasitism compared to the southwestern subspecies (Sedgwick, 2000). Habitat loss may be the primary factor leading to the extirpation of the flycatcher in Arkansas. For example, less than 1% of the tallgrass prairie remains in the Grand Prairie Natural Division (Heitmeyer et al., 2000) where Audubon found the bird (Audubon, 1831, 1839; Arthur, 1937). Most of the area now is converted to agricultural fields (Heitmeyer et al., 2000). Willow Flycatchers were common in the Grand Prairie and in other places in the state until the mid-1950s (Howell, 1911; Wheeler, 1924; Baerg, 1951; Meanley, 1952; James and Neal, 1986). However, since then nearly all suitable breeding habitat has been gradually converted for other land uses, and no breeding on the Grand Prairie has been observed since 1969, although some birds lingered at the last nesting site, Konecny Grove Natural Area, until 1982 (James and Neal, 1986). One nest near Rogers, Arkansas, (Arkansas Audubon Society Bird Records File) is the only nest found between 1969 and the present study in 2002. This present study therefore represents the re-discovery of nesting Willow Flycatchers, which were thought to have disappeared or nearly so, as successful nesting birds in Arkansas after 1969.

In addition to habitat loss due to agriculture, general habitat degradation also strongly influenced the extirpation of the Willow Flycatchers from Arkansas. Fire suppression has led to shrubby areas succeeding to more mature woody habitat with structure not suitable for flycatcher nesting. Excessively frequent fire is a problem also. Willow Flycatchers nest in shrubby habitat bordering fallow fields and prairie patches (Sedgwick, 2000). Prairie preserves are regularly burned to manage against invasion of woody vegetation. These fires often sweep through the fringing shrubby vegetation that the flycatcher seeks. Nearby

standing or flowing water is also a commonly-found component of the bird's nesting habitat (Sedgwick, 2000). Land drainage projects have adversely affected these conditions.

Our documentation of the presence of this species will help shape conservation efforts at Baker Prairie. The Arkansas Natural Heritage Commission and The Nature Conservancy have built fire lines around the sites of Willow Flycatcher territories so that habitat would not be lost during prescribed burns in 2003. In addition, woody vegetation along fencerows that is too tall (> 2.5 m) for the flycatchers will be burned or mechanically removed. These actions should help maintain Willow Flycatcher habitat and help create additional habitat (Sedgwick, pers. comm.). Habitat in existing territories will be burned in a few years to avoid succession that would lead to unsuitable breeding habitat.

We will continue to monitor the Willow Flycatcher population at Baker Prairie to determine population trends. In addition, it is possible that the area will begin to act as a source population for colonizing shrubby areas along fencerows in adjacent pasture lands. More thorough surveys will be conducted in these areas over the next few years to determine if colonization by the flycatcher occurs. Though the current numbers are small, there may be enough suitable habitat to eventually support 10 or more breeding pair in this area, which could be adequate for a stable population (Sedgwick, pers. comm.).

We believe that our study could indicate that the eastern population of the Willow Flycatcher is expanding southward and/or that small, isolated remnant populations in Arkansas have gone undetected. More intensive monitoring needs to be conducted at the Lake Bentonville area near Rogers, Arkansas, to determine occurrence, breeding success, frequency of use, potential for population growth, and needed management strategies. Further, habitat in extreme northeast Arkansas needs to be investigated for nesting Willow Flycatchers. Indeed, three Willow Flycatchers with brood patches were captured in Craighead County in the summer of 2003 suggesting that a small breeding population of that species likely occurs there (Bednarz, pers. comm.). Finally, the Buffalo National River, because its hydrologic processes are largely intact, should also be more closely surveyed in areas where seasonal floods create open shrubby habitat.

ACKNOWLEDGMENTS.—We thank Jack Stewart, Max Parker, Martha Milburne, and Sally Jo Gibson for monitoring efforts that helped in determining when to begin the field season and where to look for the flycatchers. Comments and suggestions by W. Baltosser and J. Bednarz greatly improved the manuscript. We also thank Tom Foti, Joe Neal, Scott Simon, Mike Mlodinow, and Theo Witsell for their input.

Literature Cited

Aldrich, J. W. 1951. A review of the races of the Traill's flycatcher. Wilson Bull. 63:193-194.

American Ornithologists' Union. 1973. Thirty-second supplement to the American Ornithologist' Union checklist of North American birds. Auk 90:411-419.

American Ornithologists' Union. 1998. Check-list of North American birds, 7th ed. Am. Ornithologists' Union, Washington, D.C.

Arkansas Natural Heritage Commission. 2001. Annu. Rept. 2001. 190 pp.

Arthur, S. C. 1937. Audubon, an intimate life of the American woodsman. Harmanson Publ., New Orleans.

Audubon, J. J. 1831. Ornithological Biography. Vol. 1. A. & C. Black, Edinburgh.

Audubon, J. J. 1839. Ornithological Biography. Vol. 5. A. & C. Black, Edinburgh.

Baerg, W. J. 1951. Birds of Arkansas. Univ. Arkansas Agric. Exp. Sta., Bull. No. 258 (rev.), 188 pp.

Bibby, C. J., N. D. Burgess, and **D. A. Hill.** 1997. Bird census techniques. Academic Press, Inc., San Diego, California.

Brewster, W. 1895. Notes on certain flycatchers of the genus *Empidonax*. Auk 12:157-163.

Browning, M. R. 1993. Comments on the taxonomy of *Empidonax traillii* (willow flycatcher). West. Birds 24:241-257.

Foti, T. 1971. The Grand Prairie. Ozark Soc. Bull. 4:6-11.

Heitmeyer, M. E., L. H. Fredrickson, and **S. King.** 2000. An evaluation of ecosystem restoration for the Grand Prairie of Arkansas. A Report Prepared for: U.S. Army Corps of Engineers, Memphis District. 72 pp.

Howell, A. H. 1911. Birds of Arkansas. U.S. Dept. Agric., Biol. Surv. Bull. No. 38, 100 pp.

James, D. A., and **J. C. Neal.** 1986. Arkansas birds, their distribution and abundance. Univ. Arkansas Press, Fayetteville, Arkansas.

James, F. C. 1974. Threatened native birds of Arkansas, Pp. 107-122 *In* Arkansas Natural Area Plan. Arkansas Dept. Planning, Little Rock, Arkansas.

Lancia, R. A., J. D. Nichols, and **K. H. Pollock.** 1994. Estimating the number of animals in wildlife populations. Pp. 215-253 *In* T.A. Bookout, ed. Research and management techniques for wildlife ad habitats. Fifth ed. The Wildl. Soc., Bethesda, Maryland.

Marsh, M. 1978. Baker Prairie, Critical habitat for Grasshopper Sparrow and Ornate Box Turtle. Ozark Soc. Bull. 12:10-11.

Meanley, B. 1952. Notes on nesting Traill's Flycatcher in eastern Arkansas. Wilson Bull. 64:111-112.

Mumford, R. E., and **Keller, C. E.** 1984. The birds of Indiana. Ind. Univ. Press, Bloomington, Indiana.

Sauer, J. R., J. E. Hines, and **J. Fallon.** 2001. The North American Breeding Bird Survey, Results and Analysis 1966 - 2000. Version 2001.2, USGS Patuxent Wildlife Research Center, Laurel, Maryland. (http://www.mbr-pwrc.usgs.gov/bbs/bbs.html)

Sedgwick, J. A. 2000. Willow Flycatcher (*Empidonax traillii*). *In* The Birds of North America, No. 533 (A. Poole and F. Gill, eds.). The Birds of North America, Inc., Philadelphia, Pennsylvania.

Sutton, G. M. 1967. Oklahoma birds. Univ. Okla. Press, Norman, Oklahoma.

U.S. Fish and Wildlife Service. 1995. Final rule determining endangered status for the Southwestern Willow Flycatcher. Fed. Reg. 60:10694-10715 (February 27, 1995).

Wheeler, H. E. 1924. The birds of Arkansas. Ark. Bureau Mines, Manufacturers, Agric., Little Rock, 177 pp.

White, M. 1995. A Birder's Guide to Arkansas. Am. Birding Assoc., Inc., Colorado Springs, Colorado.

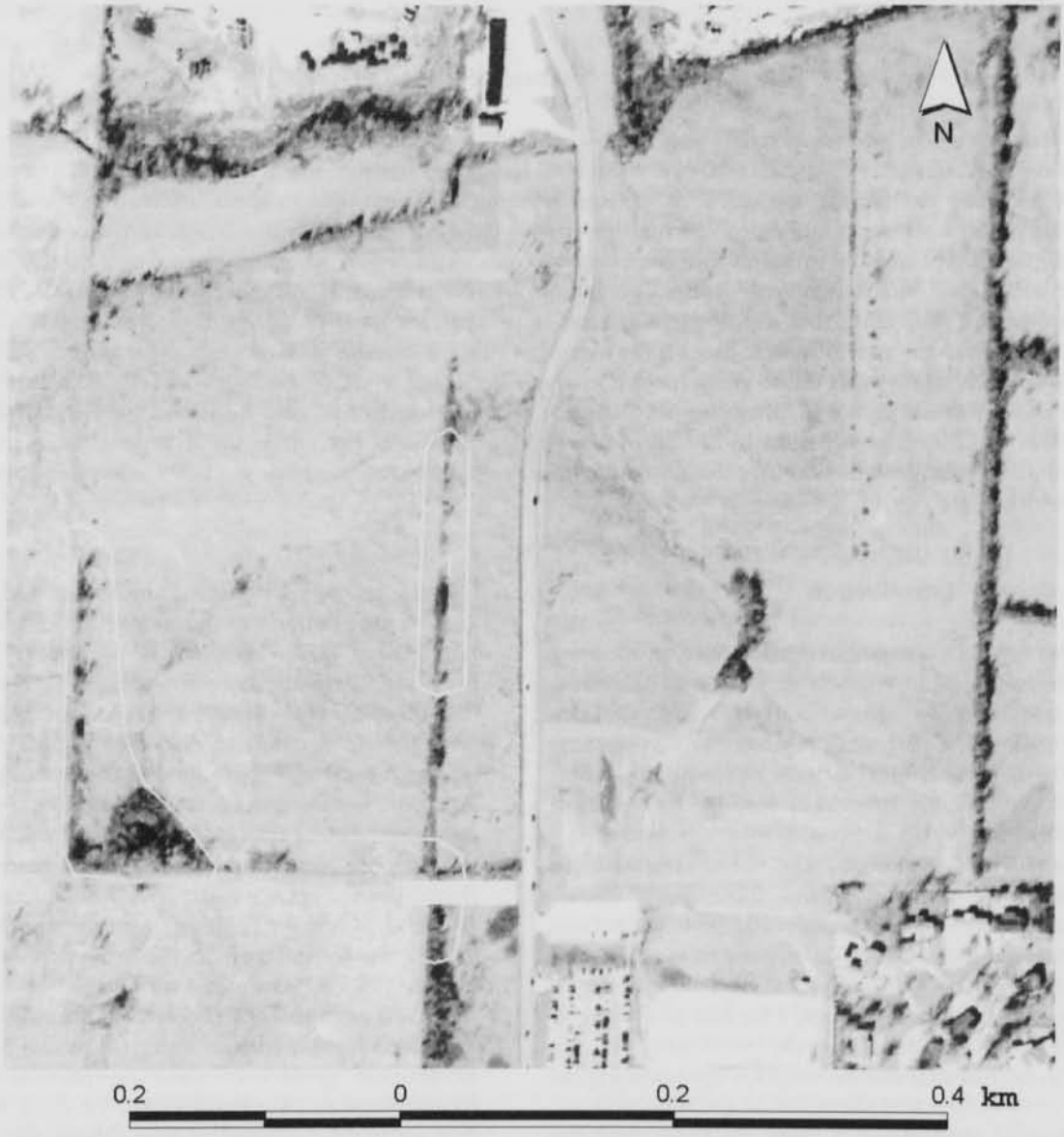

Fig. 1. Aerial photo of Harrison shows the location of three Willow Flycatcher territories at Baker Prairie Natural Area in 2002. Goblin Drive bisects the area from north to south.

The Use of Irradiated and Formalin-fixed *Trichomonas vaginalis* to Examine Protective Immune Responses in the Mouse Intraperitoneal Model

Terryl L. Hostetler and **James J. Daly***
Department of Microbiology
and Immunology
University of Arkansas for
Medical Sciences
Little Rock, AR 72205

Timothy J. O'Brien
Department of Obstetrics
and Gynecology
University of Arkansas for
Medical Sciences
LittleRock, AR 72205

Max L. Baker
Department of Radiology
University of Arkansas
for Medical Sciences
Little Rock, AR 72205

*Corresponding Author

Abstract

Gamma irradiated *Trichomonas vaginalis* was used to initiate a protective immune response in mice by intraperitoneal inoculation using host mortality as the measure of virulence. Irradiated trichomonads of a virulent strain gave some immune protection but no more so than the use of formalin-fixed, virulent trichomonads. A formalin-fixed virulent strain combined with complete Freund's adjuvant (CFA) gave complete protection. Metabolically produced antigens do not appear to be important in conferring protective immunity in these experiments. A common laboratory strain of *T. vaginalis* (ATCC 30001) was used as an avirulent control. It gave no protection against a virulent strain. Combining CFA with ATCC 30001 (avirulent) gave partial protection indicating that a protective antigen is present, but needed an immune stimulant to be detected. IgG analysis corresponded to the mortality results with the avirulent strain being the weakest responder and the strongest being the formalin-fixed virulent strain with CFA. Western blot analysis indicated a band of about 31-kDa that was present using the protocols that showed from partial to complete protection. This band was not present using the avirulent strain but appeared with the addition of CFA. These results indicated that a 31-kDa protein is present in the avirulent strain but it requires an immune stimulant to be revealed. Whether this antigen confers protective immunity or not in the mouse intraperitoneal model is an open question.

Introduction

Trichomonas vaginalis, a flagellated protozoan, produces a fulminant vulvovaginitis in women. It is one of the most common venereal disease agents and is transmitted by males, who for the most part, may not have any symptoms themselves. The general clinical aspects, chemotherapy, and immunology have recently been reviewed by Krieger and Alderete (1999). The drug metronidazole has been very effective against this organism, but cases resistant to treatment and drug resistant strains have been found. Immunotherapy has been considered, but protective immunity to this parasite appears to be poor or non-existent .However, evidence for both humoral and cell-mediated immune responses have been found. This has given rise to the possibility of a vaccine or at least for an immunodiagnostic test that can be used for epidemiological purposes.

Immunological studies on *T. vaginalis* have used the mouse as the primary animal model. Three routes have been used for antigen exposure to develop an immune response and each has its positive and negative aspects: Intraperitoneal (IP) and intramuscular (IM) injections and vaginal inoculation are the routes used (Warren et al. 1960; Honigberg, 1978; Abraham et al., 1996). IM models are preferred to IP methods for antigen inoculation since IM uses ulcer development as a measure of pathology and does not cause host death as does IP. Vaginal models in mice, although more closely related to the parasites normal site of infection, are the most complex models. They require sterol injections and/or manipulation of *Lactobacillus* flora to make the vaginal vault receptive to maintaining *T. vaginalis* populations (McGrory and Garber, 1992; Abraham et al., 1996). Unfortunately, although more clinically realistic, the vaginal model suffers from the same problem as the human vagina. Direct exposure to antigen does not seem to stimulate an apparent protective immunity. However, IM injections combined with a vaginal model have been shown to provide protection reducing parasite populations in mouse vaginas (Abraham et al., 1996). It has been shown that circulating antibodies may diffuse through the vaginal mucosa and give some degree of protection, therefore giving hope for developing an anti-trichomonad vaccine. The more easily accomplished IP route has also been used

for studying immune responses but has been most effective in studying strain virulence (Honigberg, 1978). Death of the host and time of death, usually in days, have been measurements used to determine relative virulence of a strain in the IP model.

The primary objective of this study was to use irradiated *T. vaginalis* to stimulate a protective immune response using the IP model. Protective antigens may be metabolically produced rather then being part of the pathogen's cellular structure. As a rule, reproduction is halted but the organisms continue to metabolize. In some cases, reproduction has not been affected, but the pathology usually produced has been attenuated. It has been shown with a number of protozoan parasites that irradiated cells can produce a more efficient immune response than crude cellular extracts (Hostetler., 1987). The IP route was considered to be the best choice for these experiments based on ease of manipulation of the model and the fact that the environment of the peritoneal cavity would serve as a nutritionally supportive locale for irradiated trichomonad survival. Previous studies on the survival of *T. vaginalis* with gamma radiation showed a dosage whereby trichomonads would remain metabolically active but unable to reproduce (Daly et al., 1991). Different treatment protocols for preparation of antigen source were used for comparison and as controls. IgG response was measured for each of these treatments, and Western blot analysis was used to detect protein(s) that might be protective.

Materials and Methods

The experimental design include the following: (1) selection of a virulent and avirulent strain of *T. vaginalis* based on IP inoculation, (2) gamma irradiation of *T. vaginalis,* (3) determination of the length of time irradiated trichomonads would survive in vitro, (3) determination of the number and quantity of sensitizing antigen doses needed to illicit a protective immune response, (4) IgG analysis to correlate with the mortality or protection seen with challenges to the respective inoculation protocols, and (5) Western blot analysis to determine protein bands associated with protective immunity.

A. *Trichomonas vaginalis* strains and Growth Medium. *T. vaginalis* strain ATCC 30001 was used as the avirulent agent, and two isolates from clinical cases of trichomoniasis, designated C_1 and C_2, were used as the virulent strains. Trichomonads were grown in TYM medium (Diamond, 1957) with 10% heat inactivated (56° C) Seitz-filtered human serum. Serum was obtained from the clinical laboratories of the University of Arkansas for Medical Sciences Hospital.

B. Experimental animals. Female BALB/c mice were obtained from the National Center for Toxicological Research (Jefferson, AR) or purchased from SASCO Incorporated (Omaha, NE). Mice, 3 or 24 weeks of age, were used in some experiments to determine if age affects the immune response.

C. Preparation of Inocula. *T. vaginalis* strains were grown to a concentration of 10^4/ml and passaged three times at this population level to insure that cells were in the logarithmic phase of growth. Cells were harvested from 100 ml of medium at 500xg in 50 ml centrifuge tubes. The cells were resuspended and washed 3x in sterile phosphate buffered-saline (PBS – pH 7.2). The final pellet was suspended in buffer and adjusted to the final cell concentrations to be used. *T. vaginalis* were irradiated with gamma radiation from a $Cesium^{137}$ irradiator by the methods of Daly et al. (1991). Total cell counts were made in a Neubauer hemocytometer, and viable counts were with the semi-soft agar technique of Ivy (1961) as modified by Matthews and Daly (1974).

D. Trypan Blue Dye Exclusion. Fifty µl of cells to be tested was removed from irradiated and control (nonirradiated cells) culture tubes. Trypan blue dye was added to a final concentration of 0.4%. After mixing, the two suspensions were loaded into separate counting chambers, and the number of total cells and the number of cells excluding the dye were determined. Final values were from three counts.

E. Inoculation of Mice. Cell concentrations were adjusted to contain a predetermined number in 200 µl for intraperitoneal inoculation using tuberculin syringes with 26g needles. Twenty gauge needles were used with formalin-killed cells with complete Freund's adjuvant (CFA). Immunizing inocula were prepared by resuspending a pellet of cells in 0.5% formalin at 4°C for 1 hr. Irradiated cells were suspended in fresh, sterile TYM medium without serum.

F. Procurement of blood and anti-Trichomonad antibody assay. Mice were anesthetized with methoxyfurane and bled from the retroorbital plexis with heparinized capillary tubes. The tubes were centrifuged, the plasma removed, and the plasma stored at minus 20°C until use. Dilutions of plasma were done two-fold starting with 1/10 increasing to 1/256. These were placed in slide wells. Fluorescein isothiocynate conjugated with goat anti-mouse IgG (Cappel Laboratories, West Chester, PA), diluted 1/20 in PBS, was then added to the wells and incubated for 30 minutes at 37°C. The sample wells were counterstained with Evans blue dye and allowed to dry. Three controls were used - (a) normal mouse serum, (b) immune mouse serum, (c) and mouse serum with a known high titer to *T. vaginalis.* Examination of the wells was with a Zeiss flourescence microscope at X400 magnification. The antibody titer was defined as the highest dilution of serum that resulted in flourescence of the cells.

G. SDS-PAGE and Western Blot. *Preparation of trichomonad*

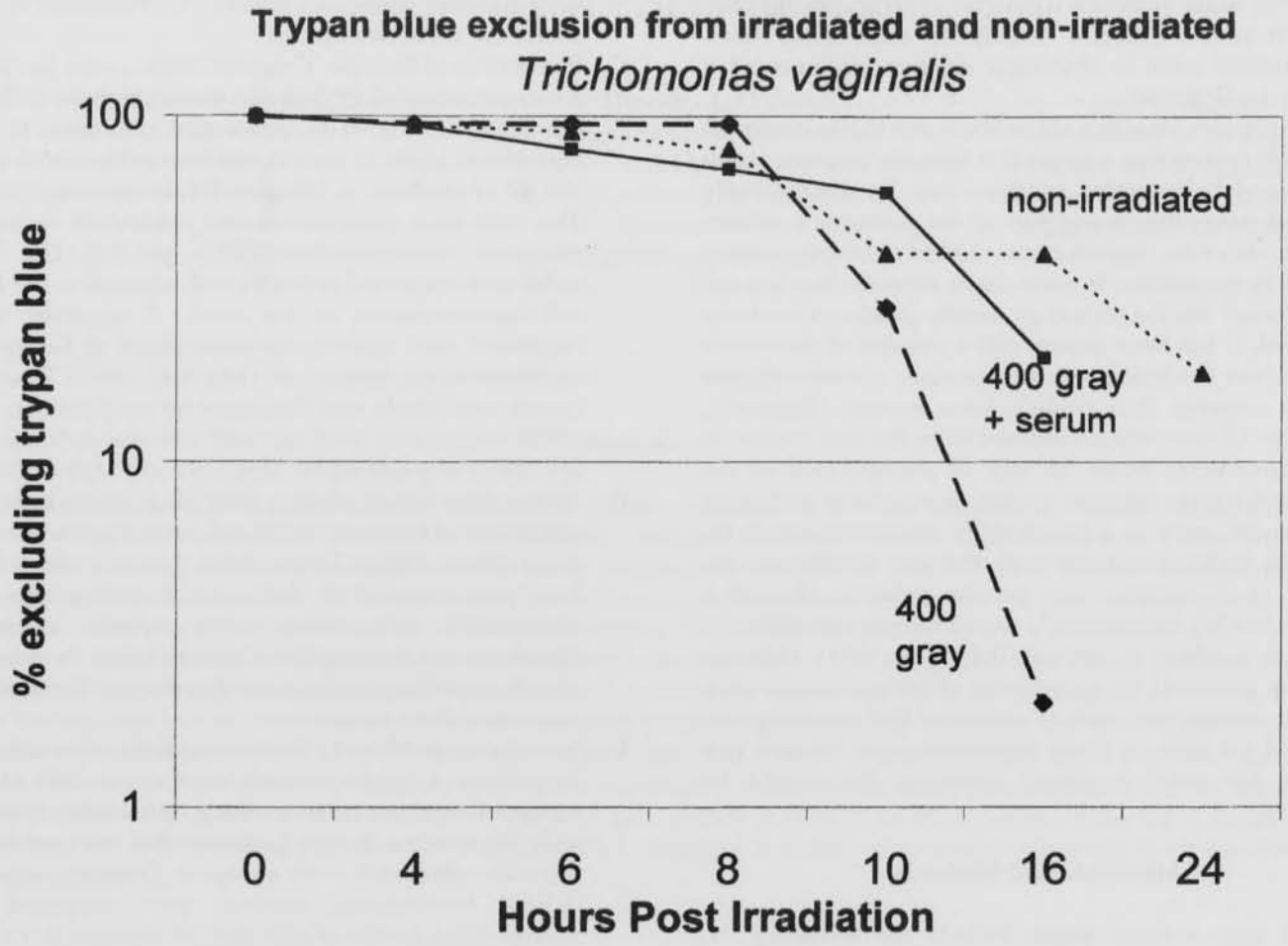

Fig. 1. Metabolic activity over time as demonstrated by trypan blue exclusion from irradiated or non-irradiated C_1 *Trichomonas vaginalis* at 37°C. The 16 hour measurements are the final data points shown because there were no viable cells at 24 hours. Cells were irradiated in TYM medium with and without serum (one experiment).

protein extracts: Cells were harvested from 2 liters of TYM medium containing 10^9 cells by a single speed Sorvol centrifuge. After washing the cells, a solution of 1% Triton x-100 was added to dissolve a portion of the pellet. The suspension was centrifuged at X2000g at 4°C to pellet the lipid component, which was discarded. The supernatant was dialyzed against 4mM tris buffer (pH 6.8) at 4°C overnight and then frozen at –70°C until used. 10^9 trichomonads yields approximately 15 mg of protein. *SDS electrophoresis*: Dialyzed extract was diluted 1:1 with tris buffer, boiled for 5 minutes, and then chilled on ice until used. A 12% polyacrilamide gel with a 5% stacking gel with one wide well and one narrow well was prepared, and 1.6 ml of extract was placed into the wide well. High and low molecular weight standards were loaded into the narrow well. An initial current of 70 mAmps was applied until the samples were out of the well at which time the current was increased to 120 mAmps. The current was discontinued when the dye front reached the bottom edge of the gel. *Transblot of proteins*: The proteins in the gel were transblotted onto nitrocellulose overnight at 30 volts. The nitrocellulose was removed from the transblot cell and a strip containing the molecular weight standards and a section of the well of the sample was stained with amido black. *Western Blot*: The nitrocellulose that remained unbound to protein was blocked by incubation in "blotto" (Carnation Instant Milk, 5%) at 4°C for 4 hours. Strips containing the protein samples were cut from the nitrocellulose and incubated at 4°C overnight with serum from the various treatment groups that had been diluted 1:150 or 1:500

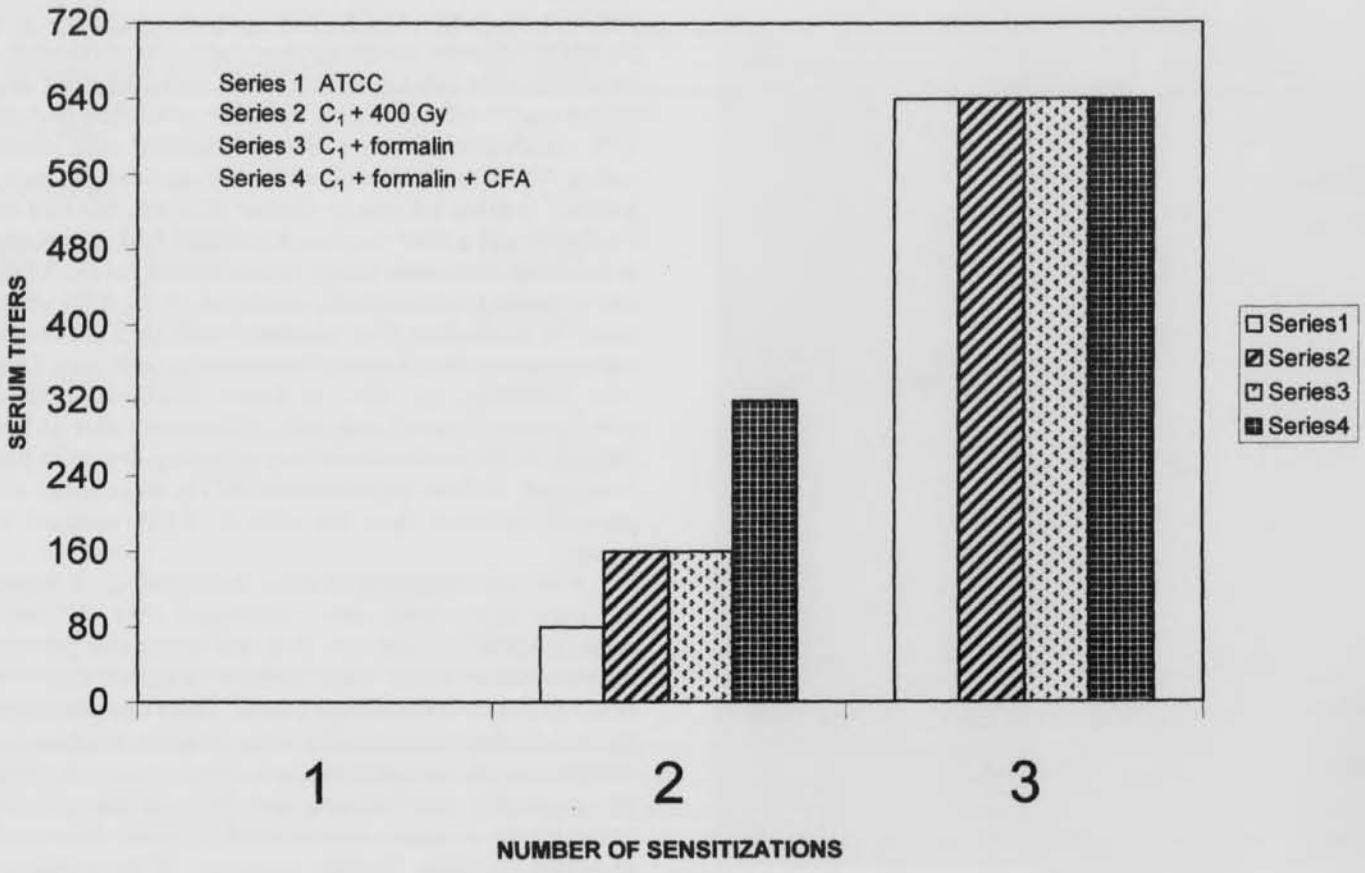

Fig. 2. Development of serum IgG titers in 24 week-old mice to *Trichomonas vaginalis* by four sensitization protocols. Titers were determined by indirect immunoflourescence using *T. vaginalis* C_1 as the antigen source. Each group represents pooled plasma samples from 5 mice.

in blotto. The strips were washed in fresh blotto at 4°C at 15 minute intervals to remove primary mouse antibody. Secondary antibody (rabbit anti-mouse) was diluted 1:600 in blotto, added to the strips, and incubated at 4°C for 2 hours. Strips were then washed in blotto and 20 µl of I^{125} labeled *Staphylococcus aureus* protein A (ICN Laboratories, Irvine, CA) was added which was first diluted 1:40 in PBS). The strips were then incubated at 4°C for 1 hour, washed once in blotto and then exposed to x-ray film for 8 hours at −70°C.

Results

ATCC strain 30001 of *Trichomonas vaginalis* did not produce mortality or outward signs of sickness or distress three weeks post-inoculation when injected with a range of 10^6 to 10^7 cells (Table 1). Necropsy results showed no pathology in the peritoneal cavity. C_1 was isolated from a patient from University Hospital and caused death in 2 to 5.8 days with dosages ranging from 10^6 to 2 x 10^7 (Table 1). ATCC 30001 was then used as the avirulent control in these experiments and C_1 as the virulent strain. As C_1 was maintained in culture it began to lose virulence after several months passage in TYM medium. When the average mortality in mice of C_1 reached 28 days, it was decided to replace this strain with a newly isolated one designated C_2. Loss of virulence during cultivation is well known with *T. vaginalis* (Honigberg, 1978). Different dosages of C_1 (or C_2) ranging from 10^3 to 10^7 cells showed a threshold for producing death in mice at 10^6 cells. This inoculation size was selected since a larger inoculum might overwhelm any acquired immune response seen using mortality of mice as a criterion.

In order to determine if irradiated trichomonads could

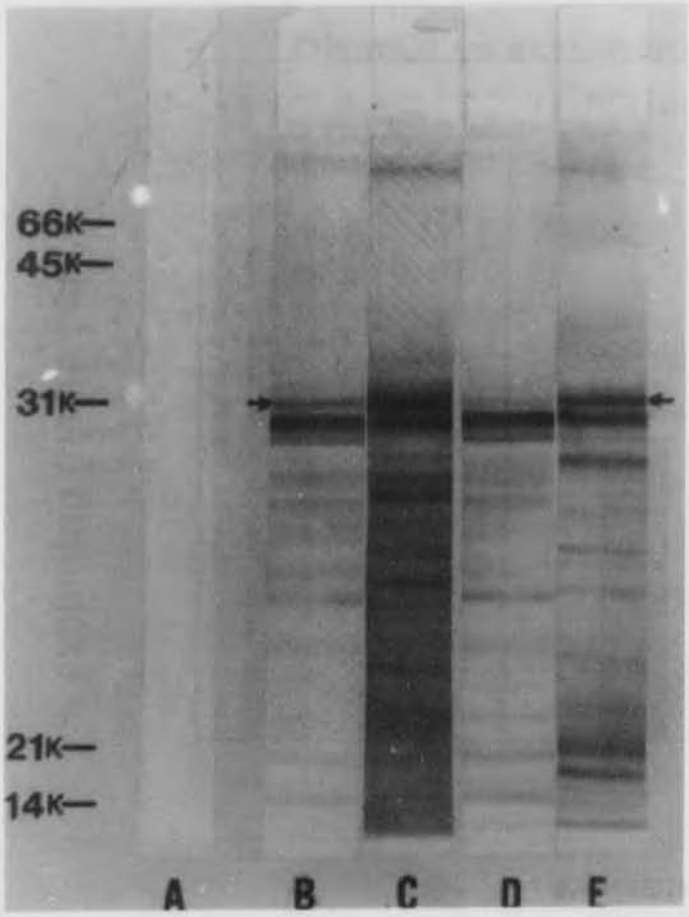

Fig. 3. Western blot analysis of serum from different mouse treatment groups sensitized with *Trichomonas vaginalis* antigen preparations. A protein extract from *T. vaginalis* C_2 was separated according to molecular weight by SDS-Page. The sensitization protocols used to obtain the sera for each lane were (A) Normal mouse serum (control – no antigen inoculated); (B) Formalin-fixed *T. vaginalis* ATCC 30001+ CFA (partial protection); (C) Formalin-fixed *T. vaginalis* C_2 + CFA (complete protection); (D) Irradiated *T. vaginalis* C_2 (partial protection); (E) Formalin-fixed *T. vaginalis* C_2 (partial protection).

produce a protective immunity through IP inoculation, a radiation dose had to be found where the organisms could survive, but not cause mortality in mice. The ability of *T. vaginalis* to produce mortality after radiation was determined by exposing 10^6 C_1 trichomonads in TYM medium to 100, 200, 400, and 800 Gy, respectively (Table 2). Mortalities of mice averaged 3.6, 5.8, and 5.8 days after 0, 100, and 200 Gy. No survival was seen in mice inoculated with trichomonads exposed to 400 and 800 Gy. Since very high dosages of radiation can cause cellular disruption and disintegration of *T. vaginalis*, a trypan blue dye assessment was made to determine if the cells would still remain metabolically active and for how long after exposure to 400 Gy (400 Gy is not a sterilizing dose since 13% of the cells can reproduce after 500 Gy – Daly et al., 1991). Figure 1 shows the percent of cells excluding dye after given time periods at 37°C incubation. One set of non-irradiated cells (control) was in TYM medium without serum additive (to prevent growth), another set was in similar medium, but had been irradiated and a third set, also irradiated, had serum added to duplicate conditions inside the peritoneal cavity. All three sets remained metabolically active at 70 to 80% after 12 hours of incubation. The irradiated cells in TYM medium without serum then began to lose activity with only 1.8% of cells excluding dye after 16 hours; irradiated cells with added serum followed with only 25% activity after 16 hours. Neither of the irradiated sets was excreting dye at 24 hours. As a result of these experiments 400 Gy was chosen as the primary radiation dose for cells in TYM medium with serum.

After one sensitizing dose of irradiated C_1 *T. vaginalis*, the mice (n = 5/set) were challenged with 10^6 cells of nonirradiated C_1. This one dose did not confer protection because those mice died earlier (3.4±0.5 days) than unsensitized controls (4.0±0.0 days). Since one sensitization did not produce protection, a series of three inoculations of irradiated cells was administered, once a week, to increase the possibility of obtaining protective immunity. These preparations included formalinized C_2 with the immune stimulant complete Freunds adjuvant (CFA), formalinized C_2 without CFA, live avirulent ATCC 30001, formalinized ATCC 30001 with CFA, and a sublethal dose (10^4) of C_2 (Table 3). Three sensitizing doses of irradiated cells did produce some measure of protective immunity in the mice that received irradiated cells as did the formalin-fixed C_2 cells and the formalin-fixed avirulent cells with CFA. The best protection was conferred with the use of virulent C_2 formalinized cells with added CFA.

IgG titers of adult mice showed that antibody response using irradiated cells correlated with the mortality studies (Fig. 2). CFA stimulated a faster response but the titer was the same as all other titers, which did not differ after three weeks. The avirulant ATCC 30001 control showed the least stimulatory effect as would be expected from the mortality studies, but the serum titer was also the same as the others at the end of three weeks. Passive transfer of immunity was tried with serum from these mice, but it was unsuccessful. Three passages of sublethal dosages of 10^3, 10^4, and 10^5 cells of C_1 were also used, but these showed no IgG titer after the first week, 1:160 titer for only the 10^5 dose after weeks 2 and 3, and 1:80 for the lower dosages for week 3 only. The data indicate that the amount of antigen administered is important in the IgG response.

The Use of Irradiated and Formalin-fixed *Trichomonas vaginalis* to Examine Protective Immune Responses in the Mouse Intraperitoneal Model

Table 1. The effect of different intraperitoneal doses of *Trichomonas vaginalis* strains ATCC 30001 and C_1 in five BALB/c mice (N = 5/dose).

Inoculum (No.of trichomonads)*	Inoculum	Percent Survival	Days to Death
PBS (control)	PBS	100	-----
ATCC 30001 1 x 10^6	C_1 1 x10^3	100	----
ATCC 30001 2.5 x 10^6	C_1 1 x10^4	100	----
ATCC 30001 5 x 10^6	C_1 1 x10^5	100	----
ATCC 30001 1 x 10^7	C_1 1 x10^6	0	5.8
	C_1 4 x10^6	0	4.0
	C_1 7 x10^6	0	4.0
	C_1 1 x10^7	0	4.0
	C_1 2 x10^7	0	2.0

*100% survival

Table 2. The mean time to death of female female Balb/c mice after intraperitoneal injection of *Trichomonas vaginalis* C_1 that were irradiated with different doses of ionizing radiation. Inoculum size was 10^6 for all groups, five mice in each group.

Radiation dose (Gray)	No. mice surviving/group	Mean time to death (days ± SD)
0	0/5	3.6 ± 1.9
100	0/5	5.8 ± 1.4
200	0/5	5.6 ± 1.3
400	5/5	----'
800	5/5	----

The Western blot analysis of serum from mouse treatment groups with different levels of protection can be seen in Figure 3. There were a large number of different molecular weight proteins recognized by serum from all the mouse treatment groups. There were, however, some differences in the size of the proteins that were demonstrated by this procedure. In the three treatment groups sensitized with either virulent strain (C_1 or C_2) that exhibited partial or complete protection (gamma irradiated, formalin-killed, and formalin-killed plus CFA), there were IgG antibodies to a *T. vaginalis* protein with an approximate molecular weight of 31,000 (arrow, Fig. 3). This band did not appear in the serum from animals that were sensitized with the avirulent strain of ATCC 30001 (Hostetler, 1987). However, when serum from mice that were sensitized with the avirulent strain plus CFA was used as the antibody source, this 31-kDa protein was also seen (arrow, Fig. 3). Thus in all cases where protective immunity was demonstrated, antibodies to this protein were seen.

Table 3. The percent survival of BALB/C different aged mice after intraperitoneal challenge with live C_1 or C_2 virulent strains of *Trichomonas vaginalis* after sensitizing the mice with different protocols. Ten mice were used for each group except where noted. Three separate sensitizing inoculations for each group were done a week apart. All sensitizations were accomplished with 10^6 cells unless noted.

Sensitization Protocol	Percent Surviving	Challenge
	Young[b] (3 weeks-old)	Adult[c] (24 weeks-old)
ATCC 30001 (live avirulent)	0	0[a]
ATCC 30001 formalin-fixed + complete Freund's adjuvant	60	---
Sublethal (10^4 cells), Virulent strain	0	0
Virulent strain, Formalin-fixed	20	60
Virulent strain, Gamma radiated (400 Gy)	20	40
Virulent strain, Formalin-fixed + complete Freund's adjuvant	100	100[d]

[a] 5 mice used
[b] C1 (2×10^3 cells) used to challenge
[c] C2 (1×10^6 cells) used to challenge
[d] 20 mice used

Discussion

Radiation was first used to attenuate a parasitic protozoan for vaccination purposes by Wallace and Sanders in 1966 (Hostetler, 1987) using the murine parasite, *Trypanosoma lewisi*. Since then there have been a number of successful immunizations using this technique with important parasitic protozoa such as *Leishmania, Plasmodium, Toxoplasma*, and *Eimeria* (Daly et al., 1991), including a study in which protective immunity in human volunteers was developed using irradiated sporozoites of *Plasmodium falciparum* (Egan et al., 1993). In the present study, however, the use of irradiated *Trichomonas vaginalis* in the mouse IP model did not offer any advantage over other methods of antigen preparation used in the study. It was originally hypothesized that perhaps metabolic or other short-lived antigens might produce a better immune response than fixed or otherwise killed trichomonads. Failure to improve on killed antigenic preparations is due either to the lack of metabolically-produced protective immunogens or the inability of the trichomonads to survive long enough in the peritoneal cavity to produce enough antigens to stimulate a protective response. *In vitro*, the cells were only able to survive 16 hours as indicated by trypan blue exclusion, but it is not known what the survival is *in vivo* in the peritoneum. The use of a much greater inoculum size of irradiated trichomonads might resolve this. However, the ability of the avirulent, formalin–killed ATCC strain to confer some protective immunity, when used with CFA, supports the idea of a structural antigen more so than a metabolic one. Also, the intraperitoneal route of antigen administration used in this study is artificial since the natural site of infection and where the most obvious pathology is produced is the human vagina. It would be of interest to see if radioattenuated *T. vaginalis* could stimulate an immune response, protective or otherwise, in the mouse vagina (or in human volunteers) by inoculation directly into the vagina or by the IM route.

The protective immunity, if any, to *Trichomonas vaginalis* in human females is poorly understood. IgG, IgA, and IgM to *T. vaginalis* have all been found in both vaginal washings and serum samples from patients or mouse models (Su,

1982; Alderete, 1984; Cogne et al., 1985; Wos and Watt, 1986; Bhatt et al., 1992; Paintla et al., 2002) as has IgE (Su, 1982). In this study the only immunoglobulin response measured was IgG in mouse serum. The IgG response correlated well with the degree of protection obtained with the different protocols and may indicate a protective role, but IgA and IgM were not examined and these may be involved in the protective immune responses seen. Cell-mediated immunity (CMI) may also play a role. A mouse footpad assay for delayed type hypersensitivity has shown strong responses for formalin-fixed virulent strains, with and without CFA, and irradiated virulent cells (Hostetler, 1987). CMI responses to *T. vaginalis* such as phagocytosis by neutrophils have been found (Rein et al., 1980; Mason and Forman, 1982), The cytokines TNF-α, IL2, LTB4, αINF, and IL8 have been found to be stimulated by *T. vaginalis* as well (Shaio and Lin, 1995 ; Shaio et al., 1995; Paintla et al., 2002). A role for complement has also been found (Alderete and Kasmala, 1986; Caterina et al., 1999). Regardless, in spite of evidence from the above cited studies, the immune response in the vagina does not seem to confer obvious protective immunity. Complicating possible protective immunity is that the trichomonads can absorb host proteins that could act as a protective barrier against antibodies (or CMI mechanisms) directed to surface receptors (Peterson and Alderete, 1982). The variation, as observed in this study with virulence, and more specifically with protein-epitopes (Alderete et al., 1987; Dailey and Alderete, 1991; Fiori et al., 1992) may also be a mechanism for immune avoidance.

The protective immune responses seen so far have not been proven to be linked to any specific antigens conferring protection although associations have been inferred. A number of studies have focused on the most quantitatively significant antigens (Addis et al., 1999) and those that might be associated with virulence such as *T. vaginalis* proteinases (Alderete et al., 1991a, 1991b), cell membrane surface proteins (Alderete, 1987; Alderete, 1999), and heat shock antigens (Bozner, 1997; Davis-Haymer et al., 2000). Most of these antigens have been high molecular weight proteins (>100,000) but smaller immunogens have been found. Of special interest is a 30-kDa proteinase detected by Arroyo and Alderete (1995). Inhibition of this proteinase and another proteinase of 65-kDa resulted in decreased levels of *T. vaginalis* cytoadherence and totally abolished contact-dependant cytotoxicity. It may be that the 31-kDa protein in the present study and the 30-kDa proteinase are the same. Live ATTC 30001 did not stimulate a visible antibody response to this 31-kDA band. Although when stimulated with CFA, the ATCC strain revealed this band showing that the protein was present but in much smaller amounts. This 31-kDa protein may be coincidental with immune protection or may be associated with a loss of virulence and not related to protective immunity. Isolation of this protein in sufficient quantity for immunization studies is needed to determine if it plays a any role in protective immunity.

ACKNOWLEDGMENTS.—The authors wish to thank Drs. Roger G. Rank (Dept. of Microbiology and Immunology, Univ. Ark. for Med. Sci.), Dean W. Roberts (National Center for Toxicological Research), and Dale V. Ferguson (Dept. of Biology, Univ. of Arkansas at Little Rock) for their advice and assistance on this project.

Literature Cited

Abraham, M. C., M. Desjardins, L. G. Filion, and **G. E. Garber.** 1996. Inducible immunity to *Trichomonas vaginalis* in a mouse model of vaginal infection. Infect. Immun. 64:3571-3575.

Addis, F, M., P. Rappelli, A. M. P. de Andrade, F. M. Rita, M. M. Colombo, P. Cappuccinelli, and **P. L. Fiori.** 1999. Identification of *Trichomonas vaginalis* α-actin as the most common immunogen recognized by sera of women exposed to the parasite. J. Infect. Dis. 180:1727-1730.

Alderete, J. F. 1984. Enzyme linked immunosorbent assay for detecting antibody to *Trichomonas vaginalis.* infection. Br. J. Vener. Dis. 60:164-170.

Alderete, J. F. 1987. *Trichomonas vaginalis* NYH286 phenotypic variation maybe coordinated for a repertoire of trichmonad surface immunogens. Infect. Immun. 55:1957-1962.

Alderete, J. F. 1999. Iron modulates phenotypic variation and phosphorylation of P270 in double-strnded RNA virus-infected *Trichomonas vaginalis.* Infect. Immun. 67:4298-4302.

Alderete, J. F., P. Demes, A. Gombosova, M. Valent, A. Yanoska, H. Fabusova, L. Kasmala, G. E. Garza, and **E. C. Metcalfe.** 1987. Phenotypes and protein epitope phenotype variation among fresh isolates of *Trichomonas vaginalis.* Infect. Immun. 55:1037-1041.

Alderete, J. F., and **L. Kasmala.** 1986. Monoclonal antibody to a major glycoprotein immunogen mediates differential complement-independent lysis of *Trichomonas vaginalis.* Infect. Immun. 53:697-699.

Alderete, J. F., E. Newton, C. Dennis, J. Engbring, and **K. A. Neale.** 1991a. Vaginal antibody of patients with trichomoniasis is to a prominent surface immunogen of *Trichomonas vaginalis.* Genitourin. Med. 67:220-225.

Alderete, J. F., E. Newton, C. Dennis, and **K. A. Neale.** 1991b. The vagina of women infected with *Trichomonas vaginalis* has numerous proteinases and antibody to trichomonad proteinases. Genitourin. Med. 67:469-474.

Arroyo, R., and **J. F. Alderete.** 1995. Two *Trichomonas vaginalis* surface proteinases bind to host epithelial cells and are related to cytoadherence and cytotoxicity. Arch. Med. Res. 26:279-285.

Bhatt, R., D. Pandit, and **L. Deodhar.** 1992. Detection of serum anti-trichomonal antibodies in urogenital trichomoniasis by immunofluorescence. J. Postgrad. Med. 38:72-74.

Bozner, P. 1997. Immunological detection and subcellular localization of Hsp70 and Hsp60 homologs in *Trichomonas vaginalis.* J. Parasitol. 83:224-229.

Caterina, P., D. Lynch, R. B. Ashman, A. Warton, and **J. M. Papadimitriou.** Complement-mediated regulation of *Trichomonas vaginalis* infection in mice. Exp. Clin. Immunogenet. 16:107-116.

Cogne, M., P. Brassuer, and **J. J. Ballet.** 1985. Detection and characterization of serum antitrichomonal antibodies in urogenital trichomoniasis. J. Clin. Microbiol. 21:588-592.

Dailey, D. C., and **J. F. Alderete.** 1991. The phenotypically variable surface protein of *Trichomonas vaginalis* has a single, tandemly repeated immunodominant epitope. Infect. Immun. 59:2083-2088.

Daly, J. J., M. L. Baker, T. Hostetler, and **P. L. Guthrie.** 1991. The effect of ionizing radiation on the viability of *Trichomonas vaginalis.* Comp. Biochem. Physiol. 98a:259-263.

Davis-Hamer, S. R., P. H. Shah, R. W. Finley, J. C. Meade, and **W. B. Lushbaugh.** Antigenicity of *Trichomonas vaginalis* heat-shock proteins in human infections. Parasitol. Res. 86:115-120.

Diamond, L. S. 1957. The establishment of various trichomonads of animals and man in axenic cultures. J. Parasitol. 47:488-490.

Egan, J. E., S. L. Hoffman, J. D. Haynes, J. C. Sadoff, I. Schneider, G. E. Grau, M. H. Hollingdale, W. R. Ballou, and **D. M. Gordon.** 1993. Humoral immune responses to volunteers immunized with irradiated *Plasmodium falciparum* sporozoites. Am. J. Trop. Med. Hyg. 49:166-173.

Fiori, P L., C. Manca, and **P. Cappuccinelli.** 1992. Phenotypic variation of surface antigenic determinants in *Trichomonas vaginalis* detected by monclonal antibodies. Microbiologia 15:27-235.

Honigberg, B. M. 1978. Trichomonads of importance in human medicine, 275-454, *In,* Parasitic protozoa, vol. 2. (J.P. Krier ed.) Academic Press, Inc., New York.

Hostetler, T. L. 1987. The use of irradiated and formalin-fixed *Trichomonas vaginalis* to examine protective immune responses in the mouse model. Unpubl. Masters Thesis. Univ. Ark. Med. Sci., Little Rock. 84 pp.

Ivey, M. J. 1961. Growth characteristics of clones of *Trichomonas* in solid medium. J. Parasitol. 47:539-544.

Krieger, J. N., and **J. F. Alderete.** 1999. *Trichomonas vaginalis* and Trichomoniasis, 587-604, *In,* Sexually Transmitted Diseases, 3rd ed. (Holmes, K. K. et al., eds.) McGraw Hill, New York, New York.

Matthews, R. S., and **J. J. Daly.** 1974. *Trichomonas gallinae.* Use of solid medium to test survival under various environmental conditions. Exptl. Parasitol. 36:288-298.

Mason, P. R., and **L. Forman.** 1982. Polymorphonuclear cell chemotaxis to secretions of pathogenic and nonpathogenic *Trichomonas vaginalis.* J. Parasitol. 71:457-462.

McGrory, T., and **G. E. Garber.** 1992. Mouse intravaginal infection with *Trichomonas vaginalis* and role of *Lactobacillus acidophilus* in sustaining infection. Infect. Immun. 60:2375-2379.

Paintla, M. K., S. Kaur, I. Gupta, N. K. Ganguly, R. C. Mahjan, and **N. Malla.** 2002. Specific IgA response, T-cell subtype and cytokine profile in experimental intravaginal trichomoniasis. Parasitol. Res. 88:338-343.

Peterson, K. M., and **J. F. Alderete.** 1982. Host plasma proteins on the surface of pathogenic *Trichomonas vaginalis.* Infect. Immun. 37:755-762.

Rein, M. F., J. A. Sullivan, and **G. L. Mandell.** 1980. Trichomonad activity of human polymorphonuclear neutrophils: Killing by disruption and fragmention. J. Infect. Dis. 142:575-585.

Shaio, M. F., and **P. R. Lin.** 1995. Influence of humoral immunity on leucotirene B4 production by neutrophils in response to *Trichomonas vaginalis* stimulation. Parasit. Immunol. Res. 17:127-133.

Shaio, M. F., P. R. Lin, J. Y. Liu, and **K. D. Yang.** 1995. Generation of interleukin-8 from human monocytes in response to *Trichomonas vaginalis* stimulation. Infect. Immun. 63:3864-3870.

Su, K. E. 1982. Antibody to *Trichomonas vaginalis* in human cervicovaginal secretions. Infect. Immun. 37:852-857.

Warren, L. G., W. B. Kitzman, and **E. Hake.** 1960. Induced resistance of mice to subcutaneous infection with *Trichomonas gallinae* (Rivolta, 1878). *In*: Hostetler, T. (1987).

Wos, S. M., and **R. M. Watt.** 1986. Immunoglobulin isotypes of anti-*Trichomonas vaginalis* antibodies in patients with vaginal trichomoniasis. J. Clin. Microbiol. 24:790-795.

Genetic Relationships of Some Common Arkansas Freshwater Sunfishes (Centrarchidae: *Lepomis*) Inferred From Restriction Endonuclease Analysis of Mitochondrial DNA

Ronald L. Johnson*
Department of Biological Sciences
Arkansas State University
State University, AR 72467

K. Ashlei Williams
University of Arkansas Medical School
4301 W. Markham, Slot 501
Little Rock, AR 72205

*Corresponding Author

Abstract

Geographic isolation and habitat specialization has aided in the evolution and maintenance of genetic integrity of the lepomid sunfishes (*Lepomis*: Centrarchidae) of North America. Our goal was to measure genetic distances between four of the eleven extant sunfish species by using mitochondrial DNA analysis. Mitochondrial DNA restriction fragment length polymorphisms (RFLPs) were examined in bluegill (*L. macrochirus*), redear sunfish (*L. microlophus*), longear sunfish (*L. megalotis*), and green sunfish (*L. cyanellus*) using 15 restriction endonucleases. The largemouth bass (*Micropterus salmoides*) was used as an outgroup. The phylogeny inferred from Dollo parsimony cladistic analysis largely concurred with published results from allozyme analyses and the fossil record, yet was inconsistent with published anatomical analyses. Genetic distances between species ranged from 0.1627 to 0.3328. The green sunfish was the basal member of the genus, whereas the bluegill was the most diverged from the largemouth bass. These four species diverged over a broad time frame, with estimated times of speciation occurring during Miocene (8.14 - 16.64 mya).

Introduction

The family Centrarchidae originated within the Mississippi River system of North America. Included among the Centrarchidae are the sunfishes, genus *Lepomis*, which are the most diverse group of this family, with eleven described species (Avise and Smith, 1977). Several attempts have been made to classify the phylogenetic relationships of the sunfishes, yet there have been inconsistencies between proposed phylogenies. Bluegill (*L. macrochirus* Rafinesque) have been suggested as a more recently derived species within the genus based upon the fossil record (Miller, 1965; Mabee, 1988) and allozyme analysis (Avise and Smith, 1977). However, Branson and Moore (1962) proposed that the longear sunfish (*L. megalotis* Rafinesque) was more recently diverged based on comparisons of the acoustico-lateralis system. Each of the studies above places the green sunfish as the basal member of the genus.

The research reported here focused on four species common to Arkansas and throughout much of the Mississippi river drainage system: green sunfish (*L. cyanellus* Rafinesque), bluegill sunfish, longear sunfish, and redear sunfish (*L. microlophus* Gunther). Our goal was to assess the concordance of mitochondrial DNA sequence divergence to previous models developed from anatomic and genetic evidences.

Materials and Methods

Single populations of bluegill (n = 18), redear sunfish (n = 12) and green sunfish (n = 14) were studied from private farm ponds near the Arkansas State University campus, and longear sunfish (n = 10) were collected from the South Fork of the Spring River. Mitochondria and mitochondrial DNA (mtDNA) were isolated and analyzed from liver tissue using techniques described by Johnson et al. (2002). Purified mtDNA was digested for 7 h at 37° C using 15 restriction endonucleases (*Bam*HI, *Bgl*I, *Bgl*II, *Csp*45I, *Dra*I, *Eco*RI, *Eco*RV, *Him*DIII, *Mlu*I, *Pst*I, *Pvu*II, *Sal*I, *Sca*I, *Xba*I, *Xho*I), under conditions recommended by the supplier (Promega Corp.). Fragment sizes generated were determined through the use of a least-squares fit program (Schaeffer and Sederoff, 1981). Variables measured included genome size, percentage genome analyzed, nucleon diversity (Nei and Tajima, 1981) and nucleotide sequence divergence (Nei and Li, 1979). Times of divergence were estimated from observed levels of sequence divergence using a divergence rate of 2% per million years (Brown et al., 1979). A phenogram. was constructed by the unweighted pair group method (UPGMA; Sokal and Sneath, 1963) using matrices of distance values with NTSYS-PC: Numerical Taxonomy and Multivariate Analysis System (Rohlf, 1990) as well as an inferred phylogenetic tree using the Dollo parsimony algorithm in Phylogeny Inference Package (PHYLIP; Felsenstein, 1993). The dominant haplotype of the northern

Genetic Relationships of Some Common Arkansas Freshwater Sunfishes (Centrarchidae: *Lepomis*) Inferred From Restriction Endonuclease Analysis of Mitochondrial DNA

Table 1. MtDNA genetic analysis for sunfishes of the genus *Lepomis*.

Common Name	N	Restriction Fragments	Genome Size (bp) ± SE	Percent Genome Sampled	Number of Haplotypes	Nucleon Diversity
Green sunfish	14	40	16,958 ± 182	1.42%	7	0.64
Bluegill 18	58	16,642 ± 130	2.09%	9	0.67	
Longear sunfish	10	31	16,639 ± 135	1.12%	7	0.78
Redear sunfish	12	53	16,671 ± 164	1.91%	6	0.62

Table 2. Number of restriction fragments generated from mtDNA for *Lepomis* species sampled. Abbreviations are as follows: Green, green sunfish; Blue, bluegill; Long, longear sunfish; and Red, redear sunfish. Total number of polymorphisms identified by an individual restriction endonuclease in parentheses.

Restriction Endonuclease		Common Name Green	Blue	Long	Red
*Bam*HI	(4)	2	0	2	1
*Bgl*I	(7)	3-4	3-4	0-1	3
*Bgl*II	(5)	1	2	2	2
*Csp*45I	(6)	0	2-3	3	3
*Dra*I	(5)	3	5	0	3-4
*Eco*RI	(2)	0-1	1	0-1	1
*Eco*RV	(4)	0	3	2	5
*Hin*dIII	(5)	3	4-5	3	4-5
*Mlu*I	(2)	1	0	0-1	0
*PSt*I	(7)	2	3-4	2-3	3-4
*Pvu*II	(3)	2	2	0	0
*Sal*I	(4)	1-2	0,2	0	1
*Sca*I	(6)	4-5	3	2-3	5
*Xba*I	(6)	5	3-4	1-2	3
*Xho*I	(4)	1-2	2	0,2	2

largemouth bass (*Micropterus salmoides salmoides* Lacepede; Johnson et al., 2002), a representative of the genus most closely related to *Lepomis* (Branson and Moore, 1962; Avise and Smith, 1977), was used as an outgroup to root the tree.

Results and Discussion

The total number of restriction fragments generated using 15 restriction endonucleases was 140, with ranges of 31 for longear sunfish to 58 for bluegill (Table 1). From 1.12 to 2.09 percent of the mtDNA genome was surveyed. Seven of the restriction endonucleases did not identify recognition sequences within individual species (*BamH*I bluegill; *Csp45*I, green sunfish; *Dra*I, longear sunfish; *Eco*RV, green sunfish; *Mlu*I, bluegill and redear sunfishes; *Pvu*II, redear and longear sunfishes; and *Sal*I, longear sunfish). *Bgl*I, *Csp*45I, *Dra*I, *Eco*RV, *Hin*dIII, *Pst*I, *Sca*I and *Xba*I generated higher numbers of polymorphisms (Table 2). The enzymes *Bgl*I and *Pst*I were particularly informative phylogenetically, with large numbers of restriction sites and high polymorphism between species (Table 2). Conversely, the restriction endonucleases *Eco*RI and *Mlu*I were less informative, with zero to one restriction site. However, no profile for an individual restriction endonuclease was shared by all species (Table 3).

Mean genome size (Table 1) ranged from 16,639 (± 135 SE) base pairs for longear sunfish to 16,958 (± 182 SE) base pairs for green sunfish. These estimates are similar to those found for blugill (16,200 bp) by Avise et al. (1984) and for the shadow bass, *Ambloplites rupestris* (16,751 bp; Johnson and Cavenaugh, 2003), yet lower than that found for six species of *Micropterus*, another centrarchid genus (range of 17,346 to 17,779; Johnson et al., 2002).

A total of 29 haplotypes was identified among the 54 individuals (Table 1). A single haplotype was dominant for each species, with all other haplotypes found in single individuals (Table 3). Haplotype diversity was similar for all species studied, with h values ranging from 0.62 to 0.78 (Table 1). Nucleon diversity was similar to that found for

Table 3. Dominant composite mtDNA haplotypes observed for *Lepomis* species studied. Order of restriction endonucleases in columns as follows: *Bam*HI, *Bgl*I, *Bgl*II, *Csp*45I, *Dra*I, *Eco*RI, *Eco*RV, *Hin*dIII, *Mlu*I, *Pst*I, *Pvu*II, *Sal*I, *Sca*I, *Xba*I, and *Xho*I. Asterisks indicate restriction profiles which are invariant for that restriction endonuclease and samples. All variant haplotypes not listed were represented by single individuals.

Common Name	N	Haplotype													
Green sunfish	8	E*	L	B*	D*	C*	F	B*	A*	D*	D*	C*	A	D	C*	F
Bluegill	10	F*	H	E	K	0*	F*	K*	K	B*	K	N*	C	E*	L	F*
Longear sunfish	4	G*	E	1*	0*	B*	B	L*	N*	B*	M	B*	C*	G*	N	G
Redear sunfish	7	B*	J*	E*	N*	A	F*	A*	M	B*	A	B*	G*	C*	A*	F*

Table 4. Mitochondrial DNA sequence divergence (above diagonal) and estimated time of divergence in millions of years (below diagonal) for *Lepomis* species studied. Standard errors of the mean in parentheses beneath the means.

Species	1	2	3	4	5
1. Green sunfish	***	0.3328	0.3228	0.2778	0.3216
		*** (0.0012)	(0.0017)	(0.0010)	(0.0011)
2. Bluegill	16.64	***	0.2187	0.1627	0.4166
	(0.01)		*** (0.0019)	(0.0006)	(0.0003)
3. Longear sunfish	16.17	10.94	***	0.2453	0.5763
	(0.01)	(0.01)		*** (0.0010)	(0.0005)
4. Redear sunfish	13.89	8.14	12.27	***	0.3277
	(0.01)	(0.01)	(0.01)		*** (0.0067)
5. Largemouth bass	16.08	20.83	28.82	16.39	***
	(0.01)	(0.01)	(0.01)	(0.01)	

several *Micropterus* species (Johnson et al., 2002; range of 0.46 to 1.00), but the diversity was higher relative to other micropterid studies (population range of 0.07 to 0.37; Nedbal and Philipp, 1994; Snyder et al., 1996). The relatively high genetic heterogeneity values observed in the present study and in Johnson et al. (2002) may be attributed in part to the larger number of restriction endonucleases utilized (15 versus 7-8 in previous studies), which provided a better opportunity to detect genetic variability.

Estimated nucleotide sequence divergence, standard error, and time of divergence for *Lepomis* and *Micropterus* are found in Table 4. Divergence values ranged from 0.1627 for bluegill and redear to 0.3328 for the bluegill and green sunfish. These congeneric values are similar to that found in the genus *Micropterus* (Johnson et al., 2002). Data indicated that the green sunfish is most closely related to the outgroup largemouth bass (0.3216), whereas the longear was most genetically distinct from the largemouth bass (0.5763).

Estimated time of divergence for the species of *Lepomis* studied ranged from 8.14 to 16.64 million years ago (Table 4). According to our estimates, the point of divergence between *M. salmoides* and *Lepomis* was during the late Oligocene to Miocene (16-29 mya), which is more recent than observed in the fossil record, which traces both genera

Genetic Relationships of Some Common Arkansas Freshwater Sunfishes (Centrarchidae: *Lepomis*) Inferred From Restriction Endonuclease Analysis of Mitochondrial DNA

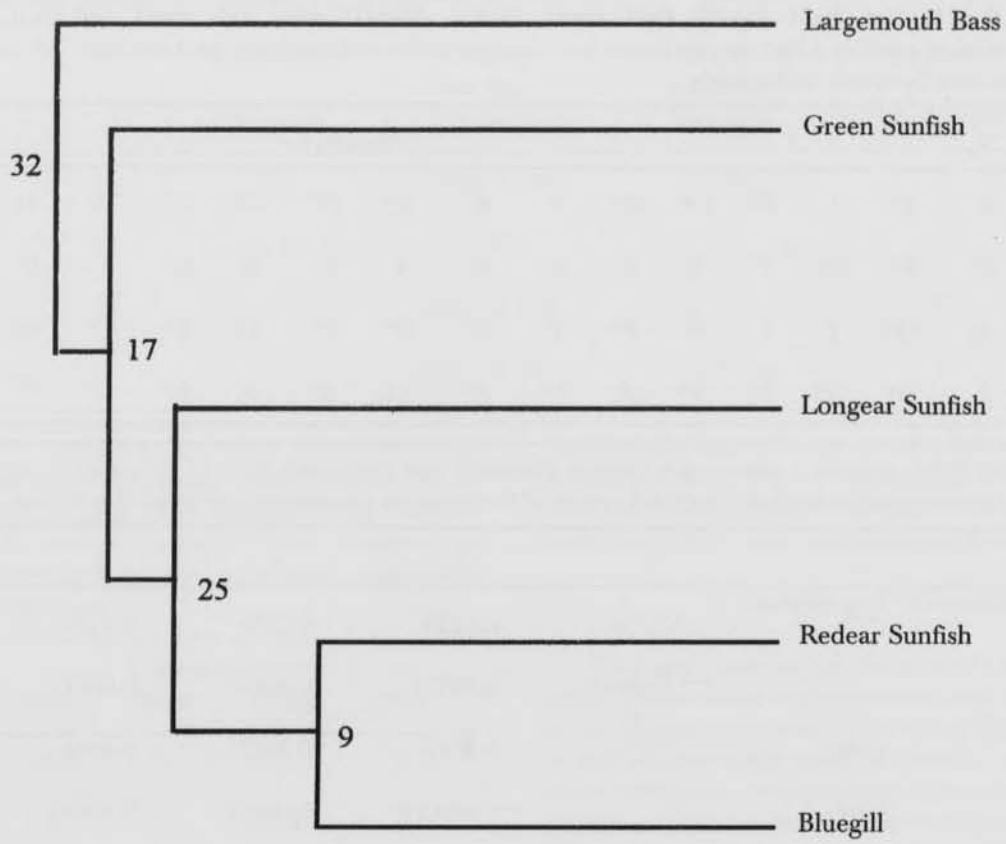

Fig. 1. Cladogram of character state matrices for presence/absence of presumptive restriction sites utilizing the Dollo parsimony algorithm. Each of the 29 equally most parsimonious trees (144 steps) were consistent to the species level.

back to the Eocene (37-58 mya, Smith, 1962; Wainwright and Lauder, 1992; Wilson and Williams, 1992). Conversely, individual species analyzed have earlier divergence times than those found in the fossil record. For example, our data indicates the green sunfish diverged from the redear sunfish 14 mya. The fossil record suggests the divergence of the green sunfish 4-6 mya (Smith, 1962). The time frames determined here also predate fossil records for redear and longear sunfishes (Smith, 1962). Additionally, the bluegill has been proposed as a more recently derived species (2-4 mya) [Miller, 1965; Mabee, 1988], which is consistent with our phylogenetic tree, but not with our estimated time of divergence (8.14 mya). It must be noted, however, that the fossil record of fish is not always complete (Wilson and Williams, 1992) and that the molecular clock of 2% per million years has not been consistent through all taxa (Grewe et al., 1990). Lastly, and most importantly, these estimates are based on single populations within each species, and therefore the values obtained are at best estimations of the divergence periods between these particular populations rather than the species as a whole.

Construction of a cladogram generated utilizing the Dollo parsimony algorithm program (Figure 1) revealed that the green sunfish was most similar to the largemouth bass and the bluegill the most distant. A UPGMA dendrogram derived from the average genetic distances between species is consistent with the cladogram. A cophenetic correlation of 0.87 was obtained, indicative of a good fit between the tree generated and the data matrix (Rohlf, 1990).

Both the best-fit cladogram and the phenogram concur with the consensus of research, which shows the green sunfish as the basal member of the genus (Branson and Moore, 1962; Avise and Smith, 1977). However, Branson and Moore (1962) studied the acoustico-lateralis system and proposed that the longear was more recently diverged, instead of the bluegill as found in our data, allozyme

analysis (Avise and Smith, 1977) and the fossil record (Miller, 1965; Mabee, 1988, Wainwright and Lauder, 1992). Whereas allozyme analysis by Avise and Smith (1977) showed the longear and redear sunfishes to be grouped with the green sunfish, our data suggest a closer relationship of these two species with the bluegill.

Future study of the genus *Lepomis* at the population, subspecies, and species levels is required to further our understanding of the historical biogeography of this genus. Additional population data may very well alter the proposed relationships of these taxa. Genetic analysis of within-species population divergence of mtDNA has only been performed on bluegill mtDNA (Avise and Saunders, 1984; Avise et al., 1984; Chapman, 1989). Population studies, particularly of sympatric populations, can provide insight as to possible source taxa of those species having restricted ranges.

ACKNOWLEDGMENTS.—We would like to thank C. Hutts, M. Oltmann, and C. McGrath for technical assistance and for assistance in the collection of specimens. We also thank A. Grippo, L. Hilburn, J. Loutsch, and L. Olson for their constructive criticisms of earlier drafts of this manuscript. This work was supported by grants from the Silo Undergraduate Research Foundation and Arkansas State University.

Literature Cited

Avise, J. C., E. Bermingham, L. G. Kessler, and **N. C. Saunders.** 1984. Characterization of mitochondrial DNA variability in a hybrid swarm between subspecies of bluegill sunfish (*Lepomis macrochirus*). Evol. 33:931-941.

Avise, J. C., and **N. C. Saunders.** 1984. Hybridization and introgression among species of sunfish (*Lepomis*): Analysis by mitochondrial DNA and allozyme markers. Genetics 108:237-255.

Avise, J. C., and **M. H. Smith.** 1977. Gene frequency comparisons between sunfish (Centrarchidae) populations at various stages of evolutionary divergence. Syst. Zool. 26:319-335.

Branson, B. A., and **G. A. Moore.** 1962. The lateralis components of the acoustico-lateralis system in the sunfish family Centrarchidae. Copeia 1962:1-108.

Brown, W. M., M. George, Jr., and **A. C. Wilson.** 1979. Rapid evolution of animal mitochondrial DNA. Proc. Nat. Acad. Sci. 76:1967-1971.

Chapman, R. W. 1989. Mitochondrial and nuclear gene dynamics of intraspecific populations of *Lepomis macrochirus*. Genetics 123:399-404.

Felsenstein, J. 1993, Phylip (Phylogeny Inference Package). Version 3.5 1. Univ. Washington, Seattle.

Grewe, P. M., N. Billington, and **P. D. N. Hebert.** 1990. Phylogenetic relationships among members of *Salvelinus* inferred from mitochondrial DNA divergence. Can. J. Fish. Aq. Sci. 47:984-991.

Johnson, R. L., and **C. Cavenaugh.** 2003. Genetic similarity of shadow and Ozark basses (*Ambloplites*) as determined by mitochondrial DNA analysis. J. Arkansas Acad. Sci. 57:(in press).

Johnson, R. L., J. B. Magee, and **T. A. Hodge.** 2002. Phylogenetics of freshwater black basses (Centrarchidae: *Micropterus*) inferred from restriction endonuclease analysis of mitochondrial DNA. Biochem. Gen. 39:395-496.

Mabee, P. M. 1988. Supraneural and predorsal bones in fishes: Development and homologies. Copeia 1988:827-838.

Miller, R. R. 1965. Quaternary freshwater fishes of North America. Pp. 569-581, *In* The Quaternary of the United States (H.E.Wright, Jr. and D.G. Frey eds.). Princeton Univ. Press, Princeton. 459 pp.

Nedbal, A. M., and **D. P. Philipp.** 1994. Differentiation of mitochondrial DNA in largemouth bass. Trans. Am. Fish. Soc. 123:460-468.

Nei, M., and **W. H. Li.** 1979. Mathematical models for studying genetic variation in terms of restriction endonucleases. Proc. Nat. Acad. Sci.76:5269-5273.

Nei, M., and **F. Tajima.** 1981. DNA polymorphisms detectable by restriction endonucleases. Genetics 97:147-165.

Rohlf, F. F. 1990. NTSYS-PC: Numerical Taxonomy and Multivariate Analysis System. Version 1.60. Exeter Publishing, Setauket.

Schaeffer, H. E., and **R. R. Sederoff.** 1981. Improved estimation on DNA fragment lengths from agarose gels. Ann. Biochem. 115:113-122.

Smith, C. L. 1962. Some Pliocene fishes from Kansas, Oklahoma, and Nebraska. Copeia 1962:505-520.

Snyder, J. A., G. C. Garman, and **R. W. Chapman.** 1996. Mitochondrial DNA variation in native and introduced populations of smallmouth bass, *Micropterus dolomieui*. Copeia 1996:995-998.

Sokal, R. R., and **P. H. A. Sneath.** 1963. Principles of numerical taxonomy. Freeman, San Francisco. 359 pp.

Wainwright, P. C., and **G. V. Lauder.** 1992. The evolution of feeding biology in sunfishes (Centrarchidae). Pp. 472-491, *In* Systematics, historical ecology, and North American freshwater fishes (R.L. Mayden, ed.). Stanford University Press, Stanford. 969 pp.

Wilson, M. V. H., and **R. G. Williams.** 1992. Phylogenetic, biogeographic, and ecological significance of early fossil records of North American freshwater teleostean fishes. Pp. 224-246, *In* Systematics, historical ecology, and North American freshwater fishes (R.L. Mayden, ed.). Stanford University Press, Stanford. 969 pp.

On the Rare Endemic *Hydrophyllum brownei* Kral & Bates (Browne's Waterleaf): New Population Information and a Recommendation for Change in Status

Travis D. Marsico
University of Arkansas Herbarium (UARK)
Biomass Research Center 141
Fayetteville, AR 72701

Abstract

Hydrophyllum brownei Kral & Bates (Browne's waterleaf), newly described in 1991, is endemic to the Ouachita Mountain Natural Division of Arkansas. For the purpose of better understanding population parameters within which *H. brownei* grows, ranges of shade values, population extents, and population distance relationships to streams were measured. *Hydrophyllum brownei* grows in extremely high shade, in populations of widely varying sizes, and always in association with a stream system. In order to list species associated with *H. brownei*, vouchers of species assemblages were collected at the *H. brownei* sites visited. The species is designated as critically imperiled globally because of its extreme rarity (G1). It is also extremely rare in Arkansas (S1) according to NatureServe and the Arkansas Natural Heritage Commission. Previously unknown populations were discovered in this study, and a recommendation to lower species rarity rank is made. However, based upon information gathered about population parameters, it is recommended that the species be reduced in status only to the global rank of G2 (imperiled globally because of rarity) and the state rank of S2 (very rare). *Hydrophyllum brownei* is currently known from 26 distinct sites, nine of which were discovered in 2002. Because *H. brownei* is a rare endemic to the Ouachita Mountains, continued intermittent monitoring of its populations is advised.

Introduction

Hydrophyllum brownei (Browne's waterleaf) is a recently described species endemic to the Ouachita Mountain Natural Division of Arkansas (Kral and Bates, 1991). It is characterized by deeply pinnately lobed leaves that often appear basal, a solitary, sometimes branched erect stem and peduncle, a dense multi-flowered cymose inflorescence that appears head-like, white to pale or bright lavender flowers, long-exerted stamens (Fig. 1), pubescence throughout, and a distinctive tuberous rootstock (Figs. 2, 3). Listed as a new discovery for Arkansas in 1951 (Moore, 1951), but known from a specimen made by George Engelmann in 1837 (Kral and Bates, 1991), early *H. brownei* collections were identified as *Hydrophyllum macrophyllum* Nutt. The distinctive tuberous rootstock, which is the most conspicuous feature that distinguishes *H. brownei* from the very similar *H. macrophyllum* and all other *Hydrophyllum* species, was not collected by early botanists (Figs. 2, 3). Bates collected the root material and recognized this and other differences enabling Kral and Bates (1991) to describe *H. brownei*. It is now thought that *H. macrophyllum* is restricted to a range east of the Mississippi River and that all collections from Arkansas are actually *H. brownei*. Because populations of the supposed *H. macrophyllum* were only of rare occurrence in Arkansas, *H. macrophyllum* was a species tracked by the Arkansas Natural Heritage Commission (ANHC). After the description of *H. brownei*, both species were tracked by the state. Now that all Arkansas specimens have been reviewed and annotated as *H. brownei*, and there is no record of *H. macrophyllum* in the state, ANHC removed *H. macrophyllum* from their tracking list in early 2003, allowing all the focus to be on *H. brownei* (Theo Witsell, personal communication). The species commands attention because it is not only rare in the state, but it is an Arkansas endemic, known only from the Ouachita Mountains and the Valley and Ridge (often lumped with the Ouachitas) Provinces.

Fig. 1. *Hydrophyllum brownei* inflorescence. Note the long-exerted stamens.

On the Rare Endemic *Hydrophyllum brownei* Kral & Bates (Browne's Waterleaf): New Population Information and a Recommendation for Change in Status

Fig. 2. Entire *Hydrophyllum brownei* plant.

In North America, *Hydrophyllum* consists of nine species with both eastern and western assemblages, divided by the Great Plains. It is thought that the genus may have been more continuous in the past, but increasingly arid conditions in the mid-continent caused the separation into eastern and western assemblages (Beckmann, 1979). *Hydrophyllum brownei* falls into the eastern assemblage of species, but it is the only species in the eastern assemblage that is confined to an area west of the Mississippi River. All *Hydrophyllum* species, including *H. brownei*, are perennials except for *H. appendiculatum*, which is a biennial species (Beckmann, 1979).

Shade is an important factor for *Hydrophyllum* species (Beckmann, 1979), and no species completely departs from the characteristic mesophytic nature of the genus (Constance, 1942). FTN Associates (2001) noted that although the amount of shade is variable at *H. brownei* sites, all populations grew under dense riparian hardwood shade. Beckmann (1979) stated, "Rigorous habitat requirements for shade and moist, porous substrate coupled with unsophisticated seed dispersal restrict encroachment into new habitats." In other parts of the country where temperatures are not as high, there is more rainfall, and/or evaporation is not as significant, shade and moisture are not necessarily tied directly to streams, and *Hydrophyllum* species

Fig. 3. Rootstock of a *Hydrophyllum brownei* plant. Note that the tubers produce fibrous roots apically, which may be again tuberous.

are not confined to stream-sides. In the Ouachita Mountains, however, the combination of shade and moisture is limited, severely restricting suitable habitat for *H. brownei*.

Since its description in 1991, little work has been done to understand the distribution and extent of *H. brownei*. The first work on the species after the initial publication was a survey conducted for ANHC (Hoang, 1999), followed by a status survey for the U. S. Fish and Wildlife Service (FTN Associates, 2001).

Hydrophyllum brownei has been designated as critically imperiled globally because of extreme rarity (G1) and designated as extremely rare in Arkansas (S1) by NatureServe and ANHC (Theo Witsell, personal communication). The basis for its classification is the number of distinct populations, viability of the populations, number of individuals in the populations, extent of the populations and geographical range, population trends, current and suspected future threats, inherent susceptibility to threats, and number of protected occurrences (Stein et al., 2000).

Materials and Methods

In this study most of the known sites were visited, and using information from previous work and field observations, a search was conducted for other populations. For a better understanding of how and where *Hydrophyllum brownei* populations are distributed and in what conditions the individuals are growing, certain population parameters were measured. From 13 May through 26 May 2002, most of the sites summarized by FTN Associates (2001) were revisited in order to determine the boundaries of the populations, count individuals, and take measurements on physical attributes of the sites. At each site, the bounds of the population were determined by pacing off the area and

Table 1. Location information for the 26 known *Hydrophyllum brownei* populations. Sites with an asterisk (*) were not visited in this study, and sites with a plus (+) were subdivided.

County	Brief site ID	7.5' Quad and TRS
Garland	Mazarn Creek	Pearcy Quad, T3S, R22W, Sec 25, center
*Howard	Cossatot River East of AR 4	Baker Springs Quad, T5S, R30W, Sec 26, NW 1/4
*Howard	Cossatot River North of AR 4	Baker Springs Quad, T5S, R30W, Sec 27, NE 1/4
Montgomery	Winding Stairs Trail, LMR	Athens Quad, T4S, R27W, Sec 32, NE 1/4
Montgomery	Buttermilk Springs Road and Collier Creek	Caddo Gap Quad, T3S, R24W, Sec 31, SE 1/4
Montgomery	Buttermilk Springs	Caddo Gap Quad, T4S, R24W, Sec 6, NW 1/4
Montgomery	North side of Caddo River in Black Springs	Norman Quad, T3S, R25W, Sec 30, center
Montgomery	Polk Creek Crossing on Pole Thicket Road	Norman Quad, T3S, R25W, Sec 31, NW 1/4
Montgomery	Southeast of chicken house on Rojo Lane	Norman Quad, T3S, R25W, Sec 31, SW 1/4
+Montgomery	Lick Creek NE of Gaston Road Bridge	Norman Quad, T3S, R26W, Sec 24, NW 1/4 and Sec 13, SW 1/4
Montgomery	Caddo Hills School	Norman Quad, T4S, R25W, Sec 12, NW 1/4
Montgomery	Mt. Gilead Church Road at Polk Creek Crossing	Norman Quad, T4S, R26W, Sec 1, NW 1/4 and Sec 2, NE 1/4
Montgomery	East of Opal on FR 5133	Pine Ridge Quad, T2S, R27W, Sec 30, SW 1/4
+Montgomery	Kates Creek	Pine Ridge Quad, T2S, R27W, Sec 32, NW 1/4
Montgomery	Caddo River on Mt. Gilead Church Road	Polk Creek Mtn. Quad, T3S, R26W, Sec 26, SW 1/4
Montgomery	AR 8 and Caddo River, near Jct. of FR 73	Polk Creek Mtn. Quad, T3S, R26W, Sec 28, SW 1/4
Montgomery	Caddo River Campsite	Polk Creek Mtn. Quad, T3S, R27W, Sec 25, SE 1/4
Montgomery	Polk Creek west of FR 73	Polk Creek Mtn. Quad, T4S, R26W, Sec 4, SW 1/4 and Sec 5, SE 1/4
*Pike	Little Missouri River	Athens Quad, T5S, R27W, Sec 17, NE 1/4
+Polk	Big Fork Natural Area	Big Fork Quad, T3S, R28W, Sec 10, SE 1/4
*Polk	Cossatot River at Gillham Springs	Eagle Mtn. Quad, T4S, R30W, Sec 15, SW 1/4 and Sec 22, NW 1/4
*Polk	Big Fork NW of Opal	Pine Ridge Quad, T2S, R28W, Sec 21, NW 1/4
Polk	Big Fork in Opal	Pine Ridge Quad, T2S, R28W, Sec 28, SE 1/4
Saline	Steel Bridge Road at Saline River	Lake Norrell Quad, T1S, R15W, Sec 8, NW 1/4
*Sevier	Cossatot River	Gillham Dam Quad, T7S, R30W, Sec 19, NW 1/4
*Yell	Petit Jean River	Blue Mtn. Dam Quad, T5N, R25W, Sec 15, NE 1/4

Table 2. Summary statistics of the measured population parameters for the 22 sites visited.

	Distance of individuals nearest stream (m)	Distance of individuals farthest from stream (m)	Minimum elevation above stream (m)	Population length (m)	Population width (m)	Population area (m2)	Percent canopy cover
Max	82	98	8.5	305	70	10120	99.480
Min	1	7	1	14	6	126	84.400
Median	4.5	30	2	64.5	15	666	96.925
Mode	3	15	1	100	9	270	98.960
Mean	11.727	34.095	2.045	89.182	23.095	2575.476	95.625
Standard Deviation	19.255	20.455	1.610	75.157	16.861	3322.827	4.493

Table 3. Most commonly collected taxa at *Hydrophyllum brownei* sites visited. Nomenclature follows PLANTS National Database.

Taxon Name	No. of Sites at Which Collected (22 Total)
Festuca subverticillata	17
Osmorhiza longistylis	14
Galium aparine	13
Viola pubescens	11
Elymus virginicus var. *virginicus*	10

using a Garmin E-Trex GPS. Because of the unforeseen state of senescence of individuals within the populations, counts of plants were not conducted. Population extent therefore was determined as the area within which individuals were found. Distance measurements also were taken of the individuals within populations that were observed growing closest to and farthest from their associated streams. In addition to linear distances, the individuals nearest the streams were measured for the minimum elevational distance above streams at which the populations grew. A concave spherical densiometer was used to determine the percent canopy cover of the populations. In addition to canopy cover, a list of canopy species was made at each site. Voucher specimens of associated vascular plant species were collected and later identified. Measurements made were summarized to determine the range, arithmetic mean, median, and mode of the population parameters.

Results

In addition to visiting known sites, seven previously unknown populations of *H. brownei* were located by the author, one by Theo Witsell, and one by Susan Hooks in 2002. There are now 26 distinct *H. brownei* sites known (Table 1). In this study, 19 of the 26 populations were visited. Three of the 19 sites visited were arbitrarily broken into paired sub-sites due to geographic features such as slopes, streams, or roads separating individuals within populations. The results presented are based upon visits to a total of 22 sites and sub-sites (Table 1).

Summary statistics are given for seven population parameters measured at the 22 sites visited (Table 2). In the majority of the populations visited, individuals closest to the stream channel were within 10 m of the stream (Fig. 4A). Although populations are restricted to true mesic and riparian habitat, depending on the size of the floodplain, individuals may grow a sizable distance from the stream

Table 4. Canopy cover species recorded from the 22 *Hydrophyllum brownei* sites visited. Nomenclature follows PLANTS National Database.

Taxon Name	No. of Sites Recorded	Taxon Name	No. of Sites Recorded
Liquidambar styraciflua	17	*Ilex opaca*	2
Platanus occidentalis	16	*Juniperus virginiana*	2
Ulmus spp.	13	*Lindera benzoin*	2
Acer negundo	9	*Acer saccharum*	1
Carya spp.	8	*Albizia julibrissin*	1
Celtis sp.	8	*Arundinaria gigantea*	1
Carpinus caroliniana	7	*Asimina triloba*	1
Fraxinus sp.	7	*Cercis canadensis*	1
Tilia americana	6	*Cornus florida*	1
Juglans nigra	4	*Cornus drummondii*	1
Magnolia tripetala	4	*Fagus grandifolia*	1
Ostrya virginiana	4	*Nyssa sylvatica*	1
Quercus falcata	4	*Prunus serotina*	1
Quercus rubra	4	*Quercus michauxii*	1
Robinia pseudoacacia	4	*Quercus nigra*	1
Pinus echinata	3	*Salix nigra*	1
Quercus alba	3	*Sideroxylon lanuginosum*	1
Gleditsia triacanthos	3	*Taxodium distichum*	1

channel (up to 100 m away). *Hydrophyllum brownei* grows in populations of varying sizes from just over 100 m^2 to over one hectare, but over half of the sites visited had population extents less than 1000 m^2 (Fig. 4B). None of the populations visited had individuals growing high above the stream channel (Table 2). High shade values (mean = 95.6%, sd = 4.49) appear to be required for the growth of individuals, as indicated from the sites visited (Fig. 4C).

Three hundred and forty-six voucher collections of species growing in association with *H. brownei* were made in May 2002. One hundred and thirteen unique taxa are represented by the collections and are listed alphabetically by family in the Appendix. The species associated with *H. brownei* at the sites visited are typical of shaded riparian or mesic areas. Table 3 shows the herbaceous species collected in the greatest number in May 2002. Although these species are common associates of *H. brownei*, interpretation of this list must be done with care. For example, *Toxicodendron radicans* (poison ivy) probably grows at nearly every site, but it is usually under-collected. Also, certain species that grow with *H. brownei* that were not reproductive at the time the sites were visited are underrepresented as well. Both Kral and Bates (1991) and FTN Associates (2001) list "typical" plants growing with *H. brownei*. The non-grass species that were most commonly collected in this study are also present in the handful of species listed by them. However, both commonly collected grass species (*Festuca subverticillata* and *Elymus virginicus* var. *virginicus*) were lacking from their lists (Table 3).

Only seven introduced taxa were collected from the sites (Appendix). It was surprising that so few introduced species were collected, as riparian areas are usually thought of as prime habitat for invaders. However, it must be noted that three of these *Lonicera japonica* (Japanese honeysuckle), *Ligustrum sinense* (Chinese privet), and *Microstegium vimineum* (Nepalese browntop) are recognized as aggressive invasives. The Appendix supplies a list of all the taxa collected at *H. brownei* populations in May 2002, but it does not depict the abundance of any individual species at one site or any one species among the sites.

The canopy species recorded at the sites are typical of riparian and mesic habitats in the Ouachita Mountains (Table 4). The term canopy as used here refers to those species that shade *H. brownei* and includes those species typically referred to as sub-canopy species. The two most commonly cited species *Liquidambar styraciflua* (sweetgum) and *Platanus occidentalis* (American sycamore) typify riparian areas in the Ouachita Mountains. *Albizia julibrissin* (mimosa) was the only introduced "canopy" species recorded. *Arundinaria gigantea* (cane) was listed as a canopy species at one site because of the tremendous amount of shade it provided the *H. brownei* plants growing below it.

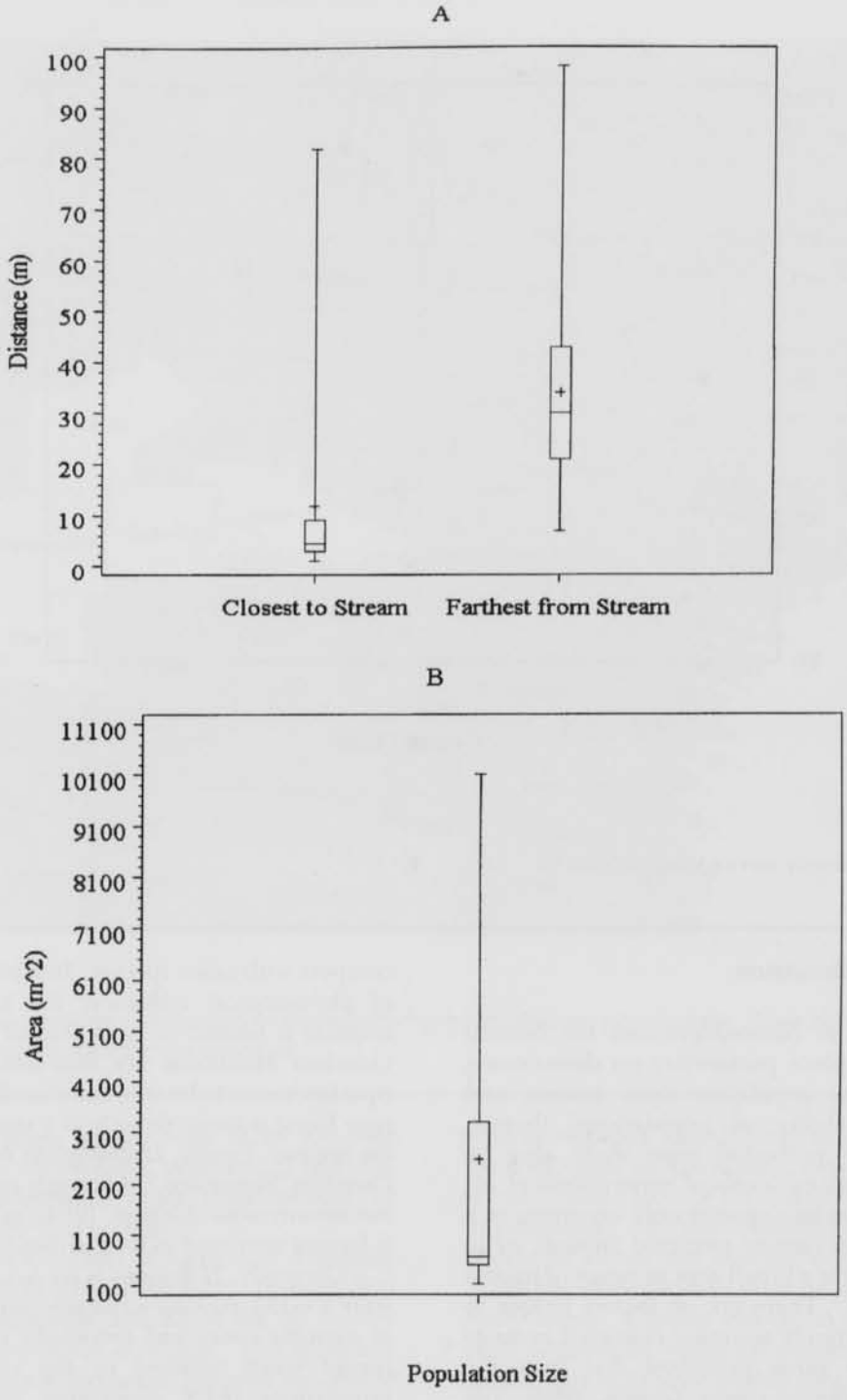

Fig. 4A. Box-plots for selected population parameters. From lowest to highest the box-plot displays the minimum value, the first quartile, the second quartile or median, the third quartile, and the maximum value observed. The + displays the arithmetic mean. (A) Summary of distances *H. brownei* plants grew from streams, (B) range of population areas.

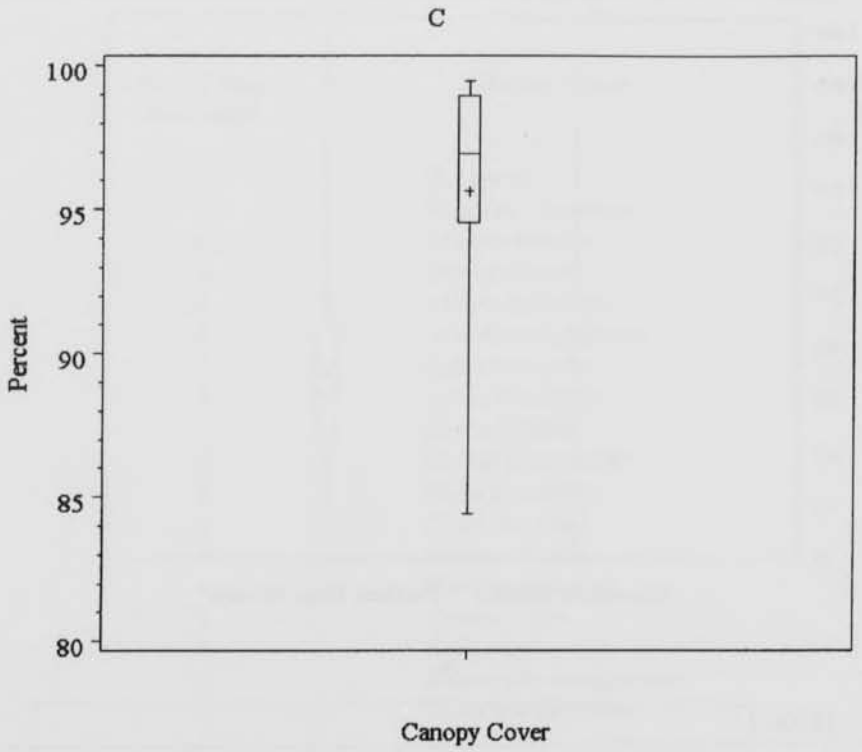

Fig. 4B. High levels of canopy cover were measured.

Discussion

The ranking system of NatureServe and the Natural Heritage network helps place parameters on determining rarity, but in addition to population sizes, extents, and species ranges, the viability of populations, threats, population trends, and protected sites must also be considered when determining levels of rarity (Stein et al., 2000). Rarity may be due to a species only occurring in a small or localized area, in rare or restricted habitats, or in overall low abundance over a broad area or range of habitat (Rabinowitz et al., 1986). There are no factors unique to rare plants. Rare plants simply are more restricted in range and/or number by the same processes that limit the distributions of more common plants (Gaston, 1994). The limited range of *H. brownei* could be due, at least in part, to a narrow tolerance range to physical factors in the environment. Likely candidates for the causes of *H. brownei*'s limited range are its requirements for high shade levels, its need for close proximity to water for seed dispersal (Beckmann, 1979), and its limited ability to compete with other species. In addition to its limited range of physiological tolerance, the habitat that *H. brownei* requires is limited in its region of growth. Although the Ouachita Mountains are dissected by drainages, suitable riparian/mesic habitat is not abundant. Often drier mixed pine forest is found directly at a stream or drainage bank in the region. Finally, *Hydrophyllum brownei* is endemic to the Ouachita Mountains. Although endemism and rarity are not synonymous (Gaston, 1994), as an endemic, *H. brownei* is further restricted in its distribution.

Currently, *H. brownei* is an Arkansas inventory element with a G1S1 ranking–critically imperiled globally because of extreme rarity and extremely rare in Arkansas. After recent work resulted in the confirmation of known populations (FTN Associates, 2001) and discovery of previously unknown sites, the species may be better represented by a reduction in status to the global rank of G2 (imperiled globally because of rarity) and the state rank of S2 (very rare). *Hydrophyllum brownei* is now known from 26 distinct sites. Based upon number of occurrences alone, the species would now fall into the categories of G3 (found

Fig. 5. Arkansas counties showing distribution of known *Hydrophyllum brownei* populations. Numbers in parentheses represent the number of known populations for the counties.

locally in a restricted range, usually with 21 to 100 sites known) and S3 (rare to uncommon, between 20 and 100 sites). However, considerations other than number of occurrences must be taken into account.

As an endemic to the Ouachita Mountains of Arkansas, the species requires an extra level of attention. *Hydrophyllum brownei* has a very small range, and 22 of the 26 known populations grow within a radius of 30 km. The species is known from eight counties in Arkansas, but over two-thirds of the known populations are from Montgomery and Polk counties alone (Fig. 5). It was also found that within its small range, *H. brownei* was greatly restricted to areas no more than 100 m from stream courses. Although no immediate pressures from development are threatening the species, the majority of the populations (at least 16) are located on private land holdings. In addition, not all populations are equally vigorous, and although some populations number in the thousands of individuals, others have been found with fewer than 20 (FTN Associates, 2001; Marsico, unpublished). It was determined that populations vary widely in extent but that the majority of them are small. Small population extent must be considered when assessing rarity status. Climate change in the area or even a small scale catastrophe could have a serious impact on the entire species due to its very limited range. Still, the G1S1 ranking is clearly no longer appropriate. It is recommended that the species status be reduced only to the less critical G2S2 ranking based on the small range and inconsistent vigor of the populations.

Continued monitoring and searches to find further *H. brownei* populations are also recommended. However, the prime time for searching discussed by both Kral and Bates

(1991) and FTN Associates (2001), May, is too late for accurate individual plant counts. Flowering individuals remain observable above ground for a much longer time than non-flowering individuals. As long as an investigator is familiar with the species, populations can be found from mid-March through May. Therefore, counts of individuals for monitoring purposes should be conducted early in the season from mid-April to early May. It may be that ratios of flowering individuals to non-flowering individuals will prove difficult to determine, as those plants that do not flower in a given year senesce much earlier than those that do flower. In addition, it is a possibility that certain individuals are dormant through an entire growing season, remaining underground as a viable rootstock, as in certain members of Asclepiadaceae (Alexander et al., 1997) and some other herbaceous perennials. Future searches may result in recommendations for further lowering of rarity ranking if populations continue to be located. At the present time, however, G2S2 is the most appropriate ranking for *H. brownei*. Additional investigations and studies of natural history, ecology, distribution patterns, and conservation genetics are warranted to better understand this rare Arkansas endemic.

ACKNOWLEDGMENTS.—I must first and foremost acknowledge the Ouachita National Forest, which provided the grant to the University of Arkansas Herbarium to fund a portion of this project. I also thank the Arkansas Native Plant Society for funding. The Ouachita Mountains Biological Station provided an excellent place to stay and work while in the field. I appreciate the OMBS more than I can say. Dr. Johnnie Gentry's discussions stimulated my thinking as to the directions this project could take, and his listening ear is always appreciated. Thanks to Sarah Nunn for her help in identifications and review of this manuscript. I also appreciate the assistance received from the University of Arkansas Center for Statistical Consulting. Susan Hooks, Terry McKay, and Theo Witsell all provided information to locations of known *H. brownei* populations. Finally, I gladly thank my wife, Katie, for her unceasing support, attentive listening (if only pretending) to rants, concerns, and formulation of ideas, time with me in the field, and hours of assistance upon my return.

Literature Cited

Alexander, H. M., N. A. Slade, W. D. Kettle. 1997. Application of mark-recapture models to estimation of the population size of plants. Ecology 78: 1230-1237.

Beckmann, R. L., Jr. 1979. Biosystematics of the genus *Hydrophyllum* L. (Hydrophyllaceae). Amer. J. Bot. 66:1053-1061.

Constance, L. 1942. The genus *Hydrophyllum* L. Amer. Mid. Nat. 27:710-731.

FTN Associates. 2001. Species status survey–*Hydrophyllum brownei* Kral & Bates. Prepared for US Fish and Wildlife Service, Conway (Arkansas) Field Office–Unpublished document.

Gaston, K. J. 1994. Rarity. Chapman & Hall, London, United Kingdom.

Hoang, L. 1999. Survey for *Hydrophyllum brownei*. Unpublished report to the Arkansas Natural Heritage Commission.

Kral, R., and **V. Bates.** 1991. A new species of *Hydrophyllum* from the Ouachita Mountains of Arkansas. Novon 1:60-66.

Moore, D. M. 1951. Some new records for the Arkansas flora. Proc. Arkansas Acad. Sci. 4:61-63.

Rabinowitz, D., S. Cairns, and **T. Dillon.** 1986. Seven forms of rarity and their frequency in the flora of the British Isles. Pages 182-204, *In* Conservation Biology (M. E. Soule, editor). Sinauer Associates, Inc., Sunderland, Massachusetts. xii + 584 pp.

Stein, B. A., L. S. Kutner, and **J. S. Adams (editors).** 2000. Precious Heritage: the Status of Biodiversity in the United States. Oxford University Press, Inc., New York, New York. xxv + 399 pp.

Appendix–List of vascular plant taxa collected from *Hydrophyllum brownei* populations, May 2002. Nomenclature follows PLANTS National Database.

Origin	Family	Species
N	Acanthaceae	*Ruellia strepens*
N	Aceraceae	*Acer negundo*
N	Anacardiaceae	*Toxicodendron radicans*
N	Annonaceae	*Asimina triloba*
N	Apiaceae	*Chaerophyllum procumbens* var. *procumbens*
N		*Cryptotaenia canadensis*
N		*Osmorhiza longistylis*
N		*Sanicula canadensis*
N		*Sanicula odorata*
N	Aquifoliaceae	*Ilex decidua*
N		*Ilex opaca*
N	Araceae	*Arisaema dracontium*
N		*Arisaema triphyllum*
N	Aristolochiaceae	*Asarum canadense*
N	Aspleniaceae	*Asplenium platyneuron*
N	Asteraceae	*Heliopsis helianthoides*
N		*Krigia dandelion*
N		*Packera obovata*
N	Berberidaceae	*Podophyllum peltatum*
N	Betulaceae	*Carpinus caroliniana*
N	Boraginaceae	*Cynoglossum virginianum*
N		*Myosotis verna*
N	Brassicaceae	*Arabis laevigata* var. *laevigata*
I	Caprifoliaceae	*Lonicera japonica*
N		*Symphoricarpos orbiculatus*
I	Caryophyllaceae	*Stellaria media*
N	Celastraceae	*Euonymus americana*
N	Commelinaceae	*Tradescantia ernestiana*
N		*Tradescantia ohiensis*
N	Cornaceae	*Cornus drummondii*
N		*Cornus florida*
N	Crassulaceae	*Sedum ternatum*
N	Cyperaceae	*Carex amphibola*
N		*Carex blanda*
N		*Carex jamesii*
N		*Carex oligocarpa*
N		*Carex oxylepis* var. *oxylepis*
N		*Carex retroflexa*
N		*Carex rosea*
N		*Carex texensis*
N	Dryopteridaceae	*Cystopteris protrusa*
N		*Onoclea sensibilis*
N		*Polystichum acrostichoides*
N	Ebenaceae	*Diospyros virginiana*
N	Fabaceae	*Cercis canadensis* var. *canadensis*
N		*Robinia pseudoacacia*
N	Fagaceae	*Quercus falcata*
N		*Quercus michauxii*
N		*Quercus shumardii* var. *shumardii*
N	Fumariaceae	*Corydalis flavula*
N	Gentianaceae	*Frasera caroliniensis*
N	Geraniaceae	*Geranium maculatum*
N	Hamamelidaceae	*Hamamelis vernalis*
N		*Liquidambar styraciflua*
N	Hippocastanaceae	*Aesculus glabra*
N	Hydrophyllaceae	*Hydrophyllum brownei*
N		*Nemophila phacelioides*
N		*Phacelia hirsuta*
N	Iridaceae	*Iris cristata*
N	Lamiaceae	*Monarda russeliana*
N		*Prunella vulgaris* ssp. *lanceolata*
N		*Scutellaria elliptica* var. *elliptica*
N	Lauraceae	*Lindera benzoin*
N		*Sassafras albidum*
N	Liliaceae	*Allium canadense* var. *canadense*
N		*Polygonatum biflorum*
N		*Trillium viridescens*
N	Loganiaceae	*Spigelia marilandica*
N	Magnoliaceae	*Magnolia tripetala*
N	Menispermaceae	*Calycocarpum lyonii*
N		*Cocculus carolinus*
I	Oleaceae	*Ligustrum sinense*
N	Ophioglossaceae	*Botrychium virginianum*
N	Papaveraceae	*Sanguinaria canadensis*
N	Platanaceae	*Platanus occidentalis*
N	Poaceae	*Arundinaria gigantea*
N		*Bromus pubescens*
N		*Diarrhena obovata*
N		*Dichanthelium boscii*
N		*Dichanthelium commutatum*
N		*Elymus virginicus* var. *virginicus*
N		*Festuca subverticillata*
N		*Melica mutica*
I		*Microstegium vimineum*
N		*Poa sylvestris*
N	Polemoniaceae	*Phlox divaricata* ssp. *laphamii*
N		*Polemonium reptans*
I	Polygonaceae	*Rumex obtusifolius*
N	Ranunculaceae	*Ranunculus recurvatus*
N		*Thalictrum revolutum*
N	Rhamnaceae	*Berchemia scandens*
N		*Frangula caroliniana*
I	Rosaceae	*Duchesnea indica*

Origin	Family	Species	Origin	Family	Species
N		*Geum canadense*	N		*Ulmus americana*
I		*Potentilla recta*	N		*Ulmus rubra*
N	Rubiaceae	*Galium aparine*	N	Violaceae	*Viola affinis*
N		*Galium circaezans*	N		*Viola pubescens*
N		*Galium triflorum*	N		*Viola sororia*
N	Sapotaceae	*Sideroxylon lanuginosum*	N		*Viola striata*
N	Smilacaceae	*Smilax glauca*	N	Vitaceae	*Parthenocissus quinquefolia*
N		*Smilax rotundifolia*	N		*Vitis cinerea* var. *cinerea*
N	Staphyleaceae	*Staphylea trifolia*	N		*Vitis vulpina*
N	Tiliaceae	*Tilia americana* var. *caroliniana*			
N	Ulmaceae	*Ulmus alata*			

I = Introduced N = Native

Geographic Distribution Records for Scolopendromorph Centipedes (Arthropoda: Chilopoda) from Arkansas, Oklahoma, and Texas

Chris T. McAllister
Department of Biology
Texas A&M University-Texarkana
Texarkana, TX 75505

Rowland M. Shelley
Research Laboratory
North Carolina State Museum of Natural Sciences
4301 Reedy Creek Rd.
Raleigh, NC 27607

James T. McAllister, III
Brookhaven College
3939 Valley View Lane
Dallas, TX 75244

*Corresponding Author

Abstract

During 2001-2003, we collected eight species of scolopendromorph centipedes from 17 counties of Arkansas (AR), seven counties of Oklahoma (OK), and 17 counties of Texas (TX). The following taxa were collected: *Cryptops leucopodus* (Rafinesque) from Bowie and Cass counties, TX, and Pulaski County, AR; *Hemiscolopendra marginata* (Say) from Columbia, Garland, Hempstead, Little River, Pike, Polk, and Yell counties, AR, and Cass, Cherokee, Coryell, Houston, Johnson, Kimble, Marion, Nacogdoches, Smith, and Tom Green counties, TX; *Scolopocryptops rubiginosus* L. Koch from Bowie and Dallas counties, TX; *Scolopocryptops sexspinosus* (Say) from Clark, Columbia, Conway, Faulkner, Hot Spring, Garland, Miller, Montgomery, Polk, Pope, and Pulaski counties, AR, LeFlore and McCurtain counties, OK, and Marion, Red River, and Rusk counties, TX; *Scolopendra heros* Girard from Atoka, Major, and McCurtain counties, OK; *Scolopendra polymorpha* Wood from Woodward County, OK; *Theatops posticus* (Say) from Montgomery County, AR, Choctaw, Marshall, and McCurtain counties, OK, and Cass, Dallas, Freestone, Hopkins, Houston, Red River, and Titus counties, TX; and *Theatops spinicaudus* (Wood) from Garland, Hot Spring, Little River, Pike, and Scott counties, AR, and Atoka, Choctaw, and McCurtain counties, OK. Most significantly, our records of *S. rubiginosus* are well outside its distributional range as depicted in Shelley (2002). A total of 43 new county records is documented, including 14 in Arkansas, nine in Oklahoma, and 20 in Texas.

Introduction

Shelley (2002) recently provided a faunistic monograph on North American scolopendromorph centipedes. It represented the most comprehensive synopsis to date of this important centipede order that includes three families, eight genera, and 21 species. Records of Arkansas, Oklahoma, and Texas scolopendromorphs and centipedes of other orders have never before been consolidated; there are a few reports scattered in miscellaneous papers, and most of the Arkansas records that exist are ones provided by Charles H. Bollman (Bollman, 1888, 1893). Chamberlin (1931, 1942, 1943) and Chamberlin and Muliak (1941) also reported on some chilopods of Oklahoma, Arkansas, and Texas, and Reddell (1965, 1970) provided checklists of centipedes inhabiting caves in Texas. Hoffman and Shelley (1996) reported distributional information on *Hemiscolopendra marginata*, the range of which encompasses most of Arkansas, southeastern Oklahoma, and Texas. Shelley (1990) noted some Arkansas records of *Theatops posticus* and records of the tribe Plutoniuminae were provided by Shelley (1997). The purposes of this paper are to document some distributional information on scolopendromorph centipedes of the Ark-La-Tex and to report additional Arkansas, Oklahoma, and Texas localities for eight species.

Materials and Methods

Between October 2001 and September 2003, we collected centipedes in 17 counties (Clark, Columbia, Conway, Faulkner, Garland, Hempstead, Hot Spring, Johnson, Little River, Miller, Montgomery, Pike, Polk, Pope, Pulaski, Scott, and Yell) of Arkansas, seven counties (Atoka, Choctaw, LeFlore, Major, Marshall, McCurtain, and Woodward), of Oklahoma and 17 counties (Bowie, Cass, Cherokee, Coryell, Dallas, Freestone, Hopkins, Houston, Johnson, Kimble, Marion, Nacogdoches, Red River, Rusk, Smith, Titus, and Tom Green) of Texas. The majority of specimens were taken from damp areas off trails in pine and hardwood forests by overturning decaying logs, leaf litter, and stones with potato rakes. Centipedes were also collected by peeling bark off rotting logs and stumps. At each locale, specimens were placed in individually labeled vials containing 70% ethanol and returned to the laboratory for preliminary processing and sorting. Centipedes were shipped to the second author (RMS) and identified to species. Voucher specimens were deposited in the North Carolina State Museum of Natural Sciences (NCSM).

Results and Discussion

A total of eight species of centipedes, representing five genera and three families within the order Scolopendromorpha, was found during our survey. The most common species collected was *Hemiscolopendra marginata* (Say, 1821) reported from seven Arkansas and 10 Texas counties. A complete list of taxa collected is presented below and annotated with distributional and ecological information. Specimens collected by the first and third authors are indicated by the initials CTM and JTM, respectively.

Annotated List

Family Scolopendridae

Scolopendra heros Girard, 1853. **OKLAHOMA**: **Atoka County,** 4.8 km E Springtown, off OK St. Hwy. 43, under trash pile, 4 April 2002, CTM & BSC 405 class. **Major County**, Whitlaw Ranch, 20.6 km SW Waynoka off US 412, 13 September 2003, S. Barclay. **McCurtain County**, Beaver's Bend State Park, David Boren Trail, 3 June 2003, CTM & BSC 405 class. Although expected statewide and reported previously from 21 counties in Oklahoma (see Shelley, 2002), these represent new county records.

Scolopendra polymorpha Wood, 1861. **OKLAHOMA: Woodward County**, Ft. Supply WMA, 1.6 km S. Ft. Supply off US 183, 12 September 2003, Z. D. Ramsey (**new county record**). Except for the eastern periphery, the species is expected statewide in Oklahoma, albeit it has been previously reported from only 13 counties (Shelley, 2002).

Hemiscolopendra marginata (Say, 1821). **ARKANSAS: Columbia County**, Logoly State Park, 28 December 2001, CTM & JTM (**new county record**). **Garland County**, vic. Bear off Brady Mountain Road, 6 April 2002, CTM (**new county record**). **Hempstead County**, 3.2 km W Springhill off AR St. Hwy. 355, 14 February 2002, C. S. Harris (**new county record**). **Little River County**, Wilton off US St. Hwy. 71, #1 April 2003, A. Shoemake. **Pike County**, Daisy State Park, Lake Greeson, 10 February 2002, CTM; and Crater of Diamonds State Park, 10 February 2002, CTM. **Polk County**, Pioneer Cemetery Historic Site, 2.4 km W. Queen Wilhelmina State Park along AR St. Hwy. 88 on Rich Mountain, 11 June 2002, CTM & J. L. Hollis; and Grannis, off US 71, 19 April 2003, S. Singer (**new county record**). **Yell County**, Sunlight Bay Park, Lake Nimrod, 24 December 2002, CTM & JTM (**new county record**). **TEXAS: Cass County**, 1.6 km E TX St. Hwy. 8, off FM 955, 29 October 2002, D. Moore. **Cherokee County**, Rusk-Palestine State Park, 1 March 2003, CTM & G. Torres (**new county record**). **Coryell County**, Mother Neff State Park, 25 January 2002, CTM. **Houston County**, 29.0 km E Crockett, Ratcliff Recreation Area off TX St. Hwy. 7 at 4-C Trail, 1 March 2003, CTM & G. Torres. **Johnson County**, Cleburne State Park, 25 January 2002, CTM (**new county record**). **Kimble County**, South Llano River State Park, 22 February 2003, CTM. **Marion County**, 6.4 km NW Jefferson and Lake O' the Pines, 3 February and 8 March 2003, D. Moore (**new county record**). **Nacogdoches County**, jct. county rd. 628 and FM 2782, Stephen F. Austin Interpretive Trail, 1 March 2003, CTM & G. Torres. **Smith County**, Tyler State Park, 22 March 2003, D. Moore (**new county record**). **Tom Green County**, San Angelo State Park, 28 November 2002, CTM (**new county record**). This is a widespread species whose range extends from the northern periphery of Arkansas westward into Texas to Presidio County (Hoffman and Shelley, 1996). The species has been reported previously from 41 counties of Texas and is expected to be nearly statewide in distribution in Arkansas, having been reported previously from 20 counties (Shelley, 2002). We report herein 10 new county records, five each from Arkansas and Texas.

Family Scolopocryptopidae

Scolopocryptops sexspinosus (Say, 1821). **ARKANSAS: Clark County**, 4.8 km NE Caddo Valley, off AR St. Hwy. 283, 31 January 2003, CTM (**new county record**). **Columbia County**, Logoly State Park, 28 December 2002, CTM & JTM. **Conway County**, Petit Jean State Park, 24 December 2002, CTM & JTM (**new county record**). **Faulkner County**, Woolly Hollow State Park on Huckleberry Trail, 25 December 2002, CTM & JTM (**new county record**). **Garland County**, vic. Bear off Brady Mountain Road, 4 April 2002, CTM; and 4.8 km W Crystal Springs off US 270, Charlton Recreation Area, 11 June 2002, CTM (**new county record**). **Hot Spring County**, Lake DeGray State Park, 1 February 2002, CTM (**new county record**). **Miller County**, 1.6 km S Genoa off AR St. Hwy. 196, 14 February 2002, C. S. Harris (**new county record**). **Montgomery County**, Mount Ida, 28 May 2003, CTM & JTM. **Polk County**, 3.2 km N Mena off US 88, Earthquake Trail, 13 August 2003, CTM. **Pope County**, 9.7 km N Hector off AR St. Hwy. 27, 24 June 2002, CTM. **Pulaski County**, 3.2 km S Sweet Home off AR St. Hwy. 365, 27 December 2002, CTM & JTM. **OKLAHOMA: LeFlore County,** Choctaw Nation historic site off OK St. Hwy 1 on Rich Mountain, 3 April 2003, CTM & Z. Ramsey (**new county record**). **McCurtain County**, Beaver's Bend State Park, 1 March 2002, CTM; and 11.3 km S Smithville off US 259 on county rd. 891, 11 September 2002, CTM & J. Kessler. **TEXAS: Marion County**, 6.4 km NW Jefferson, 22 December 2002, D. Moore (**new county record**). **Red River County**, 19.3 km N Clarksville, off TX Hwy 37, 26 April 2003, CTM & G. Torres (**new county record**). **Rusk County**, vic. Mt. Enterprise off US 84, Griff Ross Trail, 27 February 2003, CTM & G. Torres (**new county record**). This is the most common scolopendromorph centipede in eastern North America and its range includes all of

Arkansas, the eastern half of Oklahoma, and eastern and east-central Texas (Shelley, 2002); however, we report 10 new county records herein.

Scolopocryptops rubiginosus L. Koch, 1878. **TEXAS: Bowie County**, Texarkana off I-30, S. Cowhorn Creek Loop, 16 January 2003, CTM (**new county record**). **Dallas County**, Cedar Hill State Park, 21 January and 16 November 2002, CTM (**new county record**). **Red River County**, 19.3 km N Clarksville, off TX Hwy 37, 26 April 2003, CTM & G. Torres (**new county record**). In Texas, the species was previously known only from the northern fringe of the state along the Red River in Grayson County and a disjunct record from the south in San Patricio County (Shelley, 2002). Our new records (Fig. 1) are well outside the range as depicted in Shelley (2002; Fig. 108), and the Bowie County, Texas, record suggests its possible occurrence in adjacent parishes of extreme northwestern Louisiana that would represent a new state record.

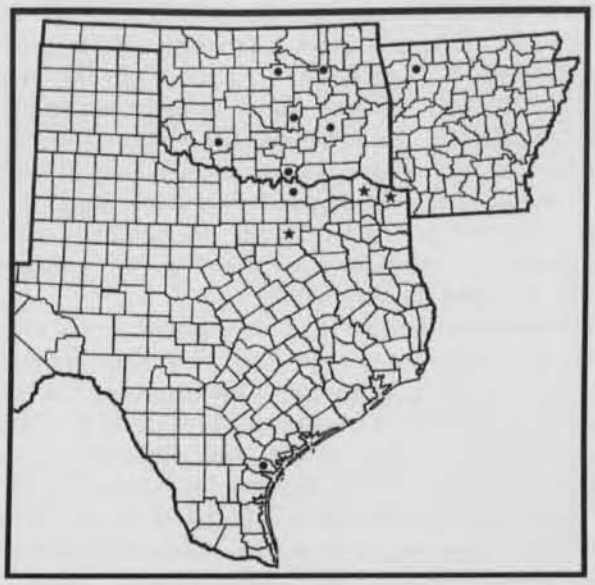

Fig. 1. Distribution of *Scolopocryptops rubiginosus* in Arkansas, Oklahoma, and Texas. Previous records (dots); new records (stars).

Family Cryptopidae

Theatops posticus (Say, 1821). **ARKANSAS: Montgomery County**, Mount Ida, 28 May 2003, CTM & JTM (**new county record**). **OKLAHOMA: Choctaw County**, Raymond Gary State Park, 24 April 2003, CTM & G. Torres (**new county record**). **Marshall County**, Buncombe Creek Recreation Area off OK Hwy. 99, 25 April 2003, CTM & G. Torres (**new county record**). **McCurtain County**, Beaver's Bend State Park, Boren Trail, 3 June 2003, CTM (**new county record**). **TEXAS: Cass County**, 1.6 km E TX St. Hwy. 8 on FM 955, 29 October 2002, D. Moore (**new county record**). **Dallas County**, Cedar Hill State Park, Talala Trail, 21 January 2002 and 16 November 2002, CTM (**new county record**). **Freestone County**, Fairfield Lake State Park, 21 December 2002, CTM & JTM (**new county record**). **Hopkins County**, Cooper Lake State Park-South Sulphur Unit, 3 January 2003, CTM (**new county record**). **Houston County**, 29.0 km E Crockett, Ratcliff Recreation Area off TX St. Hwy. 7 at 4-C Trail, 1 March 2003, CTM & G. Torres (**new county record**). **Red River County**, 19.3 km N Clarksville, off TX Hwy 37, 26 April 2003, CTM & G. Torres (**new county record**). **Titus County**, vic. Cookville at White Oak Creek, 20 September 2003, M. Cameron (**new county record**). Part of the range of this species includes an area extending from the Atlantic coast to the eastern periphery of the Central Plains in Seminole County, Oklahoma, and Limestone County, Texas, south of Dallas (Shelley, 1990). The Dallas and Marshall county sites reported here are the farthest west the species has been documented in northcentral Texas and southcentral Oklahoma, respectively. Although expected statewide in Arkansas, it is now known from only four counties of the state and only five counties in Oklahoma; in Texas, it is expected throughout the eastern one quarter of the state (Shelley, 1997).

Theatops spinicaudus (Wood, 1862). **ARKANSAS**: **Garland County**, vic. Bear off Brady Mountain Road, 6 April 2002, CTM. **Hot Spring County**, Lake DeGray State Park, 1 February 2002, CTM. **Little River County**, Wilton off US Hwy. 71, 6 February 2003, A. Shoemake (**new county record**). **Pike County**, Crater of Diamonds State Park, 10 February 2002, CTM. **Scott County**, 3.7 km SW "Y" City off US 71/270, 5 April 2003, CTM & Z. D. Ramsey (**new county record**). **OKLAHOMA**: **Atoka County**, McGee Creek State Park off OK St. Hwy. 3, 31 October 2002, CTM (**new county record**). **Choctaw County**, vic. Fort Towson off US 70, 18 April 2002, CTM (**new county record**). **McCurtain County**, Beaver's Bend State Park, David Boren Trail, 21 March 2002 and 3 June 2003, CTM; and 11.3 km S Smithville off US 259 on county road 891, 13 September 2002, CTM & J. Kessler. Interestingly, *T. spinicaudus* is considered to have statewide distribution in Arkansas, except for the extreme southern tier of counties, and has been reported previously from 24 counties of the state (Shelley, 1997). In Oklahoma, *T. spinicaudus* was previously known only from McCurtain and Muskogee counties (Shelley, 1997, 2002). The species has yet to be reported from Texas (Shelley, 2002) but these records suggest it may occur in the extreme northeast part of the state in the Ark-La-Tex region.

Cryptops leucopodus (Rafinesque, 1820). **ARKANSAS: Pulaski County**, Pinnacle Mountain State Park, 26 December 2001, CTM & JTM; and 3.2 km S Sweet Home

off AR St. Hwy. 364, 27 December 2001, CTM & JTM. **TEXAS: Bowie County**, Texarkana, off I-30, S. Cowhorn Creek Loop, 16 January 2003, CTM (**new county record**). **Cass County**, 1.6 km E TX St. Hwy. 8 off FM 955, 29 October 2002, D. Moore (**new county record**). It is expected statewide in Arkansas, but authentic specimens have been reported from only eight counties; in Texas, it is found in the northeastern one-fourth of the state and has been reported previously from 16 counties; and in Oklahoma, *C. leucopodus* is expected in the southeastern one-third of state (Shelley, 2002).

ACKNOWLEDGMENTS.—The first author would like to thank the Arkansas Game and Fish Commission for scientific collecting permit #1480, the Oklahoma Department of Wildlife Conservation for scientific collecting permit #3376, all the various State Park personnel for helpful assistance, and M. Whitlaw for access to his ranch. We also thank numerous TAMU-T biology students, especially S. Barclay, M. Cameron, J. Kessler, D. Moore, A. Shoemake, S. Singer, G. Torres, and Z. Ramsey for assistance in collecting. This study was supported by a TAMU-T Faculty Senate Enrichment Grant #200900 to CTM.

Literature Cited

Bollman, C. H. 1888. A preliminary list of the myriapods of Arkansas, with descriptions of new species. Entomol. Amer. 4:1-8.

Bollman, C. H. 1893. The Myriapoda of North America. Bull. U.S. Nat. Mus. 46:1-210.

Chamberlin, R. V. 1931. On a collection of chilopods and diplopods from Oklahoma. Entomol. News 42:97-104.

Chamberlin, R. V. 1942. Notes on a collection of centipedes chiefly from Louisiana, Arkansas, and Missouri (Chilopoda). Entomol. News 53:184-188.

Chamberlin, R. V. 1943. Some records and descriptions of American chilopods. Proc. Biol. Soc. Washington 56:97-108.

Chamberlin, R. V., and **S. Muliak.** 1941. On a collection of centipeds from Texas, New Mexico, and Arizona (Chilopoda). Entomol. News 51:107-110, 125-128, 156-158.

Hoffman, R. L., and **R. M. Shelley.** 1996. The identity of *Scolopendra marginata* Say (Chilopoda: Scolopendromorpha: Scolopendridae). Myriapodologica 4:35-42.

Reddell, J. R. 1965. A checklist of the cave fauna of Texas. I. The Invertebrata (exclusive of Insecta). Texas J. Sci. 17:143-187.

Reddell, J. R. 1970. A checklist of the cave fauna of Texas. IV. Additional records of Invertebrata (exclusive of Insecta). Texas J. Sci. 21:389-415.

Shelley, R. M. 1990. The centipede *Theatops posticus* (Say) (Scolopendromorpha: Cryptopidae) in the southwestern United States and Mexico. Canadian J. Zool. 68:2637-2644.

Shelley, R. M. 1997. The holarctic centipede subfamily Plutiniuminae (Chilopoda: Scolopendromorpha: Cryptopidae) (*nomen correctum* Ex subfamily Plutoniinae Bollman, 1893). Brimleyana 24:51-113.

Shelley, R. M. 2002. A synopsis of the North American centipedes of the order Scolopendromorpha (Chilopoda). Virginia Mus. Nat. Hist. Mem. No. 5:1-108.

Millipeds (Arthropoda: Diplopoda) of The Ark-La-Tex. III. Additional Records From Arkansas

Chris T. McAllister*
Department of Biology
Texas A&M University-Texarkana
Texarkana, TX 75505

Rowland M. Shelley
Research Laboratory
North Carolina State Museum of Natural Sciences
4301 Reedy Creek Rd.
Raleigh, NC 27607

James T. McAllister, III
Brookhaven College
3939 Valley View Lane
Dallas, TX 75244

*Corresponding Author

Abstract

As part of an on-going effort by the second author (RMS) to elucidate the North American diplopod fauna, we collected millipeds in 14 Arkansas counties between April 2002 and October 2003. Additional information for these species is recorded from the holdings at the University of Arkansas Arthropod Museum along with unpublished records from other institutions in the second author's files. The following species were identified: *Abacion tesselatum*, *A. texense*, *Aliulus caddoensis*, *Apheloria virginiensis ?reducta*, *Auturus evides*, *A. louisianus louisianus*, *Brachycybe lecontei*, *Brachyiulus lusitanus*, *B. pusillus*, *Cambala minor*, *Desmonus pudicus*, *Eurymerodesmus birdi birdi*, *E. polkensis*, *E. pulaski*, *E. serratus*, *Narceus americanus*, *Oriulus venustus*, *Oxidis gracilis*, *Pseudopolydesmus pinetorum*, *P. serratus*, and *Virgoiulus minutus*. A different and potentially new species of *Pseudopolydesmus* was collected in the entrance to Searcy Cave, Independence County. Three new state and 68 new county records are documented.

Introduction

This contribution is the third in a series of works on the Diplopoda of the Ark-La-Tex area in the southcentral United States. The first two (McAllister et al. 2002a, b) documented species occurring in western, central, and southern Arkansas, and eastern and southeastern Oklahoma. In addition, Shelley et al. (2003) provided a description of *Abacion wilhelminae* (Callipodida: Abacionidae), a new species from Rich Mountain, Polk County, Arkansas. Most recently, Shear (2003a, b) described three new species of chordeumatid millipeds in Arkansas. Prior to these reports, nearly 50 years had elapsed since the last such documentation for these states (Causey, 1955), which was primarily restricted to northwestern Arkansas and northeastern Oklahoma. There are also many reports that list species of millipeds inhabiting caves of Arkansas (McDaniel and Smith, 1976; Youngsteadt and Youngsteadt, 1978; McDaniel et al., 1979; Dunivan et al., 1982; Peck and Peck, 1982). Although a consolidated listing has never been prepared, these states harbor a speciose milliped fauna as evidenced by records in taxonomic papers and range descriptions in the latest continental checklist (Hoffman, 1999). Our work in the Ark-La-Tex is part of a larger effort by RMS to document the North American fauna as a whole, and we report here additional Arkansas localities for 22 species/subspecies.

Materials and Methods

Between April 2002 and October 2003, we collected millipeds in 14 counties of northern, western, and southwestern Arkansas: Clark, Cleburne, Conway, Craighead, Faulkner, Garland, Independence, Little River, Montgomery, Polk, Pope, Pulaski, Stone, and Yell. Most were discovered in damp areas along trails in pine and hardwood forests by overturning decaying logs and leaf litter with potato rakes. A few specimens were uncovered by peeling bark from rotting logs and stumps. At each locality, specimens were placed in individually labeled vials containing 70% ethanol and returned to the laboratory for preliminary processing and sorting. They were then shipped to RMS and identified to the lowest taxonomic level, the most important features being aspects of the male genitalia (aperture and gonopods). Voucher specimens were deposited in the North Carolina State Museum of Natural Sciences (NCSM). Supplemental material exists in the holdings of the following repositories:

FMNH – Field Museum of Natural History, Chicago, Illinois,

FSCA – Florida State Collection of Arthropods, Gainesville, Florida,

MCZ – Museum of Comparative Zoology, Harvard University, Cambridge, Massachusetts,

MEM – Mississippi Entomological Museum, Mississippi State University, Starkville, Mississippi,

MPM – Milwaukee Public Museum, Milwaukee, Wisconsin,

NMNH – National Museum of Natural History, Smithsonian Institution, Washington, DC,

OKSU - Emerson Entomological Museum, Oklahoma State University, Stillwater, Oklahoma,

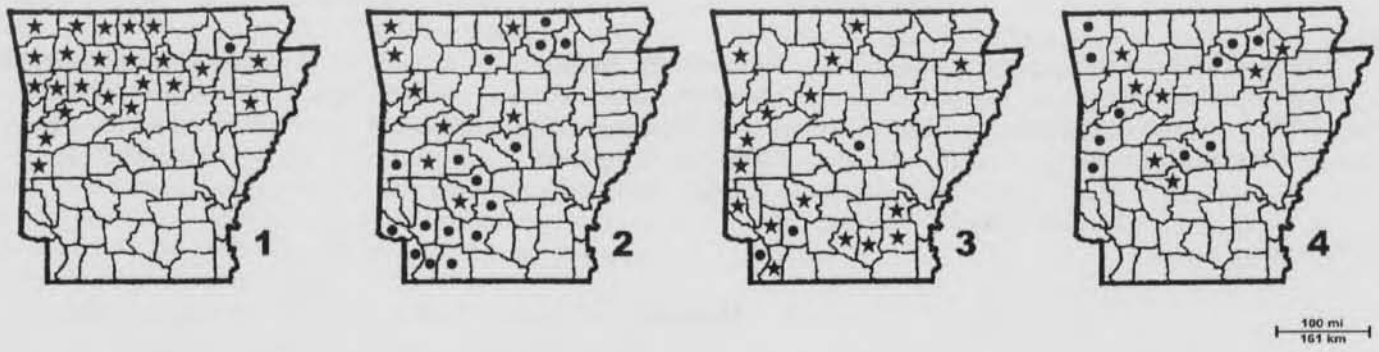

Figs. 1-4. Distributions of four milliped taxa in counties of Arkansas. 1. *Apheloria virginiensis ? reducta.* 2. *Pseudopolydesmus pinetorum.* 3. *Virgoiulus minutus.* 4. *Brachycybe lecontei.* Stars = new records. Dots = previous records.

UAAM – University of Arkansas Arthropod Museum, Fayetteville, and Arkansas,

UCO – University of Colorado Museum, Boulder, Colorado.

Results and Discussion

Distributional information is reported for 22 milliped species and subspecies, representing 13 genera, 13 families, and six orders, including a potentially new species of *Pseudopolydesmus.* Sixteen counties are cited for *Virgoiulus minutus* (Brandt, 1841), 15 of which are from samples in the FSCA and UAAM. The species collected and examined are listed below along with pertinent distributional information. Missing locality data was not provided on vial labels, and specimens collected by the first and third authors are indicated by the initials CTM and JTM, respectively. Arkansas county distribution maps are provided for some poorly documented species (Figs. 1-4).

List of Species

Order Polydesmida, Family Xystodesmidae

Apheloria virginiensis ?reducta Chamberlin, 1939. Baxter Co., juv., September 1977 (UAAM); and Lake Norfolk, ♂, 2 September 1952 (FSCA) (new county record). Benton Co., juv., 23 March and 23 September 1990, D. Pope, Perona (UAAM) (new county record). Boone Co., 2 juvs., 12 March 1990 (UAAM) (new county record). Carroll Co., Lake Leatherwood, 2♀, 21 November 1950 (FSCA) (new county record). Cleburne Co., Big Creek Natural Area E of Wilburn, ♂, 6 June 1978, D. M. Johnson (NCSM); and 9.6 km SSW Drasco, ♂, juv., 20 March 1979, D. Hildebrandt, M. Plonczynski (MPM) (new county record). Conway Co., 8.0 km N St. Vincent, off AR Hwy 95, ♀, 24 June 2002, CTM (NCSM) (new county record). Craighead Co., 18 March 1990, D. Mason (UAAM); and Jonesboro, ♂♂, ♀♀, 17 March 1962, N. B. Causey, and ♂♂, ♀♀, 30 October 1966, M. Hite (FSCA) (new county record). Crawford Co., 4.8 km SW Rudy, 2♂, 3 April 1969, O. Sanders (FSCA) (new county record). Cross Co., 19.2 km N Levesque, ♂♂, ♀♀, 18 April 1957, N. B. Causey (FSCA); and 8 km N Scottsville, ♀, 6 February 1955 (FSCA) (new county record). Franklin Co., Ft. Douglas, Hurricane Cr., 2♂, 12 April 1964, P. Porter (FSCA) (new county record). Independence Co., 2.1 km W Cushman, ♂, 5 March 1973, R. M. Blaney (FSCA) (new county record). Johnson Co., 22 April 1977, R. Mays (UAAM); and nr. Yale, ♀, 17 August 1981, D. C. Arnold (OKSU) (new county record). Logan Co., Mount Magazine, ♂, ♀, 28 October 1950 (FSCA) and 16 June 1990 (UAAM); and Cove Lake, ♂, 14-20 May 1989, T. L. Schiefer, Porter (MEM) (new county record). Madison Co., Combs, ♂, April 1953 (FSCA) (new county record). Marion Co., 14 October 1990 (UAAM) (new county record). Newton Co., ♂, ♀, 25 August 1950, N. B. Causey (FSCA) (new county record). Polk Co., Rich Mountain, 4♀, 7 September 1950 (FSCA) (new county record). Pope Co., 9.7 km N Hector, off AR Hwy. 27, 2 ♂, 3 ♀, 24 June 2002, CTM (NCSM) (new county record). Scott Co., 6.4 km W "Y" City, ♀, 24 October 1963, L. Hubricht (NCSM) (new county record). Searcy Co., ♂, 24 August 1950, N. B. Causey (FSCA) (new county record). Stone Co., vic. Fifty-six, off AR Hwy. 14, ♂, 1 July 2002, CTM (NCSM) (new county record). Van Buren Co., Clinton, ♂, 16 August 1960, M. Ferguson (MCZ) (new county record). Washington Co., Lake Weddington Preserve, ♀, 11 August 1956, N. B. Causey (FSCA); and Prairie Grove, ♂, 3♀, M. Hite (FSCA) (new county record). The type locality of *A. reducta* is Imboden, Lawrence County, Arkansas, in the foothills of the Ozark

Mountains (Chamberlin, 1939). Hoffman (1999) reduced *reducta* to subspecific status under *A. virginiensis*, the most widely ranging species in the genus. This species ranges from the vicinities of Milwaukee, Wisconsin, and Montreal, Quebec, to southern Virginia and Kentucky and southeastern Oklahoma (Hoffman, 1999; McAllister et al., 2002b; unpublished specimens collected and examined by the second author). We provisionally assign our specimens to this subspecies pending completion of a generic revision. *Apheloria virginiensis ?reducta* is now known from 24 of 75 (32%) Arkansas counties (Fig. 1) and appears to be relatively common in the well collected mountainous northern and western parts of the state; the southernmost record is that from McCurtain County, Oklahoma (see McAllister et al., 2002b). Investigations are needed in the coastal plain of southern and southeastern Arkansas to determine whether this colorful milliped also occurs in that corner of the state.

Family Euryuridae

Auturus evides (Bollman, 1887). Cleburne Co., 3.7 km W Concord at Wolf Bayou Cutoff on county rd. 90, ♂, 19 April 2002, M. McCallum (NCSM). Shelley (1982) previously reported *A. evides* from Cleburne County and 14 additional Arkansas counties, mostly in the northern part of the state in the Ozarks. In addition, McAllister (2002b) reported the species from three localities in Little Rock, Pulaski County, south of the Arkansas River.

Auturus louisianus louisianus (Chamberlin, 1918). Polk Co., Shady Lane Rec. Area, ♂♂, 18 June 1953, D. Dowling (NCSM); and 1.6 km N Mena, off AR Hwy. 88, ♂, 24 December 2002, CTM, JTM (NCSM). This milliped occurs exclusively south of the Arkansas River (Shelley, 1982), and the latter specimen was taken from the East End Visitor Information Station trail in pine and oak forest. McAllister et al. (2002b) previously reported this subspecies from Polk Co., and Shelley (1982) revised the genus and summarized locality records for Arkansas.

Family Eurymerodesmidae

Eurymerodesmus birdi birdi Chamberlin, 1931. Madison Co., 3.2 km N Crosses, ♂, 7 March 1953, R. S. Chase (FSCA) (new county record). Polk Co., vic. Big Fork at Ouachita Mountains Biological Station, ♂, 21 April 2002, CTM (NCSM); Pioneer Cemetery, vic. Queen Wilhelmina State Park off AR St. Hwy. 88, ♂, ♀, 11 June 2002, CTM (NCSM); and 1.6 km N Mena, East End Visitor Center Interpretative trail, off AR St. Hwy. 88, ♂, 24 December 2002, CTM, JTM (NCSM). Yell County, Mt. Nebo State Park near summit of Mt. Nebo, ♂, 6 May 1961, M. Hite (FSCA) (new county record). In Arkansas, *E. b. birdi* is known only from western counties, as Shelley (1990) recorded it from Benton, Carroll, Logan, Polk, Pope, and Washington counties. It also occurs in southwestern Missouri and into central and eastern Louisiana. These records suggest potential occurrence in southern and southeastern Arkansas, which is still relatively uninvestigated.

Eurymerodesmus polkensis (Causey, 1952). Yell Co., Sunlight Bay Park, Lake Nimrod, 3.2 km S Plainview, ♂, ♀, 4 juvs., 24 December 2002, CTM, JTM (NCSM) (new county record). This species was previously known only from Montgomery, Polk, and Scott counties, Arkansas (Shelley, 1990). Its discovery to the northeast in adjacent Yell County suggests widespread occurrence in the west-central part of the state.

Eurymerodesmus pulaski (Causey, 1950). Pulaski Co., Little Rock, University of Arkansas at Little Rock campus, ♂, 5 April 2002, M. McCallum (NCSM); and w. Little Rock, off Asher Avenue, Rosedale Addition, 4200 Gilman St., 2 ♂, 12 December 2002 and 1 February 2003, CTM (NCSM). This milliped is still known only from Pulaski County, Arkansas (Shelley, 1990; McAllister et al., 2002b).

Eurymerodesmus serratus (Shelley, 1990). Faulkner Co., 1.6 km N Cato, off AR St. Hwy. 89 on Cato Road at Cato Apostolic Jesus Name Church, ♂, 25 December 2002; and Woolly Hollow State Park, 11.3 km NE Greenbrier, off AR St. Hwy. 285, ♂, 25 December 2002, CTM, JTM (NCSM) (new county record). The latter locality is about 40 km N of the type locality, Cato, just south of the Faulkner County line in Pulaski County (Shelley, 1990).

Family Paradoxosomatidae

Oxidis gracilis (C. L. Koch, 1847). Miller Co., Doddridge, ♂♂, 6 April 2002 and 4 October 2002, N. Solley (NCSM). Stone Co., Fifty-six, Rowland Cave, ♂♂, ♀♀, juvs., 1 July 2003, CTM (NCSM). Thousands of this commonly introduced species were observed near the entrance of this Ozarkian cave and fewer numbers were seen on cave walls into the twilight zone. However, none were found in the dark zone of the cave.

Family Polydesmidae

Pseudopolydesmus sp. Independence Co., entrance to Searcy Cave, 9.6 km N Batesville off AR St. Hwy. 167, ♂♂, 1 July 2002 and 30 June 2003, CTM (NCSM). These narrow, small-bodied males are distinct from other species known from Arkansas, particularly *P. pinetorum*, which is widespread and larger-bodied. Judging from aspects of the gonopods, they appear to represent a new species, but there are seven nominal species in Louisiana, Arkansas, and Missouri whose identities are uncertain, and perhaps one of these names applies. While *Pseudopolydesmus* has not been revised, the species occurring primarily east of the Mississippi River have

been defined in faunal studies (Shelley, 1978, 1988; Hoffman, 1974, 1999). Species occurring to the west of this watercourse are still poorly known, and modern drawings of the diagnostic features are not available. This genus needs comprehensive review, and lacking such, our determination of a new species is provisional.

Pseudopolydesmus pinetorum (Bollman, 1888). Baxter Co., nr. Henderson, ♂, 14 May 1982, P. R. Miller (MEM) (new county record). Benton Co., Siloam Springs, 4 ♂, 3 ♀, 9 April 1955, Hastings (FSCA) (new county record). Clark Co., 5.1 km NW Caddo Valley off AR Hwy 283, ♂, ♀, 26 October 2003, CTM (NCSM) (new county record). Craighead Co., Jonesboro, ♂, 17 March 2002, S. E. Trauth (NCSM) (new county record). Faulkner Co., Woolly Hollow State Park, 11.3 km NE Greenbrier, off AR Hwy 285, ♂, ♀, CTM, JTM (NCSM) (new county record). Franklin Co., White Rock Mtn., ♂, 23 June 1944 (NMNH) (new county record). Garland Co., Hot Springs, ♂♂, ♀♀(NMNH); and Charleton Recreation Area, off US 270, ♂, ♀, 11 June 2002, CTM (NCSM). Independence Co., 2.1 km W Cushman, Cushman (Blowing) Cave, ♂, 30 June 2003, CTM (NCSM). Montgomery Co., ♂, 31 March-8 April 1956, S. Finkelstein (FSCA); Camp Albert, 16 km NW Langley, ♂, ♀, 1979, H. W. Robison (NCSM); Mount Ida, ♂, 28 May 2003, CTM & JTM (NCSM) (new county record). Polk Co., 8 km N Scottsville, ♂, 6 February 1955, B. Owen (FSCA). Pulaski Co., Little Rock, 4200 Gilman Street, ♂, 8 March 2003, CTM (NCSM) and Little Rock, ♂♂, ♀♀, Hutcherson (NMNH). Washington Co., Lake Weddington, ♂, 1 May 1956, N. B. Causey (FSCA); Cove Creek Valley, 6♂, 7♀, 9 January 1956, M. Hite (FSCA); Johnson, ♂, 1957 (FSCA); and Carhoerker Cave, 2♂, (NMNH) (new county record). Yell Co., Sunlight Bay Park, Lake Nimrod, vic. Plainview, ♂, ♀, 24 December 2002, CTM, JTM (NCSM) (new county record). *Pseudopolydesmus pinetorum* is the most common polydesmid in woodlands west of the Mississippi River and has been reported previously from Columbia, Dallas, Garland, Hempstead, Hot Spring, Lafayette, Little River, Miller, Nevada, Ouachita, Polk, and Pulaski counties (Fig. 2) (Causey, 1955; McAllister et al., 2002a, b); the type locality is Little Rock, Pulaski County (Bollman, 1888). The species is also known from Arkansas cave sites, including Richardson Cave (Fulton Co.), Clay Cave (Izard Co.), Davis Pit (Searcy Co.), and Center Cave (Sharp Co.) (McDaniel and Smith, 1976; Youngsteadt and Youngsteadt, 1978; Dunivan et al., 1982).

Pseudopolydesmus serratus (Say, 1821). Pulaski Co., w. Little Rock, off Asher Ave., 4200 Gilman Street, 2♂, 1 February 2003, CTM (NCSM) (new state record). The most common species east of the Mississippi River and particularly along the east coast, *P. serratus* occurs sporadically to the west; this is the first record from Arkansas.

Family Sphaeriodesmidae

Desmonus pudicus (Bollman, 1888). Hempstead Co., 2 juvs., 25 April 1977, R. T. Allen (UAAM) (new county record). Pulaski Co., Pinnacle Mountain State Park, ♀, 25 January 1988, R. T. Allen (UAAM). Washington Co., Fayetteville, Mt. Sequoyah, ♂, 6 October 1949, N. B. Causey (FSCA). *Desmonus pudicus* is well known from Pulaski County, as Little Rock is its type locality (Bollman, 1888). In Arkansas, it is known also from Benton, Carroll, Clark, Columbia, Conway, Johnson, Newton, Pike, Polk, Sebastian, Sevier, and Washington counties (Causey, 1958; Shelley, 2000). Even though Hempstead is a new county record for *D. pudicus* in Arkansas, its discovery there is consistent with the overall distribution, which extends southward through Texas into Nuevo Leon, Mexico.

Order Spirostreptida, Family Cambalidae

Cambala minor Bollman, 1888. Lawrence Co., Imboden, ♂, ♀, Fall 1930, B. C. Marshall (NMNH) (new county record). Little River Co., Wilton off US Hwy. 71, ♂, 22 March 2003, A. R. Shoemake (NMNH) (new county record). Polk Co., Ouachita trail off AR St. Hwy. 88, ♂, 4♀, 2 juvs., 9 November 2002, CTM (NCSM). Previous Arkansas records for this cool weather species span the length and breadth of the state and include sites in Benton, Clay, Columbia, Garland, Howard, Nevada, Ouachita, Polk, Pulaski, Randolph, Stone (Roasting Ear Cave), Union, and Washington counties (McDaniel and Smith, 1976; Shelley 1979; McAllister et al., 2002a, b). Thus, *Cambala minor* occurs statewide in Arkansas.

Order Callipodida, Family Abacionidae

Abacion tesselatum Rafinesque, 1820. Cleburne Co., 3.7 km W Concord at Wolf Bayou Cutoff on county rd. 90, ♂, 19 April 2002, M. McCallum (NCSM). Shelley (1984, Fig. 12) previously reported the species from Benton, Cleburne, Cross, Jefferson, Polk, Stone, and Washington counties, Arkansas.

Abacion texense (Loomis, 1937). Conway Co., 8.0 km N St. Vincent, off AR Hwy 95, ♂, ♀, 24 June 2002, CTM (NCSM) (new county record). This site is the farthest east in Arkansas that *A. texense* has been reported from previously. On distribution maps, Shelley (1984) and Shelley et al. (2003) depicted its occurrence in Clark, Franklin, Hempstead, Madison, Montgomery, Newton, Pike, Saline, Scott, and Washington counties, and McAllister et al. (2002a) added a record from Miller County. *Abacion texense* also occurs in northeastern and central Mississippi (Shelley, 1984), so it should be expected in southeastern Arkansas.

Order Julida, Family Julidae

Brachyiulus pusillus (Leach, 1815). Pulaski Co., w. Little Rock, Rosedale Edition, off Asher Ave., 4200 Gilman Street, 2 ♂, ♀, 1 February 2003, CTM (NCSM) (new state record). This species is native to western Europe and offshore islands and has been introduced into Easter Island, St. Helena, Argentina, and South Africa (Blower, 1985; Hoffman, 1999). In North America it has been recorded from New York, Ohio, and four provinces of Canada: Newfoundland, Nova Scotia, Quebec, and Ontario (Bailey 1928; Williams and Hefner, 1928; Shelley, 1988, 2002), but some of these records may represent misidentifications of *B. lusitanus* Verhoeff, 1898 (Hoffman, 1999).

Brachyiulus lusitanus Verhoeff, 1898. Pulaski Co., w. Little Rock, Rosedale Edition, off Asher Ave., 4200 Gilman Street, ♂, 8 March 2003, CTM (NCSM). Sevier Co., Horatio, ♂, 11 April 1955, D. N. Griffin (FSCA) (new state record). With the most recent discovery of *B. lusitanus* in Pulaski County, and the older sample in the FSCA, Arkansas becomes the first state in which both species of *Brachyiulus* have been documented.

Family Parajulidae

Aliulus caddoensis Causey, 1950. Polk Co., Queen Wilhelmina State Park off AR St. Hwy 88, ♂, 12 September 2002, CTM, J. Kessler (NCSM). The type locality is an unspecified site in Caddo County, Oklahoma, west of Oklahoma City, but *A. caddoensis* has been previously reported from Dallas, Howard, Pike, Polk, and Sebastian counties, Arkansas (Causey, 1950, 1953), so the species occurs over a 400 km distance in both mixed prairie and forested/mountainous ecosystems. There is very little anatomical difference between *A. caddoensis* and *A. carrollus* (Causey, 1950), which occurs to the north in Benton, Carroll, Searcy, and Washington counties (Hoffman, 1999), and the two names may be synonymous, with *A. carrollus* being the type species and holding taxonomic priority. The second author is evaluating these and other names as part of a summary paper on the tribe Aniulini.

Oriulus venustus (Wood, 1864). Craighead Co., Jonesboro, ♂, 12 March 2001, S. E. Trauth (NCSM) (new county record). Shelley (2002) reported *O. venustus* from Baxter, Benton, Clay, Drew, Monroe, Pulaski, and Washington counties, so it occurs throughout Arkansas except for the southwest corner.

Family Blaniulidae

Virgoiulus minutus (Brandt, 1841). Baxter Co., 2 ♀, September 1977 (UAAM). Bradley Co., ♀, 14 December 1964 (FSCA) and 2.4 km S Warren, 11 August 1977, juv., R. Chenowith (UAAM). Calhoun Co., 10.0 km E Hampton, ♀, juv., 19 February 1977, R. Chenowith (UAAM). Clark Co., 3 juvs., 14 April 1977, R. T. Allen (UAAM). Craighead Co., juv., 1 September 1977 (UAAM). Drew Co., juv., 10 August 1977 (UAAM). Hempstead Co., 5 juvs., 25 February 1977 (UAAM). Lafayette Co., juv., 25 February 1977 (UAAM). Lincoln Co., 1.4 km E Cleveland Co., line off St. Hwy 11, 4 juvs., 19 February 1977, R. Chenowith (UAAM). Logan Co., Mount Magazine, sinkhole, juv., 24 July 1990, B. Leary (UAAM). Nevada Co., juv., 25 February 1977 (UAAM). Polk Co., juv., 13 April 1977, R. T. Allen (UAAM). Pope Co., 2.4 km N jct. St. Hwys 16 and 27, 4 juvs., 21 October 1977, R. Chenowith (UAAM). Pulaski Co., Little Rock, ♀, 16 March 1962, N. B. Causey (FSCA). Scott Co., juv., 9 December 1976 (UAAM). Searcy Co., juv., December 1976 (UAAM). Sevier Co., 4 juvs., 13 April 1970, R. T. Allen (UAAM). Washington Co., Cave Creek Valley, 2♀, January 1956 (FSCA), and Prairie Cove, AR Hwy. 1, 8♀, M. Hite (FSCA). In their studies of the Blaniulidae, Enghoff and Shelley (1979) and Enghoff (1984) only gave the states of occurrence without specific localities, as did Hoffman (1999) in his summary range statement. In Arkansas, *V. minutus* was previously known only from Pulaski (Bollman, 1888), Miller, and Nevada counties (McAllister et al., 2002b). We provide a county distribution for the species (Fig. 3). The other counties listed above, except for Nevada and Pulaski counties, constitute new county records.

Order Platydesmida, Family Andrognathidae

Brachycybe lecontei (Wood, 1864). Garland Co., 3.7 km SE Hot Springs, 27 August 1966 (FSCA), and off Brady Mtn. Rd. vic. Bear, 4 April 2002, CTM (NCSM) (new county record). Hot Spring Co., 32 km N Arkadelphia, along AR Hwy. 7, 24 July 1982, S. K. Wu (UCO) (new county record). Independence Co., Magness, Hutcherson (NMNH), and 4.8 km SE Sandtown at Searcy Cave, 24 April 1976, D. M. Johnson (new county record). Johnson Co., 8 km N Clarksville, Kings Canyon, 26 April 1936, L. Hubricht (NMNH), and 12.8 km N Clarksville, 29 May 1982, R. L. Brown (MEM) (new county record). Lawrence Co., Imboden, 23 April 1936, B. C. Marshall (NMNH), and Ravenden, B. C. Marshall (NMNH) (new county record). Madison Co., 26 May 1985, Blackwood (OKSU) (new county record). Polk Co., Rich Mtn., 26 April 1936, L. Hubricht (NMNH), Mena, January 1956, A. L. McMillan (FSCA), and 1.6 km N Mena off St. Hwy. 88, Visitor Center, 13 August 2003, CTM (NCSM). Pope Co., 9.7 km N Hector off AR Hwy 27, 24 June 2002, CTM (NCSM) (new county record). Pulaski Co., Little Rock, C. F. Baker (NMNH). Previous county records reported for *B. lecontei* include Benton, Izard, Logan, Polk, Pulaski, Saline, Scott, Sharp (Center Cave #2), Stone, and Washington counties (Gardner, 1975; McDaniel and Smith, 1976; McAllister et al., 2002b), indicating that the species occurs from northwestern and west-

central Arkansas to central and northeastern Arkansas (Fig. 4). We did not record sexes because this milliped is the only representative of the Platydesmida in the state that can be authentically identified with either gender and/or with juveniles.

Order Spirobolida, Family Spirobolidae

Narceus americanus (Beauvois, 1805). Garland Co., Brady Mtn. Campground, Lake Ouachita, ♂, 4 April 2002, CTM (FMNH); and 4.8 km W Crystal Springs at Charlton Recreation Area off US Hwy. 270, ♂, 11 June 2002, CTM (NCSM) (new county record). Little River Co., Wilton off US Hwy. 71, juv., 22 March 2003, A. R. Shoemake (NCSM) (new county record). Pope Co., 9.7 km N Hector off AR St. Hwy. 27, ♀, 24 June 2002, CTM (NCSM) (new county record). Keeton (1960) recorded *N. americanus* from Faulkner, Hempstead, Lawrence, Logan, Montgomery, Pulaski, Saline, and Yell counties, and McDaniel and Smith (1976) reported the species from the twilight zone of Cushman Cave (Independence Co). McAllister et al. (2002a) reported it from Ouachita County and noted the relative rarity of specimens from west of the Mississippi River, but this milliped is nevertheless expected statewide in Arkansas.

ACKNOWLEDGMENTS.—We thank the Arkansas Game and Fish Commission for scientific collecting permit #1480 and State Park personnel for helpful assistance. We also thank M. McCallum (LSU-Shreveport), A. Shoemake (TAMU-T), N. Solley (TAMU-T), and S. E. Trauth (Arkansas State Univ.) for providing milliped specimens, H. W. Robison (Southern Arkansas Univ.) for donating a sample of *P. pinetorum* to the NCSM, and W. Wilkes for allowing CTM access to Searcy Cave. The following curators and collection managers loaned specimens from the indicated collections to the second author: FSCA, G. B. Edwards; MEM, T. L. Schieffer; MPM, J. P. Jass; NMNH, J. A. Coddington; OKSU, D. C. Arnold; UAAM, J. K. Barnes; and UCO, S. K. Wu. This study was supported by a TAMU-T Faculty Senate Enrichment Grant #200900 to CTM.

Literature Cited

Bailey, J. W. 1928. The Chilopoda of New York state with notes on the Diplopoda. Bull. New York State Mus. No. 276:1-50.

Blower, J. G. 1985. *Millipedes. Keys and notes for the identification of the species.* E. J. Brill, London. 242 pp.

Bollman, C. H. 1888. A preliminary list of the myriapods of Arkansas, with descriptions of new species. Entomol. Amer. 4:1-8.

Causey, N. B. 1950. New genera and species of millipeds-Paraiulidae (Juloidea). Proc. Arkansas Acad. Sci. 3:45-58.

Causey, N. B. 1953. On five new North American millipeds and records of some established species. Amer. Midl. Nat. 50:152-158.

Causey, N. B. 1955. New records and descriptions of polydesmoid millipeds (Order Polydesmida) from the eastern United States. Proc. Biol. Soc. Washington 68:21-30.

Causey, N. B. 1958. Pill millipeds (Desmonidae, Polydesmida) in the United States. Proc. Biol. Soc. Washington 71:173-178.

Chamberlin, R. V. 1939. On some diplopods of the family Fontariidae. Bull. Univ. Utah 30 (2) [Biol. Ser., 5 (3)]:1-19.

Dunivan, J. D., C. R. Tumlison, and **V. R. McDaniel.** 1982. Cave fauna of Arkansas: further records. Proc. Arkansas Acad. Sci. 36:87-88.

Enghoff, H. 1984. A revision of the Nopoiulinae, with notes on the classification of blaniulid millipedes (Diplopoda: Julida: Blaniulidae). Senck. biol. 64:393-427.

Enghoff, H., and **R. M. Shelley.** 1979. A revision of the millipede genus *Nopoiulus* (Diplopoda, Julida: Blaniulidae). Ent. Scand. 10:65-72.

Gardner, M. R. 1975. Revision of the millipede family Andrognathidae in the nearctic region (Diplopoda: Platydesmida). Mem. Pacific Coast Entomol. Soc. 5:31-53.

Hoffman, R. L. 1974. A new polydesmid milliped from the southern Appalachians, with remarks of the status of *Dixidesmus* and a proposed terminology for polydesmid gonopods. Proc. Biol. Soc. Washington 87:345-350.

Hoffman, R. L. 1999. Checklist of the millipeds of North and Middle America. Virginia Mus. Nat. Hist. Spec. Pub. No. 8:1-584.

Keeton, W. T. 1960. A taxonomic study of the milliped family Spirobolidae (Diplopoda: Spirobolida). Mem. American Entomol. Soc. No. 17:1-146.

McAllister, C. T., C. S. Harris, R. M. Shelley, and **J. T. McAllister, III.** 2002a. Millipeds (Arthropoda: Diplopoda) of the Ark-La-Tex. I. New distributional and state records for seven counties of the West Gulf Coastal Plain of Arkansas. J. Arkansas Acad. Sci. 56:91-94.

McAllister, C. T., R. M. Shelley, and **J. T. McAllister, III.** 2002b. Millipeds (Arthropoda:Diplopoda) of the Ark-La-Tex. II. Distributional records for some species of western and central Arkansas and eastern and southeastern Oklahoma. J. Arkansas Acad. Sci. 56:95-98.

McDaniel, V. R., and **K. L. Smith.** 1976. Cave fauna of Arkansas: selected invertebrate taxa. Proc. Arkansas Acad. Sci. 30:57-60.

McDaniel, V. R., K. N. Paige, and **C. R. Tumlison.** 1979. Cave fauna of Arkansas: additional invertebrate and vertebrate records. Proc. Arkansas Acad. Sci. 33:84-85.

Peck, S. B., and **J. H. Peck.** 1982. Invertebrate fauna of Devils Den, a sandstone cave in northwestern Arkansas. Proc. Arkansas Acad. Sci. 36:46-48.

Shear, W. A. 2003a. *Branneria bonoculus*, n. sp., a second species in the North American milliped family Branneriidae (Diplopoda: Chordeumatida: Brannerioidea). Zootaxa 233:1-7.

Shear, W. A. 2003b. The milliped family Trichopetalidae, Part 1: Introduction and genera *Trigenotyla* Causey, *Nannopetalum* n. gen., and *Causeyella* n. gen. (Diplopoda: Chordeumatida, Cleidogonoidea). Zootaxa 321:1-36.

Shelley, R. M. 1978. Millipeds of the eastern Piedmont region of North Carolina, U.S.A. (Diplopoda). J. Nat. Hist. 12:37-79.

Shelley, R. M. 1979. A synopsis of the milliped genus *Cambala*, with a description of *C. minor* Bollman (Spirostreptida: Cambalidae). Proc. Biol. Soc. Washington 92:551-571.

Shelley, R. M. 1982. Revision of the milliped genus *Auturus* (Polydesmida: Platyrhacidae). Canadian J. Zool. 60:3249-3267.

Shelley, R. M. 1984. A synopsis of the milliped genus *Abacion* Rafinesque (Callipodida: Caspiopetalidae). Canadian J. Zool. 62:980-988.

Shelley, R. M. 1988. The millipeds of eastern Canada (Arthropoda: Diplopoda). Canadian J. Zool., 66:1638-1663.

Shelley, R. M. 1990. Revision of the milliped family Eurymerodesmidae (Polydesmida: Chelodesmidea). Mem. Amer. Ent. Soc. 37:1-112.

Shelley, R. M. 2000. Revision of the milliped subfamily Desmoninae (Polydesmida: Sphaeriodesmidae). Myriapodologica 6:27-54.

Shelley, R. M. 2002. The millipedes of central Canada (Arthropoda: Diplopoda), with reviews of the Canadian fauna and diplopod faunistic studies. Can. J. Zool.,80:1863-1875.

Shelley, R. M., C. T. McAllister, and **J. L. Hollis.** 2003. A new milliped of the genus *Abacion* Rafinesque, 1820 from Arkansas, U.S.A. (Callipodida: Abacionidae). Zootaxa 170:1-7.

Williams, S. R., and **R. A. Hefner.** 1928. The millipedes and centipedes of Ohio. Ohio Biol. Surv. Bull. 18:92-146.

Youngsteadt, N. W., and **J. O. Youngsteadt.** 1978. A survey of some cave invertebrates from northern Arkansas. Arkansas Cave Stud. 1:1-13.

A Herpetofaunal Inventory of Arkansas Post National Memorial, Arkansas County, Arkansas

Malcolm L. McCallum
Red River Watershed Institute
Museum of Life Sciences
Department of Biological Sciences
Louisiana State University in Shreveport
One University Place
Shreveport, LA 71115

Stanley E. Trauth and Robert G. Neal
Department of Biological Sciences
Arkansas State University
State University, AR 72467-0599

Vernon Hoffman
University of Arkansas
Community College
P.O. Box 3350
Batesville, AR 72501

Abstract

The Arkansas Post National Memorial (ARPO) is a unique historical landmark with an interesting herpetofaunal community. We conducted an amphibian and reptile inventory of this national park from 2000-2002. We found eight amphibian and 21 reptilian species inhabiting the park. These included eight species not previously identified at ARPO. Overall species richness was highest at Alligator Slough, although the northern portion of ARPO was relatively rich. Aquatic trophic guilds included 7 (36.8%) piscivores, 7 (36.8%) omnivores, 4 (21.1%) insectivores, and one (5.3%) carnivore. The terrestrial trophic guilds included 13 (76.5%) insectivores, 2 (11.8%) carnivores, and 1 (5.9%) each of omnivores and generalized carnivores. We provide a species list, analysis of the distributions, diversity relationships and the trophic guilds present at ARPO, including management recommendations for the conservation of the herpetofauna community at ARPO.

Introduction

Even relatively small National Park Service lands may provide potential refuges for amphibian and reptilian species. The U.S. Congress passed the National Parks Omnibus Management Act in 1998 in response to concerns about the status of biodiversity in the nation's national park system (National Research Counsel 1992). This act called for baseline inventory data for parks throughout the nation. Arkansas Post National Memorial (ARPO) in southeastern Arkansas (Arkansas County) was one of these areas lacking data.

Arkansas Post was designated as a national memorial in 1960. It spans approximately 302 ha (747 acres) of which 451 acres is federal land. The habitat is dominated by bottomland hardwood forest, backwater slough, and big river habitat. The surrounding land use is typical of the Mississippi Delta, being composed of rice and soybean production. Crop dusting is performed adjacent to the park throughout the growing season. Recreational use at ARPO was estimated at 49,087 visitors in 1999. Nearly all the natural habitat in the Mississippi Delta has been modified or fragmented by agriculture. Habitat fragmentation and alteration have been implicated as primary factors influencing amphibian declines (Pechmann and Wilbur, 1994; Blaustein et al., 1994) and biodiversity declines in general (Heywood, 1992). Many amphibian and reptilian populations are best described as metapopulations (Levins, 1969; Hanski and Gilpin, 1997) whose stability is dependent upon a balance between population extirpation and recolonization (Johnson et al., 2002). Although the habitats at ARPO are not virgin lands, their setting in the Delta makes ARPO an important conservation area; thus, habitat management to limit disturbance may allow ARPO to act as ecological source for refueling adjacent populations (Weins, 1996). Despite its importance as a biodiversity holding ground, little is known about ARPO's wildlife and plant communities.

During 21-23 of April 2000 we undertook a short-term herpetofaunal survey at ARPO with the cooperation of park personnel. Despite its small size, an array of amphibians and reptiles was found at the park. Several species of turtles, lizards, and frogs were plentiful. The preliminary inventory resulted in four new county records for amphibians and reptiles at the park (red milk snake [*Lampropeltis triangulum syspila*], Graham's crayfish snake [*Regina grahamii*], northern fence lizard [*Sceloporus undulatus hyacinthinus*], and the marbled salamander [*Ambystoma opacum*]).

Additional inventory work at ARPO provided a more thorough, survey in 2001-2002. This study attempted to identify at least 90% of the amphibian and reptilian species utilizing ARPO. The primary objective of that investigation was to provide an up-to-date assessment of species richness at the park. Secondary objectives involved the estimation of relative abundance, delineation of local ranges for each species, collection and deposition of voucher specimens, and the implementation of survey methods that would insure a 90% repeatability of the project.

Materials and Methods

We followed up our preliminary inventory with a primary inventory from fall 2001 through summer 2002. Data from both surveys were combined for this report. Our primary terrestrial inventory methods included road cruising (Karns, 1986) and general search and seizure activities (Vogt and Hine, 1982). Aquatic methods included dip netting, seining (Karns, 1986), and the use of minnow (Karns, 1986) and turtle traps (Legler, 1960). We employed a seven-member team during most visits. Most common and scientific names are based on Moriarty (2000).

We visited the park on 8-9 August 2001, 19-20 October 2001, 15 March 2002, 12-14 April 2002, and, 7-8 May 2002. A sampling grid of primary and secondary points for ARPO (Fig. 1) was designed for our use by the long-term ecological monitoring (LTREM) staff stationed at the NPS Heartland Inventory and Monitoring headquarters in Republic, Missouri. At each primary point on the sampling grid, four secondary points were identified in each of the primary compass directions from the primary point. Coverboard use was adapted from Grant et al. (1992). We alternately placed two wood and two tin coverboards at each secondary point to account for potential differences in their quality as amphibian and reptilian attractants. Each coverboard plot was visited at least once during the study. Twelve of the 37 primary points were designated as coverboard plots, and time-area constrained searches (TACS) were used at 13 primary points. Eleven of the primary points were eliminated from the study because they fell outside the park boundary or in water bodies. Point 28 was near shore, so we placed cover boards along the shoreline at this sight. Both points 7 and 15 had a secondary point removed for the same reason as described above. If a primary grid point appeared in a heavily wooded area, then coverboards were not applied, and we instead designated that point for TACS. The TACS technique was a modification of the "time constrained search and seizure method" and the "quadrant search and seizure;" utilized by Campbell and Christman (1982).

Four secondary points, designated as described above, were identified. An 8 m^2 plot was delineated at each secondary point and searched systematically for 10 minutes. All logs, rocks, and other debris were returned to their original position after turning. Each primary point was recorded using a Trimble GeoExporer 3 Global Positioning

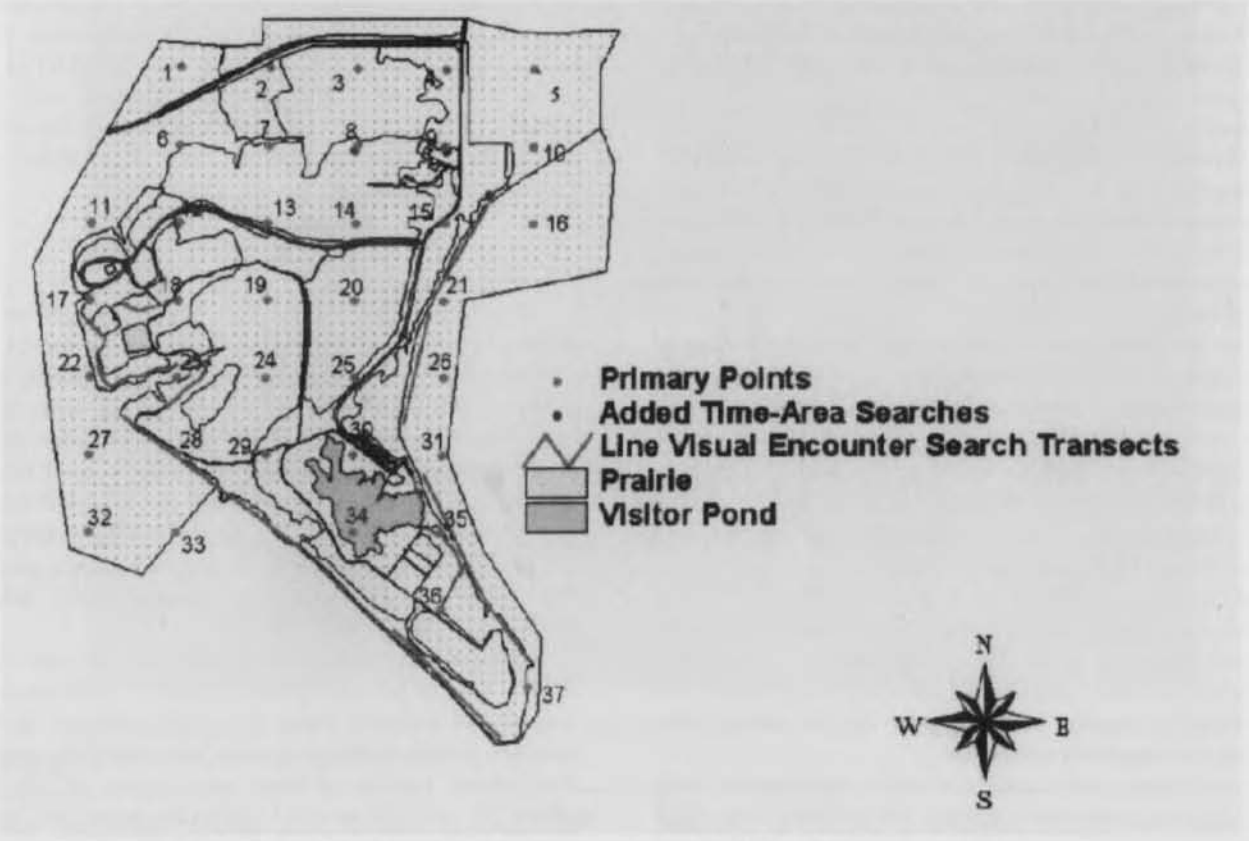

Fig. 1. Map of Arkansas Post National Memorial showing primary points and other search areas.

Table 1. Amphibians of Arkansas Post National Memorial.
Key: (+++++) = Commonly encountered, (+) = Rare, (?) = unverified observation

Amphibia	Family		Relative Abundance
Anura	Bufonidae	American Toad (*Bufo americanus*)	+++
		Fowler's Toad (*Bufo fowleri*)	+++++
		Northern Cricket Frog (*Acris crepitans*)	+++++
		Spring Peeper (*Pseudacris crucifer*)	+++
		Cope's Gray Treefrog (*Hyla chrysoscelis*)	+
		Green Treefrog (*Hyla cinerea*)	++++
	Microhylidae	Eastern Narrowmouth Toad (*Gastrophryne carolinensis*)	+++
	Ranidae	Bullfrog (*Rana catesbeiana*)	+++
		Bronze Frog (*Rana clamitans clamitans*)	++++
		Southern Leopard Frog (*Rana sphenocephala*)	+++++
Caudata	Ambystomatidae	Marbled Salamander (*Ambystoma opacum*)	+
	Plethodontidae	Western Slimy Salamander (*Plethodon albagula*)	?

System (GPS) portable hand-held unit at the highest accuracy possible given the conditions at the time. No less than 150 data point readings were collected with the GPS for each primary point, and these were saved as a single file for each grid point.

Generalized search and seizure methodology was utilized throughout the entire park in addition to the other two methods. All trails and east-west/north-south transects between coverboard plots were hiked. Both day and night road cruising were implemented on all park roads and on roads adjacent to the park. Animals were recorded as encountered.

Turtle trapping was implemented in the vicinity of primary point 1 on 12-14 April 2002. The water depth in other locations was too shallow to adequately sample by this method. We placed two turtle traps near basking logs where turtles were observed. Dip netting was implemented in roadside ditches, Alligator Slough (AS), and in the Visitor Center Lake (VCL), and in a small backwater pond northeast of the VCL.

Spotlighting was used at AS and on the VCL to observe frogs and alligators. The eye-shine from these animals is easily seen using a spotlight or high-intensity flashlight. These lights are also helpful in capturing amphibians and reptiles at night because the light prevents the animal from seeing the investigator's approach.

In most cases, only a single voucher specimen of each species observed was taken during the primary inventory. These specimens were preserved (Pisani, 1973) and deposited in the National Park Service Heartland Division Special Collection within the Arkansas State University Museum of Zoology herpetology collection. Specimens with their numbers were entered into an electronic Microsoft Access database for reference. A map of ARPO with all primary points and designated special areas (with labels) is shown in Fig. 1. We utilized ArcView 3.0 as the geographic information system (GIS) to analyze species richness throughout the park.

Results

The preliminary inventory yielded eight amphibian species (one salamander and seven anurans) and 21 reptilian species (one crocodilian, six turtles, five lizards, and nine snakes). The extensive inventory found eight additional species including three anurans, one salamander, two turtles, and two snakes. Six species were represented by a single observation/specimen. These were the marbled salamander (*Ambystoma opacum*), red milk snake (*Lampropeltis triangulum syspila*), green anole (*Anolis carolinensis*), rough green snake (*Opheodrys aestivus*), and the western slimy salamander (*Plethodon albagula*; Tables 1 and 2).

Overall herpetofaunal species richness was highest at AS (vicinity of primary points 22 and 23) followed by VCL (vicinity of primary point 34). The northern two rows of primary points at the park were also relatively species rich. Amphibian species richness was highest at AS (primary points 22 and 23), at VCL (primary point 34), and in the vicinity of primary points 1, 6, and 7. The American alligator was observed nesting at Alligator Slough (Fig. 2).

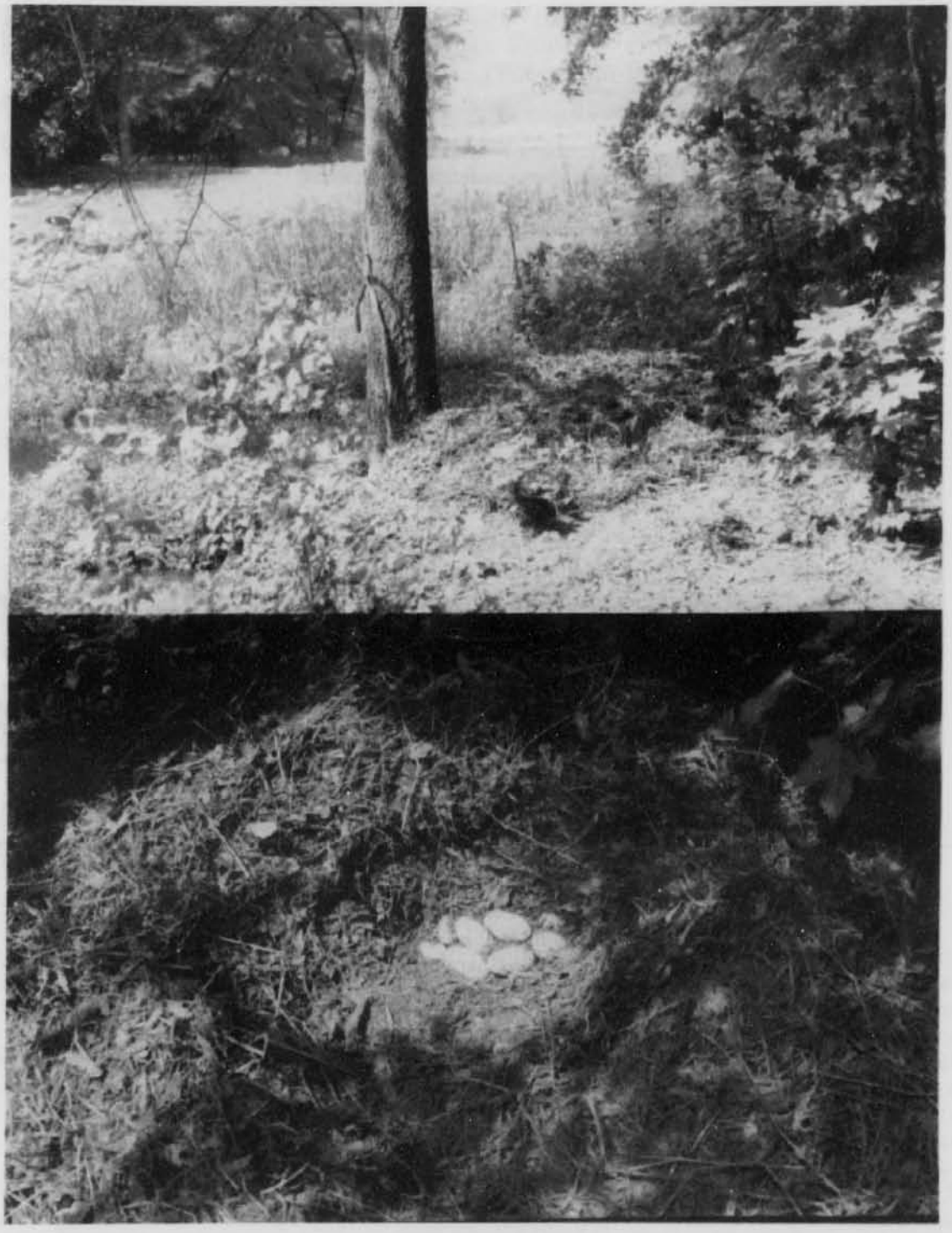

Fig. 2. The American alligator nest (at base of tree) and eggs at Alligator Slough (7 Aug 2001), Arkansas Post National Memorial. Eggs were covered after photograph was taken.

Trophic guilds at ARPO and in the surrounding counties (Arkansas and Desha counties) are provided in Fig. 3. Aquatic trophic guilds in the surrounding counties included 12 (36.4%) piscivores, 11 (33.3%) omnivores, 9 (27.3%) insectivores, and one (3%) carnivore. Terrestrial trophic guilds in the surrounding counties included 21

Table 2. Reptiles of Arkansas Post National Memorial.
Key: (+++++) = Commonly encountered, (+) = Rare, (?) = unverified observation

Reptilia	Family		Relative Abundance
Squamata	Phrynosomatidae	Northern Fence Lizard (*Sceloporus undulatus hyacinthinus*)	+++
	Scincidae	Five-lined Skink (*Eumeces fasciatus*)	++++
		Broadhead Skink (*Eumeces laticeps*)	+++
		Ground Skink (*Scincella lateralis*)	+++++
	Colubridae	Eastern Racer (*Coluber constrictor*)	+++
		Speckled Kingsnake (*Lampropeltis getula*)	+++
		Red Milk Snake (*Lampropeltis triangulum*)	+
		Green Water Snake (*Nerodia cyclopion*)	+++++
		Yellowbelly Water Snake (*Nerodia erythrogaster flavigaster*)	++++
		Broad-banded Water Snake (*Nerodia fasciata confluens*)	++++
		Diamondback Water Snake (*Nerodia rhombifer*)	++++
		Rough Green Snake (*Opheodrys aestivus*)	+
		Graham's Crayfish Snake (*Regina grahamii*)	+++
		Western Ribbon Snake (*Thamnophis proximus*)	++
	Viperidae	Western Cottonmouth (*Agkistrodon piscivorus*)	++++
Testudines	Chelydridae	Common Snapping Turtle (*Chelydra serpentina*)	++++
	Emydidae	Common Map Turtle (*Graptemys geographica*)	++
		Eastern River Cooter (*Pseudemys concinna*)	+++++
		Three-toed Box Turtle (*Terrapene carolina triunguis*)	++++
		Red-eared Slider (*Trachemys scripta*)	+++++
	Kinosternidae	Common Musk Turtle (*Sternotherus odoratus*)	++
		Razorback Musk Turtle (*Sternotherus carinatus*)	++++
Crocodilia	Alligatoridae	American Alligator (*Alligator mississippiensis*)	++

Table 3. Species richness at Alligator Slough.

Species	Inhabitant	Observed In Vicinity
American Alligator	X	
Black Racer	X	
Broad-banded Water Snake	X	
Broadhead Skink	X	
Bronze Frog	X	
Bullfrog	X	
Common Musk Turtle	X	
Common Snapping Turtle	X	
Diamondback Water Snake		X
Eastern Narrowmouth Toad		X
Five-lined Skink	X	
Graham's Crawfish Snake	X	
Green Treefrog		X
Green Water Snake	X	
Ground Skink	X	
Marbled Salamander		X
Northern Cricket Frog	X	
Northern Fence Lizard	X	
Razorback Musk Turtle	X	
Red Milk Snake		X
River Cooter		X
Southern Leopard Frog	X	
Speckled Kingsnake	X	
Three-toed Box Turtle	X	
Western Cottonmouth	X	
Western Ribbon Snake		X
Western Slimy Salamander	X	
Yellowbelly Water Snake	X	

(67.7%) insectivores, six (19.4%) carnivores, three (9.7%) generalized carnivores, and one (3.2%) omnivore. The aquatic trophic guilds at ARPO included seven (36.8%) piscivores, seven (36.8%) omnivores, four (21.1%) insectivores, and one (5.3%) carnivore. The terrestrial trophic guilds at ARPO included 13 (76.5%) insectivores, two (11.8%) carnivores, and 1 (5.9%) each of omnivores and generalized carnivores.

Discussion

The most important habitat resource for herpetofauna in the park is the area surrounding and including AS. No other part of ARPO is nearly as rich. Species abundance in this area was also much higher than anywhere else in the park. Twenty-one species (Table 3) were found in this area, representing 57% of the total richness. Another seven species were observed close enough to AS to derive benefits from its habitats. This suggests that 76% of the amphibians and reptiles at ARPO may utilize the habitats of AS. Although they could not be identified, several species of basking turtles were observed swimming in AS. All seven turtle species observed at the park probably utilize this area to some extent. Six species of amphibians were observed at AS representing 50% of the amphibian species richness on ARPO. Twenty-two species of reptiles were observed at AS representing 88% of the reptilian species richness at the park.

At least one American alligator and its nest were observed within the area of AS. The single nest was first sighted on 7 August 2001 (Fig. 4). We counted 22 hatchlings in the vicinity of the nest 10 months later on 7 May 2002. The hatchlings remained in close association with their nest for the next several months. A second pod of hatchlings (no nest was found in this area) was observed in the VCL around the same time, but the following spring none of these individuals was present. It appeared that all hatchlings from this second pod probably died during the winter. This suggests AS may be an important source habitat for

Table 4. Species richness at Visitor Center Lake.

Species	Inhabitant
American Alligator	X
Bronze Frog	X
Common Map Turtle	X
Diamondback Water Snake	X
Eastern Narrowmouth Toad	X
Green Treefrog	X
Northern Cricket Frog	X
River Cooter	X
Southern Leopard Frog	X

American alligators. We observed populations of ghost shrimp in AS so dense that our dipnet contained nearly a liter of the invertebrates following one scoop on 7 August 2002. The abundance of ghost shrimp and other invertebrates in the waters of this location undoubtedly provides a rich, high-caloric diet to prepare the hatchlings for the winter months. This single factor may have been sufficient to relate the survivorship differences observed between the two pods during our study.

The high species richness at AS may also be due to lower levels of visitors in this area as compared to other parts of the park. Alligator Slough has only one small dirt footpath. Other areas have paved paths with mowed borders. This probably leads to heavier traffic and higher potential for human interaction with the wildlife. The natural attractiveness of AS makes it an important natural resource at ARPO.

The VCL provides an important resource for the herpetofaunal community of ARPO. Eleven species were observed here representing 30% of the total species richness at ARPO (Table 4). Diamondback water snakes were particularly abundant here. As mentioned previously, hatchling alligators were present here on 7August 2001, but were not observed in April 2002. Eastern narrowmouth toads (*Gastrophryne carolinensis*), northern cricket frogs (*Acris*

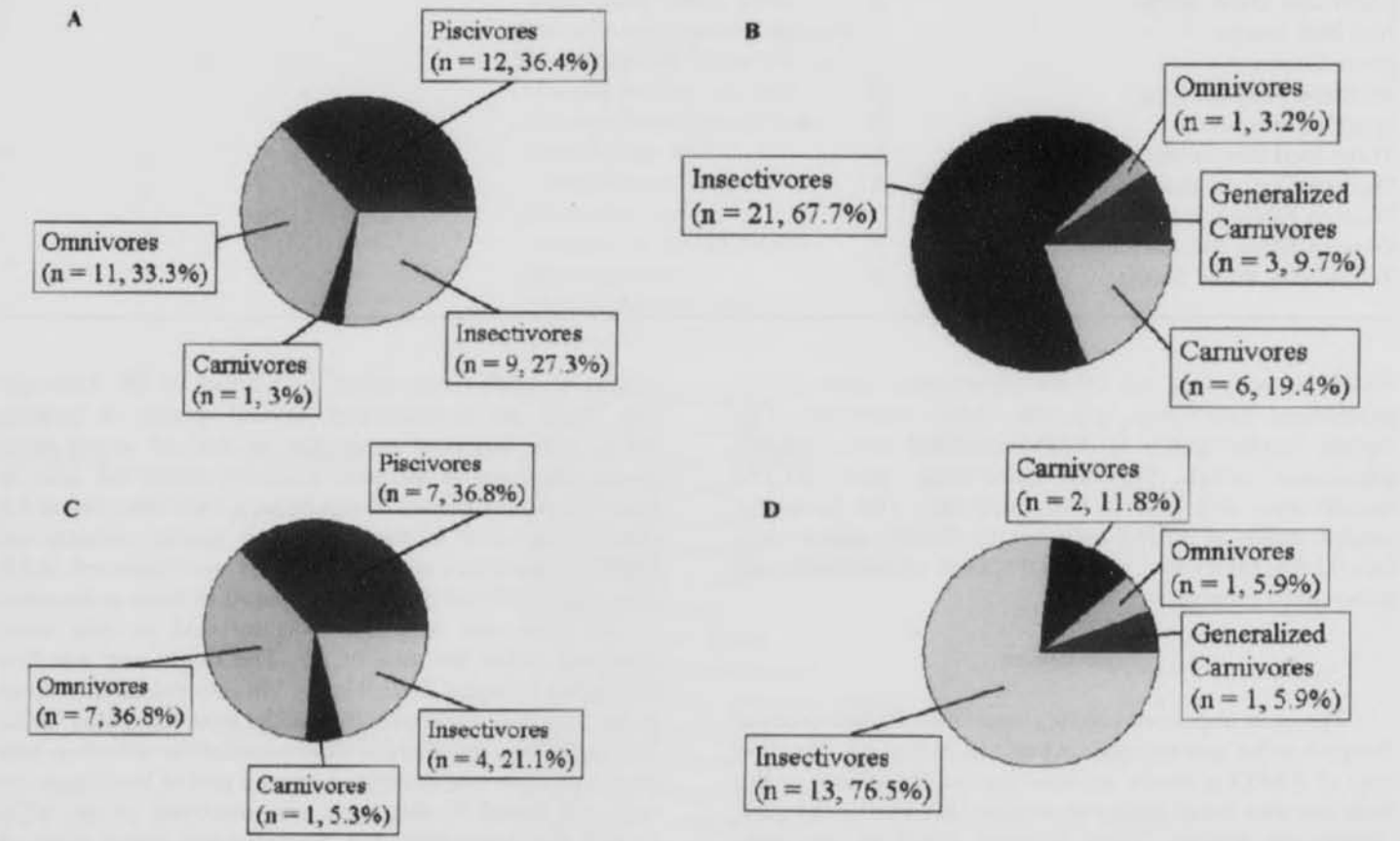

Fig. 3. Aquatic and terrestrial herpetofaunal trophic guilds in Arkansas and Desha counties. A) Aquatic Arkansas-Desha, B) Terrestrial Arkansas-Desha, C) Aquatic ARPO, D) Terrestrial ARPO.

crepitans), green treefrogs (*Hyla cinerea*), bronze frogs (*Rana clamitans*), bullfrogs (*Rana catesbeiana*), and southern leopard frogs (*Rana sphenocephala*) were observed calling at this location. Except for the eastern narrowmouth toad, all amphibians and reptiles present at the pond were essentially aquatic species. The pond is entirely surrounded by mowed lawn grass. In most areas the grass is mowed to the water's edge. Human activity at this small lake is heavy. These factors may be suppressive to amphibian and reptilian populations that might otherwise inhabit the terrestrial habitats adjacent to VCL.

The forested areas at ARPO are highly fragmented. The largest tracts of forested land appear in the areas of highest species richness. Fewer than 10 northern cricket frogs were observed in mowed areas away from the forest edge. Arkansas Post has large tracts of mowed habitat for human use distributed in the central region of the park. This creates an atoll-shaped forest habitat within this region. This type of habitat distribution is typically expected to possess lower than average species diversity (MacArthur and Wilson, 1967).

The low richness and abundance of ambystomatid salamanders are important to address. A single marbled salamander was recovered during the preliminary inventory from habitats adjacent to AS. No adults or larvae were observed during the entire primary inventory. In fact, no fishless ephemeral ponds are present at ARPO. Such ponds are essential for maintenance of ambystomatid populations.

In all trophic guilds present at ARPO we observed fewer species present than occur in the surrounding counties. This is partly due to the limited habitat diversity present at ARPO compared to the surrounding area. The aquatic trophic guilds of ARPO were relatively similar to the guild breadths present in the surrounding counties. In both, piscivores were the most common groups, being comprised primarily of snake species. Aquatic omnivores were the second most represented guild and were represented primarily by turtles. Additional aquatic sampling might increase the representation of omnivores through additional turtle species being revealed. The terrestrial trophic guilds at ARPO were more represented by insectivores than the surrounding counties. This probably arose from our inability to collect more carnivores from the park. Carnivorous species represented 19.4% of the herpetofauna in the surrounding counties. Snakes are the primary group of carnivores comprising this guild. Among these, the timber rattlesnake and pygmy rattlesnake are unlikely to occur at ARPO except as transients. Park officials have observed the northern copperhead at ARPO, further monitoring is likely to recover this species.

Species diversity is the variety of species present combined with their relative abundances. Species diversity is believed to decrease when ecological integrity is compromised (Feinsinger, 2001). The use of species richness alone, without adequate consideration of relative abundance, can lead to inappropriate decisions regarding natural resource management (Feinsinger, 2001). It is, therefore, important that continued long-term monitoring occur at ARPO in order to insure the accuracy and precision of the resultant data set supporting future decision-making. Our brief, one-year study is primarily a species inventory and, except in a few cases, provides limited abundance information.

Management Recommendations

We believe the following management recommendations are necessary to conserve the herpetofaunal diversity at ARPO: 1) Construct up to five small, temporary wildlife ponds in forested areas to promote ambystomatid populations. 2) Supplement currently depauperate marble salamander populations with egg clutches from nearby populations (IUCN guidelines state that reintroductions into areas where species are functionally extirpated is acceptable). A small effort has high probability of restoring the park's populations. 3) Alligator Slough should be considered a special biological resource of the park and should be monitored routinely. Avoid human use improvements in this area. 4) Timber management should include a forest floor management plan so that sufficient logs, woody debris, and other refugia are available as amphibian and reptilian habitats. This should further include significant expansion of the forested areas of the park at the expense of the mowed lawn areas. 5) Establish a long-term, population monitoring plan for the park. 6) Alter human access and management by encouraging people to remain on the sidewalks, especially around VCL. An example of this may include posting warning signs for venomous snakes and alligators. These signs may discourage most people from entering the habitat proper. This would not prevent people from enjoying the visual beauty of such areas and would definitely contribute to its preservation over the long term.

ACKNOWLEDGMENTS.—We thank Kevin Eads, Ben Wheeler, Ben Ball, Robyn Konvalinka, and Charles McDowell for assistance during the inventory, the Arkansas Game and Fish for scientific collection permits, and the National Park Service for technical assistance and funding (Grant #Q6370010459).

Literature Cited

Blaustein, A. R., D. B. Wake, and **W. P. Sousa.** 1994. Amphibian declines: judging stability, persistence, and susceptibility of populations to local and global extinctions. Conserv. Biol. 8:60-71.

Campbell, H. W., and **S. P. Christman.** 1982. Field techniques for herpetofaunal community analysis. Pp. 193-200, *In:* Scott, N.J., Jr. (ed.), Herpetological communities. Wildlife Research Report 13, U.S. Fish and Wildlife Service, U.S. Depart. Inter.

Feinsinger, P. 2001. Designing field studies for biodiversity conservation. Island Press. Washington, D.C. 212 pp.

Grant, B. W., A. D. Tucker, J. E. Lovich, A. M. Mills, P. M. Dixon, and **J. W. Gibbons.** 1992. The use of coverboards in estimating patterns of reptile and amphibian biodiversity. Pp. 379-403, *In:* D. R. McCullough and R.H. Barnett (eds.). Wildlife 2001. Elsvier Sci. Publ. London, England. 608 pp.

Hanski, I. A., and **M. E. Gilpin.** 1997. Metapopulation biology: ecology, genetics, and evolution. Academic Press. San Diego, California. 358 pp.

Heywood, V. H. 1992. Global biodiversity assessment. Cambridge Univ. Press. New York, New York. 1140 pp.

Johnson, C. M., L. B. Johnson, C. Richards, and **V. Beasley.** 2002. Predicting the occurrence of amphibians: An assessment of multiple-scale models. Pp. 157-170, *In*: Scott, M. J., P. J. Heglund, and M. L. Morrison (eds.). Predicting species occurrences: issues of accuracy and scale. Island Press. Washington, D.C. 1090 pp.

Karns, D. R. 1986. Field herpetology: methods for the study of amphibians and reptiles in Minnesota. Univ. Minnesota James Ford Bell Mus. Nat. Hist. Occas. Pap. 18:1-88.

Legler, J. M. 1960. A simple and inexpensive device for trapping aquatic turtles. Utah Acad. Proc. 37:63-66.

Levins, R. 1969. Some demographic and genetic consequences of environmental heterogeneity for biological control. Bull. Entomol. Soc. Amer. 15:237-240.

MacArthur, R. H., and **E. O. Wilson.** 1967. The theory of island biogeography. Princeton Univ. Press. Princeton, New Jersey. 352 pp.

Moriarty, J. J. 2000. Scientific and standard common English names of amphibians and reptiles of North America north of Mexico with comments regarding confidence in our understanding. Herpetol. Circ. 29:1-89.

National Research Counsil. 1992. Science and the National Parks. National Academy Press. Princeton, New Jersey. 76 pp.

Pechmann, J. H. K., and **H. M. Wilbur.** 1994. Putting declining amphibian populations in perspective: Natural fluctuations and human impacts. Herpetologica 50:65-84.

Pisani, G. R. 1973. A guide to preservation techniques for amphibians and reptiles. Herpetol. Circ. No. 1, Soc. Study Amphib. Rept. St. Louis, Missouri. 46 pp.

Vogt, R. C., and **R. L. Hine.** 1982. Evaluation of techniques for assessment of amphibian and reptile populations in Wisconsin. Pp. 201-217, *In:* Scott, N.J., Jr. (ed.), Herpetological communities. Wildl. Research Report 13, U.S. Fish and Wildl. Serv., U.S. Depart. Int.

Weins, J. A. 1996. Wildlife in patchy environments: Metapopulations, mosaics, and management. Pp. 53-84, *In*: D.R. McCullough (ed.). Metapopulations and wildlife conservation. Island Press. Washington, D.C. 506 pp.

PID Stabilization of a Position-Controlled Robot Manipulator Acting Independently or in Collaboration with Human Arm

Anindo Roy*
Department of Applied Sciences
University of Arkansas at Little Rock
Little Rock, AR 72204

Kamran Iqbal
Department of Systems Engineering
University of Arkansas at Little Rock
Little Rock, AR 72204

*Corresponding Author

Abstract

In this paper we develop framework for PID stabilization of a robot manipulator when using an object independently or in collaboration with a human arm. In both applications, the manipulator is equipped with a wrist sensor represented by an impedance. A second order manipulator transfer function along each coordinate direction is assumed. The aim of the paper is to design a PID controller when measurement of contact force, available via wrist sensor, is used to command the position-controlled manipulator to a desired position and/or force profile. Necessary and sufficient conditions for stability of the closed-loop system are developed using Hermite-Biehler Theorems. The theorems have been used to analyze stability of polynomials defined over the set of real numbers. An algorithm for synthesis of PID controllers using linear matrix inequalities is developed. The theoretical framework presented in this paper can be easily adapted to other low order manipulator transfer functions.

Introduction

Robot manipulators are used in a number of industrial and service applications (Hunt, 1983; Synder, 1985; Engelberger, 1989; Tao et al., 1990; Luh and Zheng, 1987; Zheng and Luh, 1989; Al-Jarrah and Zheng, 1996; Al-Jarrah and Zheng, 1997). In most cases, where the objective is to manipulate an inertial object, a robot can be considered as a positioning device that decouples the motion along each coordinate direction, and can be approximated with a second order transfer function (Xu and Paul, 1988; Al-Jarrah and Zheng, 1996; Kazerooni, 1990). Also, in position and/or force control applications, a high impedance wrist-sensor is normally used as end-effector, which can be effectively modeled with impedance. The wrist-sensor stiffness is usually high, on the order of 10^5 oz-in.

The arm-manipulator coordination problem visualizes a human arm and a robot manipulator jointly handling an inertial object in unstructured workspace. A human operator can acquire visual knowledge of the environment relatively quickly, possess the necessary intelligence to analyze the situation, and take quick and effective decisions. In the arm-manipulator coordination scheme, the intelligence of the arm helps perform complex functions (e.g., task planning, obstacle avoidance, etc.) while the manipulator performs the load sharing function. The arm-manipulator coordination for load sharing has been has been previously discussed by researchers (Al-Jarrah and Zheng, 1996; Al-Jarrah and Zheng, 1997; Kazerooni, 1990; Iqbal and Zheng, 1997; Iqbal and Zheng, 1999; Ikeura and Inooka, 1995; Ikeura and Mizutani, 1998; Rahman et al., 1999) and several solutions to the problem, (e.g., compliant motion control, reflexive motion control, and model predictive control) have been proposed. For example, the manipulator was required to possess negative stiffness to ensure compliance in load sharing tasks (Al-Jarrah and Zheng, 1996). In the reflexive motion control scheme (Al-Jarrah and Zheng, 1997), a supervisory loop was added that acted like a force control to the compliant controller to compensate for the sluggishness of the robot. The controller thus anticipated the arm movement, and applied timely corrections to improve the manipulator response. Model predictive control strategies have also been proposed to solve the arm-manipulator coordination problem (Iqbal and Zheng, 1997; Iqbal and Zheng, 1999). In predictive control schemes, the observed manipulator output was used in an optimizing controller to command the manipulator such that the predicted arm force went to zero.

In this paper we study the stability and controller design of the closed-loop system formed by the positioning manipulator, the wrist-sensor, and a PID controller. A secondary loop is added due to the presence of the human arm. We use the Hermite-Biehler framework (Roy and Iqbal, 2002; Datta et al., 1999; Ho et al., 2000) to analyze the stability of the closed-loop system. Hermite Biehler and generalized Hermite-Biehler Theorems characterize the stability of a given polynomial and provide information on right half-plane (RHP) root locations. We show how the characteristic polynomial of the robot-sensor and arm-manipulator plants can be cast in the Hermite-Biehler framework. The paper then discusses synthesis of the PID controller for the problem. A general analysis-synthesis

PID Stabilization of a Position-Controlled Robot Manipulator Acting Independently or in Collaboration with Human Arm

framework is developed that can be applied to similar plant models.

Methods

Notation.--In the following, $\wedge$ denotes logical AND, $\vee$ denotes logical OR, $\Re=(-\infty,\infty)$, $\Re^{+}=(0,\infty)$, $\Re^{-}=(-\infty,0)$, $\{\Re\neq 0\}=\Re^{+}\cup\Re^{-}$, I_{+} denotes the set of non-negative integers, $\Re^{m\times n}$ denotes a $m\times n$ real matrix, C denotes the set of complex numbers, and $\varnothing$ denotes a null set.

Problem Formulation and Stability Analysis.--The arm-manipulator coordination problem can be visualized as a human arm and a robot manipulator jointly handling an inertial object (Fig. 1). The manipulator is modeled as a

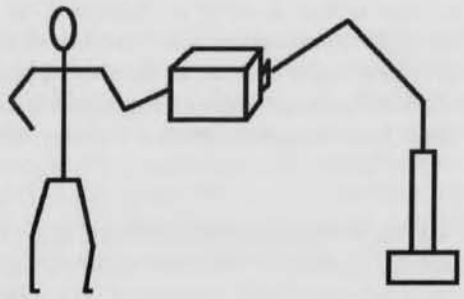

Fig. 1. The conceptual visualization of the arm-manipulation coordination problem; a human arm and a robot manipulator jointly hanlde an inertial object.

positioning device, which decouples the dynamics of the robot and provides position tracking in Cartesian coordinates. In particular, for the Puma 560 robot, a natural frequency of 2 Hz can be assumed (Xu and Paul, 1988; Al-Jarrah and Zheng, 1996; Kazerooni, 1990). A high-impedance wrist sensor is used to sense the environmental forces and moments.

The human arm is modeled as a black box neglecting the behavior of the musculo-skeletal system (Kazerooni, 1990). The arm possesses an impedance, which arises from the visco-elastic properties of the biological muscles. The desired arm trajectory is planned in the central nervous system, and no apriori knowledge of it is assumed. Further, it is assumed that the speed of manipulation task is small, such that the Coriolis and other nonlinear effects can be neglected. It is further assumed that the only forces acting on the object are the arm force (f_a), the manipulator force (f_m), and the force of gravity (f_g). Then the dynamics of the problem (Fig. 2) can be solved from Newton's laws of motion represented by the following equations, where in order to simplify the analysis, only a one-dimensional view of the problem is considered.

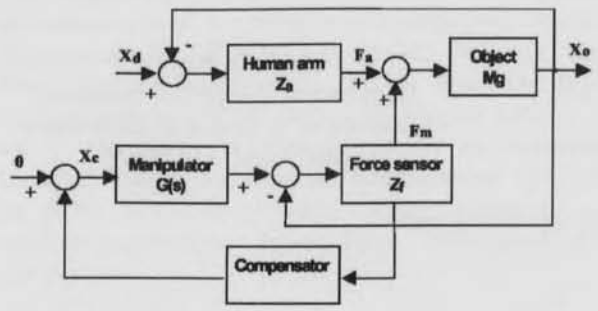

Fig. 2. Block diagram representation of the arm-manipulator coordination problem.

$$m\ddot{x}_o = f_a + f_m$$

$$f_a = k_a(x_d - x_o) + c_a(\dot{x}_d - \dot{x}_o)$$

$$f_m = k_m(Gx_c - x_o)$$

where f_a denotes arm force, f_m denotes manipulator force, k_a is arm stiffness, c_a is arm damping (assumed as viscous), k_m is manipulator (wrist-sensor) stiffness, x_d is desired object position, x_c is manipulator command, x_o is the object position, and $G(s)$ represents the manipulator transfer function given as

$$G(s) = \frac{\omega_n^2}{s^2 + 2\xi\omega_n s + \omega_n^2}.$$

The transfer functions relating manipulator command to arm-force and manipulator force are given by

$$\frac{f_a}{x_c} = -\frac{k_m(c_a s + k_a)}{ms^2 + c_a s + (k_a + k_m)}G(s) \text{ and}$$

$$\frac{f_m}{x_c} = \frac{mk_m s^2}{ms^2 + c_a s + (k_a + k_m)}G(s).$$

Finally, the position of the object being manipulated is given as

$$x_o = \frac{(c_a s + k_a)x_d + k_m x_c G(s)}{ms^2 + c_a s + (k_a + k_m)}$$

where in the steady state, the object position is given by $(k_a x_d + k_m x_c) / (k_a + k_m)$. Since $k_m >> k_a$, the object position will be primarily determined by the manipulator command (x_c). By commanding the manipulator to eliminate the arm force, we can ensure that $x_c = x_d = x_o$ (Iqbal and Zheng, 1997; Iqbal and Zheng, 1999). Accordingly, in the arm-manipulator coordination problem (i.e., the regulation

problem) our objective is to reduce the arm force to zero. In the absence of the human arm, when the manipulator interacts with the environment, the sensor output can be controlled using a generalized force input of the form $f_g = ms^2 x_c$, such that

$$\frac{f_m}{f_g} = \frac{k_m}{ms^2 + k_m} G(s)$$

where the above representation defines a tracking problem. In the following our effort would be to develop a general framework that can handle the above as well as other similar situations. Accordingly we consider a possibly unstable process given by the following transfer function

$$G_p(s) = \frac{n_p}{d_p}(s) = \frac{\omega_n^2 (as + b)}{(ms^2 + cs + k)(s^2 + 2\xi\omega_n s + \omega_n^2)} \quad (1)$$

where the first part represents a general second order transfer function, and the second part represents a position-controlled manipulator. We assume that the process given by equation (1) is controlled through unity gain feedback by a PID controller whose transfer is given by

$$G_c(s) = \frac{n_c}{d_c}(s) = \frac{K_d s^2 + K_p s + K_i}{s} \quad (2)$$

Then, the closed-loop characteristic polynomial is given as

$$\psi(s) = s d_p(s) + (K_i + s^2 K_d) n_p(s) + s K_p n_p(s) \quad (3)$$

Define $\tilde{A} = \{a, b, k, c, m, \xi, \omega_n\}$ to be the set of all system constants, and let $\kappa = \{K_p, K_i, K_d\}$ represent the controller parameters; then the design problem is defined as, given $\tilde{A}$, determine

$$\tilde{\kappa} \ni \mathrm{Re}[s_\psi] < 0 \, \forall s_\psi, \left\{ s_\psi \,\middle|\, \psi(s_\psi) = 0 \right\}$$

Hermite-Biehler Theorems.--In this section we state the Hermite-Biehler and the generalized Hermite-Biehler Theorems (Datta et al., 1999; Ho et al., 2000).

Theorem 1 (Hermite-Biehler Theorem): Let

$$\delta(s) = \sum_{i=0}^{n} \delta_i s^i, \ \delta_i \in \Re \, \forall i.$$

Write $\delta(s) = \delta_e(s^2) + \delta_o(s^2)$ where $\delta_{e,o}(s^2)$ are the components of $\delta(s)$ made up of even and odd powers of s, respectively. Let ω_{ej} denote the real non-negative distinct zeros of $\delta_e(-\omega^2)$ and let ω_{ok} denote the real non-negative distinct zeros of $\delta_o(-\omega^2) \forall j,k$, both arranged in ascending order of magnitude. Then $\delta(s)$ is Hurwitz stable if and only if δ_n and δ_{n-1} are of the same sign, all the zeros of $\delta_e(-\omega^2)$, $\delta_e(-\omega^2)$ are real and distinct, and the non-negative real zeros satisfy the interlacing property given by $0 < \omega_{e1} < \omega_{o1} < \omega_{e2} < \omega_{o2} < \cdots$

Theorem 2: Let $\delta(s) = \sum_{i=0}^{n} \delta_i s^i, \ \delta_i \in \Re \, \forall i$. Write $\delta(s) = \delta_e(s^2) + \delta_o(s^2)$ where $\delta_{e,o}(s^2)$ are the components of $\delta(s)$ made up of even and odd powers of s, respectively. For every $\omega \in \Re$, denote $\delta(jw) = p(\omega) + jq(\omega)$ where $p(\omega)$ and $q(\omega)$ are given by $p(\omega) = \delta_e(-\omega^2)$ and $q(\omega) = \delta_o(-\omega^2)$; let ω_{ej} denote the real non-negative distinct zeros of $\delta_e(-\omega^2)$, and let ω_{ok}, denote the real non-negative distinct zeros of $\delta_o(-\omega^2) \forall j,k$, both arranged in ascending order of magnitude. Then the following conditions are equivalent:

(1) $\delta(s)$ is Hurwitz stable,

(2) δ_n and δ_{n-1} are of the same sign, and

$$n = \mathrm{sgn}[\delta_0]\left[\mathrm{sgn}[p(0)] + 2\sum_{i=1}^{m} (-1)^i \mathrm{sgn}[p(\omega_{oi})]\right], \ n = 2m \, \forall m \in I_+, \ \omega_{om} = \infty$$

$$n = \mathrm{sgn}[\delta_0]\left[\mathrm{sgn}[p(0)] + 2\sum_{i=1}^{m} (-1)^i \mathrm{sgn}[p(\omega_{oi})]\right], \ n = 2m+1 \, \forall m \in I_+.$$

(33) δ_n and δ_{n-1} are of the same sign, and

$$n = 2\,\mathrm{sgn}[\delta_0]\left[\sum_{i=1}^{m} (-1)^{i-1} \mathrm{sgn}[q(\omega_{ei})]\right], \ n = 2m \, \forall m \in I_+$$

$$n = 2\,\mathrm{sgn}[\delta_0]\left[\sum_{i=1}^{m+1} (-1)^{i-1} \mathrm{sgn}[q(\omega_{ei})]\right], \ n = 2m+1 \, \forall m \in I_+, \ \omega_{em+1} = \infty$$

The classical Hermite-Biehler Theorem fails to provide any further information when the polynomial is not Hurwitz. However, the generalized Hermite-Biehler Theorem (Datta et al., 1999; Ho et al., 2000) ascertains Hurwitz stability and at the same time provides information about the number of RHP roots, if any.

Theorem 3 (Generalized Hermite-Biehler Theorem): Let $\delta(s) = \sum_{i=0}^{n} \delta_i s^i, \ \delta_i \in \Re \, \forall i$ with a root at the origin of multiplicity k. Let $0 < \omega_{o1} < \omega_{o2} \cdots < \omega_{om-1}$ be the zeros of $q(\omega)$ that are real, distinct and nonnegative. Also, define $\omega_0 = 0$, $\omega_{om} = \infty$, and $p^{(k)}(\omega_0) = \left(\frac{d^k}{d\omega^k} p(\omega) \right)\Big|_{\omega = \omega_0}$.

Then,

$$\sigma[\delta(s)] = (-1)^{m-1}\left[\mathrm{sgn}[p^{(k)}(\omega_0)] + 2\sum_{i=1}^{m-1} (-1)^i \mathrm{sgn}[p(\omega_{oi})] + (-1)^m \mathrm{sgn}[p(\omega_{om})]\right] \mathrm{sgn}[q(\infty)], \ n = 2m$$

$$\sigma[\delta(s)] = (-1)^{m-1}\left[\mathrm{sgn}[p^{(k)}(\omega_0)] + 2\sum_{i=1}^{m-1} (-1)^i \mathrm{sgn}[p(\omega_{oi})]\right] \mathrm{sgn}[q(\infty)], \ n = 2m+1 \, \forall m \in I_+$$

where $q(\omega)$ is defined in Theorem 2, and $\sigma[\delta(s)] = n_\delta^{(L)} - n_\delta^{(R)}$ $n_\delta^{(L)}$ and $n_\delta^{(R)}$ denote the number of open left-half plane (LHP) and RHP roots of $\delta(s)$. The proof of the theorems can be found in the literature (Datta et al., 1999; Ho et al., 2000).

A Framework for Controller Synthesis.--Based on Hermite-Biehler Theorems, the following procedure is adapted for PID controller design of the unity gain feedback

system. The plant and controller transfer functions are given as $G_p(s) = n_p(s)/d_p(s)$, $G_c(s) = n_c(s)/d_c(s)$, where $n_c(s) = K_d s^2 + K_p s + K_i$, $d_c(s) = s$. Let

$$\delta(s) = \psi(s)n_p(-s) = sd_p(s)n_p(-s) + (K_i + K_d s^2)n_p(s)n_p(-s) + K_p sn_p(s)n_p(-s) \quad (4)$$

Then, it can be verified that $\sigma[\delta(s)] = \sigma[\psi(s)] - \sigma[n_p(s)]$. Let $m_\psi = \Theta[\psi(s)]$ denote the order of $\psi(s)$, then the number of RHP poles of $\psi(s)$ is given by $n_\psi^{(R)} = \frac{1}{2}\{m_\psi - \sigma[\psi(s)]\}$.

It is easy to see that, if $\psi(s)$ is to be Hurwitz, then $\sigma[\psi(s)] = m_\psi$, and $\sigma[\delta(s)] = m_\psi - \sigma[n_p(s)]$. Note that $\delta(j\omega) = p(\omega) + jq(\omega)$ where the polynomials are $p(\omega) = p_1(\omega) + (K_i - K_d\omega^2)p_2(\omega)$ and $q(\omega) = q_1(\omega) + K_p q_2(\omega)$. Therefore, let $m_q = \Theta[q(\omega)]$ and $\tilde{m}_q \le m_q$ be the number of distinct, nonnegative, real zeros of $q(\omega)$ for some value of $K_p \in (-\infty, \infty)$, and define

$$\tilde{I}_i = \text{sgn}\left[p_1(\omega_{oi}) + (K_i - K_d\omega_{oi}^2)p_2(\omega_{oi})\right] \in \{-1, 1\}\ \forall i \in [1, \tilde{m}_q],$$

$$\tilde{I}_0 = \text{sgn}[p_1(0) + K_i p_2(0)] \in \{-1, 0, 1\},$$

$\rho = m_\psi - \sigma[n_p(s)]$, $\gamma = (-1)^{\tilde{m}_q - 1}\,\text{sgn}[q(\infty)]$, and

$$\alpha = \frac{1}{2}\{m_\psi + \Theta[n_p(s)]\}.$$

Then, if $\psi(s)$ is to be Hurwitz, there must be a feasible solution to either of the following equations (Roy and Iqbal, 2002; Datta et al., 1999; Ho et al., 2000):

$$\rho = \left[\tilde{I}_0 + 2\sum_{i=1}^{\tilde{m}_q - 1}(-1)^i \tilde{I}_i + (-1)^{\tilde{m}_q}\tilde{I}_{\tilde{m}_q}\right]\gamma,\ \alpha \in I_+ \text{ and} \quad (5)$$

$$\rho = \left[\tilde{I}_0 + 2\sum_{i=1}^{\tilde{m}_q - 1}(-1)^i \tilde{I}_i\right]\gamma,\ \alpha \notin I_+. \quad (6)$$

Assuming that a solution to equations (5) or (6) can be found, we denote this feasible set as $g^* = \{\tilde{I}_i\} \neq \varnothing\ \forall i \in [0, \tilde{m}_q]$. Then, a non-empty stabilizing PID set $S_{\tilde{K}} = \{K_p, [\underline{K}_i, \overline{K}_i], [\underline{K}_d, \overline{K}_d]\}$ for some $K_p \in (-\infty, \infty)$ can be computed from a set of linear inequalities developed as $(g^*)\cdot\{[P_1] + [P_2][\kappa]\} > 0$, i.e., $\text{sgn}\{[P_1] + [P_2][\kappa]\} = g^*$, where the matrices $[P_1] \in \Re^{\tilde{m}_q \times 1}$, $[P_2] \in \Re^{\tilde{m}_q \times 2}$ and $[\kappa] \in \Re^{2\times 1}$ are defined as

$$[P_1] = [\,p_1(0) \quad p_1(\omega_{o1}) \quad p_1(\omega_{o2}) \quad \cdots \quad p_1(\omega_{o\tilde{m}_q - 1})\,]^T \quad (7)$$

$$[P_2] = \begin{bmatrix} p_2(0) & p_2(\omega_{o1}) & p_2(\omega_{o2}) & \cdots & p_2(\omega_{o\tilde{m}_q - 1}) \\ 0 & -\omega_{o1}^2 p_2(\omega_{o1}) & -\omega_{o2}^2 p_2(\omega_{o2}) & \cdots & -\omega_{o\tilde{m}_q - 1}^2 p_2(\omega_{o\tilde{m}_q - 1}) \end{bmatrix}^T, \text{ and} \quad (8)$$

$$[\kappa] = [K_i \quad K_d]^T. \qquad S_{\tilde{K}} \in \Re \quad (9)$$

Note that in the preceding analysis $S_{\tilde{K}} \in \Re^+$, has been assumed. In practice, to facilitate tuning, we may require that $S_{\tilde{K}} \in \Re^+ \left| \{(g^*)\cdot\{[P_1] + [P_2][\kappa]\} > 0\right\} \neq \varnothing$.

Necessary Conditions for Stability.--In this section we shall determine the necessary condition for the existence of K. To this effect, re-write equation (1) as

$$G_p(s) = \frac{n_p}{d_p}(s) = \frac{a_1 s + a_0}{s^4 + b_3 s^3 + b_2 s^2 + b_1 s + b_0}. \quad (10)$$

Define $\{a\} = \{a_0, a_1\}$ and $\{b\} = \{b_0, b_1, b_2, b_3\}$. Note that for the given problem $m_\psi = 5$, $\rho = 4$, $\alpha = 3$, and the polynomial

$$q(\omega) = \omega\tilde{q}(\omega) = \frac{a_1}{a_0}\left[(a_0 - b_3 a_1)\omega^5 + \{(b_1 a_1 - b_2 a_0) + K_p a_1^2\}\omega^3 + (b_0 a_0 + a_0^2)\omega\right] \quad (11)$$

Using equation (11) we determine that $q(\infty) = \frac{a_1(a_0 - b_3 a_1)}{a_0}$ such that $\gamma = (-1)^{\tilde{m}q - 1}s_o$, where $s_o = \text{sgn}\left[\frac{a_1(a_0 - b_3 a_1)}{a_0}\right]$; then, if $\psi(s)$ is to be Hurwitz stable, we must have (Roy and Iqbal, 2002; Ho et al., 2000):

$$(-1)^{\tilde{m}_q - 1}\left[\tilde{I}_0 + 2\sum_{i=1}^{\tilde{m}_q - 1}(-1)^i \tilde{I}_i + (-1)^{\tilde{m}_q}\tilde{I}_{\tilde{m}_q}\right]s_o = \rho \quad (12)$$

where $\tilde{I}_i = \begin{cases} \tilde{I}_0 \in \{-1, 0, 1\},\ i = 0 \text{ and } \tilde{m}_q \text{ is the number of roots} \\ \tilde{I}_i \in \{-1, 1\},\ i \neq 0 \end{cases}$

$q(\omega, K_p)$ that are real, nonnegative, and distinct, given as $\omega_0 = 0$, and the four roots of the equation $\tilde{q}(\omega, K_p) = 0$ are given as

$$\omega_{1,2,3,4}^2 = \lambda_{1,2} = \frac{b_2 a_0 - b_1 a_1 - K_p a_1^2 \pm \sqrt{\Delta}}{2(a_0 - b_3 a_1)} \quad (13)$$

where $\lambda = \omega^2$ and define

$\Delta(K_p) = \{(b_1 a_1 - b_2 a_0) + K_p a_1^2\}^2 - 4a_0(b_0 + a_0)(a_0 - b_3 a_1)$.

Let $0 \le \tilde{m}^* \le 4$ be the number of roots of $\tilde{q}(\omega, K_p) = 0$ that are real, nonnegative, and distinct; then the stability results for the various cases of $\tilde{m}_q$ are summarized in Table 1. The necessary conditions for stability of the closed-loop system defined by equations (1) and (2) are given by the following theorem.

Theorem 4: Let Ω be a logical set defined as $\Omega = \text{sgn}[\Delta] \neq -1 \wedge \sum_i \text{sgn}[\lambda_i] \ge 0$; then, the necessary condition for a set of stabilizing PID controllers for the process given by (1) is $\Omega \neq \varnothing$.

Proof: From Table 1, the conditions for $g^* \neq \varnothing$ are

$$\tilde{m}^* = \begin{cases} 1 \Leftrightarrow \text{sgn}[\Delta] \neq -1 \wedge \prod_i \text{sgn}[\lambda_i] = -1 \\ 2 \Leftrightarrow \text{sgn}[\Delta] \neq -1 \wedge \prod_i \text{sgn}[\lambda_i] \ge 0. \end{cases}$$

Combining the two conditions and recognizing that

$$\prod_i \text{sgn}[\lambda_i] = -1 \vee \prod_i \text{sgn}[\lambda_i] \ge 0 \equiv \sum_i \text{sgn}[\lambda_i] \ge 0,$$

we obtain the result $g^* \neq \varnothing \Leftrightarrow \Omega \neq \varnothing$.

Q.E.D.

The following lemmas illustrate how the necessary conditions are determined for the problem.

Lemma 1: $\text{sgn}[\Delta] \neq -1$ if and only if $K_p \in S^*(K_p)$ where Δ is as defined above, and

$$S^*(K_p) = \begin{cases} (-\infty, \min\{k_{1,2}^*\}) \cup [\max\{k_{1,2}^*\}, \infty), & k_{1,2}^* \in \Re \\ (-\infty, \infty), & k_{1,2}^* \in C \end{cases}$$

where $k_{1,2}^*$ are the roots of Δ.

Proof: From equation (13), we note that we can write Δ as a quadratic in K_p,

$\Delta = a_1^4 K_p^2 + 2a_1^2(b_1a_1 - b_2a_0)K_p + c = \prod_i (K_p - k_i^*)$, where

$c = (b_1a_1 - b_2a_0)^2 - 4a_0(b_0 + a_0)(a_0 - b_3a_1)$. Then, it can be seen that $\Delta \geq 0 \; \forall K_p \in (-\infty, \min\{k_{1,2}^*\}) \cup [\max\{k_{1,2}^*\}, \infty)$ and $\Delta < 0 \; \forall K_p \in (\min\{k_{1,2}^*\}, \max\{k_{1,2}^*\})$. Therefore,

$\text{sgn}[\Delta] \neq -1 \forall K_p \in (-\infty, \min\{k_{1,2}^*\}) \cup [\max\{k_{1,2}^*\}, \infty) = S^*(K_p)$.

However, it can be verified that for $\forall k_{1,2}^* \in C$,

$\Delta > 0 \forall K_p \Rightarrow \text{sgn}[\Delta] \neq -1 \Rightarrow S^*(K_p) = (-\infty, \infty)$.

Q.E.D.

Lemma 2: For $\sum_i \text{sgn}[\lambda_i] \geq 0$ the range of K_p is given by the following range $\{K_p \in \overline{S}(K_p)\} \vee K_p \in \begin{cases} \widetilde{S}(K_p) & \text{for } s_1 = -1 \\ \varnothing & \text{for } s_1 = 1 \end{cases}$

where $\overline{S}(K_p) = \left(-\infty, \dfrac{b_1|a_1| - b_2|a_0|}{a_1^2} \right]$, $\widetilde{S}(K_p) = \left(\dfrac{b_1|a_1| - b_2|a_0|}{a_1^2}, \infty \right)$,

and $s_1 = \text{sgn}\left[\dfrac{a_0(b_0 + a_0)}{(a_0 - b_3a_1)} \right]$.

Proof: Note that

$$\lambda_{1,2} = \frac{b_2a_0 - b_1a_1 - K_pa_1^2 \pm \sqrt{\Delta}}{2(a_0 - b_3a_1)} = \frac{B(K_p) \pm \sqrt{\Delta}}{\overline{A}(\{a\}, \{b\})} = \overline{B}_1(K_p) \pm \overline{B}_2(K_p) \quad (14)$$

where $\overline{B}_1(K_p) = \dfrac{B_1(K_p)}{\overline{A}}$, $\overline{B}_2(K_p) = \dfrac{\sqrt{\Delta}}{\overline{A}}$.

Then, regardless of the value of sgn $[\overline{A}]$, since

$\Delta \geq 0 \; \forall K_p \in S^*(K_p)$,

$$\sum_i \text{sgn}[\lambda_i] \geq 0 \equiv \text{sgn}[\overline{B}_1] = 1 \vee \left\{ \text{sgn}[\overline{B}_1] = -1 \wedge \text{sgn}[|\overline{B}_1| - |\overline{B}_2|] = -1 \right\}$$

But $\text{sgn}[\overline{B}_1] = 1$ if and only if $K_p \in \overline{S}(K_p)$, while $\text{sgn}[\overline{B}_1] = -1 \Leftrightarrow K_p \in \widetilde{S}(K_p)$. However,

$$\text{sgn}\left[|\overline{B}_1| - |\overline{B}_2| \right] = -1 \equiv \text{sgn}[\overline{B}_1^2 - \overline{B}_2^2] = \text{sgn}\left[\frac{a_0(b_0 + a_0)}{(a_0 - b_3a_1)} \right] = s_1 = -1.$$

Since s_1 is a function that is independent of K_p, we have

$$\left\{ K_p \middle| \text{sgn}\left[|B_1| - |B_2| \right] = -1 \right\} = \begin{cases} (-\infty, \infty) & \text{for } s_1 = -1 \\ \varnothing & \text{for } s_1 = 1 \end{cases} \text{ or,}$$

$$\text{sgn}[\overline{B}_1] = -1 \wedge \text{sgn}\left[|\overline{B}_1| - |\overline{B}_2| \right] = -1 \Rightarrow \{K_p \in \overline{S}(K_p)\} \vee K_p \in \begin{cases} S(K_p) & \text{for } s_1 = -1 \\ \varnothing & \text{for } s_1 = 1 \end{cases}.$$

Q.E.D.

Theorem 5 (Necessary Condition): The process given by equation (1) is stabilizable, i.e., $\exists g^* \neq \varnothing$ if and only if $K_p \in S(K_p)$ where is evaluated as

(i) $$S(K_p) = \begin{cases} S^*(K_p) & \text{for } s_1 = -1 \\ S^*(K_p) \cap \overline{S}(K_p) & \text{for } s_1 = 1 \end{cases} \quad \forall k_{1,2}^* \in \Re,$$

(ii) $$S(K_p) = \begin{cases} (-\infty, \infty) & \text{for } s_1 = -1 \\ \overline{S}(K_p) & \text{for } s_1 = 1 \end{cases} \quad \forall k_{1,2}^* \in C$$

where $S^*(K_p)$ and $\overline{S}(K_p)$ are as defined in Lemma 1 and Lemma 2.

Proof: (i) From Lemma 1 and Lemma 2 we get

$$\text{sgn}[\Delta] \neq -1 \wedge \sum_i \text{sgn}[\lambda_i] \geq 0 \equiv K_p \in S^*(K_p) \cap \overline{S}(K_p) \cup \begin{cases} \widetilde{S}(K_p) & \text{for } s_1 = -1 \\ \varnothing & \text{for } s_1 = 1 \end{cases}.$$

Substituting the above condition in the result of Theorem 4, we obtain

$$g^* \neq \varnothing \Leftrightarrow K_p \in S^*(K_p) \cap \overline{S}(K_p) \cup \begin{cases} \widetilde{S}(K_p) & \text{for } s_1 = -1 \\ \varnothing & \text{for } s_1 = 1 \end{cases}$$

$$\Rightarrow S(K_p) = \begin{cases} S^*(K_p) \cap \{\overline{S}(K_p) \cup \widetilde{S}(K_p)\} & \text{for } s_1 = -1 \\ S^*(K_p) \cap \overline{S}(K_p) & \text{for } s_1 = 1 \end{cases}.$$

Since $\overline{S}(K_p) \cup \widetilde{S}(K_p) = (-\infty, \infty) = \Re$ and $S^*(K_p) \cap (-\infty, \infty) = S^*(K_p)$, we obtain

$$S(K_p) = \begin{cases} S^*(K_p) & \text{for } s_1 = -1 \\ S^*(K_p) \cap \overline{S}(K_p) & \text{for } s_1 = 1 \end{cases}.$$

(ii) Observe from Lemma 1 that $\forall k_{1,2}^* \in C$, $S^*(K_p) = (-\infty, \infty)$. Using this result in (i), and recognizing that $(-\infty, \infty) \cap \overline{S}(K_p) = \overline{S}(K_p)$, the result follows. Q.E.D.

Sufficient Conditions for Stability.--We now determine the sufficient conditions for the existence of the stabilizing PID set. We note that sufficient conditions for the PID to exist are given by (Roy and Iqbal, 2002; Ho et al., 2000)

$$(g^*) \cdot \{[P_1] + [P_2][\widetilde{\kappa}]\} > 0 \neq \varnothing \quad (15)$$

where the real matrices $[P_1]$, $[P_2]$, and $[\widetilde{\kappa}]$ are defined by equations (7)-(9). From Table I we know that $g^* \neq \varnothing \Leftrightarrow \widetilde{m}_q = 2, 3$. Define

$$f = \frac{a_1 \max(\lambda_i)^3 + (a_0b_3 - a_1b_2)\max(\lambda_i)^2 + (|K_i|a_1^2 - a_0b_1)\max(\lambda_i) + |K_i|a_0^2}{\max(\lambda_i)(a_1^2 \max(\lambda_i) + a_0^2)},$$

$$\bar{f} = \frac{a_1 \max(\lambda_i)^3 + (a_0b_3 - a_1b_2)\max(\lambda_i)^2 - (|K_i|a_1^2 - a_0b_1)\max(\lambda_i) - |K_i|a_0^2}{\max(\lambda_i)(a_1^2 \max(\lambda_i) + a_0^2)},$$

$$\eta_{1,2} = \frac{a_1\lambda_{1,2}^3 + (a_0b_3 - a_1b_2)\lambda_{1,2}^2 + (|K_i|a_1^2 - a_0b_1)\lambda_{1,2} + |K_i|a_0^2}{\lambda_{1,2}(a_1^2\lambda_{1,2} + a_0^2)},$$

and $S_\eta = \left(\min\{\eta_{1,2}\}, \max\{\eta_{1,2}\}\right)$, $S_{\overline{\eta}} = \left(\min\{\overline{\eta}_{1,2}\}, \max\{\overline{\eta}_{1,2}\}\right)$

The following lemma develops the sufficiency condition.

Lemma 3: A stabilizing PID set $\widetilde{\kappa}$, for the process in equation (10) exists only under the following conditions: for a given $K_p \in S(K_p)$,

1) If $\tilde{m}^* = 1$, then $\begin{cases} K_i \in (0,\infty),\ K_d \in (f,\infty) \text{ when } \gamma = 1 \\ K_i \in (-\infty,0),\ K_d \in (-\infty,\bar{f}) \text{ when } \gamma = -1. \end{cases}$

2) If $\tilde{m}^* = 2$, then

(a) If $\sum_i \text{sgn}[\lambda_i] = 1$, then $\begin{cases} K_i \in (0,\infty),\ K_d \in (f,\infty) \text{ when } \gamma = 1 \\ K_i \in (-\infty,0),\ K_d \in (-\infty,\bar{f}) \text{ when } \gamma = -1. \end{cases}$

(b) If $\sum_i \text{sgn}[\lambda_i] = 2$, then $\begin{cases} K_i \in \Re^+,\ K_d \in S_\eta \text{ when } \gamma = 1 \\ K_i \in \Re^-,\ K_d \in S_{\bar{\eta}} \text{ when } \gamma = -1. \end{cases}$

Proof: 1) From Table 1, for $\tilde{m}^* = 1$,
$\text{sgn}[\Delta] \neq -1 \wedge \prod_i \text{sgn}[\lambda_i] = -1 \equiv \text{sgn}[\Delta] \neq -1 \wedge \sum_i \text{sgn}[\lambda_i] = 0.$
But from Theorem 4 and Theorem 5, we have
$\text{sgn}[\Delta] \neq -1 \wedge \sum_i \text{sgn}[\lambda_i] \geq 0 \forall K_p \in S(K_p).$
Therefore, whenever $\tilde{m}^* = 1$, $\sum_i \text{sgn}[\lambda_i] \geq 0 \forall K_p \in S(K_p)$.
Using this result in equation (13), we deduce $\omega_{o1} = \sqrt{\max(\lambda_i)}$.

Furthermore, from equations (5)-(7) and the set of linear inequalities, we obtain

$$\begin{cases} K_i > 0,\ K_d > \dfrac{p_1(\omega_{o1}) + |K_i| p_2(\omega_{o1})}{\max(\lambda_i) p_2(\omega_{o1})} \text{ when } \gamma = 1 \\ K_i < 0,\ K_d < \dfrac{p_1(\omega_{o1}) - |K_i| p_2(\omega_{o1})}{\max(\lambda_i) p_2(\omega_{o1})} \text{ when } \gamma = -1. \end{cases}$$

Substituting ω_{o1} in the expressions of $p_{1,2}(\omega)$ (Datta et al., 1999), we obtain

$$\frac{p_1(\omega_{o1}) + |K_i| p_2(\omega_{o1})}{\max(\lambda_i) p_2(\omega_{o1})} = f \text{ and } \frac{p_1(\omega_{o1}) - |K_i| p_2(\omega_{o1})}{\max(\lambda_i) p_2(\omega_{o1})} = \bar{f}.$$

2a.) If $\sum \text{sgn}[\lambda_i] = 1$, then $\{\omega_i\} = \{0, 0, 2\Re \neq 0\}$. Then the root distribution of $q(\omega, K_p)$ is $\{0, 0, 0, 2\Re \neq 0\}$.
Therefore the roots that qualify for the computation of equation (15) are $\{\omega_0 = 0, \omega_{o1} = \sqrt{\max(\lambda_i)}\}$, and the proof follows from equation (1) of Lemma 3.
2b.) The proof is on similar lines as (2a) except that for $\sum_i \text{sgn}[\lambda_i] = 2$, the dimensions in equations (5) and (6) increase by one. It is known from equation (13) that for $\sum_i \text{sgn}[\lambda_i] = 2$, $\omega_{o1,2} = \sqrt{\lambda_{1,2}}$. The result follows from (2a) in conjunction with equation (15) and making substitution for $\omega_{o1,2}$.
Q.E.D.
The stability results of Lemmas 1, 2, and 3 are summarized in the following theorem.

Theorem 6 (Main result on stabilization): The process given by equation (10) is stabilizable with a PID controller if and only if $K_p \in S(K_p)$ and if the ranges of K_i, K_d are chosen according to the following situations:
(a) If $\sum_i \text{sgn}[\lambda_i] = 0,1$ and $\gamma = 1$, then $K_i \in \Re^+$, $K_d \in (f,\infty)$.
(b) If $\sum_i \text{sgn}[\lambda_i] = 0,1$ and $\gamma = -1$, then $K_i \in \Re^-$, $K_d \in (-\infty,\bar{f})$.
(c) If $\sum_i \text{sgn}[\lambda_i] = 2$ and $\gamma = 1$, then either $(K_i \in \Re^+,\ K_d \in S_\eta)$, or $(K_i \in \Re^-,\ K_d \in S_{\bar{\eta}})$ whichever is non-empty.
(d) If $\sum_i \text{sgn}[\lambda_i] = 2$ and $\gamma = -1$, then $(K_i \in \Re^+,\ K_d \in S_\eta)$, or $(K_i \in \Re^-,\ K_d \in S_{\bar{\eta}})$ whichever is non-empty.
Proof: For closed-loop stability we know that the necessary condition for the existence of a stabilizing PID controller is given by Theorem 5, i.e., $K_p \in S(K_p)$. Furthermore, (a) and (b) are the results of Lemma 3(1) and 3(2a), while (c) and (d) follow from Lemma 3(2b). Q.E.D.

The following algorithm is proposed to determine the stabilizing PID set for the problem:
(i) Use the Theorem 5 to calculate $S(K_p)$. Constraint the value of K_p to $K_p = K_{p0} \in S(K_p)$.
(ii) Calculate the value of $\sum_i \text{sgn}[\lambda_i]$ and γ. Note that γ is given as

$$\gamma = (-1)^{\tilde{m}_q - 1} s_o = \begin{cases} -s_o \text{ for } \sum_i \text{sgn}[\lambda_i] = 0,1 \\ s_o \text{ for } \sum_i \text{sgn}[\lambda_i] = 2 \end{cases}.$$

Accordingly, calculate f (or $\bar{f}$) or S_η (or $S_{\bar{\eta}}$).
(iii) Use Theorem 6 to evaluate the stabilizing PID set.

Remark 1: From Theorem 6 and the above algorithm, we can write the stabilizing PID set as
$\forall K_p = K_{p0} \in S(K_p)$,
(a) $S_K = \{K_{p0}, \Re^+, (f,\infty)\}$ or $S_K = \{K_{p0}, \Re^-, (-\infty,\bar{f})\}$ for $\sum_i \text{sgn}[\lambda_i] = 0,1$ and $\gamma = \pm 1$.
(b) $S_K = \{K_{p0}, \Re^+, S_\eta\}$ or $S_K = \{K_{p0}, \Re^-, S_{\bar{\eta}}\}$ for $\sum_i \text{sgn}[\lambda_i] = 2$ and $\gamma = \pm 1$.

Remark 2: Note that f, $\bar{f}$, η, and $\bar{\eta}$ are a linear function of K_i as,

$$f, \bar{f} = \pm \frac{(a_1^2 \max(\lambda_i) + a_0^2)}{\max(\lambda_i)(a_1^2 \max(\lambda_i) + a_0^2)} |K_i| + \frac{a_1 \max(\lambda_i)^2 + (a_0 b_3 - a_1 b_2)\max(\lambda_i)^2 - a_0 b_1 \max(\lambda_i)}{\max(\lambda_i)(a_1^2 \max(\lambda_i) + a_0^2)},$$

$$\eta_{1,2},\ \bar{\eta}_{1,2} = \pm \frac{(a_1^2 \lambda_{1,2} + a_0^2)}{\lambda_{1,2}(a_1^2 \lambda_{1,2} + a_0^2)} |K_i| + \frac{a_1 \lambda_{1,2}^3 + (a_0 b_3 - a_1 b_2)\lambda_{1,2}^2 - a_0 b_1 \lambda_{1,2}}{\lambda_{1,2}(a_1^2 \lambda_{1,2} + a_0^2)}.$$

Therefore, a constrained point value of $K_i \in \Re^\pm$ generates an interval of K_d, and the bounds of the interval depend linearly on K_i. This concept is illustrated in Figure 3.

Results

Example 1. We consider the arm-manipulator problem when the process parameters are given as
$\tilde{A} = \{a, b, k, c, m, \xi, \omega_n\} = \{-10^3, -10^2, 101, 10, 1, 0.25, 2\}$

and the process is controlled by a PID controller. Therefore, $\{a\} = \{-400, -4000\}$ and $\{b\} = \{404, 141, 115, 11\}$. Then $s_1 = -1$ and $\Delta = 10^{11}(2560K_p^2 - 165.76K_p + 2.68) \Rightarrow k_{1,2}^* \in C$. Using Lemma 1, $S^*(K_p) = (-\infty, \infty)$, and from Theorem 5, $S(K_p) = S^*(K_p) = (-\infty, \infty)$. Let $K_p = K_{p0} = 1$, then $\Delta = 2.3969 \times 10^{14}$. From equation (13) we obtain $\lambda_1 = -355.09$, $\lambda_2 = 1.04 \times 10^{-4} \Rightarrow \sum_i \text{sgn}[\lambda_i] = 0$, and max $(\lambda_i) = 1.04 \times 10^{-4}$. Therefore, $\tilde{m}_q = 2 \Rightarrow \gamma = (-1)^1 \text{sgn}\{436000\} = -1$. Then from Theorem 6, $K_i \in \Re^- = (-\infty, 0)$ and $K_d \in (-\infty, \bar{f})$ where the value of $\bar{f}$ depends on the constrained value of K_i. The stabilizing PID set is given by $S_\kappa = \{1, (-\infty, 0), (-\infty, \bar{f})\}$. For example, constraining the value of $K_i = -1$, we obtain $\bar{f} = -9615.03$ and from Lemma 3, the stabilizing PID set is given by $S_\kappa = \{1, -1, (-\infty, -9615.03)\}$. As a further example, the closed-loop system is simulated for $\tilde{\kappa} = \{1, -1, -10^4\}$, and the response is shown in Figure 4.

Example 2. $(\tilde{A} > 0)$ Consider a manipulator-sensor process given by equation (1) with a process parameter set $\tilde{A} = \{10^3, 10^2, 101, 10, 1, 0.25, 2\}$. Then $s_1 = s_0 = -1$, $\Delta = 10^{11}(2560K_p^2 + 165.76K_p + 3.2441) \Rightarrow k_{1,2}^* \in C$. From Lemma 2, $S^*(K_p) = (-\infty, \infty)$, and from Theorem 5, we find that $S(K_p) = S^*(K_p) = (-\infty, \infty)$. Let $K_p = K_{p0} = 1$, then $\Delta = 2.7290 \times 10^{14}$. From equation (13) we obtain $\lambda_1 = -378.87$, $\lambda_2 = 0.0229 \Rightarrow \sum_i \text{sgn}[\lambda_i] = 0$, and max $(\lambda_i) = \lambda_2 = 0.0229$. Thus $\tilde{m}_q = 2 \Rightarrow \gamma = (-1)^1 s_0 = 1$. From Theorem 6 we obtain $K_i \in \Re^+ = (0, \infty)$ and $K_d \in (\bar{f}, \infty)$ where the value of $\bar{f}$ similarly depends on the constrained value of K_i. The stabilizing PID set is given by $S_\kappa = \{1, (0, \infty), (\bar{f}, \infty)\}$. Constraining the value of $K_i = 1$, we obtain $\bar{f} = 3.1199$ and from Lemma 3, the stabilizing PID set is given by $S_\kappa = \{1, 1, (3.1199, \infty)\}$. The closed-loop system is simulated for $\tilde{\kappa} = \{1, 1, 4\}$ and is shown in Figure 5.

Example 3. $(k, c < 0)$ Let an unstable manipulator-sensor process be given by the following parameters: $\tilde{A} = \{10^3, 10^2, -101, -10, 1, 0.25, 2\}$. Then $s_1 = 1, s_0 = -1$, and $\Delta = 10^{11}(2560K_p^2 - 166.78K_p + 2.7137) \Rightarrow k_{1,2}^* \in \Re$. From Lemma 1 and Lemma 2, $S^*(K_p) = (-\infty, 0.0336) \cup [0.0316, \infty)$ and $\bar{S}(K_p) = (-\infty, -0.0326)$. Furthermore, from Theorem 5 we obtain $S(K_p) = S^*(K_p) \cap \bar{S}(K_p) = (-\infty, -0.0326)$. Let $K_p = K_{p0} = -1$, then $\Delta = 2.7290 \times 10^{14}$. From equation (13) we obtain $\lambda_1 = -2.17$, $\lambda_2 = 381.10 \Rightarrow \sum_i \text{sgn}[\lambda_i] = 0$, and max $(\lambda_i) = \lambda_2 = 381.10$. Therefore, $\tilde{m}_q = 2 \Rightarrow \gamma = (-1)^1 s_0 = 1$. From Theorem 6, $K_i \in \Re^+ = (0, \infty)$ and $K_d \in (f, \infty)$ where the value of f depends on the constrained value of K_i. The stabilizing PID set is given by $S_\kappa = \{-1, (0, \infty), (f, \infty)\}$. Constraining the value of $K_i = 1$, we obtain $f = 0.1249$ and, from Lemma 3, the stabilizing PID set given by $\{-1, 1, (0.1249, \infty)\}$. The closed-loop system is simulated for $\tilde{\kappa} = \{-1, 1, 0.5\}$ and is shown in Figure 6.

Conclusions

In conclusion, this paper discusses PID controller stabilization of a robot manipulator equipped with a wrist sensor in an unstructured work environment. The problem is formulated in a general framework that can also be used for other similar applications. Necessary and sufficient conditions for stability are derived using the analytical framework of Hermite-Biehler Theorem that is based on the interlacing property of the even and odd parts of the characteristic polynomial. The controller synthesis involves solution of a set of linear matrix inequalities (LMIs) that can be solved on the computer. We propose an algorithm that conveniently solves for controller parameters given the plant model. Our simulation results for the robot-manipulator examples show that the controller, when used in conjunction with the position-controlled manipulator, effectively reduces the arm effort during manipulation tasks. The approach, albeit conservative in terms of being model specific, is successful in identifying a set of all stabilizing PID controllers for the given problem.

Literature Cited

Al-Jarrah, O. M., and **Y. F. Zheng.** 1996. Arm-manipulator coordination for load sharing using compliant control. Proc. IEEE Int. Conf. on Robotics and Automation. Minneapolis, Minnesota, USA. 2:1000-1005.

Al-Jarrah, O. M., and **Y. F. Zheng.** 1997. Arm-manipulator coordination for load sharing using reflexive motion control. Proc. IEEE Int. Conf. on Robotics and Automation. Albuquerque, New Mexico, USA. 2:2326-2331.

Datta, A., M. Ho, and **S. P. Bhattacharyya.** 2000. *Structure and Synthesis of PID Controllers.* Springer-Verlag, New York, USA. 43-52 pp.

Engelberger, J. F. 1989. *Robotics in Service.* MIT Press, Cambridge, Massachusetts, USA. 21-25 pp.

Ho, M., A. Datta, and **S. P. Bhattacharyya.** 2000. A New Approach to Feedback Design. Unpublished Research Report. Texas A&M University, Texas, USA. 121-146 pp.

Hunt, V. D. 1983. *Industrial Robotics Handbook.* Industrial Press, New York, USA. 16-22 pp.

Ikeura, R., and **H. Inooka.** 1995. Variable impedance control of robot for cooperation with a human. Proc. IEEE Int. Conf. on Robotics and Automation. Nagoya, Aichi, Japan. 3:3097-3102.

Ikeura, R., and **K. Mizutani.** 1998. Control of robot cooperating with human motion. Proc. IEEE Int. Workshop on Robotics and Human Communications. Takamatsu, Kagawa, Japan. 1:525-529.

Iqbal, K., and **Y. F. Zheng.** 1997. Use of prediction control

in arm-manipulator coordination. Proc. IEEE Int. Symp. on Intelligent Control. Istanbul, Turkey. 1:409-414.

Iqbal, K., and **Y. F. Zheng.** 1999. Arm-Manipulator Coordination for Load Sharing Using Predictive Control. Proc. IEEE Int. Conf. on Robotics and Automation. Detroit, Michigan, USA. 2:2539-2544.

Kazerooni, H. 1990. Human-robot interaction via the transfer of power and information signals. IEEE Transactions on Systems, Man, and Cybernetics. 20(2):450-463.

Luh, J. Y. S., and **Y. F. Zheng.** 1987. Constrained relation between two coordinated industrial robots for motion control. Int. J. of Robotic Research. 6(3):60-70.

Rahman, M., R. Ikeura, and **K. Mizutani.** 1999. Investigating the impedance characteristics of human arm for development of robots to cooperate with human operators. Proc. IEEE Int. Conf. on System, Man and Cybernetics. Tokyo, Japan. 2:676-681.

Roy, A., and **K. Iqbal.** 2003. PID stabilization for a single-link inverted pendulum with multiple feedback delays using the Hermite-Biehler Theorem. Proc. IEEE Conf. on Systems, Man, and Cybernetics. Washington, D.C., USA. 1:642-648.

Snyder, W. E. 1985. *Industrial Robots: Computer Interfacing and Control.* Prentice-Hall, New Jersey, USA. 23-43 pp.

Tao, J. M., J. Y. S. Luh, and **Y. F. Zheng.** 1990. Compliant coordination control of two moving industrial robots. IEEE Transactions on Robotics and Automation. 6(3):322-325.

Xu, Y., and **R. P. Paul.** 1988. On position compensation and force control stability of a robot with compliant wrist. Proc. IEEE Int. Conf. on Robotics and Automation. Philadelphia, Pennsylvania, USA. 2:1173-1178.

Zheng, Y. F., and **J. Y. S. Luh.** 1989. Optimal load distribution for two industrial robots handling a single object. ASME Journal of Dynamic System, Measurement, and Control. 111: 232-237.

Table 1. Stability results for various cases of roots of $\widetilde{q}(\omega, K_p)$

$\widetilde{m}^*$	Possible $\{\omega_i\}$ for $g^* \neq \varnothing$	Condition on sign of Δ
0	$\{\varnothing\}$	Not applicable
1	$\{2\Re, 2C\}$	$\text{sgn}[\Delta] \neq -1 \wedge \prod_i \text{sgn}[\lambda_i] = -1$
2	$\{4\Re \neq 0\}, \{0, 0, 2\Re \neq 0\}$	$\text{sgn}[\Delta] \neq -1 \wedge \prod_i \text{sgn}[\lambda_i] \geq 0$
3, 4	$\{\varnothing\}$	Not applicable

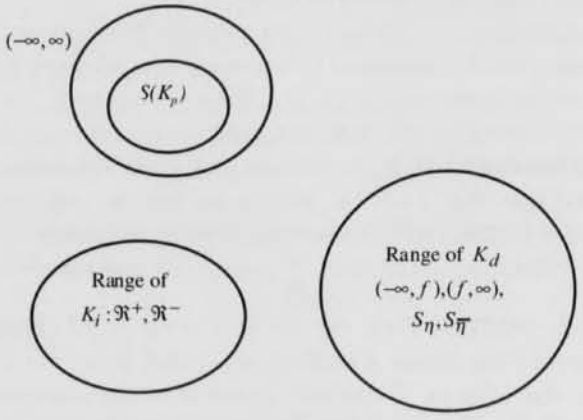

Fig. 3. A set diagram illustrating the concept of the algorithm derived from Theorem 6.

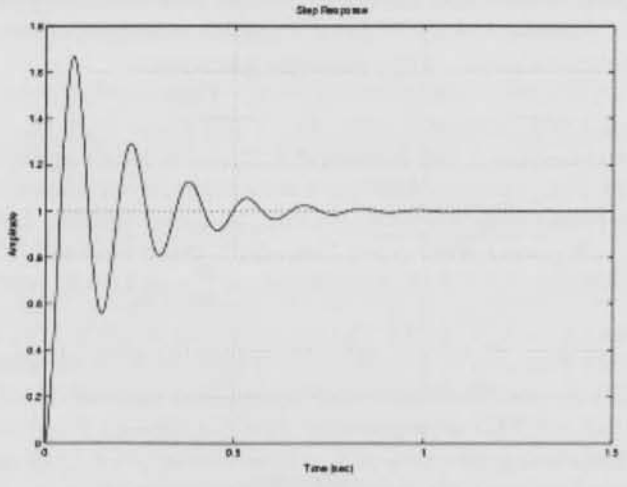

Fig. 4. Closed-loop step response with $\widetilde{\kappa} = \{1, -1, -10^4\}$ when $a, b < 0$. The choice of parameters represents robot acting in collaboration with human arm.

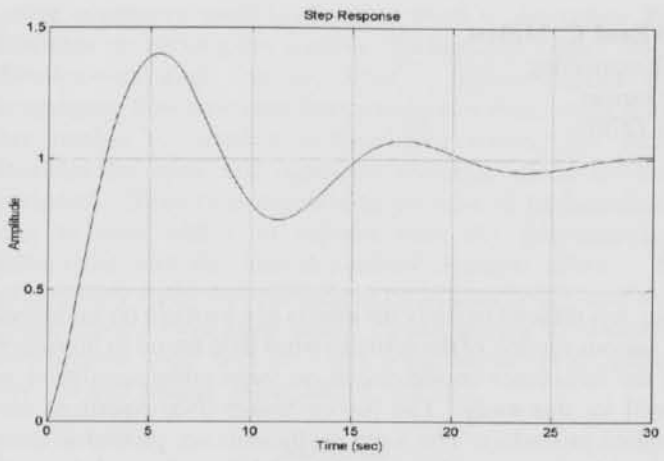

Fig. 5. Closed-loop step response with $\widetilde{\kappa} = \{1, 1, 4\}$ when $\widetilde{A} > 0$. The choice of parameters represents robot manipulator alone.

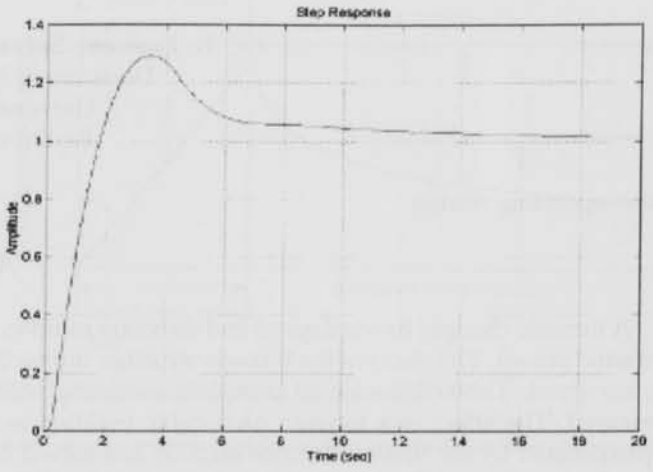

Fig. 6. Closed-loop step response with $\widetilde{\kappa} = \{-1, 1, 0.5\}$ when $k, c < 0$. The choice of parameters represents a possibly unstable sensor response.

Computer Modeling of Tornado Forces on a Cubic Building Using Large Eddy Simulation

R. Panneer Selvam* and **Paul C. Millett**
Department of Civil Engineering
University of Arkansas
Fayetteville, AR 72701

*Corresponding Author

Abstract

A tornado changes its wind speed and direction rapidly; therefore, it is difficult to study the effects of a tornado on buildings in a wind tunnel. The status of the tornado-structure interaction and various models of the tornado wind field found in literature are surveyed. Three dimensional computer modeling work using the turbulence model based on large eddy simulation is presented. The effect of a tornado on a cubic building is considered for this study. The Navier-Stokes (NS) equations are approximated by the finite difference method and solved by an implicit procedure. The force coefficients are plotted in time to study the effect of Rankine combined vortex model. The tornado is made to translate at a 0° and 45° angle, and the grid resolution is refined. Some flow visualizations are also reported to enhance understanding of the flow behavior around the cube.

Introduction

Tornadoes cause millions of dollars in property damage every year in the USA. In order to mitigate this damage, it is necessary to design buildings that are more resistant to tornadoes. The first requirement for accomplishing this goal is a better knowledge of the tornado-structure interaction and tornado-induced loads on buildings. Since the tornado changes its wind speed and direction rapidly, it is difficult to study the effects of a tornado on a building in a wind tunnel. Mehta et al. (1976) calculated tornado forces on buildings from post-storm damage investigations. The maximum wind speed in the tornadic wind was determined from the calculation of equivalent straight-line wind capable of such building failure. A drawback to this procedure is that the force coefficients are considered to be constant in time, whereas in the case of a tornado, the force coefficients change in time, which produces more damage comparatively.

In recent years, computational wind engineering has been developed to such an extent that wind flows around buildings can computed considering the effects of viscosity and turbulence. The results from computation compare reasonably well with experimental results for straight boundary layer (SBL) wind (Selvam, 1992). In this work, the current status of the forces on buildings due to tornadoes is reviewed. Research conducted in the wind tunnel as well as the use of computer models is reported. Different tornado wind field models that can be used for tornado-structure interaction study are surveyed. Some of the recent work conducted in our laboratory investigating the tornado effects on a building is also reported.

The specific objectives of this study are as follows:

- To survey the tornado-structure interaction research up to date.
- To survey tornado-wind field models that can be used in computer models.
- To model the tornado-structure interaction using the large-eddy simulation turbulence model in a three-dimensional environment.
- To visualize the flow around a cube and to report the time dependent force coefficients.

Literature Review.--The amount of research aimed at determining exactly how tornadoes affect buildings has been incredibly meager over the past few decades. Although there have been numerous attempts to heighten this knowledge by a variety of different avenues (theoretical and experimental), a widely agreeable and conclusive solution has not yet been achieved. Because of a tornado's rotational and translational interaction with a building, the wind speed and direction are ever-changing with respect to the building while in the vicinity of the tornado wind field (Selvam and Millett, 2002). As a result, inertial forces are present and perhaps even dominant, unlike in quasi-static wind conditions (Wen and Chu, 1973). Wen, using Kuo's (1971) tornado model, calculated the time-dependant forces on a building using a semi-emperical equation which includes drag and inertia. Dutta et al. (2002) conducted similar theoretical calculations with an actual tornado record and the Finite Element Method. Although this work is useful in determining the dynamic effect, no attention is given to the flow-structure interaction. Much work has been devoted to surveying the resulting structural damage produced by tornadoes (Mehta et al., 1976) in an attempt to

calculate tornado loadings by calculating the straight winds capable of such damage. Studies have been conducted using laboratory models of vortex wind to determine the loadings on rectangular models (Jischke and Light, 1983; Bienkiewicz and Dudhia, 1993). These studies do investigate flow-structure interaction; however, since they are unable to simulate a translating vortex, the wind loadings are static and again the dynamic effects are not included. Numerical simulations promise to be beneficial due to their ability to capture both the flow-structure interaction and the time-dependant dynamic effects. A preliminary study was carried out by Wilson (1977), and on-going reports have been issued by our group: (McDonald and Selvam, 1985; Selvam, 1993, 2002; Selvam et al., 2002; Selvam and Millett, 2002; Millett, 2003).

Methods

Tornado wind field modeling.--The simplest model that can satisfy the Navier-Stokes equations for tornado wind field model is the Rankine-Combined vortex model (RCVM) as reported in Lewellen (1976). In the RCVM, the tangential velocity varies linearly up to radius r_{max}, i.e. $V_\theta = \alpha r$, where r is the radius from the center of tornado and α is a constant (Fig. 1). At radii larger than r_{max}, V_θ varies as $\alpha r^2_{max}/r$. In this computational simulation, a translational velocity, V_t, with respect to the building is superimposed onto the RCVM wind field in addition to a vertical logarithmic variation to account for the boundary layer as reported by Selvam (1993). Considering that the origin of both the x- and y-axis is at the center of the building, and the z axis on the ground, and time, t, is zero when the center of the tornado coincides with center of the building, the velocity components in the x and y directions are expressed as follows:

For any approach angle of tornado translation:

$$\begin{aligned} V_x &= [V_{tx} + (V_{ty}t - y)\alpha]^*Z_f \quad \text{for } r \le r_{max};\\ V_x &= [V_{tx} + (V_{ty}t - y)C]^*Z_f \quad \text{for } r > r_{max}, \text{ and}\\ V_y &= [V_{ty} + (x - V_{tx}t)?]^*Z_f \quad \text{for } r \le r_{max};\\ V_y &= [V_{ty} + (x - V_{tx}t)C]^*Z_f \quad \text{for } r > r_{max} \end{aligned} \qquad (1)$$

where V_{tx} = x-component of Vt; V_{ty} = y-component of Vt; $C = \alpha r^2_{max}/r^2$; $r^2 = (x\text{-}V_t t)^2 + y^2$; $Zf = u^* \ln((z+z0)/z0)/\kappa$.

Here u^* is the frictional velocity, which is determined from the known velocities at the known height, $\kappa = 0.4$, z0 is the roughness length of the ground, and z is the height from the ground. In this work, z0 has been set equal to 0.00375, and Zf is considered to be one at the top of the cube.

Fluid-structure interaction modeling.--Turbulence in fluid flow can be considered in computational fluid dynamics (CFD) by direct simulation (DS), large eddy simulation (LES), and Reynolds averaged equations as surveyed by Selvam (1998). Reynolds averaged equations are applied in many fields of engineering and science. These equations solve for Reynolds averaged stresses using transport equations or simple equations. One form of Reynolds averaged equation is the k-ε model. Selvam (1993) in his earlier work on tornado effects on buildings used this turbulence model. The large eddy simulation turbulence model is based on the filtered Navier-Stokes equations. Direct simulation requires a large number of grid points, and hence it is possible to apply to wind engineering problems for low Reynolds number flow (Selvam and Qu, 2000). The turbulence for this work is modeled using the large eddy simulation. The Navier-Stokes equations using LES used with this CFD simulation program can be obtained by referencing Selvam (1998) and Selvam et al. (2002)

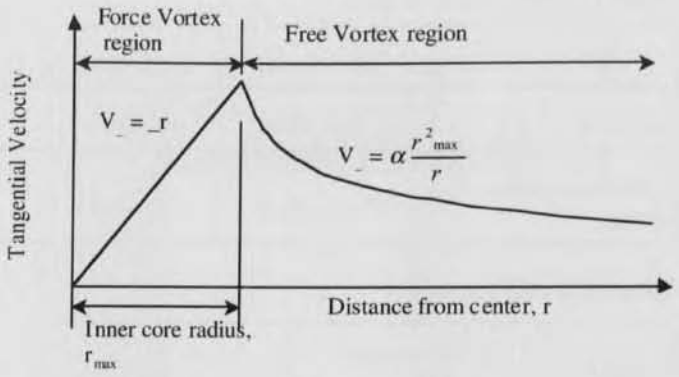

Fig. 1. Tangential Velocity (V_) for RCVM

Problem geometry and boundary conditions.--A plan view of the relative position of the tornado with respect to the building is shown in Figure 2. The tornado translates across in the x-direction. The width of the cube is assumed

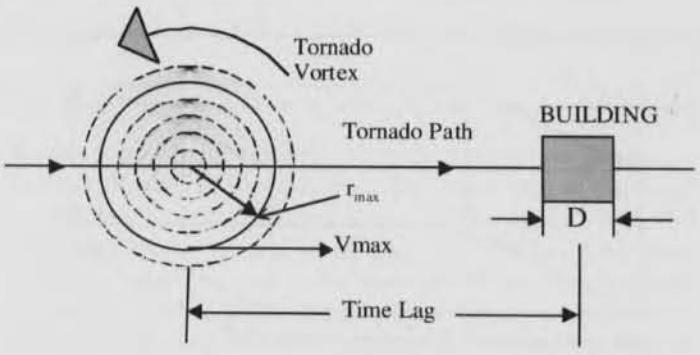

Fig. 2. Schematic of plan view of dynamics of flow field for 3D program.

Table 1. Tornado parameters

	_ (see Fig. 1)	r_{max} (see Fig. 1)	V_1 (trans. vel.)	V (tang. vel.)	$V_{max} = V_1 + V_-$
SI units	1.5 (constant)	*61 meters*	*45.4 mph*	_ * r_{max} = *204 mph*	*250 mph*
Non-Dimensional units	1.5 (constant)	3.0 units	1 unit/sec	4.5 units/sec	5.5 units/sec

Table 2. Grid Properties

GRID	Computational Region	Points on bldg. face	Min. Spacing next to bldg.	Total # of points
A	61 x 61 x 37	10 x 10 x 10	0.0720 H	137,677
B	103 x 103 x 56	20 x 20 x 10	0.0104 H	594,104
C	131 x 131 x 69	30 x 30 x 20	0.0078 H	1,184,109
D	155 x 155 x 69	40 x 40 x 20	0.0055 H	1,657,725

to be 20.3 m. To nondimensionalize the problem, the width of the cube (H), the translational velocity, and the density of air are set at 1 nondimensional (ND) unit. With that assumption, the parameters of the tornado are assigned the values presented in Table 1.

The boundary of the computational domain is located at a reasonable distance away from the cube. The domain has a size of 30 units × 30 units x 10 units as shown in Figure 3. The dimensions of the grids that were generated for this study are presented in Table 2. On the surface of the cube, the velocities are considered to be zero, i.e. no-slip condition. At each time step the interior velocities and pressures are computed by solving the NS equations.

Nomenclature.--The nomenclature used in this study is given below:

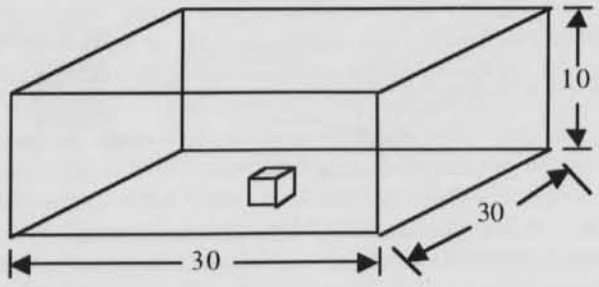

Fig. 3. Isometric view of computational domain.

$$Cx = Fx/[0.5\rho V^2 A] \quad Cy = Fy/[0.5\rho V^2 A]$$
$$Cz = Fz/[0.5\rho V^2 A] \quad Cp = \Delta P/[0.5\rho V^2 A] \qquad (4)$$

Here, Cx, Cy and Cz are the computed force coefficients in the x, y, and z directions, respectively, and Cp is the mean pressure coefficient. F_x, F_y, and F_z are the respective forces in the x, y and z directions, V is the reference velocity, ρ is the density of air, ν is the kinematic viscosity of air, and ΔP is the pressure difference, P – P(ref) [P(ref) is equal to 0.0]. The reference velocity is the maximum velocity in the tornado wind field, which is the equal to $V_\theta + V_t$. The forces are computed by integrating the pressures on the wall in each direction.

Results and Discussion

Tornado-Structure Interaction.--The primary advantage of CFD modeling of the tornado-structure interaction is the capability to investigate the wind characteristics from any angle at any instant in time. Figure 4 below displays the interaction of the tornadic wind (45° approach) and a cubic building (at the 90% of building height) at various instances in time (t = 7 sec, 10 sec, 13 sec) for a time lag of 10 sec. The time lag is the amount of time from beginning of simulation until when the center of the tornado coincides with the center of the building.

Figures 4b,c above illustrate the flow separation near the building due to the multiple sharp corners of the cubic building. The resulting vortex shedding produces highly localized negative pressure regions on the walls of the

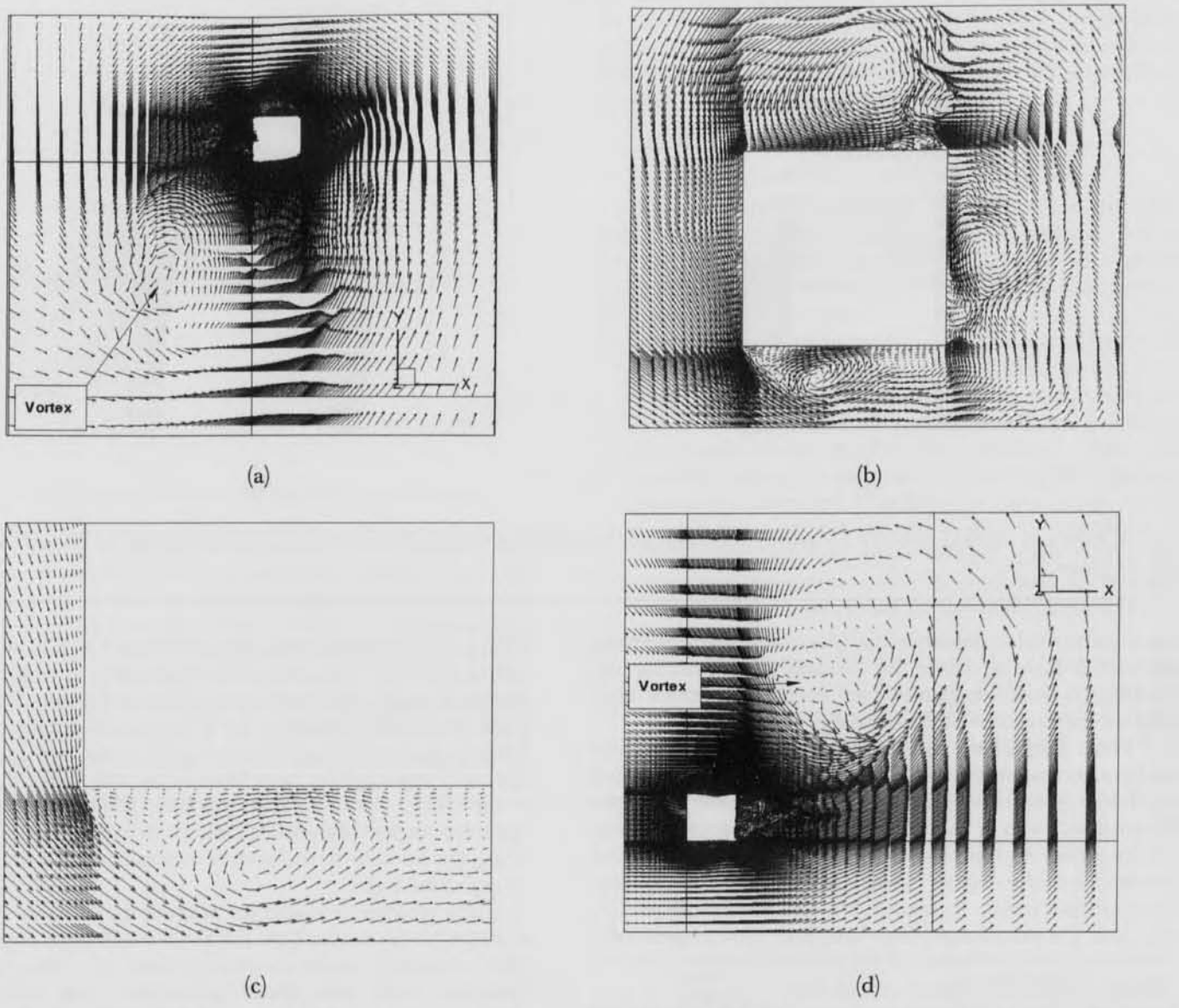

Fig. 4. XY-plane view of tornado velocities (45° approach angle, Grid C, time lag = 10 sec.) at (a) 7 sec.; (b) 10 sec.; (c) 10 sec, close-up of SW corner flow separation; (d) 13 sec.

building (see Fig. 5), which is in agreement with experimental results (Jischke and Light, 1983). Typically the walls of a building, unlike the roof, are not designed to withstand such high suction forces.

The rotational wind created by a tornado produces large suction forces on the roof of a cubic building. When the vortex core is completely surrounding the cubic building, the vertical force coefficient is the highest (see Fig. 7a). The numerical simulations performed in this work may perhaps shed some light on why this occurs. It is shown in Figure 5 that large amounts of vertical wind are produced around all sides of the building. This is a result of the wind converging toward the vertical axis of the vortex. With the building interaction, the wind is converted from horizontal to highly concentrated vertical wind all around the roof corners of the building. As the high-velocity vertical wind flows past the corners of the building, flow separation occurs just above the entire roof surface (as seen by the turbulent wake above the building in Fig. 5a). It has been observed in laboratory simulations (Bienkiewicz and Dudhia, 1993) and

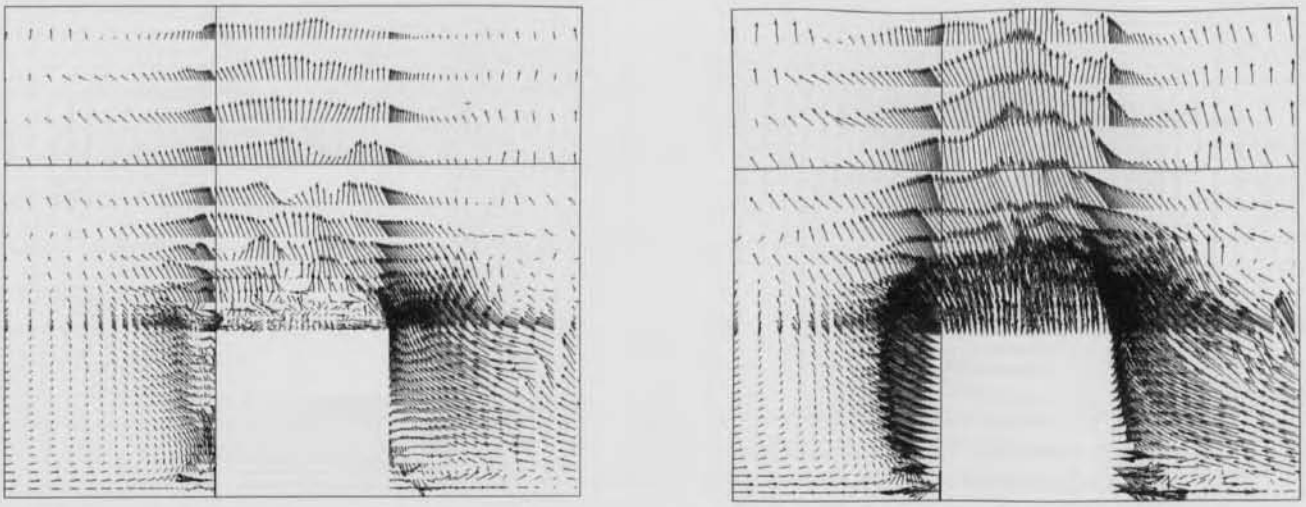

(a) (b)

Fig. 5. Views of vertical velocity for grid C with tornado surrounding building (time = time lag) with (a) the xz-plane, and (b) the yz-plane.

these numerical simulations that the atmospheric pressure above the building while the tornado is surrounding the building is more negative than inside the vortex core without the presence of the building.

Force Coefficients on Building.--The computed force and pressure coefficients, Cx, Cy, Cz, and Cp, are presented in Table 3 for the proposed RCVM model with the dimensions given in Table 1 for a 0° and 45° approach with all the grids. As can be seen in Figure 6, the more refined meshes produce higher force coefficients and pressure coefficients. With a 0° approach angle, the maximum Cx, Cy, and Cz values are 0.82, 1.36, and 1.81, respectively. With a 45° approach angle, the maximum Cx, Cy, and Cz values are 1.33, 1.24, and 1.71, respectively. For the two approach angles, the maximum force coefficients for the walls are similar; however, the 0° approach applies more force to the wall perpendicular to the y-axis, and the 45° approach angle applies more force to the wall perpendicular to the x-axis. The Cz values are fairly similar for the two approach angles with peak values of 1.81 and 1.71 occurring while the tornado is completely surrounding the building (time = time lag).

Table 3. Force and pressure coefficients

GRID	TORN. APPR.	Cx	Cy	Cz	Cp
A	0°	0.65	0.67	1.27	-1.60
B	0°	0.73	1.06	1.67	-1.90
C	0°	0.78	1.26	1.66	-2.20
D	0°	0.82	1.36	1.81	-2.20
A	45°	1.00	0.49	1.23	-1.50
B	45°	1.11	0.77	1.45	-2.40
C	45°	1.33	0.99	1.71	-2.40
D	45°	1.05	1.24	1.68	-2.82
SBL	0°	0.76	0.00	0.87	-1.20
SBL	45°	0.94	0.90	0.89	-2.00

This program was also run without the tornado vortex in order to determine how the force coefficients compare with quasi-static wind conditions (Table 3). The results compare well with those calculated with full-scale measurements, wind tunnels, and CFD. The Cx, Cy, Cz, and Cp values for the 0° angle of approach (aoa) are 0.76, 0.00, 0.87, and -1.20; and for the 45° aoa they are 0.94, 0.90, 0.89, and -2.00. For comparison, the tornado produces 45% higher overall force on a single wall and 100% higher overall suction force on the roof than quasi-static wind. This trend is similar to that reported in Selvam et al. (2002). In addition, a dynamic factor also needs to be included because of the rapid change in the applied direction of the forces (Cx and Cy) during a short period of time (Fig. 7a).

The maximum localized pressure coefficient, Cp, is also found to be higher during the tornado event than in quasi-static wind conditions. During straight wind, the largest local suction pressures occur on the roof behind the windward edge (0° and 45°). For a tornado, large local

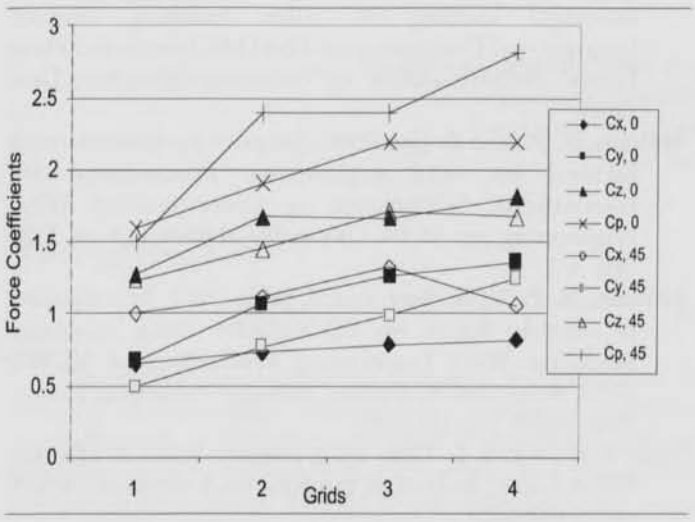

Fig. 6. Convergence of force and pressure coefficients

suction pressures occur in multiple locations (Fig. 7b), behind wall corners and along the entire roof section due to flow separation from the sharp corners. It is observed that only the most refined grids show these local gradients in pressure due to the high concentration of grid points near the building that can capture the vortex formations near the building shown in Figure 4. It is necessary to point out that the Vref used in equation (4) is the maximum velocity in the domain ($V_\theta + V_t$). This velocity is never actually applied to the building because the r_{max} is greater than the building length (see Fig. 2). As a result, the coefficients calculated in this study are perhaps underestimated for an appropriate comparison with straight boundary layer wind.

Conclusions

In this paper, the status of the tornado-structure interaction was presented briefly. A three-dimensional study on tornado-structure interaction is conducted using computational fluid dynamics. The following conclusions are arrived from this work:

1. A translating tornado produces higher overall forces on the walls (45% more) and roof (100% more) of a building than quasi-steady wind. In addition, these forces change magnitude and direction quickly when the tornado core is near the building. Also, the localized suction pressures on the building envelope are greater and generated in multiple locations, unlike those caused by straight wind. For computational simulations, only the most refined grids (with high concentration of points near the building) are needed for a convergence of results for this highly unsteady and turbulent flow.
2. More simulations will be made by changing such variables as size and shape of building (square to various rectangular shapes, low-rise, mid-rise, and high-rise), the number of buildings in the domain, as well as

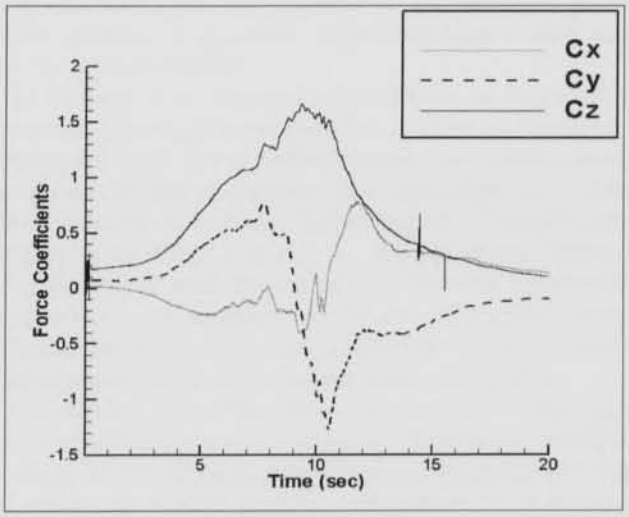

(a)

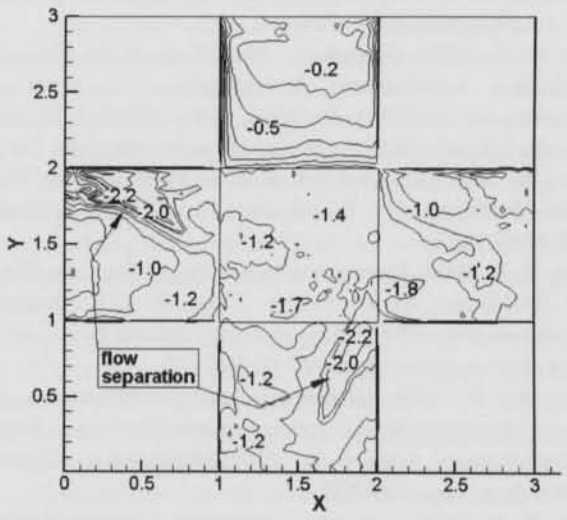

(b)

Fig. 7. (a) Time variation of force coefficients due to RCVM (grid C, approach = 0o); (b) pressure coefficients around cubic building for time = 10 sec (grid C, approach = 0o).

tornado parameters such as translational velocity, core size, and maximum tangential wind speed. The more data collected with these experiments, the closer we will be to determining exactly how any tornado effects any type of building.

Literature Cited

Bienkiewicz, B., and **P. Dudhia.** 1993. Physical modeling of tornado-like vortex and tornado effects on building loading. Seventh U.S. Conf. Wind Eng., UCLA, CA, June 27-30:95-104.

Dutta, P. K., A. K. Ghosh, and **B. L. Agarwal.** 2002. Dynamic response of structures subjected to tornado loads by FEM. J. Wind Eng. Ind. Aerodynamics 90:55-69.

Jischke, M. C., and **B. D. Light.** 1983. Laboratory simulation of tornadic wind loads on a rectangular model structure. J. Wind Eng. Ind. Aerodynamics 13:371-382.

Kuo, H. L. 1971. Axisymmetric Flow in the Boundary Layer of a Maintained Vortex. J. Atmospheric Sci. 28:20-41.

Lewellen, W. S. 1976. Theoretical models of the tornado vortex. Proceedings of the Symposium on Tornadoes, Edited by: R.E. Peterson, Texas Tech University, Lubbock, June 22-24:107-143.

McDonald, J. R., and **R. P. Selvam.** 1985. Tornado forces on building using the boundary element method. Proceedings: Fifth U.S. National Conference on Wind Engineering, Texas Tech University, Lubbock, TX.

Mehta, K. C., J. E. Minor, and **J. R. McDonald.** 1976. Wind Speed Analysis of April 3-4 Tornadoes. J. Struc. Div., ASCE 102:1709-1724.

Millett, P. C. 2003. Computer Modeling of the Tornado-Structure Interaction: Investigation of Structural Loading on a Cubic Building. Unpublished Master's Thesis. University of Arkansas, Fayetteville, AR. 176 pp.

Selvam, R. P. 1992. Computation of Pressures on Texas Tech Building. J. Wind Eng. Ind. Aerodynamics (43):1619-1627.

Selvam, R. P. 1993. Computer Modeling of Tornado Forces on Buildings. Proceedings: The 7th U.S. National Conference on Wind Engineering, Edited by: Gary C. Hart, Los Angeles, June 27-30:605-613.

Selvam, R. P. 1998. Computational procedures in grid based computational bridge aerodynamics. Bridge Aerodynamics, Larsen, A. and Esdahl (eds), Balkema, Rotterdam, pp. 327-336.

Selvam, R. P. 2002. Computer modeling of tornado forces on buildings. Proceedings of the Second International Symposium on Advances in Wind & Structures, C.K. Choi et. al. (Ed.), Techno-Press, Korea, 2002: 105-114.

Selvam R. P., and **P. C. Millett.** 2002. Computer modeling of the tornado-structure interaction: investigation of structural loading on cubic building. Second International Conference on Fluid Mechanics and Fluid Power; Indian Institute of Technology-Roorkee, Dec. 12-14.

Selvam, R. P., and **Z. Qu.** 2000. Adaptive hp-finite element method for wind engineering. Proceedings: 3rd International Symposium on Computational Wind Engineering, pp. 61-64, University of Birmingham, UK, Sep. 4-7.

Selvam, R. P., U. K. Roy, and **Y. Jung.** 2002. Investigation of tornado forces on 2D cylinder using computer modeling. Wind Engineering, Proceedings of NCWE 2002, Edited by: K. Kumar, Phoenix Publishing House, New Delhi, pp. 342-353.

Wen Y. K., and **S. L. Chu.** 1973. Tornado Risks and Design Wind Speed, Journal of the Structural Division, ASCE (99):2409-2421.

Wilson, T. 1977 Tornado Structure Interaction: A Numerical Simulation. Report: UCRL-52207, Distribution Category: UC-11, 80, Lawrence Livermore Laboratory, University of California, Livermore.

Rec12 (Spo11) Recombinase of Fission Yeast Promotes a Backup, Distributive Pathway for Chromosome Segregation in Meiosis I

Wallace D. Sharif, Mari K. Davidson, and **Wayne P. Wahls***
Department of Biochemistry and Molecular Biology
University of Arkansas for Medical Sciences
Little Rock, AR 72205

*Corresponding Author

Abstract

We studied the relationship between recombination and segregation in the fission yeast *Schizosaccharomyces pombe*. In meiosis, chromosomes undergo two rounds of segregation to produce haploid meiotic products. Crossover meiotic recombination (chiasmata) promotes chromosome segregation during meiosis I; achiasmatic chromosomes often suffer nondisjunction in meiosis I. Rec12 protein is a topoisomerase II ortholog that introduces double-strand DNA breaks that initiate recombination. The *rec12* null (deletion) and active site (Y98F) mutants lack recombination and crossovers, and consequently suffer meiosis I nondisjunction. However, null mutants chromosomes segregate to opposite poles more frequently than predicted. Thus, fission yeast has a backup, "distributive segregation" pathway that can function in the absence of Rec12 and Rec12-dependent chiasmata. Interestingly, presence of catalytically-inactive Rec12 protein (Y98F) enhances the fidelity of distributive segregation. We hypothesize that Rec12 protein activates a checkpoint that promotes use of the distributive segregation pathway.

Introduction

Meiosis is a specialized form of cellular differentiation in which a single diploid cell gives rise to four haploid meiotic products. Subsequent post-meiotic differentiation gives rise to haploid cells such as sperm, eggs, pollen, and ascospores. The biological imperative, sex, brings together haploid gametes to generate zygotic diploids which may enter the diploid cell cycle.

In meiosis, homologous chromosomes undergo DNA replication, pair with their partners to form a "bivalent," experience a high rate of recombination, and subsequently undergo two rounds of chromosome segregation to produce haploid meiotic products. Homologous chromosomes segregate from their partners in a reductional division during meiosis I, and during meiosis II sister chromatids segregate from one-another in an equational division similar to mitosis. There is an intimate connection between meiotic recombination and meiotic chromosome segregation.

Crossover recombination (reciprocal exchange) generates physical connections, called "chiasmata," between homologs. These physical connections provide the primary mechanism to ensure proper segregation of homologs during meiosis I (Hawley, 1988). Chiasmata oppose spindle tension during meiosis I and are thought to help orient the paired homologous chromosomes (bivalent) on the metaphase I plate (Hassold and Hunt, 2001). When homologous chromosomes lack chiasmata (crossovers) they often experience nondisjunction and segregate randomly from their partners. Studies of model organisms and humans support the view that chiasmata are important for segregation of chromosomes in meiosis I (Antonarakis et al., 1986; Hawley et al., 1994; Rockmill and Roeder, 1994; Koehler et al., 1996; Hassold and Hunt, 2001; Molnar et al., 2001).

While chiasmatic segregation is widely used to partition chromosomes in meiosis I, there are a few organisms that lack crossovers (chiasmata) on chromosomes. As an alternative strategy, these organisms use achiasmatic or "distributive" mechanisms for chromosome segregation in meiosis I (Grell, 1976; Carpenter, 1991; Dernburg et al., 1996; Koehler and Hassold, 1998). Such distributive segregation systems can partially or almost fully support faithful segregation of chromosomes during meiosis I in the absence of recombination. However, it is not clear whether distributive segregation occurs in organisms that rely upon chiasmatic segregation.

It is difficult to study mutations affecting meiotic chromosome segregation because the probability of obtaining viable meiotic products is inversely proportional to the power of chromosome number. Most products of such meioses are aneuploid (*i.e.*, have the wrong number of chromosomes) and inviable. In fission yeast, however, there are only three pairs of chromosomes. As a consequence, random assortment can produce, at a relatively high frequency, meiotic products that receive at least one copy of each chromosome and are hence viable (Krawchuk et al., 1999). We have taken advantage of this feature of *S. pombe* biology to study the relationship between crossover

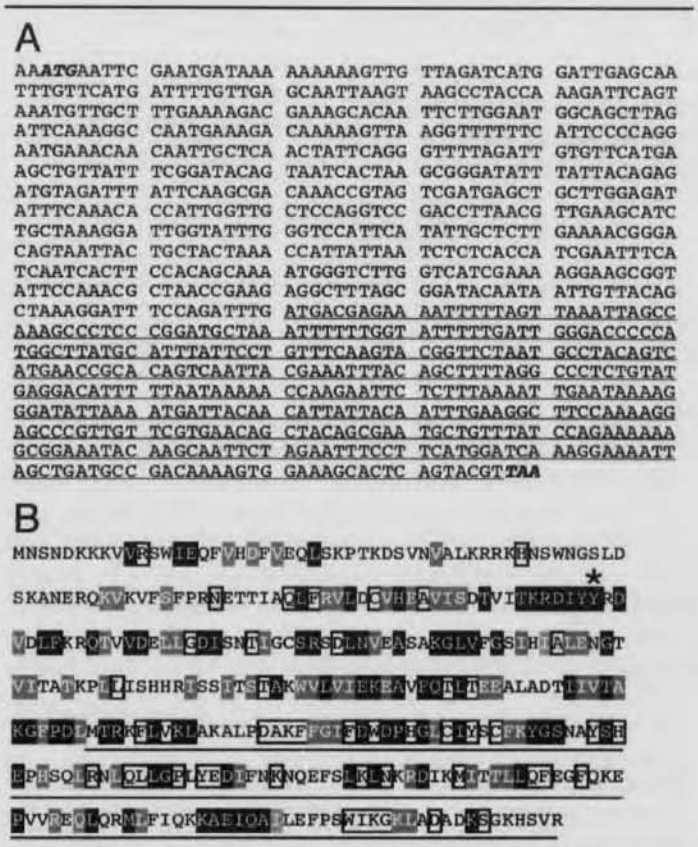

Fig. 1. Revised sequence of rec12+ open reading frame and homology of Rec12 protein to type II topoisomerases. (A) DNA sequence of complementing *rec12*$^{+}$ cDNA clone showing positions of the ATG start codon (italics), TAA stop codon (italics), and region reported previously to encode the Rec12 protein (underlined) (Lin and Smith, 1994). (B) Amino acid sequence of Rec12 protein showing residues that are identical (black boxes), conserved (gray boxes), or conserved in family members other than Rec12 (open boxes). Also shown is the position of the active site tyrosine (*) and the region reported previously to encompass Rec12 (underlined). Alignments evaluated proteins from *S. pombe* (P40384), *Neurospora crassa* (Q9P6Y7), *Coprinus cinereus* (Q9P4D2), *Homo sapiens* (Q9NQM7), *Mus musculus* (Q9QZS1), *Arabidopsis thaliana* (AAL01152), *Drosophila melanogaster* (O77205), *Caenorhabditis elegans* (Q22236), and *Saccharomyces cerevisiae* (P23179).

recombination (chiasmata) and chromosome segregation (Krawchuk et al., 1999; Sharif et al., 2002). We found that Rec12 protein is essential for recombination (chiasmata) and chiasmatic chromosome segregation, and also functions to promote an alternative, backup distributive segregation pathway in the presence of achiasmatic chromosomes.

Materials and Methods

S. pombe culture--Culture media and genetic methods were as described (Gutz et al., 1974; Krawchuk et al., 1999).

Intron mapping and sequence analysis.--Cells harboring the *pat1-114*^{ts} allele were induced to enter meiosis (Wahls and Smith, 1994) and were collected after 3 hours of meiotic induction. Genomic DNA and total RNA were prepared (Kon et al., 1998) and subject to PCR and RT-PCR using primers flanking each putative intron. Full-length *rec12*$^{+}$ cDNA was obtained using RT-PCR using primers designed to amplify the *rec12*$^{+}$ cDNA from the first ATG in exon 1 to a position +142 bp downstream of the stop codon in exon 5. RT-PCR products were cloned by blunt-end ligation into pCR-Blunt (Invitrogen Corp.) and both strands were subject to DNA sequencing (GenBank accession no. AF195027). Conceptual translation of the cDNA open reading frame was used to infer the sequence of Rec12 protein. Protein sequences homologous to that of *S. pombe* Rec12 were identified with a NCBI Blast search (Altschul et al., 1997) using matrix BLOSUM62 and were aligned using T-COFFEE (Notredame et al., 2000). Output was prepared using a 50% threshold for identical and conserved residues.

Construction of *rec12-D13::ura4*$^{+}$ and *rec12-Y98F* alleles. A PCR based gene targeting approach (Bähler et al., 1998) was used to delete the *rec12*$^{+}$ coding region and replace it with the *ura4*$^{+}$ gene (Sharif et al., 2002). Candidates were screened with a combination of PCR analysis, restriction digestion, and DNA sequencing to identify those with successful allele replacement. The *rec12-Y98F* allele was constucted by site-directed mutagenesis of plasmid-born *rec12* (Sharif et al., 2002). Replacement of the endogenous *rec12*$^{+}$ locus with the *rec12-Y98F* allele was achieved by transformation and a pop-in, pop-out approach (Francesconi et al., 1993). Transformation, forward selection, and reverse selection were as described (Grimm et al., 1988; Francesconi et al., 1993). Candidates were screened as described above.

Recombinant frequency determination. Mating, meiosis, and preparation of free spores were as previously (Kon et al., 1997). Intergenic and intragenic recombinant frequencies were determined as described (Kon et al., 1997; Krawchuk et al., 1999). Because diploid spores could contain complementing markers and be mistaken for recombinants, they were excluded from recombinant frequency determinations. Recombinant frequencies from mutltiple inervals spanning approximately 20% of the genome (Sharif et al., 2002) were used to calculate the average number of crossovers per genome per meiosis.

Diploid spore isolation and haploidization analysis. Identification of diploid spore colonies and their haploidization were as described (Krawchuk et al., 1999). Fifty haploidized colonies derived from each diploid spore

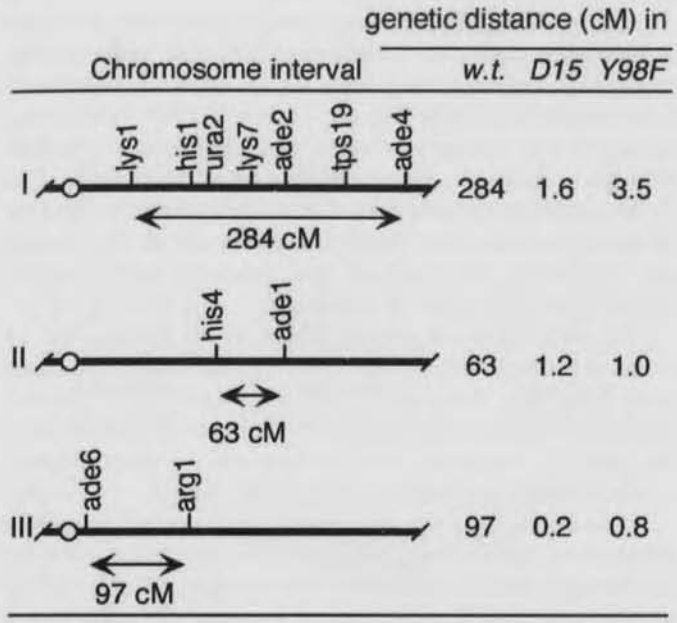

Fig. 2. Effects of Rec12 upon crossover recombination and formation of chiasmata. Intergenic recombinant frequencies were determined in *rec12* mutants (Sharif et al., 2002) and were converted to genetic map distances using the formula of Haldane (Haldane, 1919). These were compared to published map distances in wild-type cells (NCI Entrez Genome) (Munz, 1994). The genetic map distances (*i.e.*, % frequency of crossovers/chiasmata) between the most distal marker pairs are indicated. The average number of crossovers/chiasmata per meiosis (bottom panel) was extrapolated from the average values for all intervals tested (encompassing ~20% of the genome).

colony were replica plated to differentially supplemented minimal media to genotype the *lys1* and *ade6* loci (Sharif et al., 2002). The *tps13* alleles were scored by replica plating colonies onto rich (YEA) media and testing for growth at permissive (22°C) and restrictive (35°C) temperatures (Sharif et al., 2002).

Microscopy. Asci from meiotic cultures were fixed with 70% ethanol at -20°C for at least 15 minutes, washed with H_2O, and stained with 4,6-diamidino-2-phenylindole (DAPI) at a final concentration of 1 µg/ml. Cells were examined by differential interference contrast (DIC) and fluorescence (DAPI) microscopy with a Zeiss axiophot (Carl Zeiss, Thornwood, NY). Images were analyzed using the MetaMorph software package (Universal Imaging, West Chester, PA).

Results

Rec12 is a meiotic ortholog of archaebacterial Topoisomerase VI.--The *rec12-117* mutant of fission yeast exhibits a 6-fold reduction in crossover recombination (De Veaux et al., 1992). The *rec12* mRNA is induced only during meiosis and was reported to encode an orphan protein of 139 amino acids (Lin and Smith, 1994). However, our analysis of the DNA sequence revealed the presence of consensus sequences for splicing and five potential exons, suggesting that *rec12* encodes a larger protein. PCR analysis of genomic DNA and RT-PCR analysis of mRNA from meiotic cells, using primers flanking the putative introns, confirmed the presence of four introns (Sharif et al., 2002).

The confirmed presence of introns suggested that *rec12* encodes a protein larger than originally reported. In order to confirm the intron/exon assignments, we cloned and sequenced a cDNA (Fig. 1A) and introduced it into expression vectors (Maundrell, 1993) in such a way that the first ATG in predicted exon 1 would be used for translation. This construct complemented the recombination defect of *rec12-117* mutants (Sharif et al., 2002), confirming that the cDNA encodes a functional Rec12 protein of 345 amino acids in length. The revised protein sequence shares homology with a family of eukaryotic proteins (Spo11) and belongs to the type-II topoisomerase family (Fig. 1). Rec12/Spo11 is most closely related to the Top6A (catalytic) subunit of archaebacterial topoisomerases, suggesting that Rec12/Spo11 might catalyze meiosis-specific double-strand breaks that initiate recombination.

DNA sequence analysis revealed that the *rec12-117* allele had a single missense mutation in exon 5 (our unpublished observations). We therefore used *in vitro* mutagenesis and gene replacement to construct two new alleles of *rec12* expressed from the endogenous locus (Sharif et al., 2002). The *rec12-D15* (deletion of 1.5 kbp; null) allele removed the entire *rec12* coding region. Tyrosine-98 was of particular interest because it is in the most conserved region of the Rec12 protein and it is in the same position as the active site tyrosine in type-II topoisomerases (Fig. 1B). The *rec12-Y98F* (active site) allele was designed to express full length Rec12 protein in which a single tyrosine at position 98 was replaced with phenylalanine (Fig. 1B).

Rec12 and its active site tyrosine are essential for recombination.--Fission yeast has three pairs of chromosomes. We analyzed the frequency of intergenic recombination for multiple intervals encompassing approximately 20% of the genome to determine the requirements for Rec12 in crossover (chiasmata) formation (Fig. 2). Recombinant frequencies were determined for intervals on all three chromosomes, for intervals close to a centromere, for interstitial intervals, and for distal intervals to determine whether there was any regional and/or

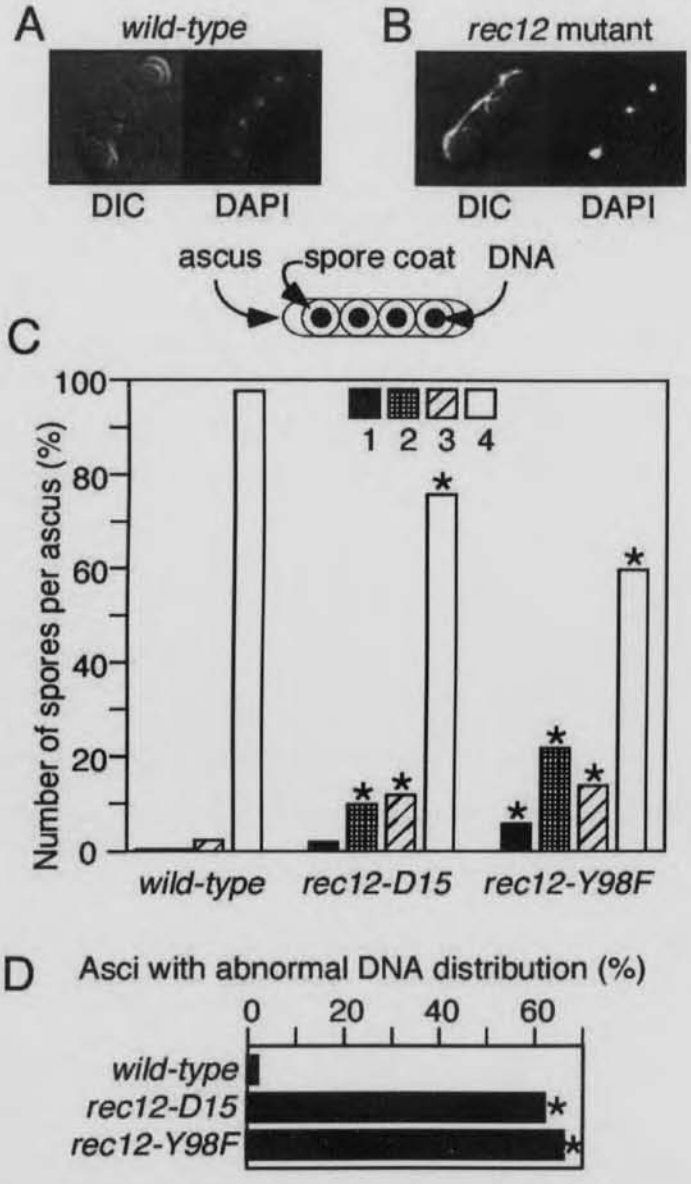

Fig. 3. Cytological phenotypes of *rec12* mutant meioses. Asci from (A) wild-type and (B) *rec12* mutant meiotic cultures were characterized by differential interference contrast (DIC) and DNA fluorescence (DAPI) microscopy (Krawchuk et al., 1999; Sharif et al., 2002). The ascus wall, spore coat, and DNA distribution can be visualized. (C) The number spores per ascus was determined as a measure of the efficiency with which the *rec12* mutants complete meiosis. (D) Frequency of aberrant DNA segregation; asci were scored for aberrant number, intensity, or distribution of DAPI fluorescent signals as in panel B. Data in panels C and D are from analysis of more than 300 asci per genotype and frequency values significantly different from those of wild-type cells (test between two proportions) are indicated (*)

chromosomal specificity (Sharif et al., 2002).

The *rec12-D15* (null) mutants were profoundly deficient in recombination–they exhibited a 256-fold reduction in average recombinant frequency for all intervals, relative to those in wild-type cells (Fig. 2). The *rec12-Y98F* (active site) mutants were similarly affected and exhibited a 263-fold reduction in recombination, relative to wild-type cells (Fig. 2). Recombination was affected in all intervals tested and on all three chromosomes. These data prove that Rec12 protein and its active site tyrosine are essential for crossover recombination (reciprocal exchange).

In each *S. pombe* meiosis there is an average of 44 crossovers distributed on the three chromosomes and those crossovers are distributed without interference (Munz, 1994). A 250-fold reduction in recombination would leave less than 0.1 crossovers per chromosome, so chromosomes in *rec12* mutant meioses are achiasmatic (Fig. 2).

Rec12 and its active site tyrosine are required for meiotic chromosome segregation.–Differential interference contrast microscopy and fluorescence microscopy using a DNA-specific dye (DAPI) were used to examine the phenotypes of asci from wild-type and *rec12* mutant meioses (Sharif et al., 2002). In wild-type cells, meioses produced asci with four well-rounded spores and equivalent DNA content in each spore (Fig. 3A). While the *rec12* mutants lacked chiasmata, they were proficient for meiosis; most cells clearly underwent two meiotic divisions, and the majority of cells formed asci with visible spores (Fig. 3B, 3C). However, gross defects in chromosome segregation and ascus morphology were apparent (Fig. 3D). The heterogeneity of phenotypes suggested that chromosome segregation was random in one or both of the meiotic divisions, as has been described for other mutations affecting meiotic chromosome segregation (Krawchuk et al., 1999). The additional defects in spore formation may be a secondary consequence of chromosome segregation errors, as ascospore formation in *S. pombe* is controlled by the spindle pole body of the meiosis II spindle (Hirata and Shimoda, 1994).

Aberrant chromosome segregation should produce meiotic products that are aneuploid (*i.e.*, have the wrong complement of chromosomes). In *S. pombe*, haploids and diploids are viable, nullisomic aneuploids (missing one or more chromosomes) are inviable, and disomic or polysomic aneuploids (having extra chromosomes) are unstable and rapidly lose the extra chromosome(s) (Niwa and Yanagida, 1985). Since *S. pombe* has only three pairs of chromosomes random assortment can, by chance, result in a relatively high frequency of meiotic products that receive at least one copy of each chromosome and hence are viable (Krawchuk et al., 1999). Similarly, some meiotic products might receive, by chance, at least two copies of each chromosome and thus produce viable diploids. We therefore determined the frequency of spore viability and of meiotic diploidy as

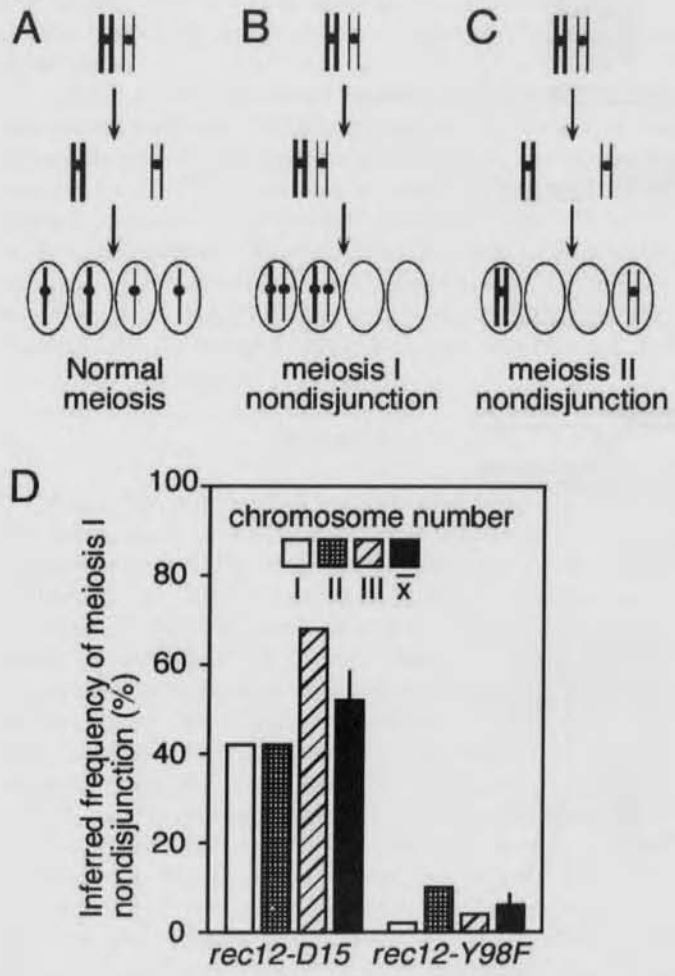

Fig. 4. Segregation patterns of chromosomes. (A) In a normal meiosis two rounds of chromosome segregation produce haploid meiotic products (B) Meiosis I nondisjunction produces disomic (or diploid) meiotic products that are heterozygous for centromere-linked markers. (C) Meiosis II nondisjunction produces disomic (or diploid) meiotic products that are homozygous for centromere-linked markers. (D) Frequency of meiosis I nondisjunction in *rec12* mutants. Diploid spore colonies were genotyped for heteroallelic, centromere-linked markers on each of the three chromosomes (Krawchuk et al., 1999; Sharif et al., 2002). The frequency of meiosis I nondisjunction was inferred from the frequency of diploid meiotic products heterozygous for centromere-linked markers (Sharif et al., 2002).

genetic measures of chromosome segregation errors (Krawchuk et al., 1999).

Most (97 ± 21%) of the spores from wild-type meioses were viable. Less than half (41 ± 5%) of the spores from *rec12-D15* (null) meioses were viable, suggesting that 59% of the products failed to receive at least one copy of each chromosome (*i.e.*, were nullisomic). This value is very close to the expected frequency of nullisomics (58%) if segregation were entirely random in one of the two meiotic divisions. Interestingly, spore viability was significantly lower (20 ± 6%) from crosses of the *rec12-Y98F* mutants than from *rec12-D15* mutant crosses, suggesting that *rec12-Y98F* may encode a separation-of-function mutation (see below).

Very few (0.3 ± 0.1%) of the spores from wild-type meioses were diploid. As predicted, the *rec12-D15* (null) and *rec12-Y98F* (active site) mutants produced an elevated frequency of diploid meiotic products (9 ± 4% and 12 ± 1%, respectively) (Sharif et al., 2002). The spore viability data, spore diploidy data, and cytological data (Fig. 3) demonstrate that chromosomes segregate aberrantly in the absence of Rec12 protein and its active site tyrosine. Importantly, the recovery of viable diploid meiotic products from *rec12* mutant meioses permitted us to infer the meiotic division in which chromosomes segregated aberrantly.

Loss of Rec12 protein causes meiosis I nondisjunction and reveals presence of a backup, distributive segregation pathway.– Meiotic diploids derived from nondisjunction of chromosomes during meiosis I should contain chromosomes that are heterozygous for centromere-linked markers (Fig. 4B). Precocious separation of sister chromatids during meiosis I would also produce diploids that are predominantly heterozygous for centromere-linked markers (not shown). Meiotic diploids that result from mis-segregation during meiosis II should contain chromosomes that are homozygous for centromere-linked markers (Fig. 4C). Since fluorescence *in situ* hybridization revealed no defects in sister chromatid cohesion in *rec12* mutants (Nabeshima et al., 2001), one can use the frequency of heterozygous diploids as a direct measure of the frequency of meiosis I nondisjunction.

Individual diploid spore colonies were haploidized, and fifty individual haploid derivatives from each diploid spore colony were scored for heteroallelic, centromere-linked markers on each of the three chromosomes (Sharif et al., 2002). Approximately 50% of the diploid spore colonies from *rec12-D15* mutant meioses were heterozygous for centromere-linked markers on each of the three chromosomes (Fig. 4D), demonstrating that these diploids arose as a consequence of meiosis I nondisjunction. However, this frequency of meiosis I nondisjunction is only half that expected for achiasmatic chromosomes. Distributive segregation occurs when achiasmatic chromosomes segregate away from their homologous partners (during meiosis I) at a frequency that is higher than the frequency of random assortment. The lower-than-expected frequency of nondisjunction in meiosis I in the *rec12-D15* mutants suggests that *S. pombe* has a backup,

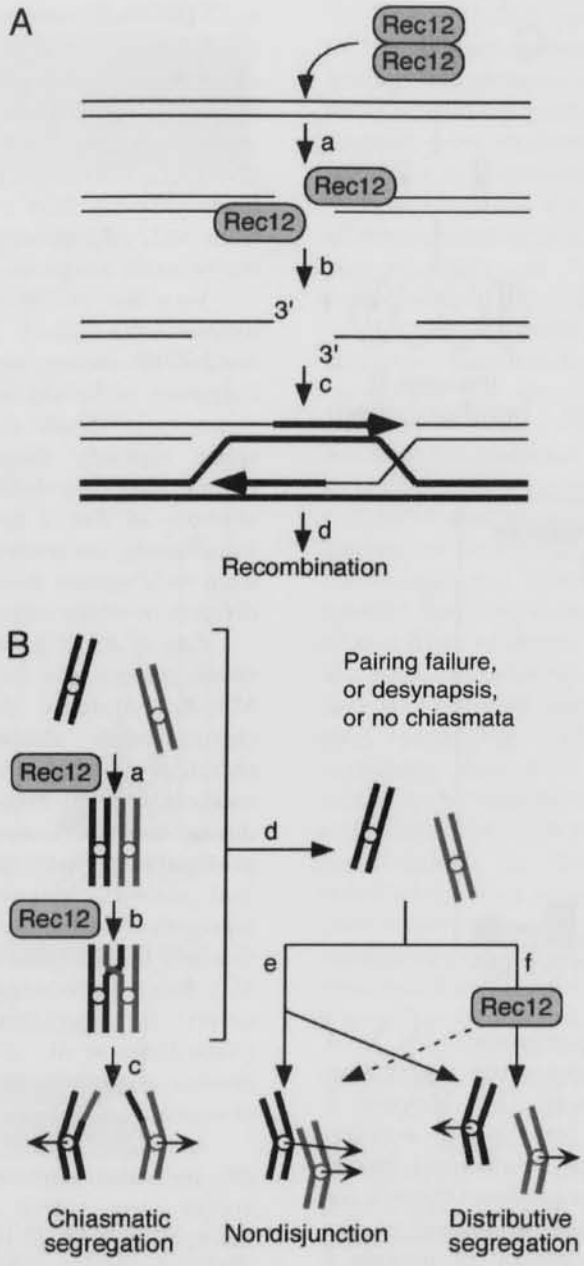

Fig. 5. Models for multiple functions of Rec12 in meiotic chromosome dynamics. (A) Initiation of recombination: Wild-type Rec12 protein is the catalytic subunit of a recombinase holoenzyme that introduces recombinogenic double-strand DNA breaks (*a*). Those breaks are processed to generate 3' single-stranded DNA tails (*b*) that can invade a homologous chromosome and prime DNA synthesis (*c*). Subsequent processing (*d*) produces recombinant products with or without reciprocal exchange (crossing over) of flanking markers, as originally proposed (Szostak et al., 1983). Reciprocal exchanges produce chiasmata which help hold paired homologs together. (B) Chiasmatic and distributive segregation: Rec12 protein may promote interhomolog pairing interactions (*a*) (Cha et al., 2000; Romanienko and Camerini-Otero, 2000). Wild-type Rec12 protein is essential to initiate recombination and crossover formation (*b*), which are in turn essential for chiasmatic segregation during meiosis I (*c*). Various defects can lead to achiasmatic chromosomes (d). In the absence of Rec12, achiasmatic chromosomes experience both meiosis I nondisjunction and distributive segregation (*e*). However, when achiasmatic chromosomes are present, catalytically-inactive Rec12 (and presumably also wild-type Rec12) promotes function of the backup, distributive segregation pathway (*f*).

distributive (achiasmatic) pathway of chromosome segregation that can function in the absence of Rec12 protein and Rec12-dependent crossover recombination (chiasmata).

Rec12 protein promotes function of the distributive segregation pathway.--While meioses lacking Rec12 protein frequently suffered meiosis I nondisjunction, the active site mutants (*rec12-Y98F*) produced meiotic diploids with nearly normal meiosis I segregation patterns (Fig. 4D). This difference is not related to crossover frequency, because the two mutants exhibit identical deficiencies in meiotic recombination (Fig. 2). Thus, the presence of catalytically-inactive Rec12 protein promotes the function of the distributive segregation pathway.

Discussion

The *rec12* gene has five exons and encodes a protein of 345 amino acids in length that shares homology with type-II topoisomerases (Fig. 1) (Keeney, 2001; Sharif et al., 2002). In eukaryotes, topoisomerase-II enzymes function as a homodimer that introduces a double-strand DNA break, passes a second DNA strand through the break, and religates the broken ends. A catalytic domain introduces the breaks, and an ATPase domain is required for conformational changes involved in strand passage and religation (Fortune and Osheroff, 2000). In prokaryotes, type-II topoisomerases function as a heterotetramer in which the catalytic and ATPase functions are in separate polypeptides. Rec12/Spo11 shares the highest homology with the Top6A subunit of archaebacterial enzymes (Fig. 1) (Keeney, 2001; Sharif et al., 2002). However, there is no obvious homolog for Top6B in most eukaryotes, including fission yeast. This makes sense in terms of models for meiotic recombination (Szostak et al., 1983) because initiation of recombination does not require DNA strand passage and religation activities like those carried out by canonical type-II topoisomerases (Fig. 5A).

Meiotically-induced double-strand DNA breaks have been demonstrated in budding yeast and in fission yeast (Sun et al., 1989; Cao et al., 1990; Zenvirth and Simchen, 2000). Rec12/Spo11 enzyme almost certainly catalyzes these breaks: First, it shares homology with topoisomerases (Fig. 1). Second, Rec12 and its active site tyrosine are essential for recombination (Fig. 2) (Sharif et al., 2002). Third, Rec12/Spo11 becomes covalently linked by a phosphotyrosine linkage to the 5' end of the meiotic double-strand DNA breaks ((De Massy et al., 1994; Keeney and Kleckner, 1995; Liu et al., 1995); our unpublished observations). Proteins homologous to Rec12 (Spo11) are found in a wide range of eukaryotes and available evidence suggests that the initiation of meiotic recombination by Rec12/Spo11-dependent double-strand DNA breaks is conserved (Dernburg et al., 1998; McKim and Hayashi-Hagihara, 1998; Baudat et al., 2000; Romanienko and Camerini-Otero, 2000). Double-strand DNA breaks initiate repair synthesis from the homologous chromosome, leading to recombination intermediates that can be resolved with or without reciprocal exchange of flanking markers (crossing over) (Fig. 5A).

Because *rec12-D15* (null) and *rec12-Y98F* (active site) mutants lack recombination (Fig. 2), their chromosomes are achiasmatic and would be expected to suffer nondisjunction during meiosis I. Indeed, the *rec12-D15* (null) mutants fail to properly segregate their chromosomes (Fig. 3), and they exhibit significant levels of meiosis I nondisjunction (Fig. 4D). However, the frequency of meiosis I nondisjunction observed is only half of that expected–in half of the instances in which homologs should suffer nondisjunction, they end up segregating to opposite poles (Fig. 4D). We conclude that fission yeast has a distributive (achiasmatic) chromosome segregation system. This distributive system partially circumvents the meiosis I segregation errors of achiasmatic chromosomes and can function in the complete absence of Rec12 protein and Rec12-dependent crossovers (chiasmata).

Distributive segregation has been reported in organisms with naturally-occurring achiasmatic chromosomes and in a few other experimental circumstances (Carpenter, 1973; Dawson et al., 1986; Hawley et al., 1992; Hawley and Theurkauf, 1993; Hawley, 1996; Molnar et al., 2001). Our results indicate that a pathway for distributive segregation exists (and is fairly robust) in an organism that normally uses chiasmatic segregation. While Rec12 protein and Rec12-dependent crossovers (chiasmata) are not required for distributive segregation, catalytically-inactive Rec12 markedly increases the fidelity of distributive segregation (Fig. 4D) (Sharif et al., 2002). Presumably wild-type Rec12 protein can do so as well, although this has not been demonstrated directly. Thus, Rec12 has two key roles in meiotic chromosome segregation. It generates chiasmata to promote chiasmatic segregation, and when things go awry, it promotes distributive segregation of achiasmatic chromosomes (Fig. 5B).

There are two non-mutually exclusive hypotheses regarding how Rec12 promotes distributive segregation. First, Rec12/Spo11 may have a structural function for meiotic interhomolog interactions prior to and after initiation of recombination (Romanienko and Camerini-Otero, 2000). For example, Rec12 may help hold bivalents together in the absence of crossovers. This would be akin to the role of heterochromatin in distributive segregation in *Drosophila* (Carpenter, 1973; Carpenter, 1991; Hawley and Theurkauf, 1993). Second, Spo11/Rec12 may activate a "meiosis I nondisjunction/distributive segregation" checkpoint that provides time for the backup, distributive

segregation pathway to be established. For example, Rec12 and other components of the recombinase complex are in the right place at the right time to sense whether or not crossovers (chiasmata) are successfully generated. Rec12-dependent signal transduction (*e.g.*, checkpoint activation) would provide a parsimonious way to promote the backup, distributive segregation pathway in the presence of achiasmatic chromosomes.

ACKNOWLEDGMENTS.—Work in our laboratory is supported by funds from the National Institutes of Health (NIGMS) and the Human Frontier Science Program. WDS was supported in part by a UNCF-Merck Graduate Science Research Dissertation Fellowship Award.

Literature Cited

Altschul, S. F., T. L. Madden, A. A. Schaffer, J. Zhang, Z. Zhang, W. Miller, and **D. J. Lipman.** 1997. Gapped BLAST and PSI-BLAST: a new generation of protein database search programs. Nucleic Acids Res. 25:3389-3402.

Antonarakis, S. E., A. Chakravarti, A. C. Warren, S. A. Slaugenhaupt, C. Wong, S. L. Halloran, and **C. Metaxotou.** 1986. Reduced recombination rate on chromosomes 21 that have undergone nondisjunction. Cold Spring Harbor Symp. Quant. Biol. 1:185-190.

Bähler, J., J.-Q. Wu, M. S. Longtine, N. G. Shah, A. McKenzie III, A. B. Steever, A. Wach, P. Philippsen, and **J. R. Pringle.** 1998. Heterologous modules for efficient and versatile PCR-based gene targeting in *Schizosaccharomyces pombe.* Yeast 14:943-951.

Baudat, F., K. Manova, J. P. Yuen, M. Jasin, and **S. Keeney.** 2000. Chromosome synapsis defects and sexually dimorphic meiotic progression in mice lacking Spo11. Mol. Cell 6:989-998.

Cao, L., E. Alani, and **N. Kleckner.** 1990. A pathway for generation and processing of double-strand breaks during meiotic recombination in *S. cerevisiae.* Cell 61:1089-1101.

Carpenter, A. T. 1973. A meiotic mutant defective in distributive disjunction in *Drosophila* melanogaster. Genetics 73:393-428.

Carpenter, A. T. 1991. Distributive segregation: motors in the polar wind? Cell 64:885-890.

Cha, R. S., B. M. Weiner, S. Keeney, J. Dekker, and **N. Kleckner.** 2000. Progression of meiotic DNA replication is modulated by interchromosomal interaction proteins, negatively by Spo11p and positively by Rec8p. Genes Dev. 14:493-503.

Dawson, D. S., A. W. Murray, and **J. W. Szostak.** 1986. An alternative pathway for meiotic chromosome segregation in yeast. Science 234:713-717.

De Massy, B., F. Baudat, and **A. Nicolas.** 1994. Initiation of recombination in *Saccharomyces cerevisiae* haploid meiosis. Proc. Natl. Acad. Sci. U.S.A. 91:11929-11933.

De Veaux, L. C., N. A. Hoagland, and **G. R. Smith.** 1992. Seventeen complementation groups of mutations decreasing meiotic recombination in *Schizosaccharomyces pombe.* Genetics 130:251-262.

Dernburg, A. F., K. McDonald, G. Moulder, R. Barstead, M. Dresser, and **A. M. Villeneuve.** 1998. Meiotic recombination in *C. elegans* initiates by a conserved mechanism and is dispensable for homologous chromosome synapsis. Cell 94:387-398.

Dernburg, A. F., J. W. Sedat, and **R. S. Hawley.** 1996. Direct evidence of a role for heterochromatin in meiotic chromosome segregation. Cell 86:135-146.

Fortune, J. M., and **N. Osheroff.** 2000. Topoisomerase II as a target for anticancer drugs: when enzymes stop being nice. Prog. Nucleic Acid Res. Mol. Biol. 64:221-253.

Francesconi, S., H. Park, and **T. S. Wang.** 1993. Fission yeast with DNA polymerase delta temperature-sensitive alleles exhibits cell division cycle phenotype. Nucleic Acids Res. 21:3821-3828.

Grell, R. 1976. Distributive pairing. Pp. 435-486, *In* The Genetics and Biology of *Drosophila* (M. Ashburner and E. Novitski, ed.) Academic Press, New York.

Grimm, C., J. Kohli, J. Murray, and **K. Maundrell.** 1988. Genetic engineering of *Schizosaccharomyces pombe*: a system for gene disruption and replacement using the *ura4* gene as a selectable marker. Mol. Gen. Genet. 215:81-86.

Gutz, H., H. Heslot, U. Leupold, and **N. Loprieno.** 1974. *Schizosaccharomyces pombe.* Pp. 395-446, *In* Handbook of Genetics (R. C. King, ed.) Plenum Press, New York.

Haldane, J. B. S. 1919. The combination of linkage values, and the calculation of distances between loci of linked factors. J. Genet. 8:299-309.

Hassold, T., and **P. Hunt.** 2001. To err (meiotically) is human: the genesis of human aneuploidy. Nat. Rev. Genet. 2:280-291.

Hawley, R. S. 1988. Exchange and chromosomal segregation in eukaryotes. Pp. 497-527, *In* Genetic Recombination (R. Kucherlapati and G. R. Smith, ed.) American Society for Microbiology, Washington, D.C.

Hawley, R. S. 1996. Direct efidence of a role for heterochromatin in meiotic chromosome segregation. Cell 86:135-146.

Hawley, R. S., J. A. Frazier, and **R. Rasooly.** 1994. Separation anxiety: the etiology of nondisjunction in flies and people. Human Mol. Genet. 3:1521-1528.

Hawley, R. S., H. Irick, A. E. Zitron, D. A. Haddox, A. Lohe, C. New, M. D. Whitley, T. Arbel, J. Jang, K. McKim, and **R. S. Hawley.** 1992. There are two mechanisms of achiasmate segregation in *Drosophila* females, one of which requires heterochromatic

homology. Dev. Genet. 13:440-467.

Hawley, R. S., and **W. E. Theurkauf.** 1993. Requiem for distributive segregation: achiasmate segregation in *Drosophila* females. Trends Genet. 9:310-317.

Hirata, A., and **C. Shimoda.** 1994. Structural modification of spindle pole bodies during meiosis II is essential for normal formation of ascospores in *Schizosaccharomyces pombe*: ultrastructural analysis of *spo* mutants. Yeast 10:173-183.

Keeney, S. 2001. Mechanism and control of meiotic recombination initiation. Curr. Top. Dev. Biol. 52:1-53.

Keeney, S., and **N. Kleckner.** 1995. Covalent protein-DNA complexes at the 5' strand termini of meiosis-specific double-strand breaks in yeast. Proc. Natl. Acad. Sci. U.S.A. 92:11274-11278.

Koehler, K. E., and **T. J. Hassold.** 1998. Human aneuploidy: lessons from achiasmate segregation in *Drosophila melanogaster*. Ann. Hum. Genet. 62:467-479.

Koehler, K. E., R. S. Hawley, S. Sherman, and **T. Hassold.** 1996. Recombination and nondisjunction in humans and flies. Hum. Mol. Genet. 5:1495-1504.

Kon, N., M. D. Krawchuk, B. G. Warren, G. R. Smith, and **W. P. Wahls.** 1997. Transcription factor Mts1/Mts2 (Atf1/Pcr1, Gad7/Pcr1) activates the *M26* meiotic recombination hotspot in *S. pombe*. Proc. Natl. Acad. Sci. U.S.A. 94:13765-13770.

Kon, N., S. C. Schroeder, M. D. Krawchuk, and **W. P. Wahls.** 1998. Regulation of the Mts1-Mts2-dependent *ade6-M26* meiotic recombination hotspot and developmental decisions by the Spc1 mitogen-activated protein kinase of fission yeast. Mol. Cell. Biol. 18:7575-7583.

Krawchuk, M. D., L. C. DeVeaux, and **W. P. Wahls.** 1999. Meiotic chromosome dynamics dependent upon the *rec8*$^+$, *rec10*$^+$, and *rec11*$^+$ genes of the fission yeast *Schizosaccharomyces pombe*. Genetics 153:57-68.

Lin, Y., and **G. R. Smith.** 1994. Transient, meiosis-induced expression of the *rec6* and *rec12* genes of *Schizosaccharomyces pombe*. Genetics 136:769-779.

Liu, J., T. C. Wu, and **M. Lichten.** 1995. The location and structure of double-strand DNA breaks induced during yeast meiosis: evidence for a covalently linked DNA-protein intermediate. EMBO J. 14:4599-4608.

Maundrell, K. 1993. Thiamine-repressible expression vectors pREP and pRIP for fission yeast. Gene 123:127-130.

McKim, K. S., and **A. Hayashi-Hagihara.** 1998. *mei-W68* in *Drosophila melanogaster* encodes a Spo11 homolog: evidence that the mechanism for initiating meiotic recombination is conserved. Genes Dev. 12:2932-2942.

Molnar, M., J. Bahler, J. Kohli, and **Y. Hiraoka.** 2001. Live observation of fission yeast meiosis in recombination-deficient mutants: a study on achiasmate chromosome segregation. J. Cell Sci. 114:2843-2853.

Munz, P. 1994. An analysis of interference in the fission yeast *Schizosaccharomyces pombe*. Genetics 137:701-707.

Nabeshima, K., Y. Kakihara, Y. Hiraoka, and **H. Nojima.** 2001. A novel meiosis-specific protein of fission yeast, Meu13p, promotes homologous pairing independently of homologous recombination. EMBO J. 20:3871-3881.

Niwa, O., and **M. Yanagida.** 1985. Triploid meiosis and aneuoploidy in *Schizosaccharomyces pombe*: an unstable aneuploid disomic for chromosome *III*. Curr. Genet. 9:463-470.

Notredame, C., D. G. Higgins, and **J. Heringa.** 2000. T-Coffee: A novel method for fast and accurate multiple sequence alignment. J. Mol. Biol. 302:205-217.

Rockmill, B., and **G. S. Roeder.** 1994. The yeast *med1* mutant undergoes both meiotic homolog nondisjunction and precocious separation of sister chromatids. Genetics 136:65-74.

Romanienko, P. J., and **R. D. Camerini-Otero.** 2000. The mouse *Spo11* gene is required for meiotic chromosome synapsis. Mol. Cell 6:975-987.

Sharif, W. D., G. G. Glick, M. K. Davidson, and **W. P. Wahls.** 2002. Distinct functions of *S. pombe* Rec12 (Spo11) protein and Rec12-dependent crossover recombination (chiasmata) in meiosis I; and a requirement for Rec12 in meiosis II. Cell Chromosome 1:1-14.

Sun, H., D. Treco, N. P. Schultes, and **J. W. Szostak.** 1989. Double-strand breaks at an initiation site for meiotic gene conversion. Nature 338:87-90.

Szostak, J. W., T. L. Orr-Weaver, R. J. Rothstein, and **F. W. Stahl.** 1983. The double-strand-break repair model for recombination. Cell 33:25-35.

Wahls, W. P., and **G. R. Smith.** 1994. A heteromeric protein that binds to a meiotic homologous recombination hot spot: correlation of binding and hot spot activity. Genes Dev. 8:1693-1702.

Zenvirth, D., and **G. Simchen.** 2000. Meiotic double-strand breaks in *Schizosaccharomyces pombe*. Curr. Genet. 38:33-38.

Interpolation Techniques for Overset Grids

Paul S. Sherman* and **Nathan B. Edgar**
Arkansas State University
College of Engineering
P.O. Box 1740
State University, AR 72467

*Corresponding Author

Abstract

The use of finite difference schemes in computational aeroacoustics requires the use of structured grids in computational space. Complex geometries in the physical space can be modeled using multiple overlapping grids that are transformed into computational space. In this work, finite difference schemes are used that necessitate the addition of psuedo- or ghost-points in the overlap region of the grids for closure of the difference stencil. The functional values at these ghost points must be approximated from the values at the original grid points. This paper investigates interpolation techniques for these overset grids. An n^{th} order interpolation scheme using Lagrange polynomials is applied to the one dimensional (1D) wave propagation problem to test the effects of increasing the interpolation order. This is done for both equal and unequal sized overset grids. Preliminary results from two dimensional (2D) grids will be presented.

Introduction

In computational aeroacoustics, finite difference schemes are more commonly used because they are more computationally efficient than the finite element schemes. Finite difference schemes require the use of structured grids in computational space. An unstructured grid in the physical space can be transformed (Tannehill et al., 1997) into a structured grid in the computational space. However, complex geometries in the physical space may require multiple overlapping grids. In this paper, we discuss the construction of overset grids, problems associated with their construction, 1D and 2D results which show some of the problems arising from the application of the grids, and some solutions implemented to address these problems.

For this work, we chose to model the 1D and 2D wave equations using a single pair of overlapping structured grids. In general, overlapping grids can have mismatched grid spacing (Petersson, 1999) in each direction and may not share a common point. An example of the overlap regions for 1D and 2D grids is provided in Fig. 1. The layout of multiple grids in the physical space will be dictated by the geometry to be modeled.

Overlapping regions will exist wherever multiple grids share a common boundary. Two problems/difficulties must be dealt with in the overlap region. These are closure at the overlap region and the interpolation of overlapping grid points.

Additional pseudo- or ghost-points are necessary in the overlap region of the grids in order to provide for closure of the difference stencil. Only the function values are needed at these points for the finite difference schemes to compute the derivatives within the grids. For the schemes used in this work, three ghost-points are necessary for closure. The function values for the ghost-points are determined from the function values of the grid points in the other grid.

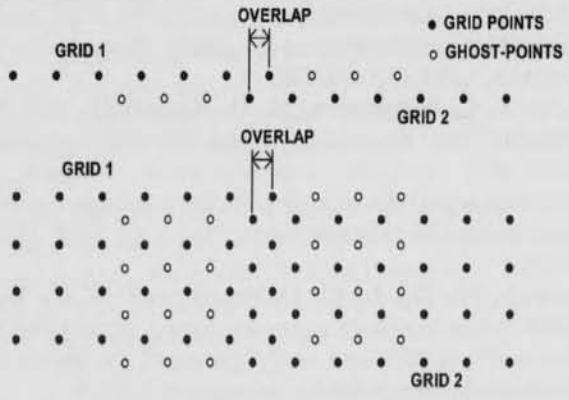

Fig. 1. Example of the overlap regions for 1D and 2D grids.

The values for the ghost-points are determined by an interpolation scheme. Although there are a variety of interpolation schemes available, we chose to use a Lagrange polynomial interpolation technique. Benefits of this technique are ease of programming, computational efficiency, and the fact that the interpolation order can be easily altered and compared.

Methods

There are three classes of numerical methods used in

this work. The first deals with the approximation of a derivative. The second deals with interpolating a functionís value with *n* known values. The third is a digital filter to remove high frequency waves.

Finite Difference Schemes.--A numerical solution to a first order partial differential equation requires the approximation of the first derivative based on the function values. A compact finite difference scheme (Lele, 1992) for a uniformly spaced grid is used which can be written in the form

$$\beta f'_{i-2} + \alpha f'_{i-1} + f'_i + \alpha f'_{i+1} + \beta f'_{i+2} = c\frac{f_{i+3} - f_{i-3}}{6\Delta x} + b\frac{f_{i+2} - f_{i-2}}{4\Delta x} + a\frac{f_{i+1} - f_{i-1}}{2\Delta x} \quad (1)$$

where f_i is the value of the function at x_i

f'_i is the derivative of f with respect to x at x_i

Δx spacing between x_i and x_{i+1}

$\alpha, \beta, a, b,$ and c are constant coefficients to be determined.

Formal truncation errors up to 10th order can be obtained by an appropriate selection of the coefficients a, b, c, α, and β. The general case having non-periodic boundary conditions requires two additional relations appropriate for the near boundary nodes. These can be obtained by setting α and/or β equal to zero and by selecting appropriate values for the coefficients a, b, and c. The full set of equations will need the function values at three ghost-points beyond the boundary of the grid.

A 10th order penta-diagonal scheme is used for the interior grid points with the following coefficients:

$$\alpha = \frac{1}{2}, \quad \beta = \frac{1}{20}, \quad a = \frac{17}{12}, \quad b = \frac{101}{150}, \quad c = \frac{1}{100}. \quad (2)$$

One of the near boundary relations is an 8th order tri-diagonal scheme with the following coefficients:

$$\alpha = \frac{3}{8}, \quad \beta = 0, \quad a = \frac{25}{16}, \quad b = \frac{1}{5}, \quad c = \frac{-1}{80}. \quad (3)$$

A dispersion-relation-preserving (DRP) scheme (Tam and Webb, 1993) with a 7-point stencil was chosen for the remaining near boundary relation. It has the following coefficients:

$$\alpha = \beta = 0, \quad \frac{a}{2} = 0.770882380518, \quad \frac{b}{4} = -0.166705904415, \quad \frac{c}{6} = 0.0208431427703. \quad (4)$$

Interpolation.--The function values at the ghost-points can be approximated using Lagrange polynomials (Hoffman, 1992) allowing the function value to be computed as a linear combination of neighboring grid points. The weighting factors are a function only of the positions of the grid points and not the function values at the grid points. Thus, the weighting factors only need to be computed once instead of with each time step. The expression for computing the function value at the ghost-point located at x_0 is

$$f(x_0) = \sum_{i=1}^{n} w_i(x_0) f(x_i) \quad (5)$$

where $$w_i(x_0) = \frac{\prod_{j=1, j\neq i}^{n} (x_0 - x_j)}{\prod_{j=1, j\neq i}^{n} (x_i - x_j)}, \quad (6)$$

Filtering.--Numerical techniques use approximations of derivatives to solve partial differential equations. The truncation error of the techniques leads to the introduction of spurious high frequency signals or noise into the results. These spurious signals travel at high wave velocity in the negative direction and can create ëfalse pulsesí when they interact with grid boundaries or other spurious signals. Lele (1992) proposed using an implicit scheme to filter the computed signal. This can be represented in the following form:

$$\beta\hat{f}_{i-2} + \alpha\hat{f}_{i-1} + \hat{f}_i + \alpha\hat{f}_{i+1} + \beta\hat{f}_{i+2} = af_i + \frac{b}{2}(f_{i+1} + f_{i-1}) + \frac{c}{2}(f_{i+2} + f_{i-2}) + \frac{d}{2}(f_{i+3} + f_{i-3}) \quad (7)$$

where $\hat{f}$ is the filtered value

f is the unfiltered value.

The coefficients are chosen based on the formal accuracy and the desired degree of control on the cutoff frequency. Two schemes, B and C, (Lele, 1992, Fig. 20) were utilized in this work. These methods have a 4th order formal truncation error and use two parameters to control the cutoff frequency of the filter. Schemes B and C have the following coefficients for the interior grid points:

$$\alpha = 0.4627507, \quad \beta = 0.2265509, \quad a = 0.8470630$$
$$b = 1.166845, \quad c = 0.3422386, \quad d = 0.02245659, \quad (8)$$

$$\alpha = 0.6522474, \quad \beta = 0.1702929, \quad a = 0.9891856,$$
$$b = 1.321180, \quad c = 0.3333548, \quad d = 0.001359850. \quad (9)$$

Explicit equations (4th order formal accuracy and exact filtering of $\omega = \pi$) for the near boundary nodes are given by the following:

$$\hat{f}_1 = \frac{15}{16}f_1 + \frac{1}{16}(4f_2 - 6f_3 + 4f_4 - f_5)$$
$$\hat{f}_2 = \frac{3}{4}f_2 + \frac{1}{16}(f_1 + 6f_3 - 4f_4 + f_5) \quad (10)$$
$$\hat{f}_3 = \frac{5}{8}f_3 + \frac{1}{16}(-f_1 + 4f_2 + 4f_4 - f_5)$$

Results and Discussion

1D Results.--For all of the 1D cases, an equal number of points are chosen on each side of the ghost-point using grid points in both of the overlapped grids as shown in Fig. 2. Also, the initial signal was a Gaussian pulse defined as

$$u = 1.0\exp\left[-(\ln 2)\left(\frac{x-18}{3}\right)^2\right]. \quad (11)$$

The first set of tests was performed with the following conditions: a linear interpolation, or 2 terms for the Lagrange polynomial interpolation; Δx for each grid is 1.0; and periodic boundary conditions (provides a wrap-around effect). The amount of overlap varied from 0 to 1 with 0.5 being the 'worst case' when considering the interpolation error. Figure 3 shows the initial pulse and the pulse after propagating for selected amounts of time for each of the overlap values. At overlap values of 0 and 1, the propagated pulse shows no discernable error after moving through the overlap region. The worst error occurs with an overlap value of 0.5 where it can be seen that the signal peak has a significant reduction, and there is a presence of high-

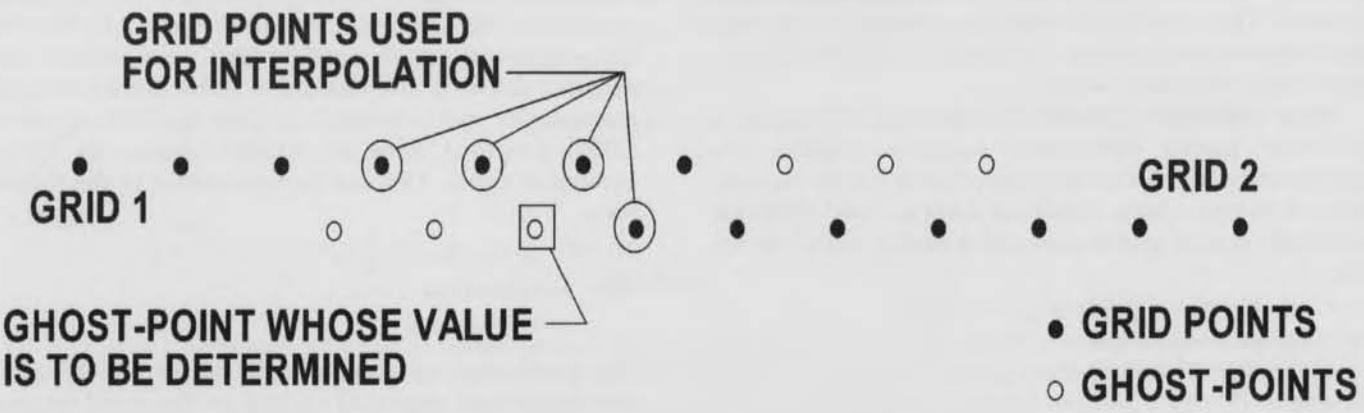

Fig. 2. Example of 1D interpolation with overlap.

Interpolation Techniques for Overset Grids

Paul S. Sherman* and **Nathan B. Edgar**
Arkansas State University
College of Engineering
P.O. Box 1740
State University, AR 72467

*Corresponding Author

Abstract

The use of finite difference schemes in computational aeroacoustics requires the use of structured grids in computational space. Complex geometries in the physical space can be modeled using multiple overlapping grids that are transformed into computational space. In this work, finite difference schemes are used that necessitate the addition of psuedo- or ghost-points in the overlap region of the grids for closure of the difference stencil. The functional values at these ghost points must be approximated from the values at the original grid points. This paper investigates interpolation techniques for these overset grids. An n^{th} order interpolation scheme using Lagrange polynomials is applied to the one dimensional (1D) wave propagation problem to test the effects of increasing the interpolation order. This is done for both equal and unequal sized overset grids. Preliminary results from two dimensional (2D) grids will be presented.

Introduction

In computational aeroacoustics, finite difference schemes are more commonly used because they are more computationally efficient than the finite element schemes. Finite difference schemes require the use of structured grids in computational space. An unstructured grid in the physical space can be transformed (Tannehill et al., 1997) into a structured grid in the computational space. However, complex geometries in the physical space may require multiple overlapping grids. In this paper, we discuss the construction of overset grids, problems associated with their construction, 1D and 2D results which show some of the problems arising from the application of the grids, and some solutions implemented to address these problems.

For this work, we chose to model the 1D and 2D wave equations using a single pair of overlapping structured grids. In general, overlapping grids can have mismatched grid spacing (Petersson, 1999) in each direction and may not share a common point. An example of the overlap regions for 1D and 2D grids is provided in Fig. 1. The layout of multiple grids in the physical space will be dictated by the geometry to be modeled.

Overlapping regions will exist wherever multiple grids share a common boundary. Two problems/difficulties must be dealt with in the overlap region. These are closure at the overlap region and the interpolation of overlapping grid points.

Additional pseudo- or ghost-points are necessary in the overlap region of the grids in order to provide for closure of the difference stencil. Only the function values are needed at these points for the finite difference schemes to compute the derivatives within the grids. For the schemes used in this work, three ghost-points are necessary for closure. The function values for the ghost-points are determined from the function values of the grid points in the other grid.

The values for the ghost-points are determined by an interpolation scheme. Although there are a variety of

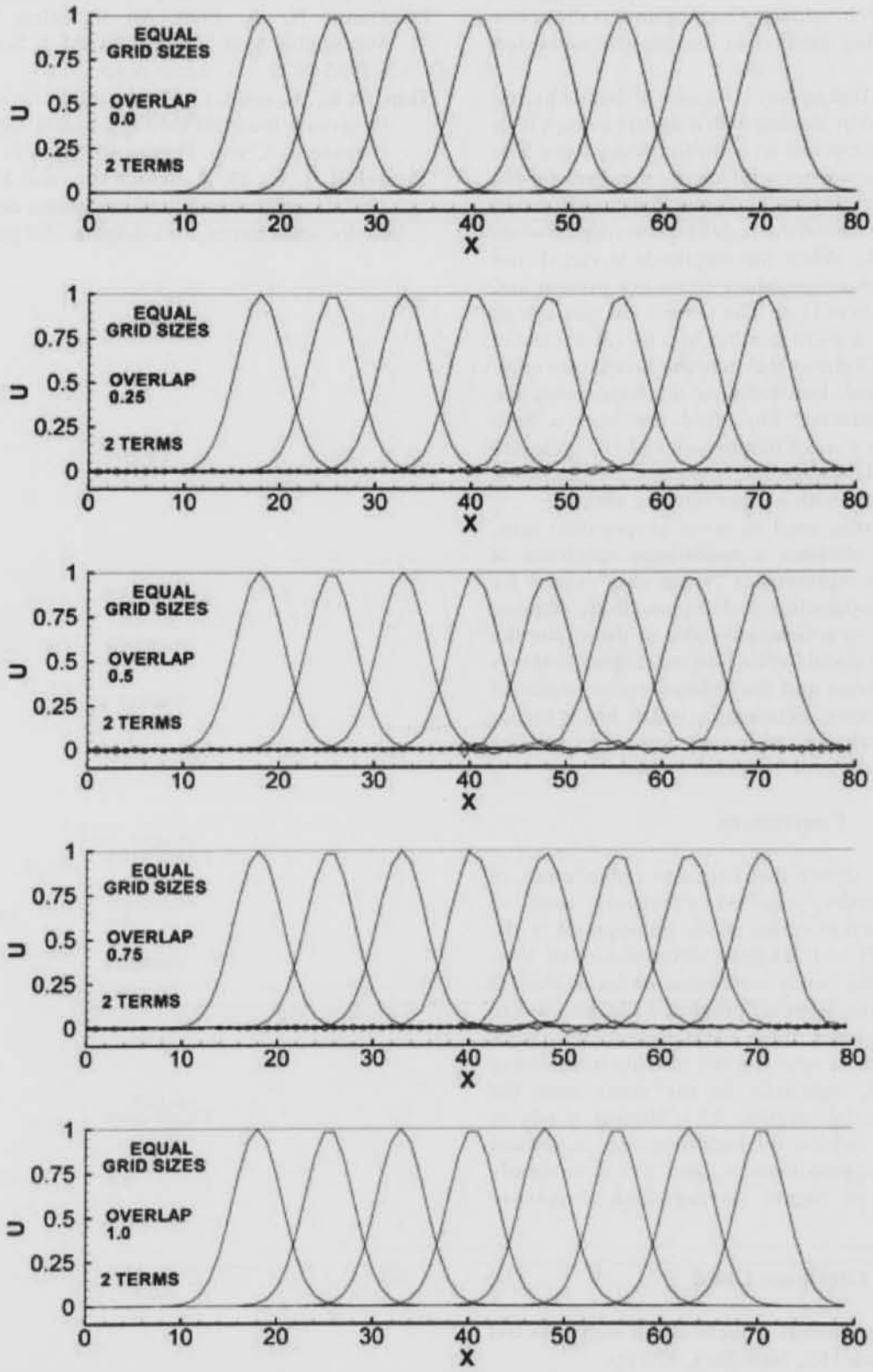

Fig. 3. Comparison of wave propagation results for the 1D case having equal grid spacing and varying amounts of overlap.

region or the upper boundary and that the ripple triggers a îfalseî pulse at the left boundary. Once again this illustrates the need for a filtering method to remove the unwanted signals.

Filtering Tests.--Testing for 1D cases of both filtering schemes was achieved by starting with a signal having a high frequency term superimposed on a low frequency term. The first test uses a high frequency with a wave number of π (25 cycles/50 grid points). Figure 12 shows that both filtering schemes completely remove the high frequency signal when at constant amplitude. When the amplitude is varied (not shown), additional lower frequency terms are present and are not completely filtered out. The second test uses a high frequency term with a wave number of 2.64 (21 cycles/50 grid points). Figure 13 shows that Scheme B removes more of the unwanted signal, but that near the boundaries, the filtering effect is reduced. The third test uses a high frequency term with a wave number of 2.14 (17 cycles/50 grid points). Figure 14 shows that Scheme C has the same trends as Scheme B but with a lesser filtering effect.

The Gaussian pulse used in wave propagation tests, both 1D and 2D, contains a continuous spectrum of frequencies. Thus, it represents a "worst case" signal for numerical wave propagation techniques. Both filtering schemes are applied to a Gaussian pulse to determine the errors induced in the signal by the filtering. Figure 15 shows the signal before filtering and the induced errors produced by each filtering scheme. Scheme C, which has a higher cutoff frequency, produces significantly less error, and the dominant error is at the near boundary nodes.

Conclusions

The results have shown that Lagrange polynomials, of sufficiently high order, can be effectively used to approximate the function values of the ghost-points in the overlap region of 1D and 2D finite difference cases. Four and six terms provide barely noticeable errors in the 1D cases, and the filtering schemes presented can be used to remove the high frequency ripple that is present. More work still needs to be done in applying the filtering to the wave propagation model, especially in the areas near the boundaries and overlap region. The filtering produces conflicting effects. It reduces the high frequency ripple that is induced by the approximations, and it non-uniformly attenuates a desired signal having high frequency components.

Literature Cited

Hoffman, J. D. 1992. Numerical methods for engineers and scientists. McGraw Hill, New York, 825 pp.

Lele, S. K. 1992. Compact finite difference schemes with spectral-like resolution. J. Comp. Physics 103:16-42.

Petersson, N. A. 1999. An algorithm for assembling overlapping grid systems. SIAM J. Sci. Comput. 20-6:1995-2022.

Tam, C. K. W., and **J. C. Webb.** 1993. Dispersion-Relation-Preserving finite difference schemes for computational acoustics. J. Comp. Physics 107:262-281.

Tannehill, J. C., D. A. Anderson, and **R. H. Pletcher.** 1997. Computational fluid mechanics and heat transfer. Taylor and Francis, Philadelphia. 792 pp.

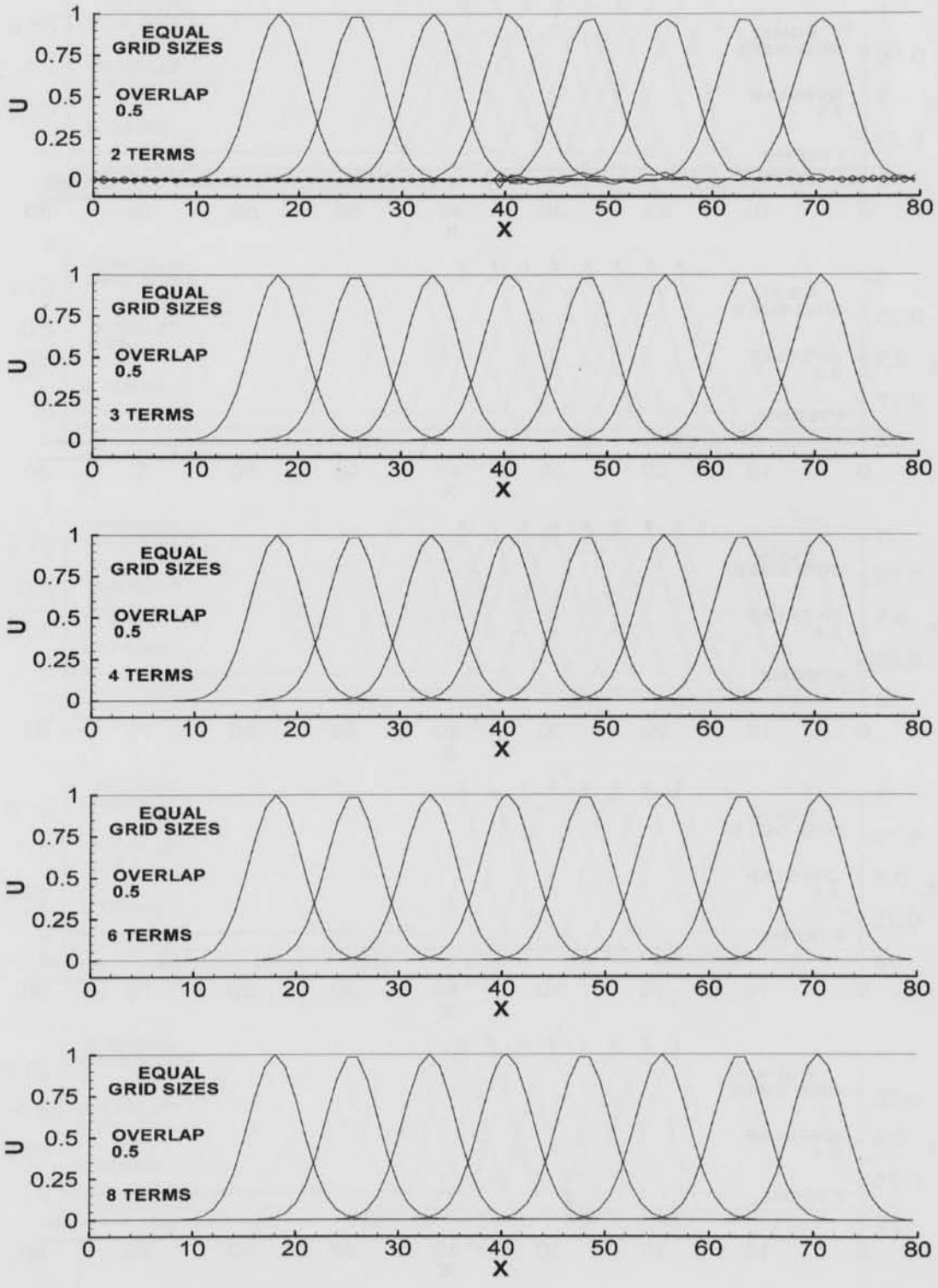

Fig. 4. Comparison of wave propagation results for the 1D case having equal grid spacing and varying interpolation order.

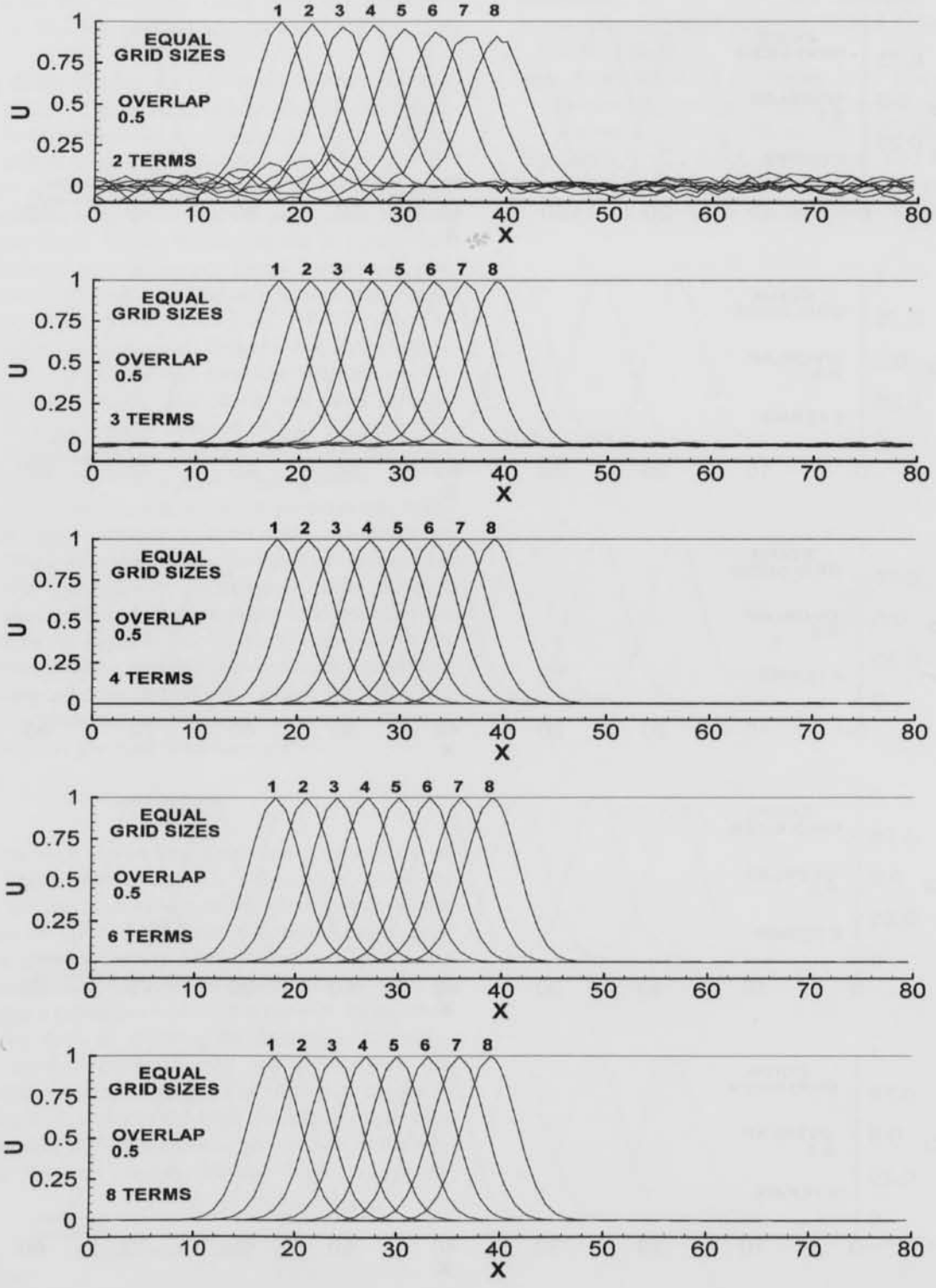

Fig. 5. Comparison of "long distance" wave propagation results for the 1D case having equal grid spacing and varying interpolation order.

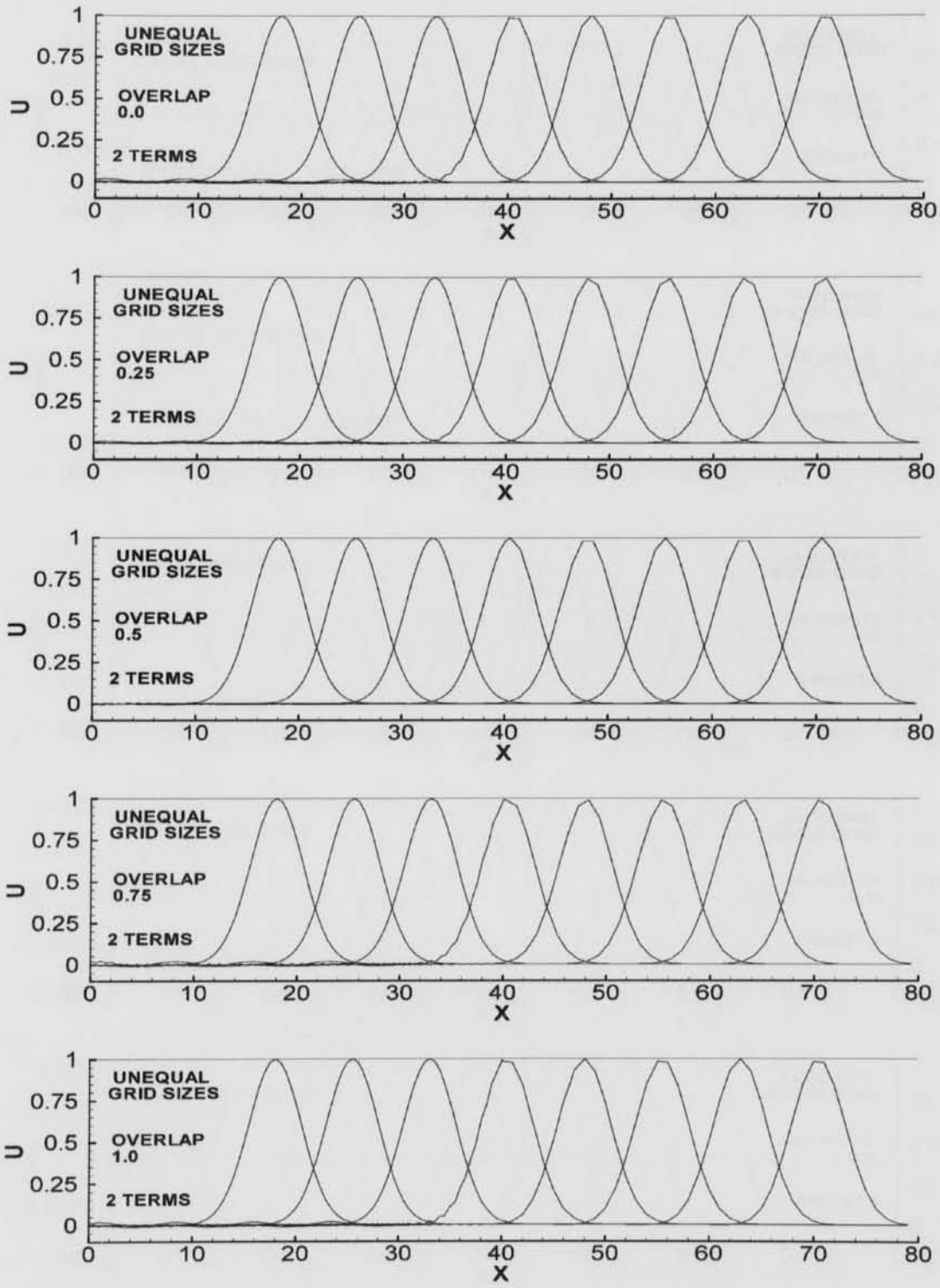

Fig. 6. Comparison of wave propagation results for the 1D case having unequal grid spacing and varying amounts of overlap.

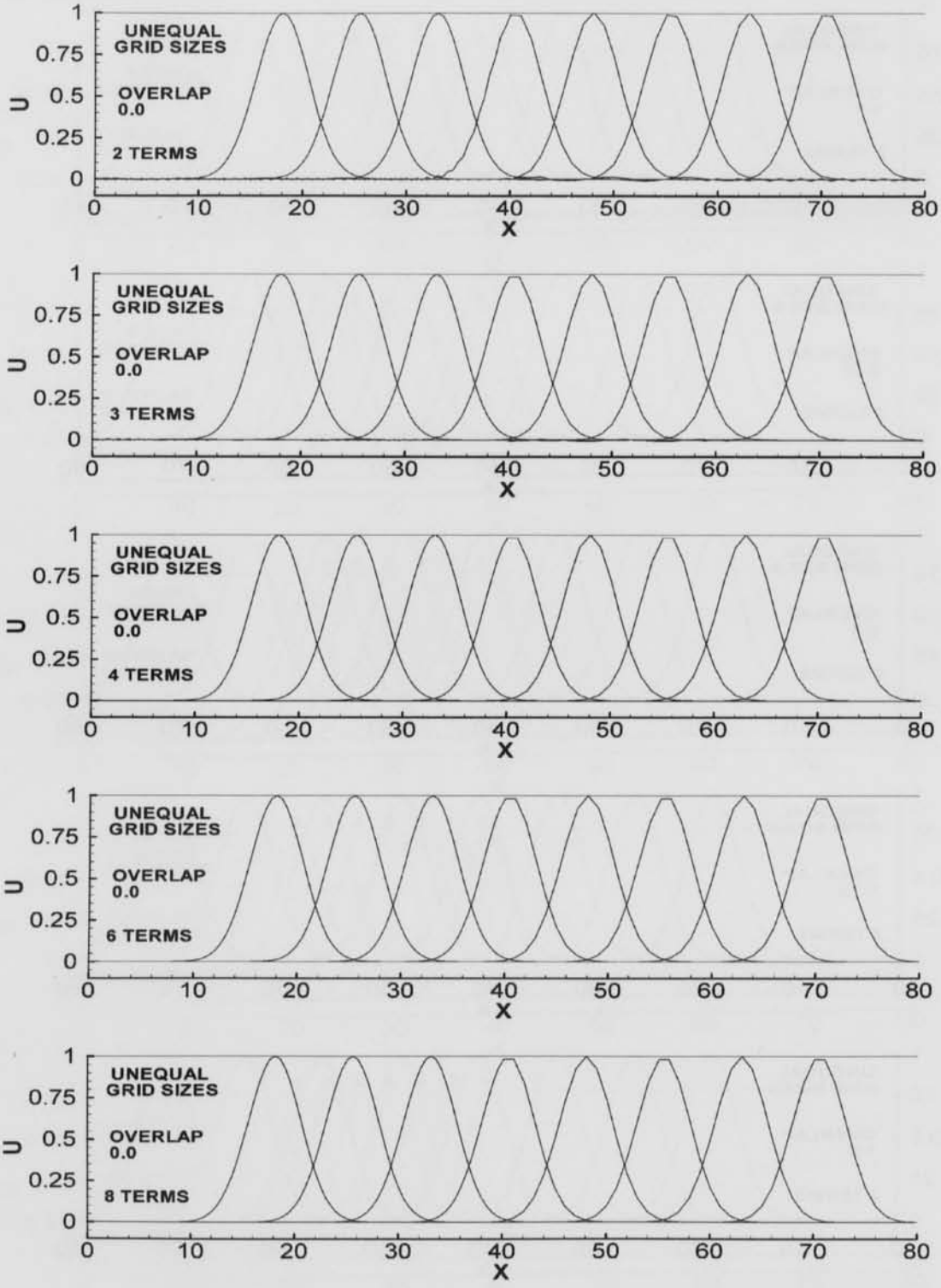

Fig. 7. Comparison of wave propagation results for the 1D case having unequal grid spacing and varying interpolation order.

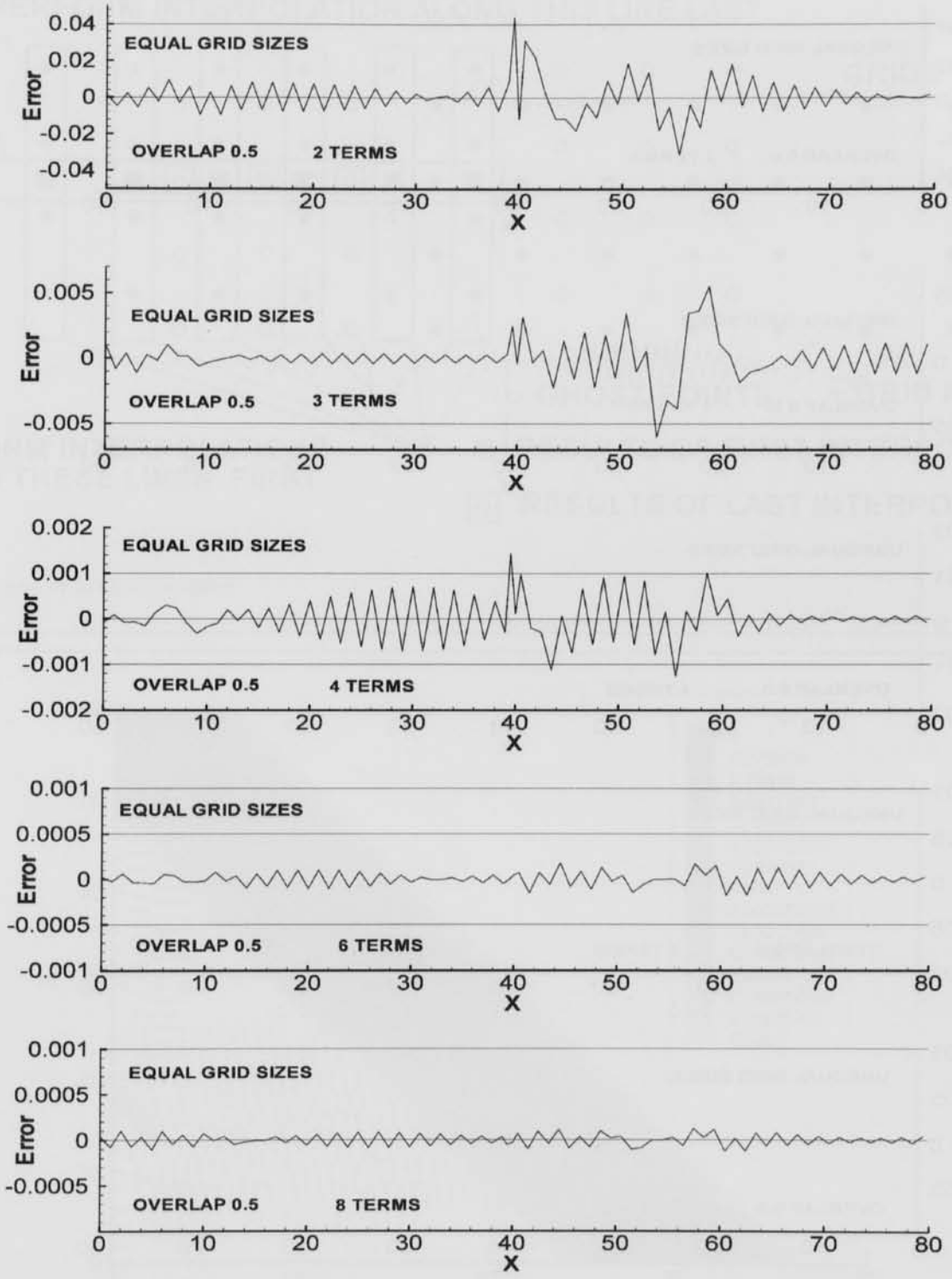

Fig. 8. Comparison of the typical errors in a propagated wave for the 1D case having equal grid spacing and varying interpolation order.

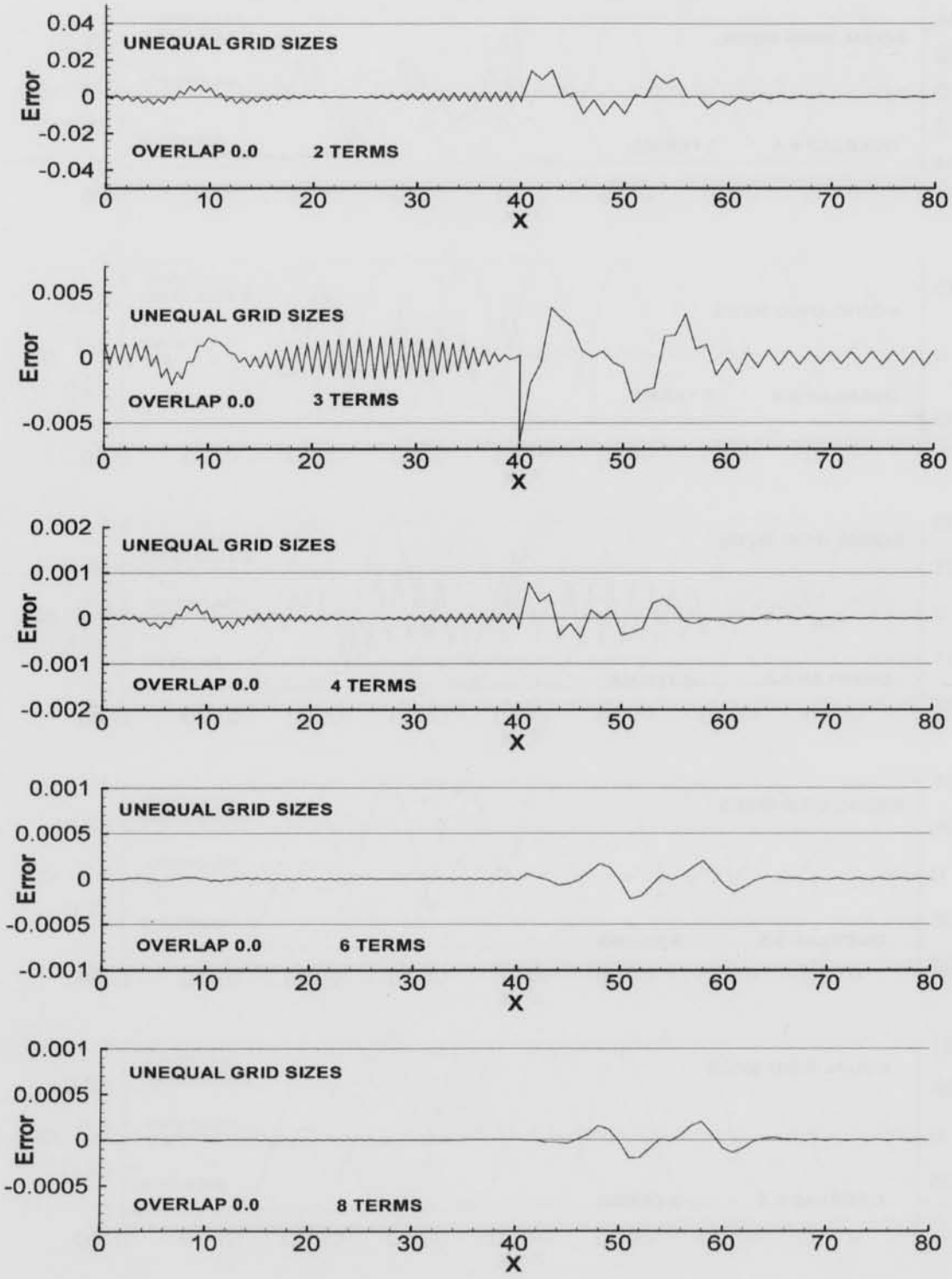

Fig. 9. Comparison of the typical errors in a propagated wave for the 1D case having unequal grid spacing and varying interpolation order.

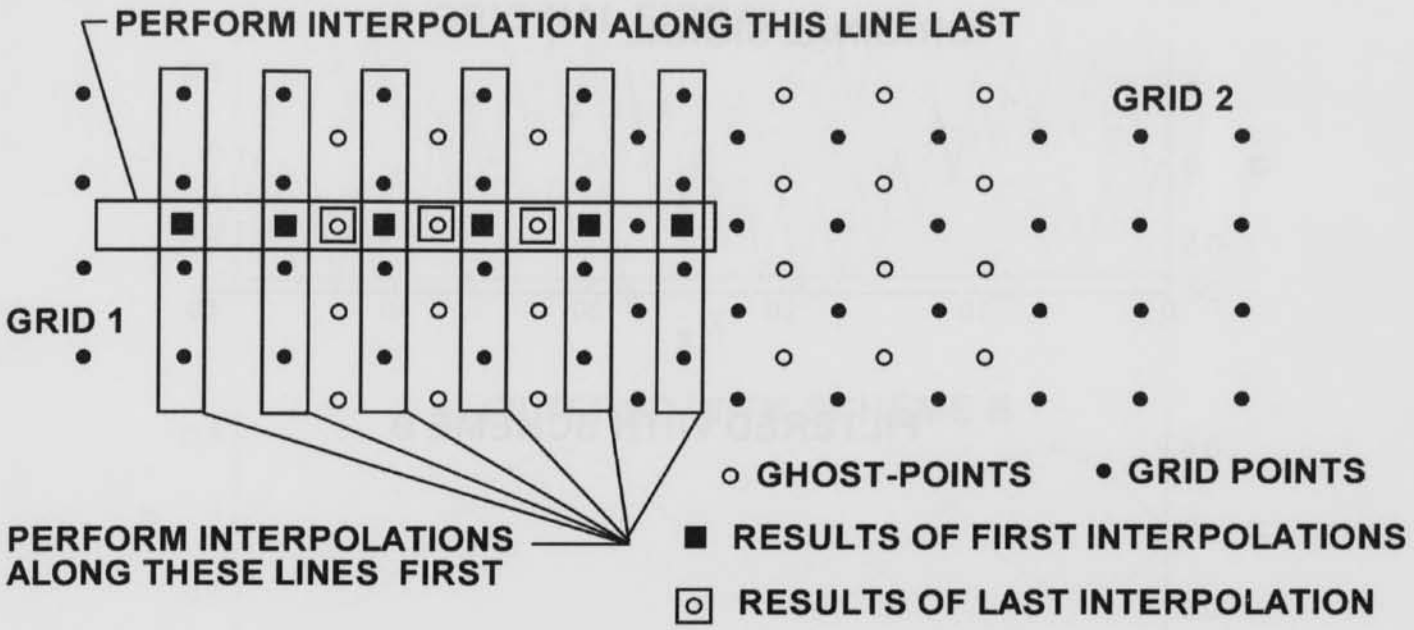

Fig. 10. Example of 2D interpolation

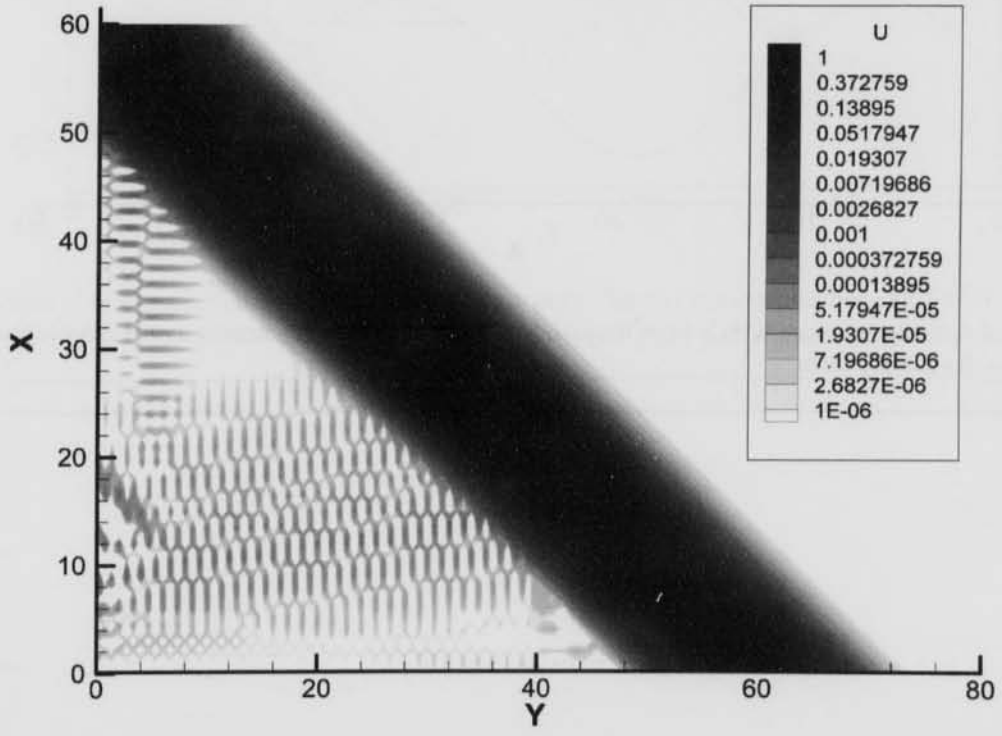

Fig. 11. Contour map of a propagated Gaussian wave after it encounters an overlap region at y = 40 and the upper boundary.

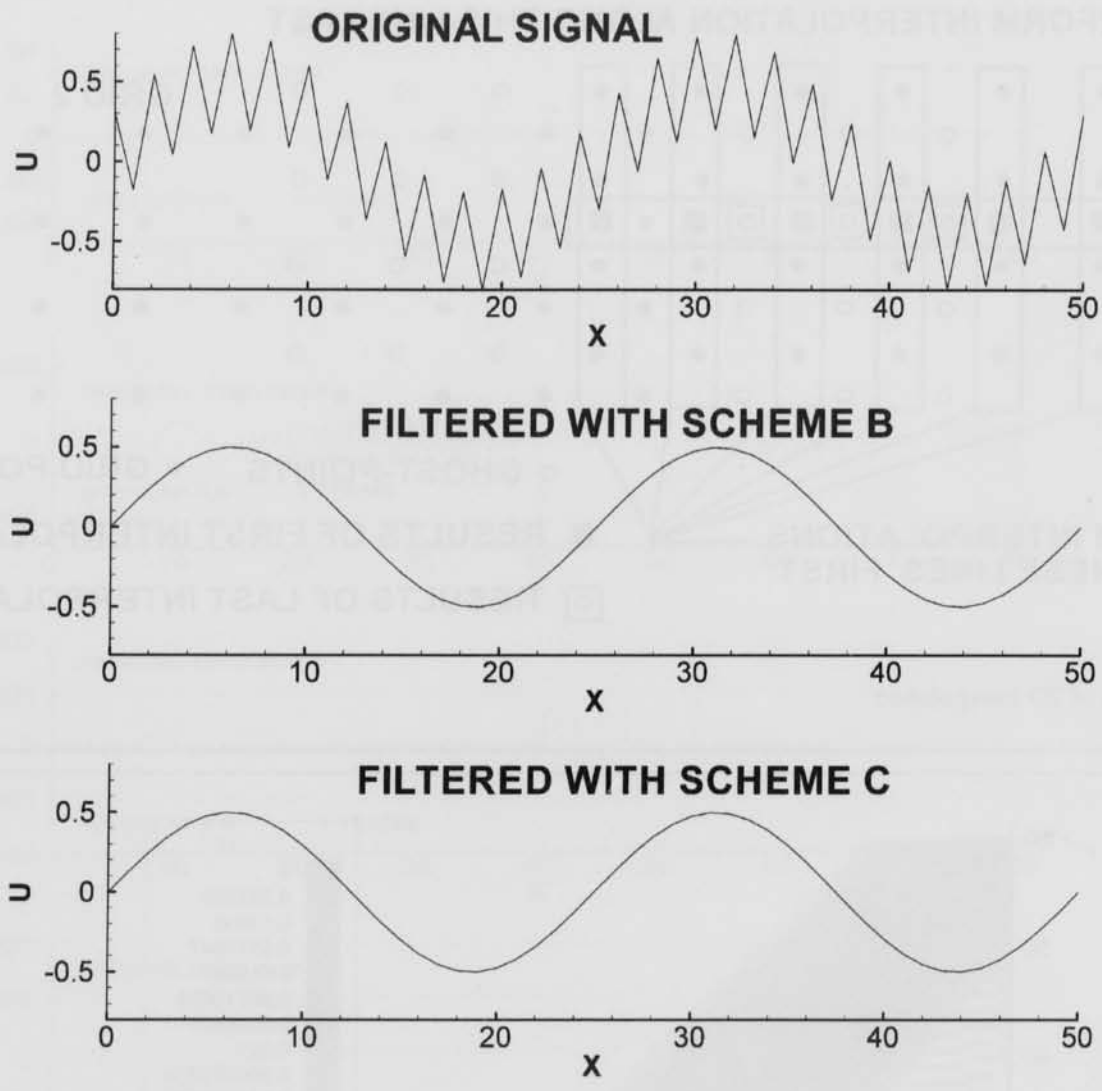

Fig. 12. Comparison of filtering schemes with a high frequency term, having a wave number of π (25 cycles/50 grid points), superimposed on a low frequency term.

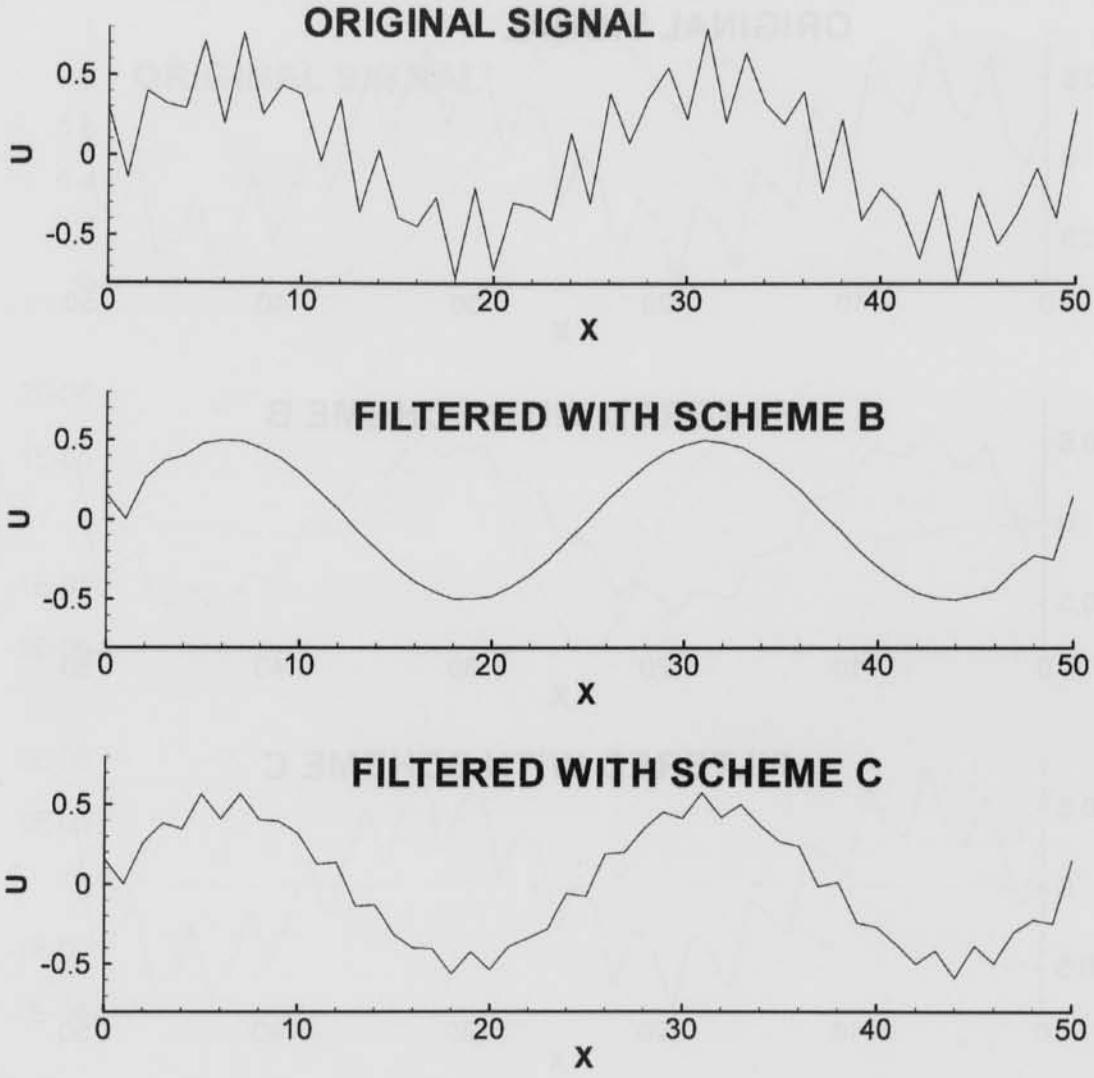

Fig. 13. Comparison of filtering schemes with a high frequency term, having a wave number of 2.64 (21 cycles/50 grid points), superimposed on a low frequency term.

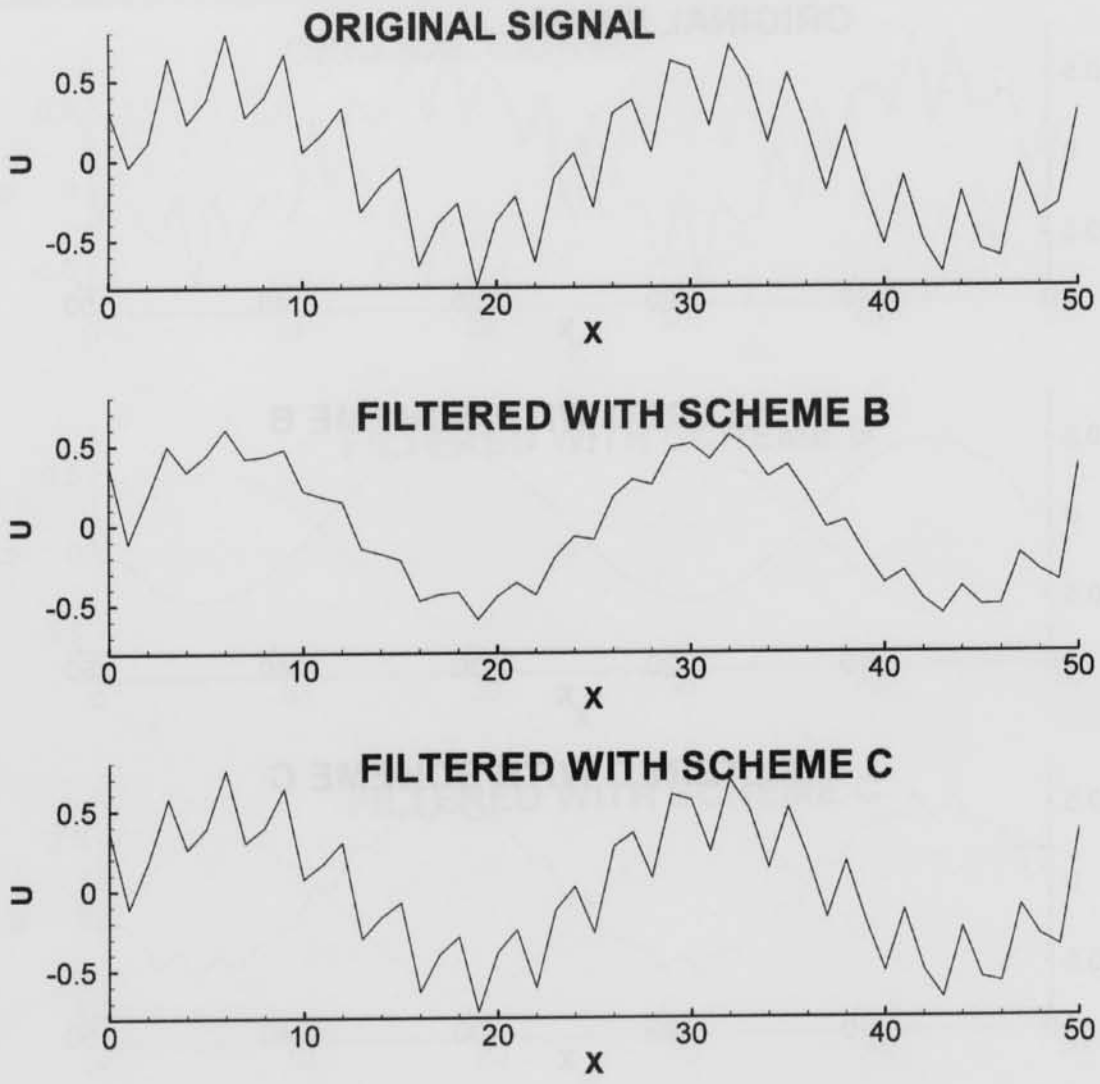

Fig. 14. Comparison of filtering schemes with a high frequency term, having a wave number of 2.14 (17 cycles/50 grid points), superimposed on a low frequency term.

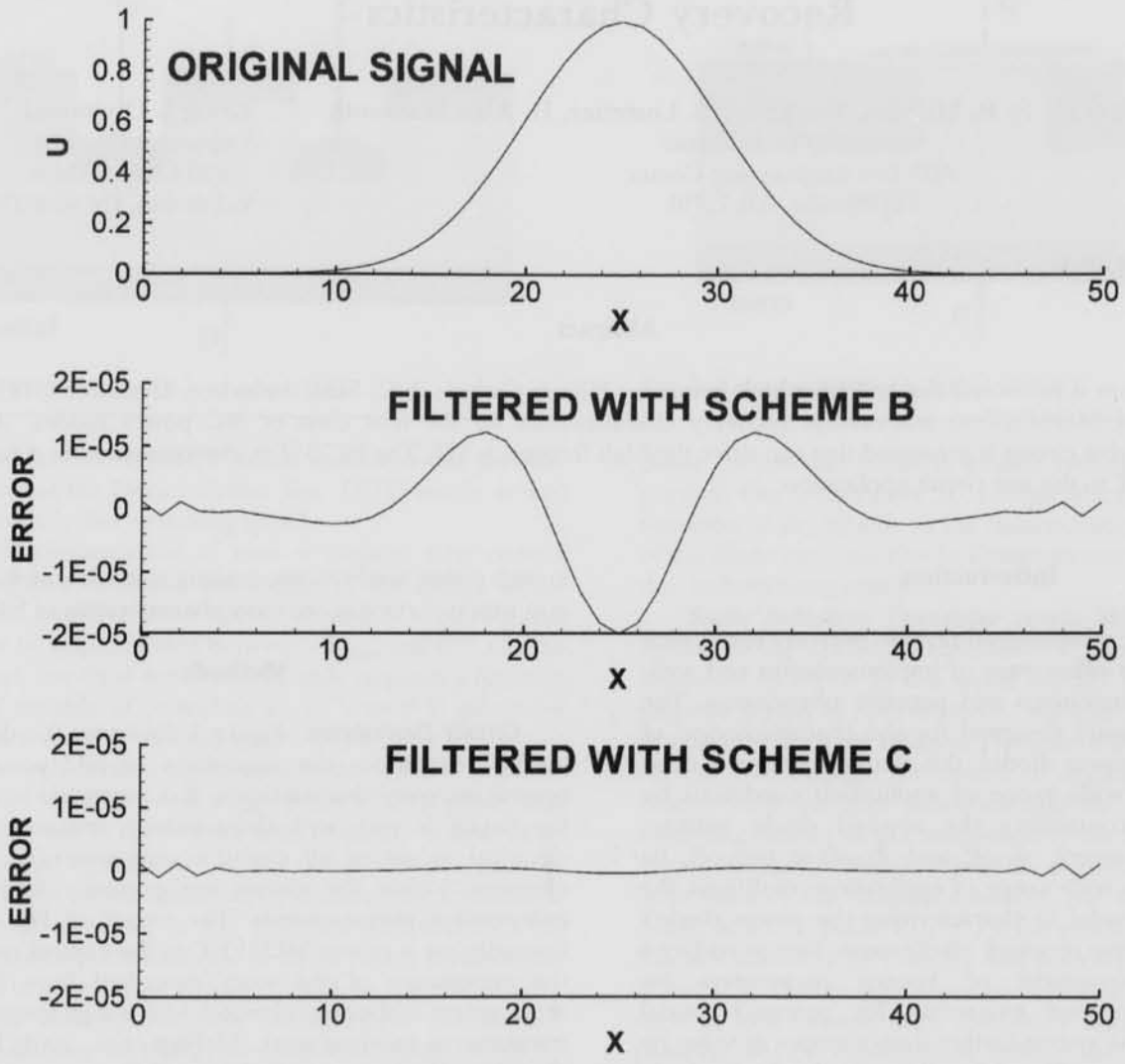

Fig. 15. Comparison of the error induced by filtering Schemes B and C after being applied to a Gaussian pulse.

A Novel High Frequency Silicon Carbide Static Induction Transistor-Based Test-Bed for the Acquisition of SiC Power Device Reverse Recovery Characteristics

Kevin M. Speer*, Ty R. McNutt, Alexander B. Lostetter, H. Alan Mantooth
University of Arkansas
3217 Bell Engineering Center
Fayetteville, AR 72701

Kraig J. Olejniczak
Valparaiso University
1900 Chapel Drive
Valparaiso, IN 46383

*Corresponding Author

Abstract

A test system is presented that utilizes a high-frequency Silicon Carbide (SiC) Static Induction Transistor (SIT) in place of the traditional MOSFET to test reverse recovery characteristics for the new class of SiC power diodes. An easily implementable drive circuit is presented that can drive the high-frequency SIT. The SiC SIT is also compared to a commonly used Si MOSFET in the test circuit application.

Introduction

In this paper, a high-speed reverse recovery test system is developed that offers ease of implementation and well-characterized components and parasitic phenomena. The system is specifically designed for the characterization of high-speed SiC power diodes; this characterization is done by emulating a wide range of application conditions by independently controlling the applied diode voltage, forward diode current, di_D/dt, and dv_D/dt at turn-off. By emulating such a wide range of application conditions, the system is very useful in characterizing the power diode's forward and reverse recovery phenomena, thus providing a controlled environment of known parameters for conducting parameter extraction for compact model development. The system further demonstrates its value by providing a means of model validation, the final step in model development (McNutt et al., 2002).

SiC PiN diodes have demonstrated reverse recovery times of 6 ns (McNutt et al., 2001; Hefner et al., 2001), and the SiC Schottky and Merged Pin Schottky (MPS) rectifiers have demonstrated even faster switching times than PiN rectifiers due to the unipolar nature of their operation range (Hefner et al., 2000). Due to the advantageous electrical properties of SiC, SiC diodes are orders of magnitude faster than application-comparable Si diodes; thus, a new test circuit was developed that can stress the SiC diodes (McNutt et al., 2002). As such, the SIT is a noteworthy candidate for the semiconductor switch in the high-speed reverse recovery test circuit shown in Fig. 1. The SIT has a lower parasitic capacitance and a faster switching speed than the conventionally-utilized power MOSFET. The primary reason for using a SIT is the aforementioned increase in switching speed; however, another amenity is the SIT's superior voltage blocking capability that legitimizes its use in high power applications, making it an ideal switch for the acquisition of reverse recovery characteristics of SiC diodes.

Methods

Circuit Description.--Figure 1 illustrates the developed test-bed circuit for the acquisition of SiC power diode reverse recovery characteristics. It is important to note that the circuit is very well characterized, meaning that the electrical values of all circuit components and parasitic elements within the circuit are precisely known after independent measurements. The circuit of Fig. 1 would normally use a power MOSFET as the control switch, but the importance of the work described here is in the replacement of the control switch with a high frequency SiC transistor; in previous work (McNutt et al., 2001; Hefner et al., 2001; Hefner et al., 2000), a 6LF6 vacuum tube was

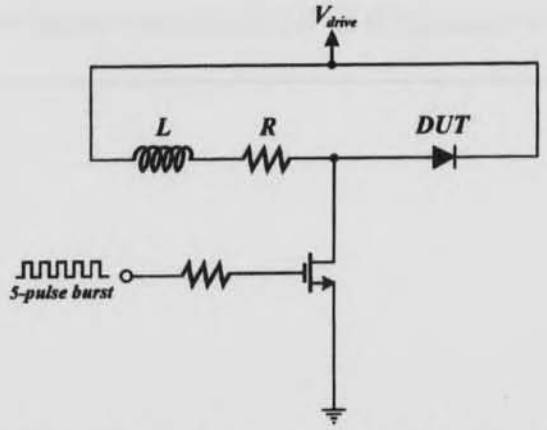

Fig. 1. Circuit diagram for the high-speed diode reverse recovery test system.

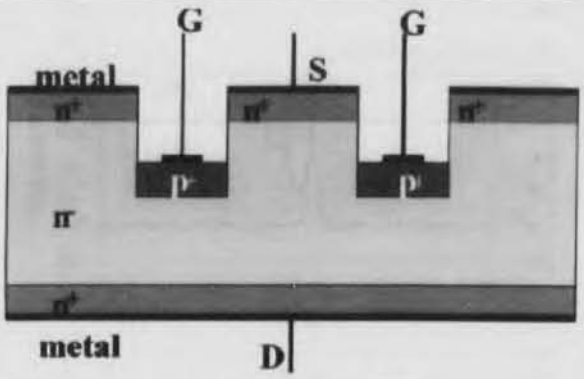

Fig. 2. Cross-section of a V-channel SIT.

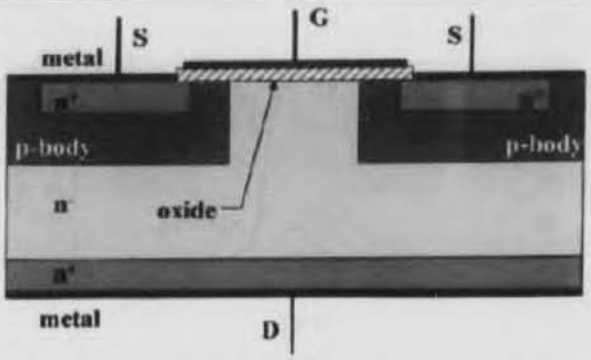

Fig. 3. Cross-section of a VDMOSFET.

substituted for the MOSFET switch to achieve low parasitic capacitance at the Device Under Test (DUT) anode as well as an extremely fast switching speed.

The implementation of such a vacuum tube control switch requires extensive knowledge of the design of the tube screen negative drive circuit, as well as requiring that the circuit be implemented between $-V_{drive}$ and 0 V. On the other hand, the three-terminal SIT only requires a function generator capable of providing a –10 V to 0 V gate-drive pulse with a variable rise/fall time.

The switch control signal used in the test-bed is a low-duty cycle, five-pulse burst, triggered by a 10 Hz pulse, thus enabling the use of the SIT for tests normally outside of its range of power operation. The five-pulse burst also reduces both DUT and switch self-heating, yielding characterization of device phenomena at the intended temperature; still further, the burst eliminates the need for power supplies that provide a large value of output current, as the output filter capacitance used to minimize the ac ripple can store a sufficient amount of charge to output adequate levels of current.

The test-bed itself allows for the performance of reverse recovery tests for various values of forward diode current, V_{drive}, di_D/dt, and dv_D/dt, where the value of forward diode current is controlled by the input pulse width to the gate drive circuit; di_D/dt is controlled by varying the value of the gate resistor; and dv_D/dt is controlled by placing various capacitors across the DUT. By independently controlling these parameters, the test circuit enables testing of the new SiC technology for the full range of application conditions: Varying the value of V_{drive} emulates the application conditions for circuits with different DC buss voltages; varying the value of di_D/dt emulates the application conditions of different speed anti-parallel switching devices; varying the value of dv_D/dt emulates the application conditions of using anti-parallel switching devices of different output capacitances; and for model parameter extraction purposes, varying the value of the forward diode current at turn-off aids in the determination of the portion of diode current that is due to emitter recombination and the portion that contributes to charge storage. In addition, variation of dv_D/dt aids in the determination of the portion of the diode recovery due to charge storage and the portion due to device capacitance.

Static Induction Transistor versus MOSFET.--A cross section of the 4H-SiC V-channel SIT used in this work is illustrated in Fig. 2. In this work, the SIT is operated in its unipolar region of operation (i.e., the gate p-n junctions do not become forward biased). The gate voltage controls the current flow through the means of depletion regions that extend from the gate junctions into the n-type channel, extending deeper as the magnitude of the negative gate-to-source voltage increases. When the depletion regions from both sides of the channel intersect, the device current is cutoff, at which point $V_{GS} = V_P$, the pinch-off voltage. The SIT is a normally ON device that is switched between –10 V and 0 V. Due to the device construction, it is commonly used in low voltage, high frequency applications, where parasitic device capacitances inhibit the turn-on/turn-off times of inferior switching devices. By keeping the duty cycle low in this application, the SIT is able to operate at these higher frequencies, thus providing the needed stress in testing the SiC diodes.

A typical VDMOSFET structure is shown in Fig. 3. High parasitic capacitances can be credited for severely limiting power MOSFETs' operation to frequencies well below those of the SITs: First, a capacitance can be seen in Figure 4 that results from overlapping areas of the gate and the source. Denoted C_{gs}, the capacitance is directly proportional to the gate-source overlap area, and thus is assumed to be constant. Secondly, and more influential to switching performance, the Miller capacitance between the gate and drain, C_{gd}, determines the gate and drain currents and the drain-to-source and gate-to-source voltages (Budihardjo et al., 1997). Lastly, the parasitic capacitance between the drain and source, C_{ds}, which is a combination of the gate oxide capacitance and the depletion layer capacitance beneath the gate, has negligible effect on

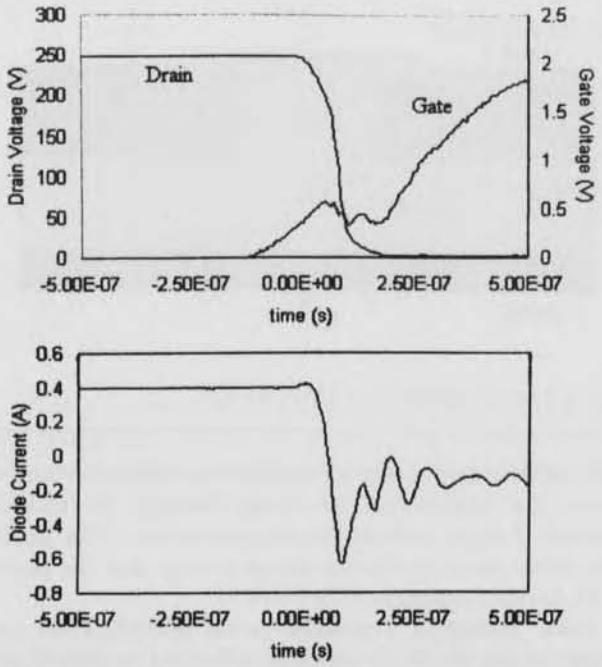

Fig. 4. Diode reverse recovery test with t_{rise}=400ns utilizing IF PG40 Si MOSFET.

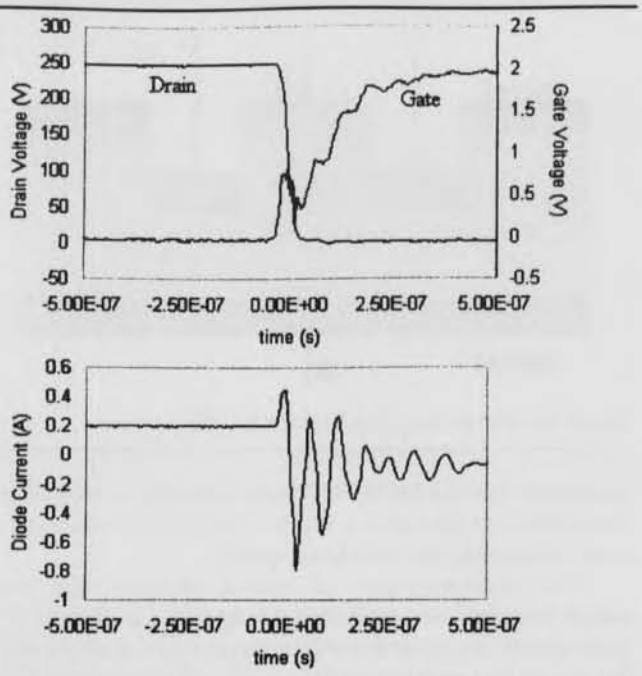

Fig. 5. Diode reverse recovery test utilizing IRF PG40 Si MOSFET with t_{rise}=5ns, demonstrating limits of MOSFET in high-speed test circuit.

switching characteristics (Mohan et al., 1995); in any event, the end result is that the combination of the larger parasitic capacitances of the MOSFET structure limits the device's switching time and thus makes the SIT the switching device of choice for high frequency applications.

SIT Test Circuit Results.--In Figs. 4, 5, and 6, an initial forward current is established in the diode before the diode is switched off by applying a constant negative di/dt with the control switch. The switch current increases linearly until the voltage reaches the voltage supply value, V_{drive}. Figure 4 and 5 illustrate the results of using a typical IRF820 Si MOSFET (International Rectifier, HEXFET Power MOSFET, Datasheet #PD-9.324O) in the test circuit of Fig. 1, and Fig. 6 shows the results of using the SiC SIT.

As functions of time, Figs. 4 and 5 show the MOSFET gate and drain/DUT voltages, directly below which are the corresponding DUT currents at turn-off. The rise time used for Fig. 4 is t_{rise} = 400 ns, and the rise time represented in Fig. 5 is t_{rise} = 5 ns. It can be seen that as the rise time of the control signal is decreased (i.e., the gate pulse is faster to reach its final value), the di/dt of the DUT at turn-off increases. For the case of the Si MOSFET, decreasing the rise time (or synonymously, increasing the di/dt of the DUT) is restricted by the parasitic capacitances of the MOSFET structure. The current waveform in Fig. 5 is a clear demonstration of this; reducing the rise time to t_{rise} = 5 ns forces large oscillations in the current waveform due to the parasitic capacitance of the MOSFET structure. Also evident from these waveforms at the MOSFET turn-on is the three-stage rise of the gate voltage.

For the case of the SiC SIT, Fig. 6 shows the results when t_{rise} = 5 ns. The capability to increase the di/dt of the DUT at DUT turn-off is improved by the reduction in parasitic capacitance of the SIT structure. The reader should note that the gate voltage waveform of Fig. 6 is a single-phase rise that reaches the maximum gate voltage value very quickly after the drain voltage decreases to its minimum value. This boldly demonstrates that the gate voltage can increase to its maximum value much faster than in the case of the MOSFET due to the severe reduction of the Miller capacitance offered by the SIT structure.

Conclusions

It is shown that a SiC SIT is capable of much faster switching speeds than the traditional power MOSFET when used in the diode characterization test-bed. Due to the device structure, the SIT provides less parasitic capacitance and, ultimately, the capability to switch at much higher frequencies, while retaining the capability to adequately stress the diode under test. In addition, the SIT offers convenience, since it boasts an easy to implement control system that does not require elaborate circuit design when compared to a vacuum tube.

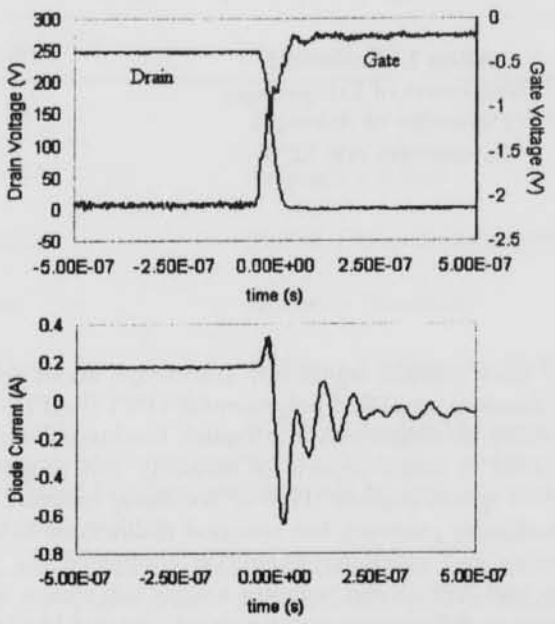

Fig. 6. High-speed diode reverse recovery test with t_{rise}=5ns utilizing SiC SIT.

Literature Cited

Budihardjo I., P. O. Lauritzen, and **H. A. Mantooth.** 1997. Performance Requirements for power MOSFET Models, IEEE Trans. on Power Electronics, pp. 36-45, vol. 12:Jan. 1997.

Hefner, A., D. Berning, J. Lai, C. Lui, and **R. Singh.** 2000. Silicon Carbide Merged PiN Schottky diode switching characteristics and evaluation for power supply applications, Conference Recordings of IEEE IAS Annual Meeting, October 2000.

Hefner, A., R. Singh, J. Lai, D. Berning, S. Bouche, and **C. Chapuy.** 2001. SiC power diodes provide breakthrough performance for a wide range of applications, IEEE Trans. on Power Electronics 16:March 2001. pp.

McNutt, T., A. Hefner, A. Mantooth, J. Duliere, D. Berning, and **R. Singh.** 2002. Parameter Extraction Sequence for SiC Schottky, Merged PiN Schottky, and PiN Power Diode Models, Conf. Rec. of IEEE Power Electronics Specialists Conf (PESC), Cairns, Australia.

McNutt, T. R., A. R. Hefner, H. A. Mantooth, J. Duliere, D. W. Berning, and **R. Singh.** 2001. Silicon Carbide PiN Schottky, and Merged Pin-Schottky Power Diode Models Implemented in the Saber Circuit Simulator, Conf. Proc. of IEEE Power Electronics Specialists Conference (PESC), pp. 2103-2108, Vancouver, Canada.

Mohan, N., T. Undeland, and **W. Robbins.** 1995. Power Electronics: Converters, Applications, and Design, New York, NY: John Wiley & Sons, Inc.

Weitzel, C., J. Palmour, C. H. Carter, K. Moore, K. Nordquist, and **L. L. Pond.** 1996. Silicon Carbide High-Power Devices, IEEE Trans. Electron Devices 43:10, 1732-1741.

Nuclear Ribosomal ITS Region Sequences for Differentiation of *Rubus* Genotypes

Eric T. Stafne* and **John R. Clark**
Department of Horticulture
University of Arkansas
Fayetteville, AR 72701

Allen L. Szalanski
Department of Entomology
University of Arkansas
Fayetteville, AR 72701

*Corresponding Author

Abstract

Previous molecular investigations into *Rubus* species diversity have yielded significant knowledge about species relatedness. However, little work has been focused at the cultivar level. Random amplified polymorphic DNA (RAPD)-PCR studies have successfully differentiated closely related cultivars. The ability to definitively distinguish blackberry and red raspberry cultivars based on other molecular methods could prove useful in many aspects of breeding and proprietary protection. In this study, the nuclear ribosomal DNA internal transcribed spacer regions (ITS) of six *Rubus* cultivars were sequenced. DNA sequencing revealed little genetic variation among blackberry cultivars, but revealed distinctions between blackberry and red raspberry cultivars. Analysis by maximum-parsimony and maximum-likelihood confirmed the small variation among blackberry cultivars, although cultivars Apache, Brazos, and APF-12 did organize a weak sub-cluster within the blackberry genotypes. However, ITS region sequences do not appear to differentiate among closely related blackberry genotypes for purposes of cultivar discrimination or plant patent protection.

Introduction

Blackberries (*Rubus* subgenus *Rubus* Watson; subgenus *Eubatus*) and red raspberries (*R. idaeus* L.; subgenus *Idaeobatus*) are economically and ecologically important fruiting plants which belong to the diverse genus *Rubus*. Most modern Eastern American blackberry cultivars were derived from diploid blackberry species *R. allegheniensis* Porter and *R. argutus* L. (Hall, 1990). Morphological differentiation between blackberries and raspberries is fairly well delineated with distinct fruiting characteristics being the primary recognition, but these identifiers are not present throughout the year (Parent and Pagé, 1992). Also, raspberry species have been used in blackberry breeding, thus donating significant traits which were not previously known in blackberry germplasm (e.g., fall-fruiting habit). Breeding of new *Rubus* cultivars has resulted in a narrowing of the genetic diversity, thus making definitive cultivar identification difficult (Jennings, 1988). However, little is known about the actual relationships among cultivars to their progenitors. Therefore, improvement in cultivar identification could be of significant benefit to verify identity and assist in confirming proprietary rights.

Since the internal transcribed spacer (ITS) region is repeated within plant nuclear genomes, amplification and sequencing of the nuclear ribosomal DNA is easily achieved (Baldwin et al., 1995). Previous studies on *Rubus* involving nuclear ribosomal DNA ITS region sequences have focused entirely at the species level (Alice, 2002; Alice and Campbell, 1999; Alice et al., 2001). Alice and Campbell (1999) reported that *Rubus* ITS sequences are mainly informative among subgenera, but variability is low between closely related species. Since the lineages of most blackberry cultivars include several distinct species, it may be possible to discriminate among the cultivars based on ITS sequences.

The objectives of this study were to distinguish blackberry and raspberry genotypes with the use of ITS sequences and also to ascertain if the results obtained would be useful for incorporation into a *Rubus* breeding program and plant patent protection.

Materials and Methods

Actively growing leaf material was sampled from six *Rubus* cultivars (Table 1) growing in the field during summer 2001 at the Univ. of Arkansas Fruit Research Substation, Clarksville or at the Agricultural Research and Extension Center in Fayetteville. All plant material was stored in a freezer (-20° C) until the DNA extraction procedure was initiated, which was generally within 24 hours. Actively growing leaf tissue (100 mg) was ground to a powder with a mortar and pestle in the presence of liquid nitrogen. DNA extraction followed manufacturer's protocols (Qiagen Dneasy Plant Mini Kit, Valencia, CA). DNA was re-precipitated with ammonium acetate (one-half of the original extraction volume) and 100% ethanol (three times the extraction volume plus the ammonium acetate). The

Table 1. Parentage and program of origination of six *Rubus* genotypes studied.

Genotype	Parentage	Program location
Apache	(SIUS 68-6-15 x Comanche) x Navaho	Fayetteville, Arkansas
APF-12[z]	Arapaho x A-830	Fayetteville
Arapaho	(A-550 x Cherokee) x A-883	Fayetteville
Brazos	Lawton x Nessberry	College Station, Texas
Heritage[y]	(Milton x Cuthbert) x Durham	Geneva, New York
Illini Hardy	NY95 x Chester Thornless	Carbondale, Illinois

[z]Unreleased breeding selection, not an item of commerce.
[y]Raspberry cultivar.

Table 2. Pairwise genetic distances among nine *Rubus* genotypes and two outgroup taxa.

No.	Genotype	1	2	3	4	5	6	7	8	9	10	11
1	APF-12			-								
2	Apache			0.009	-							
3	Brazos			0.009	0.003	-						
4	Heritage			0.039	0.036	0.038	-					
5	*R. idaeus*		0.040	0.035	0.036	0.003	-					
6	Illini Hardy		0.014	0.007	0.009	0.028	0.030	-				
7	*R. allegheniensis*	0.012	0.004	0.006	0.027	0.028	0.000	-				
8	*R. argutus*		0.012	0.006	0.008	0.030	0.032	0.001	0.000	-		
9	Arapaho			0.014	0.004	0.006	0.031	0.033	0.003	0.000	0.001	- -
10	*A. arguta*[z]		0.702	0.697	0.699	0.696	0.699	0.699	0.699	0.696	0.697	-
11	*V. corymbosum*[z]	0.705	0.708	0.706	0.703	0.705	0.703	0.703	0.705	0.704	0.287	-

[z]Outgroup taxa.

resulting DNA pellet was dried and then washed with 70% ethanol and re-suspended in 50 μL of TE buffer (pH 7.4).

The PCR reaction mixtures for each sample were comprised of 5 μL of 10X Taq buffer with $MgCl_2$ (Promega, Madison, WI), 4 μL dNTP (Pharmacia Biotechnology, Pescataway, NJ), 1 μL primer ITS 4 (5' - TCCTCCGCTTATTGATATGC- 3'), 1 μL ITS 5 (5' - GGAAGTAAAAGTCGTAACAAGG- 3') (White et al., 1990), 0.4 μL Taq polymerase (Promega), and 40 μL double distilled water all of which were master mixed to ensure uniformity among reagents. An aliquot of 48 μL was added to a 0.5 ml thin-walled microcentrifuge tube (Sarstedt, NC),

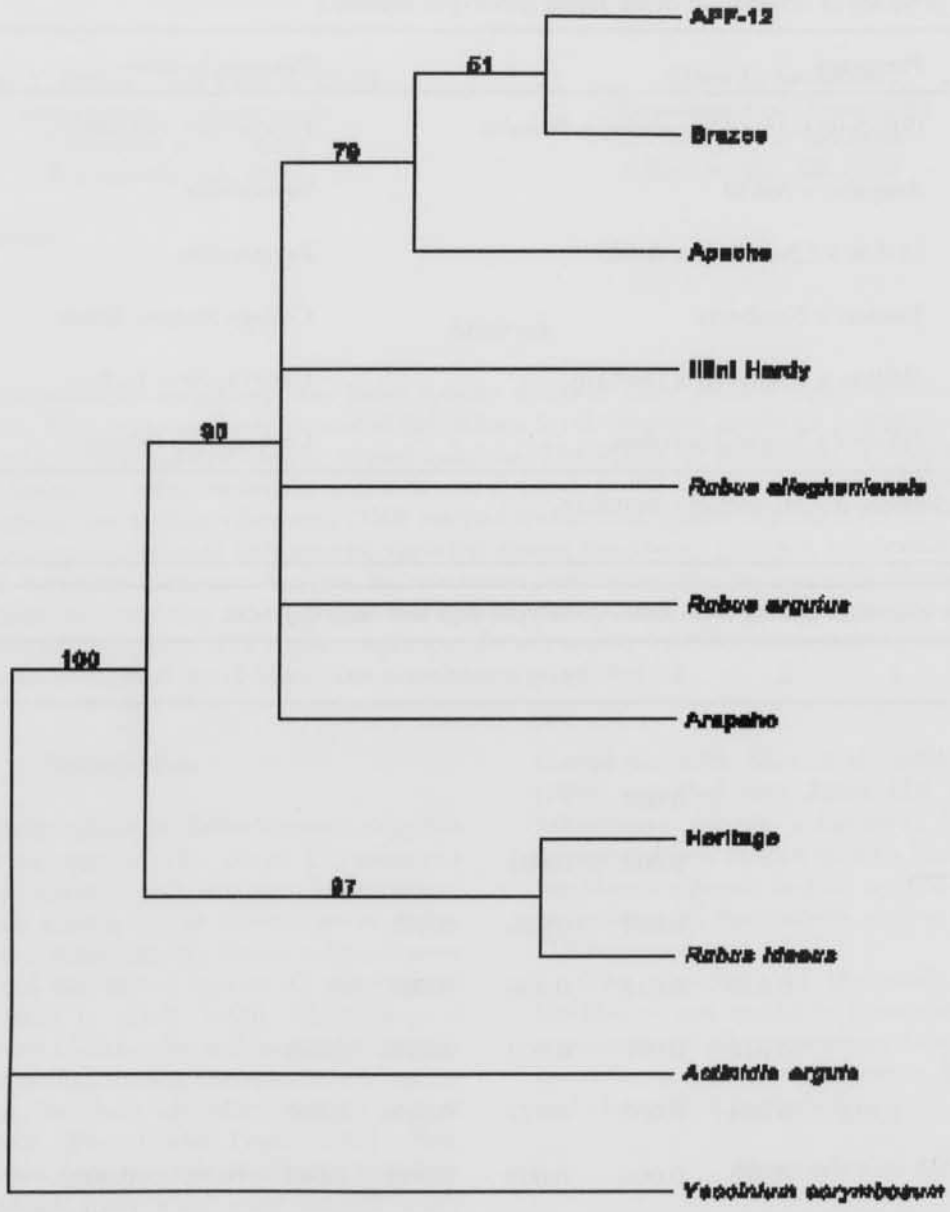

Fig. 1. Consensus parsimony tree with nine *Rubus* genotypes and two outgroups based on ITS region DNA sequences. Bootstrap values greater than 50% are indicated at nodes.

then 2 μL of template DNA was added to comprise a total reaction volume of 50 μL. A Techne Touchgene 40 x 0.5 ml (Techne Corp., Princeton, NJ) was used to perform the PCR. The thermocycling program used for this study consisted of an initial denaturation of 94 °C for 2 min., then 40 cycles of 94° C for 45 s, 46° C for 1 min, and 72° C for 1 min, followed by a final extension for 5 min at 72° C.

A 1% agarose solution (Fisher Scientific, St. Louis, MO), was placed into the gel box (Owl Scientific, Cambridge, MA) filled with 0.5X TBE buffer solution. The PCR product and dye buffer totaled 10 μl. Ten μl of 100 bp DNA ladder (Promega) was added in the first well. Ethidium Bromide was added to the buffer solution and the voltage was set at ~165 V. The electrophoresis ran for 50 min. The gel was removed and photographed in the BioDoc-It imaging system (UVP, Inc., Upland, CA).

Amplified DNA of six sample genotypes (five blackberry and one raspberry) was purified as described in

Szalanski et al. (2000). The purified DNA samples were sent to the DNA core sequencing lab at the Univ. of Arkansas (Fayetteville) to be sequenced in both directions with an ABI Prism 377 DNA sequencer. An amplified fragment of DNA between 700 and 800 bp in size was sequenced for all samples. However, to understand genetic relationships with existing Genbank DNA sequences, the sequences were reduced to 643 bp.

Sequences derived from ribosomal DNA were aligned with the Genetics Computer Group (GCG, Madison, WI) PILEUP program (gap weight = 5.0, gap length weight = 1.0) and used *Vaccinium corymbosum* L. and *Actinidia arguta* (Sieb. & Zucc.) Planch. ex Miq. as outgroups. Maximum likelihood and maximum parsimony analyses were performed with PAUP* 4.0b10 (Swofford, 2002). Bootstrap testing (100 re-sampled datasets) was used to determine tree robustness (Felsenstein, 1985).

Results and Discussion

Bases were revealed at the frequency of 0.20967, 0.28372, 0.27825, and 0.22836 for A, C, G, and T, respectively. Existing Genbank sequences for *A. arguta* (AF323836; Li et al., 2002) and *V. corymbosum* (AF419778; Powell and Kron, unpublished data) were used as outgroups. *R. idaeus* (AF0557552), *R. allegheniensis* (AF055772), and *R. argutus* (AF0557742) were existing Genbank DNA sequences that were included to compare species with the modern cultivars included in the study (Alice and Campbell, 1999). Parsimony analysis resulted in 643 total characters consisting of 147 constant characters (22.8%), 176 variable characters that were parsimony-uninformative (27.3%), and 320 parsimony-informative characters (49.7%). Pairwise genetic distances (Tajima and Nei, 1984) ranged from 0.00 ('Illini Hardy'/*R. allegheniensis* and *R. allegheniensis*/*R. argutus*) to 0.04 (APF-12/*R. idaeus*) within the *Rubus* cultivars (Table 2). Alice and Campbell (1999) reported that ITS sequence divergence among species of the blackberry subgenus averaged only 1.2%, and this appears also be a close representation of the data obtained in this study.

Only one parsimonious tree was derived from the data set (Fig. 1) with a length of 603 and a consistency index (CI) of 0.982. Bootstrap analysis indicated little divergence among blackberry cultivars and species, but suggested a weak sub-cluster of APF-12, 'Brazos', and 'Apache'. The value of 51% at the APF-12/'Brazos' node implies a very weak support for that separation. The maximum-likelihood analysis starting with the parsimonious tree found 3 trees, but all were similar and none of the changes resulted in a significant change in topology. The resulting tree was similar in topology to that of the consensus parsimony tree (data not shown). Blackberry and red raspberry genotypes were separated as distinct clusters by both the maximum-parsimony and maximum-likelihood tests. The raspberry genotypes displayed informative deletions at sites 75 and 442, whereas the blackberry genotypes had a deletion at 515 (data not shown). These are likely strong indicators for differentiating the two groups.

The phylogenetic maximum likelihood tree derived from PAUP* differentiated the subgenera *Idaeobatus* and *Eubatus* (red raspberry and blackberry, respectively), but did not recognize any notable differences within the blackberry cultivars. Thus, *Rubus* cultivar differentiation, which has been done with other molecular techniques (Stafne et al., 2003), does not appear to be viable with ITS region sequences. Blackberry cultivars containing more divergent species have yet to be tested and may show distinction from the other blackberry cultivars tested in this study.

Conclusions

The main benefit for *Rubus* appears to be if morphological ambiguity exists. ITS sequence analysis may distinguish between red raspberry and blackberry genotypes, but probably not within cultivars of those groups unless they contain highly divergent progenitor species. Since ITS sequences cannot distinguish between similar cultivars, its utility for plant patent protection is limited.

Literature Cited

Alice, L. A. 2002. Evolutionary relationships in *Rubus* (Rosaceae) based on molecular data. Acta Hort. 585:79-83.

Alice, L. A., and **C. S. Campbell.** 1999. Phylogeny of *Rubus* (Rosaceae) based on nuclear ribosomal DNA internal transcribed spacer region sequences. Amer. J. Bot. 86:81-97.

Alice, L. A., T. Eriksson, B. Eriksen, and **C. S. Campbell.** 2001. Hybridization and gene flow between distantly related species of *Rubus* (Rosaceae): evidence from nuclear ribosomal DNA internal transcribed spacer region sequences. Syst. Bot. 26:769-778.

Baldwin, B. G., M. J. Sanderson, J. M. Porter, M. F. Wojciechowski, C. S. Campbell, and **M. J. Donoghue.** 1995. The ITS region of nuclear ribosomal DNA: a valuable source of evidence on angiosperm phylogeny. Ann. Missouri Bot. Garden 82:247-277.

Felsenstein, J. S. 1985. Confidence limits on phylogenies: an approach using bootstrap. Evolution 39:783-791.

Hall, H. K. 1990. Blackberry breeding. Pp. 249-312, *In* Plant Breeding Reviews (J. Janick ed.) Vol. 8. Timber Press, Portland, Oregon.

Jennings, D. L. 1988. Raspberries and blackberries: their breeding, diseases and growth. Academic Press, London.

Li, J., H. Huang, and **T. Sang.** 2002. Molecular phylogeny and infrageneric classification of *Actinidia*

(Actinidiaceae). Syst. Bot. 27:408-415.

Parent, J. G., and **D. Pagé.** 1992. Identification of raspberry cultivars by random amplified polymorphic DNA (RAPD) analysis. HortScience 27:1108-1110.

Stafne, E. T., J. R. Clark, M. C. Pelto, and **J. T. Lindstrom.** 2003. Discrimination of Rubus cultivars using RAPD markers and pedigree analysis. Acta Hort. 2003. 626:119-124.

Swofford, D. L. 2002. PAUP*: phylogenetic analysis using parsimony (*and other methods), version 4 beta 10. Sinauer, Sunderland, Massachusetts.

Szalanski, A. L., D. S. Sikes, R. Bischof, and **M. Fritz.** 2000. Population genetics and phylogenetics of the endangered American burying beetle, *Nicrophorus americanus* (Coleoptera: Silphidae). Ann. Ento. Soc. Amer. 93:589-594.

Tajima, F., and **M. Nei.** 1984. Estimation of evolutionary distance between nucleotide sequences. Mol. Biol. Evol. 1:269-285.

White, T. J., T. Bruns, S. Lee, and **J. Taylor.** 1990. Amplification and direct sequencing of fungal ribosomal RNA genes for phylogenetics, p. 315-322. *In* PCR protocols: a guide to methods and applications. (D.G.M. Innis, J. Sninsky, and T. White, eds.). Academic Press, San Diego, California.

Experimental Channel Catfish Virus Infection Mimics Natural Infection of Channel Catfish

Robin L. Stingley and **Wayne L. Gray***
Department of Microbiology
and Immunology
University of Arkansas
for Medical Sciences
Little Rock, AR 72205

Billy R. Griffin
Stuttgart National Aquaculture
Research Center
ARS-USDA
Stuttgart, AR 72160

Reid Landes
Division of Biometry
University of Arkansas
for Medical Sciences
Little Rock, AR 72205

*Corresponding Author

Abstract

Channel catfish virus (CCV) causes a severe hemorrhagic disease in channel catfish fry and fingerlings. CCV epizootics are associated with elevated water temperatures and high mortality rates. Survivors of acute disease are latently infected with the virus. In this study, we investigated conditions effecting CCV pathogenesis and latency utilizing an experimental immersion model to simulate natural infection and a population of Arkansas catfish verified to have no prior CCV exposure. The results indicate that the Auburn-1 laboratory strain is comparable to CCV field isolates in virulence and ability to establish latent infection. The study confirms that water temperature and fish age effect susceptibility to acute infection. Twenty-four week old fish were more susceptible to acute CCV infection at 28° C than at 24° C. Eight week old fish were susceptible to disease at 24° C and 28° C. Yearling catfish, although more resistant to acute disease, were susceptible to latent CCV infection. CCV latency was established as early as 27 days following experimental infection and maintained for at least one year post infection. The CCV infection model described in this report is useful for further investigation of CCV pathogenesis and latency and for evaluation of potential antiviral therapies.

Introduction

Commercial catfish farming is a major aquaculture industry in the southern United States contributing especially to the economies of Arkansas, Mississippi, Alabama, and Louisiana. In 2002, nearly 200 Arkansas catfish operations covering 38,000 water surface acres generated over $65 million in sales (Anonymous, 2003). However, several factors, including disease, may hamper production and cause significant economic loss (Anonymous, 1997).

Channel catfish virus (CCV) disease is the leading viral disease in catfish. This herpesvirus causes an acute hemorrhagic disease in juvenile channel catfish, *Ictalurus punctatus* (Buck, 1990; Plumb, 1977). Clinical signs of the disease include erratic swimming followed by lethargy, punctate hemorrhaging at the base of fins, abdominal swelling, and exophthalmia. Internally, visceral organs such as the kidneys, intestines, and liver often exhibit hemorrhagic lesions (Wolf et al., 1972). Infectious CCV and viral DNA may be detected in kidney, intestine, liver, brain, and muscle tissues of acutely infected fish (Plumb, 1971; Gray et al., 1999a). CCV epizootics usually occur during summer months, when water temperatures exceed 25° C and channel catfish fry and fingerlings are abundant (Plumb, 1977; 1978). Outbreaks in hatchery stocks may cause high mortality of fish in infected ponds (Plumb, 1978).

Survivors of acute CCV infection are latently infected, a characteristic of herpesviruses (Plumb et al., 1981; Wise et al., 1985; Gray et al., 1999b). Viral DNA may be detected in blood, brain, intestines, kidney, liver, and peripheral blood leukocytes of latently infected fish by PCR analysis using CCV specific primers (Gray et al., 1999b).

In addition to the ability to establish latent infection in the host, CCV shares many characteristics with other herpesviruses. Morphologically, CCV is similar to other herpesviruses in size and structure (Wolf and Darlington, 1971). The overall organization of the double-stranded CCV DNA genome into unique and repeat regions is typical of herpesvirus genomes (Davison, 1992). In addition, CCV gene expression is temporally regulated in the same manner as that of other herpesviruses (Dixon and Farber, 1980; Silverstein et al., 1995, 1998; Huang and Hanson, 1998; Stingley and Gray, 2000).

CCV infection of channel catfish provides an excellent natural model to investigate herpesvirus pathogenesis and latency. Previous experimental studies of CCV pathogenesis were limited because of the inability to confirm that fish were not already latently infected. We have recently verified that catfish stocks at the Stuttgart National Aquaculture

Research Center in Stuttgart, Arkansas are negative for CCV latency, indicating that these fish have no prior exposure to CCV (Gray et al., 1999b). In this study, we have used this CCV negative catfish population to develop an experimental model of CCV infection of channel catfish that mimics natural infection.

Materials and Methods

CCV strains and propagation.--Channel catfish ovary (CCO) cells were maintained at 27° C in Eagle's minimum essential medium (EMEM) supplemented with penicillin (5,000 U/ml), streptomycin (5,000 U/ml) and 5% fetal bovine serum (FBS). The laboratory strain, CCV Auburn-1 (American Type Culture Collection VR-665), and three CCV isolates from epizootics in Mississippi were propagated in CCO cells. Viral stocks were generated by infection of confluent CCO monolayers and viral titers were determined by plaque assay on CCO cells (Stingley and Gray, 2000).

Fish infections.--Channel catfish were maintained at the Stuttgart National Aquaculture Research Center, ARS-USDA, in Stuttgart, AR. Immersion infection of 8-week old fish in 400 ml of water and immersion infection of 24-week old fish in 600 ml of water were performed with 10^7, 5 x 10^7, or 10^8 pfu of CCV for 30 min. Immersion infection of 1-year old fish was carried out in 2 liters of water with 4.5 x 10^7 pfu of CCV for 30 min. After initial immersion, fish were maintained in 30-gallon tanks at either 24° or 28° C. Fish that survived infection at 24-weeks old were maintained at the Stuttgart facility for more than 2 years post infection (p. i.).

Intraperitoneal (i. p.) injection was used to infect additional 1-year-old fish. The fish were anesthetized in 100 mg/l tricaine (3-aminobenzoic acid ethyl ester, Sigma Chemical Co.) prior to injection. Each fish was injected with 10^7, 10^4, or 10^3 pfu CCV in 100 µl EMEM, 2% FBS. Mock-infected fish were each injected with 100 µl EMEM, 2% FBS. Following infection, the fish were transferred to 30-gallon tanks and maintained at 28° C for seven to ten days.

Infectious virus assay.--Tissues (kidney and liver) were harvested and pooled in one ml EMEM, 2% FBS. The tissues were homogenized in the media and centrifuged to pellet cellular debris. Blood samples were not homogenized. Ten-fold serial dilutions of samples were applied to CCO monolayers. The cells were observed for ten days, and plaque formation, if any, was recorded.

CCV DNA detection in latently infected fish.--CCV latency in fish was confirmed by the ability to detect CCV DNA, but not infectious virus, in tissues. Total cell DNA was isolated from infected and mock-infected catfish tissues using the Wizard Genomic DNA Purification kit (Promega Corp.). Standard PCR conditions were generally used to detect CCV DNA in tissues of latently infected fish. CCV open reading frame (ORF) 3 primers (CCV genome nucleotides [nt] 4881 – 4899 and 5117 – 5136 (Davison, 1992) were designed to amplify a 256 bp PCR product from 0.5 – 1.0 µg DNA template in the 50-cycle reaction. Each cycle consisted of a denaturation step at 94° C for 1 min, annealing at 55° C for 2 min, extension at 72° C for 3 min, and a final extension at 72° C for 7 min. Amplification products were analyzed by UV illumination following electrophoresis through 1.0% agarose gels and ethidium bromide staining. To confirm the results, the DNA sequence of the PCR products was determined and demonstrated to be specific to CCV ORF 3.

Nested set PCR was required to detect CCV DNA in blood derived from latently infected fish at one year p. i. (Gray et al., 1999b). The nested-set PCR assay utilized primers within CCV open reading frame (ORF) 8. Initially "external" primers were used to amplify a 335 base pair (bp) product from 0.5 – 1.0 µg DNA template in a 50-cycle reaction using conditions as described above. Nested primers (nt 12646 – 12664 and 12801 – 12820) were employed in a subsequent reaction to generate a 175 bp product using 5 µl of the external reaction product as the template. For the nested-set PCR, 30 amplification cycles were used, each consisting of a denaturation step at 94° C for 1 min, annealing at 55° C for 3 min, extension at 72° C for 3 min, and a final extension at 72° C for 7 min. Amplification products were analyzed as described above.

Statistical analyses.--To compare the virulence of the Auburn-1 CCV strain to that of field isolates, the Kaplan-Meier estimates of the survivor distribution for each group were obtained and compared using the log rank Chi-square test. For all other survival experiments, the proportion surviving at the end of each experiment, rather than the entire curve, was used in statistical comparisons with the Fisher's Exact Test. A significance level of 5% was used to declare differences.

Results

Infection with CCV Auburn-1 strain and CCV field isolates.--The CCV Auburn-1 strain is the prototype laboratory CCV strain and has been passaged in culture for several years. To determine whether the CCV Auburn-1 is as virulent as three CCV field isolates, we compared survival rates of infected 24-week old catfish. In each tank, 20 fish were infected by immersion with 10^8 pfu of CCV and maintained at 28° C. Fish infected with the Auburn-1 strain and the CCV isolates exhibited clinical signs of CCV disease including aberrant swimming patterns and hemorrhagic lesions. The Auburn-1 strain was virulent with a 10 day survival rate (35%) that was not statistically different from the survival rates of the CCV isolates (15 to 30%) (Fig. 1).

Viral latency was examined in fish which survived

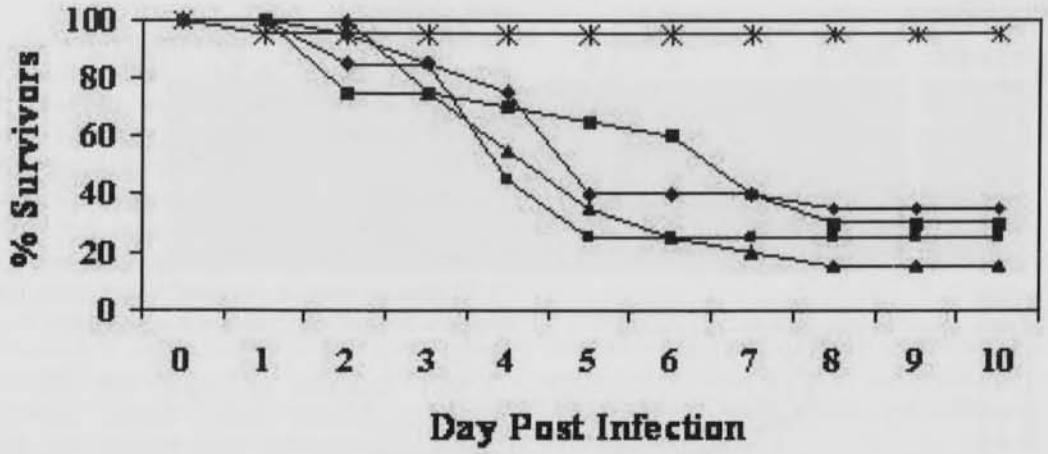

Fig. 1. Infection with CCV Auburn-1 strain is similar to that of field isolates. Survival rates are shown for channel catfish infected with Auburn-1 (diamonds), MS-1 (squares), MS-2 (triangles), MS-3 (circles) and mock-infected (*). Twenty fish in each group were infected with 10^8 pfu CCV or mock-infected by immersion in 400 ml of water for 30 min, then transferred to 30 gallon tanks and maintained at 28° C. Survival was monitored daily and mortalities were recorded. Employing Kaplan-Meier analysis, the test of equality had a p-value = 0.4417, indicating that there are no differences in the survival curves among the CCV strains.

experimental infection with Auburn-1 and the CCV isolates. At 27 days p. i., blood, kidney, and liver tissues were harvested and pooled from 3 fish infected with 10^7 pfu of the Auburn–1 strain or with each CCV isolate. Surviving fish were confirmed to have resolved the acute infection by the inability to detect infectious virus in the kidney and liver tissues by infectious virus assay. PCR analysis employing an ORF 3 primer set detected CCV DNA in blood samples of fish originally infected with the Auburn-1 strain and the CCV isolates (Fig. 2). The expected 256 bp PCR products were gel-purified and sequenced to confirm CCV specificity. Control PCR reactions using template DNA from the blood of mock-infected fish or no DNA template were negative (Fig. 2). These results demonstrated that the Auburn-1 laboratory strain and CCV field isolates cause acute disease in experimentally infected catfish and that survivors are latently infected by 27 days p. i. Subsequent experiments in this study used the Auburn-1 strain.

Parameters of experimental CCV infection.--To examine experimental parameters for CCV infection of channel catfish, we determined the effects of viral dose, fish age, and water temperature on survival rates of infected fish. In an effort to mimic natural infection as closely as possible, fish were infected by immersion in water containing specific doses of Auburn-1 CCV. Two sets of fish, 8-week old and 24-week old, were immersion-infected with 10^7, or 5×10^7 pfu of CCV at 24° or 28° C and monitored daily. Fish that died exhibited signs of CCV disease.

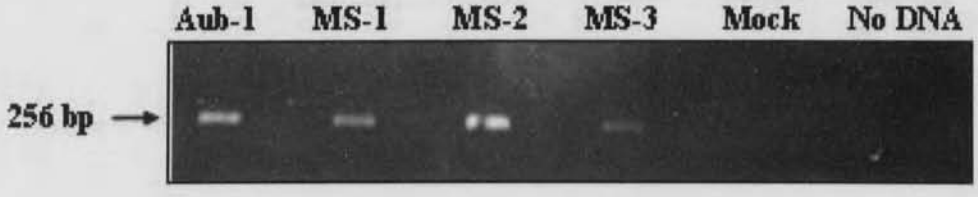

Fig. 2. Detection of CCV DNA in the blood of fish latently infected with Auburn-1 and three CCV field isolates (MS-1, MS-2, and MS-3). DNA was isolated and pooled from three infected fish and from three mock-infected fish at 27 days p. i. CCV IE 3 gene primers were used in 50-cycle PCR to detect the expected 256 bp CCV DNA amplification product upon agarose gel electrophoresis and ethidium bromide staining. Control reactions employing DNA isolated from blood of mock-infected fish and reactions which included no DNA template were included.

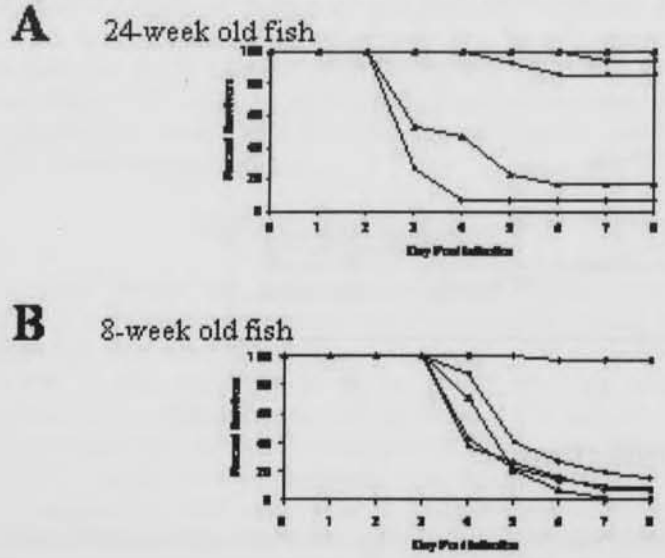

Fig. 3. Effects of age and temperature on the survival rate of CCV-infected channel catfish. Survival rates are shown 24-week old (A) and 8-week old (B) channel catfish infected with 10^7 (triangles) and 5 x 10^7 (circles) pfu CCV or mock-infected (diamonds). Each group included at least 32 fish). Infections were conducted at 24° C (open symbols) or 28°C (solid symbols). Fish were monitored and mortalities were recorded on the various days p. i.

Water temperature had a dramatic effect on the survival rate of 24-week old fish. At 24° C, 100% and 86% of 24-week old fish survived infection at 10^7 and 5 x 10^7 pfu, respectively, whereas only 17% and 7% survived infection with similar doses at 28° C (Fig. 3A). The temperature effect at both viral doses was highly significant ($p < 0.0001$) in 24-week old fish.

In contrast, this temperature effect was not observed with 8-week old fish. At 24° C, only 1% and 15% of 8-week old fish survived infection at 10^7 and 5 x 10^7 pfu, respectively, whereas at 28° C, 8% and 6% of 8-week old fish survived similar infection (Fig. 3B). No significant differences between survival rates at the two temperatures were observed at either viral dose ($p < 0.05$). The results indicate that 24-week old fingerlings were susceptible to CCV disease only at elevated water temperatures, but the younger 8-week old fish were susceptible at either 24°C or 28°C.

CCV infection of 1-year old fish.--During CCV epizootics, juvenile channel catfish exhibit symptoms of CCV disease; however, adult fish are more resistant to acute disease (Plumb, 1978; Hedrick et al., 1987). To determine whether 1-year old fish could be acutely infected with CCV, we compared survival rates in fish infected by immersion with fish infected by intraperitoneal (i. p.) injection.

Twelve 1-year old fish were i. p. injected with 100 µl EMEM, 2% FBS alone (mock-infected), or containing 10^3, 10^4, or 10^7 pfu CCV. Mock-infected fish had a 92% survival rate, whereas fish infected with 10^3, 10^4, and 10^7 pfu CCV had survival rates of only 40%, 25% and 0%, respectively (Fig. 4). As expected, yearling fish infected via immersion with 4.5 x 10^7 pfu CCV had a significantly higher survival rate. Only two of the eight fish infected by immersion did not survive (Fig. 4).

We next determined whether or not 1-year old fish infected by immersion develop latent infection despite the lack of acute disease development. Blood, kidney, and liver samples were harvested from 3 individual fish at 107 days p. i. Infectious virus assays performed on CCO monolayers confirmed that infectious CCV could not be detected in the

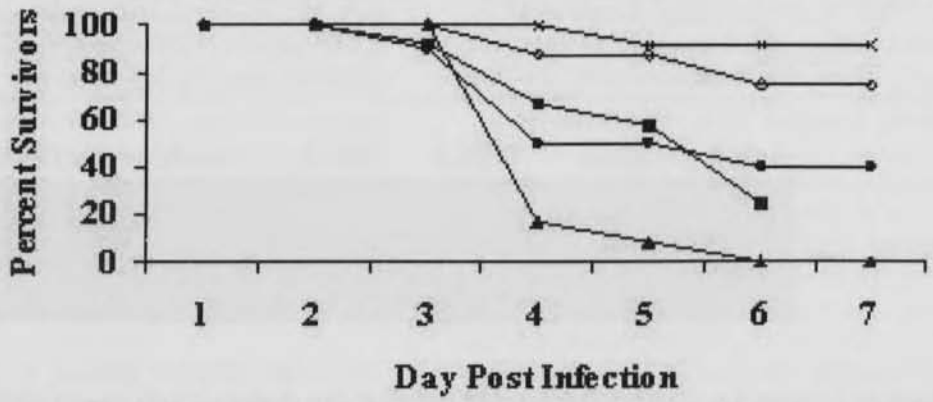

Fig. 4. CCV infection of 1-year old channel catfish. The survival rates are shown for fish that were immersion-infected with 4.5 x 10^7 pfu CCV (open diamonds) or i. p. infected with 10^3 (solid circles), 10^4 (solid squares), or 10^7 pfu i. p. (solid triangles) ptu CCV. Control fish were injected i.p. with an equivalent amount of EMEM, 2%FBS(X) on day 6 p.i., the standpipe in the tank containing fish infected with 10^4 i.p. was dislodged and all remaining fish were lost. Fish were monitored and mortalities were recorded on the various days p. i.

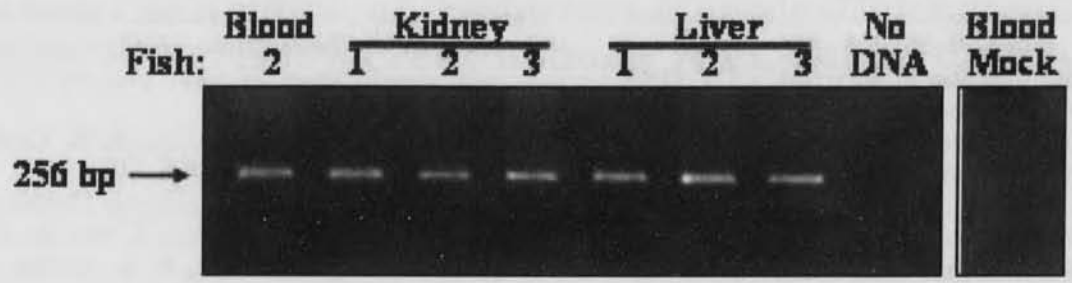

Fig. 5. Detection of CCV DNA in tissues of one year-old fish infected by immersion. DNA was isolated and pooled from the blood, kidney, and liver of three infected fish at 107 days p. i. and from the blood of three mock-infected fish. CCV IE 3 gene primers were used in 50-cycle PCR to amplify the expected 256 bp product upon agarose gel electrophoresis and ethidium bromide staining. Controls reactions using no DNA template were included.

kidney or blood of these fish. Total cell DNA isolated from the tissues served as template for PCR analysis utilizing the ORF 3 primer set. CCV DNA was detected in the blood, kidney, and liver tissues from the infected fish, but not in blood from mock-infected fish or reactions omitting the DNA template (Fig. 5). The results demonstrate that viral latency can be established in fish infected as adults.

Long-term persistence of latency following experimental CCV infection.--CCV latency is established as early as 27 days p. i. (Fig. 2). In this study, we determined whether or not viral latency is maintained for as long as one year following experimental CCV infection. Twenty-four week old fish were infected with 1 x 10^7 pfu CCV at 24° or 28° C (Fig. 3A). At one year p. i., total cell DNA was isolated from blood of surviving fish. Standard PCR employing ORF 8 external primers did not detect CCV DNA in the blood samples (Fig. 6). However, CCV DNA was detected in the blood of each of five latently infected fish examined using ORF 8 nested set PCR. CCV DNA was not detected in blood of mock-infected fish.

Discussion

This study describes an experimental model of CCV infection of channel catfish, focusing on immersion-infection to simulate conditions of natural infection. A particular advantage of this study is the use of channel catfish that were confirmed to be uninfected prior to experimental infection. Previous studies employing experimental infection of channel catfish have used fish populations with no history of CCV (Plumb et al., 1981; Hedrick et al., 1987; Nusbaum and Grizzle, 1987). However, CCV DNA has been detected in fish populations with no known exposure to CCV, indicating latent CCV infection in these fish (Wise et al.,1985). The channel catfish population used in this study has been maintained at the Stuttgart National Aquaculture Research Center without exposure to CCV. This fish population is not latently infected as confirmed by PCR analysis (Gray et al., 1999b).

The Auburn-1 strain is the prototype laboratory strain commonly used in experimental analysis of CCV. This

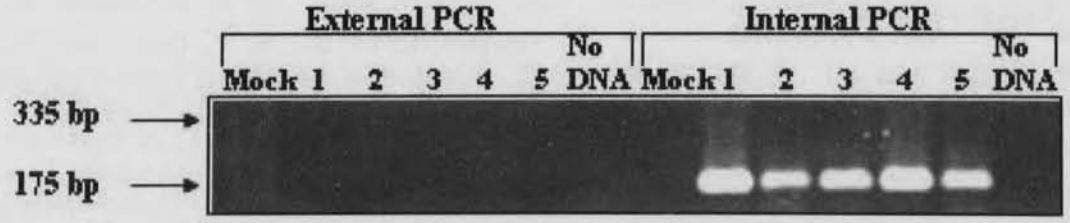

Fig. 6. Detection of CCV DNA in fish blood at one year p. i. 24-week old fish were experimentally infected by immersion with CCV. At one year p. i., total cell DNA was isolated from the blood of 5 surviving infected fish (1-5) and from mock-infected fish. PCR employing CCV ORF 8 external primers did not reveal the expected 335 bp product upon agarose gel electrophoresis. Nested-set PCR employing CCV ORF 8 internal primers amplified the expected 175 bp CCV DNA. Control reactions using DNA template from mock-infected fish or using no DNA template were included.

study confirmed that the laboratory strain is useful in mimicking natural infection. Similar to CCV field isolates, the Auburn-1 strain induced acute disease in infected fish and established latent infection in survivors. CCV DNA could be detected in the blood of latently infected fish as early as 27 days p. i. and as late as one year p. i., indicating rapid establishment and long-term persistence of viral latency.

The age of fish and water temperature effect the susceptibility of channel catfish to natural CCV infection, as evident by the fact that CCV outbreaks cause disease in juvenile catfish and occur when water temperatures exceed 25°C (Plumb, 1977, 1978). Our results support these findings and indicate that these factors also effect susceptibility during experimental infections. The 24-week old catfish were dramatically more susceptible to disease at the higher water temperature (28° C). In contrast, the 8-week old fish were susceptible to disease when infected at 24° C or 28° C. It is possible that a temperature effect on disease in 8-week old fish might be revealed by exposure to lower viral doses.

Adult catfish are more resistant to CCV infection than fry and fingerlings and do not generally develop acute CCV disease during epizootics. In our experimental model, yearling catfish were less susceptible to CCV disease than fingerlings upon immersion infection. Yearling fish are not innately resistant, as acute CCV disease could be induced by i.p. infection at relatively low doses. In the absence of acute disease following immersion infection, one-year old fish developed latent infection, as demonstrated by detection of viral DNA in the tissues by 107 days p. i. The implication is that during CCV outbreaks older fish may not die, but become latently infected and serve as a source for long term viral persistence in the population.

ACKNOWLEDGMENTS.—This study was supported by Cooperative State Research, Education, and Extension Service Grant 96-35204-3852 from the United States Department of Agriculture and from a grant from the UAMS Graduate Student Research Fund.

Literature Cited

Anonymous. 1997. USDA National Animal Health Monitoring System. Part1: Reference of 1996 U.S. catfish health and production practices. United States Department of Agriculture, Animal and Plant Health Inspection Service, Veterinary Services, National Animal Health Monitoring System, Publication N235.497

Anonymous. 2003. Catfish Production. National Agricultural Statistics Report of Feb. 6, 2003. United States Department of Agriculture.

Buck, C. 1990. Channel catfish virus- a review. ATCC Quart. Newsletter 3:1-2.

Davison, A. J. 1992. Channel catfish virus: A new type of herpesvirus. Virology 186:9-14.

Dixon, R. A. F., and **F. E. Farber.** 1980. Channel catfish virus: Physiochemical properties of the viral genome and identification of viral polypeptides. Virology 103:267-278.

Gray, W. L., R. J. Williams, and **B. R. Griffin.** 1999a. Detection of channel catfish virus DNA in acutely infected catfish, *Ictalurus punctatus* (Rafinesque), using the polymerase chain reaction. J. Fish Dis. 22:111-116.

Gray, W. L., R. J. Williams, R. L. Jordan, and **B. R. Griffin.** 1999b. Detection of channel catfish virus DNA in latently infected catfish. J. Gen. Virol. 80:1817-1822.

Hedrick, R. P., J. M. Groff, and **T. McDowell.** 1987. Response of adult channel catfish to waterborne exposures of channel catfish virus. Prog. Fish Cult. 49:181-187.

Huang, S. M., and **L. A. Hanson.** 1998. Temporal gene regulation of the channel catfish virus (Ictalurid herpesvirus 1). J. Virol. 72:1910-1917.

Nusbaum, K. E., and **J. M. Grizzle.** 1987. Uptake of channel catfish virus from water by channel catfish and bluegills. Am. J. Vet. Res. 48:375-377.

Plumb, J. A. 1971. Tissue distribution of channel catfish virus. J.Wildlife Dis. 7:213-216.

Plumb, J. A. 1977. Channel catfish virus disease. Fish Dis. Leaflet 52, U.S. Dept. of Interior.

Plumb, J. A. 1978. Epizootiology of channel catfish virus disease. Mar. Fish. Rev. 40:26-29.

Plumb, J. A., R. L. Thune, and **P. H. Klesius.** 1981. Detection of channel catfish virus in adult fish. Dev. Biol. Stand. 49:29-34.

Silverstein, P. S., R. C. Bird, V. L. Van Santen, and **K. E. Nusbaum.** 1995. Immediate-early transcription from the channel catfish virus genome: Characterization of two immediate-early transcripts. J. Virol. 69:3161-3166.

Silverstein, P. S., V. L. Van Santen, K. E. Nusbaum, and **R. C. Bird.** 1998. Expression kinetics and mapping of the thymidine kinase transcript and an immediate-early transcript from channel catfish virus. J. Virol. 72:3900-3906.

Stingley, R. L., and **W. L. Gray.** 2000. Transcriptional regulation of the channel catfish virus genome direct repeat region. J. Gen. Virol. 81:2005-2010.

Wise, J. A., P. R. Bowser, and **J. A. Boyle.** 1985. Detection of channel catfish virus in asymptomatic adult channel catfish, *Ictalurus punctatis* (Rafinesque). J. Fish Dis. 8:485-493.

Wolf, K., and **R. W. Darlington.** 1971. Channel catfish virus: a new herpesvirus of ictalurid fish. J. Virol. 8:525-533.

Wolf, K., R. L. Herman, and **C. P. Carlson.** 1972. Fish viruses: histopathologic changes associated with experimental channel catfish virus disease. J. Fish Res. Board of Canada 29:149-150.

GENERAL NOTES

Status and Distribution of Freshwater Mussels (Unionacea) Inhabiting the Saline River/Holly Creek Bottoms Area, Saline County, Arkansas

Chris L. Davidson*
200 Hazelwood Drive
Sheridan, AR 72150

Dave Gosse
The Nature Conservancy
601 N. University Avenue
Little Rock, AR 72205

*Corresponding Author

Abundance and diversity of freshwater mussels (Bivalvia: Unionacea) have been declining for the past 40 years throughout North America (Williams et al., 1993). The Nature Conservancy (TNC) has recognized 55% of North American freshwater mussels as extinct or imperiled (Master, 1990). Harris et al. (1997) recommended 22 of the 75 (29%) freshwater mussel species considered native to Arkansas for conservation status listing. Eight species are listed as federally endangered, and one is listed as federally threatened.

The Saline River begins on the east end of the Ouachita Mountains as four distinctive branches (South, North, Middle, and Alum forks). These waters converge north of Benton, Arkansas, just before the Saline River enters the Gulf Coastal Plain. The Saline River flows southward before reaching its confluence with the Ouachita River near the Arkansas-Louisiana state line. The river basin is gently rolling, and some lands adjacent to larger streams are swampy. Substrates range from cobble to gravel, sand and clayey silt in a riffle-pool environment. The total drainage basin at the Saline River/Holly Creek Bottoms Area is 223 km^2 (USGS, 1979).

The upper Saline River is one of the last major undammed rivers in the Ouachita River drainage. Arkansas Department of Environmental Quality (ADEQ) has designated the headwaters of the Saline River as an Ecologically Sensitive Waterbody. This designation provides additional protection to waterbodies known to provide habitat for endangered, threatened, or endemic species. The remainder of the Saline River is designated as an Extraordinary Resource Waterbody due to a combination of chemical, physical and biological characteristics that is characterized by scenic beauty, aesthetics, scientific values, recreation potential, and intangible social values. TNC also recognizes this segment of the Saline River as an ecoregional priority for conservation.

Davidson and Clem (2002) reported 42 species as a component of the Saline River unionid fauna, with an additional four species as a possible component. Headwater reaches of the Saline River to near Benton, Arkansas have been adequately surveyed (Harris and Gordon, 1988; Brown and Brown, 1989; U.S. Fish and Wildlife Service, 1990; U.S. Fish and Wildlife Service, 1992; Burns and McDonnell, 1992a, 1992b). Davidson and Clem (2002) surveyed 158.8 km of the Saline River from Tull, Arkansas to Arkansas Highway 15 near Warren, Arkansas. Davidson (1997) surveyed the lower 18 km of the Saline River that lies within the boundary of Felsenthal National Wildlife Refuge. A few unionid records exist for highway crossings (John Harris, pers. comm.) on the Saline River. Unsurveyed portions of the Saline River in Arkansas include a short stretch from Benton to Tull and Arkansas Highway 15 near Warren to Felsenthal National Wildlife Refuge.

The study area lies within the Saline River/Holly Creek Bottoms Area. The Holly Creek watershed comprises upland and bottomland forests along the Saline River and Holly Creek. Mature bottomland hardwoods are the dominant trees of the forest bordering the Saline River. There are two pasture locations on both sides of the river near the confluence of Holly Creek. Land bordering the Saline River is privately owned and consists of bottomland hardwoods and pastures.

The objective of this survey was to document species composition, size distribution, approximate abundance of mussel concentrations, population and community estimates in mussel beds, and location of mussel beds and concentrations. Results will provide baseline information on the status of the mussel fauna inhabiting the Holly Creek Loop in the Saline River. Data derived may be added to an Arkansas Game & Fish Commission (AGFC) mussel database. These data will allow the development of management strategies for the protection of this mussel community.

A field survey for preliminary site assessment was conducted 29 September 2001. The study area begins in the Saline River at the upstream portion of a braided channel (Sec. 26; R15W; T2S); for the purposes of this report the study area is termed the "Holly Creek Loop Area" and extends approximately 4 km downstream to the "Haskell Bridge" (Sec. 36; R15W; T2S). The entire study area was

Table 1. Mussels collected during qualitative searches of mussel beds and concentrations, approximate concentration area (m^2) and approximate density of concentrations in the Holly Creek Loop, Saline River, Arkansas.

Scientific name	B1	B2	C1	C2	C3	Total
Actinonaias ligamentina	12	25	21	28	31	120
Amblema plicata	11	3	7	0	1	22
Cyprogenia aberti	2	0	0	0	0	2
Elliptio dilatata	5	4	0	0	1	10
Fusconaia ebena	2	1	2	2	1	8
Fusconaia flava	1	2	5	0	0	8
Lampsilis cardium	3	3	6	3	1	16
Lampsilis hydiana	0	0	2	1	0	3
Lampsilis ornata	0	1	0	0	0	1
Lampsilis powelli	0	1	2	0	0	3
Lampsilis teres	0	0	1	0	0	1
Lasmigona costata	1	2	0	1	4	8
Ligumia recta	1	3	2	0	0	6
Obliquaria reflexa	0	0	1	0	0	1
Pleurobema rubrum	R*	0	0	0	0	0
Potamilus purpuratus	1	0	2	0	0	3
Ptychobranchus occidentalis	4	3	9	6	1	23
Quadrula metanevra	1	0	0	0	3	4
Quadrula pustulosa	3	3	7	0	2	15
Strophitus undulatus	0	2	1	1	0	4
Truncilla truncata	0	0	1	0	0	1
Truncilla donaciformis	1	0	0	0	0	1
Tritogonia verrucosa	1	0	2	0	0	3
Villosa lienosa	0	0	1	0	0	1
Total Individuals	49	56	72	42	45	264
Number of Species	16	13	17	7	9	24
Approximate Area (m^2)	**	**	120	30	80	230
Approximate Density (#/m^2)	**	**	6	8	6	

* R = Relict; ** Defined during quantitative analysis (see Tables 2 and 3)

surveyed for the presence of mussel resources. Due to the presence of shallow shoals, snorkeling and wading techniques were utilized to survey this segment of the Saline River. Quantitative sampling of two mussel beds identified during the preliminary site assessment was conducted on 6 June 2002.

The entire survey area was traversed in an upstream to downstream fashion to locate mussel concentrations and beds. Once mussel resources were located, bed dimensions were determined and a timed search was conducted to establish species composition and approximate abundance. Concentrations and beds were searched for 2/3 to 1 man-hour (m-h). Mussels were hand picked, bagged, identified and enumerated, and then returned to the substrate. Federally endangered and threatened species were photographed to verify identification.

Summary statistics including mean, minimum, maximum, standard deviation (SD), variance and sum were calculated for each stratum and for the entire data set. Quantitative estimates were made using the Sampford method (Huebner et al., 1990) and are outlined in Harris et al. (1993).

Mussel concentrations and beds were generally located in two physical settings: 1) riffle/run areas or 2) along descending banks immediately upstream of riffle/run areas. Mussels were located in water depths, at low flow conditions, ranging from approximately 15 cm to 1 m. Mussels were most often associated with gravel/sand. In some areas, dense mats of algae covered the gravel. Mussels in these areas appeared to be migrating upward from the gravel/sand substrate into the algal mats, which acted as sediment traps. Pools were generally devoid of mussels.

Table 2. Physical parameters, species composition and population and community estimates for Mussel Bed 1 (Unionacea) in the Saline River/Holly Creek Bottoms Area, Arkansas, 2002.

Location: Mussel Bed 1, Head of riffle, NE 1/4 SW 1/4 S25, T2S, R15W, Saline Co.
Latitude: 34.517841, Longitude: -92.567141
Stratum Size: 7 m x 12 m = 84 m^2
Substrate: Gravel
Total Samples: 5
Minimum - Maximum density (#/m^2): 4.0 - 22.0
Mean density #/m^2 (Standard deviation): 11.8 (6.8)

Species	Number Collected	Percent of Total	Population Estimate
Actinonaias ligamentina	24	41.4	403±446
Amblema plicata	2	3.4	34±55
Cyprogenia aberti	1	1.7	17±45
Elliptio dilatata	7	12.1	118±152
Fusconaia ebena	2	3.4	34±90
Fusconaia flava	2	3.4	34±90
Lampsilis cardium	2	3.4	34±90
Lasmigona costata	1	1.7	17±45
Ptychobranchus occidentalis	4	6.9	67±84
Quadrula pustulosa	7	12.1	118±90
Strophitus undulatus	5	8.6	84±123
*Villosa arkansasensis**	1	1.7	17±45
Totals	59	99.8	991±683

*Represents species not found during preliminary searches within study area

Twenty-seven species of unionids were found within the study area (Tables 1 - 3). *Actinonaias ligamentina* was dominant, accounting for 46% of the live mussels examined during preliminary searches. Numerous gravid individuals of *A. ligamentina* and *Lampsilis cardium* were observed within the study area. *Amblema plicata, L. cardium, Ptychobranchus occidentalis*, and *Quadrula pustulosa* collectively comprised 29% of the live mussels.

Mussel concentrations were defined as areas with > 0 and <10 mussels/square meter (m^2). Three mussel concentrations were identified within the survey reach (C1: Latitude 34.509686, Longitude -92.566872; C2: Latitude 34.507894, Longitude -92.567352; C3: Latitude 34.504136, Longitude -92.569044). Approximate area of mussel concentrations ranged from 30 to 120 m^2. A total of 159 specimens from three mussel concentrations found in the Holly Creek Area included 20 species (Table 1). Approximate mean abundance ranged from 5 to 8 mussels/m^2. *Actinonaias ligamentina* was dominant in each mussel concentration. Two *Lampsilis powelli*, a federally threatened species, were found in Mussel Concentration 1.

Mussel beds were defined as areas with ≥10 mussels/m^2 and > 50 m^2. Collections from two mussel beds made during preliminary searches consisted of 105 live individuals and included 19 species (Table 1), of which *Actinonaias ligamentina* (40%) numerically dominated live individuals. *Pleurobema rubrum* was found only as a relict. One individual of *Lampsilis powelli* was found in Mussel Bed 2. Two individuals of *Cyprogenia aberti*, a state special concern species, were found in Mussel Bed 1.

Sixteen 1-m^2 samples yielded 242 individuals. Mean density was 11.8 and 16.6 mussels/m^2 for Mussel Beds 1 and 2, respectively. Total bed area was 84 m^2 and 203 m^2 for Mussel Beds 1 and 2, respectively. *Actinonaias ligamentina* was the dominant species in both mussel beds. The second-most dominant species in each mussel bed was *Elliptio dilatata*. Estimated community numerical standing crop was 991±683 and 3,357±1,163 mussels per bed for Mussel Beds 1 and 2, respectively (Tables 2 and 3).

Shell dimensions were calculated for each species encountered during quantitative analysis of mussel beds (Table 4). No specimens were of legally harvestable size

Table 3. Physical parameters, species composition and population and community estimates for Mussel Bed 2 (Unionacea) in the Saline River/Holly Creek Bottoms Area, Arkansas, 2002.

Location: Mussel Bed 2, Riffle/run at head of braided channel, NE1/4 SW1/4 S25, T2S, R15W, Saline Co., Latitude: 34.515836, Longitude: -92.569088
Stratum Size: 1.) 8 m x 1 m = 128 m^2
2.) 5 m x 15 m = 75 m^2
Substrate: Gravel
Total Samples: 12
Minimum - Maximum density (#/m^2): 0.0 - 26.0
Mean density #/m^2 (Standard deviation): 1.) 14.9 (10.0)
2.) 15.8 (7.9)

Species	Number Collected	Percent of Total	Population Estimate
Actinonaias ligamentina	75	41.0	1,386±720
Amblema plicata	10	5.5	185±136
Alasmidonta marginata	1	0.5	19±40
Cyprogenia aberti	4	2.2	74±87
Elliptio dilatata	17	9.3	314±147
Fusconaia ebena	6	3.3	110±93
Fusconaia flava	6	3.3	110±85
Fusconaia/Pleurobema complex*	9	4.9	166±110
Lampsilis cardium	6	3.3	110±103
Lampsilis hydiana	1	0.5	18±39
Lampsilis powelli	1	0.5	19±40
Lasmigona costata	6	3.3	111±123
Ligumia recta	3	1.6	56±57
Ptychobranchus occidentalis	12	6.6	222±107
Potamilus purpuratus	1	0.5	18±39
Quadrula metanevra	4	2.2	74±87
Quadrula pustulosa	14	7.7	258±164
Strophitus undulatus	2	1.1	37±50
Truncilla truncata	4	2.2	73±55
Tritogonia verrucosa	1	0.5	18±39
Totals	183	100.0	3,357±1,163

* Represents species not found during preliminary searches within study area

based on size restrictions set by the AGFC.

Shells of mussels surveyed in this study appeared to be characteristic of mature populations. The presence of gravid females of several species suggested reproduction might be occurring within these populations. However, the only apparent juvenile encountered was one *Ligumia recta*. There is a need for information on size at onset of sexual maturity for mussels in the Saline River basin. This information could contribute to multi-phase management schemes, such as monitoring population dynamics, suggested by Christian et al. (2000). Future studies should investigate life history characteristics including drainage-specific growth (Christian et al., 2000) and age at sexual maturity.

The introduced Asian Clam, *Corbicula fluminea,* was found throughout the present study area. This species has invaded nearly every major river system in the United States since its introduction sometime during or before the 1920's.

One federally listed threatened species, *Lampsilis powelli*, was encountered during this survey from two new locations. *Lampsilis powelli* is an Arkansas endemic species known to occur in the four forks of the Saline River,

Table 4. Mean ($\bar{x}$) and standard deviation measurements for mussel species from Mussel Bed 1 and 2 in the Saline River/Holly Creek Bottoms Area, Arkansas, 2002.

Species	(N)	($\bar{x}$) length (mm)	S	($\bar{x}$) depth (mm)	S	($\bar{x}$) width (mm)	S
A. ligamentina	99	74.1	12.9	47.7	7.9	30.5	5.4
A. plicata	12	74.7	13.4	53.9	7.0	33.9	4.6
A. marginata	1	65.2	na[1]	33.3	na	31.7	na
C. aberti	5	48.2	19.5	38.8	2.4	24.8	1.0
E. dilatata	24	58.4	8.7	30.5	5.4	17.3	3.2
F. ebena	8	43.7	10.2	37.0	8.6	22.7	4.2
F. flava	8	41.0	14.6	32.3	10.0	23.0	7.6
F./P. complex[2]	9	49.9	5.0	38.8	4.7	27.0	3.6
L. cardium	8	80.4	13.1	52.5	5.9	39.0	5.5
L. hydiana	1	63.4	na	37.2	na	24.3	na
L. powelli	1	88.9	na	48.2	na	36.5	na
L. costata	7	97.2	16.2	49.2	7.0	26.6	4.2
L. recta	3	108.7	23.2	45.7	10.9	29.9	8.9
P. occidentalis	16	66.0	13.2	33.4	6.7	20.5	5.2
P. purpuratus	1	39.5	na	26.2	na	16.2	na
Q. metanevra	4	69.2	8.1	46.6	2.4	38.0	5.3
Q. pustulosa	21	49.3	8.4	40.7	8.2	27.7	4.0
S. undulatus	7	45.7	19.4	27.4	10.2	17.1	8.2
T. truncata	4	46.1	3.6	32.4	1.5	22.4	1.8
T. verrucosa	1	53.3	na	32.8	na	17.9	na
V. arkansasensis	1	29.8	na	18.8	na	12.9	na

[1]na = not applicable
[2]*F./P.* complex = *Fusconaia/Pleurobema* complex

mainstem Saline River upstream of Arkansas Highway 270, the Caddo River, the South Fork Ouachita River, and upper mainstem Ouachita River. *Cyprogenia aberti* and *Villosa arkansasensis*, considered imperiled globally by TNC and of Special Concern in Arkansas (Harris et al., 1997), were found within the surveyed area. Mussels exist in areas where the substrate and environmental conditions permit, but these areas are small and subject to natural or anthropogenic disturbances. Management strategies should concentrate on maintaining the quantity and/or quality of habitat throughout the study area in order to sustain viable populations.

As an ecoregional priority, TNC's prospective management activities for the Saline River (including Holly Creek Bottoms) will follow a site conservation plan and will include terrestrial community assessment and monitoring. Assessment, including the results of this study, will promote the identification of key areas such as mussel beds and concentrations and encourage recruitment of landowners or potential partners interested in compatible ecological management options. Conservation and protection of mussel resources on the Saline River may involve runoff reductions streambank stabilization, pollution control and compatible land use promotion.

In order to successfully develop long-term management for rare species populations, qualitative and quantitative monitoring of freshwater mussel populations must be conducted and tailored for target mussel species. Size and distribution data of mussel populations from the Holly Creek Loop could provide the basis for formulation of management strategies to protect reproductive mussels within the Saline River. The information obtained from monitoring activities will establish baseline data that will be used to modify future stewardship activities.

Protection or improvements in the status of mussels in the Holly Creek Loop of the Saline River require proper management of the watershed and cooperative efforts of stakeholders. Private landowners, and personnel from Aluminum Company of America (Alcoa), TNC, AGFC and ADEQ should consider efforts to stabilize existing habitats (i.e. stream bank stabilization projects) and sustain exceptional water quality. Execution of these management

strategies should improve and/or sustain the quality and quantity of vegetative cover in riparian zones, decrease siltation and subsequently improve habitat quality for mussels.

Alcoa provided access to the survey area via a gated road (Sec. 25; R15W; T2S).

Literature Cited

Brown, A. V., and **K. B. Brown.** 1989. Stream inventory of *Lampsilis powelli* populations on national forest lands. A report to the U.S.D.A. Forest Service, Ouachita National Forest, Hot Springs. 28 pp + Appendices.

Burns & McDonnell, Inc. 1992a. Distribution of the Arkansas fatmucket mussel (*Lampsilis powelli*) in the North Fork of the Saline River. Prepared for Hope Engineers, Benton, AR.

Burns & McDonnell, Inc. 1992b. Report on surveys for the Arkansas fatmucket mussel. Prepared for Hope Engineers and the Saline County Rural Development Authority, Benton, AR.

Christian, A. D., C. L. Davidson, W. R. Posey II, P. J. Rust, J. L. Farris, J. L. Harris, and **G. L. Harp.** 2000. Growth curves of four commercially valuable freshwater mussels (Bivalvia: Unionidae) in Arkansas. J. Arkansas Acad. Sci. 54:41-50.

Davidson, C. L. 1997. Analysis of mussel beds in the Little Missouri and Saline rivers, Blue Mountain, Ozark and Dardanelle lakes, Arkansas. Unpubl. M.S. Thesis. Arkansas State University. 156 pp.

Davidson, C. L., and **S. A. Clem.** 2002. The freshwater mussel resources in a selected segment of the Saline River: location, species composition and status of mussel beds. Prepared for The Nature Conservancy – Arkansas Field Office and Arkansas Game and Fish Commission. 30 pp. + Appendices.

Harris, J. L., and **M. E. Gordon.** 1988. Status survey of *Lampsilis powelli* (Lea, 1852). Prepared for the U.S. Fish and Wildlife Service, Office of Endangered Species, Jackson, MS. 44 pp. + Appendices.

Harris, J. L., P. J. Rust, S. W. Chordas, III, and **G. L. Harp.** 1993. Distribution and population structure of freshwater mussels in Lake Chicot, Arkansas. Proc. Arkansas Acad. Sci. 47:38-43.

Harris, J. L., P. J. Rust, A. C. Christian, W. R. Posey II, C. L. Davidson, and **G. L. Harp.** 1997. Revised status of rare and endangered Unionacea (Mollusca: Margaritiferidae, Unionidae) in Arkansas. Proc. Arkansas Acad. Sci. 51:66-89.

Huebner, J. D., D. F. Malley, and **K. Donkersloot.** 1990. Population ecology of the freshwater mussel *Anodonta grandis grandis* in a Precambrian shield lake. Can. J. Zool. 68:1931-1941.

Master, L. 1990. The imperiled status of North American aquatic animals. Biodiversity Network News 3:1-2, 7-8.

U. S. Fish and Wildlife Service. 1990. Endangered and threatened wildlife and plants; threatened status for the Arkansas fatmucket, *Lampsilis powelli*. Federal Register 55(66):12797-12801.

U. S. Fish and Wildlife Service. 1992. Arkansas fatmucket mussel (*Lampsilis powelli*) recovery plan. U.S. Fish and Wildlife Service, Jackson, MS. 19 pp.

U. S. Geological Survey. 1979. Drainage areas of streams in Arkansas in the Ouachita River Basin. Open file report. Little Rock, AR. 87 pp.

Williams, J. D., M. L. Warren, Jr., K. S. Cummings, J. L. Harris, and **R. J. Neves.** Conservation status of freshwater mussels of the United States and Canada. American Fisheries Society 18:6-22.

Gyratrix hermaphroditus: A State Record For Arkansas

Jane Dunn
Department of Biology
Henderson State University
Arkadelphia, AR 71999

Gyratrix hermaphroditus (Platyhelminthes, Rhabdocoela) was collected from Magnolia Manor in Clark County near Arkadelphia on 3 January 2003, constituting a new geographic distribution record for the state of Arkansas. This pond has been routinely sampled for microturbellarians since September 2001, but this was the first individual of this species observed. Magnolia Manor pond is approximately 40 years old, is surrounded by a mixture of pine and hardwoods, and has a mature stand of Asiatic lotus (*Nelumbo nucifera*) covering about 80% of the pond. The pond is approximately 50 m in diameter and 1.245 to 2 m deep at the deepest point. The substrate is silty and covered with a layer of fallen leaves and other detritus. *Gyratrix* was collected using a zooplankton net dragged along the bottom. Multiple samples were collected to include the debris stirred by the action of the net. A sample of one liter was collected, taken to the laboratory, and allowed to settle for two hours. After settling, 5 ml of bottom silt and water were placed in a watch glass and observed with a dissection microscope. Individual worms were transferred to a microscope slide for further observation utilizing a compound microscope. As fixation methods tend to destroy the epidermis or distort the location and size of the internal organs, this microturbellarian was observed and photographed alive. Chromosome numbers were not determined. Voucher specimens are in preparation to be deposited in the Queensland Museum, Brisbane, Australia.

Gyratrix hermaphroditus is well studied in contrast to many microturbellarians. Kolasa (1991) states that there are about 400 species of freshwater microturbellarians, but only 150 species have been recorded in the United States. Most freshwater microturbellarians are less than 1 mm in length, which causes them to be overlooked (Kolasa, 1991). Previous research indicates that freshwater *G. hermaphroditus* has one pair of dark brown eye spots set about the end of the first one third of the body, but some eyeless marine specimens have been described (Artois et al., 2000). A proboscis is situated anteriorly to the eyes. The mouth and pharynx rosulatus are located midventrally. The intestine, which is covered on the dorsal side by vitellaria, reaches both anteriorly and posteriorly from the mouth. The reproductive system is located in the posterior fifth of the body. The male reproductive system consists of a single testis (Fig. 1) on the side opposite the ovary, and a stylet with a sheath at the very posterior end of the animal (Fig. 2). The stylet can be used as a means of food capture (Kolasa, 1991). The female reproductive system consists of a single ovary and a large, dispersed vitteline (yolk gland) system. The nephridia are located laterally in the posterior end of the animal.

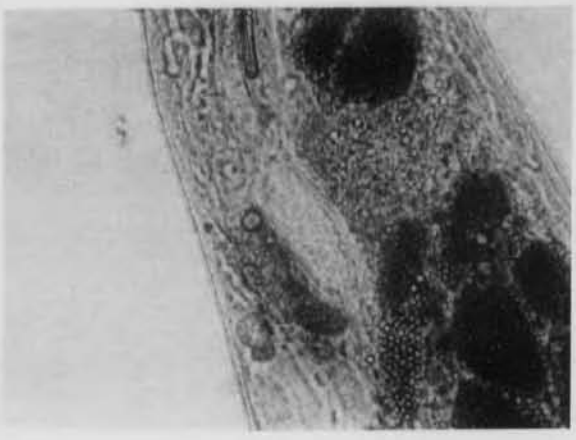

Fig. 1. Testis – *Gyratrix hermaphroditus* (1,000x).

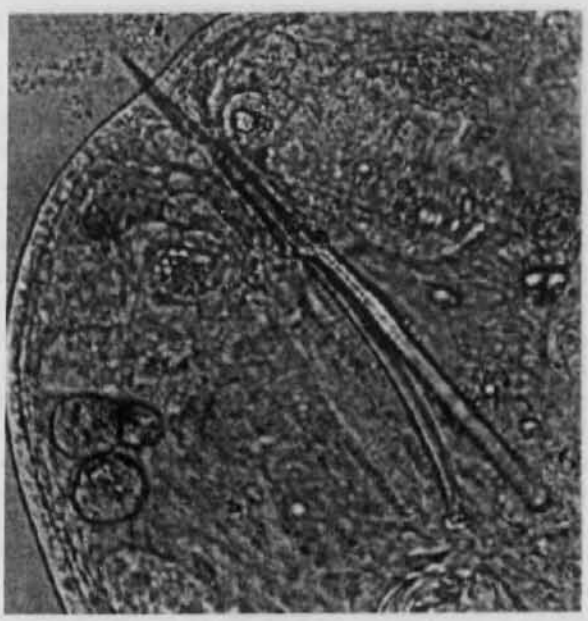

Fig. 2. Stylus and sheath – *Gyratrix hermaphroditus* (1,000X).

Gyratrix hermaphroditus has been found in marine (Curini-Gallatti and Puccinelli, 1994), freshwater (Mead and Kolasa, 1984), and brackish habitats (Therriault and Kolasa,

1999). It has been reported from North Australia (Curini-Gallatti and Puccinelli, 1990), Jamaica (Therriault and Kolasa, 1999), Hawaii (Karling et al., 1973), the North American Pacific coast (Karling et al., 1973), and from New York state (Kolasa et al., 1987). Some consider this species to consist of a "complex of sibling species" (Curini-Gallatti and Puccinelli, 1994). Specimens taken from various sites show considerable variation in dimensions of the male stylet, in chromosome number, in body color, and in presence or absence of eyes.

Curini-Gallatti and Puccinelli (1994) stated that *G. hermaphroditus* is represented in western Europe by individuals that are distinct both karyologically and ecologically. Their research indicates that individuals in marine environments have a base chromosome number of $2n = 6$, but freshwater individuals are $2n = 4$. The only contradicting results were obtained near Darwin, Northern Territory, Australia by Curini-Gallatti and Puccinelli in 1990. They found individuals in intertidal habitats with both chromosome configurations. As salinity fluctuates widely in this area at different times of the year, the coexistence of the two species could be possibly explained. According to Kolasa (1991), members of the superfamily Kalyptorhynchia are rarely found in freshwater, but *G. hermaphroditus* has been found in several different freshwater sites.

Very little, if any, research has been conducted on this order of Platyhelminthes in Arkansas. To date, four species of the genus *Stenostomum*, one species of *Microdalyellia*, and one species of *Phaenocora* have been identified from Magnolia Manor and are the subjects of further research. Four other species have been observed, but identification has not been determined. These findings, in addition to *G. hermaphroditus*, will be monitored over several years to assess the species' impact on this pond.

Literature Cited

Artois, T., W. Vermin, and **E. Schockart.** 2000. Rhabdocoela (Platyhelminthes) from the Weddell Sea (Antarctica) with the description of eight new species. Belgian J. Zool. 130:103-110.

Curini-Gallatti, C. M., and **I. Puccinelli.** 1990. The *Gyratrix hermaphroditus* species complex (Platyhelminthes: Kalyptorhynchia) in the Darwin Area (Northern Territory, Australia). Trans. Amer. Microsc. Soc. 109:368-379.

Curini-Gallatti, C. M., and **I. Puccinelli.** 1994. The *Gyratrix hermaphroditus* species complex (Platyhelminthes: Kalyptorhynchia) in the marine tropical area: first data from the Caribbean. Belgian J. Zool. 124:157-166.

Karling, T. G., V. Mack-Fira, and **J. Dorjes.** 1973. First record on marine microturbellarians from Hawaii. Zoologica Scripta. 1:251-269.

Kolasa, J. 1991. Flatworms: Turbellaria and Nemertea. Ecology and classification of North American freshwater invertebrates. (Eds. J. H. Thorpe and A. P. Covich) Academic Press, San Diego. 145-171 pp.

Kolasa, J., D. Strayer, and **E. Bannon-O'Donnell.** 1987. Microturbellarians from interstitial waters, streams, and springs, in southeastern New York. J. North Am. Benth. Soc. :125-132.

Mead, A. P., and **J. Kolasa.** 1984. New records of fresh water microturbellaria from Nigeria, West Africa. Zool. Anzeiger. 212:257-271.

Therriault, T. W., and **J. Kolasa.** 1999. New species and records of microturbellarians from coastal rock pools of Jamaica, West Indies. Archiv. Feur Hydrobiologie. 144:371-381.

Subterranean Biodiversity of Arkansas, Part 2: Status Update of the Foushee Cavesnail, *Amnicola cora* Hubricht, 1979 (Mollusca: Gastropoda: Hydrobiidae)

G. O. Graening
The Nature Conservancy
Arkansas Field Office
601 North University Avenue
Little Rock, AR 72205

In 1978 a minute snail lacking eyes and pigment (Fig. 1) was discovered in the subterranean stream of Foushee Cave, Independence County, Arkansas, by Youngsteadt and Youngsteadt (1978) and described by Hubricht (1979) as the Foushee cavesnail, *Amnicola cora*. For the next 25 years, nothing more was known of its status or distribution. To address this and other data deficiencies, a regional inventory of subterranean habitats was initiated by a multi-agency consortium (the Ozark Subterranean Biodiversity Project), the results of which are being presented in this manuscript series. A bioinventory on 18 August 2002 of Foushee Cave by the author, David Kampwerth (U. S. Fish and Wildlife Service), R. C. Schroeder and Ed Corfey (both of the Association for Arkansas Cave Studies) confirmed the presence of this cavesnail in the type locality. Cavesnails were found in abundance, primarily on the sides of rocks (Pitkin limestone) in pools and riffles having cobble substrate. A brief visual survey (1/2 hour x 4 men = 2 man-hours) of the cave stream revealed a density range of 1 to 20 cavesnails per m^2, and a total population estimate of 500 individuals. Although the cave is relatively large (1900 m of mapped passage), the available (or at least visible) stream habitat is small, and the cavesnails were apparently absent from areas close to the entrance (the twilight zone) and from stream segments with swift current.

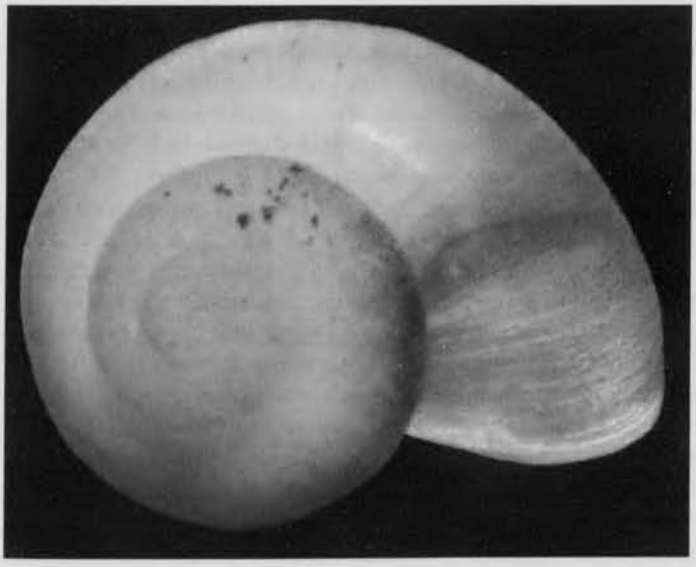

Fig. 1. The shell of *Amnicola cora*, 2 mm in diameter.

The Foushee cavesnail population coexists with a diverse subterranean community of at least 34 other animal species, totaled from this study and Youngsteadt and Youngsteadt (1978). Nine other taxa are known from Foushee Cave that are limited to groundwater habitats (stygobites) or limited to caves (troglobites): the grotto salamander (*Typhlotriton spelaeus*), a flatworm (Tricladida), a dung fly (*Spelobia tenebrarum*), a milliped (*Causeyella* sp.), a springtail (*Schaefferia alabamensis*), a sow bug (*Miktoniscus* sp.), an undescribed dipluran (*Litocampa* sp. nov.), an amphipod (*Stygobromus* sp.) and a water slater (*Caecidotea ancyla*). Also present were potential predators of the cavesnail: the cave salamander (*Eurycea lucifuga*), the dark-sided salamander (*Eurycea longicauda melanopleura*), the slimy salamander (*Plethodon albagula*), the banded sculpin (*Cottus carolinae*), and an epigean crayfish (*Orconectes* sp.). Other fauna identified in the two combined studies were an aquatic snail (Physidae), a terrestrial snail (*Polygyra lithica*), the eastern pipistrelle bat (*Pipistrellus subflavus*), a crane fly (Tipulidae), a humpbacked fly (*Megaselia cavernicola*), a heleomyzid fly (*Amoebalaria defessa*), a long-legged fly (*Neurigonella sombrea*), a dark-winged fungus gnat (*Bradysia* sp.), a chironomid (*Cricotopus* sp.), two harvestmen (*Leiobunum* sp. and *Crosbyella spinturnix*), a soil mite (*Gaeolaelaps* sp.), a cave cricket (*Ceuthophilus gracilipes*), a colonial bat (*Myotis* sp.), a round fungus beetle (*Ptomaphagus shapardi*), a rove beetle (*Quedius* sp.), a water slater (*Lirceus bicuspidatus*), and two unidentified Araneae. This richness of species, and especially the presence of ten subterranean obligates, makes Foushee Cave one the most biologically significant caves in the Ozark plateaus ecoregion to date.

Extensive efforts to inventory cave life by the author and colleagues have failed to discover any other cavesnail populations in Arkansas. *Amnicola cora* remains the only stygobitic mollusk endemic to Arkansas; it is one of approximately 11 snails found only in Arkansas (Robison and Allen, 1995; Walsh and Coles, 2002), and one of approximately 36 hydrobiid cavesnails known in North America (Hershler and Holsinger, 1990). The national

Natural Heritage Program and The Nature Conservancy consider *Amnicola cora* to be critically imperiled (rank of G1; NatureServe, 2003) and the World Conservation Union considers this cavesnail to be vulnerable to extinction (Red List rank of VU+D2; IUCN, 2003). Other related species known from the Ozark Plateaus ecoregion are the Ozark springsnail (*Fontigens aldrichi*), the enigmatic cavesnail (*Fontigens antroecetes*), and three cavesnails endemic to Missouri – the stygian cavesnail (*Amnicola stygia*), the Tumbling Creek cavesnail (*Antrobia culveri*), and the proserpine cavesnail (*Fontigens proserpina*) (Wu et al., 1997; NatureServe, 2003). Robert Hershler of the Smithsonian Institution is revising the systematics of the family Hydrobiidae using molecular evidence. Genetic analysis of hydrobiid cavesnails is necessary because their characteristic miniaturization and anatomical simplification makes phylogenetic analysis by morphological criteria alone extremely difficult (Hershler and Holsinger, 1990). To assist in this effort, four *Amnicola cora* specimens were collected and sent to Hershler and curated (USNM 1017836).

Although *Amnicola cora* was confirmed to be locally abundant, its extreme endemicity makes it vulnerable to extirpation. The landowner has controlled and limited access to the cave, which is an important strategy to abate the threat of trampling by cavers. Perhaps the greatest threat is habitat alteration, especially increased sediment and nutrient inputs. Loss of interstitial habitat by excessive sediment input is implicated in the population decline of a related species, the endangered Tumbling Creek cavesnail (USFWS, 2002). Three other hydrobiid snails – the Ouachita pebblesnail (*Somatogyrus amnicoloides*), the thicklipped pebblesnail (*S. crassilabris*), and the channelled pebblesnail (*S. wheeleri*) - each endemic to single aquatic sites in Arkansas, are thought to be extinct due to hydrologic alteration of their habitats by impoundment and hypolimnetic release (Walker, 1915; Robison and Allen, 1995).

Literature Cited

Hershler, R., and **J. R. Holsinger.** 1990. Zoogeography of North American hydrobiid cavesnails. Stygologia 5:5-16.

Hubricht, L. 1979. A new species of *Amnicola* from an Arkansas cave (Hydrobiidae). Nautilus 93:142.

NatureServe. 2003. NatureServe Explorer: An online encyclopedia of life, Version 1.8. Internet database. NatureServe, Arlington, Virginia. Accessed September 2003. Internet URL =http://www.natureserve.org/explorer.

Robison, H. W., and **R. T. Allen.** 1995. Only in Arkansas: a study of the endemic plants and animals of the state. University of Arkansas Press, Fayetteville, Arkansas. 121 pp.

U. S. Fish and Wildlife Service. 2002. Federal Register 67(157):52879-52889. Federal Register Document No. 02-20339S. August 14, 2002. Williams, Director, U. S. Fish and Wildlife Service.

Walker, B. 1915. Apical characters in *Somatogyrus* with descriptions of three new species. The Nautilus 29:37-41, 29:49-53.

Walsh, G. E., and **B. F. Coles.** 2002. Distribution and geographical relationships of the polygyrid land snails (Mollusca, Gastropoda, Polygyridae) of Arkansas. J. Arkansas Acad. Sci. 56:212-219.

World Conservation Union. 2003. The 2002 IUCN Red List of Threatened Species. Internet publication and database. International Union for Conservation of Nature and Natural Resources. Accessed September, 2003. Internet URL = http://www.redlist.org/.

Wu, S., R. D. Oesch, and **M. E. Gordon.** 1997. Missouri aquatic snails. Natural History Series, No. 5. Conservation Commission of the State of Missouri. Jefferson City, Missouri. 97 pp.

Youngsteadt, N. W., and **J. O. Youngsteadt.** 1978. Biosurvey of invertebrates in Foushee Cave, IN-371, with notes on vertebrate observations. AACtivitieS 84:12-15. The Association for Arkansas Cave Studies. Harding University, Searcy, Arkansas.

Reciprocal Translocation Reestablishes Breeding Status of Mississippi Alluvial Plain Population of Red-cockaded Woodpeckers in Arkansas

William C. Holimon*
Arkansas Natural Heritage Commission
1500 Tower Building, 323 Center Street
Little Rock, AR 72201

Warren G. Montague
Poteau Ranger District
Ouachita National Forest
USDA-Forest Service
P.O. Box 2255
Waldron, AR 72958

*Corresponding Author

The Red-cockaded Woodpecker (*Picoides borealis*) is a federally listed endangered bird species endemic to the southeastern United States. A habitat specialist that occurs only in mature, open pine woodlands, this species has declined drastically due to loss of habitat. This loss of habitat has been caused by suppression of fire that increases woody encroachment of hardwood trees, logging practices that reduce or eliminate mature pines, and land conversion resulting in habitat loss and/or fragmentation (Conner et al., 2001). A cooperative breeder, Red-cockaded Woodpecker breeding groups have plummeted by 97% following European settlement (U.S. Fish and Wildlife Service, 2000).

In Arkansas Red-cockaded Woodpeckers historically occurred throughout much of the state, with populations in the Upper West Gulf Coastal Plain, Ouachita Mountains (OM), Mississippi Alluvial Plain (MAP), and eastern portions of the Ozark Mountains (James and Neal, 1986). Intensive logging in the Ozarks likely caused the extirpation of this species from that region by the early 1900s (James and Neal, 1986; Smith and Neal, 1991). In addition, large-scale land conversion, primarily for agricultural production, has all but eliminated Red-cockaded Woodpecker habitat in the MAP (Burnside, 1983; James and Neal, 1986).

This loss of habitat nearly resulted in the extirpation of the MAP Red-cockaded Woodpecker population. Indeed, by 2000 the entire MAP population was reduced to one breeding group located at the Pine City Natural Area (PCNA) in southern Monroe County (Arkansas Natural Heritage Commission, 2001). The PCNA, currently 180 ha, supports the largest remaining remnant of high quality loblolly pine (*Pinus taeda*) forest stands remaining in the MAP. Prior to settlement, there were approximately 1,295 sq km, mostly in Monroe County, that supported extensive stands of loblolly pine forests (Sargent, 1884). There are now likely fewer than 4.05 sq km of high quality loblolly pine forests remaining in the MAP, mostly in small, highly-fragmented tracts (Tom Foti, pers. comm.).

By 2001 the breeding female of the PCNA group had vanished and the only remaining female (hatched in summer of 2000) was an offspring of the breeding male. Because males will not pair bond with their offspring, this group became nonviable as a breeding group. Without human intervention it was likely that this breeding group, and therefore the entire MAP population, would have become extirpated. Therefore on 13 September 2001, a reciprocal augmentation was completed using a 4-month-old female from the OM population, which was swapped with the 16-month-old female from PCNA. Both females were trapped, transported, and released using translocation methods established by DeFazio et al. (1987). All birds were color banded to aid subsequent identification of each individual.

The female translocated to PCNA in September 2001 successfully bred in 2002, producing two offspring. These two offspring were still using the PCNA cavity tree cluster in March of 2003. A cavity tree cluster is an aggregation of trees with cavities previously and currently used and defended by Red-cockaded Woodpeckers for the purpose of roosting and nesting (U.S. Fish and Wildlife Service, 2000). The female moved to the OM also successfully bred in that population. Thus, this reciprocal translocation of Red-cockaded Woodpeckers reestablished the single remaining group of the MAP population as a viable breeding unit and also contributed to recovery efforts for the OM population.

Though the breeding status of the MAP population has been reestablished successfully, the continued persistence of this population is precarious and will require additional conservation measures. To establish a new cavity tree cluster, artificial cavity inserts were placed in five trees at PCNA on 18 September 2002 following methods established by Allen (1991). This new cluster, located approximately 1.9 km west of the reestablished breeding group, was created to support a second breeding group. On 27 March 2003 a second reciprocal augmentation was completed using a 10-month-old female and 10-month-old male from the OM population, which were swapped for a 10-month-old female from PCNA. The pair from the OM was released in the new cluster with the hope that they will accept this site and breed there. The male from the OM was an offspring of the female that had been translocated to the OM from PCNA in 2001.

In addition, ANHC is negotiating to acquire land

adjacent to or nearby PCNA to increase the overall amount of available habitat under protection and management. Once the property is acquired, habitat restoration such as prescribed burning and planting of native loblolly pine will be conducted to create suitable Red-cockaded Woodpecker foraging and breeding habitat (U.S. Fish and Wildlife Service, 2000).

ACKNOWLEDGMENTS.—This study was supported by U.S. Fish and Wildlife Service Grant 1448-40181-02-G-063. We would like to thank Troy Bader, Nelva Bohannan, Dan Brown, Jody Gschwend, Keith Piles, Dana Ripper, Bill Shepherd and Lyndal York for providing expert field assistance.

Literature Cited

Allen, D. H. 1991. An insert technique for constructing artificial Red-cockaded Woodpecker cavities. USDA For. Serv. Gen. Tech. Rep. SE-73.

Arkansas Natural Heritage Commission. 2001. Annu. Rept. 2001. 190 pp.

Burnside, F. L. 1983. The status and distribution of the Red-cockaded Woodpecker in Arkansas. Amer. Birds 37:142-145.

Conner, R. N., D. C. Rudolph, and **J. R. Walters.** 2001. The Red-cockaded Woodpecker, surviving in a fire-maintained ecosystem. Univ. Texas Press, Austin, Texas. 363 pp.

DeFazio, J. T., M. A. Hunnicutt, M. R. Lennartz, G. L. Chapman, and **J. A. Jackson.** 1987. Red-cockaded Woodpecker translocation experiments in South Carolina. Proc. Annu. Conf. Southeast. Assoc. Fish and Wildl. Agencies 41:311-317.

James, D. A., and **J. C. Neal.** 1986. Arkansas birds, their distribution and abundance. Univ. Arkansas Press, Fayetteville, Arkansas. 402 pp.

Sargent, C. S. 1884. Report on the forests of North America (exclusive of Mexico). Govt. Print. Offc., Washington, D.C. 612 pp.

Smith, K. G., and **J. C. Neal.** 1991. Pre-settlement birds and mammals of the Interior Highlands. Pp. 77-103, *In* Restoration of Old Growth Forests in the Interior Highlands of Arkansas and Oklahoma (Henderson, D. and L.D. Hedrick, eds.). Ouachita Natl. For. and Winrock Intl. Inst. for Agric. Develop., Hot Springs, Arkansas.

U. S. Fish and Wildlife Service. 2000. Technical/Agency draft, revised recovery plan for the Red-cockaded Woodpecker (*Picoides borealis*). Atlanta, Georgia: U.S. Fish and Wildl. Serv. 229 pp.

Parameter Extraction Software For Compact Diode Model

Maruf Hossain, Edgar Cilio, Ty R. McNutt, A. B. Lostetter, and **H. Alan Mantooth***
Sic Research Group
Dept. of Electrical Engineering
Univ. of Arkansas
3217 Bell Engineering Center
Fayetteville, AR 72701

*Corresponding Author

Introduction

A reliable device model is crucial for the development and implementation of a circuit design. However, the creation of a high quality model requires a significant amount of time and money. The software package presented in this paper seeks to minimize the time and money invested in the realization of a high quality model for SiC Schottky, Merged PiN Schottky, and PiN Power diodes based on McNutt and Mantooth's Comprehensive SiC Diode model (McNutt et al., 2001, 2002). This software can be used for extraction of any other device model parameters with little modification (Ma et al., 1994; Krishna et al, 1995., Bai et al., 2001; Laux et al., 1991).

The software package is a user-friendly three-step algorithm that provides the user with efficient parameter extraction of the device. Initially, the *Slope Calculation* program determines the on-state resistance of the diode. Secondly, the ONSTMSR program carries out the on-state parameter calculation; and lastly, the TPE program performs the extraction of the transient parameters. All of the programs have been created with LabWindows/CVI with the exception of TPE, which utilizes LabWindows/CVI and Saber.

On-state Resistance Calculation.--*Slope Calculation* determines the on-state resistance of the diode. Measured data of the voltage across the diode and the current going through it have to be supplied in any type of data file. The *Slope Calculation* software analyzes the data, plots the voltage against the current, and displays the resulting curve as detailed in Fig. 2. In order to find the on-resistance, *Slope Calculation* allows the user to find the slope and inverse slope at any given point in the curve. The value obtained for the inverse slope is the on-state resistance of the diode. Figure 1 shows the output of a test run. *Slope Calculation* software allows the user to calculate the on-state resistance, for diodes and transistors. Figure 1 shows the calculation of slope for a transistor. From this figure it can be seen that the software has four check boxes at the top to allow the user to plot four different curves at the same time or any number of plots in which the user might be interested. The user can use

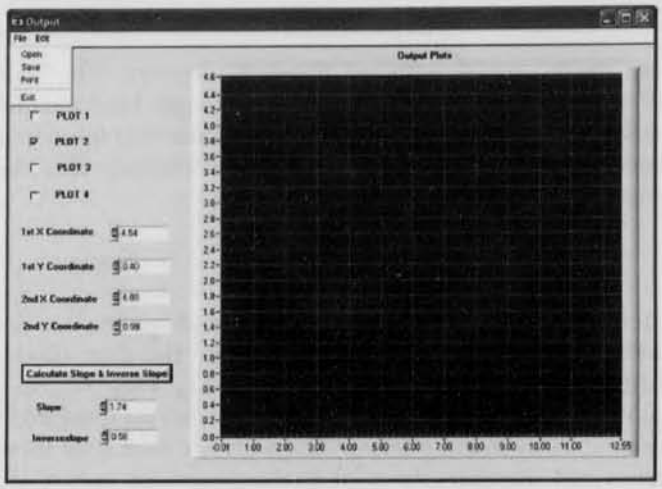

Fig. 1. Output from slope calculation software.

the two cursors to obtain two sets of data points. Those points are shown in their specific spaces called 1st X coordinate, 2nd X coordinate, 1st Y coordinate, and 2nd Y coordinate. The user is given the value of slope and inverse slope by pressing the calculate slope and inverse slope buttons. Notice that the best value for the on-state is obtained at the point where the curve starts increasing linearly. This value of resistance will be used by ONSTMSR.

On-state Parameter Calculation.--This software carries out the results of *Slope Calculation* software and uses this to extract the parameter of any diode. Figure 3 shows an on-

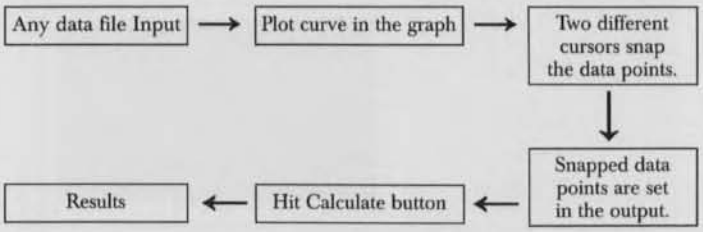

Fig. 2. Flow chart of slope calculation software.

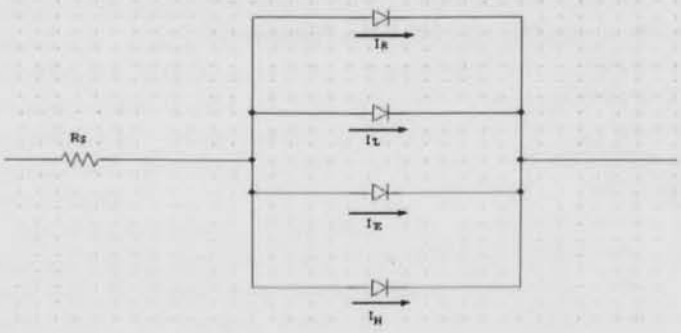

Fig. 3. On state diode model with no forward recovery.

state diode model with no forward recovery. The four different current components flow through four parallel diodes. This software extracts eight parameters of these four diodes. To extract the parameters, the software uses the formula

$$I=I_s(e^{vj/n*vt}) \qquad \text{Equation (1)}$$

where vj is the voltage across the diode, and I_S and n are the model parameters and are different for the four diodes illustrated in Fig. 3. The parameters are I_{SR}, IS_{SL}, I_{SE}, I_{SH}, n_R, n_L, n_E, and n_H. The user inputs the value for these eight parameters as initial guesses. The software then uses these values and calculates the total diode current for each diode voltage using equation (1). These current and voltage values are then plotted in the graph. Whenever the plot of the sum of all currents and voltages matches the measured current and voltage plot, the user gets the parameters from the output shown in Fig. 4. This software also allows users to

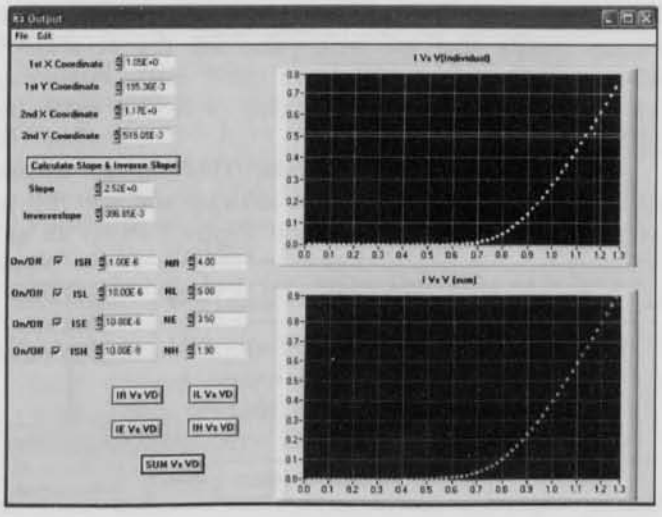

Fig. 4. Output from On-state parameter extraction software.

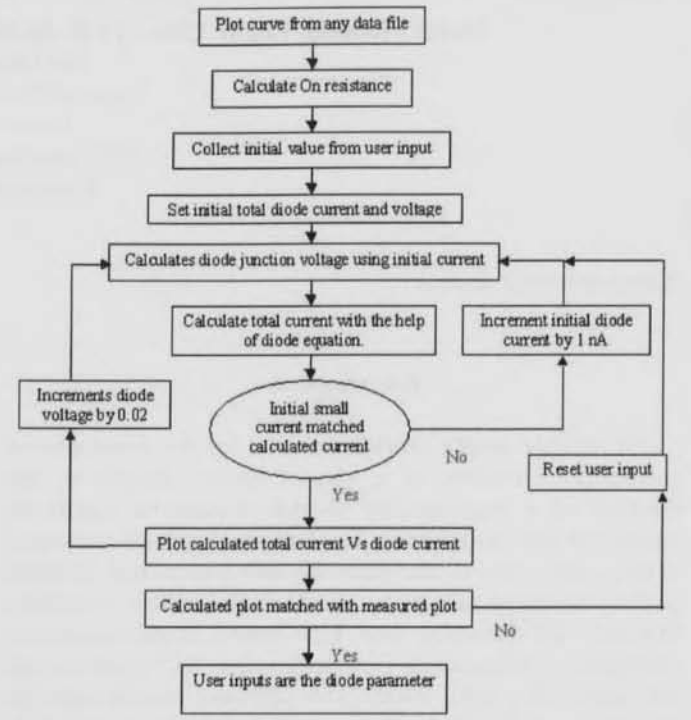

Fig. 5. Flow chart of on-state parameter calculation software.

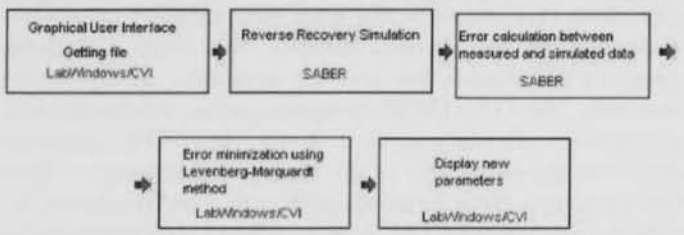

Fig. 6. Flow chart of transient parameter extraction software.

select the number of parallel diodes needed for their diode model. Figure 5 shows the flowchart for the on-state parameter calculation software. From the flowchart, it can be seen that any data file is plotted in the graph first. Then the slope calculation software calculates the on-resistance. On-resistance is the inverse slope of the curve. Next the user inputs some initial values for I_{SR}, IS_{SL}, I_{SE}, I_{SH}, n_R, n_L, n_E, and n_H to the specific box of the output. The software collects that input and uses it to calculate the diode current by Equation (1). In the process, the software calculates the diode junction voltage using the initial diode currents. After each calculation, the software plots one point of current and voltage. After each plot, the total diode voltage (V_D) is incremented by 0.02V. After plotting the entire curve, the software compares the computed plot with the experimental plot. If these two plots match, the user input values are determined to be the model parameters. Otherwise, the user

changes the input value, and the process is repeated.

Transient Parameters Extraction.--TPE extracts the parameter of the diode during the reverse recovery. This software is still under development. Nevertheless, the outline of this routine has been determined and will be implemented as described in this section. LabWindows/CVI delivers the user-interface component of the program. Initially, measured transient data of a diode reverse recovery circuit is provided to Saber. Saber will simulate the reverse recovery circuit and compare it to the measured data. Using the Levenberg-Marquardt (McNutt, 2002) optimization routine, the difference between the measured data and the simulated data will be minimized. After the minimization, the extraction software will provide the new set of parameters. During the entire process, Saber will work in batch mode. LabWindows/CVI will communicate with Saber and export parameter values and display them. Figure 6 describes the data flow manipulation that TPE will perform.

Conclusions

Parameter extraction software has been presented in this paper. This software can accurately model SiC Schottky, Mereged PiN Schottky, and PiN Power diodes based on McNutt and Mantooth's Comprehensive SiC Diode model (McNutt, 2001). The parameter extraction is carried out in three different phases: on-state resistance extraction, on-state parameter extraction, and transient parameter extraction. The software presented here provides the user a friendly environment, while delivering accurate, reliable parameters that can be use for circuit design in differing applications.

Literature Cited

Bai, Y., and **Goldsman, N.** 2001. Modeling of nonuniform SiGe heterostructure. Semiconductor Device Research Symposium, 2001 International:244-247.

Krishna, K., and **Director, S. W.** 1995. A novel methodology for statistical parameter extraction. IEEE/ACM International Conference:696-699.

Laux, S. E., and **Fischetti, V.** 1991. Simulation of small semiconductor devices using a coupled Monte Carlo-Poisson approach. Proceedings IEEE/Cornell Conference on Advance Concepts:338-346

Ma, C. L., and **Lauritzen, P. O.** 1994. A systematic technique to modeling of power semiconductor devices for power electronic simulation. Northcon/94 Conference Record:54-59.

McNutt, T. R. 2001. Silicon Carbide PiN Schottky Power Diode Models Implemented in the Saber Circuit Simulator. Conf. Proc. of IEEE Power Electronics Specialists Conference (PESC) 4:2103-2108.

McNutt, T. R., Hefner, A. R., Mantooth, H. A., Duliere, J. L., Berning, D.W., and **Singh, R.** 2002. Parameter Extraction Sequence for Silicon Carbide Schottky, Merged PiN Schottky, and PiN Power Diode Models. Conf. Proc. of IEEE Power Electronics Specialists Conference (PESC) 3:1269-1276.

Identifying Minimum *G* Aberration Designs from Hadamard Matrices of Order 28

Steffany Belcher-Novosad and **Debra Ingram***
Department of Mathematics and Statistics
Arkansas State University
State University, AR 72467

* Corresponding Author

Two-level fractional factorial designs are among the most widely used statistical experimental strategies for the simultaneous study of the effects of several variables. In general, factorial designs consist of a fixed number of levels for each of the variables (factors) under investigation and all combinations of these factor levels. The combinations of factor levels represent the conditions at which the response will be measured, and a combination of factor levels at which an experiment is to be carried out is called a *run*. Since identifying active factors is often an early phase in a sequential experimental strategy, we would like to run the fewest number of levels of the factors while still learning about their impacts. Consequently, two-level factorial designs are popular choices for "screening" – that is, identifying which of the many factors under investigation really affects the response. To study the effects of k factors each at two levels, + and -, a two-level *full* factorial design consists of all 2^k combinations of factor levels. The two-level *fractional* factorial designs specify a carefully selected subset, or fraction, of the 2^k combinations of factor levels and are therefore extremely useful when a large number of factors is being investigated and/or the experimental runs are expensive or time consuming to conduct That is, two-level fractional factorials are favored because of their *run size economy*. We consider the broad class of orthogonal two-level factorial designs that can be constructed from the columns of Hadamard matrices. A Hadamard matrix of order n, say $\boldsymbol{M}$, is an orthogonal $n \times n$ matrix with entries 1 or −1, so that $\boldsymbol{M}^T\boldsymbol{M} = n\boldsymbol{I}$ where $\boldsymbol{I}$ is the $n \times n$ identity matrix. For such a matrix to exist, n must be a multiple of four (except for the trivial cases $n = 1$ and $n = 2$), and a library of Hadamard matrices of every order up to $n = 256$ is available at N.J.A. Sloane's web site, *www.research.att.com/~njas*. For notational ease, we often use + and - to represent 1 and −1, respectively. Hadamard matrices may be normalized so the first column is all +'s. Removing this first column gives a Hadamard design, $\boldsymbol{H}$, with n runs and $n-1$ columns. The orthogonal property of Hadamard matrices means that designs constructed from the columns of Hadamard matrices have the same number of +'s and −'s in each design column and the four combinations (+, +), (+, -), (-, +), and (-, -) occur with the same frequency in every two design columns. From each Hadamard matrix of order n, there are ${}_{n-1}C_m$ possible designs of n runs and m factors. A survey on applications of Hadamard matrices in design theory can be found in Hedayat and Wallis (1978).

Aliasing of effects is the price paid for run size economy in fractional factorial designs. Two effects are aliased when it is not possible to distinguish the estimate of one effect from the estimate of the other. The *regular* fractional factorials exhibit a simple aliasing structure in that any two effects can be estimated independently or are fully aliased. For example, take a design that exhibits full aliasing between the main effect of factor A and the effect of the three-factor interaction between factors B, C, and D. The data from such a design will yield an estimate of the sum of these effects, $A + BCD$, but is not capable of distinguishing the estimate of A from the estimate of BCD. Fortunately, the effects of three-factor interactions tend to be negligible.

The regular fractional factorial designs are most commonly used and are readily available in the literature. See, for example, Wu and Hamada (2000) and Box et al. (1978). However, the number of runs in a regular design must be a power of two, leaving large gaps in the available choices of run size. In contrast, *nonregular* fractional factorial designs can be constructed for run sizes that are multiples of four, filling in the gaps in available run sizes left by the regular designs. The nonregular designs exhibit partial aliasing of effects. Using an example similar to the one above, the data from a nonregular design in which A and BCD are partially aliased with an aliasing coefficient of 1/3 will yield an estimate of the main effect of factor A plus one third the effect of the three-factor interaction BCD, denoted by $A + 1/3\ BCD$. By comparison, the aliasing coefficients in a regular design are either ±1 or 0, corresponding to effects that are fully aliased or are orthogonal (i.e., uncorrelated), respectively. The aliasing structures of nonregular designs are more complex than those of regular designs in that the number of partial aliases is much larger than the number of full aliases in a regular design, making the aliasing structure difficult to disentangle. However, partially aliased effects may be jointly estimable, as shown in Hamada and Wu (1992). Moreover, since nonregular designs can be constructed for run sizes that are multiples of four, they provide a distinct advantage over regular designs in *run size economy* and *run size flexibility*. For example, nonregular

designs of 20, 24, and 28 runs fill in the gap left by the 16-run and 32-run regular fractional factorials.

"Optimal" fractions are those for which potentially important effects are not aliased with each other. When no *a priori* knowledge exists about which effects are potentially active, the hierarchical ordering principle (Wu and Hamada, 2000) suggests that lower order effects (e.g., main effects) are more likely to be important than higher order effects (e.g., three-factor interactions). For regular designs, optimal fractions are chosen according to the well-known resolution (Box and Hunter, 1961) and minimum aberration (Fries and Hunter, 1980) criteria. These criteria cannot be applied to nonregular designs, and there were no systematic criteria for comparing different nonregular designs until recently. Deng and Tang (1999) proposed minimum *G* aberration (short for "generalized minimum aberration") for this purpose. For a subset of k columns from a Hadamard design, $s = \{c_1, c_2, \ldots, c_k\}$, define

$$J_k(s) = \left| \sum_{i=1}^{n} c_{i1} c_{i2} \ldots c_{ik} \right| \qquad (1)$$

where c_{ij} is the ith component of column c_j. $J_1(s) = J_2(s) = 0$ because the designs taken from Hadamard matrices are orthogonal. For a regular design, the only possible values of $J_k(s)$ are 0 and n, corresponding to orthogonality and full aliasing, respectively. $J_k(s)$ values between 0 and n correspond to partial aliasing, as found in nonregular designs. Values of $J_k(s)$ closer to n indicate more serious aliasing among the columns of s, and values closer to 0 indicate less serious aliasing among the columns of s. For the set $s = \{c_1, c_2, c_3\}$ of three columns, $J_3(s)/n$ is the absolute value of the aliasing coefficient of main effect c_1 and the two-factor interaction c_2c_3. Therefore, large $J_3(s)$ values provide the worst scenario – a potentially large amount of contamination of two-factor interactions on the estimation of main effects. When $n = 28$ runs, the possible values of $J_3(s)$ are 28, 20, 12, and 4. Then, for example, when $J_3(s) = 20$, the data will yield an estimate of the main effect c_1 plus (or minus) 20/28 of the effect of the two-factor interaction c_2c_3, denoted by $c_1 + 20/28\ c_2c_3$. On the other hand, when $J_3(s) = 4$, the data will yield an estimate of $c_1 + 4/28\ c_2c_3$. The potential amount of contamination of the c_2c_3 two-factor interaction on the estimation of main effect c_1 is less for lower values of $J_3(s)$.

The *confounding frequency vector* of a design is built up from its $J_k(s)$ values, and two designs of the same size are compared by their confounding frequency vectors. Let $F_k(D)$ be the vector which contains the frequencies of the different $J_k(s)$ values for design D. Define the confounding frequency vector of D as $F(D) = [F_3(D), F_4(D), \ldots, F_m(D)]$. Deng and Tang (2002) showed that only two or three leading terms in $F(D)$ are needed to classify and rank designs. Consequently, we use the abbreviated confounding frequency vector $F(D) = [F_3(D), F_4(D), F_5(D)]$ as the classification and ranking criterion. As an example, the top and second-ranked designs of $n = 24$ runs and $m = 8$ columns found by a complete search of Hadamard matrices of order 24 in Deng and Tang (2002) have (abbreviated) confounding frequency vectors $F(D_1) = [(0, 0, 0, 56)_3, (0, 0, 70, 0)_4, (0, 0, 0, 56)_5]$ and $F(D_2) = [(0, 0, 6, 50)_3, (0, 0, 52, 18)_4, (0, 0, 18, 38)_5]$. For 24 runs, the possible values of $J_k(s)$ are 24, 16, 8, and 0 and the four components of $F_k(D)$ are the number of subsets of k columns with $J_k(s) = 24$, 16, 8, and 0, in that order from left to right. The confounding frequency vectors indicate that in the second-ranked design D_2, there are six subsets of three columns for which the aliasing coefficient between the main effects and two-factor interactions is $\pm$ 8/24 = $\pm$ 1/3 whereas in the top-ranked design D_1, all the main effects can be estimated independently of two-factor interactions since each of the ${}_8C_3 = 56$ subsets of three columns yields $J_3(s) = 0$. (In practice, the last components in $F_3(D)$, $F_4(D)$, and $F_5(D)$ can be omitted since these values can be determined by the previous entries.) To compare two designs according to the minimum *G* aberration criterion, compare the entries of their confounding frequency vectors from left to right. Let r be the smallest number for which $F_r(D_1)$ not equal to $F_r(D_2)$. Use the $[i]$ nomenclature for a particular element of a vector. If $F_r(D_1)[i] < F_r(D_2)[i]$ are the leftmost entries of $F_r(D_1)$ and $F_r(D_2)$ that are not equal, then D_1 is said to have less *G* aberration than D_2, and D_1 is preferred. If no design has less *G* aberration than D_1, then D_1 is said to have minimum *G* aberration.

With a criterion now available for assessing the goodness of nonregular fractional factorial designs, methods for the construction of good designs were needed. By complete search of all possible designs from Hadamard matrices, Deng, Li, and Tang (2000) and Deng and Tang (2002) produced a comprehensive catalog of minimum *G* aberration designs of 12, 16, and 20 runs and a partial catalog of designs of 24 runs (accommodating up to eight factors). However, the number of comparisons required in a complete search for larger designs is enormous (e.g., for 28 runs and 10 factors, there are 4×10^9 designs to compare), rendering a complete search impractical. To solve this problem, efficient computational algorithms based on forward selection and backward elimination of columns of Hadamard matrices were studied in Ingram and Tang (2001). Improvements to these algorithms led to an excursion-at-target algorithm that allows the efficient exchange of columns after reaching the target design and thereby bypasses local minimum *G* aberration designs. The excursion-at-target algorithm was implemented in the construction of minimum *G* aberration designs of 24 runs for nine or more factors, and these designs are presented in Ingram (2000).

Designs of 28 runs are needed to further fill the gap in

available run sizes left by the regular designs (no regular designs exist for run sizes between $n = 16$ and $n = 32$) and to offer more run size flexibility to experimenters. However, the excursion-at-target algorithm needed some major improvements to handle the complicated 28-run case. While it performed adequately in searching the 60 nonequivalent Hadamard matrices of order 24, it lacked the efficiency and stability to effectively search the 487 nonequivalent Hadamard matrices of order 28. To increase the stability of the program, memory usage was made more efficient. More sophisticated data structures were introduced to reduce the amount of memory used in each iteration. After the searches are performed, all necessary output is written to an output file to free up the memory for the next round of searches. In addition to these changes, the algorithm is now more generalized, allowing the construction of designs for any run size. Details on the original excursion at target algorithm appear in Ingram (2000). A complete discussion of the improvements made to the original algorithm along with the S-PLUS code appear in Belcher-Novosad (2002).

The upgraded excursion-at-target algorithm has now been implemented in the construction of designs of 28 runs. Competing designs include the regular designs of 32 runs, and therefore comparisons between the best 32-run designs and the best 28-run designs are of interest. Let m denote the number of factors accommodated by a design. For $m = 6$-16, the regular 32-run designs are such that all main effects can be estimated independently of two-factor interactions. The 28-run designs for $m = 6$-16 exhibit the weakest level of partial aliasing between main effects and two-factor interactions but may compete with the 32-run designs in terms of number of clear effects (Wu and Hamada, 2000).

For $m = 17$-27, the best regular designs of 32 runs all contain full aliasing between main effects and two-factor interactions, whereas the best 28-run designs exhibit only partial aliasing between main effects and two-factor interactions. For example, the minimum or near-minimum G aberration design of 28 runs and 17 factors found by the excursion-at-target algorithm has confounding frequency vector $F(D_{28\times17}) = [(0, 0, 59, 621)_3, (0, 28, 262, 2090)_4, (0, 72, 2361, 3755)]$. The possible $J_k(s)$ values for $n = 28$ are (28, 20, 12, 4) for $k = 3, 4$ and (24, 16, 8, 0) for $k = 5$. A $J_3(s)$ value of 28 indicates full aliasing between main effects and two-factor interactions, whereas $J_3(s)$ values of 20, 12, and 4 indicate partial aliasing that decreases in severity with decreasing values of $J_3(s)$. The confounding frequency vector for design $D_{28\times17}$ shows that the most serious level of aliasing is that exhibited by the columns contained in the 59 subsets of three columns with $J_3(s)$=12. The two-factor interactions contained in these 59 subsets are partial aliases of main effects with aliasing coefficient $\pm12/28 = \pm0.43$. At the same time, the best regular design of 32 runs and 17 factors has confounding frequency vector $F(D_{32\times17}) = [(23, 0, 0, 0, 657)_3, (80, 0, 0, 0, 2300)_4, (194, 0, 0, 0, 5994)_5]$. The possible $J_k(s)$ values for n = 32 are (32, 24, 16, 8, 0) for all k. Therefore, the best design of 32 runs contains 23 subsets of three columns in which the main effects and two-factor interactions are *fully* aliased.

Table 1. $D_{28\times17}$: minimum or near-minimum G aberration design of 28 runs and 17 factors with confounding frequency vector $[(0, 0, 59, 621)_3, (0, 28, 262, 2090)_4, (0, 72, 2361, 3755_5)]$.

Run	1	2	3	4	5	6	7	8	9	10	11	12	13	14	15	16	17
1	+	+	+	+	+	-	-	-	-	-	-	-	+	+	+	+	-
2	-	-	-	-	-	+	+	+	-	-	-	-	+	+	+	-	+
3	-	-	-	-	-	-	-	-	+	+	+	+	+	+	+	+	+
4	+	-	+	+	-	-	+	-	+	-	-	+	-	+	-	+	+
5	+	-	+	-	+	+	-	-	-	-	+	-	-	-	+	+	+
6	+	-	-	+	+	-	-	+	+	+	-	-	+	-	-	+	+
7	-	+	+	-	-	-	+	+	-	-	+	+	+	-	-	+	+
8	-	+	-	+	-	+	-	+	+	+	-	+	-	-	+	+	+
9	-	+	-	-	+	+	+	-	-	+	+	-	-	+	-	+	+
10	+	-	+	-	-	-	+	+	+	+	+	-	-	+	-	-	-
11	+	-	-	+	-	+	-	+	-	-	+	+	+	-	-	-	-
12	+	-	-	-	+	+	+	-	+	+	-	+	-	-	+	-	-
13	-	+	+	+	-	+	-	-	+	-	+	+	-	+	+	-	-
14	-	+	+	-	+	-	-	+	+	+	+	-	+	-	+	-	-
15	-	+	-	+	+	-	+	-	-	+	-	+	+	+	-	-	-
16	+	+	+	-	-	-	+	+	-	+	-	+	-	-	+	+	-
17	+	+	-	+	-	+	-	+	-	+	+	-	-	+	-	+	-
18	+	+	-	-	+	+	+	-	+	-	+	+	+	-	-	+	-
19	-	-	+	+	-	+	+	-	-	+	-	-	+	-	+	+	-
20	-	-	+	-	+	+	-	+	+	-	-	+	+	+	-	+	-
21	-	-	-	+	+	-	+	+	+	-	+	-	-	+	+	+	-
22	+	+	+	-	-	+	-	-	+	+	-	-	+	+	-	-	+
23	+	+	-	+	-	-	+	-	+	-	+	-	+	-	+	-	+
24	+	+	-	-	+	-	-	+	-	-	-	+	-	+	+	-	+
25	+	-	+	+	+	+	+	+	-	+	+	+	+	+	+	-	+
26	-	+	+	+	+	+	+	+	+	-	-	-	-	-	-	-	+
27	-	-	+	+	+	-	-	-	-	+	+	+	-	-	-	-	+

Design $D_{28\times17}$ is given in Table 1. It was constructed from column numbers {1, 2, 4, 5, 6, 7, 8, 9, 13, 16, 17, 18, 19, 20, 21, 26, 27} of the 28th Hadamard matrix of order 28 (denoted had.28.28 in Sloane's library of Hadamard matrices) after normalizing and removing the first column of +'s. Complete design tables containing the minimum or near-minimum G aberration designs of 28 runs constructed by the excursion-at-target algorithm are being generated.

ACKNOWLEDGMENTS.—The authors are grateful to the referees for their useful suggestions that improved the paper. The authors also thank the Managing Editor, Associate Editor, Assistant Editor, and Editor-in-Chief. Funding for

Steffany Belcher-Novosad was provided by a SILO Undergraduate Research Fellowship.

Literature Cited

Belcher-Novosad, S. 2002. Minimum G-aberration designs from Hadamard matrices of order 28. Senior Honors Thesis. Arkansas State Univ. 100 pp.

Box, G. E. P., and **Hunter, J. S.** 1961. The 2^{k-p} fractional factorial designs, Part I. Technometrics 3:311-351.

Box, G. E. P., Hunter, W. G., and **Hunter, J. S.** 1978. Statistics for experimenters. Wiley, New York. 653 pp.

Deng, L. Y., and **Tang, B.** 1999. Generalized resolution and minimum aberration criteria for Plackett-Burman and other nonregular factorial designs. Statistica Sinica 9:1071-1082.

Deng, L. Y., and **Tang, B.** 2002. Design selection and classification for Hadamard matrices using generalized minimum aberration criterion. Technometrics 44:173-184.

Deng, L. Y., Li, Y., and **Tang, B.** 2000. Catalogue of small runs nonregular designs from Hadamard matrices with generalized minimum aberration. Comm. Stat. – Theory and Methods 29:1379-1395.

Fries, A., and **Hunter, W. G.** 1980. Minimum aberration 2^{k-p} designs. Technometrics 22:601-608.

Hamada, M., and **Wu, C. F. J.** 1992. Analysis of designed experiments with complex aliasing. J. Quality Tech. 24:130-137.

Hedayat, A., and **Wallis, W. D.** 1978. Hadamard matrices and their applications. Ann. Stat. 6:1184-1238.

Ingram, D., 2000. The construction of generalized minimum aberration designs by efficient algorithm. Ph.D. Dissertation, Univ. Memphis. 124 pp.

Ingram, D., and **Tang, B.** 2001. Efficient computational algorithms for searching for good designs according to the generalized minimum aberration criterion. Amer. J.f Math. Manage. Sci. 21:325-344.

Wu, C. F. J., and **Hamada, M.** 2000. Experiments: planning, analysis, and parameter design optimization. Wiley, New York. 630 pp.

Genetic Similarity of Shadow and Ozark Basses (*Ambloplites*) as Determined by Mitochondrial DNA Analysis

Ronald L. Johnson* and **Carrie F. Cavenaugh**
Arkansas State University
Department of Biological Sciences
State University, AR 72467

* Corresponding Author

The rock basses, *Ambloplites*, contain four nominal species and represent one of eight genera within the sunfish family (Centrarchidae). The shadow bass (*A. ariommus* Viosca) occurs in the southern plains states east and west of the Mississippi River. The range of the shadow bass west of the Mississippi River is limited to Arkansas and parts of southern Missouri and eastern Oklahoma. Several Arkansas river drainages contain the shadow bass including the Red, Ouachita, Arkansas, Illinois, Little Red, Strawberry, Spring, Black, and St. Francis river drainages (Robison and Buchanan, 1988). The Ozark bass (*A. constellatus* Cashner and Suttkus) is found in streams of the White River drainage in northern Arkansas and southern Missouri and in the Buffalo River (Robison and Buchanan, 1988). The geographic ranges of the shadow and Ozark basses are proximal to one another. The Roanoke bass (*A. cavifrons* Cope) is limited to Virginia and North Carolina (Cashner and Jenkins, 1982). Only the rock bass, *A. rupestris* Rafinesque, has an extensive range throughout much of the Mississippi River drainage.

Several morphological and anatomical features distinguish the shadow and Ozark basses including blotchy pigmentation versus irregular rows of spots, a deeper versus a more slender body depth, and the presence of less than or more than 41 lateral line scales (Robison and Buchanan, 1988). Genetic analysis of *Ambloplites* is limited to a single allozyme study. Koppleman et al. (2000) could not genetically distinguish between the shadow and rock basses, yet identified fixed allelic differences at two of 41 loci between the Ozark and shadow basses. No direct DNA comparisons have been performed on this genus. One of our research goals was to perform a genetic comparison of the *Ambloplites* species native to Arkansas (shadow and Ozark basses) using restriction endonuclease digestion of intact mitochondrial DNA (mtDNA). A second goal was to estimate the time of divergence using a commonly used mtDNA molecular clock (Brown et al., 1979).

Shadow bass were collected from the South Fork of the Spring River (n = 22), the Spring River (n = 28), and the Caddo River (n = 2), while Ozark bass (n = 24) were collected from the Buffalo River. Mitochondria and mtDNA were isolated and analyzed from liver tissue using techniques described by Johnson et al. (2002). Purified mtDNA was digested for 7 h at 37° C using 14 restriction endonucleases (*Bam*HI, *Bgl*I, *Bgl*II, *Csp*45I, *Dra*I, *Eco*RI, *Eco*RV, *Mlu*I, *Pst*I, *Pvu*II, *Sal*I, *Sca*I, *Xba*I, *Xho*I), under conditions recommended by the supplier (Promega Corp.). Fragment sizes generated were determined through the use of a least-squares fit program (Schaeffer and Sederoff, 1981). Variables measured included genome size, percentage genome analyzed, nucleon diversity (h; Nei and Tajima, 1981) and nucleotide sequence divergence (Nei and Li, 1979). Times of divergence were estimated from observed levels of sequence divergence using a rate of sequence divergence of 2% per million years (Brown et al., 1979). A phenogram was constructed by the unweighted pair group method (UPGMA; Sokal and Sneath, 1963) using matrices of distance values with NTSYS-PC: Numerical Taxonomy and Multivariate Analysis System (Rohlf, 1990) as well as an inferred phylogenetic tree using the Dollo parsimony algorithm in Phylogeny Inference Package (PHYLIP; Felsenstein, 1993). The northern largemouth bass (*Micropterus salmoides salmoides* Lacepede) and the green sunfish (*Lepomis cyanellus* Rafinesque), basal members of other centrarchid genera, were used for comparison of higher taxonomic relationships (Branson and Moore, 1962; Avise and Smith, 1977).

Mean genome size ranged from 16,676 (± 337 SE) base pairs for shadow bass to 17,170 (± 292 SE) base pairs for Ozark bass. These estimates are similar to values obtained for *Lepomis* (range 16,639 to 16,958; Johnson and Williams, 2003) and slightly lower than that obtained for *Micropterus* (range of 17,346 to 17,779; Johnson et al., 2002).

The total number of restriction fragments generated using 13 restriction endonucleases was 43, with 31 fragments identified for the Ozark bass and 32 fragments for the shadow bass. Three of the restriction endonucleases did not identify recognition sequences within individual species (*Bam*HI, Ozark bass, shadow bass; *Sal*I, shadow bass; and *Xho*I, Ozark bass and shadow bass) [Table 1]. The dominant haplotype (A) for the shadow bass was found in all three populations sampled (Caddo, South Fork and Spring rivers). Two additional haplotypes (B and C) were identified for single individuals from the South Fork (B) and the Spring River (C). Haplotype diversity for shadow bass of the South Fork was 0.15 with a diversity of 0.07 for the Spring River

Table 1. Composite haplotypes of *A. ariommus, A. constellatus, L. cyanellus* and *M. salmoides* collected from northeast Arkansas. Restriction endonucleases are in columns as follows: *Bam*HI, *Bgl*I, *Bgl*II, *Csp*45I, *Dra*I, *Eco*RI, *Eco*RV, *Mlu*I, *Pst*I, *Pvu*II, *Sal*I, *Sca*I, *Xba*I, and *Xho*I.

Species	Genotype Assignment	n
A. ariommus A	AAAAAAAAAAAAA	50
A. ariommus B	AAAAABAAAAAAA	1
A. ariommus C	AAAAAABAAAAAA	1
A. constellatus	ABAABABBABBBA	24
M. salmoides	BCABCACCBCCCB	1
L. cyanellus	CDACDCDDCBDDC	1

population. Haplotype B had a unique restriction site for the endonuclease *Eco*RV, whereas haplotype C had a unique restriction site for *Mlu*I. There was a single haplotype found within the Ozark bass sampled (h = 0.00). Unique restriction profiles between the Ozark and shadow basses were identified for the following restriction endonucleases: *Bgl*I, *Dra*I, *Pst*I, *Sal*I, *Sca*I, and *Xba*I.

Estimated nucleotide sequence divergence, standard error, and time of divergence for *Ambloplites, Lepomis,* and *Micropterus* are found in Table 2. Divergence values ranged from 0.0612 for the shadow and Ozark basses to 0.3216 for the largemouth bass and green sunfish. The divergence values for the shadow and Ozark basses are lower than that found for congeneric members within the genera *Lepomis* and *Micropterus* (Johnson and Williams, 2003; Johnson et al., 2002). Data indicated that *Ambloplites* is more similar to the largemouth bass than to the green sunfish. Estimated time of divergence for the two species of *Ambloplites* studied was 3.07 million years ago (Table 4). Unfortunately, there is no reported fossil record of *Ambloplites* on which to base a comparison. It must be noted that the molecular clock of 2% per million years has not been consistent through all taxa (Grewe et al., 1990). Additionally, these estimates are based on few populations within each species and therefore the values obtained are at best estimations of the divergence periods between these particular populations rather than the species as a whole.

Construction of a cladogram generated utilizing the Dollo parsimony algorithm program revealed that *Ambloplites* was most similar to *Micropterus* and less so to *Lepomis* (Fig. 1). A UPGMA dendrogram derived from the average genetic distances between species was consistent with that above. A cophenetic correlation of 0.76 was

Table 2. Mitochondrial DNA sequence divergence (above diagonal) and estimated time of divergence in millions of years (below diagonal) for *Ambloplites, Lepomis* and *Micropterus* studied. Standard errors of the mean in parentheses beneath the means.

Species	1	2	3	4
1. *A. ariommus*	***	0.0615	0.2044	0.1675
		*** (0.0014)	(0.0003)	(0.0030)
2. *A. constellatus*	3.07	***	0.2121	0.1371
	(0.01)		*** (0.0004)	(0.0006)
3. *L.cyanellus*	10.22	10.66	***	0.3216
	(0.01)	(0.01)		*** (0.0011)
4. *M. salmoides*	8.37	6.86	16.08	***
	(0.01)	(0.01)	(0.01)	***

obtained, indicative of a suitable fit between the tree generated and the data matrix (Rohlf, 1990). In contrast, Avise and Smith (1977) hypothesized that *Lepomis* was intermediate to *Micropterus* and *Ambloplites* based upon allozyme analysis of several centrarchid genera. However, Avise and Smith (1977) sampled the rock bass as compared to the shadow and Ozark basses, and they used the average genetic distances of ten *Lepomis* species rather than looking at a specific species (green sunfish). Future study of the genus *Ambloplites* at the population, subspecies, and species levels is required to further our understanding of the historical biogeography of this genus. Additional population data may alter the proposed relationships of these taxa.

We would like to thank J. Quinn, K. Shirley, M. Wine, C. Hutts, T. Sanders and L. Mommsen for technical assistance and for assistance in the collection of specimens. This work was supported by grants from the Silo Undergraduate Research Foundation and Arkansas State University.

Literature Cited

Avise, J. C., and **M. H. Smith.** 1977. Gene frequency comparisons between sunfish (Centrarchidae) populations at various stages of evolutionary divergence. Syst. Zool. 26: 319-335

Branson, B. A., and **G. A. Moore.** 1962. The lateralis components of the acoustico-lateralis system in the sunfish family Centrarchidae. Copeia 1962: 1-108.

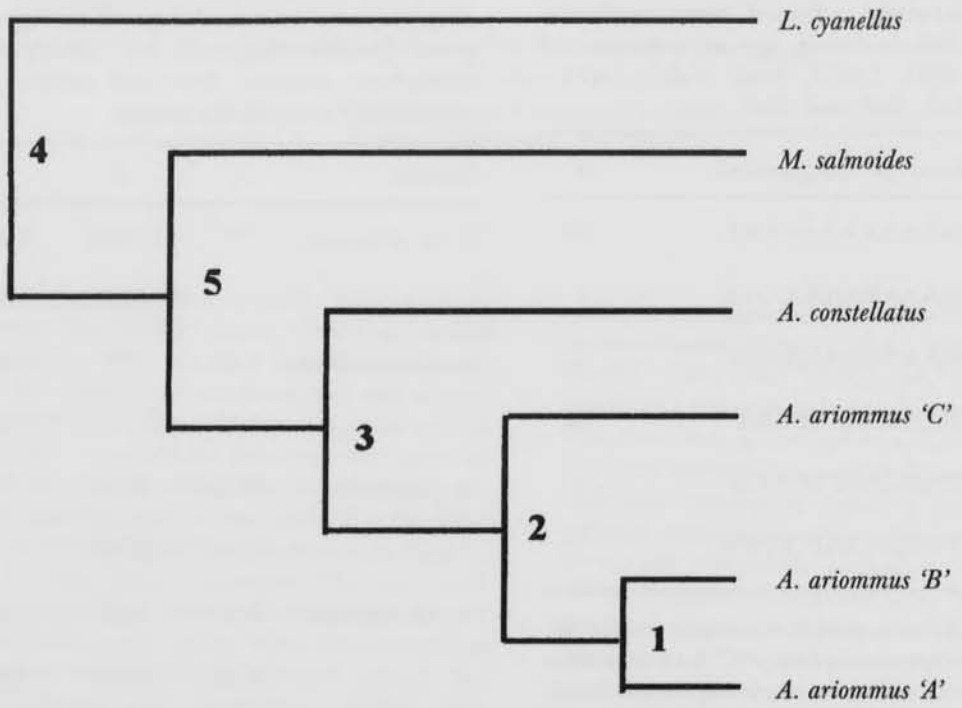

Fig. 1. Cladogram of character state matrices for presence/absence of presumptive restriction sites utilizing the Dollo parsimony algorithm. One parsimonious tree (22 steps) was generated.

Brown, W. M., M. George, Jr., and **A. C. Wilson.** 1979. Rapid evolution of animal mitochondrial DNA. Proc. Nat. Acad. Sci. 76:1967-1971.

Cashner, R. C., and **R. E. Jenkins.** 1982. Systematics of the Roanoke bass, *Ambloplites cavifrons*. Copeia 1982:581-594.

Felsenstein, J. 1993. Phylip (Phylogeny Inference Package). Version 3.51. University of Washington, Seattle.

Grewe, P. M., N. Billington, and **P. D. N. Hebert.** 1990. Phylogenetic relationships among members of *Salvelinus* inferred from mitochondrial DNA divergence. Can. J. Fish. Aq. Sci. 47:984-991.

Johnson, R. L., and **K. A. Williams.** 2003. Genetic relationships of some common Arkansas freshwater sunfishes (Centrarchidae: *Lepomis*) inferred from restriction endonuclease analysis of mitochondrial DNA. J. Arkansas Acad. Sci. 57:(in press).

Johnson, R. L., J. B. Magee, and **T. A. Hodge.** 2002. Phylogenetics of freshwater black basses (Centrarchidae: *Micropterus*) inferred from restriction endonuclease analysis of mitochondrial DNA. Biochem. Gen. 39:395-496.

Koppleman, J. B., C. M. Gale, and **J. S. Stanovick.** 2000. Allozyme and morphological variation among three nominal species of *Ambloplites* (Centrarchidae) inhabiting the Ozarks Region. Trans. Am. Fish. Soc. 129:1134-1149.

Nei, M., and **W. H. Li.** 1979. Mathematical models for studying genetic variation in terms of restriction endonucleases. Proc. Nat. Acad. Sci.76:5269-5273.

Nei, M., and **F. Tajima.** 1981. DNA polymorphisms detectable by restriction endonucleases. Genetics 97:147-165.

Robison, H. W., and **T. M. Buchanan.** 1988. Fishes of Arkansas. University of Arkansas Press, Fayetteville. 563 pp.

Rohlf, F. F. 1990. NTSYS-PC: Numerical Taxonomy and Multivariate Analysis System. Version 1.60. Exeter Publishing, Setauket.

Schaeffer, H. E., and **R. R. Sederoff.** 1981. Improved estimation on DNA fragment lengths from agarose gels. Ann. Biochem. 115:113-122.

Sokal, R. R., and **P. H. A. Sneath.** 1963. Principles of numerical taxonomy. Freeman, San Francisco. 359 pp.

Testing and Modeling Electrical Characteristics of Novel Silicon Carbide (SiC) Static Induction Transistors (SITs)

Avinash S. Kashyap, Sharmila D. Magan Lal,
Ty R. McNutt, Alexander B. Lostetter and **H. Alan Mantooth***
Silicon Carbide Research Group
Department of Electrical Engineering
University of Arkansas
3217 Bell Engineering Center
Fayetteville, AR 72701

*Corresponding Author

Introduction

The static induction transistor (SIT) was invented by Professor Junichi Nishizawa of Tohoku University in 1950. One of the main advantages of the SIT device is its high speed switching characteristics. Since no carriers are injected from the gate, switching can be performed at an extremely high speed (without storage effects) and a small gate resistance (r_g) is used for minimum high frequency signal loss. SITs have high input impedance and are voltage controlled devices, and therefore only a low drive power is required at the gate. SiC has very high voltage breakdown (2MV/cm), thermal conductivity (4.8W/cm-K), and saturation velocity ($2x10^7$ cm/s) compared to Si devices. Thus, SiC SITs are highly suited for high power applications (Lostetter, 2003).

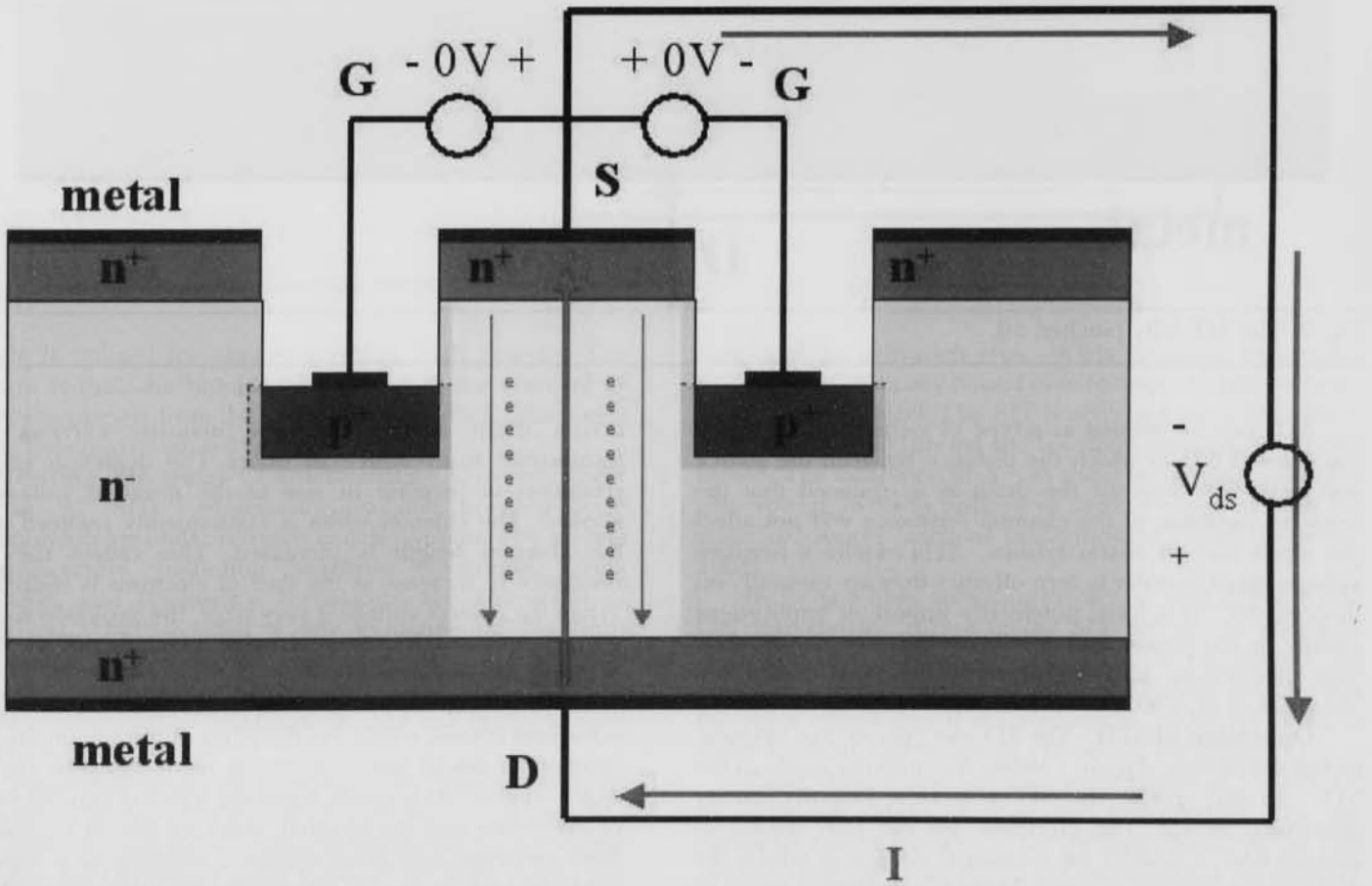

Fig. 1. The SIT operating in a unipolar forward conduction mode.

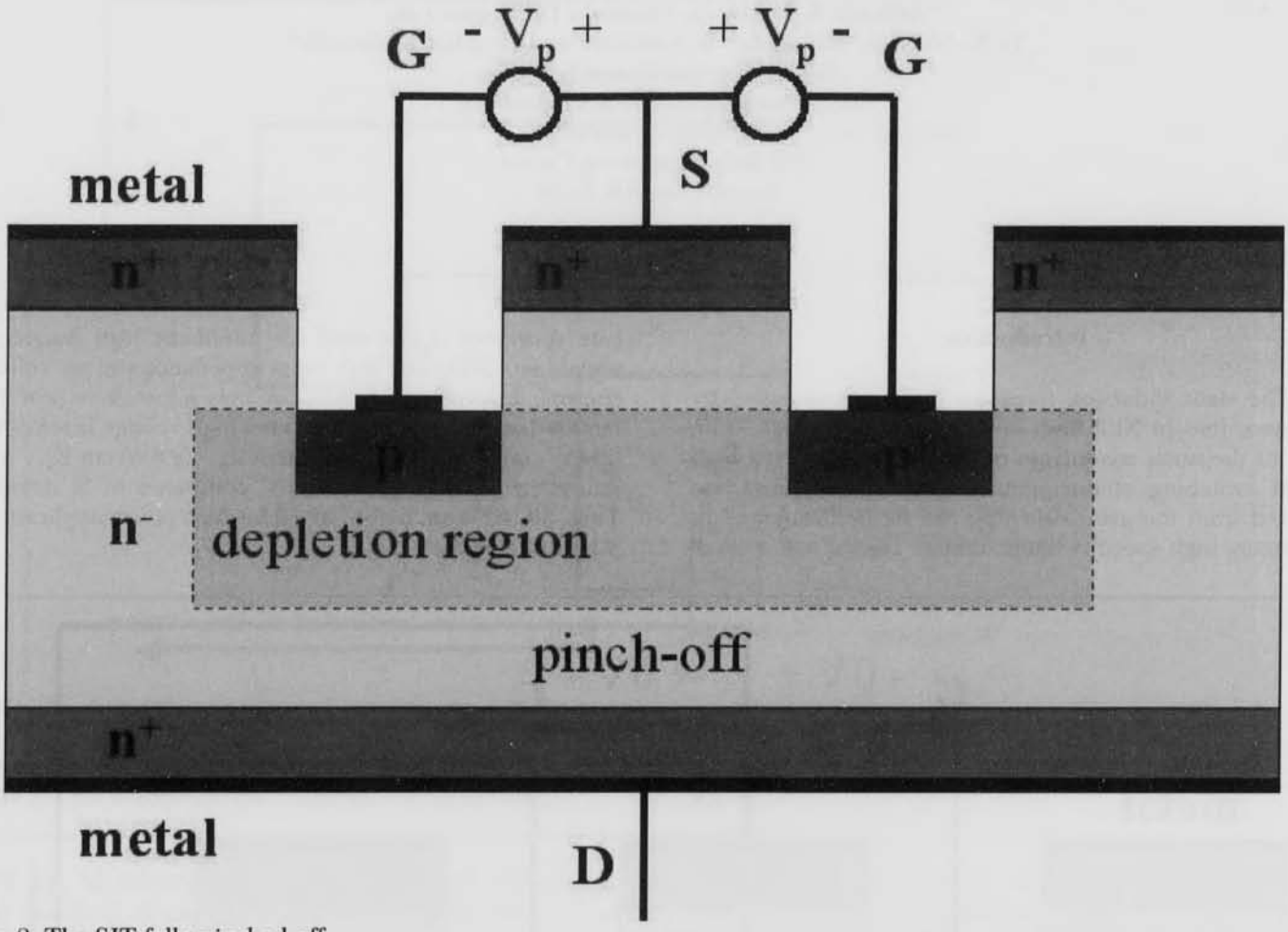

Fig. 2. The SIT fully pinched-off.

SITs can be defined as a type of v-channel field effect transistor (FET) in which the distance between the source and depletion layer of the drain is so reduced that the negative feedback of the channel resistance will not affect the direct current characteristics. SITs require a negative voltage signal in order to turn off since they are normally-on devices. SiC SITs have potentially important applications mainly in the power and aerospace industry due to their high-temperature and high-current handling capabilities (Neudeck et al., 2002).

Operation of SITs.--The SIT can operate as a unipolar or bipolar device. Figure 1 shows the unipolar mode of the SIT. In this mode, the SIT acts as a majority carrier (electrons) device. The electrons are the only means of current flow. Consider an n-channel device in which the drain and source are shorted. There is a depletion region in the gate-source interface and when a voltage is applied across drain and source, the majority carriers are transported from source to drain. The depletion region continues to increase in size as the negative voltage is applied. The channel width is consequently reduced, and the channel length is increased. This causes the on-resistance to increase as the flow of electrons is restricted. When the reverse voltage is very large, the depletion region grows large enough to meet, thereby "pinching off" the flow of current as shown in Fig. 2.

In the bipolar mode of operation, the gate-source region is forward biased, which has the effect of turning on the p-n junction (a diode) into conduction mode between the p^+ and n- region. As a result, holes are injected into the body of the device and the channel, reducing the on resistance. Both electrons and holes conduct, resulting in a bipolar mode as seen in Fig. 3. Generally, the unipolar mode is used for high frequency applications whereas the bipolar

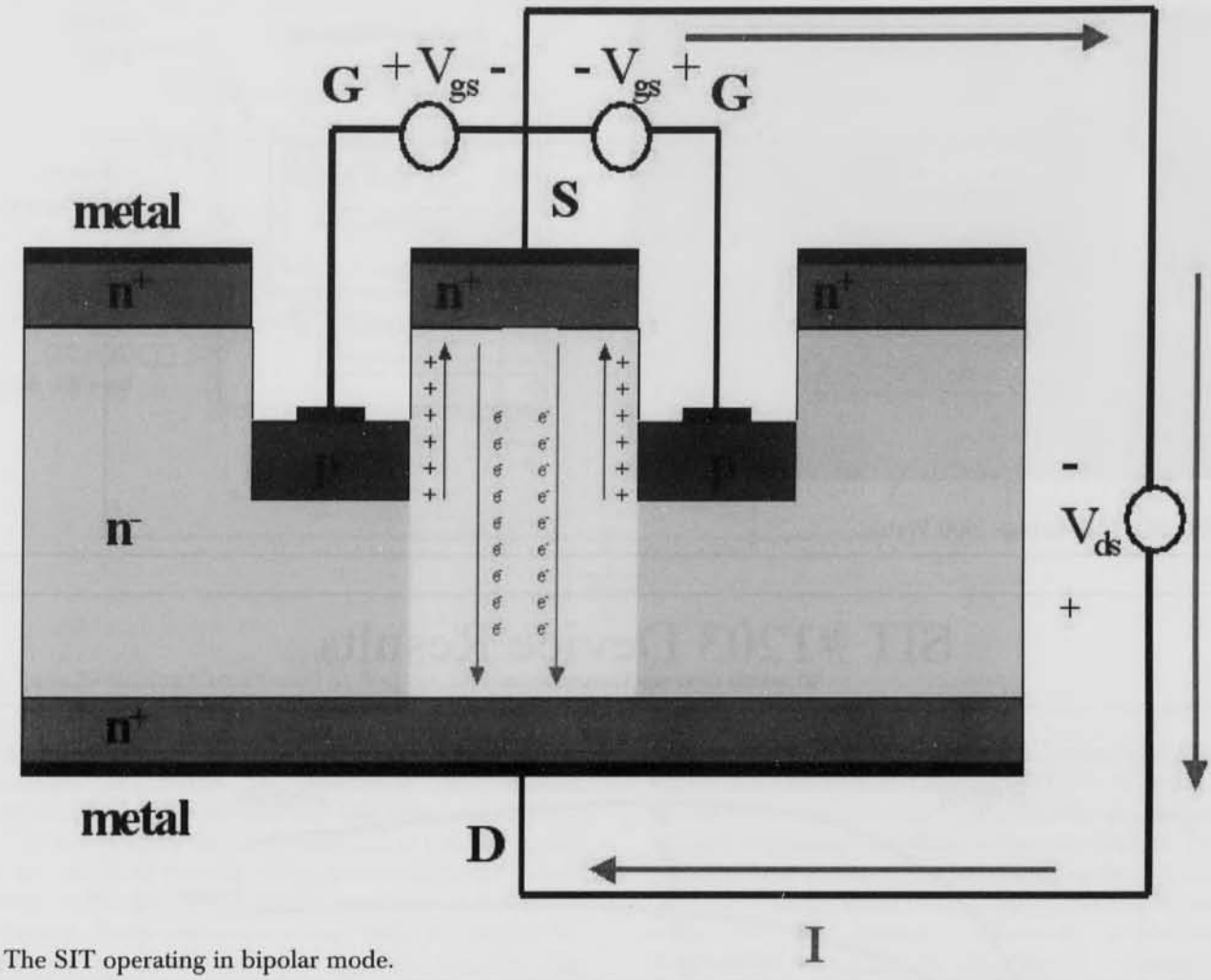

Fig. 3. The SIT operating in bipolar mode.

mode is utilized for circuits handling high power. The reason is that, the bipolar mode requires the removal of minority carriers from the bulk substrate, which takes more time, thus maximum frequency is reduced.

Testing Electrical Characteristics.-- Currently there are no SiC SITs commercially available, however these components are under research and development by several manufacturers, including Northrop Grumman, Cree, Infineon, and Rockwell. Fortunately, the University of Arkansas (UA) obtained a few experimental Northrop Grumman static induction transistors and Cree Schottky diodes. The UA Silicon Carbide group has begun to utilize these components by building a SiC SIT half-bridge as seen in Fig. 4.

Figure 5 illustrates the experimentally obtained turn-On characteristic curves of one of the SIT devices. These SiC SITs were developed by Northrop Grumman for use in low voltage, high frequency radar applications. Note that in this figure the transition region consists of the cut-off area (Off state) and the activation area. When the drain and source junctions are inversely biased (due to negative gate voltage), the SIT device is off. The SIT is activated when the source junction is forward biased and the drain junction is reversed biased. The saturation area (On state) takes place when the gate voltage is made positive or zero resulting in both the drain and source junctions being forward biased (Lostetter, 2003).

By using a basic switching circuit (as seen in Fig. 6) the On characteristic curves of the SIT device are obtained. Note that the driving circuit in Fig. 6 determines the switching speed of the circuit. RS is the output resistance in the drive circuit and it is necessary to make RS small in order to obtain fast switching (Tatsuta et al., 1995).

Using Ohm's Law and the measurement of V_{DS} vs. ID for different values of V_{GS} and temperature, the on-resistance can be obtained. For instance, based on the ON characteristic curve in Fig. 5, the on-resistance for this SIT device at room temperature will be 2Ω. Theoretically, the

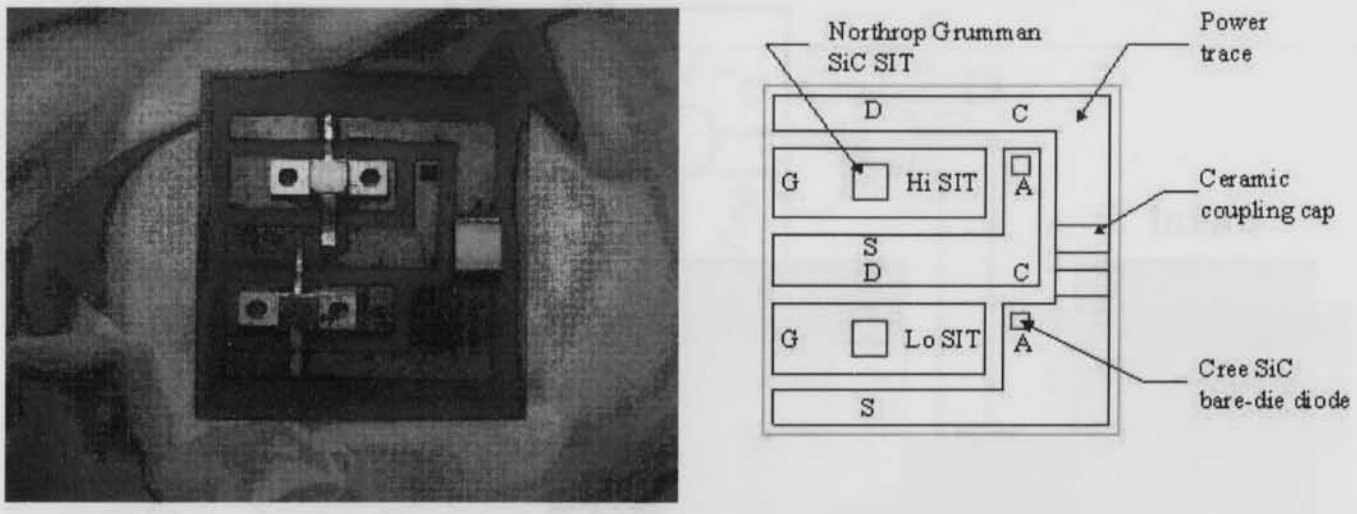

Fig. 4. SiC SIT Half-Bridge (500 Watts).

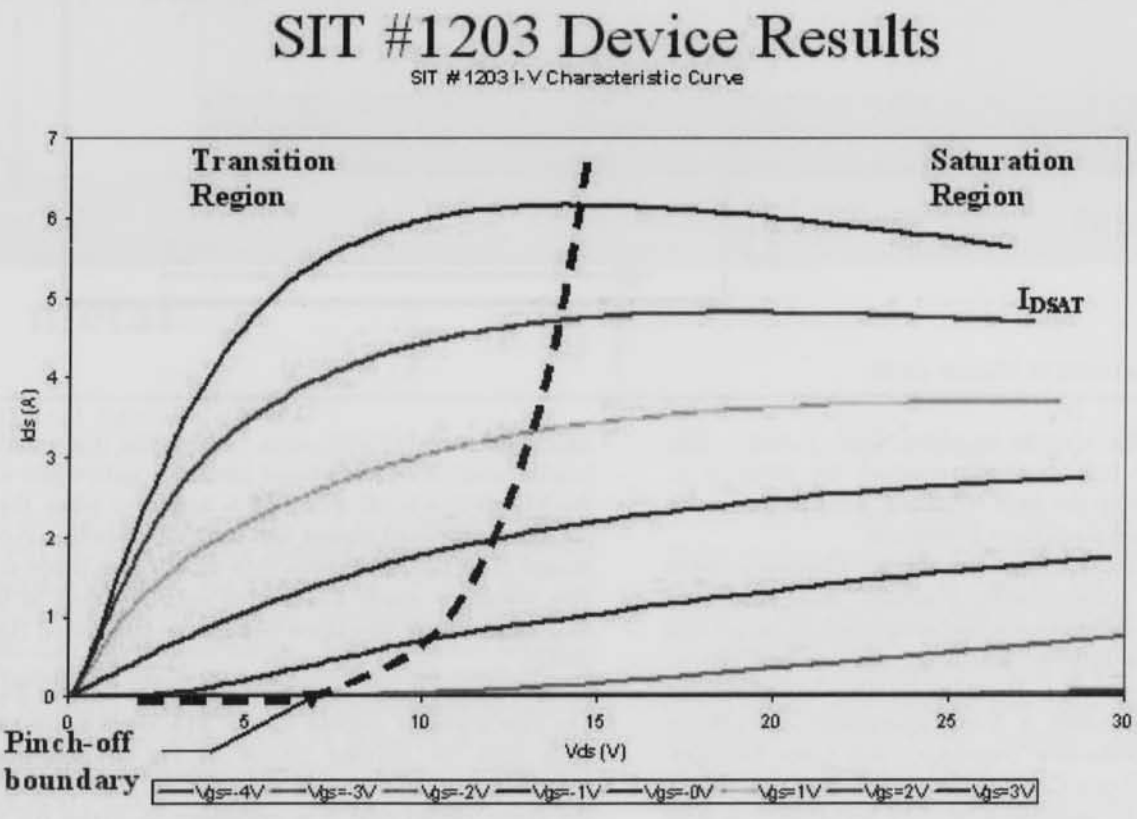

Fig. 5. SIT #1203 I-V ON characteristic curve.

on resistance will go down as temperature increases because of the negative current/temperature characteristics.

The voltage amplification ratio (μ) is the ratio of the potential change of V_{DS} and V_{GS}.

$$\mu = \left|\frac{V_{DS}}{V_{GS}}\right|$$

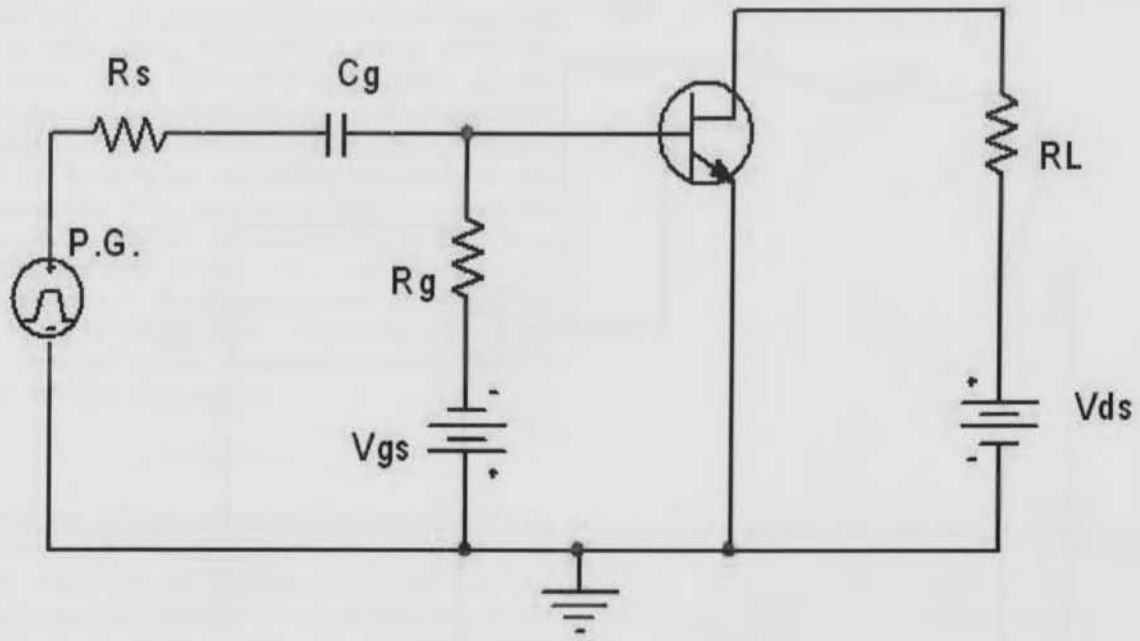

Fig. 6. Basic Switching Circuit used to find the ON resistance of the SIT.

Another basic circuit, as seen in Fig. 7, is under construction in order to determine the mutual transconductance of the SIT device. The drain current, I_{D1}, can be obtained when Switch 1 is placed at Position 1, and Switch 2 is placed in Position 2; I_{D2} is obtained when Switch 1 is placed at Position 2, and Switch 2 is placed at Position 1. The mutual transconductance can then be found by applying the measured values of I_{D1} and I_{D2} into the following formula:

$$g_m = \frac{I_{D1} - I_{D2}}{\Delta V_{GS}}$$

The SIT's response time (that is, delay time, rise time, storage time, and fall time) can be obtained by examining the measured input current and voltage versus the output. The delayed time is the time required for the output to reach 10% of the maximum amplitude starting at the time of the application of the input pulse. The rise time is the time required for the output to go from 10% to 90% of the maximum amplitude. The storage time is the time required for the output to decrease to 90% of the maximum amplitude after the input pulse disappears. Finally, the fall time is the time required for the output to decrease from 90% to 10% of the maximum amplitude.

Modeling Characteristics.--Given the increasing popularity of SiC devices, compact circuit simulation models are in great demand so that commercial simulators can include them in their model libraries. The MSCAD Laboratory at the University of Arkansas uses the MAST Hardware Description Language (HDL) (Vlach., 1992) to model these devices. MAST is a flexible language that can be used to generate excellent behavioral models. The model parameters and means of extraction for the SiC SITs have been identified (Scozzie et al., 1994). As stated previously, some of the primary electrical parameters are transconductance (g_m), the drain/source saturation current (I_{DSS}), the threshold voltage (V_t), the lumped resistance parameter (r_s), gate-source junction capacitance at zero bias (c_{gs}), and gate-drain junction capacitance at zero bias (c_{gd}). The term gm is defined as the maximum transconductance at zero gate voltage and uses a value of I_{DSS} that is the average of the current in the saturation region of the device for zero gate voltage. Figure 8 shows the equivalent circuit for the SIT model that can be used for analyses. V_t was extracted from the data using the square-root of the I_D vs. V_{GS} curve, in which the slope of the curve is extrapolated to the x-axis, and V_t is defined as the intercept. V_t is the externally applied voltage to achieve pinch-off. The lumped resistance parameter (r_s) will be modeled using the EMPEROR technique (Wen et al., 1992). The characteristic equations that are used to model the SIT are as follows:

Cut-off region ($V_{GS}-V_{to} \le 0$) : $i_d = 0$

Linear region ($0<V_{DS}<V_{GS}-V_{to}$):$i_d = g_{ml} V_{DS} * [2(V_{GS}-V_{to})-V_{DS}]$

Saturation region ($0< V_{GS}-V_{to} \le V_{DS}$):$i_d = g_{ms} * [V_{GS}-V_{to}]2 * [1+ \zeta V_{DS}]$

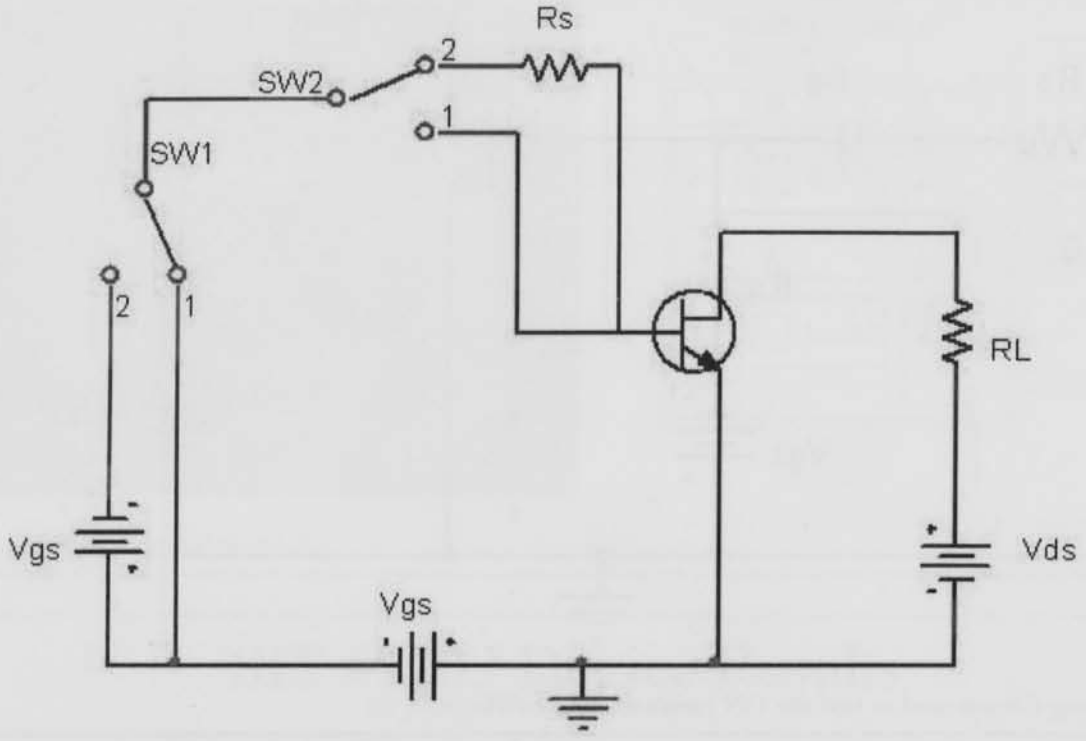

Fig. 7. Basic switching circuit used to find the mutual transconductance of the SIT.

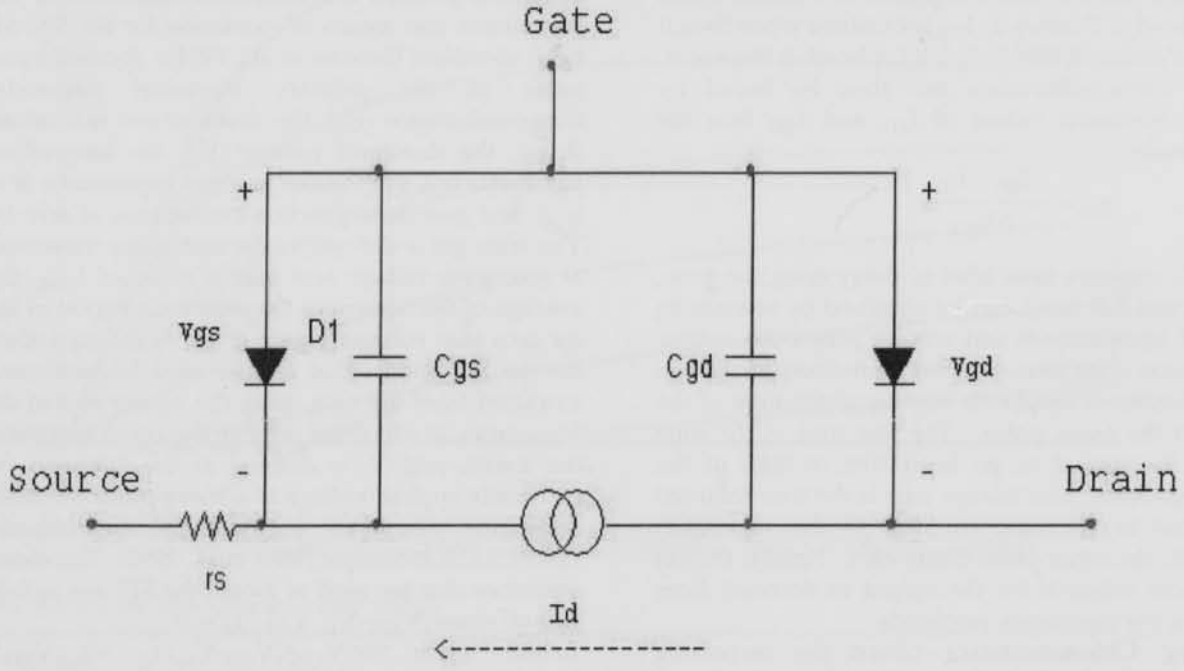

Fig. 8. Equivalent circuit for the SIT model.

where ζ is the pinch-off parameter that has been introduced in the model, for modeling the the SIT pinch-off effect. The transconductance of the SITs varies at the active and the saturation regions. These parameters and their extraction aid in making a robust model that can be used extensively in simulators. Temperature dependent modeling is also needed, since the SITs operate at high temperatures (theoretically up to 600°C). Repeated testing of the SITs at room temperature has already been performed at the MSCAD Laboratory. High-temperature study will be carried out at the HiDEC facility. The models will then be validated with actual device measurements with the SITs provided by the UA collaborators.

Conclusions

Currently, the SiC research that is being performed by the UA is increasingly demonstrating the versatility of these wide band gap devices. Before SiC SITs can be commercially launched, issues such as modeling and device physics need to be demonstrated. The characterization study currently under investigation has shown the excellent power density handling capabilities of these devices. The model of the SIT under development will be a very useful tool for power electronic circuit designers.

Literature Cited

Lostetter, A. B. 2003. The design, fabrication and analysis of half-bridge multichip power modules (MCPM) utilizing advanced laminate, silicon carbide and diamond-like carbon technologies. Published by Univ. Arkansas. Ph.D. Dissertation. Univ. Arkansas, Fayetteville. 450 pp.

Neudeck, P. G., Liang-Yu Chen., and **R. S. Okojie.** 2002. High-temperature electronics - a role for wide bandgap semiconductors? Proc. IEEE, 90:1065 -1076

Scozzie C. J., C. W. Tipton, W. M DeLancey, J. M. McGarrity, and **F. B. McLean.** 1994. High temperature stressing of SiC JFETs at 3000C, Reliability Physics Symp. 32:351-358.

Tatsuta M., E. Yamanaka, and **J. Nishizawa.** 1995. High frequency – High Power Static Induction Transistor, IEEE Industry Applications Magazine 1(2):40-45.

Vlach, M. 1991. Analogy Inc. Application Notes–Model Fundamentals. Analogy Inc. Beaverton, OR. 346 pp.

Wen C. S., M. Guldahl, L. P. Sadwick, R. Kent, and **H. Gaffur.** 1992. Measurement and parameter extraction of sub-micron VLSI MOSFET test structures. Proc. Int. Conf. Microelectronic Test Structures 5:196-201

DNA Sequence Analysis of the Freshwater Mussel *Lampsilis hydiana* (Bivalvia: Unionidae) in Select Ozark and Ouachita Mountain Streams of Arkansas

Jennifer A. Lewter* **and Allen L. Szalanski**
Department of Entomology
University of Arkansas
Fayetteville, AR 72701

Tsunemi Yamashita
Department of Biology
Arkansas Tech University
Russellville, AR 72801

*Corresponding Author

Nearly 300 species of freshwater mussels are found in North America; this represents the greatest diversity of freshwater mussels in the world (Williams et al., 1993; Lydeard and Mayden, 1995). Although it is not clearly understood which environmental and historical factors have fostered such diversity in North America, there is scientific evidence of anthropogenic factors causing the rapid decline of many species of freshwater mussels (Neves et al., 1997). The unionid mussels have recently become one of the most endangered freshwater organisms in North America (Williams et al., 1993; Stein and Flack, 1997; Master et al., 1998). The primary threats to these mussels include pollution, increased sedimentation from stream alterations, loss of fish species that host the parasitic unionid larvae (glochidia), and the introduction of the exotic zebra mussel (*Dreissena polymorpha*) (Williams et al., 1993; King et al., 1999). To date, there has been very little research done on the genetic diversity of unionid mussels (Liu et al., 1996; Roe and Lydeard, 1998). The traditional method of classifying taxa based on physical characteristics is challenging with mussels because they do not have many distinguishing features (Lydeard and Roe, 1998). Furthermore, knowing the exact geographical range of an endangered species (or sub-species) can provide insight as to which anthropogenic factors may be the most detrimental to the organism's survival (Roe et al., 2001). Finally, conservational laws and methods cannot be implemented until the endangered organism(s) is properly classified and its geographical range is known (Lydeard and Roe, 1998).

The objective of this study was to examine a ~300 bp region of mitochondrial DNA in the 16s rRNA gene of *Lampsilis hydiana* and compare our results with those of Turner et al. (2000). Previous to this study, the only genetics research available for this species was done by Turner et al. (2000) who found five haplotypes using the 16S rRNA gene.

Since *L. hydiana* can be found in many different streams in Arkansas, we hypothesized that the *Lampsilis* populations would exhibit a population structure that reflects isolation-by-distance. For example, populations that are further apart geographically have greater genetic variation than populations that are closer together which could potentially interbreed.

Mussel Samples.--*Lampsilis hydiana* mussels were collected from the North and Middle forks of the Illinois Bayou and the South Fourche La Fave River of Arkansas (Table 1.) Live specimens were brought back to the Department of Biology, Arkansas Tech Univ. in Russellville, AR and were killed by immersion in a jar of 95% ethanol and stored at -20° C.

DNA Extraction, Sequencing and Sequencing Analysis.--DNA was extracted from a small piece of muscular foot tissue (<1 cm^3) using the following phenol/chloroform extraction protocol. Nine hundred µL of Lifton Buffer (0.2M sucrose, 0.05M EDTA, 0.1M Tris, 0.5% SDS) was added to a 50 mL plastic tube with foot tissue. Forty-five µL of Proteinase K (Promega, Madison, WI) were added and the tissue was homogenized with a glass stirring rod and placed on ice for one hour. One hunded µL of 8M potassium acetate was added and the samples were vortexed briefly and again chilled on ice for one hour. The solution was transferred to a new microtube and centrifuged at 14000 RPM for fifteen minutes. Supernatant was transferred to a new microtube, 2 µL of RNAse (Promega), were added to the new tube, and it was incubated at room temperature for twenty minutes. One hundred µL chloroform/isoamyl alcohol (CIA) and 300 µL of equilibrated phenol was added, samples were vortexed, incubated at room temp for five minutes, and centrifuged at 14000 RPM for five min. The aqueous phase was pipetted to a new microtube, 400 µL CIA were added, and the sample was vortexed and centrifuged at 14000 RPM for five min. The aqueous phase was pipetted to a new microtube, then 100 µL of 3M sodium acetate were added. Three hunded µL of isopropanol was added, and sample was stored at –20°C for three days. The samples were then centrifuged at 14000 RPM for 30 minutes, then 1 mL of chilled 70% ETOH was added to the DNA pellet. The samples were spun at 14000 RPM for five minutes, supernatant removed and the DNA pellet was rewashed with 1 mL chilled 70% ETOH and was centrifuged for five min. Supernatant was removed and the DNA pellet was allowed to air dry for at least fifteen minutes. Finally, 200 µL of distilled H_2O were added, DNA was resuspended for two hours at room temperature and then stored at 4°C.

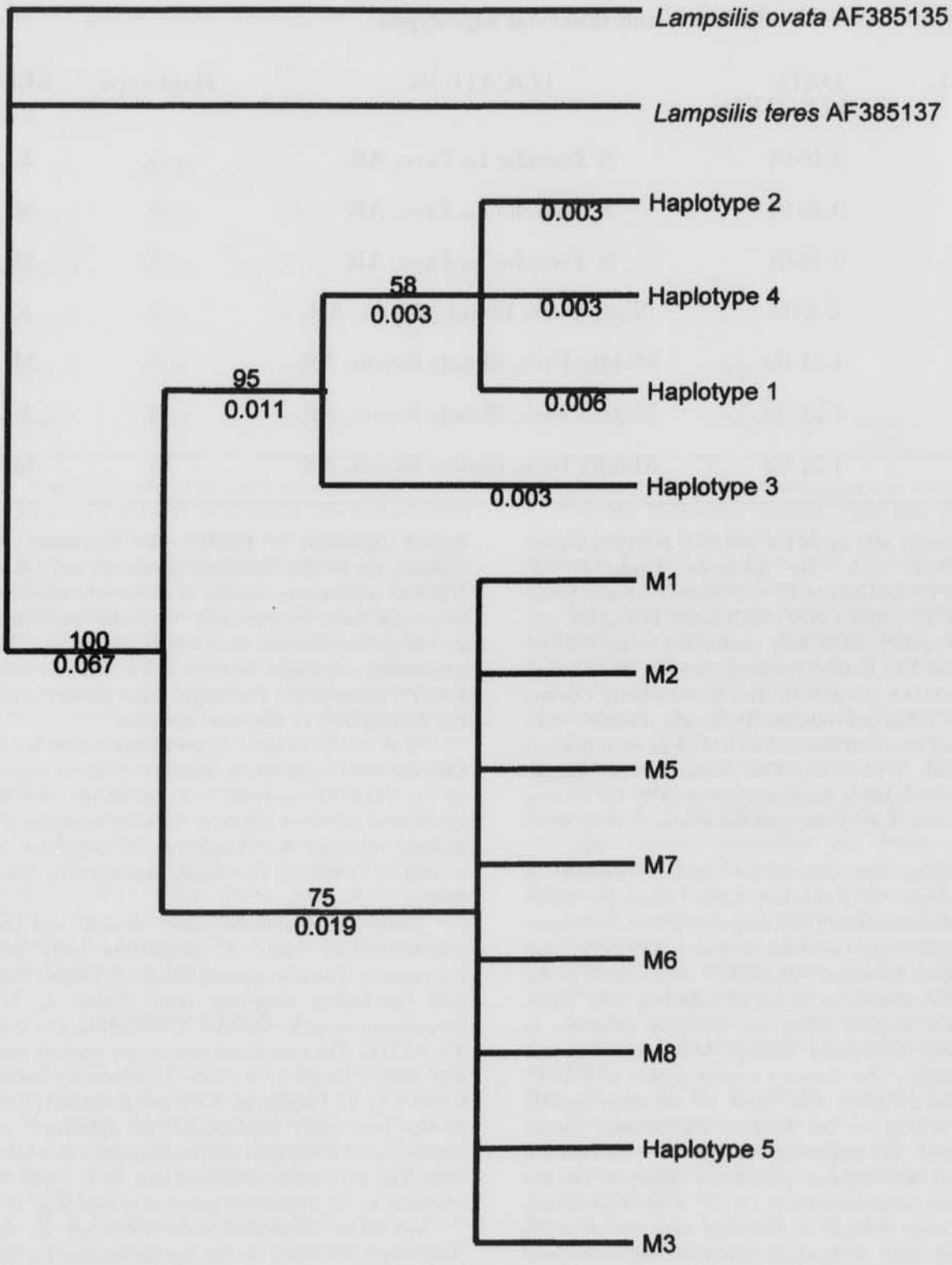
Lampsilis ovata AF385135
Lampsilis teres AF385137
Haplotype 2
0.003
58
0.003
Haplotype 4
0.003
95
0.011
Haplotype 1
0.006
Haplotype 3
0.003
M1
100
0.067
M2
M5
M7
75
0.019
M6
M8
Haplotype 5
M3

Table 1. Specimens used in this study and observed haplotypes.

MUSSEL ID	DATE COLLECTED	LOCATION	Haplotype	SEX
M1	9-16-01	S. Fourche La Fave, AR	5	F
M2	9-16-01	S. Fourche La Fave, AR	5	M
M3	9-16-01	S. Fourche La Fave, AR	5	M
M5	4-4-02	North Fork, Illinois Bayou, AR	5	F
M6	4-21-02	Middle Fork, Illinois Bayou, AR	5	M
M7	4-21-02	Middle Fork, Illinois Bayou, AR	5	F
M8	4-21-02	Middle Fork, Illinois Bayou, AR	5	M

Approximately 400 bp of the mtDNA 16S rRNA gene were amplified with the primers 16sint3-L (5' –TGAGCGTVCTAAGGTAGC- 3') (Turner et al., 2000) and 16sint4-H (5' –AKCCAACATCGAGGTCGCAA –3') (Turner et al., 2000). PCR was conducted using 9.25 µl DH_2O, 3.0 µl of 10X Buffer (Promega), 0.5 µl DNTP, 0.5 µl BSA, 0.5 µl DMSO, 0.5 µl formalin, and 0.4 units *Thermus aquaticus (Taq)* DNA polymerase (Promega). Primers were added at a final concentration of 20 µM (5 µl each primer) and mixed with 5 µl DNA. The thermal cycler profile consisted of 30 cycles of denaturation at 94°C for 30 sec, annealing at 50°C for 30 sec, and extension at 72°C for 1 min.

PCR products were sent to the Graduate Institute of Technology, Univ. of Arkansas, Little Rock for DNA sequencing. Mitochondrial DNA sequences from freshwater mussels *Lampsilis ovata* (GenBank accession AF385135) and *L. teres* (GenBank accession AF 385137) were added to the *L. hydiana* DNA sequences to act as outgroup taxa. DNA sequences were aligned using the PILEUP program in GCG (Genetics Computer Group, Madison, WI) and adjusted manually. The distance matrix option of PAUP* 4.0b10 (Swofford, 2001) was used to calculate genetic distances according to the Kimura 2-parameter model (Kimura, 1980) of sequence evolution. Maximum likelihood and unweighted parsimony analysis on the alignments were conducted using PAUP* 4.0b10 (Swofford, 2001). Gaps were treated as missing data or as a 5th character state and a random addition sequence was employed. The reliability of trees was tested with a bootstrap test (Felsenstein, 1985). Parsimony bootstrap analysis included 1,000 resamplings using the Branch and Bound algorithm of PAUP*. For maximum likelihood analysis, the default likelihood parameter settings were used (HKY85 6-parameter model of nucleotide substitution, and empirical base frequencies), with the exception of the transition/transversion ratio which was set to 2.345. These parameters were used to carry out a heuristic search using PAUP*, using either the single most parsimonious tree as the starting tree, or step-wise addition.

PCR products were approximately 400 bp in length. One hundred eighteen nucleotide characters were excluded in the PILEUP analysis, and out of the 309 remaining characters, 251 were constant. All seven samples of *Lampsilis hydiana* matched the 'haplotype 5' sequence (GenBank accession AF191569) previously published by Turner et al., (2000).

Thirty-one characters were variable and parsimony-uninformative, while 27 characters were parsimony-informative. Pairwise genetic distances ranged from 0.00 to 0.07 (excluding outgroup taxa) (Table 2). Nucleotide frequencies were A = 0.38817, C = 0.20102, G = 0.18934 and T = 0.22147. The maximum parsimony analysis resulted in a tree with a length of 64 and a consistency index (CI) of 0.969 (Fig. 1). Haplotype 5 formed a distinct clade relative to the four other haplotypes. No difference was found between excluding gaps and treating gaps as a 5th character state. The maximum likelihood tree, -ln L = 690.49790, was identical to the maximum parsimony tree (Fig. 1).

We have confirmed that there are *L. hydiana* of 'haplotype 5' located in the South Fourche La Fave River, and this same haplotype is found in the North and Middle forks of the Illinois Bayou. Since sample sizes were small, future research should be conducted including more

Table 2. Pairwise genetic distances among the 5 haplotypes *Lampsilis hydiana* and 2 *Lampsilis* outgroup taxa.

		1	2	3	4	5	6	7
1	*L. ovata*	-						
2	*L. teres*	0.044	-					
3	Haplotype 2	0.124	0.112	-				
4	Haplotype 4	0.124	0.112	0.007	-			
5	Haplotype 1	0.121	0.108	0.010	0.010	-		
6	Haplotype 3	0.117	0.104	0.007	0.007	0.010	-	
7	Haplotype 5	0.124	0.107	0.038	0.038	0.041	0.031	-

specimens from each site. The geographical range of *L. hydiana* is not clearly defined, so it would also be beneficial to sample as many different Arkansas streams and rivers as possible. Other molecular markers such as the nuclear ITS region may also be used to detect sequence diversity. Nuclear protein genes are believed to evolve at a slower rate than mitochondrial genes, so it is important to note that nuclear markers may reflect different stages of evolutionary history than mitochondrial markers (Machordom et al., 2003). Other researchers working with freshwater mussels suggest that if different populations within the same species are found (i.e., no gene exchange is possible between them), they should be managed as separate conservation units, particularly by avoiding relocating the mussels (King et al., 1999). It is essential to protect the genetic lineages of unionids that have been evolving over thousands of years.

ACKNOWLEDGMENTS.—We thank Jobi Brown and Kendall Moles for collecting samples. This project was funded in part by the Arkansas Tech University Physical and Life Sciences Endowment Fund.

Literature Cited

Felsenstein, J. 1985. Confidence limits on phylogeneties: An approach using the bootstrap. Evolut. 39:783-791.

Kimura, M. 1980. A simple method for estimating evolutionary rate of base substitutions through comparative study of nucleotide sequences. J. Molec. Evolut. 16:111-120.

King, T. L., M. S. Eackles, B. Gjetvaj, W. R. Hoeh. 1999. Intraspecific phylogeography of *Lasmigona subviridis* (Bivalvia: Unionidae): Conservation implications of range discontinuity. Molec. Ecol. 8:S65-S78.

Liu, H-P., J. B. Mitton, and **S. J. Herrmann.** 1996. Genetic differentiation in and management recommendations for the freshwater mussel *Pyganodon grandis*. Amer. Malacolog. Bull. 13:117-124.

Lydeard, C., and **K. J. Roe.** 1998. Phylogentic Systematics: The missing ingredient in the conservation of freshwater unionid bivalves. Fisheries 23: 16-17.

Lydeard, C., and **R.L. Mayden.** 1995. A diverse and endangered aquatic ecosystem of the Southeast United States. Conser. Biol. 9:800-805.

Machordom, A., R. Araujo, D. Erpenbeck, and **M. Ramos.** 2003. Phylogeography and conservation genetics of endangered European Margaritiferidae (Bivalvia:Unionoidea.) Biol. J. Linn. Soc. 78:235-252.

Master, L. L., S. R. Flack, and **B. A. Stein**. 1998. *Rivers of Life: Critical Watersheds for Protecting Freshwater Biodiversity.* The Nature Conservancy, Arlington, VA.

Neves, R. J., A. E. Bogan, J. D. Williams, S. A. Ahlstedt, and **P. Hartfield.** 1997. Status of aquatic mollusks in the Southeastern United States: A downward spiral of diversity. In: *Aquatic fauna in Peril: the Southeastern Perspective* (eds Benz, G.W., Collins, D.E.), pp.43-85. Special publication 1. Southeast Aquatic Research Institute, Lenz Design and Communications, Decatur, GA.

Roe, K. J., P. D. Hartfield, and **C. Lydeard.** 2001. Phylogeographic analysis of the threatened and endangered superconglutinate-producing mussels of the genus *Lampsilis* (Bivalvia: Unionidae.) Molec. Ecol. 10:2225-2234.

Roe, K. J., and **C. Lydeard.** 1998. Molecular systematics of the freshwater mussel genus *Potamilus* (Bivalvia: Unionidae.) Malacologia 39:195-205.

Stein, B. A., and **S. R. Flack.** 1997. *1997 species report card: the state of U.S. plants and animals.* The Nature

Conservancy, Arlington, VA.

Swofford, D. L. 2001. PAUP*: Phylogeny Analysis Using Parsimony (* and other methods), version 4.0b10. Sinauer Associates, Sunderland, MA.

Turner, T. F., J. C. Trexler, J. L. Harris, and **J. L. Haynes.** 2000. Nested cladistic analysis indicates population fragmentation shapes genetic diversity in a freshwater mussel. Genetics 154:777-785.

Turner, T. F., J. C. Trexler, J. L. Harris, and **J. L. Haynes.** 2000. Nested cladistic analysis indicates population fragmentation shapes genetic diversity in a freshwater mussel. Genetics 154:777-785.

Williams, J. D., M. L. Warren Jr., K. S. Cummings, J. L. Harris, and **R. J. Neves.** 1993. Conservation status of freshwater mussels of the United States and Canada. Fisheries 18:6-22.

Yang, Z. 1994. Maximum likelihood phylogenetic estimation from DNA sequences with variable rates over sites: Approximate methods. J. Molec. Evol. 39:306-314.

Acoustic Mapping of Aquatic Vegetation in Lakes: An Example from Northwest Arkansas

Angela M. Polly
Tennessee Valley Authority
1101 Market St.
HB 2A-C
Chattanooga, TN 37402-2801

Stephen K. Boss*
Department of Geosciences
113 Ozark Hall
University of Arkansas
Fayetteville, AR 72701

*Corresponding Author

Lake Wedington Recreation Area is located in Washington County in northwest Arkansas (Fig. 1). The lake is accessible in the Ozark National Forest 17.7 km west of Fayetteville, on State Highway 16. The normal pool of Lake Wedington lies at an elevation of 342 m (1,121 ft; Fig. 1) and has a maximum depth of approximately 12 m (Fig. 2; Table 1). In 1937, an artificial dam was constructed across the drainage leading to the Illinois River to create Lake Wedington. The lake has been drained occasionally throughout its history as a means of controlling aquatic macrophytes, composed primarily of aquatic algae and an aquatic vascular plant, *Potamogeton natans* (floating-leaf pondweed; Lindman, 1901; Owen, 1952; Fig. 3). Two previous studies of Lake Wedington were completed in 1952 (Allman, 1952; Owen, 1952). Allman (1952) focused on the relationship between water chemistry and spring phytoplankton blooms using temperature, dissolved oxygen, pH, and nitrate. Owen (1952) provided a number of morphometric measures of the lake and also reported water quality parameters similar to those of Allman (1952) from July 1950 to June 1951. Most recently, Polly (2001) conducted a detailed bathymetric and sedimentation survey of Lake Wedington utilizing a dual frequency (28 and 200 kHz) echo sounding system. The acoustic mapping system deployed by Polly (2001) is typically utilized to discriminate bedrock and lacustrine sediment fill, providing detailed maps of bathymetry (Fig. 2) and sediment thickness (Polly and Boss, 2000; Polly, 2001). However, this short note reports on the observation of distinctive yet anomalous acoustic signatures on a number of echo sounder profiles from the Polly (2001) survey, and the correlation of these acoustic anomalies with dense growths of aquatic plants. As such, results presented here provide a novel and potentially cost-effective method for lake managers to map distributions of aquatic plants.

Polly's (2001) survey of bathymetry and sediment thickness of Lake Wedington was conducted during June 2000 as a research project for her M.S. degree in Geosciences. Lake elevation at the time of the survey was 342 m. The survey utilized a Knudsen Engineering, Ltd. Model 320 B/P Dual Frequency (28 and 200 kHz) Echo Sounding System deployed from an 8-m pontoon boat maintained by the Department of Geosciences at the University of Arkansas – Fayetteville for limnological research. During lake surveys, the boat travels at approximately 2 m/s. The transducer of the echo sounding system transmits acoustic energy to the lake bottom from which it reflects to be detected again by the transducer. The two-way travel time (i.e. time for sound to travel from the transducer to the lake floor and back to the transducer) of the acoustic impulse is recorded by the system and converted to depth according to the following relationship:

$$D = \frac{t}{2} v$$

where D = depth (m), t = two-way travel time (s), and v = p-wave velocity (m/s) (Robinson and Coruh, 1988). In order to solve this equation, the p-wave velocity through water must be known. This velocity will vary with water temperature, but because Lake Wedington is relatively shallow, choosing an average velocity for the entire water column (despite temperature changes) results in minimal error (<0.15 m, or <1.25%, in the deepest part of the lake). For this study, the echo sounding system was calibrated in known water depth at the lake's boat dock and the p-wave velocity was determined to be 1,480 m/s, a typical value obtained in fresh water (Robinson and Coruh, 1988). The echo sounder emitted and recorded six pulses every second. These data were averaged to obtain one sounding for each second of the lake survey, resulting in 15,324 soundings throughout the lake basin.

Table 1. Morphometric parameters of Lake Wedington derived from bathymetric survey and GIS analyses.

Parameter	Units
Fetch	1,000 m
Area	279,243 m^2 (69 acres)
Maximum Depth	12.4 m
Mean Depth	6.0 m
Shoreline Length	4,192 m
Volume of Lake	1,675,458 m^3
Watershed Area	10,198,440 m^2

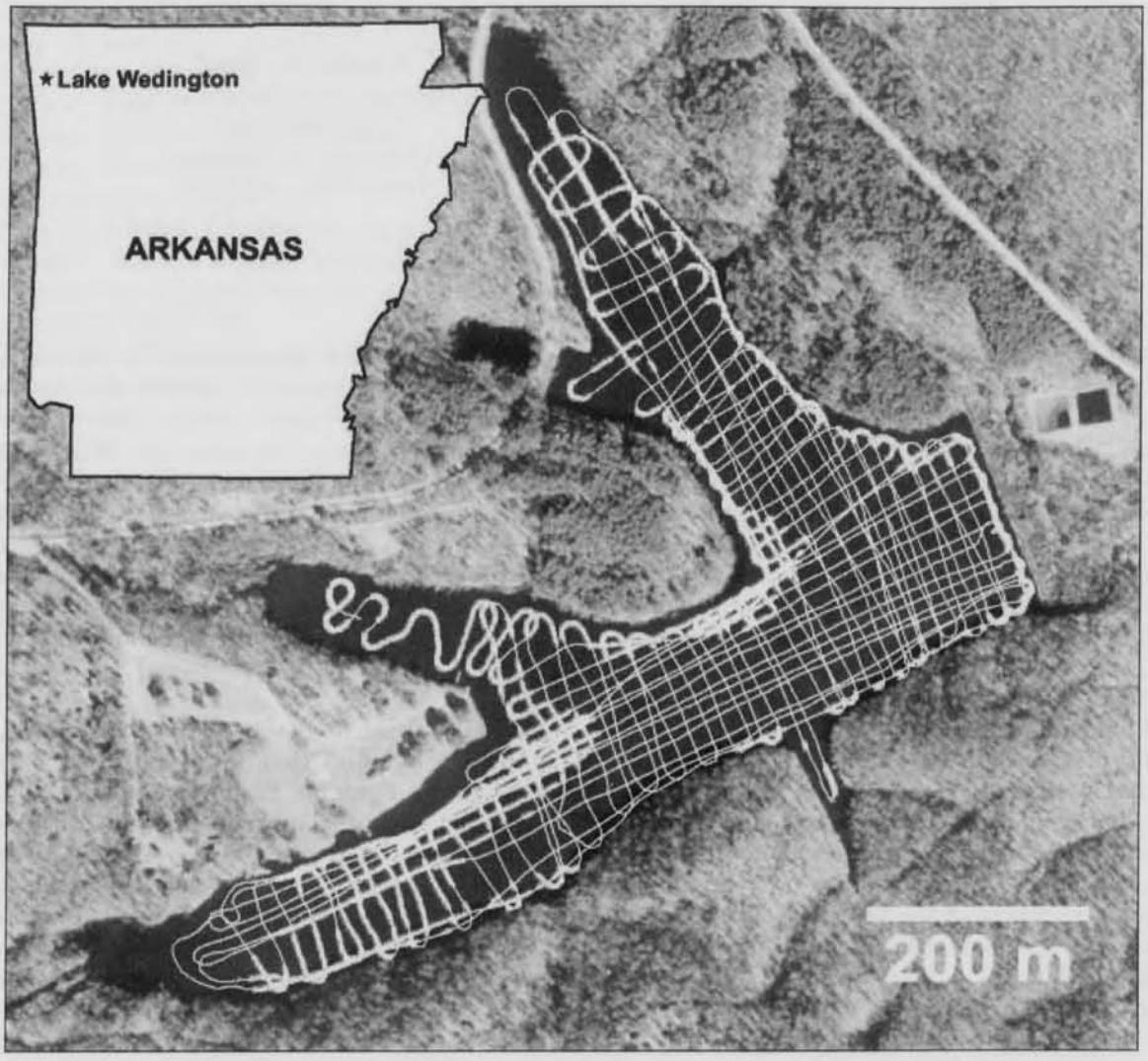

Fig. 1 Illustration showing location of Lake Wedington in northwest AR superimposed on aerial photograph of Lake Wedington and showing echo sounder survey track lines (white lines) and portions of track lines exhibiting anomalous acoustic signatures (bold white lines). Prominent road curving along north shore of Lake Wedington is AR State Highway 16.

Accurate positioning of the echo sounding survey within the lake basin was obtained using a Trimble Pathfinder Pro XRS Global Positioning System (GPS). Data obtained using this receiver were differentially corrected using the differential GPS radio beacon in Sallisaw, Oklahoma to provide location data with 2 to 3 m horizontal accuracy. Positions were automatically logged from the GPS receiver every five seconds during the survey. Following the survey, GPS data were interpolated to provide geographic coordinates (latitude and longitude) for each second of the survey, and these interpolated data were merged with echo sounder data and used to generate the bathymetric map (Fig. 2).

Various lake morphometric parameters were derived directly from survey data by importing these data to Geographic Information System (GIS) software (Table 1). In addition, a number of echo sounder profiles displayed anomalous acoustic signatures indicative of scattering of the acoustic impulse within the water column (Fig. 4). Locations of all echo sounder profiles or portions of profiles displaying this distinctive acoustic signature were displayed as an overlay on the overall map of survey tracklines (Fig. 1). The distribution of these anomalous echo profiles showed that all were associated with relatively shallow water (<5 m) along the lake margins or in the northern lake arms. Field inspection of the distribution of these profiles and visual

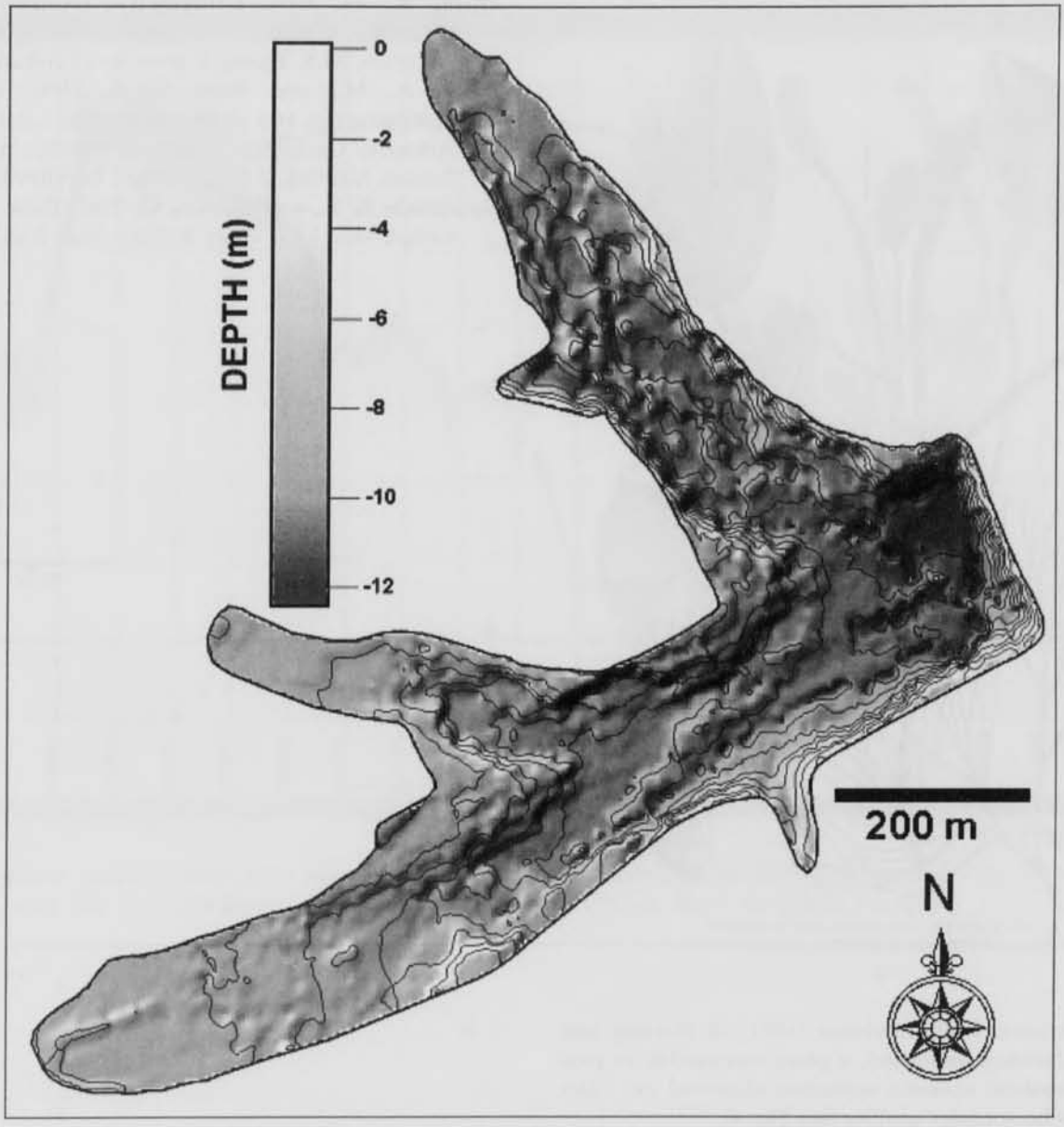

Fig. 2. Detailed bathymetric map of Lake Wedington, Washington County, Arkansas derived from dual frequency echo sounder survey of Polly (2001).

examination of the nearshore regions of the lake indicated that this signature resulted from scattering of the acoustic impulse by dense growths of aquatic vegetation.

These results indicate that the speed and efficiency of similar geophysical surveys could provide lake managers with a novel method to assess the distribution and abundance of aquatic plants throughout a lake basin. In addition, it would be possible to conduct repeat surveys several times through a growing season to determine changes in the distribution and abundance of lacustrine flora. As such, lake managers might find a powerful analytical tool in the application of acoustic geophysical methods for conducting assays of lake macroflora. Future studies will focus on quantifying the species composition of vegetation responsible for observed acoustic anomalies in Lake Wedington, and analyzing acoustic signatures that might correspond to individual plant species.

Fig. 3. Illustration from Lindman (1901) of floating leaf pondweed (*Potamogeton natans*), a plant responsible in part for the anomalous acoustic signature observed on Lake Wedington echo sounder profiles (see Fig. 4).

Literature Cited

Allman, J. F. 1952. Phytoplankton studies of Lake Wedington. Unpubl. M.S. Thesis, University of Arkansas, Fayetteville, Arkansas. 30pp.

Lindman, C. A. M. 1901. Bilder ur Nordens Flora [translated "Pictures of Nordic Flora"], Stockholm, Sweden. 650pp.

Owen, B. G. 1952. Limnological studies in Arkansas IV. Chemical-physical and biological features of Lake Wedington in its thirteenth and fourteenth years of impoundment. Unpubl. M.S. Thesis, University of Arkansas, Fayetteville, Arkansas. 43pp.

Polly, A. M. 2001. Bathymetry, sedimentation, and chemistry of Lake Wedington, Washington County, Arkansas. M.S. Thesis, University of Arkansas. 75pp.

Polly, A. M., and **Boss, S. K.** 2000. Bathymetry, sedimentation, and water chemistry of Lake Wedington, Arkansas: Geological Society of America South-Central Section Meeting, 2-5 April 2000, Fayetteville, AR

Robinson, E. S., and **Coruh, C.** 1988. Basic Exploration Geophysics: John Wiley & Sons, New York. 562pp.

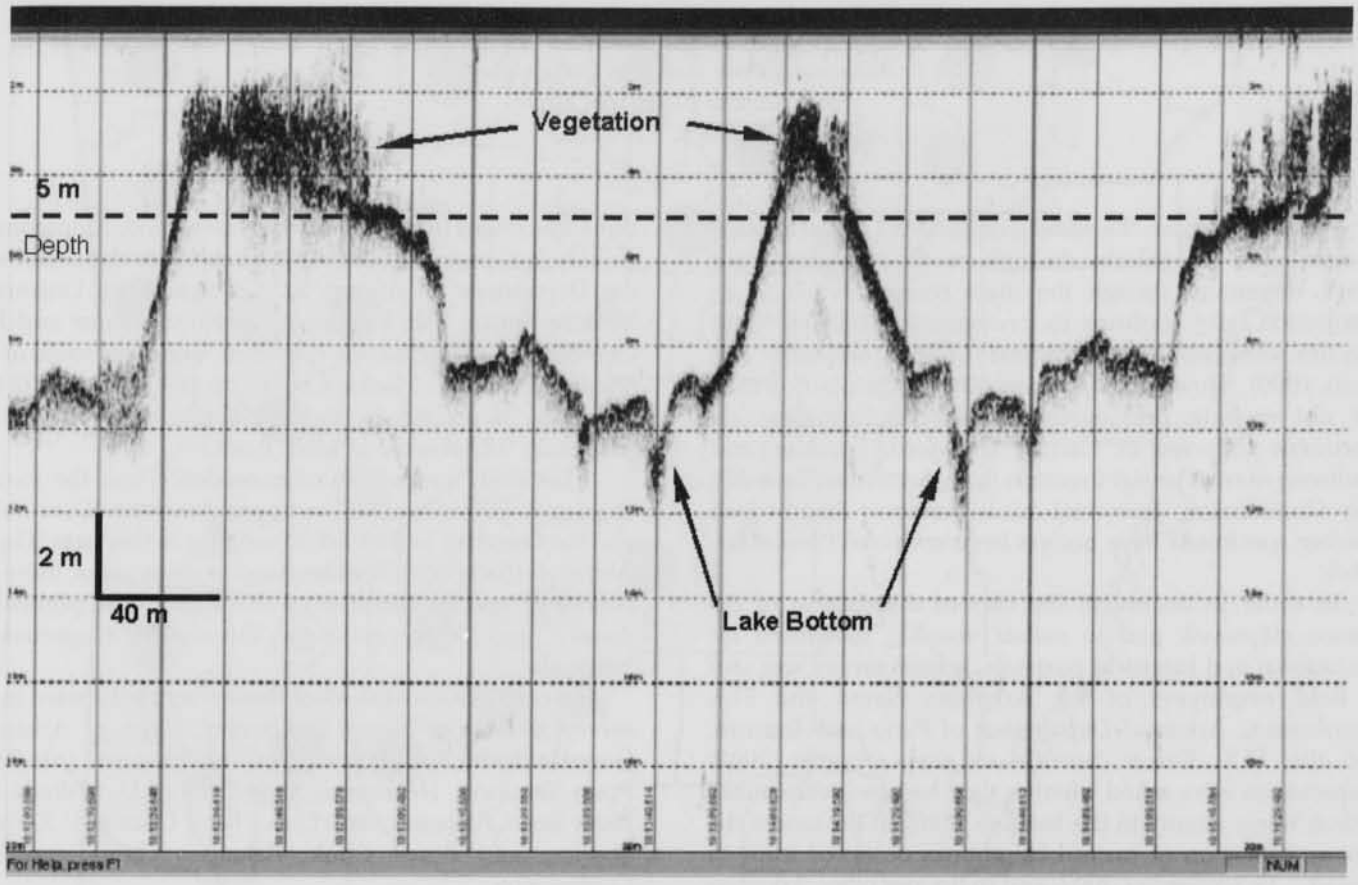

Fig. 4. Example of dual frequency echo sounder profile from Lake Wedington (depth on the vertical axis) showing acoustic signature of rocky lake floor and aquatic vegetation in shallow water (<5 m deep) along lake margins.

New Records of the Eastern Chipmunk (*Tamias striatus*) from Arkansas

D. Blake Sasse
Arkansas Game and Fish Commission
2 Natural Resources Drive
Little Rock, AR 72205

Within Arkansas, the eastern chipmunk (*Tamias striatus*) is distributed irregularly throughout the Ouachita and Ozark mountains though the most recent review of its distribution only confirms its presence in 21/49 (43%) of counties where appropriate habitat is found (Sealander and Heidt, 1990). However, the accompanying distribution map did not include previously published information on specimens collected in Carroll, Crawford, Franklin, and Madison counties or sight records from Arkansas Game and Fish Commission personnel in 10 counties from which voucher specimens have not yet been collected (Sealander, 1956).

In order to document the current distribution of the eastern chipmunk and to collect voucher specimens for educational and historical purposes, a mail survey was sent to field employees of the Arkansas Game and Fish Commission, Arkansas Department of Parks and Tourism, and the U.S. Forest Service in early August 2002. Respondents were asked whether they had seen chipmunks in their home county in the last five years, to document the date and location of eastern chipmunks observed from 15 August – 15 September 2002, and to list any other Arkansas counties in which this species was observed in the last five years. Willing respondents from counties lacking historical records of eastern chipmunk presence were asked to attempt to collect specimens for deposit in a museum.

A total of 223 surveys was received from 71/75 (95%) Arkansas counties. During the 15 August - 15 September 2002 survey period 36 respondents observed eastern chipmunks in 21 counties including new county records for Newton, Perry, Searcy, Sebastian, and Sharp counties. Eastern chipmunks have been observed in the last five years by 95/223 (43%) of respondents in 42/75 (56%) of counties, primarily in the Ozark and Ouachita mountains and the Arkansas River valley. These sightings account for new county records from Clay, Conway, Grant, Howard, Lonoke, Scott, Van Buren, and White counties.

One previously unpublished museum specimen collected by C.M. James on 24 October 1989 in Cleburne County was located in the Vertebrate Museum of the University of Arkansas at Little Rock. A specimen from Clark County was taken in 1991 (Tumlison et al., 1992) and three additional specimens from this county have been deposited in the collection at Henderson State University since then. Four new specimens were collected during this study. Mr. Richard Graham, U.S. Forest Service, collected three specimens in the vicinity of Greenwood, Montgomery County in September 2002, which have been deposited with the Department of Biology at Arkansas State University. Wildlife Officer Tim Davenport, Arkansas Game and Fish Commission, collected one specimen four miles south of Pot Shoals Net Pens in Marion County on 19 October 2002 that has been deposited in the Vertebrate Museum of the University of Arkansas at Little Rock.

This study provides further evidence that the eastern chipmunk is confined to the upper Arkansas River valley and the Ouachita and Ozark Mountains in this state (Fig. 1). Although this species is widespread in these areas, there is a paucity of specific research on the habitat use, population density, and demographics of the eastern chipmunk in Arkansas.

I would like to thank all of those who participated in the survey as well as Nancy McCartney, Univ. of Arkansas; Gary Heidt and Robert Sikes, Univ. of Arkansas-Little Rock; Renn Tumlison, Henderson State Univ.; J.D. Wilhide and Drew Reed, Arkansas State Univ.; Betty Crump, U.S. Forest Service; and Bruce Cook, Arkansas Game and Fish Commission.

Literature Cited

Sealander, J.A. 1956. A provisional check-list and key to the mammals of Arkansas (with annotations). Am. Midl. Nat. 56: 257-296.

Sealander, J.A., and G.A. Heidt. 1990. Arkansas Mammals: Their natural history, classification, and distribution. Univ. of Arkansas Press, Fayetteville. 308 pp.

Tumlison, R., M. Karnes, and M. Clark. 1992. New records of vertebrates in southwestern Arkansas. Proc. Arkansas Acad. Sci. 46: 109-111.

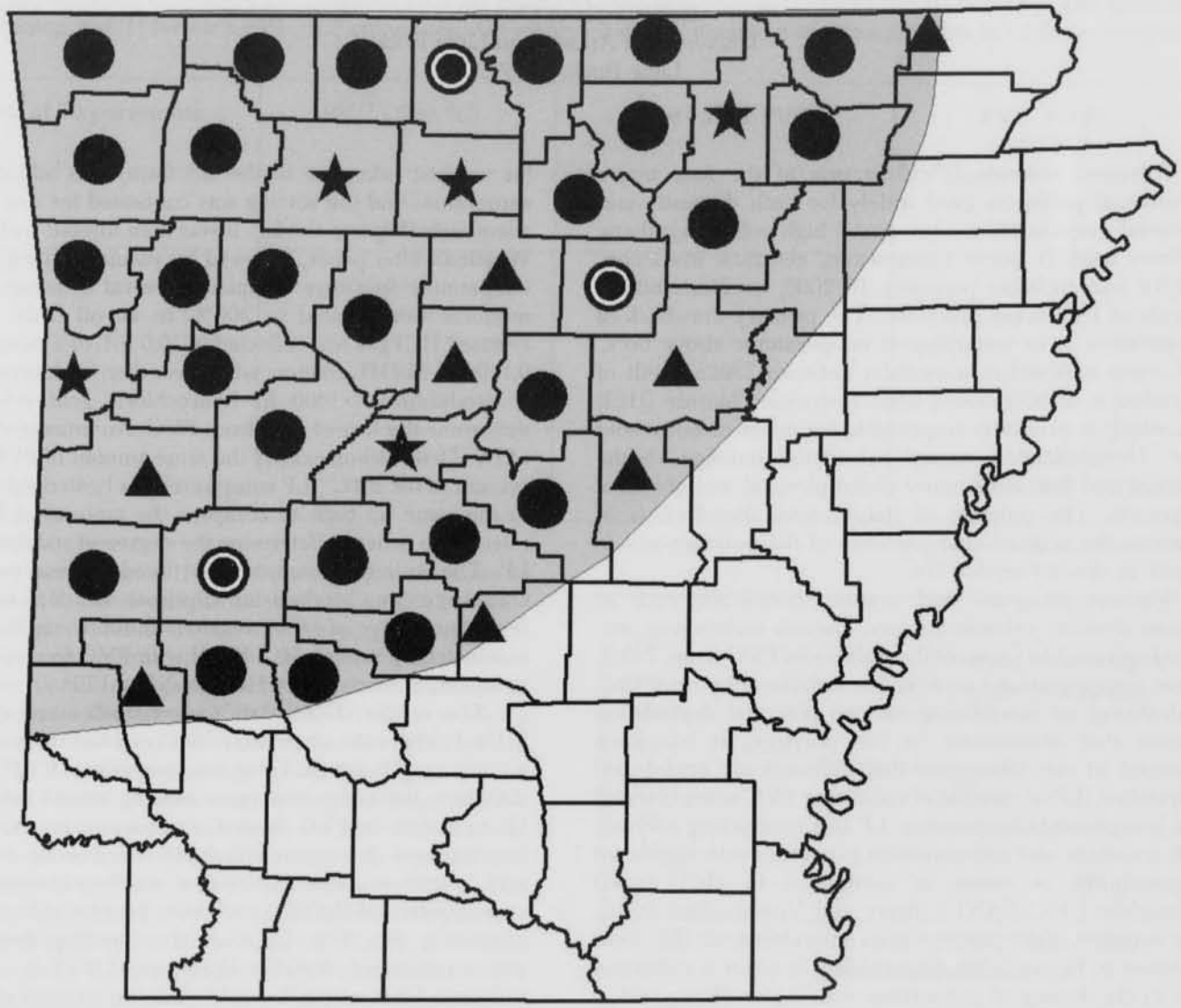

Fig. 1. Distribution of the eastern chipmunk (*Tamias striatus*) in Arkansas (modified from Sealander and Heidt, 1990). Solid circles represent counties with previously published voucher specimens whereas double circles represent specimens reported for the first time in this study. Sight records from 1997-2002 (triangles) and 15 August – 15 September 2002 (stars) are shown for counties lacking voucher specimens.

Stabilization of Polyvinyl Chloride by Some Conducting Polymers

Amit Shah, Brian C. Berry and **Ali U. Shaikh**
Department of Chemistry
University of Arkansas at Little Rock
Little Rock, AR 72204

Polyvinyl chloride (PVC) is one of the four major commercial polymers used widely for both domestic and industrial purposes. It is a low cost – high volume synthetic polymer used in home construction, electrical insulation, and for various other purposes. In 2000, over one billion pounds of PVC were produced. The primary drawback of the polymer is its instability at temperatures above 60°C and when exposed to ultraviolet radiation. As a result of degradation, PVC releases toxic hydrogen chloride (HCl) gas, which is primarily responsible for death in household fires. Destabilization causes substantial damage to the material and loss of its many useful physical and chemical properties. The purpose of stabilization, therefore, is to maintain the original characteristics of the polymer and to ensure its desired service life.

Various inorganic and organic chemicals, such as barium stearate, calcium stearate, barium carboxylate, etc. have been used to improve the stability of PVC (Ivan, 1996). These compounds act as arrestive stabilizers by removing, neutralizing, or inactivating various potential degradation sources that accumulate in the polymer. It has been observed in our laboratory that lignosulfonic acid-doped polyaniline (LP) is capable of stabilizing PVC when blended at a low percent composition. LP is a conducting polymer with anti-static and anti-corrosion properties with significant dispersibility in water as compared to HCl doped polyaniline (HCl-PANI) (Berry and Viswanathan, 2001). The structure of the polymer in its emeraldine salt (ES) form is shown in Figure 1. It's dispersibility in water is enhanced due to the doping of polyaniline with lignosulfonic acid, a highly water-soluble compound.

Studies were conducted by mixing LP with PVC at 5%, 10%, 20% and 30% (by mass of LP : PVC). Five grams of finely powdered untreated (unstabilized) PVC was poured into 100 mL distilled water in a beaker under constant stirring to produce a suspension. A measured amount of LP (as a moist cake and in the ES form) was added to the suspension, and the stirring was continued for one hour to adequately disperse the LP. It was then filtered with No. 42 Whatman filter paper, followed by vacuum drying at room temperature to assure complete removal of moisture. The mixtures were heated to 200°C in an oil bath, and the released HCl gas was collected in 10.0 mL of a standardized 0.1000 M NaOH solution, which was then back titrated with a standardized 0.1000 M hydrochloric acid solution to determine the loss of HCl from PVC. An untreated sample of PVC (containing exactly the same amount of PVC as was present in the PVC : LP composite) was heated side by side in the same oil bath to compare the amount of HCl gas released in order to determine the degree of stabilization by LP. The untreated sample was tested as received. Each composite was studied in triplicate to determine the reproducibility of the results. Similar studies were conducted by mixing HCl-PANI with PVC to compare the stabilization efficiency of HCl -PANI and LP.

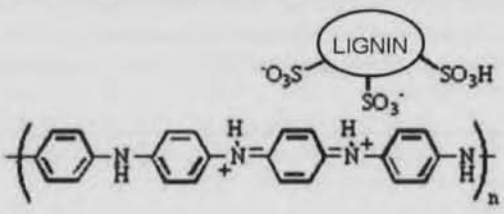

Fig. 1. Structure of LP in theEmeraldine Salt (ES) form.

The results of the stabilization studies are shown in Table 1, where the observed molarity of NaOH is shown as a function of % weight LP in the composites. If LP acts as a stabilizer, the composite upon heating would release less HCl gas than the PVC alone. Consequently, less NaOH will be consumed. A titration with the standardized hydrochloric acid, therefore, would reveal a smaller change in the concentration of NaOH. Obviously, the PVC:LP composite containing 5 - 20% LP showed a smaller decrease in concentration of NaOH. Therefore, LP does act as a stabilizer. One notices, however, that the absolute change in concentration varied slightly on a day-to-day basis for the same amount of PVC used in comparing the results of various composites. For example, the same amount of PVC used in conjunction with 5% and 10% composites showed an average molarity of 0.06987 M and 0.07282 M NaOH respectively, a difference of about 4%. The reproducibility of each composite measurement performed in triplicate, however, was within 0.5%.

Because of the variations as described above, it was considered more appropriate to plot the difference in molarity of NaOH (molarity of NaOH for PVC : LP composite vs. molarity of NaOH for PVC alone) as a function of weight percent stabilizer. As a result, the effect of day to day variation was minimized. The results are shown in Figure 2. The difference in molarity was found to be maximum for the 5% LP composite, indicating that maximum stabilization occurs with this composite. With

Table 1: Stabilization of PVC by LP. Released HCl gas from PVC was absorbed in 0.1000M NaOH Solution. The Molarity of the remaining NaOH for each PVC : LP composite with relative standard deviation of measurements in triplicate is reported.

No. of Experiments	PVC (200 ^{0}C)	% of LP in PVC	PVC + LP (200 ^{0}C)
1	0.0755 ±0.0034	5	0.0903 ±0.0020
2	0.0747 ±0.0025	10	0.0880 ±0.0021
3	0.0772 ±0.0015	20	0.0870 ±0.0005
4	0.0782 ±0.0025	30	0.0717 ±0.0017

increasing percentage of LP in the composite, the stability decreases. It is, therefore, concluded that about 5% PVC: LP composite gives the best stability. We plan to study still lower composite percentages (1% through 4%) to precisely determine the LP composite with maximum stability. In order to assess the effect of HCl-PANI (which is also a conducting polymer) on PVC stability, similar data for HCl-PANI : PVC composites are also plotted in Figure 2. One notices that the stability increases as the percentage of HCl-PANI in the composite is increased, but the effect is not as significant as with LP. Clearly, doping with lignosulfonic acid has a profound effect on the stabilization of PVC. The mechanism by which LP acts as a stabilizer is being further investigated in our laboratory. Also, the structural changes that occur in PVC during degradation and stabilization are also being studied by ultraviolet and infrared spectroscopy as well as by thermogravimetric analysis.

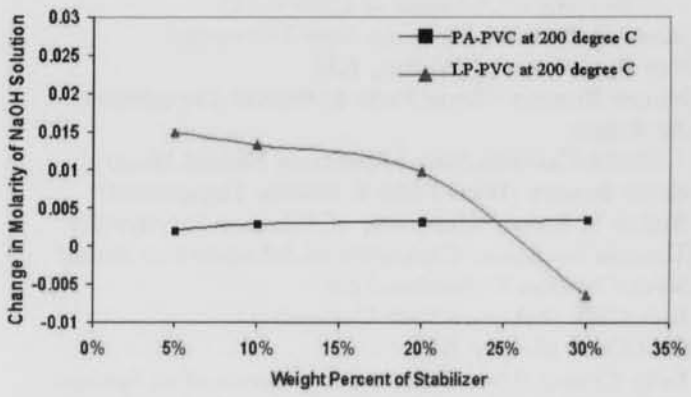

Fig. 2. The SIT fully pinched-off

References

Berry, B. C. and **T. Viswanathan.** 2001. Lignosulfonic acid-doped polyaniline – a Conductive polymer. Pp. 21-41, *In* Chemical Modification, Properties and Usage of Lignin (Hu T. Q., ed.), Plenum Publishers, New York, NY. 291 pp.

Ivan, B. 1996. Thermal stability, degradation and stabilization mechanisms of poly (vinyl chloride). Pp. 19-32 *In* Polymer Durability; Advances in Chemistry Series 249 (Clough, R, L. N. C. Billingham, and K. T. Gillen, eds.) American Chemical Society, Washington, D.C. 728 pp.

PUBLICATION POLICIES AND SUGGESTIONS FOR AUTHORS

The *JOURNAL* OF THE ARKANSAS ACADEMY OF SCIENCE appears annually. It is the policy of the Arkansas Academy of Science that 1) at least one of the authors of a paper submitted for publication in the *JOURNAL* must be a member of the Arkansas Academy of Science, 2) that only papers presented at the annual meeting are eligible for publication, and 3) that the manuscript is due at the time of presentation. In accordance with this policy, manuscripts submitted for publication should be given to the section chairman at the time the paper is being presented. Correspondence after this time should be directed to Dr. Chris T. McAllister, Managing Editor, *J. Arkansas Academy of Science*, Department of Biology, Texas A&M University-Texarkana, Texarkana, TX 75505.

Each submitted paper should contain results of original research, embody sound principles of scientific investigation, and present data in a concise yet clear manner. The COUNCIL OF BIOLOGY EDITORS STYLE MANUAL, published by the American Institute of Biological Sciences, is an example of a convenient and widely consulted guide for scientific writers. Authors should strive for directness and lucidity, achieved by use of the active voice. Special attention should be given to consistency in tense, unambiguous reference of pronouns, and to logically placed modifiers. It is strongly recommended that all authors 1) inspect the existing format for feature articles and general notes in the *JOURNAL OF THE ARKANSAS ACADEMY OF SCIENCE* and follow that format while drafting their submission, and 2) submit their manuscript to another qualified person for a friendly review to appraise it for clarity, brevity, grammar, and typographical errors.

Preparation of Manuscript

The author should submit three copies of the manuscript, tables, and figures. A diskette containing manuscript, table and figure files **MUST** also accompany submitted materials. If at all possible save the document as a Microsoft Word 6.0 document. The figures should be saved as tif, jpeg, or eps files. Manuscripts must be double spaced on 8-1/2 x 11 inch bond paper with at least one inch margins on all sides. Do not staple pages together. Do not hyphenate words on the right-hand margin; do not submit word processed copy printed with justified right-hand margins. Set words in italics that are to be in italics (e.g., scientific names). If co-authored, designate which author is to receive correspondence and at what address.Correspondence author should also include e-mail address, daytime telephone number and fax number. Minimum font size is 12 for text.

An abstract summarizing in concrete terms the methods, findings and implications discussed in the body of the paper must accompany a feature article. The abstract should be completely self-explanatory.

A feature article comprises approximately six or more typewritten pages. A *JOURNAL* printed page is equal to approximately three and one-half typewritten pages and the author is assessed a PAGE CHARGE (see Procedure section). A separate title page, including authors names and addresses should be included with the manuscript. Feature articles are divided into the following sections: abstract, introduction, materials and methods, results, discussion, conclusions, acknowledgments, and literature cited. These sections should be centered. Subheadings should begin at the left -hand margin, but more than one subheading should be avoided.

A general note is usually one to five typewritten pages and rarely utilizes subheadings. A note should have the title at the top of the first page with the body of the paper following. Abstracts are not used for general notes.

Abbreviations: Use of abbreviations and symbols can be ascertained by inspection of recent issues of the *JOURNAL*. Suggestions for uniformity include the use of numerals before units of measurements (5 m), but nine animals (10 or numbers above, such as 13 animals). Abbreviations must be defined the first time they are used. The metric system of measurements and weights must be employed.

The literature cited section should take the following form:

Davis, D. H. S. 1993. Rhythmic activity in the short-tailed vole, *Microtus*. J. Anim. Ecol. 2:232-238.

Hudson, J. W., and **J. A. Rummell.** 1966

Fleming, T. H. 1969. Population ecology of three species of neotropical rodents. Unpublished Ph.D. Dissertation. Univ. Michigan, Ann Arbor. 231 pp.

Jones, I. C. 1957. The adrenal cortex. Cambridge Univ. Press, London, 316 pp.

Wright, P. L. 1966. Observations on the reproductive cycle of the American badger (*Taxidea taxus*). Pp. 27-45, *In* Comparative biology of reproduction in mammals (I. W. Rowlands, ed.) Academic Press, London. xxi + 559 pp.

Tables and Illustrations: Tables and figures (line drawings, graphs, or black and white photographs) should not repeat data contained in the text. The author must provide numbers and short legends for illustrations and tables and place reference to each of them in the text. Legends for figures should be typed on a separate piece of paper at the end of the manuscript. Do not run tables in the text. **Illustrations must be of sufficient size and clarity to permit reduction to standard page size (or 1/2 page);** ordinarily they should be no larger then twice the size of intended reduction and whenever possible no larger than a manuscript page for ease of handling. Photographs must be printed on glossy paper. Sharp focus and high contrast are essential for good reproduction. Figures and labeling must be of professional quality. Notations identifying author, figure number, and top of print must be made on the back of each illustration. All illustrations must be submitted in duplicate. Tables must be of professional quality when submitted. Note preferred placement of figures and tables in the margins of the manuscript. Do not submit original artwork, photos, tables or figures with review copies of the manuscript.

Review Procedure

Evaluation of a paper submitted to the *JOURNAL* begins with a critical reading by the Managing Editor. The paper is then submitted to referees for checking of scientific content, originality, and clarity of presentation. Attention to the preceeding paragraphs will greatly speed up this process. Judgments as to the acceptability of the paper and suggestions for strengthening it are sent to the author. If the paper is tentatively accepted, the author will rework it, where necessary, and return two copies of the revised manuscript together with the original to the Managing Editor. Usually a time limit for this revision will be requested. If the time limit is not met, the paper may be considered to be withdrawn by the author and rejected for publication. All final decisions concerning the acceptance or rejection of a manuscript are made by the Managing Editor and/or Editor-in-Chief.

When a copy of the proof, original manuscript, and reprint order blanks reach the author, they should be carefully read for errors and omissions. The author should mark corrections on the proof and return both the proof and manuscript to the Managing Editor within 48 hours or the proof will be judged correct. Printing charges accruing from excessive additions to or changes in the proofs must be assumed by the author. Reprint charges are placed with the printer, not the Managing Editor. Page changes are $50 printed page. These changes and excessive printing charges will be billed to the author by the Academy of Science ($4.00 per word). A page charge will be billed to the author of errata.

ABSTRACT COVERAGE

Each issue of the *JOURNAL* is sent to several abstracting and review services. The following is a partial list of this coverage.

Abstracts in Anthropology
Abstracts of North America Geology
Biological Abstracts
Chemical Abstracts
Mathematical Reviews
Recent Literature of the Journal of Mammalogy
Science Citation Index
Sport Fishery Abstracts
Zoological Record
Review Journal of the Commonwealth Agricultural Bureau

BUSINESS AND SUBSCRIPTION INFORMATION

Remittances and orders for subscriptions and for single copies and changes of address should be sent to Dr. Jeff Robertson, Secretary, *J. Arkansas Academy of Science*, Department of Physical Science, Arkansas Tech University, 1701 N. Boulder, Russellville, AR 72801-2222.

Members receive one copy with their undergraduate membership of $15.00, regular membership of $30.00, sustaining membership of $35.00, sponsoring membership of $45.00 or life membership of $200.00. Institutional members and industrial members receive two copies with their membership of $100.00. Library subscription rates for 1997 are $25.00. Copies of most back issues are available. The Secretary should be contacted for prices.

TABLE OF CONTENTS